



Virginia Commonwealth University
VCU Scholars Compass

Theses and Dissertations

Graduate School

2022

Asymmetric CuH-catalyzed Reductive Coupling of Alleneamides with Carbonyl Electrophiles and the Mechanistic Investigation into the Suzuki-Miyaura Cross-couplings of Electron-Deficient Systems

Samantha L. Gargaro
Virginia Commonwealth University

Follow this and additional works at: <https://scholarscompass.vcu.edu/etd>

 Part of the [Organic Chemistry Commons](#)

© The Author

Downloaded from

<https://scholarscompass.vcu.edu/etd/7182>

This Dissertation is brought to you for free and open access by the Graduate School at VCU Scholars Compass. It has been accepted for inclusion in Theses and Dissertations by an authorized administrator of VCU Scholars Compass. For more information, please contact libcompass@vcu.edu.

**Asymmetric CuH-catalyzed Reductive Coupling of Alleneamides with
Carbonyl Electrophiles & Mechanistic Investigation into the Suzuki-Miyaura
Cross-coupling Reaction of Electron-Deficient Systems**

A dissertation submitted in partial fulfillment of the requirements for the degree of
Doctor of Philosophy at Virginia Commonwealth University

by

Samantha Leigh Gargaro

Bachelor of Science, Washington State University, 2018

Advisor and Dissertation Director: Dr. Joshua D. Sieber

Assistant Professor, Department of Chemistry

Committee: Dr. Joshua D. Sieber, Dr. Julio Alvarez, Dr. Brian Fuglestad, Dr. Frank Gupton

Virginia Commonwealth University

Richmond, Virginia

December 2022

© Samantha L. Gargaro 2022

All Rights Reserved

ABSTRACT

ASYMMETRIC CU-CATALYZED REDUCTIVE COUPLING OF ALLENEAMIDES WITH CARBONYL ELECTROPHILES & MECHANISTIC INVESTIGATION INTO THE SUZUKI- MIYAJIMA CROSS-COUPLING REACTION OF ELECTRON-DEFICIENT SYSTEMS

A dissertation submitted in partial fulfillment of the requirements for the degree of
Doctor of Philosophy at Virginia Commonwealth University.

By Samantha L. Gargaro, Ph.D.

Virginia Commonwealth University, 2022

Advisor: Dr. Joshua D. Sieber, Assistant Professor, Department of Chemistry

Most natural products and other biologically active small molecules contain multiple stereogenic heteroatoms throughout their carbon scaffold. As a result, methods to install these multi-heteroatom functionalities efficiently are highly desirable. Reductive coupling reactions have been studied extensively, and reductive allylation has been a key method for generating chiral secondary and tertiary allylic alcohols. This work focuses on utilizing naturally abundant and inexpensive Cu for the asymmetric reductive coupling of alleneamides with carbonyl electrophiles to access highly functionalized multi-heteroatom scaffolds that are difficult to produce via traditional methods. Described herein are methods for these asymmetric reductive coupling

reactions. Chapter 1 describes the development of CuH-catalyzed methods for the regio- and diastereoselective reductive coupling of *N*-based allenes and carbonyl electrophiles. The method reported was the first disclosed to access the novel linear product in the reaction with ketones, as well as directly access both the traditional branched product and the novel linear product from the same system by simply tuning the ligand. Initial projects utilized stereocontrol by a chiral auxiliary, whereas subsequent projects focused on the development of chiral-ligand controlled methods utilizing an achiral alleneamide. Chapter 2 describes the branched- and enantioselective borylative Cu-catalyzed reductive coupling of an achiral alleneamide with aldehyde electrophiles utilizing B₂(pin)₂ as the reductant. The intermediate of these reactions contains a boronate handle that allows for further derivatization and access to a wide array of dissonant 1,2-aminoalcohol motif-containing products based solely on the workup. This work is high-yielding with high diastereo- and enantiocontrol.

The Suzuki-Miyaura cross-coupling reaction is a highly utilized method for generating biaryl molecules in both industrial and academic settings. Traditional boronic acid homocoupling side product generation in these systems is due to O₂ intrusion during the reaction. However, during attempts to couple two electron-deficient fragments under anaerobic conditions, the boronic acid homo-coupling and aryl halide dehalogenation side products were both observed in similarly high yields. Chapter 3 describes the discovery and development of a novel anaerobic mechanism for the generation of aryl boronic acid homo-coupling product in the Suzuki-Miyaura cross-coupling reaction of electron-deficient systems. The discovery, mechanistic investigation, and scope of the optimized reaction are discussed.

This work is dedicated to

Joseph Gargaro

Rowan Gargaro

Jamie Ginter

Kevin Ginter

Kyrstin Ginter

In loving memory of

Alli Hanson

Doreen Parker

ACKNOWLEDGMENTS

I would like to take the time to thank my advisor, Dr. Joshua D. Sieber, for his guidance, patience, and unparalleled knowledge. This endeavor would not have been possible without you, and I will carry much of what I have learned in your lab with me going forward.

I would like to express my appreciation to my committee for your invaluable insight and constructive advice.

My fellow Sieber group members, for your friendship, collaboration, and help in gathering data for projects regarding Chapter 1.

Mrs. Elizabeth Carey, M.S., for being an incredible teacher and inspiring me to pursue a degree in the sciences. For embodying women in science and for the passion and enthusiasm brought to the subject material.

Dr. Maryanne Collinson for advocating for me when it came to parental leave after the birth of my son. Without your dedication, I may not have been able to make it this far.

Joseph, my loving husband, for all of your unwavering support and for being an amazing partner, father, and cheerleader. Rowan, you have driven this project for longer than you know.

My parents, Jamie and Kevin Ginter, for always believing in me and supporting me, for your unyielding love and support have gotten me so far. For emphasizing the importance of education, and always wanting your children to achieve their full potential. My sister, Kyrstin, for her support, love, and silliness.

All of my family, every one of you has supported me in one way or another; I know you are always there cheering me on and have helped make this possible. I love you all; work hard, get smart.

To my in-laws, namely Heather and Joey, for your support and willingness to child-sit so that I could write this dissertation.

The team at VCU Innovation Gateway, namely Magda Morgan and Brittaney Ritchie, for helping me realize my passion for Intellectual Property and inspiring the pivot in career path that I have since chosen.

And finally, for an endless supply of caffeine and proper mental health diagnosis and treatment for keeping me alert and sane enough to finish this feat. These last four and a half years seem to have simultaneously droned on and flown by. It's hard to believe my time here has come to an end.

TABLE OF CONTENTS

ABSTRACT	III
ACKNOWLEDGMENTS.....	VI
TABLE OF CONTENTS	VIII
LIST OF FIGURES.....	X
LIST OF TABLES.....	XI
LIST OF SCHEMES	XII
LIST OF ABBREVIATIONS	XIII
CHAPTER 1.....	1
I. INTRODUCTION.....	1
II. BACKGROUND.....	2
A. <i>Chiral Molecules and the Importance of Selective Syntheses</i>	2
B. <i>Highly-Functionalized Natural Products and Biologically Active Molecules</i>	3
C. <i>Retrosynthetic Analysis and Consonant/Dissonant Theory</i>	3
D. <i>Umpolung</i>	5
E. <i>Reductive coupling</i>	5
F. <i>Allylation</i>	6
III. RESEARCH PLAN AND RATIONALE	9
A. <i>Research Plan</i>	9
B. <i>C- vs N-based Allene</i>	9
IV. DEVELOPMENT OF A LINEAR-SELECTIVE AUXILIARY-CONTROLLED REDUCTIVE COUPLING.....	10
A. <i>Reaction Discovery</i>	10
B. <i>Substrate Scope</i>	14
V. DEVELOPMENT OF BRANCHED-SELECTIVE AUXILIARY-CONTROLLED METHOD	15
A. <i>Reaction Discovery</i>	15
B. <i>Reaction Development</i>	16
C. <i>Substrate Scope</i>	18
VI. STEREO- AND REGIOCHEMICAL MODEL.....	19
A. <i>Effect of Oxazolidinone Structure on Regioselectivity</i>	19
B. <i>Regio- and Stereochemical Model</i>	20
VII. DEVELOPMENT TOWARDS A LINEAR-SELECTIVE ENANTIOSELECTIVE METHOD.....	23
VIII. DEVELOPMENT TOWARDS AN ENANTIOSELECTIVE REDUCTIVE COUPLING METHOD WITH CF ₃ -KETONES	26
IX. CONCLUSIONS	30
X. EXPERIMENTAL METHODS	30
CHAPTER 2.....	42
I. INTRODUCTION.....	42
II. BACKGROUND.....	43
A. <i>Review of Reductive Coupling and Reductant Source</i>	43
B. <i>Rationale Behind Choice of Alleneamide</i>	44
III. DEVELOPMENT OF ENANTIOSELECTIVE BORYLATIVE AMINOALLYLATION.....	45
A. <i>Research Plan</i>	45
B. <i>Overall Reaction Development</i>	46
C. <i>Protonation Workup – Traditional branched 1,2-aminoalcohol generation</i>	51
D. <i>Oxidation workup – Methyl ketone synthesis</i>	53
E. <i>Suzuki-Miyaura Cross-coupling – 1,1-disubstituted olefin synthesis</i>	55
F. <i>Synthetic Applications – Aldol and Hydroboration</i>	59

G. Stereochemical Model.....	60
IV. CONCLUSIONS	61
V. EXPERIMENTAL PROCEDURES	62
CHAPTER 3.....	100
I. INTRODUCTION.....	100
II. BACKGROUND.....	101
A. Heterogeneous vs. Homogeneous Catalysis.....	101
B. Covalent-Organic Frameworks (COFs)	102
C. Fluorinated Pharmaceuticals.....	102
D. Suzuki-Miyaura Cross-Coupling.....	103
E. Typical homocoupling mechanism with O ₂	106
F. Electron-deficient coupling and why it is inherently difficult	107
III. EXPERIMENTAL DESIGN AND REACTION DEVELOPMENT	108
A. Initial Plan and Troubleshooting; Early Attempts	108
B. Homocoupling	111
C. Stoichiometric studies to ensure and propose an anaerobic mechanism	114
D. Mechanistic insight and proposed pathway	115
E. Cross coupling	118
F. Future Work.....	119
IV. CONCLUSIONS	120
V. EXPERIMENTAL PROCEDURES	121
APPENDIX A1. SELECT NMR SPECTRA FROM CHAPTER 1	128
APPENDIX A2. SELECT NMR SPECTRA FROM CHAPTER 2	142
APPENDIX A3. SELECT NMR DATA FOR CHAPTER 3	181
REFERENCES	207
VITA	224

LIST OF FIGURES

<i>Figure 1.1. Highly functionalized and structurally diverse natural products and biologically active molecules.</i>	<i>3</i>
<i>Figure 1.2. Consonant and dissonant theory in 1,n-substituted molecular frameworks.</i>	<i>4</i>

LIST OF TABLES

Table 1.1. Solvent survey for the development of a linear-selective method. ^a	11
Table 1.2. Ligand survey for the development of the linear-selective method ^a	13
Table 1.3. Branched-selective reductive coupling ligand survey ^a	17
Table 1.4. Ligand survey for the development of enantioselective linear-selective method.	24
Table 1.5. Ligand survey for the development of enantioselective linear-selective method with CF ₃ -ketones.	28
Table 2.1. Cu-catalyzed borylative aminoallylation ligand optimization. ^[a]	47
Table 2.2. Cu-catalyzed borylative aminoallylation reaction temperature optimization. ^[a]	48
Table 2.3. Cu-catalyzed borylative aminoallylation base optimization. ^[a]	49
Table 2.4. Cu-catalyzed borylative aminoallylation solvent optimization. ^[a]	50
Table 2.5. Cu-catalyzed borylative aminoallylation boronate optimization. ^[a]	51
Table 2.6. Oxidative workup optimization. ^[a]	54
Table 2.7. Suzuki-Miyaura reaction optimization. ^[a]	56
Table 2.8. Suzuki-Miyaura telescoping process optimization. ^[a]	56
Table 2.9. Further optimization of the telescoped Suzuki-Miyaura reaction and development of GP-4. ^[a]	58
Table 3.1. Ligand survey for the Suzuki-Miyaura cross-coupling reaction of the electron-deficient system.	110

LIST OF SCHEMES

<i>Scheme 1.1.</i> Overall method development for CuH-catalyzed reductive coupling reactions of alleneamides and carbonyl electrophiles.	2
<i>Scheme 1.2.</i> Overview of reductive allylative coupling.....	6
<i>Scheme 1.3.</i> Progression of the development of reductive allylative coupling.	7
<i>Scheme 1.4.</i> Buchwald's CuH-catalyzed reductive allylation method and working mechanistic hypothesis.	8
<i>Scheme 1.5.</i> Design for regiodivergency in allylative reductive coupling (this work):	10
<i>Scheme 1.6.</i> Linear-selective Substrate scope ^a	15
<i>Scheme 1.7.</i> Branched-selective method substrate scope. ^a	18
<i>Scheme 1.8.</i> Effect of oxazolidinone structure on regioselectivity.	19
<i>Scheme 1.9.</i> Stereo- and regiochemical model for the CuH-catalyzed reductive coupling methods.	20
<i>Scheme 1.10.</i> Driving forces for regioselectivity.	21
<i>Scheme 2.1.</i> Overall reaction development of the Cu-catalyzed borylative aminoallylation.....	43
<i>Scheme 2.2.</i> Effect of reductant source on product generation.....	43
<i>Scheme 2.3.</i> Borylcupration of C-based allenes as demonstrated by Hoveyda.	44
<i>Scheme 2.4.</i> Previous work in reductive aminoallylation utilizing a hydride reductant source.	44
<i>Scheme 2.5.</i> Borylative reductive aminoallylation research plan.	45
<i>Scheme 2.6.</i> Enantioselective borylative aminoallylation employing the protonolysis workup. ^[a]	52
<i>Scheme 2.7.</i> Enantioselective borylative aminoallylation, utilizing the oxidative workup. ^[a]	54
<i>Scheme 2.8.</i> Enantioselective borylative aminoallylation, utilizing Suzuki-Miyaura cross-coupling application. ^[a] ..	59
<i>Scheme 2.9.</i> Further synthetic applications of the reductive coupling products via a diastereoselective boron-mediated aldol reaction and diastereoselective hydroboration.	60
<i>Scheme 2.10.</i> Stereochemical model for preferential generation of anti-diastereomer over the syn-diastereomer....	61
<i>Scheme 3.1.</i> Suzuki-Miyaura Cross-coupling and competitive boronic acid homocoupling.	101

LIST OF ABBREVIATIONS

1,2-DME	1,2-dimethoxyethane
API	Active pharmaceutical ingredient
σ^*	sigma anti-bonding orbital
Ac ₂ O	acetic anhydride
ACN	Acetonitrile
AcOH	acetic acid
B(Et) ₃	Triethylborane
B ₂ (pin) ₂	bis(pinacolato)diboron
BINAP	2,2'-bis(diphenylphosphino)-1,1'-binaphthalene
BINOL	1,1'-binaphthalene-2,2'-diol
brsm	based on recovered starting material
CMD	Concerted metalation deprotonation
COF	Covalent organic framework
DIBAL	diisobutylaluminum hydride
DMF	N,N-dimethylformamide
dppf	bis(diphenylphosphino)ferrocene
dr	diastereomeric ratio
ee	enantiomeric excess
equiv	equivalents
er	enantiomeric ratio
EtOAc	ethyl acetate
EtOH	ethanol
H8-BINOL	Hydrogenated binol
HPLC	high performance liquid chromatography
iPr	Isopropyl-
MeOH	methanol
MeTHF	2-Methyl tetrahydrofuran
MOF	Metal organic framework
MS	molecular sieves
n.d.	not determined
n/a	not applicable
NaO ^t Bu	Sodium <i>tert</i> -butoxide
<i>n</i> -BuLi	<i>n</i> -butyllithium
NHC	<i>N</i> -Heterocyclic carbene
NMR	nuclear magnetic resonance spectroscopy

PCy ₃	tricyclohexylphosphine
Pd ₂ (dba) ₃	tris(dibenzylideneacetone)dipalladium
pin	pinacol
pyr	pyridine
RBF	round-bottom flask
rt	room temperature
TBHP	<i>tert</i> -butyl hydrogen peroxide
TBS	<i>tert</i> -butyldimethylsilyl
TBSOTf	<i>tert</i> -butyl dimethylsilyl triflate
TCDI	thiocarbonyl diimidazole
TEA	triethylamine
TEP	Tolman Electronic Parameter
THF	tetrahydrofuran
THP	tetrahydropyran
TLC	thin-layer chromatography
TMANO	trimethylamine N-oxide
UHP	urea hydrogen peroxide

CHAPTER 1

Development of Asymmetric CuH-Catalyzed Reductive Couplings of Alleneamides with Carbonyl Electrophiles

I. Introduction

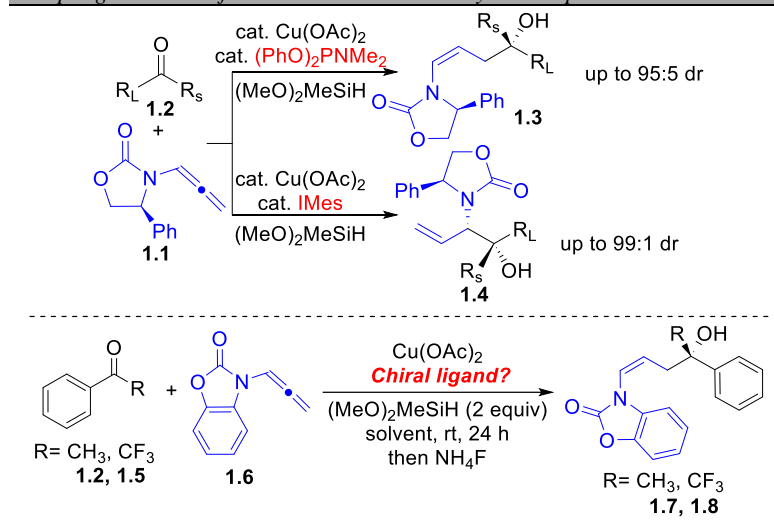
Many biologically active organic molecules and pharmaceuticals contain several stereogenic carbons and multiple heteroatoms throughout their carbon framework.¹⁻¹⁰ These stereogenic chiral centers affect the molecule's overall three-dimensional shape, and as a result, stereoisomers of the same molecule can have drastically different biological activity.¹¹ Therefore, selective syntheses of these complex molecules and the ability to control the regio-, stereo-, or enantioselectivity of C-C bond formation is essential in modern organic synthesis and has been a challenging endeavor for organic chemists over the years.

When considering chiral architectures containing multiple stereogenic carbon atoms bearing heteroatom substitution (*e.g.*, *N*, *O*), the polarization effects these electron-withdrawing groups can exert over the entire molecule can create synthetic challenges to the desired scaffold when applying traditional methods. Particularly challenging heteroatom substitution patterns must then be formed via non-traditional means, and reductive coupling reactions (*i.e.*, cross-electrophile coupling) have been extensively studied as an efficient synthetic method for these non-traditional C-C bond formations.^{9,12-17} While this has been an intense area of study, methods to impart multiple stereocenters while installing multiple heteroatoms in single steps still need development.

This research builds upon the CuH-catalyzed portfolio to-date, by switching the traditional reactivity of the fragments, in an effort to access new reactivity in the system as well as develop methods to install multiple heteroatoms to generate increasingly complex products containing dissonant functionalities.^{18,19} Utilizing inexpensive and widely available starting materials, the development of Cu-catalyzed methods for the regio- and diastereoselective reductive coupling of *N*-based allenes (alleneamides) and carbonyl electrophiles are herein described (**Scheme 1.1-Top**). These methods were the

first disclosed to access the novel linear product **1.3** in the reaction with ketones **1.2**, as well as directly access both the traditional branched product **1.4** and the novel linear product **1.3** from the same system by simply tuning the ligand. The initial projects utilized stereocontrol by a chiral auxiliary (**1.1**) whereas subsequent projects focused on the development of chiral-ligand controlled methods utilizing an achiral alleneamide (**1.6**, **Scheme 1.1-Bottom**).

Scheme 1.1. Overall method development for the CuH-catalyzed reductive coupling reactions of alleneamides and carbonyl electrophiles.



II. Background

A. Chiral Molecules and the Importance of Selective Syntheses

Chirality within organic molecules is significant, as it greatly affects the biological activity and other pharmacokinetic properties of bioactive organic molecules and Active Pharmaceutical Ingredients (APIs).¹¹ This is due to stereogenic carbons containing four distinct substituents, and the effect of their orientation on the overall three-dimensional shape of the isomer.¹¹ There are countless examples of enantiomers of the same molecule exhibiting drastically different biological activity, including the infamous case of Thalidomide. The Thalidomide racemate, brought to market in the 1950s, was available over-the-counter for the treatment of multiple conditions, including morning sickness in pregnant mothers.²⁰ It was later discovered that the (*R*)-enantiomer of Thalidomide was the active form of the hypnotic drug; the (*S*)-enantiomer was not an active hypnotic, but instead was teratogenic, causing over 10,000 infants to be born

with limb malformations and other birth defects.²¹ As isomers of organic molecules can exhibit drastically different pharmacokinetic properties,²² guidelines and regulations for drug development have changed to favor single isomer drug compositions and emphasize the development of selective syntheses.²³ For these reasons, it is imperative to have a wide set of methods for generating single isomers selectively, through regio-, diastereo- or enantioselective means.¹¹

B. Highly-Functionalized Natural Products and Biologically Active Molecules

Nature is quite skilled and efficient at producing highly functionalized and complex molecules. Most natural products and biologically active small molecules contain multiple heteroatoms spread throughout their carbon framework;^{3-7,17,24-26} examples are given in **Figure 1.1**. These highly functionalized complex scaffolds require a heavy amount of planning into their synthesis, as each route must be carefully crafted to ensure viability and selectivity for each step. Therefore, developing methods to selectively install multiple heteroatoms in minimal steps is invaluable.^{4-6,8-10}

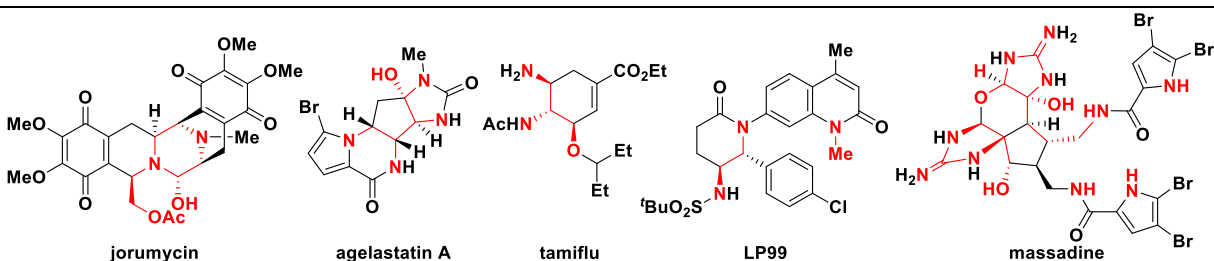


Figure 1.1. Highly functionalized and structurally diverse natural products and biologically active molecules.

C. Retrosynthetic Analysis and Consonant/Dissonant Theory

Before attempting to synthesize complex organic molecules, the planning stage must be approached carefully to determine efficient routes and viable selective methods to the desired molecule. Current standard practice for determining synthetic routes for organic molecules is the use of retrosynthetic analysis. The concept of retrosynthetic analysis was developed by E. J. Corey in the 1960s, winning him the Nobel Prize in 1990.²⁷ Using the steps that he proposes,²⁸ key disconnections (known as “strategic bonds”) are identified by working backwards from the desired target molecule, and the molecule is broken down into

simple intermediates, referred to as “synthons”. This process allows for the direct and efficient identification of possible routes that may then be explored in the forward synthetic direction.

When designing these synthetic routes, the electronics of the desired bond disconnection also needs to be considered. For instance, a strategic bond lying on a path between two functional groups creating a matched chain polarization should be easier to form via traditional methods compared to a strategic bond where the chain polarization is mismatched by the two functional groups causing traditional methods to be ineffective. In the 1970's, Evans conceptualized this idea and designated the terms Consonant and Dissonant Charge Affinity, and the phrase Consonant/Dissonant Theory, also known as Polar Bond Theory (**Figure 1.2**).^{18,19} Recently, this theory has been elegantly laid out in a review by Reisman,²⁹ and application of the concept was described by Seebach.³⁰

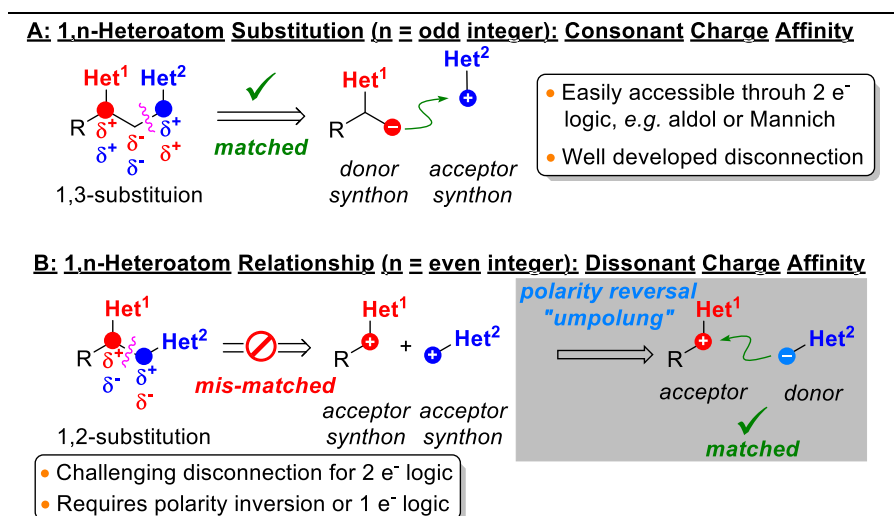


Figure 1.2. Consonant and Dissonant Theory in 1,n-substituted molecular frameworks.

According to the Evans construct, each functional group in a molecule polarizes the carbon framework in a certain way, impacting the overall electronic distribution across the carbon chain of the molecule. When multiple functional groups are present, each group leads to a specific carbon chain polarization that may either reinforce (consonant) or conflict (dissonant) each other. When considering *N*- or *O*-heteroatom substituents that are electron-withdrawing by nature, the scenario in **Figure 1.2** is produced. For a 1,n-substitution pattern between two electron-withdrawing functional groups, if *n* is an odd integer, a consonant charge affinity results (**Figure 1.2A**), and strategic bonds lying along this path

may be more easily synthesized via traditional two-electron methods and generally are well-known. However, if *n* is an even integer, a dissonant charge affinity results (**Figure 1.2B**) creating a scenario that is more difficult to construct via traditional methods relying on two-electron mechanistic pathways. In these cases where dissonant relationships exist, non-traditional methods, such as umpolung (polarity-reversal)³⁰ or radical^{31–35} chemistry are more suited from a strategic design perspective.

D. Umpolung

While ubiquitous, the 1,2- and 1,4-substitution of heteroatoms are inherently difficult to access via traditional two-electron processes, as they have a dissonant relationship caused by the conflicting electronic pattern throughout the molecule.^{19,30} As a result, one process to better access these functionalities is the method of polarity umpolung³⁰, or polarity reversal, to access previously hard-to-reach dissonant functional group pairs. The term umpolung, meaning "pole reversal" in German, was first coined by Seebach³⁶ in 1974 for the chemical modification of a functional group with the aim of reversing the traditional polarity of that functional group within a molecule to access hidden reactivity, **Figure 1.2B**. Umpolung-based approaches have become the go-to method for generating these dissonant scaffolds.^{37–41}

E. Reductive coupling

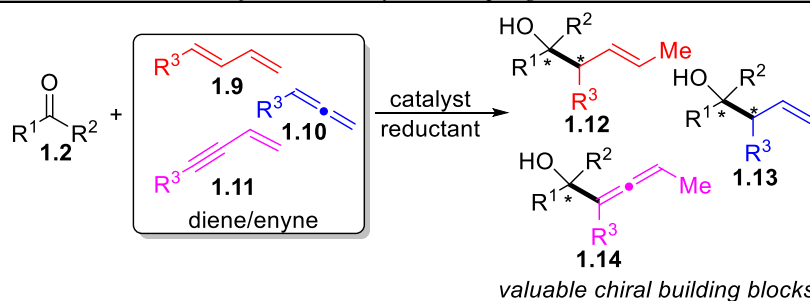
The classic method for generating C-C bonds includes the redox-neutral coupling of a nucleophilic (electron-rich) species and an electrophilic (electron-deficient) species.⁴² Other methods have been developed to utilize different coupling partners. One of these methods includes reductive coupling, or "cross-electrophile" coupling, in which two electrophilic fragments are coupled; both getting reduced in the process.^{12,14,43–46} As both fragments get reduced, a stoichiometric reductant must be used to turn over the catalyst.¹² Common reducing agents include BEt_3 , R_3SiH , H_2 , or $\text{B}_2(\text{pin})_2$. Reductive coupling reactions have been seen more recently as an elegant way to bring together new coupling partners,¹² and reductive allylation has been a favorite of these reactions, as an olefin and heteroatom are generated – both of which can be further functionalized.

F. Allylation

i. Pioneering work in allylation – H.C. Brown, 1980's

A powerful coupling method for the installation of a stereogenic carbon-heteroatom bond is through the catalytic reductive allylative coupling of carbonyl electrophiles and conjugated unsaturated hydrocarbons (**Scheme 1.2**).^{15,47–49} Early work in stereoselective allylation, such as the work of H.C. Brown in the 1980s,^{50–52} employed the generation of a stoichiometric chiral allylmetal nucleophile **1.15** in a separate step to be used in the allylation reaction with an aldehyde or ketone to generate the chiral alcohol (**Scheme 1.3A**).

Scheme 1.2. Overview of Reductive Allylative coupling.

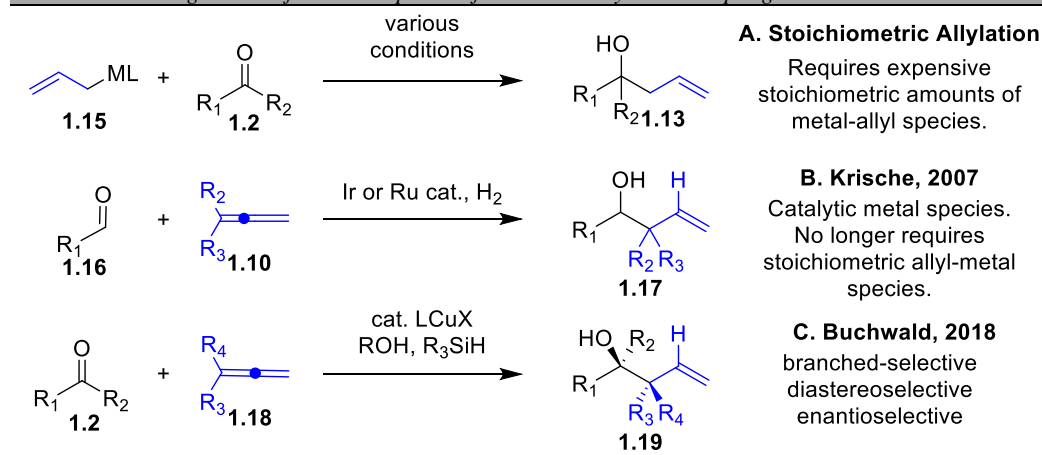


This combined process required 3 steps and over 3 days in order to form the allylborane starting material. While this pioneering method allowed for the generation of allylic alcohols, this process has some drawbacks including the requirement of stoichiometric amounts of metal-allyl species, which is expensive and time-consuming, as the metal-allyl species had to be generated separately prior to use.

ii. Development of catalytic methods for allylation

The use of stoichiometric allyl-species for allylations lasted nearly 40 years,^{53,54} prior to the development of methods for the *in situ* generation of the catalytic allyl-species. Since then, catalytic methods have emerged to generate the reactive allylmetal species *in situ* from an unreactive allyl source and a metal catalyst. Commonly used reactive allylmetal species include Boron^{55–59}, Silicon^{60,61}, and Tin^{62–65}-based, and many methods have utilized umpolung approaches to employ the allyl electrophile as a nucleophile^{37–41}.

Scheme 1.3. Progression of the development of Reductive Allylative Coupling.



However, reductive coupling strategies^{15,47–49} that generate the reactive allylmetal from unsaturated hydrocarbons via hydrometalation, in particular, are extremely powerful, atom-economical approaches for the synthesis of chiral homoallylic alcohols.^{66–73}

iii. *Krische's formation of metal-allyl species in situ*

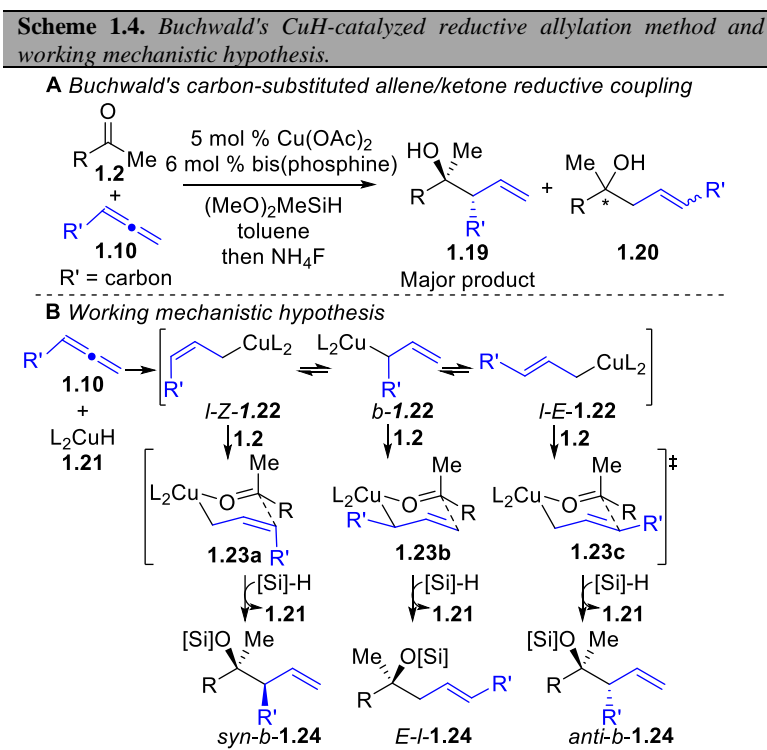
Pioneering work by Krische (**Scheme 1.3B**) enabled a method to circumvent the use of pre-formed allyl-metal reagents through the use of catalytic Ir^{74,75} or Ru⁷⁶ for the addition of dimethylallene to an aldehyde electrophile to generate secondary allylic alcohols **1.17**. This reductive coupling strategy included the use of H₂ as the stoichiometric reductant. Hydrometalation of the allene forms the metal allyl complex *in situ*. Mitigating the use of stoichiometric quantities of pre-formed organometallic reagents led to improvements in atom economy and functional group tolerance; however, both Ir and Ru are still costly precious metals at \$154 and \$15 per gram, respectively.⁷⁷ As a result, catalytic versions using cheaper, more readily available metals still needed to be developed.

iv. *Buchwald's orthogonal method using CuH*

Copper hydride (CuH) has been studied extensively over the years⁷⁸ but has only recently been explored as a catalyst for reductive coupling reactions.⁷⁹ In this regard, CuH-catalyzed reductive coupling of unsaturated hydrocarbons and carbonyl electrophiles has emerged as a method to generate chiral alcohols. In 2018, Buchwald developed an elegant method for generating chiral tertiary allylic alcohols **1.19** via the reductive coupling between allenes^{80–82} **1.10** or 1,3-dienes⁸³ **1.9** and ketone or imine

electrophiles (**Scheme 1.3C**). As ketones are less reactive than aldehydes, this reaction worked with and thus utilized catalytic copper, an inexpensive and widely available alternative to precious metals (Cu costs <\$0.01 per gram).⁷⁷

This work used a copper catalyst with chiral bis(phosphine) ligands to couple an achiral allene to ketone electrophiles to generate the *anti*-diastereomer of the branched tertiary allylic alcohol product **1.19**. Utilization of silane (*e.g.* (MeO)₂MeSiH) as the reductant, forms CuH *in situ* after reacting with catalytic copper, as demonstrated in **Scheme 1.4B**. Hydrocupration across the external olefin of the allene then begins the reductive coupling cycle. Buchwald has shown that the addition to the ketone is the rate-limiting step,⁸³ meaning that the three possible intermediates of **1.22** may be present in rapid equilibrium.⁸⁴ After coupling of intermediate **1.22** with the carbonyl electrophile **1.2**, likely through chair-like transition states **1.23a,b,c**, and turnover by silane, the O-Si products **1.24** are obtained. This method selectively generated the *anti*-branched product *anti-b-1.24* as the major product in high diastereo- and enantioselectivity.



III. Research Plan and Rationale

A. Research plan

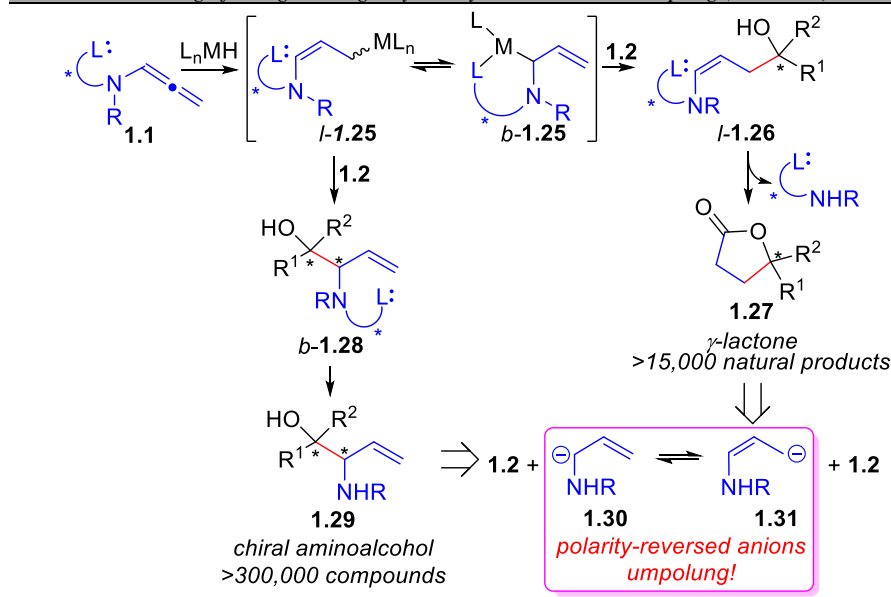
While not confirmed by Buchwald, we initially hypothesized that the intermediates in **Scheme 1.4B** may be in rapid equilibrium and that the observed major product obtained by Buchwald (*anti-b-1.24*) was a result of Curtin-Hammett kinetics whereby **1.23c** represents the lowest energy transition structure. Furthermore, of significance is the fact that linear products had never been produced from such reductive coupling methods using ketone electrophiles. Therefore, our group initially became interested in developing a method to generate the novel linear product utilizing a similar approach to Buchwald, which had not been reported with ketones. According to the above Curtin-Hammett selectivity proposal, selective generation of the linear product *E-l-1.24* would require a way to favor transition structure **1.23b** to achieve this goal. While Buchwald had previously shown that generation of both the linear and branched products are possible when utilizing imine electrophiles⁸⁰ by switching the *N*-substituent on the imine, this is not possible with ketone electrophiles. As a result, developing a new strategy for accessing the novel linear product using ketone electrophiles is necessary.

B. C- vs N-based allene

In order to enable a linear selective process, we needed to determine how to favor reaction through the branched copper(allyl)-intermediate species *b-1.22* that is likely uphill in energy due to increased steric interactions compared with linear copper(allyl)-intermediates *l-Z-1.22* and *l-E-1.22*. To solve this problem, we proposed that the equilibrium between these nucleophilic species could be influenced by the use of a chelating group tethered to the allene by a heteroatom to allow for subsequent cleavage of the chelating group (**Scheme 1.5**). The tethered ligand should help stabilize the branched (allyl)Cu intermediate *b-1.25* through coordination to copper. Then, reaction with the ketone *via* a six-membered chair-like transition state would generate the linear product **1.26**, containing an enamine group, representing a masked aldehyde functionality to provide useful dissonant chiral 1,4-hydroxyaldehyde equivalents. If the chelating group utilized is chiral, it could help enable stereocontrol over the newly formed stereocenter of **1.26**. Cleavage

of that chiral tethered chelating group could then generate the 1,4-lactone **1.27** – an important motif that is present in over 15,000 natural products.⁸⁵

Scheme 1.5. Design for regiodivergency in allylative reductive coupling (this work):



Alternatively, we reasoned that the branched product **1.28** may also be accessible under conditions that may inhibit coordination of the directing group (*e.g.* high coordination number at Cu) which would enable synthesis of the highly useful dissonant 1,2-aminoalcohol motif **1.29** that is present in over 300,000 compounds including over 2,000 natural products and over 80 FDA-approved drugs.⁸⁶ The development of synthetic methods to access these ubiquitous functionalities has been a rising topic in the field of organic chemistry.^{87–99}

IV. Development of a Linear-Selective Auxiliary-Controlled Reductive Coupling

A. Reaction Discovery

Our initial goal was to bias the selectivity of the reductive coupling reaction of allenes to carbonyl electrophiles to generate the novel linear product by forming a system that favors reactions through the branched substituted copper(σ -allyl) nucleophile. With this aim, we developed a *N*-based allene containing a chelating group that could coordinate to copper. We began with the Evans' chiral auxiliary¹⁰⁰-derived alleneamine **1.1** because: (1) it is inexpensive and readily commercially available; (2) it had been synthesized previously and was known in the literature;¹⁰¹ and (3) we hoped that the carbonyl of the

oxazolidinone would be a sufficient enough coordinating group^{102,103} to Cu to stabilize the transition state needed to generate the linear product **1.3a**. To keep copper at a low-enough coordination state to allow chelation by the oxazolidinone, the reaction conditions needed to facilitate this and thus reflect these goals. Conditions that would be conducive to keeping copper at a low coordination state include the use of non-coordinating solvents, as well as monodentate ligands.

An investigation into the solvent effect was initially performed to determine the most appropriate solvent choice for further reaction optimization (**Table 1.1**). The results were obtained in collaboration with Raphael Klake and Dr. Joshua Sieber. Non-coordinating aprotic solvents were surveyed as an effort to keep the coordination state of copper low (entries 1, 2, 5, and 6).¹⁰⁴ However, regioselectivity had marginal impact based on solvent choice. While a more polar solvents such as dichloromethane effectively gave no selectivity over linear and branched products and poor yield (entry 3), use of polar coordinating solvent THF (entry 4) gave comparable linear:branched selectivity to that of non-coordinating solvents such as toluene (entry 5,6), MTBE (entry 1), or dioxane (entry 2).

Table 1.1. Solvent survey for the development of a linear-selective method.^a

Reaction scheme showing the reaction of oxazolidinone **1.1** and ketone **1.2a** to form linear product **1.3a** and branched product **1.4a**. Reagents: 5 mol % Cu(OAc)₂, 6 mol % P(*t*-Bu)₃•HBF₄, 5.5 mol % KO*t*-Bu, Me(MeO)₂SiH, solvent, rt.

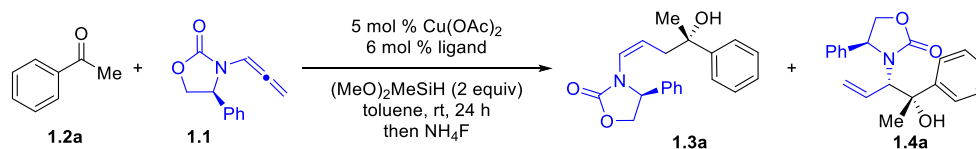
Entry	Solvent	<i>l</i> : <i>b</i> ^b	% yield 1.3a ^c	dr 1.3a ^b
1	MTBE	78:22	52	92:8
2	Dioxane	76:24	62	93:7
3	CH ₂ Cl ₂	58:42	33	91:9
4	THF	75:25	33	93:7
5	toluene	76:24	61	93:7
6 ^d	toluene	74:26	60	93:7

^aReactions performed as described in the general catalyst screening procedure. ^bDetermined by ¹HNMR spectroscopic analysis on the unpurified reaction mixture. ^cDetermined by quantitative ¹HNMR analysis on the unpurified reaction mixture. ^d10 mol % of P(*t*-Bu)₃•HBF₄ and 10 mol % of KO*t*-Bu was used.

While solvent choice had minimal impact on regio- and diastereoselectivity, reaction yield was significantly impacted. As the solvent became increasingly non-polar (entries 4, 1, 2, 5, respectively), an increase in yield was observed. The best overall results were observed with toluene (entry 5), which was therefore chosen as the model solvent choice. Increasing the ligand loading to 10 mol% (entry 6) led to no improvements, so 6 mol% ligand was kept as the optimal ligand loading.

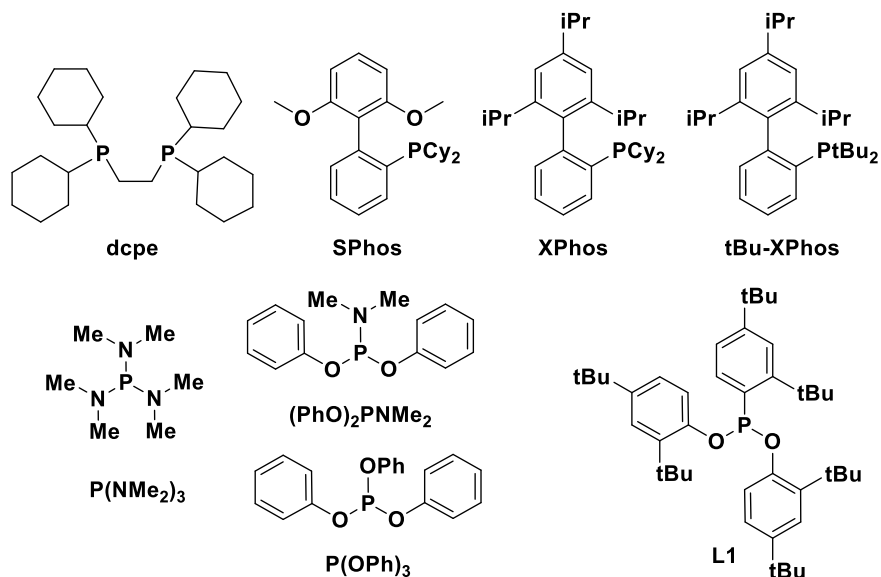
We then began an investigation into the ligand used in an effort to favor the linear product, as per our proposal, (**Table 1.2**). The results given in **Table 1.2** were performed by Dr. Joshua Sieber and two undergraduates in the laboratory (Skyler Gentry and Sharon Elele). Monodentate trialkyl phosphines showed modest favorability toward the linear product **1.3a** (entries 1, 3, 4). Dcpe, a common bidentate ligand for CuH-reductive coupling reactions,⁸⁰⁻⁸³ favored the generation of the undesired branched product (entry 2) consistent with inhibition of oxazolidinone coordination by increasing the coordination number at Cu through use of a chelating ligand. After completing this comprehensive survey varying the steric and electronic properties of various ligands, a general trend was observed based on the electron-donating ability of the ligand used. The Tolman Electronic parameter^{105,106} can be used as a common value for comparison of the electron-donating ability of ligands. The Tolman Electronic parameter value represents the ν_{CO} stretching frequency of a $\text{LNi}(\text{CO})_3$ complex obtained by Infrared Spectroscopy (IR). It is a measurement of the strength of CO triple bond as impacted by the strength of backbonding to Ni that varies based on the electron-donating ability of the ligand L. Larger TEP values represent stronger CO bonds implying reduced backbonding to Ni which is less electron-rich due to reduced electron-donation by the ligand L. Linear selectivity was observed to increase using ligands with less electron-donating ability. This observation is consistent with oxazolidinone-Cu coordination being important for linear selectivity since as the ligand used becomes less electron-donating, copper would be expected to become more Lewis acidic, which would promote coordination of the carbonyl of the oxazolidinone to copper and overall result in increased linear selectivity.

Table 1.2. Ligand survey for the development of the linear-selective method^a



Entry	Ligand	TEP ^b	Cone angle ^c	<i>l:b</i> ^d	dr linear ^d	% yield linear ^d
1	PCy ₃	2056	170	80:20	84:16	68
2	dcpe	--	142	23:77	84:16	14
3	P(<i>t</i> -Bu) ₃	2056	182	76:24	93:7	61
4	P(adam) ₃	2052	--	71:29	93:7	71
5	Sphos	--	--	9:91	68:32	7
6	Xphos	--	--	12:88	N.D.	5
7	<i>t</i> -BuXPhos	--	--	26:74	N.D.	5
8	P(<i>o</i> -tol) ₃	2067	194	70:30	81:19	14
9	P(NMe ₂) ₃	2062	157	83:17	87:13	79
10	P(OEt) ₃	2076	109	92:8	83:17	90
11	(PhO) ₂ PNMe ₂	--	--	97:3	90:10	97
12	L1	--	--	97:3	92:8	89
13	P(OPh) ₃	2085	128	99:1	89:11	76
14	P(C ₆ F ₅) ₃	2091	184	99:1	85:15	12

^a**1.2a** (0.25 mmol) and **1.1** (0.30 mmol) in 0.5 mL of toluene. See the Experimental Information for details. ^bTolman electronic parameter of $\text{LNi}(\text{CO})_3$ complex.^{105,106} ^cLigand cone angle obtained from literature.¹⁰⁵ ^dDetermined by ¹HNMR spectroscopy on the unpurified reaction mixture.

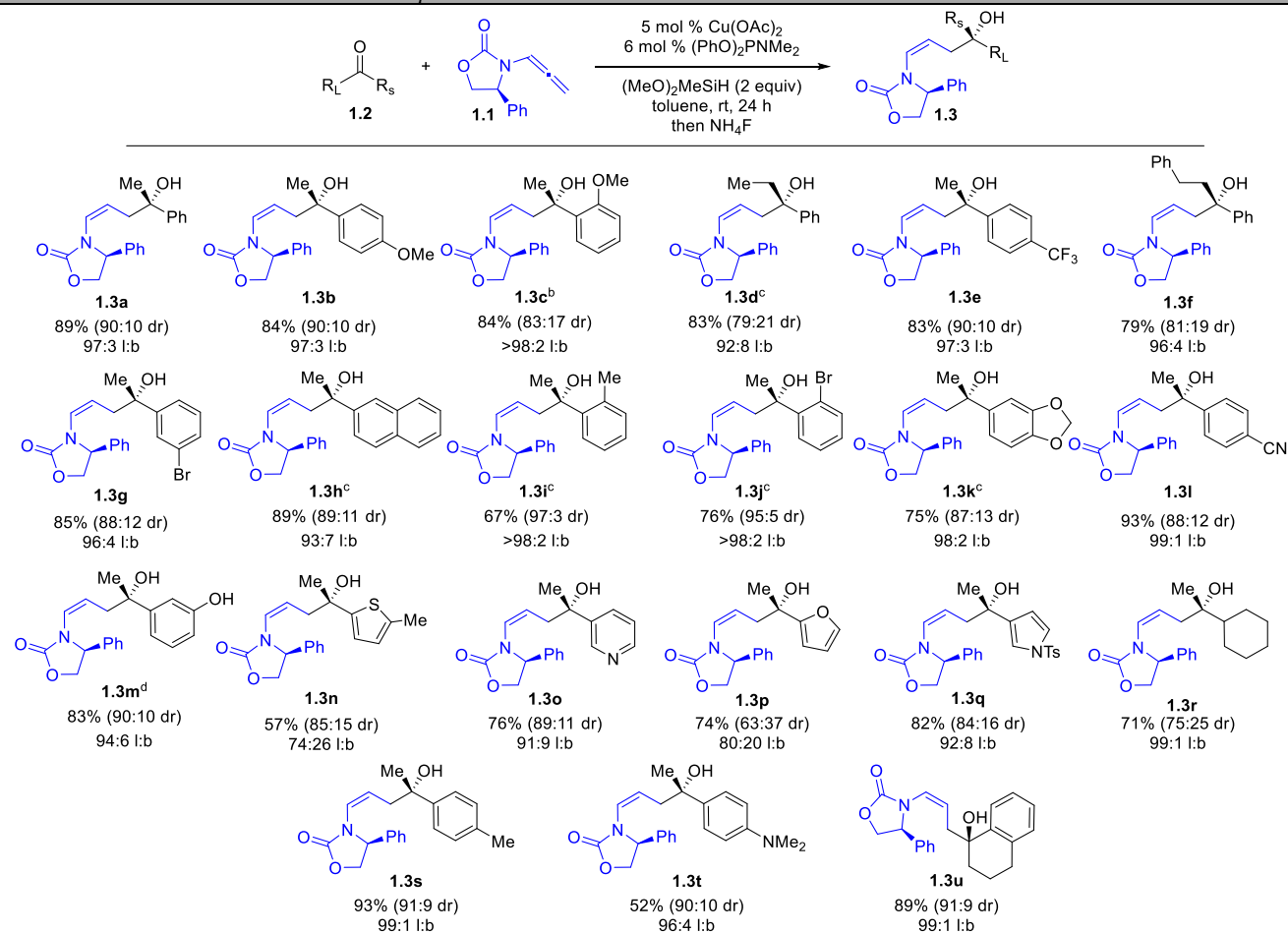


There was a rough correlation between ligand cone angle and diastereocontrol with larger ligands affording higher diastereoselectivity (compare entries 1, 3, 4, 9, 10, 12, and 13). This aspect will be further analyzed in *Section VI: stereo- and regiochemical model*. The highest linear selectivity and yield were obtained by phosphoramidite (PhO)₂PNMe₂ (entry 11). This phosphoramidite ligand was then selected as the optimal ligand to probe the substrate scope in the reaction.

B. Substrate Scope

After the reaction conditions were optimized, the scope of the reaction was examined by varying the ketone electrophile (**Scheme 1.6**). These results were obtained in collaboration with another graduate student in the lab, Raphael Klake. The reaction is highly linear selective and worked well for a wide variety of ketones including electron-rich (**1.3b,c,k,m**) and electron-poor arenes (**1.3e,o**). Analysis of the substrate scope determined that a variety of functional groups including nitriles (**1.3l**), amines (**1.3**), and free hydroxyl groups (**1.3**) were well tolerated. This is essential for the wide applicability of this reaction, as well as the ability to subsequently further functionalize the product. Lower yield was observed for the sterically hindered *ortho*-substituted aromatic ketones (**1.3c,i,j**), which required heating for full conversion. Sterically hindered ketones may have lower yield, but still give high regio- and diastereoselectivity. The five-membered heteroarenes (**1.3n,p,q**) examined offered slightly lower yield, with modest selectivity. This could be due to a combination of the steric difference between 6- and 5-membered aromatic rings as well as the electronic difference between arene and heteroarene systems.

When the size difference between the small and large R groups on the ketone reactant is made less significant, where the two R groups are closer in size, such as the examples of propiophenone **1.3d** and 2-phenylacetophenone **1.3f**, the regio- and diastereoselectivity are both reduced. The stereo- and regiochemical model for this reaction will be further analyzed in *Section VI: Stereo- and regiochemical model*. This method that we developed allowed us to form the novel linear product from these reductive coupling reactions with carbonyl electrophiles that had previously not been accessible.

Scheme 1.6. Linear-selective Substrate scope^a

^aPercent yield represents isolated yield of linear product as a mixture of two diastereomers on 0.5 mmol scale of **1.2** using 1.2 equiv of **1.1**. Diastereomeric ratios (dr) and linear:branched ratios (l:b) were determined by ¹H NMR spectroscopy on the unpurified reaction mixture. ^bReaction performed at 60 °C. ^cReaction performed at 40 °C. ^d4.0 equiv of Me(MeO)₂SiH used.

V. Development of Branched-Selective Auxiliary-Controlled method

A. Reaction Discovery

Based on our original proposal and previously developed linear-selective reductive coupling mechanism, we set out to develop a branched-selective coupling method to generate pharmaceutically-relevant chiral 1,2-aminoalcohol scaffolds. Our linear-selective work demonstrated that monodentate ligands that were less electron-donating favored linear product formation **1.3** presumably due to coordination of the oxazolidinone carbonyl to copper.¹⁰⁷ Based on this work, more electron-donating ligands^{105,106} that may inhibit oxazolidinone binding to Cu, or chelating ligands that may saturate copper's

coordination number were hypothesized to lead to branched product **1.4** selectively using the same Evans' auxiliary-derived allene **1.1**.

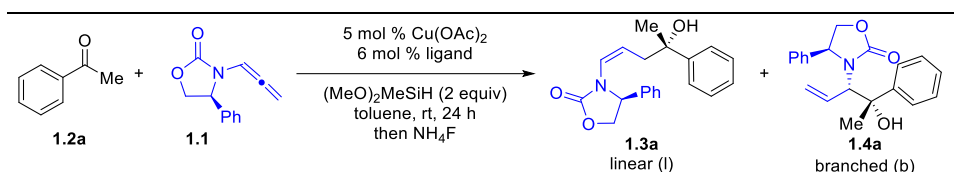
B. Reaction Development

We predicted that by using a ligand that could destabilize the coordinating ability of the oxazolidinone, a branched-selective process may be enabled through favoring reaction through the less sterically hindered transition structures **1.23a** or **1.23c** ($R' = X_c$, **Scheme 1.4**) from reaction with the linear substituted Cu(σ -allyl) nucleophile **1.22a** or **1.22c**. A survey of bidentate and electron-donating ligands was examined in collaboration with Dr. Joshua Sieber and Raphael Klake for this system (**Table 1.3**). Phosphines and phosphoramidite ligands, such as $P(OPh)_3$ (entry 1) and $(PhO)_2PNMe_2$ (entry 2) respectively, selectively generated the linear product, as seen in our previous work. Dcpe (entry 5), a common ligand used in reductive coupling reactions,⁸⁰⁻⁸² favored the generation of branched product, but with low yield, regio-, and diastereoselectivity.

The use of more coordinating solvents did not aid in the reaction, as seen in entries 6 and 7. In our proposal, use of a coordinating solvent could have helped in our goal of favoring the branched product, as solvent coordination could saturate copper, preventing further coordination from the oxazolidinone carbonyl, and thus inhibit linear product formation. While this could occur, the effect of using coordinating solvent was not great enough to see any visible difference in selectivity.

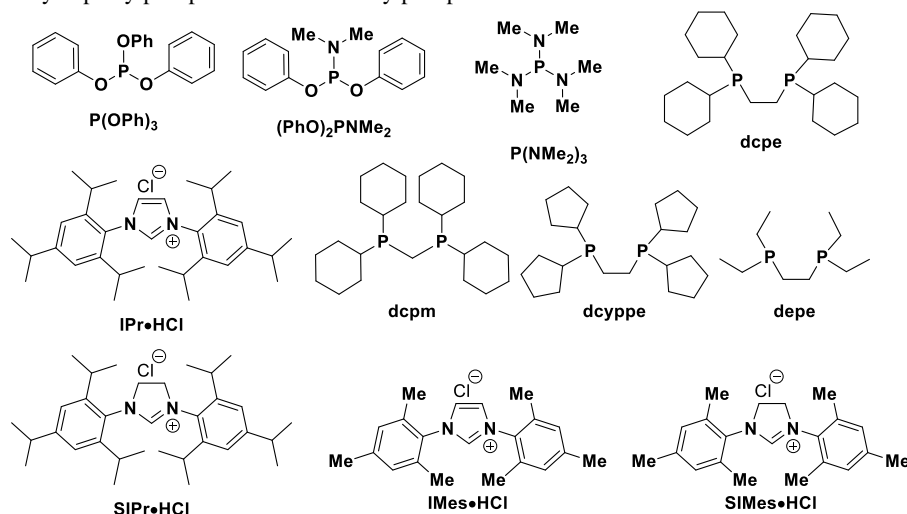
Ligand bite angles represent the measured ligand-metal-ligand bond angle in which bidentate ligands attach to the metal; these values can be used as a measure of sterics effects around the metal center and have the potential to greatly affect the reaction.¹⁰⁸ The bite angle in this case did not have an effect on the reaction. This aspect was probed by surveying ligands with increasingly larger bite angles (seen in entries 5, 8, 9, and 10); however, the larger bite angle did not change the yield, dr, or regioselectivity in any comprehensive manner.

Table 1.3. Branched-selective reductive coupling ligand survey^a



Entry	Ligand	TEP ^b	Yield b 1.4a ^c	Dr 1.4a ^c	b:l ^c
1	P(OPh) ₃	2085	<2	--	1:99
2	(PhO) ₂ PNMe ₂	--	2	--	3:97
3	P(NMe ₂) ₃	2062	16	88:12	17:83
4	PCy ₃	2056	17	93:7	20:80
5	dcpe	--	47	53:47	77:23
6	dcpe w/ DME	--	28	59:41	65:35
7	dcpe w/ THF	--	24	60:40	53:47
8	dcpm ^d	--	25	92:8	39:61
9	dcyppe ^e	--	32	54:46	66:34
10	depe ^f	--	27	57:43	50:50
11	IPr	2052	70	87:13	87:13
12	SIPr	2052	15	82:18	99:1
13	IMes	2051	76	93:7	83:17
14	SIMes	2052	78	92:8	89:11

^aA1 (0.25 mmol) and 1 (0.30 mmol) in 0.5 mL of toluene. ^bTolman electronic parameters obtained from literature.^{105,106} ^cDetermined by ¹HNMR spectroscopy on the unpurified reaction mixture using dimethylfumarate as a standard. ^dDicyclohexylphosphinomethane. ^eDicyclopentylphosphinoethane. ^fDiethylphosphinoethane.

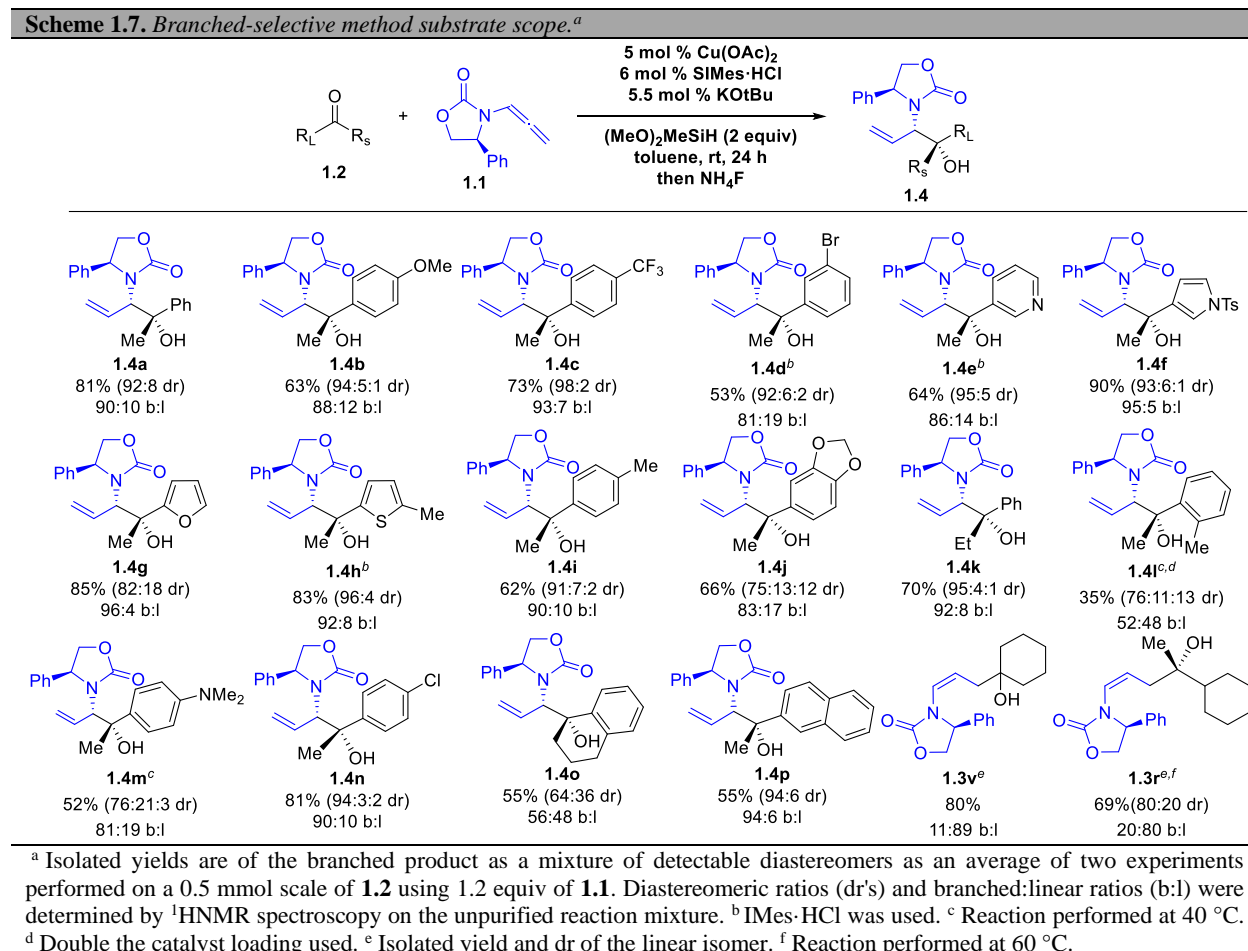


Finally, the use of electron-rich *N*-heterocyclic carbene ligands (NHC's) allowed for the selective production of the branched product (Table 1.3, entries 13 and 14). NHC's, such as IMes and SIMes, are sterically bulky and highly electron-donating ligands¹⁰⁶ that allow for inhibition of oxazolidinone

coordination to the Cu-catalyst, leading to branched product **1.4a** selectivity. IMes and SIMes, for the purposes of this method, gave similarly high yields, with high stereoselectivity and diastereoselectivity.

C. Scope of Reaction – Substrate scope

Once the branched-selective method was developed and optimized, we set out to probe the scope of the reaction (**Scheme 1.7**). The reactions were performed in collaboration with fellow graduate students Raphael Klake and Kevin Burns.



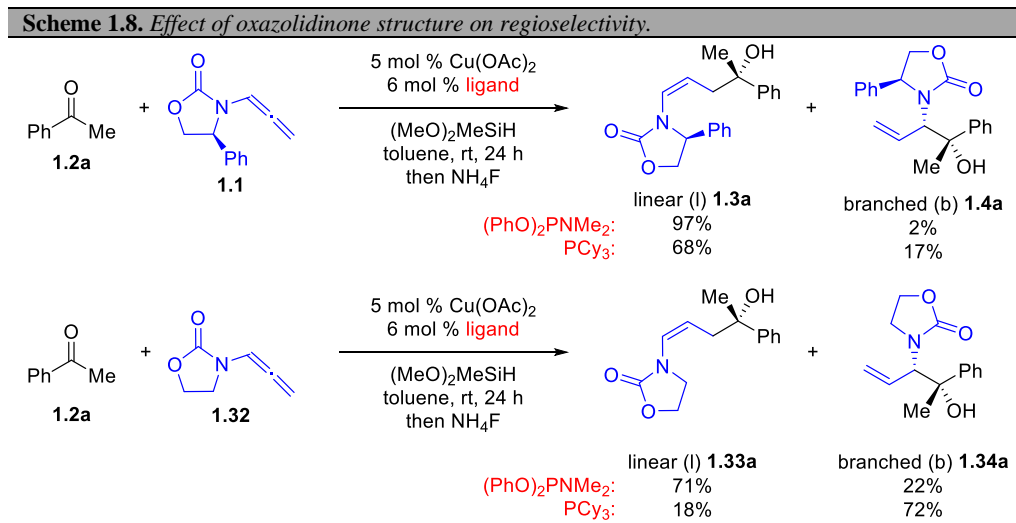
The reaction tolerated electron-rich and electron-poor aryl ketones, and was tolerant of arylhalides **1.4n**, heterocycles **1.4e,f,g,h**, and amines **1.4m**. The reaction using NHC's is highly branched selective, but very sensitive to sterics. Aryl ketones containing a *meta*-substituent generated lower yield with lower regioselectivity, **1.4d**, **1.4j**. Also, *ortho*-substituted aryl ketones **1.4l** were not well tolerated and gave near

equal yields of branched and linear product, even with heating at 40°C and double the catalyst loading. Finally, sp³-containing aliphatic ketones, such as cyclohexyl methyl ketone **1.3r**, and cyclic ketones, such as cyclohexanone **1.3v**, generated greater yields of the linear product.

VI. Stereo- and Regiochemical model

A. Effect of Oxazolidinone Structure on Regioselectivity

With the data from these two consecutive projects in hand, we set out to understand what factors govern the regio- and stereoselectivity of these reductive coupling reactions in more detail. For the purpose of this system, regioselectivity is defined as the ratio of the linear and branched products generated, as determined by ¹HNMR spectroscopy on the unpurified crude reaction mixture. Diastereoselectivity is then defined as the ratio of the diastereomers of the respective linear or branched product produced in these reactions, as determined by ¹HNMR spectroscopy on the unpurified crude reaction mixture. Because the chiral allenamide contains a stereocenter, the diastereomers produced from these reactions are effectively enantiomers after the chiral auxiliary is cleaved, as only one stereocenter would remain.

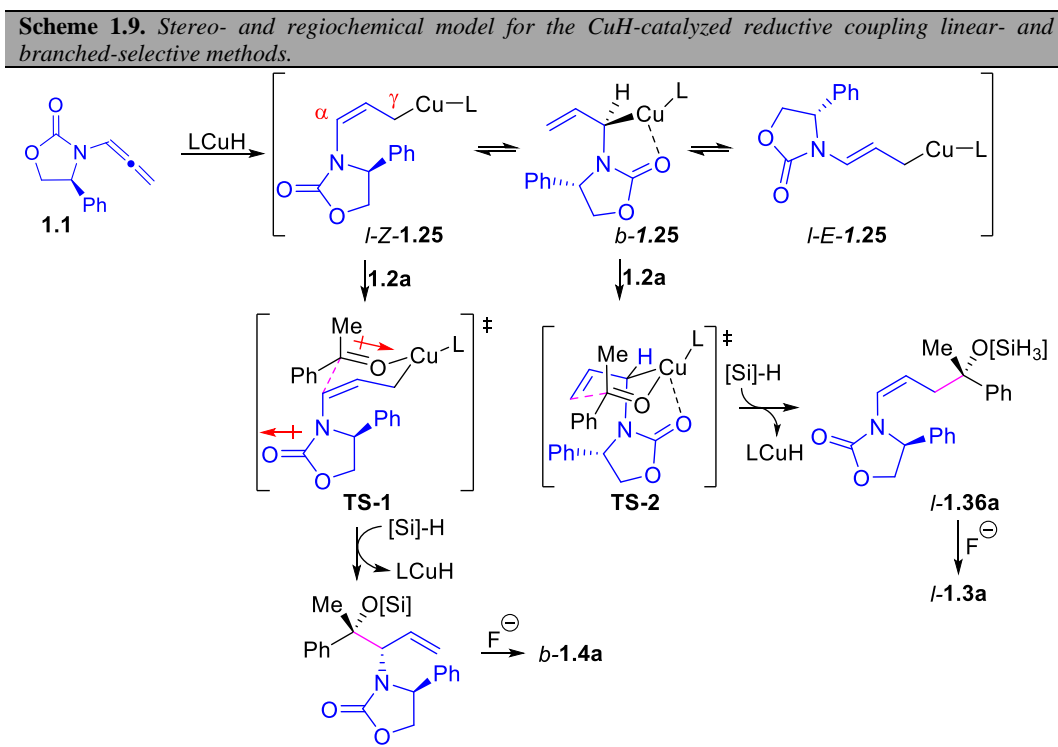


The effect of the oxazolidinone structure on regioselectivity was investigated by examining the yield and selectivity of the reaction of large and small oxazolidinone-based allenamides with phosphine ligands of varying electron-donating ability. Chiral allenamide **1.1** allowed for selective generation of the linear product **1.3a** for both the optimized linear-selective phosphoramidite ligand and electron-rich PCy₃.

However, when the smaller achiral oxazolidinone-based alleneamide (**1.32**, **Scheme 1.8**) was tested, the optimized linear-selective ligand generated the linear product **1.33a** with less regioselectivity than the chiral alleneamide **1.1**. Also, when this achiral alleneamide **1.32** was used with electron-rich ligands, such as both PCy₃ and SIMes, the reaction generated the branched product **1.34a** selectively. This is proposed to be due to the minimization of the A_{1,3}-interaction that will be discussed in the next section.

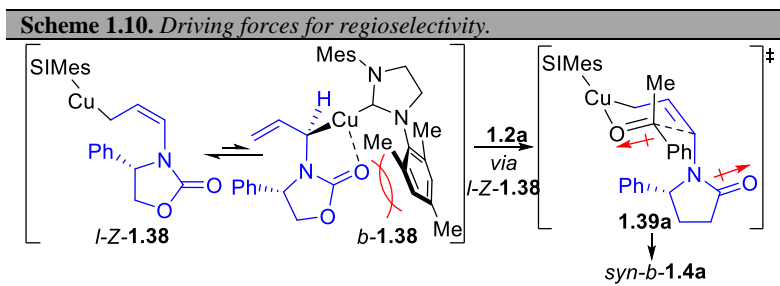
B. Regio- and Stereochemical Model

Equipped with the linear- and branched-selective reaction methods developed, we were able to analyze the data to propose a stereo- and regiochemical model (**Scheme 1.9**). This work showed that less electron-donating phosphine ligands generate the linear product selectively, through γ -addition of the branched Cu(allyl) complex *b*-**1.25** to ketone **1.2a** via a six-membered chair-like transition state **TS-2** with the oxazolidinone group in an axial position and coordinated to copper for selective reaction to the Si-face of **1.2a**.



Initial hydrocupration is mechanistically proposed to occur trans to the large oxazolidinone group,¹⁰⁹ leading to the *Z*-geometry of the σ -(allyl)Cu complex *l-Z-1.25*. Because the turnover limiting step in copper-catalyzed reductive coupling reactions between allenes and ketones is believed to be the addition of the Cu-allyl species to the ketone electrophile,⁸⁰⁻⁸² the *Z*- σ -(allyl)Cu complex *l-Z-1.25* can equilibrate prior to coupling with the ketone. The regioselectivity is proposed to be a competition in the equilibrium between the strength of the oxazolidinone coordination to copper and the magnitude of the $A_{1,3}$ -strain present. Thus, linear selectivity is due to the favoring of branched σ -(allyl)Cu complex *b-1.25* over the linear σ -Cu(allyl) complex *l-Z-1.25*, because of the allylic $A_{1,3}$ -strain present and the directing effect of the oxazolidinone.

As the phosphine ligand's electron-donating ability decreases, the linear selectivity increases, leading to an increased favoring of the α - σ -Cu(allyl) complex *b-1.25* due to the increased electrophilic nature of the copper in these states. Also, it should be noted that the size of the oxazolidinone affects the magnitude of the $A_{1,3}$ -interactions. Larger oxazolidinone-derived alleneamides, such as **1.1**, generate more $A_{1,3}$ -strain, which leads to a preference for linear product formation, as demonstrated in **Scheme 1.8**, when comparing the effect of the oxazolidinone in the reaction. Because the use of both electron-rich and electron-deficient phosphine ligands with alleneamide **1.1** provides linear selectivity, the primary interaction leading to linear selection is the $A_{1,3}$ -strain present in intermediate **1.37**.



Ligand electronics still play an essential role, as weakening the electron-donating ability of the ligand used leads to an increase in linear selectivity, most likely due to the enhanced ability of the oxazolidinone carbonyl to coordinate to copper as copper becomes more electrophilic. As NHC ligands are

employed, **Scheme 1.10**, the initial hydrocupration occurs in the same manner as with the phosphine ligands, but the coordination of the oxazolidinone carbonyl of *b*-**1.38** to copper is prevented both by the strong electron-donating ability of the ligand and by the steric shielding by the bulky mesitylene group of the carbene ligand.¹⁰⁶ This steric shielding effect using NHC ligands is evidenced by the use of SIPr, an electronically similar yet more sterically demanding ligand compared to SIMes, leading to higher branched selectivity but with poorer diastereoselectivity (**Table 1.3**, entry 12). The larger, more sterically hindering SIPr allows for even further steric shielding of the copper atom.

The inhibition of the oxazolidinone carbonyl coordination to copper results in the preference of the generation of linear σ -(allyl)Cu complex *l*-**Z-1.38**, which then couples to the ketone in a dipole-minimizing¹¹⁰⁻¹¹² Zimmerman-Traxler 6-membered chair-like^{83,113} transition state, generating the branched product **1.4a**. In this case, the effects of employing the NHC ligand are stronger than those of the A_{1,3}-strain present in the linear(allyl)Cu complex *l*-**Z-1.25**, resulting in the selective formation of the branched product. However, when more sterically demanding ketones, such as cyclic, *ortho*-substituted, and dialkyl ketones are analyzed, **Scheme 1.7**, lower branched selectivity is observed. This decrease in regioselectivity is most likely due to an increase in steric interactions in the transition state **1.39a**, by the presence of *ortho*-substitution and non-planar groups on the ketone, causing a higher energy transition state to generate the branched product that would be harder to overcome, leading to a shift in the equilibrium to favor the linear product.

This proposed stereo- and regiochemical model accounts for the correct major products and diastereomers formed in each reaction, serving as stereochemical proof of oxazolidinone coordination to copper in the transition state. Further computational analysis of the mechanism by our collaborators has shown that the reaction outcome is a product of Curtin-Hammett control,¹¹⁴ as the stereochemical outcome is a direct result of the transition states in **Scheme 1.9** having the lowest energy pathways.⁸⁴

Overall, a delicate balance in the equilibrium determines the regio- and stereo-selectivity in these copper-catalyzed reductive coupling reactions between alleneamides and ketones. This balance is dominated by A_{1,3}-interactions – which can be influenced by the size of the oxazolidinone group, as well

as the strength of the oxazolidinone carbonyl coordination to copper – which is influenced by the ligand electron-donating ability as well as the possibility of steric shielding by large, bulky ligands.

VII. Development Towards a Linear-Selective Enantioselective Method

A. Chiral alleneamide vs chiral ligand control

The two works described thus far have utilized a chiral auxiliary-derived alleneamide as the allyl coupling partner. This pre-installed chirality serves to impart stereocontrol throughout the course of the reaction. This method is useful when necessary but is not an ideal choice due to the low efficiency in atom economy, as it requires more chiral material to be carried through the reaction. Instead, stereocontrol by a chiral Cu-catalyst is ideal and allows the catalytic use of chiral materials over the stoichiometric methods reported previously. For this reason, our next endeavor was to develop an enantioselective reductive coupling method to generate the linear product by way of chiral-catalyst control.

B. Linear-selective enantioselective reaction development

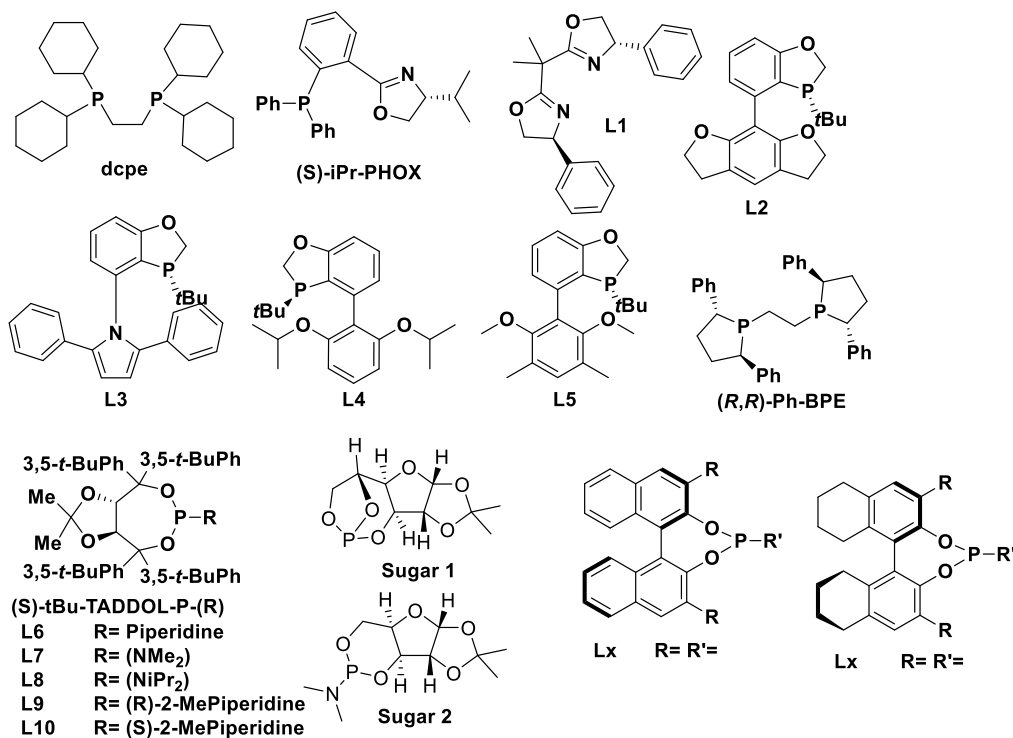
The goal of this work was to develop a chiral catalyst that enabled the linear-selective asymmetric reductive coupling with ketone electrophiles. Buchwald's group has published an enantioselective catalyst-controlled branched-selective reaction of this nature using *C*-based allenes,⁸² but our focus was to use alleneamides to generate the novel linear product enantioselectively while installing multiple heteroatoms.

From the regio- and stereochemical model presented in **Section VI**, linear product generation is favored with the use of large oxazolidinones due to an increase in $A_{1,3}$ -strain that helps shift the equilibrium. reductive coupling product. With this knowledge in hand, we set out to generate a catalyst-controlled enantioselective linear-selective reductive coupling method and began by utilizing the bulky fused-phenyl alleneamide **1.6** (Table 1.4) to help skew the reaction towards the linear product **1.7a**.

Table 1.4. Ligand survey for the development of enantioselective linear-selective method.

Reaction scheme: 1.2a + 1.6 $\xrightarrow[\text{then NH}_4\text{F}]{\text{Cu(OAc)}_2, \text{Ligand}, \text{(MeO)}_2\text{MeSiH (2 equiv), solvent, rt, 24 h}}$ 1.7a

Entry	Ligand	Yield (L/B)	L : B	ER	EE
1	DCPE	49.3% B	n.d	50:50	0
2	(S)-iPr-PHOX	8% B	<1 : 99	-	-
3	L1	2% B	<1 : 99	-	-
4	L2	9% B	18 : 82	-	-
5	L3	1.5% B	>1 : 99	-	-
6	L4	1.5	54 : 46	-	-
7	L5	2	37 : 63	-	-
8	(R,R)-PhBPE	23.8% B	29 : 71	-	-
9	L6	16	54.5 : 45.5	-	-
10	L7	28	69 : 31	46 : 54	8
11	L8	59	87.5 : 12.5	48.5 : 51.5	3
12	L9	49	88 : 12	47 : 53	6
13	L10	5	29.5 : 70.5	-	-
14	Sugar 1	69	>99:1	49.7:50.3	0.6
15	Sugar 2	28	95:5	57:43	14
16	H(BINOL)-P(NMe ₂) (MonoPhos)	73	92:8	50:50	0
17	(Me)BINOL-P(NMe ₂)	71	>99:1	47:53	6
18	(Br)BINOL-P(NMe ₂)	74	98.7:1.3	46.5:53.5	7
19	(Ph)BINOL-P(NMe ₂)	84	>99:1	50:50	0
20	(p-tBuPh)BINOL-P(NMe ₂)	86	98:2	53:47	6
21	(Ph ₃ Si)BINOL-P(NMe ₂)	20	n.d.	45:55	10
22	(Anthro)-BINOL-P(NMe₂)	62	>99:1	65:35	30
23	(Anthro)BINOL-P(NEt ₂)	78	97.2:2.8	49 : 51	2
24	H8-BINOL-P(NMe ₂)	71	97.5:2.5	54:46	8
25	(3,5-dimethylphenyl)-H8-BINOL-P(NMe ₂)	65	95:5	56:44	12
26	(3,5-bis(trifluoromethyl)phenyl)-H8-BINOL-P(NMe₂)	91	97.5:2.5	65:35	30
27	(mesityl)-H8-BINOL-P(NMe ₂)	45	92:8	60:40	20



We commenced the investigation into the reductive coupling between the fused phenyl allenamide **1.6** and acetophenone **1.2a** by examining various chiral ligands to determine the optimal ligand for this system (**Table 1.4**). Use of bidentate ligands (entries 1-5, 8) in this system yielded high branched selectivity, which aligns with our previous stereo- and regiochemical model presented in **Section VI**. Initially, BINOL-derived ligands were screened for this reaction due to their classification as privileged ligands – chiral ligands containing a C₂-axis – which allow for chiral control of multiple reaction types,¹¹⁵ and their electronic similarities to (PhO)₂PNMe₂, the optimal ligand in the linear-selective process employing chiral allenamides. The BINOL-derived ligands examined were prepared by previous group member Kevin Burns, according to literature procedures.^{116–122}

As seen in **Table 1.4**, the standard ligand classes examined gave decent yield, however, none demonstrated high enantioselectivity. The best enantioselectivity initially observed was with the use of 3,3'-Anthracenyl-BINOL-P-NMe₂ (entry 21) with an er of 65:35. A trend in the effect of the ligand sterics on enantioselectivity was noticed, as increasingly larger groups in the 3,3'-position of the BINOL-backbone (entries 16, 17, 19, 20, 22); however, these changes induced little impact on enantioselectivity.

From here, we became familiar with recent work in allylation from the Meek group,¹²³ in which the investigators were getting much better results in their allylation system with the hydrogenated H8-BINOL derivatives. The saturated external rings of the H8-BINOL system leads to a change in the rotation axis, changing the interaction of the ligand at the metal center, which affects the rest of the reaction system.¹²⁴ The H8-BINOL ligand system poses the additional benefit of being easier to synthesize than the traditional BINOL ligands. With this knowledge, we set out to try it for ourselves. A series of H8-BINOL ligands were prepared in collaboration with an undergraduate researcher in our lab (Christian Knott), in accordance to the literature,^{123,125-128} and examined in this system. Our current results reflect that (3,5-bis(trifluoromethyl)phenyl)-H8-BINOL-P-NMe₂ (entry 26) is the best performing ligand thus far, with the same enantioselectivity as Anthracene-BINOL-PNMe₂, but with a stark increase in yield and regioselectivity. To this point, an optimal ligand to favor high linear selectivity enantioselectively has yet to be identified; The search remains and is an ongoing effort in the Sieber Lab.

VIII. Development towards an Enantioselective Reductive Coupling Method with CF₃-ketones

A. Fluorine in APIs

Fluorinated organic compounds are prevalent in the pharmaceutical industry for the development of new medicines due to the C-F bond's innate ability to increase lipophilicity and metabolic stability.^{129,130} The C-F bond cannot be metabolized *in vivo*, and therefore the C-F substituted drug would be more potent and longer-lasting in the body than the drug itself.^{131,132} The electronegativity of fluorine creates a strong dipole and low-lying C-F σ^* orbital,¹³⁰ available for hyperconjugative donation, while the small radius of fluorine poses similar steric effects as hydrogen. The formed dipoles can allow for conformational control via alignment and minimization of dipoles. The electronegativity of the C-F bond influences the pK_a of the molecule and increases the lipophilicity, making the F-substituted drug more easily able to enter cells and thus be more bioavailable.¹³³

Due to the factors mentioned above, it is crucial to utilize fluorinated species in chemical reactions to generate fluorinated drug molecules. With this premise, we wanted to apply trifluoroacetophenone (**1.5a**) to the reductive coupling reactions employing allenamides. The use of trifluoroacetophenone and other CF₃-ketones **1.5** would allow for the generation of CF₃-aminoalcohols, a relevant medicinal chemistry scaffold. The ability to synthesize these fluorinated compounds would open doors to new fluorinated drug scaffolds with simplified synthetic routes.

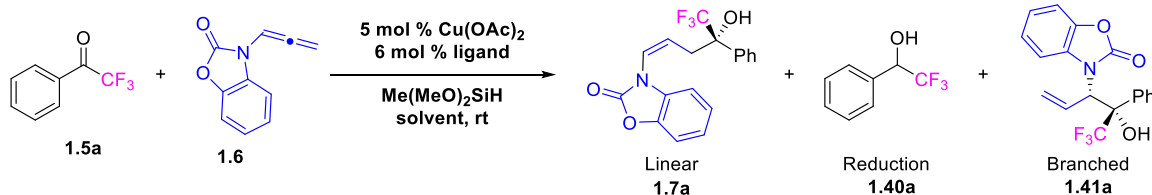
B. Reaction optimization and ligand survey using CF₃-ketones

A ligand survey for the same achiral fused-phenyl allenamide **1.6** was performed and showed a higher yield of linear than branched products, but with high levels of CF₃-ketone reduction **1.40a** (**Table 1.5**). The best enantioselectivity achieved thus far utilized a BINOL-derived ligand.

The most significant issue consistently seen thus far is the high generation of CF₃-ketone reduction **1.40** which arises from the increased reactivity of the trifluoromethyl ketone (**1.5a**). This should be avoidable by the slow addition of ketone **1.5a** overtime via syringe-pump addition, slowing the competing ketone reduction process by making the ketone to catalyst ratio incredibly small within the reaction. Syringe-pump addition has been used in our lab in similar reactions using aldehydes¹³⁴ and greatly decreases the generation of the reduction product.

The TADDOL core (**Table 1.5**, entries 24-37) has shown a significant impact on the reactivity, as the rate of CF₃-ketone reduction is suppressed. The H8-BINOL ligand systems will also be examined for this reaction. Once an optimal ligand for this system has been identified, the reaction conditions must still be optimized, and future CF₃-ketones analyzed can either be commercially purchased or prepared via various literature procedures.¹³⁵ This reaction seems to be naturally linear-selective; however, the development of either branched- or linear-selective methods would be novel.

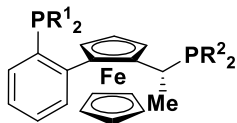
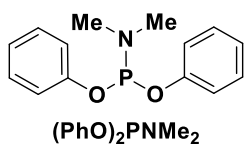
Table 1.5. Ligand survey for the development of an enantioselective linear-selective method for coupling with CF₃-ketones.



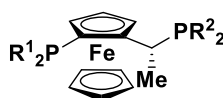
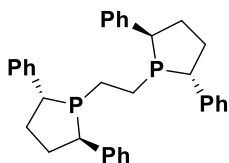
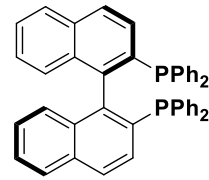
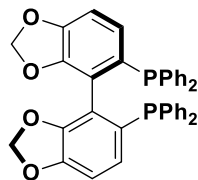
Entry	Ligand	% Yield L 1.7a	L : Red : B	ER 1.7a	EE 1.7a
1	(PhO) ₂ P(NMe ₂)	45	48 : 52 : 0	50:50	0
2	Walphos-008 (W8)	0	0 : 100 : 0	-	-
3	(R)-SEGPhos	<1	1 : 99 : 0	-	-
4	(R)-BINAP	2	3 : 97 : 0	-	-
5	(R)-BINOL-(2'-Me-thq)	5	9 : 85 : 6	74:26	48
6	JosiPhos-006	6	9 : 91 : 0	-	-
7	(R,R)-PhBPE	19	31 : 69 : 0	-	-
8	Only silane and CF ₃ ketone	0	0 : 100 : 0	-	-
9	(R) – Monophos (L11)	11	35 : 40 : 25	57 : 43	14
10	(R)-(Me)BINOL-P(NMe ₂) (L12)	47	74 : 26 : 0	48 : 52	4
11	(R)-Ph-BINOL-P(NMe ₂) (L13)	26	40 : 60 : 0	45 : 55	10
12	(R)-BINOL-P(^t Bu) (L14)	34	50 : 50 : 0	46 : 54	8
13	(R)-BINOL-(2'-Me-thq) ^b	28	30 : 63 : 7	43 : 57	14
14	[(S)-BINOL]P-Ethyl-P[(S)-BINOL] (L15)	33	55 : 45 : 0	51 : 49	2
15	(S)-Antphos	17	17 : 83 : 0	60 : 40	20
16	L16	4.5	14 : 61 : 25	39 : 61	22
17	(R)-H8-BINOL-P(NMe ₂)	40	58.5:41.5:0	46 : 54	8
18	(R)-VAPOL-P(NMe ₂)	32	41 : 53 : 6	61 : 39	22
19	(R)-VANOL-P(NMe ₂)	32	36 : 53:11	54 : 46	8
20	(R)-BIDIME	16	20 : 80 : 0	52 : 48	4
21	(R,R)- <i>i</i> Pr-BIDIME	16	29 : 68 : 4	48 : 52	4
22	(R)-SIPHOS	25	32 : 68 : 0	44 : 56	12
23	(S)-PipPhos	39	66 : 34 : 0	45 : 55	10
24	(S)-TADDOL-P-(NMe ₂)	36	50 : 50 : 0	38 : 62	24
25	(S)- <i>t</i> Bu-TADDOL-P(NMe ₂) (L7)	89	92 : 8 : 0	30 : 70	40
26	(S)- <i>t</i> Bu-TADDOL-P(NiPr ₂) (L8)	51	58 : 42 : 0	39 : 61	22
27	(S)- <i>t</i> Bu-TADDOL-P(Ph) (L17)	95	95 : 5 : 0	34 : 66	32
28	(S)- <i>t</i> Bu-TADDOL-P(2'-Me-thq) (L18)	65	68 : 28 : 4	45 : 55	10
29	(S)- <i>t</i> Bu-TADDOL-P-Piperidine (L6)	85	91 : 9 : 0	28 : 72	44
30	(S)- <i>t</i> Bu TADDOL-P((S)-2-methyl-piperidine) (L10)	80	85 : 15 : 0	30.5 : 69.5	39
31	(S)- <i>t</i> Bu-TADDOL-P((R)-2-methyl-piperidine) (L9)	60	77 : 23 : 0	37 : 63	26
32	(S)- <i>t</i> Bu-TADDOL-P(NMe ₂), ran at 1M (L7)	63%, 8% Red	88 : 12 : 0	29 : 71	42
33	(S)- <i>t</i> Bu-TADDOL-P(NMe ₂), ran at 0.1M (L7)	13.5, 40% SM	79 : 12 : 9	31 : 69	38
34	(S)-Xylyl-TADDOL-P(NMe ₂) (L19)	62	67 : 33 : 0	34 : 66	32
35	(S)-Xylyl-TADDOL-P(Ph) (L20)	78	80 : 20 : 0	46 : 54	8
36	(S)-Xylyl-TADDOL-Piperidine (L21)	73	75 : 25 : 0	40 : 60	20
37	1-Naphthyl-TADDOL-P(NMe ₂)	24	32:66:2	43 : 57	14

^aDetermined by ¹HNMR spectroscopy on the unpurified reaction mixture using dimethylfumarate as the analytical standard.

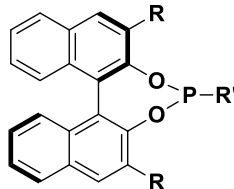
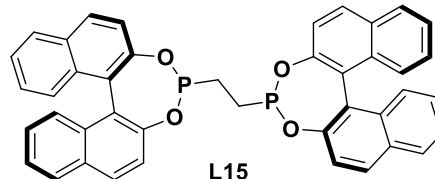
^b Half of ketone added initially, half added after 8 hours.



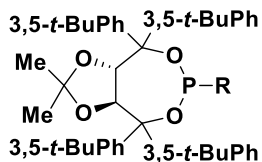
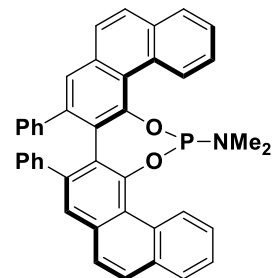
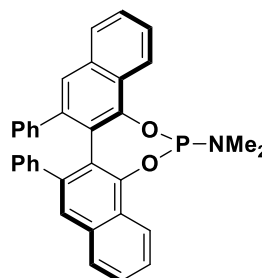
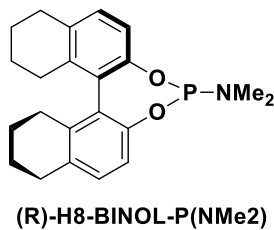
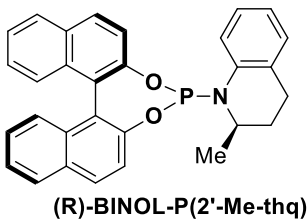
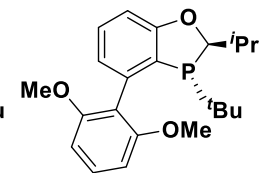
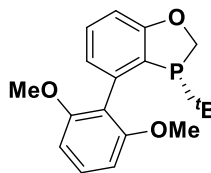
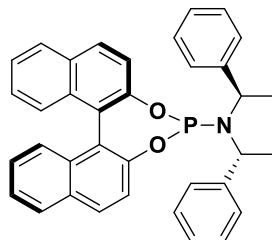
R¹ = 3,5-(CF₃)₂-Ph, R² = Cy



R¹ = 3,5-(CF₃)₂-Ph, R² = Cy



R = H, R' = (NMe₂)
 R = Me, R' = (NMe₂)
 R = Ph, R' = (NMe₂)
 R = H, R' = (tBu)



L6 R = Piperidine

L7 R = (NMe₂)

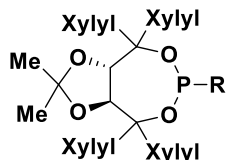
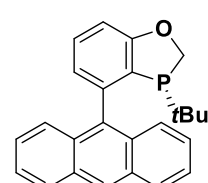
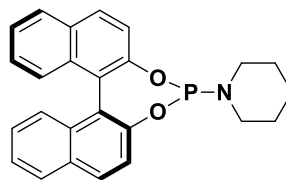
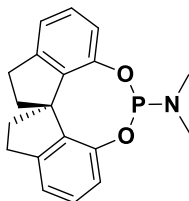
L8 R = (NiPr₂)

L9 R = (R)-2-MePiperidine

L10 R = (S)-2-MePiperidine

L17 R = Phenyl

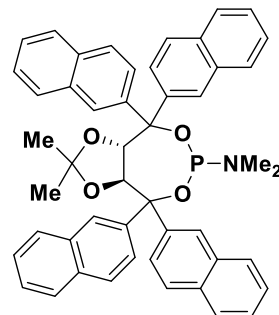
L18 R = 2'-methyl-tetrahydroisoquinoline



L19 R = (NMe₂)

L20 R = Phenyl

L21 R = Piperidine



IX. Conclusions

Through the work described, we developed regiodivergent and diastereoselective reductive coupling methods to generate dissonant functional group pairs. These methods are the first disclosed to generate the novel linear product **1.3**, as well as directly access both the traditional branched product and the novel linear product from the same system by simply tuning the ligand. The use of a chiral auxiliary-derived alleneamide **1.1** allows the stereocontrol over the newly formed stereocenter, generating the desired products each with high diastereoselectivity. Simple removal of the auxiliary gives access to the dissonant branched aminoalcohol and linear hydroxyaldehyde equivalent products. This method involves the use of inexpensive and readily available starting materials, as well as the ability to generate increasingly complex products containing dissonant functionalities.

In addition to the generation of the chiral auxiliary-controlled system for generating the branched and linear products diastereoselectively, the ongoing development of an enantioselective linear-selective method to couple fused-phenyl alleneamides **1.6** with ketones **1.2** and trifluoromethyl ketones **1.5** was here described. This work is still in progress and will require the development and analysis of new ligand systems to yield higher enantioselectivity for the reaction with ketones. In the coupling of trifluoromethyl ketones, the use of syringe-pump addition of the CF₃-ketone will most likely be the solution to increase the yields to an acceptable degree to allow for further optimization of the reaction, while preventing the generation of the CF₃-ketone reduction product **1.40**.

X. Experimental Methods

A. General

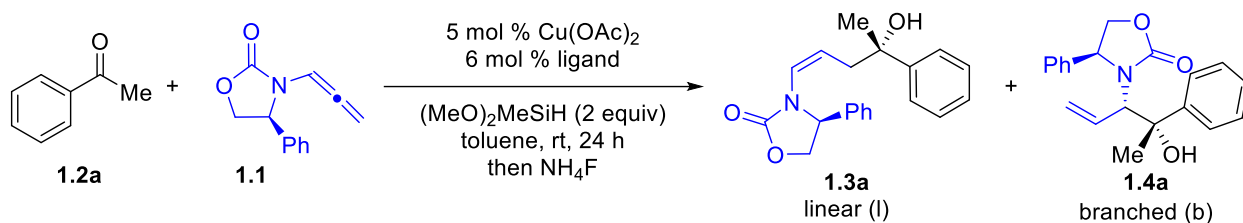
¹H NMR spectra were recorded on Bruker 600 MHz spectrometers. Chemical shifts are reported in ppm from tetramethylsilane with the solvent resonance as an internal standard (CDCl₃: 7.26 ppm, C₆D₆: 7.15 ppm; MeOD: 4.78 ppm). Data are reported as follows: chemical shift, integration, multiplicity (s = singlet, d = doublet, t = triplet, q = quartet, p = pentet, h = hextet, hept = heptet, br = broad, m = multiplet), and coupling constants (Hz). ¹³C NMR was recorded on a Bruker 600 MHz (151 MHz) instrument with complete proton decoupling. Chemical shifts are reported in ppm from tetramethylsilane with the solvent as the internal standard (CDCl₃: 77.0 ppm, C₆D₆: 128.4 ppm; MeOD: 49.2 ppm). Liquid chromatography was performed using forced flow (flash chromatography) on silica gel purchased from Silicycle. Thin layer

chromatography (TLC) was performed on glass-backed 250 μm silica gel F254 plates purchased from Silicycle. Visualization was achieved using UV light, a 10% solution of phosphomolybdic acid in EtOH, or potassium permanganate in water followed by heating. HRMS was collected using a Jeol AccuTOFDARTTM mass spectrometer using DART source ionization. Specific rotations were measured on a JASCO P2000 digital polarimeter. All reactions were conducted in oven or flame dried glassware under an inert atmosphere of nitrogen or argon with magnetic stirring unless otherwise noted. Solvents were obtained from VWR as HPLC grade and transferred to septa sealed bottles, degassed by Ar sparge, and analyzed by Karl-Fischer titration to ensure water content was < 600 ppm. $\text{Me}(\text{MeO})_2\text{SiH}$ was purchased from Alfa Aesar and used as received. Allenamides were prepared in one step as described in the literature.¹³⁶ $(\text{PhO})_2\text{PNMe}_2$ was prepared from hexamethylphosphorous triamide (HMPT) and phenol according to the literature procedure,¹³⁷ and the density was determined experimentally (1.10 g/cm^3). Ketones were purchased from Sigma Aldrich, TCI America, Alfa Aesar, or Oakwood Chemicals and used as received. All other materials were purchased from VWR, Sigma Aldrich, Combi-Blocks, Alfa-Aesar, or Strem Chemical Company and used as received.

B. Experimental Procedures

i. Linear procedures

General catalyst screen procedure for the reaction between acetophenone and allenamide 1.1 (Table 1.1 and 1.2):



To a 20 mL crimp-cap vial with stir-bar in an Ar-filled glove-box was charged 2.3 mg (0.013 mmol) of $\text{Cu}(\text{OAc})_2$, and 0.015 mmol of ligand. Toluene (0.5 mL) was then charged, and the mixture was stirred for 5 min. Allenamide **1.1** (60.4 mg, 0.300 mmol) followed by acetophenone (29.0 μL , 30.0 mg, 0.250 mmol) was then charged, and the vial was sealed with a crimp-cap septum and removed from the glove-box. The reaction was then cooled in an ice bath, and dimethoxymethylsilane (61 μL , 2 equiv) was charged by syringe (*caution: dimethoxymethylsilane should be handled in a well-ventilated fume hood because it is known to cause blindness. Syringes were quenched with 2M NaOH, gas evolution!, prior to disposal*). The mixture was then allowed to warm to rt and stirred for 24 h. The reaction was then quenched by the addition of 95 mg of NH_4F and 1.5 mL of MeOH followed by agitation at rt for 30 min – 1 h. To the mixture was then charged 5 mL of 5% NaHCO_3 followed by extraction with DCM (2x4mL). The combined organics were dried with Na_2SO_4 and concentrated *in vacuo*. To the crude residue was charged dimethylfumarate (10 – 15 mg), and the mixture was diluted in ~0.5 mL of CDCl_3 . Further dilution of an aliquot and analysis by NMR was used to determine the yield, dr, and b/l ratio.

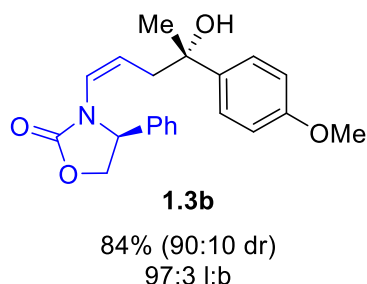
Modified procedure for the use of ligand salts (P(*t*-Bu)₃): To a 20 mL crimp-cap vial with stir-bar in an Ar-filled glove-box was charged 0.015 mmol P(*t*-Bu)₃•HBF₄ and 1.5 mg (0.013 mmol) of KO^tBu. Toluene (0.5 mL) was then charged, and the mixture stirred for 5 min. To the vial was then charged 2.3 mg (0.013 mmol) of Cu(OAc)₂, and the mixture was stirred an additional 5 min. The remaining reagents were then charged and the reaction performed as described above.

General procedure for the linear selective Cu(phosphoramidite) catalyzed reductive coupling (Scheme 1.6).

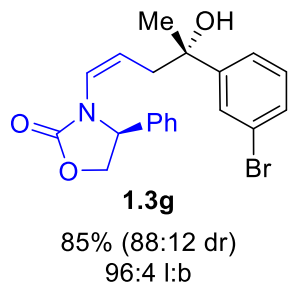
To a 20 mL crimp-cap vial with stir-bar in an Ar-filled glove-box was charged 4.5 mg (0.025 mmol) of Cu(OAc)₂ and 1.0 mL of toluene. (PhO)₂PNMe₂ was then charged by gas-tight syringe (7.75 μL, 0.033 mmol), and the mixture was stirred for 10 min. Allene **1.1** (0.121 g, 0.600 mmol) was then added, followed by the ketone (0.500 mmol), and the vial was sealed with a crimp-cap septum and removed from the glove-box. The reaction was then cooled in an ice bath, and dimethoxymethylsilane (0.12 mL, 1.0 mmol) was charged by syringe (*caution: dimethoxymethylsilane should be handled in a well-ventilated fume hood because it is known to cause blindness. Syringes were quenched with 2M NaOH, gas evolution!, prior to disposal*). The mixture was then allowed to warm to rt and stirred for 24 h. The reaction was then quenched by the addition of 190 mg of NH₄F and 2.5 mL of MeOH followed by agitation at rt for 30 min – 1 h. To the mixture was then charged 10 mL of 5% NaHCO₃ followed by extraction with CH₂Cl₂ (2x5mL). The combined organics were dried with Na₂SO₄ and concentrated *in vacuo*. An aliquot of the crude mixture was analyzed by ¹HNMR spectroscopy to determine the dr and the l/b ratio. The crude residue was then purified by flash chromatography on silica gel to afford the desired product.

ii. Analytical data for the reductive coupling products

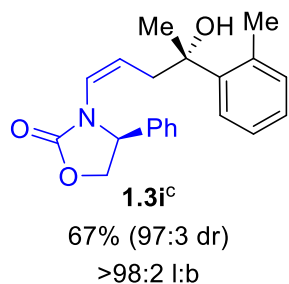
Other compounds that are not characterized here were made and characterized by other group members.^{107,138}



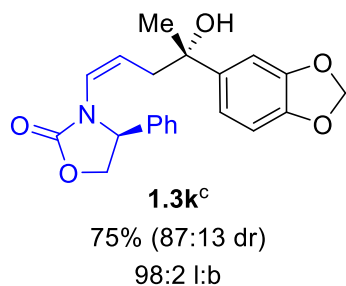
(S)-3-((S,Z)-4-hydroxy-4-(4-methoxyphenyl)pent-1-en-1-yl)-4-phenyloxazolidin-2-one (1.3b): According to the linear-selective general procedure, the product was purified by silica gel chromatography (eluent: 20 – 60% EtOAc in hexanes) to provide 148.7 mg (84%) of **1.3b** as a thick glass as a 90/10 mixture of diastereomers. Stereochemistry was determined by analogy to that of **1.3a**. *R_f* = 0.24 (50% EtOAc/hexanes). [α]_D²⁵ = + 19.19 (*c* 0.285, CHCl₃); ¹HNMR (CDCl₃, 600 MHz) δ: 7.30 – 7.42 (m, 5H), 7.31 (dd, *J* = 8.5 Hz, *J* = 6.8 Hz), 6.84 (d, *J* = 8.9 Hz, 2H), 5.70 (d, *J* = 8.8 Hz, 1H), 5.05 (td, *J* = 8.8 Hz, *J* = 6.7 Hz, 1H), 4.96 (dd, *J* = 8.7 Hz, *J* = 6.7 Hz, 1H), 4.68 (t, *J* = 8.8 Hz, 1H), 4.17 (dd, *J* = 8.7 Hz, *J* = 6.7 Hz, 1H), 3.79 (s, 3H), 3.39 (s, 1H), 2.66 (dd, *J* = 15 Hz, *J* = 9.0 Hz, 1H), 2.54 (ddd, *J* = 8.1 Hz, *J* = 6.6 Hz, *J* = 1.6 Hz), 1.51 (s, 3H) ppm. ¹³C NMR (151 MHz, CDCl₃): δ 158.2, 156.7, 139.8, 137.8, 129.4, 129.1, 126.5, 126.0, 123.3, 121.3, 113.4, 73.0, 70.2, 61.6, 55.3, 41.9, 31.0 HRMS (DART) *m/z* calcd for C₂₁H₂₄NO₄ [M + H]⁺: 354.1705; Found [M + H]⁺: 354.1716.



(S)-3-((S,Z)-4-(3-bromophenyl)-4-hydroxypent-1-en-1-yl)-4-phenyloxazolidin-2-one (1.3g): According to the linear-selective general procedure, the product was purified by silica gel chromatography (eluent: 20 – 50% EtOAc in hexanes) to provide 169.8 mg (84.5%) of *l*-**1.3g** as a thick glass as an 88/12 mixture of diastereomers. Stereochemistry was determined by analogy to that of *l*-**1.3a**. $R_f = 0.35$ (50% EtOAc/hexanes). $[\alpha]_D^{25} = +5.51$ (*c* 0.265, CHCl₃); ¹HNMR (CDCl₃, 600 MHz) δ : 7.59 – 7.61 (m, 1H), 7.32 – 7.43 (m, 5H), 7.24 (dd, *J* = 8.3 Hz, *J* = 1.4 Hz, 2H), 7.18 (t, *J* = 7.9 Hz, 1H), 5.65 (d, *J* = 8.8 Hz, 1H), 5.02 (td, *J* = 9.2 Hz, *J* = 6.3 Hz, 1H), 4.95 (dd, *J* = 8.7 Hz, *J* = 7.2 Hz, 1H), 4.70 (t, *J* = 8.9 Hz, 1H), 4.19 (dd, *J* = 8.8 Hz, 7.1 Hz, 1H), 3.90 (s, 1H), 2.72 (dd, *J* = 10 Hz, *J* = 9.5 Hz, 1H), 2.53 (ddd, *J* = 8.0 Hz, *J* = 6.2 Hz, *J* = 1.7 Hz, 1H), 1.51 (s, 3H) ppm. ¹³C NMR (151 MHz, CDCl₃): δ 156.8, 150.3, 137.5, 129.7, 129.6, 129.4, 129.2, 128.2, 126.5, 123.7, 123.6, 122.5, 121.4, 72.8, 70.2, 61.8, 41.7, 31.1. HRMS (DART) *m/z* calcd for C₂₀H₂₁BrNO₃ [M + H]⁺: 402.0705; Found [M]⁺: 402.0699.

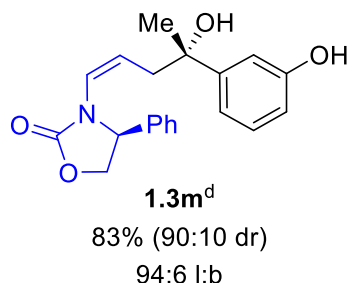


(S)-3-((S,Z)-4-hydroxy-4-(o-tolyl)pent-1-en-1-yl)-4-phenyloxazolidin-2-one (1.3i): According to the linear-selective general procedure performed at 40 °C for 24 h, the product was purified by silica gel chromatography (eluent: 10 – 50% EtOAc in hexanes) to provide 126.8 mg (75%) of *l*-**1.3i** as an off white solid as a 97/3 mixture of diastereomers. Stereochemistry was determined by analogy to that of *l*-**1.3a**. $R_f = 0.34$ (40% EtOAc/hexanes). $[\alpha]_D^{25} = +21.9$ (*c* 0.315, CHCl₃); ¹HNMR (CDCl₃, 600 MHz) δ : 7.44 – 7.48 (m, 1H), 7.35 – 7.42 (m, 3H), 7.24 (dd, *J* = 8.0 Hz, *J* = 1.4 Hz, 2H), 7.10 – 7.16 (m, 3H), 5.72 (d, *J* = 8.8 Hz, 1H), 5.09 (td, *J* = 8.7 Hz, *J* = 6.5 Hz, 1H), 4.94 (dd, *J* = 8.7 Hz, *J* = 6.5 Hz, 1H), 4.68 (t, *J* = 8.8 Hz, 1H), 4.18 (dd, *J* = 8.8 Hz, *J* = 6.5 Hz, 1H), 3.15 (s, 1H), 2.77 (ddd, *J* = 8.4 Hz, *J* = 6.9 Hz, *J* = 1.6 Hz, 1H), 2.74 (ddd, *J* = 8.0 Hz, *J* = 6.8 Hz, *J* = 1.1 Hz, 1H), 2.50 (s, 3H), 1.58 (s, 3H) ppm. ¹³C NMR (151 MHz, CDCl₃): δ 156.7, 144.6, 137.8, 135.1, 132.6, 129.4, 129.1, 126.9, 126.5, 126.3, 125.7, 123.4, 121.4, 74.5, 70.2, 61.6, 39.8, 29.7, 22.5. HRMS (DART) *m/z* calcd for C₂₁H₂₄NO₃ [M + H]⁺: 338.1756; Found [M + H]⁺: 338.1767.



(S)-3-((S,Z)-4-(benzo[d][1,3]dioxol-5-yl)-4-hydroxypent-1-en-1-yl)-4-phenyloxazolidin-2-one (1.3k): According to the linear-selective general procedure performed at 40 °C for 24 h, the product was purified by silica gel chromatography (eluent: 10 – 50% EtOAc in hexanes) to provide 153.4 mg (83%) of *l*-**1.3k** as a thick glass as a 88/11 mixture of diastereomers. $R_f = 0.26$ (40% EtOAc/hexanes). $[\alpha]_D^{25} = +4.99$ (*c* 0.515, CHCl₃); ¹HNMR (CDCl₃, 600 MHz) δ : 7.35 – 7.44 (m, 3H), 7.24 (dd, *J* = 8.3 Hz, *J* = 1.3 Hz, 2H), 6.94 (d, *J* = 1.6 Hz, 1H), 6.88 (dd, *J* = 8.2 Hz, *J* = 1.7 Hz, 1H), 6.74 (d, *J* = 8.2 Hz, 1H), 5.93 (s, 2H), 5.69 (d, *J* = 8.8 Hz, 1H), 5.06 (td, *J* = 8.9 Hz, *J* = 6.7 Hz, 1H), 4.97 (dd, *J* = 8.7 Hz, *J* = 7.0 Hz, 1H), 4.69 (t, *J* = 8.8 Hz, 1H), 4.17 (dd, *J* = 8.8 Hz, *J* = 6.9 Hz, 1H), 3.52 (s, 1H), 2.66 (dd, *J* = 15 Hz, *J* =

9.0 Hz, 1H), 2.51 (ddd, $J = 7.8$ Hz, $J = 6.5$ Hz, $J = 1.4$ Hz, 1H), 1.49, (s, 3H) ppm. ^{13}C NMR (151 MHz, CDCl_3): δ 156.6, 156.5, 138.1, 134.2, 129.3, 129.0, 128.3, 127.1, 126.5, 122.4, 121.2, 120.8, 111.1, 74.0, 70.1, 61.4, 55.3, 39.4, 27.5. HRMS (DART) m/z calcd for $\text{C}_{21}\text{H}_{20}\text{NO}_4$ $[\text{M} - \text{OH}]^+$: 350.1392; Found $[\text{M} - \text{OH}]^+$: 350.1417.

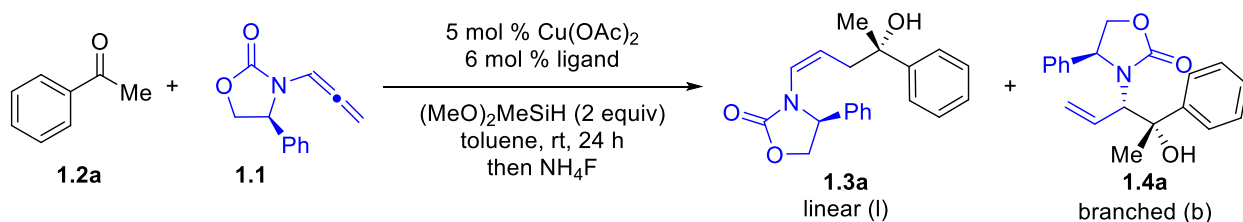


(S)-3-((S,Z)-4-hydroxy-4-(3-hydroxyphenyl)pent-1-en-1-yl)-4-phenyloxazolidin-2-one (l-1.3m): According to the linear-selective general procedure using 4.0 equiv of $(\text{MeO})_2\text{MeSiH}$, the product was purified by silica gel chromatography (eluent: 10 – 60% EtOAc in hexanes) to provide 141.1 mg (83%) of *l*-**1.3m** as a foam as a 90/10 mixture of diastereomers. $R_f = 0.18$ (40% EtOAc/hexanes). $[\alpha]_D^{25} = +9.12$ (c 0.49, CHCl_3); ^1H NMR (CDCl_3 , 600 MHz) δ : 7.35 – 7.44 (m, 3H), 7.24 (dd, $J = 8.2$ Hz, $J = 1.9$ Hz, 2H), 7.18 (t, $J = 7.9$ Hz,

1H), 6.95 – 7.01 (m, 1H), 6.92 (d, $J = 7.7$ Hz, 1H), 6.69 (dd, $J = 7.4$ Hz, 1.9 Hz, 1H), 5.65 (d, $J = 8.6$ Hz, 1H), 5.07 (td, $J = 9.0$ Hz, $J = 6.6$ Hz, 1H), 4.93 (dd, $J = 8.6$ Hz, $J = 7.1$ Hz, 1H), 4.70 (t, $J = 18$ Hz, 1H), 4.18 (dd, $J = 8.8$ Hz, $J = 7.1$ Hz, 1H), 3.80 (s, 1H), 2.69 (dd, $J = 15$ Hz, $J = 9.2$ Hz, 1H), 2.56 (dd, $J = 15$ Hz, $J = 6.4$ Hz, 1H), 1.52 (s, 3H) ppm. ^{13}C NMR (151 MHz, CDCl_3): δ 157.3, 156.4, 149.1, 137.6, 129.35, 129.30, 129.1, 126.6, 123.1, 121.7, 116.5, 113.8, 112.4, 73.9, 70.4, 61.6, 41.6, 30.1. HRMS (DART) m/z calcd for $\text{C}_{20}\text{H}_{22}\text{NO}_4$ $[\text{M} + \text{H}]^+$: 340.1549; Found $[\text{M} - \text{OH}]^+$: 340.1529.

iii. Branched procedures

General catalyst screen procedure for the reaction between acetophenone and allenamide 1.1 (Table 1.3):



To a 20 mL crimp-cap vial with stir-bar in an Ar-filled glove-box was charged 2.3 mg (0.013 mmol) of Cu(OAc)_2 , and 0.015 mmol of ligand. Toluene (0.5 mL) was then charged, and the mixture was stirred for 5 min. Allenamide **1.1** (60.4 mg, 0.300 mmol) followed by acetophenone (29.0 μL , 30.0 mg, 0.250 mmol) was then charged, and the vial was sealed with a crimp-cap septum and removed from the glove-box. The reaction was then cooled in an ice bath, and dimethoxymethylsilane (61 μL , 2 equiv) was charged by syringe (*caution: dimethoxymethylsilane should be handled in a well-ventilated fume hood because it is known to cause blindness. Syringes were quenched with 2M NaOH, gas evolution!, prior to disposal*). The

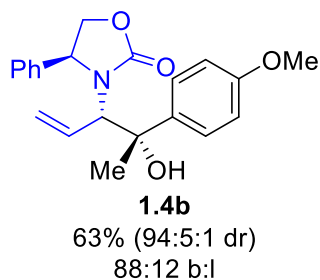
mixture was then allowed to warm to rt and stirred for 24 h. The reaction was then quenched by the addition of 95 mg of NH₄F and 1.5 mL of MeOH followed by agitation at rt for 30 min – 1 h. To the mixture was then charged 5 mL of 5% NaHCO₃ followed by extraction with DCM (2x4mL). The combined organics were dried with Na₂SO₄ and concentrated *in vacuo*. To the crude residue was charged dimethylfumurate (10 – 15 mg), and the mixture was diluted in ~0.5 mL of CDCl₃. Further dilution of an aliquot and analysis by NMR was used to determine the yield, dr, and b/l ratio.

Modified procedure for the use of ligand salts (NHC ligands or P(*t*-Bu)₃): To a 20 mL crimp-cap vial with stir-bar in an Ar-filled glove-box was charged 0.015 mmol of NHC•HCl or P(*t*-Bu)₃•HBF₄ and 1.5 mg (0.013 mmol) of KO^tBu. Toluene (0.5 mL) was then charged, and the mixture stirred for 5 min. To the vial was then charged 2.3 mg (0.013 mmol) of Cu(OAc)₂, and the mixture was stirred an additional 5 min. The remaining reagents were then charged and the reaction performed as described above.

General procedure for the branched-selective Cu(NHC) catalyzed reductive coupling (Scheme 1.7).

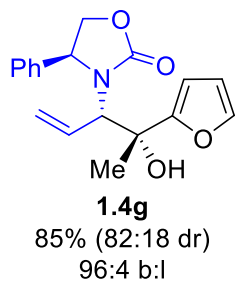
To a 20 mL crimp-cap vial with stir-bar in an Ar-filled glove-box was charged 4.5 mg (0.025 mmol) of Cu(OAc)₂, 11.1 mg (0.0325 mmol) of SIMes•HCl, and 3.1 mg (0.028 mmol) of KO^tBu. Toluene (1.0 mL) was then added, and the mixture was allowed to stir for 15 min. Allene **1.1** (0.121 g, 0.600 mmol) was then added, followed by the ketone (0.500 mmol), and the vial was sealed with a crimp-cap septum and removed from the glove-box. Dimethoxymethylsilane (0.12 mL, 1.0 mmol) was then charged by syringe (*caution: dimethoxymethylsilane should be handled in a well-ventilated fume hood because it is known to cause blindness. Syringes were quenched with 2M NaOH, gas evolution!, prior to disposal*) at rt, and the mixture was then allowed to stir for 24 h. The reaction was then quenched by the addition of 190 mg of NH₄F and 2.5 mL of MeOH followed by agitation at rt for 30 min – 1 h. To the mixture was then charged 10 mL of 5% NaHCO₃ followed by extraction with CH₂Cl₂ (2x5mL). The combined organics were dried with Na₂SO₄ and concentrated *in vacuo*. An aliquot of the crude mixture was analyzed by ¹H NMR spectroscopy to determine the dr and the l/b ratio. The crude residue was then dry-loaded onto silica gel using CH₂Cl₂ and purified by flash chromatography on silica gel to afford the desired product.

iv. Analytical data for the reductive coupling products



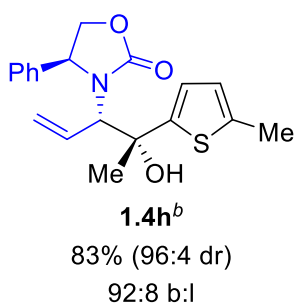
(S)-3-((3S,4S)-4-hydroxy-4-(4-methoxyphenyl)pent-1-en-3-yl)-4-phenyloxazolidin-2-one (1.4b): According to the branched-selective general procedure, the product was purified by silica gel chromatography (eluent: 0 – 30% EtOAc in hexanes) to provide 129.1 mg (63%) of **1.4b** in 87 wt% purity by quantitative ¹H NMR spectroscopy using dimethylfumurate as analytical standard as a white solid as a 95/5 mixture of diastereomers (allene rearrangement products *N*-allyl and *N*-propenyl 4-phenyloxazolidin-2-one could not be removed by chromatography). Analytically and diastereomerically pure material could be obtained by slurrying the material in 10 vol. of hot 10% EtOAc in hexanes followed by cooling to rt in 64% recovery of the major

diastereomer. The recrystallized product had a melting point of 142.0 – 146.2°C. The stereochemistry was assigned by analogy to that of **1.4a**. $R_f = 0.09$ (20% EtOAc/hexanes). $^1\text{H NMR}$ (CDCl_3 , 600 MHz) δ : 7.39 (t, $J = 7.5$ Hz, 1H), 7.31 (t, $J = 7.8$ Hz, 2H), 7.04 (d, $J = 8.5$ Hz, 2H), 6.86 (d, $J = 7.4$ Hz, 2H), 6.79 (d, $J = 8.9$ Hz, 2H), 6.52 (br s, 1H), 6.20 (dt, $J = 17$ Hz, $J = 10$ Hz, 1H), 5.48 (dd, $J = 10$ Hz, $J = 1.1$ Hz, 1H), 5.20 (d, $J = 17$ Hz, 1H), 4.68 (t, $J = 9.3$ Hz, 1H), 4.45 (t, $J = 8.9$ Hz, 1H), 3.98 (dd, $J = 9.4$ Hz, $J = 9.0$ Hz, 1H), 3.85 (s, 3H), 3.35 (d, $J = 9.5$ Hz, 1H), 1.32 (s, 3H) ppm. $^{13}\text{C NMR}$ (151 MHz, CDCl_3): δ 159.9, 158.2, 138.1, 135.4, 130.9, 129.4, 129.1, 128.6, 126.3, 121.0, 113.2, 75.17, 70.77, 68.09, 61.67, 55.31, 29.27. HRMS (DART) m/z calcd for $\text{C}_{21}\text{H}_{22}\text{NO}_3$ [$\text{M} - \text{OH}$] $^+$: 336.1600; Found [$\text{M} - \text{OH}$] $^+$: 336.1632.



(S)-3-((3S,4S)-4-hydroxy-(4-furan-2-yl)pent-1-en-3-yl)-4-phenyloxazolidin-2-one (1.4g): According to the branched-selective general procedure, the product was purified by silica gel chromatography (eluent: 0 – 30% EtOAc in hexanes) to provide 148.7 mg (78%) of **1.4g** in 82.5 wt% purity by quantitative $^1\text{H NMR}$ spectroscopy using dimethylfumarate as analytical standard as a white solid as a 98/2 mixture of diastereomers (allene rearrangement products *N*-allyl and *N*-propenyl 4-phenyloxazolidin-2-one

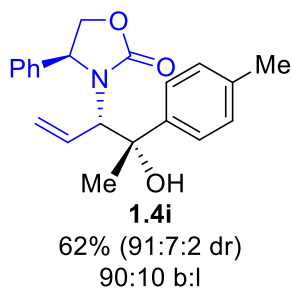
could not be removed by chromatography). Analytically and diastereomerically pure material could be obtained by slurrying the material in 10 vol. of hot 10% EtOAc in hexanes followed by cooling to rt in 70% recovery of the major diastereomer. The recrystallized product had a melting point of 125.3 – 129.4°C. The stereochemistry was assigned by analogy to that of **1.4a**. $R_f = 0.29$ (25% EtOAc/hexanes). $^1\text{H NMR}$ (CDCl_3 , 600 MHz) δ : 7.28-7.48 (m, 4H), 7.25 (s, 1H), 6.88 (d, $J = 6.9$ Hz, 2H), 6.81 (s, 1H), 6.37 (dd, $J = 17$ Hz, $J = 2.8$ Hz, 2H), 6.19 (dt, $J = 17$ Hz, $J = 9.8$ Hz, 1H), 5.47 (d, $J = 10$ Hz, 1H), 5.18 (d, $J = 17$ Hz, 1H), 4.70 (t, $J = 10$ Hz, 1H), 4.54 (t, $J = 9.0$ Hz, 1H), 4.04 (t, $J = 9.2$ Hz, 1H), 3.35 (d, $J = 9.8$ Hz, 1H), 1.34 (d, $J = 0.9$ Hz, 3H) ppm. $^{13}\text{C NMR}$ (151 MHz, CDCl_3): δ 158.3, 140.9, 135.8, 129.9, 129.5, 129.1, 128.2, 121.6, 110.5, 105.7, 121.1, 73.1, 71.2, 66.73, 61.83, 26.11. HRMS (DART) m/z calcd for $\text{C}_{18}\text{H}_{18}\text{NO}_4$ [$\text{M} + \text{H}$] $^+$: 314.1392; Found [$\text{M} + \text{H}$] $^+$: 314.1392.



(S)-3-((3S,4S)-4-hydroxy-4-(5-methylthiophen-2-yl)pent-1-en-3-yl)-4-phenyloxazolidin-2-one (1.4h): According to the branched-selective general procedure employing $\text{IMes}\cdot\text{HCl}$ as ligand, the product was purified by silica gel chromatography (eluent: 0 – 40% EtOAc in hexanes) to provide 165.2 mg (83%) of **1.4h** in 86 wt% purity by quantitative $^1\text{H NMR}$ spectroscopy using dimethylfumarate as analytical standard as a white solid as a 96/4 mixture of diastereomers (allene rearrangement products *N*-allyl and *N*-propenyl 4-phenyloxazolidin-2-

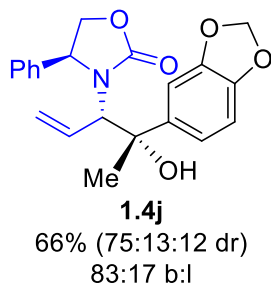
one could not be removed by chromatography). Analytically and diastereomerically pure material could be obtained by slurrying the material in 10 vol. of hot 10% EtOAc in hexanes followed by cooling to rt in 40% recovery of the major diastereomer. The recrystallized product had a melting point of 100.0 – 103.1°C. The stereochemistry was assigned by analogy to that of *syn-b*-**12a**. $R_f = 0.18$ (20% EtOAc/hexanes). $^1\text{H NMR}$ (CDCl_3 , 600 MHz) δ : 7.43 – 7.34 (m, 1H), 7.29 (t, $J = 7.7$ Hz, 2H), 6.88 (d, $J = 7.6$ Hz, 2H), 6.79 (br s, 1H), 6.59 (dd, $J = 2.3$ Hz, $J = 1.0$ Hz, 1H), 6.41 (d,

$J = 3$ Hz, 1H), 6.18 (dt, $J = 17$ Hz, $J = 9.8$ Hz, 1H), 5.45 (d, $J = 10$ Hz, 1H), 5.19 (d, $J = 17$ Hz, 1H), 4.70 (dd, $J = 9.1$ Hz, $J = 8.9$ Hz, 1H), 4.53 (t, $J = 9.0$ Hz, 1H), 4.08 (dd, $J = 9.0$ Hz, $J = 8.9$ Hz, 1H), 3.26 (d, $J = 10$ Hz, 1H), 2.47 (s, 3H), 1.40 (s, 3H) ppm. ^{13}C NMR (151 MHz, CDCl_3): δ 160.2, 148.5, 137.8, 135.8, 130.6, 129.3, 129.0, 128.3, 124.9, 122.8, 121.3, 74.64, 71.14, 68.99, 61.74, 29.67, 15.34. HRMS (DART) m/z calcd for $\text{C}_{19}\text{H}_{20}\text{NO}_2\text{S}$ $[\text{M} - \text{OH}]^+$: 326.1215; Found $[\text{M} - \text{OH}]^+$: 326.1237.



(S)-3-((3S,4S)-4-hydroxy-4-(4-methylphenyl)pent-1-en-3-yl)-4-phenyloxazolidin-2-one (1.4i): According to the branched-selective general procedure, the product was purified by silica gel chromatography (eluent: 0 – 30% EtOAc in hexanes) to provide 134.8 mg (58%) of **1.4i** in 73 wt% purity by quantitative ^1H NMR spectroscopy using dimethylfumarate as analytical standard as a white solid as a 92/8 mixture of diastereomers (allene rearrangement products *N*-allyl and *N*-propenyl 4-phenyloxazolidin-2-one could not be removed by chromatography).

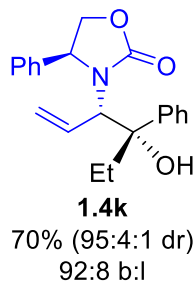
Analytically pure material could be obtained by slurrying the material in 10 vol. of hot 10% EtOAc in hexanes followed by cooling to rt in 20% recovery of the major diastereomer. The recrystallized product had a melting point of 115.3 – 116.6°C. The stereochemistry was assigned by analogy to that of **1.4a**. $R_f = 0.28$ (25% EtOAc/hexanes). ^1H NMR (CDCl_3 , 600 MHz) δ : 7.39 (d, $J = 7.3$ Hz, 1H), 7.30 (t, $J = 7.6$ Hz, 2H), 7.07 (d, $J = 7.9$ Hz, 2H), 7.01 (d, $J = 7.9$ Hz, 2H), 6.84 (d, $J = 7.6$ Hz, 2H), 6.48 (br s, 1H), 6.20 (dt, $J = 17$ Hz, $J = 9.8$ Hz, 1H), 5.48 (dd, $J = 10$ Hz, $J = 1.4$ Hz, 1H), 5.20 (dd, $J = 17$ Hz, $J = 1.4$ Hz, 1H), 4.68 (t, $J = 9.2$ Hz, 1H), 4.44 (t, $J = 8.9$ Hz, 1H), 3.97 (dd, $J = 9.4$ Hz, $J = 8.9$ Hz, 1H), 3.38 (d, $J = 9.6$ Hz, 1H), 2.39 (s, 3H), 1.33 (s, 3H) ppm. ^{13}C NMR (151 MHz, CDCl_3): δ 160.1, 143.1, 136.1, 135.6, 131.0, 129.5, 129.2, 128.8, 128.7, 125.3, 121.2, 75.50, 70.93, 68.21, 61.82, 29.42, 21.24.



(S)-3-((3S,4S)-4-(benzo[d][1,3]dioxol-5-yl)-4-hydroxypent-1-en-3-yl)-4-phenyloxazolidin-2-one (1.4j): According to the branched-selective general procedure, the product was purified by silica gel chromatography (eluent: 0 – 30% EtOAc in hexanes) to provide 155.3 mg (70%) of **1.4j** in 83 wt% purity by quantitative ^1H NMR spectroscopy using dimethylfumarate as analytical standard as a white solid as a 85/15 mixture of diastereomers (allene rearrangement products *N*-allyl and *N*-propenyl 4-phenyloxazolidin-2-one could not be removed by chromatography).

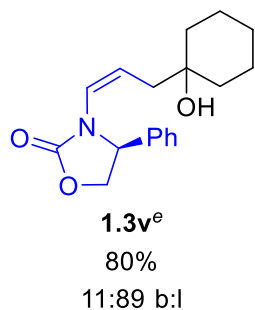
Analytically pure material could be obtained by slurrying the material in 10 vol. of hot 10% EtOAc in hexanes followed by cooling to rt in 70% recovery of the major diastereomer. The recrystallized product had a melting point of 159.2 - 166.1°C. The stereochemistry was assigned by analogy to that of **1.4a**. $R_f = 0.12$ (25% EtOAc/hexanes). ^1H NMR (CDCl_3 , 600 MHz) δ : 7.44-7.38 (m, 2H), 7.35 (t, $J = 7.6$ Hz, 2H), 6.92 (dd, $J = 7.4$ Hz, $J = 1.2$ Hz, 2H), 6.70 (d, $J = 8.2$ Hz, 1H), 6.63 (d, $J = 7.9$ Hz, 1H), 6.59 (br s, 1H), 6.52 (br s, 1H), 6.20 (dt, $J = 17$ Hz, $J = 9.8$ Hz, 1H), 5.99 (dd, $J = 25$ Hz, $J = 0.8$ Hz, 2H), 5.49 (dd, $J = 10$ Hz, $J = 0.5$ Hz, 1H), 5.21 (dd, $J = 17$ Hz, $J = 0.9$ Hz, 1H), 4.68 (t, $J = 9.3$ Hz, 1H), 4.49 (t, $J = 8.9$ Hz, 1H), 4.05 (dd, $J = 9.2$ Hz, $J = 9.2$ Hz, 1H), 3.30 (d, $J = 9.6$ Hz, 1H), 1.30 (s, 3H) ppm. ^{13}C NMR (151 MHz, CDCl_3): δ 160.1, 147.3, 146.3, 140.3,

135.4, 130.9, 129.7, 129.2, 128.8, 121.3, 118.5, 107.8, 106.5, 101.1, 75.52, 70.94, 68.22, 61.92, 29.59 ppm.



(S)-3-((3S,4S)-4-hydroxy-4-phenylhex-1-en-3-yl)-4-phenyloxazolidin-2-one (1.4k): According to the branched-selective general procedure, the product was purified by silica gel chromatography (eluent: 0 – 30% EtOAc in hexanes) to provide 104 mg (61%) of **1.4k** in 99 wt% purity by quantitative ^1H NMR spectroscopy using dimethylfumarate as analytical standard as a white solid as a 97/3 mixture of diastereomers (allene rearrangement products *N*-allyl and *N*-propenyl 4-phenyloxazolidin-2-one could not be removed by chromatography).

Analytically pure material could be obtained by slurrying the material in 10 vol. of hot 10% EtOAc in hexanes followed by cooling to rt in 17% recovery of the major diastereomer. The recrystallized product had a melting point of 123.0 – 125.1°C. The stereochemistry was assigned by analogy to that of **1.4a**. $R_f = 0.24$ (25% EtOAc/hexanes). ^1H NMR (CDCl_3 , 600 MHz) δ : 7.40 (tt, $J = 7.7$ Hz, $J = 1.4$ Hz, 1H), 7.33 (t, $J = 7.9$ Hz, 2H), 7.23 – 7.28 (m, 3H), 7.07 (br s, 1H), 6.87 (d, $J = 7.4$ Hz, 2H), 6.42 (br s, 1H), 6.17 (dt, $J = 17$ Hz, $J = 9.8$ Hz, 1H), 5.47 (dd, $J = 10$ Hz, $J = 1.4$ Hz, 1H), 5.21 (dd, $J = 17$ Hz, $J = 1.0$ Hz, 1H), 4.69 (t, $J = 9.2$ Hz, 1H), 4.41 (t, $J = 8.9$ Hz, 1H), 3.96 (dd, $J = 9.2$ Hz, $J = 8.9$ Hz, 1H), 3.42 (d, $J = 9.6$ Hz, 1H), 1.85 (sextet, $J = 7.3$ Hz, 1H), 1.43 (m, 1H), 0.54 (t, $J = 7.3$ Hz, 3H) ppm. ^{13}C NMR (151 MHz, CDCl_3): δ 159.9, 143.3, 135.4, 131.0, 129.4, 129.0, 128.8, 127.9, 126.4, 125.9, 121.0, 77.90, 70.64, 68.08, 61.50, 33.63, 7.49.



(S,Z)-3-((3-(1-hydroxycyclohexyl)prop-1-en-1-yl)-4-phenyloxazolidin-2-one (1.3v): According to the branched-selective general procedure employing IMes•HCl as ligand, the product was purified by silica gel chromatography (eluent: 20 – 60% EtOAc in hexanes) to provide 120.3 mg (80%) of **1.3v** as a thick wax. $R_f = 0.17$ (40% EtOAc/hexanes). ^1H NMR (CDCl_3 , 600 MHz) δ : 7.33-7.43 (m, 3H), 7.26 (d, $J = 4.3$ Hz, 2H), 5.89 (d, $J = 8.9$ Hz, 1H), 5.27 (dt, $J = 16$ Hz, $J = 8.1$ Hz, 1H), 5.09 (dd, $J = 8.8$ Hz, $J = 6.2$ Hz, 1H), 4.69 (t, $J = 8.8$ Hz, 1H), 4.17 (dd, $J = 8.8$ Hz, $J = 6.1$ Hz, 1H), 2.23 (br s, 1H), 2.20 (d, $J = 7.9$ Hz, 2H), 1.48 – 1.65 (m, 5H), 1.37 – 1.46 (m, 2H), 1.30 – 1.37 (m, 2H), 1.18 – 1.27 (m, 1H) ppm. ^{13}C NMR (151 MHz, CDCl_3): δ 156.8, 138.3, 129.5, 129.2, 126.6, 123.3, 119.6, 70.82, 70.29, 61.50, 38.23, 37.66, 25.93, 22.36, 22.34. HRMS (DART) m/z calcd for $\text{C}_{18}\text{H}_{24}\text{NO}_3$ $[\text{M} + \text{H}]^+$: 302.1756; Found $[\text{M} + \text{H}]^+$: 302.1768.

v. Linear selective Fused Phenyl allene Procedures

General procedure for the enantioselective linear selective Cu-catalyzed reductive coupling.

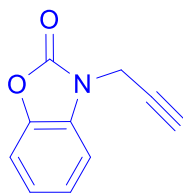
To a 20 mL crimp-cap vial with stir-bar in an Ar-filled glove-box was charged 2.2 mg (0.0125 mmol) of $\text{Cu}(\text{OAc})_2$ and 0.5 mL of toluene. Ligand was then added (0.016 mmol), and the mixture was stirred for 10 min. Allene **1.6** (52.0 mg, 0.300 mmol) was then added, followed by acetophenone **1.2a** (29.2 μL , 0.250 mmol), and the vial was sealed with a crimp-cap septum and removed from the glove-box. The reaction was then cooled in an ice bath, and

dimethoxymethylsilane (0.061 mL, 0.500 mmol) was charged by syringe (*caution: dimethoxymethylsilane should be handled in a well-ventilated fume hood because it is known to cause blindness. Syringes were quenched with 2M NaOH, gas evolution!, prior to disposal*). The mixture was then allowed to warm to rt and stirred for 24 h. The reaction was then quenched by the addition of 95 mg of NH₄F and 2.5 mL of MeOH followed by agitation at rt for 30 min – 1 h. To the mixture was then charged 10 mL of 5% NaHCO₃ followed by extraction with CH₂Cl₂ (2x5mL). The combined organics were dried with Na₂SO₄ and concentrated *in vacuo*. An aliquot of the crude mixture was analyzed by ¹HNMR spectroscopy to determine the the l/b ratio. The crude residue was then purified by flash chromatography on silica gel to afford the isolated product. The enantioselectivity of the ligand was determined by chiral HPLC on the isolated product.

General procedure for the development of the enantioselective linear selective Cu-catalyzed reductive coupling with CF₃-ketones.

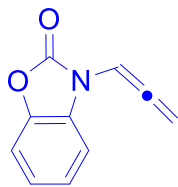
To a 20 mL crimp-cap vial with stir-bar in an Ar-filled glove-box was charged 2.2 mg (0.0125mmol) of Cu(OAc)₂ and 0.5 mL of toluene. Ligand was then added (0.016 mmol), and the mixture was stirred for 10 min. Allene **1.6** (52.0 mg, 0.300 mmol) was then added, followed by trifluoromethyl phenyl ketone **1.5** (35.1 μL, 0.250 mmol), and the vial was sealed with a crimp-cap septum and removed from the glove-box. The reaction was then cooled in an ice bath, and dimethoxymethylsilane (0.061 mL, 0.500 mmol) was charged by syringe (*caution: dimethoxymethylsilane should be handled in a well-ventilated fume hood because it is known to cause blindness. Syringes were quenched with 2M NaOH, gas evolution!, prior to disposal*). The mixture was then allowed to warm to rt and stirred for 24 h. The reaction was then quenched by the addition of 95 mg of NH₄F and 2.5 mL of MeOH followed by agitation at rt for 30 min – 1 h. To the mixture was then charged 10 mL of 5% NaHCO₃ followed by extraction with CH₂Cl₂ (2x5mL). The combined organics were dried with Na₂SO₄ and concentrated *in vacuo*. An aliquot of the crude mixture was analyzed by ¹HNMR spectroscopy to determine the the l/b ratio. The crude residue was then purified by flash chromatography on silica gel to afford the isolated product. The enantioselectivity of the ligand was determined by chiral HPLC on the isolated product.

vi. Analytical data for the fused phenyl allene products



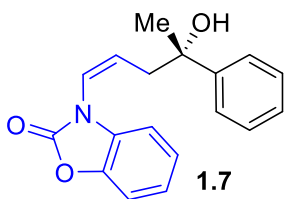
form the allene.

3-(prop-2-yn-1-yl)benzo[d]oxazol-2(3H)-one (Alkyne): Prepared according to the literature.¹³⁹ To a flame-dried rbf, was added 2-benzoxazolidinone (37.0mmol, 5.0g), propargyl bromide (1.3eq, 5.36mL), and K₂CO₃ (1.5eq, 7.67g) under inert atmosphere. The reagents were then dissolved in 90mL acetone, and refluxed overnight. The product was then extracted with EtOAc and the resulting organic layers were washed with water. The combined organic layers were dried over Na₂SO₄, concentrated to afford 5.60g of the crude alkyne in 88% yield. The crude alkyne was used directly in the next step to



1.6

3-(propa-1,2-dien-1-yl)benzo[d]oxazol-2(3H)-one (1.6): In a flame-dried rbf, the alkyne (18.9mmol, 3.27g) and 40mL anhydrous THF were added with stirring. To the rbf was then charged KO^tBu (0.3 eq, 636.1mg), and the reaction was allowed to stir at 65°C overnight. At the end of the reaction period, the reaction mixture was allowed to cool to room temperature, diluted with MTBE, and filtered through celite, and concentrated to afford a crude solid. The allene was isolated via column chromatography (0-10% EtOAc/Hexanes) to afford 2.01g as a white solid in a 61.4% yield. ¹HNMR (600MHz, CDCl₃): 7.48-7.45 (m, 1H), 7.23-7.21 (m, 1H), 7.17-7.15 (m, 2H), 7.10 (t, *J* = 6.7 Hz, 1H), 5.70 (d, *J* = 6.7 Hz, 2H) ppm.

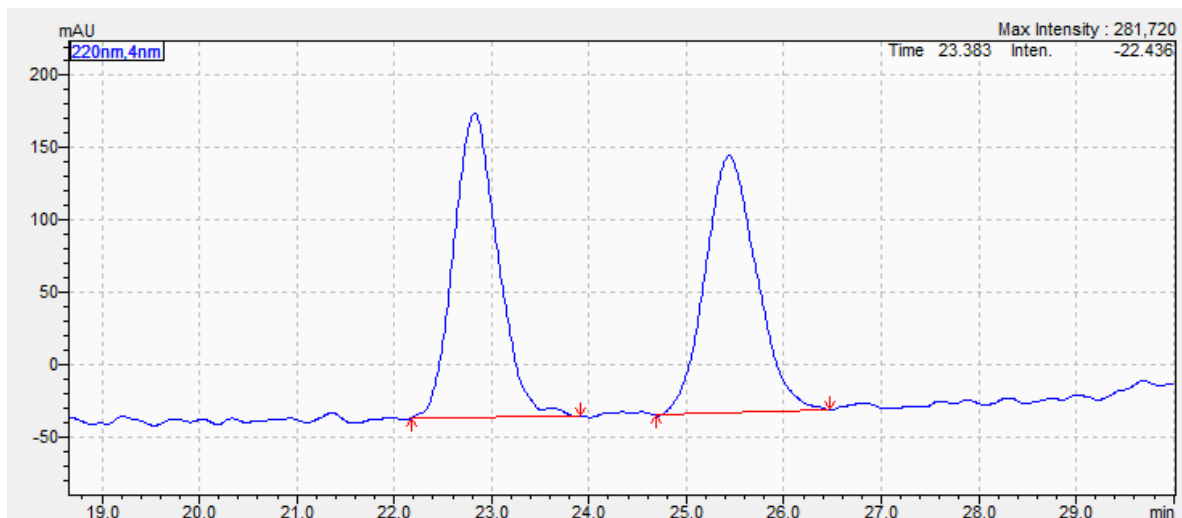


1.7

(S,Z)-3-(4-hydroxy-4-phenylpent-1-en-1-yl)benzo[d]oxazol-2(3H)-one (1.7): Isolated via column chromatography (0-20% EtOAc/Hexanes) to afford the product as a clear oil. ¹HNMR (600MHz, CDCl₃): 7.46 (d, *J* = 7.6Hz, 2H), 7.23 (t, *J* = 7.5Hz, 2H), 7.24-7.21 (m, 2H), 7.18-7.15 (m, 2H), 6.88-6.86 (m, 1H), 6.18 (d, *J* = 8.3 Hz, 1H), 5.78 (q, *J* = 7.8Hz, 1H), 3.1 (br s, 1H), 2.71 (ddd, *J* = 7.79, *J* = 2.4, *J* = 1.2 Hz, 2H), 1.60 (s, 3H) ppm.

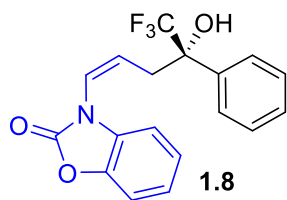
Chiral HPLC Analysis (Chiralpak AD-3 x 250 mm, heptane/isopropanol = 95/5, flow rate = 1.0 ml/min, λ = 220nm) tR = 22.8 (major), 25.4 (minor):

Racemate:



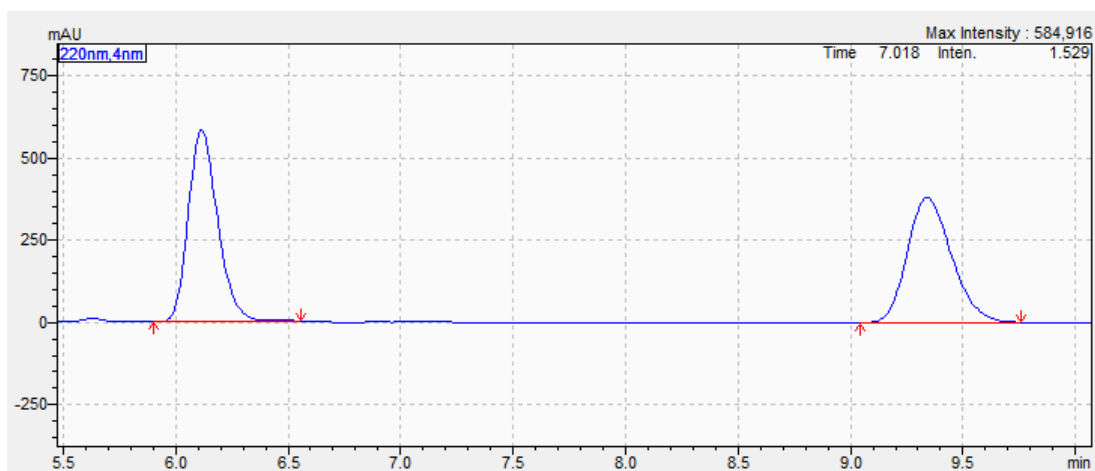
Ret. Time	Area%	Height	Conc.
22.827	50.414	210440	0.000
25.440	49.586	178385	0.000
	100.000	388825	0.000

(*S,Z*)-3-(5,5,5-trifluoro-4-hydroxy-4-phenylpent-1-en-1-yl)benzo[d]oxazol-2(3*H*)-one (1.8): Isolated via column chromatography (0-40% EtOAc/Hexanes). White solid, $R_f=0.38$ (25% EtOAc/Hexanes). $^1\text{H NMR}$ (600 MHz, CDCl_3): 7.67 (d, $J = 7.9$ Hz, 2H), 7.43 (t, $J = 7.2$ Hz, 2H), 7.38 (t, $J = 7.2$ Hz, 1H), 7.29-7.26 (m, 1H), 7.22 (dd, $J = 5.0$ Hz, $J = 4.2$ Hz, 2H), 6.98-6.95 (m, 1H), 6.18 (ddd, $J = 8.9$ Hz, $J = 1.2$ Hz, $J = 0.8$ Hz, 1H), 5.50-5.45 (m, 2H), 3.17 (dd, $J = 14.5$ Hz, $J = 10.8$ Hz, 1H), 2.98 (ddd, $J = 15.1$ Hz, $J = 5.2$ Hz, $J = 1.6$ Hz, 1H) ppm. $^{19}\text{F NMR}$ (CDCl_3): -80.17 ppm.



Chiral HPLC Analysis (Chiralpak AD-3 x 250 mm, heptane/isopropanol = 80/20, flow rate = 1.0 ml/min, $\lambda = 220\text{nm}$) tR = 6.11 (major), 9.34 (minor):

Racemate:



Ret. Time	Area%	Height	Conc.
6.115	50.562	582456	0.000
9.341	49.438	379554	0.000
	100.000	962011	0.000

Asymmetric Reaction, using L9 ((*S*)-tBu-TADDOL-P((*R*)-2-Me-Piperidine):



Ret. Time	Area%	Height	Conc.
6.102	34.832	1070924	0.000
9.272	65.168	1295912	0.000
	100.000	2366836	0.000

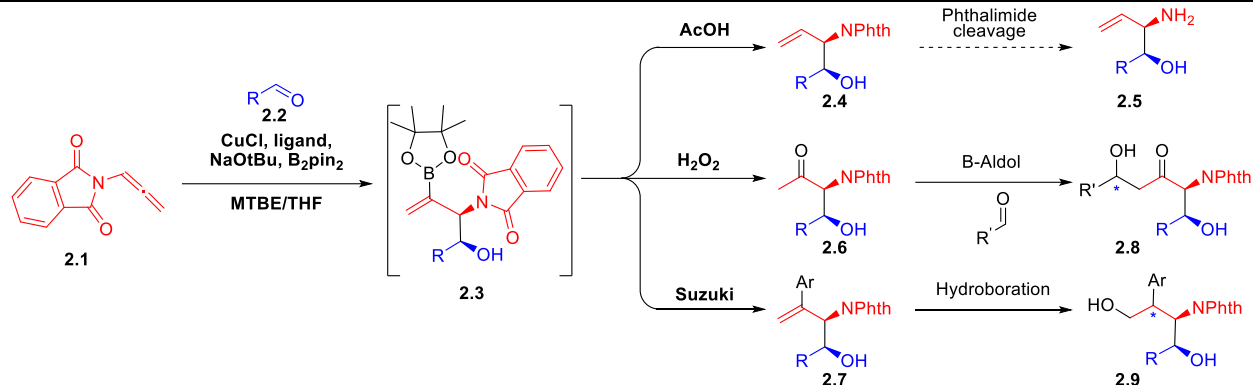
CHAPTER 2

Borylative Aminoalcohol Synthesis by Enantioselective Cu-Catalyzed Reductive Coupling of Alleneamides and Aldehydes

I. Introduction

Important biologically active organic compounds, including natural products and pharmaceuticals, often contain multiple oxygen and nitrogen heteroatoms within their carbon framework.¹⁻¹⁰ Furthermore, the chiral 1,2-aminoalcohol motif is a ubiquitous and significant scaffold often present in these bioactive natural products and APIs.³⁻⁷ As a result, asymmetric installation of these functional group pairs while installing additional functionality for subsequent diversification has been an important endeavor in organic synthesis.⁸⁻¹⁰ However, their mismatched electronics and classification as dissonant functional group pairs make accessing these scaffolds via traditional methods difficult (See *Chapter 1, Background, Consonant/Dissonant Theory*).²⁹ For this reason, alternative methods utilizing umpolung³⁰ α,γ -aminoanions¹⁴⁰⁻¹⁴⁴ and radicals³¹⁻³⁵ (See *Chapter 1, Background, Umpolung*) to generate these scaffolds have been a hot area of study for organic chemists. Of these methods, reductive coupling reactions (See *Chapter 1, Background, Reductive Coupling*) have been extensively developed as efficient synthetic methods for the formation of these respective umpolung carbon-carbon bonds.¹² Towards this end, we developed a strategy based on the Cu-catalyzed enantioselective borylative aminoallylation of aldehydes using an *N*-substituted allene (alleneamide) **2.1** to access boryl-substituted 1,2-aminoalcohol intermediates **2.3** for diversification to chiral heteroatom-rich organic compounds. The reported reaction, **Scheme 2.1**, provides access to a variety of highly functionalized chiral 1,2-aminoalcohol products from the same readily available starting materials with high enantioselectivity (>95:5 er).

Scheme 2.11. Overall reaction development of the Cu-catalyzed borylative aminoallylation.

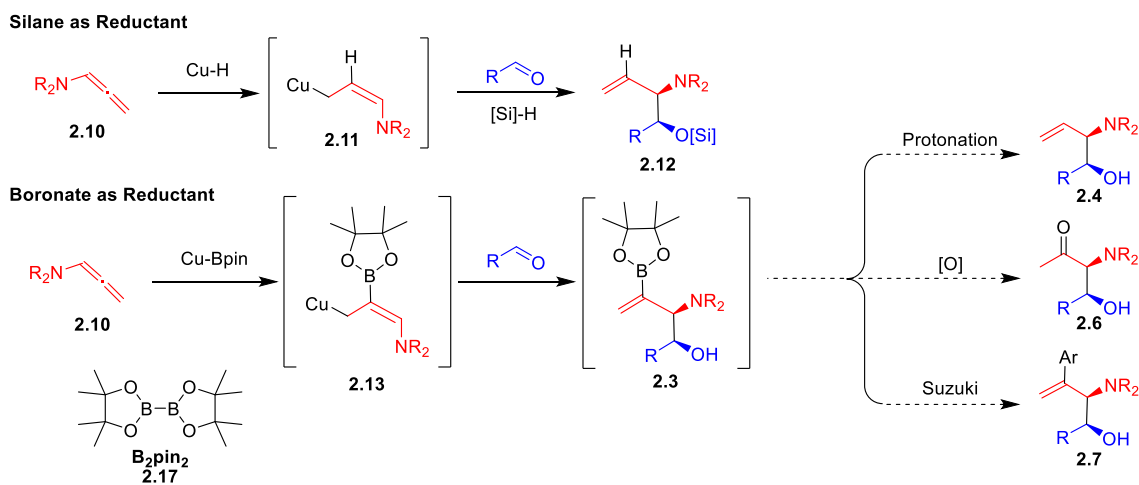


II. Background

A. Review of Reductive Coupling and Reductant Source

As covered in *Chapter 1, Background*, reductive coupling reactions have been extensively studied as methods to form C-C bonds between two electrophilic fragments and thereby require a stoichiometric reductant to turn over the catalyst.¹² In our previous work, including all projects in Chapter 1, silane was used as the reductant to affect coupling processes catalyzed by Cu(hydride) (**Scheme 2.2A**).

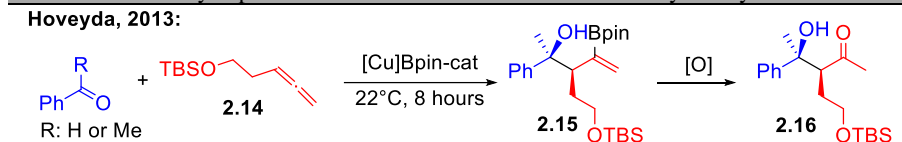
Scheme 2.12. Effect of reductant source on product generation.



Alternatively, we proposed that analogous reactions may be performed employing a boronate reductant as well through catalysis by a Cu-B(pin) catalyst generated from B₂(pin)₂ by oxygen-boron exchange¹⁴⁵ (**Scheme 2.2B**). Mechanistically, borylcupration¹⁴⁵ of the least hindered olefin of the allene leads to the analogous boryl Cu(allyl) complex **2.13** that may generate the branched vinyl boronate intermediate **2.3** after reaction with a carbonyl electrophile. The value in this approach stems from the

variety of synthetic transformations available to the C-B bond for advanced diversification of intermediate **2.3** to a variety of different chiral scaffolds (*e.g.*, **2.4**, **2.6**, **2.7**) from the same building blocks. Furthermore, the use of aldehydes is not typically supported by Cu-catalysis utilizing a hydride reductant source, due to CuH's preference for reducing the highly reactive aldehyde.^{146,147} This aldehyde reduction can be avoided via the use of B₂pin₂ as the reductant source, as CuBpin is much larger than CuH, making it slower to react.

Scheme 2.13. Borylcupration of C-based allenes as demonstrated by Hoveyda.



Previously, Hoveyda has reported a method coupling carbon-substituted allenes with aldehydes, using a Cu(I) catalyst and B₂(pin)₂, **Scheme 2.3**.¹⁴⁸ This work generated the borylative branched product **2.15** selectively, which they then oxidized to the methyl ketone **2.16** via NaBO₃·4H₂O. We envisioned being able to apply a similar method using *N*-substituted allenes.

B. Rationale behind choice of alleneamide

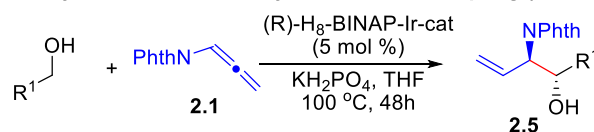
With current methods allowing for generation of substituted allylic organometallic reagents in a catalytic fashion from unsaturated hydrocarbons,^{12,15,47–49,149} catalytic asymmetric access to the allylic 1,2-aminoalcohol motif through reductive coupling methods have recently emerged, **Scheme 2.4**.^{84,86,107,138,150–}

154

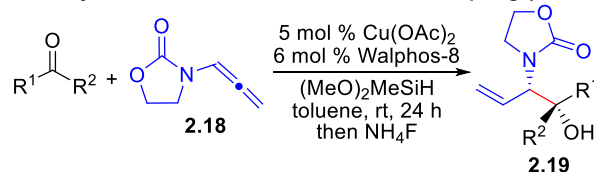
Krische's group⁸⁶ has recently applied their pioneering hydrogen autotransfer technique for the coupling of phthalimido-allene **2.1** and primary aliphatic alcohols to afford the *anti*-aminoalcohol precursor **2.4**, with high enantioselectivities, using Ir-catalysis. While these methods are useful, the development of an analogous method using cheaper, more abundant Cu in place of costly Ir, as well as

Scheme 2.14. Previous work in reductive aminoallylation utilizing a hydride reductant source.

Ir-catalyzed reductive aldehyde/allenimide coupling (Krische)



Cu-Catalyzed reductive ketone/allenamide coupling (Sieber)



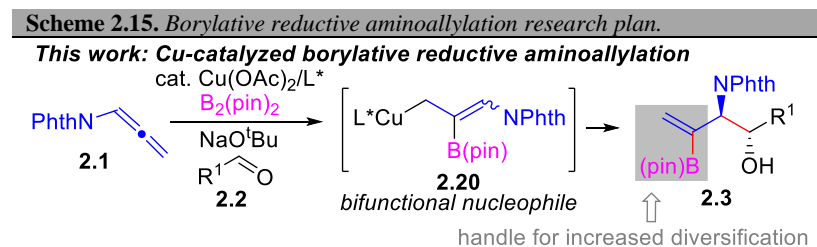
methods utilizing commercially available aromatic and aliphatic aldehydes would be desirable for accessing these dissonant motifs.

Additionally, our group reported a Cu-catalyzed enantioselective¹⁵¹ method using ketone electrophiles with allenamide **2.18** to produce *syn*-aminoalcohol surrogate **2.19** and have also demonstrated this process under chiral auxiliary control.^{84,107,138,150} The chiral auxiliary used was cheap, but not atom economical – as stoichiometric chiral material had to be carried through the reaction. The enantioselective method suffered from difficult cleavage of the carbamate group and an undesired rearrangement product leading to reduced enantioselectivities for some ketones. We aimed to resolve this issue by employing the achiral phthalimide scaffold **2.1** that was not compatible with Cu(hydride) catalyzed reductive coupling reactions due to partial reduction of the phthalimide moiety and represents a readily cleavable *N*-protective group.

III. Development of Enantioselective Borylative Aminoallylation

A. Research Plan

During the course of our development of the Cu-catalyzed asymmetric reductive coupling reactions of ketones and allenamides utilizing silane reductants (Chapter 1),^{84,107,138,150,151} we reasoned that application of a diboron reagent as the reductant (*e.g.* B₂(pin)₂) in these reactions may offer significant benefits in the ability to access heteroatom-rich organic scaffolds.^{148,155} We reasoned that borylcupration of **2.1** should be a viable pathway to access the bifunctional nucleophilic α,γ -aminoanion **2.20**, ultimately leading to boryl-substituted aminoalcohol intermediate **2.3** in a straightforward manner, as laid out in **Scheme 2.5**.



Due to the wide array of transformations that can be imparted on the C-B bond^{156–159} to access a variety of functionalities, **2.3** represents a highly valuable intermediate for asymmetric synthesis of complex 1,2-aminoalcohol containing chiral scaffolds.

Inspired by the work of Hoveyda¹⁴⁸ and Krische⁸⁶, the achiral phthalimide-derived alleneamide **2.1** was sought as a solution for the enantioselective reductive coupling reactions, as it can be easily cleaved and does not pose the threat of rearrangement, unlike previous efforts.¹⁵¹ The choice of B₂(pin)₂ as the reductant allows for the use of aldehydes as the coupling partner, as well as the ability to access a multitude of different products via the vinyl-boronate intermediates generated.

Herein, we report the development of a borylative Cu-catalyzed reductive coupling method of phthalimido-allene **2.1** with aldehydes **2.2** that provides access to a wide set of uniquely diversified dissonant chiral 1,2-aminoalcohol motif-containing products in an enantioselective fashion.¹⁶⁰

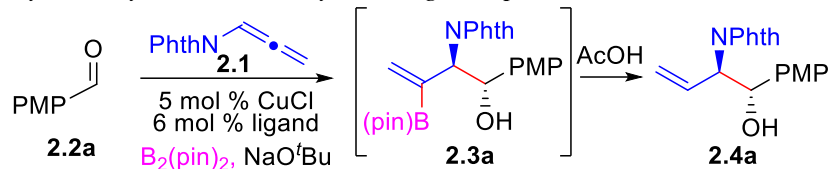
B. Overall Reaction Development

Investigation into this proposed novel reductive coupling of phthalimido-allene **2.1** with *p*-anisaldehyde **2.2a** was initially optimized through a study of ligand and solvent effects, as well as investigation into various bases, additives, and diboronate reductants (*e.g.*, B₂pin₂, B₂eg₂, B₂pg₂, B₂neo₂). B₂(pin)₂, B₂(eg)₂, B₂(pg)₂, B₂(neo)₂; **Tables 2.1 – 2.5**). In order to compare the results of each of these optimization efforts, the vinyl boronate intermediate **2.3a** was protonated by treatment with AcOH to generate the quintessential branched 1,2-aminoalcohol product **2.4a**.

The ligand effect was first investigated (**Table 2.1**). A series of various commercially available chiral bis(phosphine) ligands were evaluated in the reaction. BINAP and Segphos-type ligands (entries 2, 3, and 4) generated the desired product **2.4a** with high diastereocontrol, however, with poor enantioselectivity. *N*-Heterocyclic carbene (NHC) ligands (entries 5, 6, and 7) were not successful in generating the product, with yields below 10%. Josiphos-type ligands (entries 12, 13, and 14) generated the desired product in varying yields and diastereoselectivities, albeit with moderate enantioselectivities. (*R,R*-

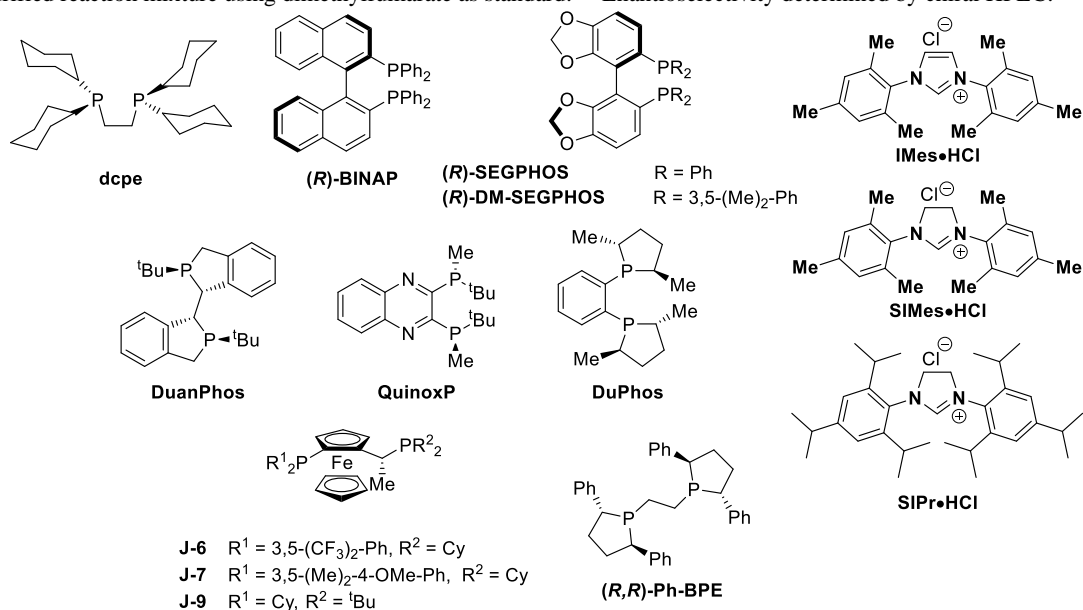
PhBPE (entry 15) was identified as the optimal ligand for this transformation among those tested, in terms of diastereocontrol, as well as enantioselectivity.

Table 2.6. *Cu-catalyzed borylative aminoallylation ligand optimization.*^[a]



Entry	Ligand	Equiv NaO ^t Bu	% Yield of 2.4a ^[b]	Dr of 2.4a ^[b]	Er of 2.4a ^[c]
1	Dcpe	1	22	70:30	50:50
2	(R)-BINAP	1	39	97:3	38:62
3	(R)-SegPhos	1	53	99:1	23:77
4	(R)-DM-SegPhos	1	47	95:5	28:72
5	IMes	1	4	--	--
6	SIMes	0.25 eq, KOtBu	5	--	--
7	SIPr	0.25 eq, KOtBu	8	--	--
8	DuanPhos	1	36	89:11	27:73
9	QuinoxP	1	9	99:1	--
10	Methyl DuPhos	1	18	63:37	n.d.
11	Ethyl DuPhos	1	17	66:34	22:78
12	J-9	1	9	58:42	--
13	J-7	1	33	67:33	19:81
14	J-6	1	55	86:14	20:80
15	(R,R)-PhBPE	1	53	99:1	93:7

^[a]Aldehyde **2.2a** (0.100 mmol, 1 equiv), allene **2.1** (0.105 mmol, 1.05 equiv), CuCl (5 mol %), ligand (6 mol %), NaO^tBu (0.100 mmol, 1 equiv), $B_2(\text{pin})_2$ (0.110 mmol, 1.1 equiv), in 0.6 mL of THF. ^[b]Determined by ¹HNMR spectroscopy on the unpurified reaction mixture using dimethylfumarate as standard. ^[c]Enantioselectivity determined by chiral HPLC.



The temperature of reaction was next examined (**Table 2.2**) by running the standard reaction with the same conditions at room temperature (22), 40, and 60 °C. As the temperature of reaction increased, a notable decrease in the yield was observed, as well as a more mild decrease in enantioselectivity (compare entries 2 and 3 with entry 1). With this observation, the optimal reaction temperature was determined to be room temperature (22°C).

Table 2.7. *Cu-catalyzed borylative aminoallylation reaction temperature optimization.*^[a]

Entry	Temp. (°C)	% Yield of 2.4a ^[b]	Dr of 2.4a ^[b]	Er of 2.4a ^[c]
1	22	53	99:1	92.5:7.5
2	40	40	99:1	91:9
3	60	38	98:2	87:13

^[a]Aldehyde **2.2a** (0.100 mmol, 1 equiv), allene **2.1** (0.105 mmol, 1.05 equiv), CuCl (5 mol %), (*R,R*)-Ph-BPE (6 mol %), NaO^tBu (0.100 mmol, 1 equiv), B₂(pin)₂ (0.110 mmol, 1.1 equiv), in 0.6 mL of THF. ^[b]Determined by ¹HNMR spectroscopy on the unpurified reaction mixture using dimethylfumarate as standard. ^[c] Enantioselectivity determined by chiral HPLC.

The effect of the base was then investigated (**Table 2.3**). The initial amount evaluated was 20 mol% of NaO^tBu, as gathered from literature.¹⁴⁸ Several catalytic amounts of NaO^tBu, as well as stoichiometric and excess amounts were evaluated. Excess equivalents of base were determined to lead to the decomposition of reaction components (entries 6 and 7). The optimal yield and enantioselectivity was obtained when using 1 equivalent of NaO^tBu.

The cation of the base was also investigated, to determine if there was a cation effect that could be exploited. The use of 1 equiv of KO^tBu or LiO^tBu led to lower yields overall (entries 8 and 9), however, LiO^tBu generated the product with equal – if not slightly better – enantioselectivity compared to NaO^tBu.

Table 2.8. *Cu*-catalyzed borylative aminoallylation base optimization.^[a]

Entry	NaO ^t Bu equiv	% Yield of 2.4a ^[b]	Dr of 2.4a ^[b]	Er of 2.4a ^[c]
1	0.04	10	95:5	--
2	0.2	37	95:5	89:11
3	0.5	47.5	99:1	83:17
4	0.75	47.1	99:1	95:5
5	1.0	53	99:1	92.5:7.5
6	2	Decomp.	--	--
7	4	Decomp.	--	--
8	1 equiv KO ^t Bu	22	99:1	83:17
9	1 equiv LiO ^t Bu	25	99:1	97:3

^[a]Aldehyde **2.2a** (0.100 mmol, 1 equiv), allene **2.1** (0.105 mmol, 1.05 equiv), CuCl (5 mol %), (*R,R*)-Ph-BPE (6 mol %), NaO^tBu, B₂(pin)₂ (0.110 mmol, 1.1 equiv), in 0.6 mL of THF. ^[b]Determined by ¹HNMR spectroscopy on the unpurified reaction mixture using dimethylfumarate as standard. ^[c] Enantioselectivity determined by chiral HPLC.

The next aspect of the reaction to be evaluated was the solvent (**Table 2.4**). The analysis of the reaction solvent demonstrated that the diastereoselectivity was not affected by solvent, as all generated the branched product **2.4a** with 99:1 diastereoselectivity. It can be assumed that the effect of the ligand on diastereoselectivity outweighs the effect of the solvent in this case. Polar solvents, including ACN (entry 1), DMF (entry 2), and DCM (entry 3), generated the desired product in poor yields and with poor enantiocontrol. THF (entry 5) gave the highest yield overall. The additional non-polar methyl of MeTHF (entry 6) did not lead to any beneficial effects. However, the enantioselectivity could be increased when switching from THF to MTBE (entry 5 vs 8). As a result, it was determined that by performing the reaction in a 1:1 mixture of MTBE:THF, both enantioselectivity and yield could be improved providing desired product **2.4a** in 75% yield with high stereoselectivity (entry 10).

Table 2.9. Cu-catalyzed borylative aminoallylation solvent optimization.^[a]

Entry	Solvent	B ₂ pin ₂ equiv	% Yield of 2.4a ^[b]	Dr of 2.4a ^[b]	Er of 2.4a ^[c]
1	ACN	2	7	99:1	N.D.
2	DMF	2	37	99:1	50:50
3	CH ₂ Cl ₂	1.1	7	99:1	42:58
4	1,2-DME	2	51	99:1	89:11
5	THF	2	65	99:1	95:5
6	MeTHF	2	64	99:1	94:6
7	Dioxane	1.1	29	99:1	89:11
8	MTBE	2	54	99:1	97.5:2.5
9	Toluene	1.1	41	99:1	85:15
10	50/50 MTBE/THF	2	75	99:1	98:2
11	50/50 MTBE/MeTHF	1.1	66	99:1	97:3

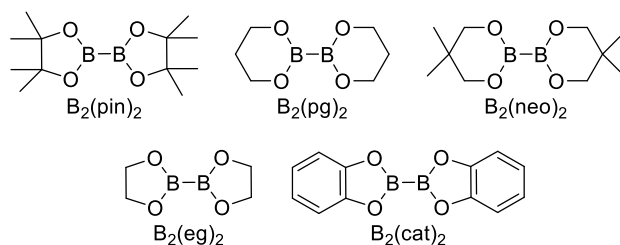
^[a]Aldehyde **2.2a** (0.100 mmol, 1 equiv), allene **2.1** (0.105 mmol, 1.05 equiv), CuCl (5 mol %), (*R,R*)-Ph-BPE (6 mol %), NaO^tBu (0.100 mmol, 1 equiv), B₂(pin)₂, in 0.6 mL of solvent. ^[b]Determined by ¹HNMR spectroscopy on the unpurified reaction mixture using dimethylfumarate as standard. ^[c] Enantioselectivity determined by chiral HPLC.

Finally, the boronate was investigated (**Table 2.5**). Initial investigation began with 1.1 equivalents of B₂(pin)₂, as obtained from literature methods.¹⁴⁸ Increasing the boronate to 2 equivalents (entry 2), led to an increase in the yield of **2.4a**, as well as the enantioselectivity. Additional amounts of B₂(pin)₂ (entries 3 and 4) led to a significant loss in yield. Other boronate esters were examined; each led to a drastic reduction in yield, as well as a reduction in diastereo- and enantioselectivity (entries 5-8).

Table 2.10. Cu-catalyzed borylative aminoallylation boronate optimization.^[a]

Entry	Diboron (equiv)	% Yield of 2.4a ^[b]	Dr of 2.4a ^[b]	Er of 2.4a ^[c]
1	B ₂ (pin) ₂ (1.1)	53	99:1	92.5:7.5
2	B ₂ (pin) ₂ (2)	75	99:1	98:2
3	B ₂ (pin) ₂ (3)	52	99:1	95:5
4	B ₂ (pin) ₂ (4)	52	99:1	98:2
5	B ₂ (pg) ₂ (2)	28	95:5	88:12
6	B ₂ (neo) ₂ (2)	19	99:1	88.5:11.5
7	B ₂ (eg) ₂ (2)	24	88:12	--
8	B ₂ (cat) ₂ (2)	20	97:3	--

^[a]Aldehyde **2.2a** (0.100 mmol, 1 equiv), allene **2.1** (0.105 mmol, 1.05 equiv), CuCl (5 mol %), (*R,R*)-Ph-BPE (6 mol %), NaO^tBu (0.100 mmol, 1 equiv), diboron in 0.6 mL of 50/50 THF/MTBE. ^[b]Determined by ¹HNMR spectroscopy on the unpurified reaction mixture using dimethylfumarate as standard. ^[c] Enantioselectivity determined by chiral HPLC.



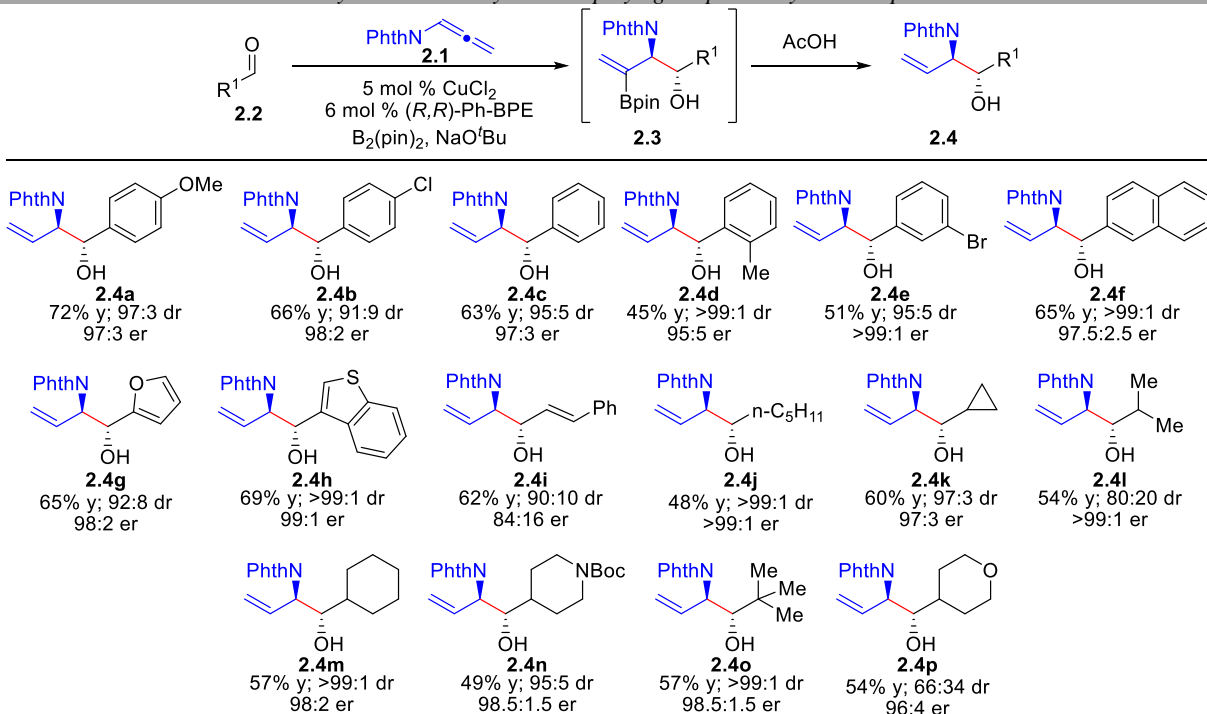
Following an extensive optimization campaign, examining various solvents, boronates, bases, and stoichiometry of the reactants, the optimal conditions were identified, as laid out in **Scheme 2.6**.

C. Protonation Workup – Traditional branched 1,2-aminoalcohol generation

With the optimal conditions in hand, the generality of the borylative aminoallylation reaction with aldehydes was next investigated using a protonolysis workup of borylated intermediate **2.3** to afford product **2.4**, the product of formal reductive coupling with a hydride reductant (**Scheme 2.6**). This is significant because aldehydes are problematic substrates in Cu-catalyzed reductive coupling with hydride-reducing agents due to the preference for aldehyde reduction.^{146,147,161} Overall, this process also enables access to identical products as produced by Krische's⁸⁶ method (**Scheme 2.4.1**) without the use of expensive precious metals or high reaction temperatures.

Both electron-rich and electron-deficient aromatic aldehydes performed well (**2.4a-f**), and the reaction was accommodating to heteroaromatic aldehydes (**2.4g, h**). The yield was somewhat decreased when sterically hindered aromatic aldehydes (**2.4d**) or aliphatic aldehydes (**2.4j-o**) were utilized. Notably, excellent diastereo- and enantioselectivities could be obtained when employing aliphatic aldehydes bearing small R¹-groups (**2.4j, k**), and reduced diastereocontrol was only observed when R¹ was *i*-Pr (**2.4l**) or THP (**2.4p**). Overall, all of the reaction products were obtained with enantioselectivities of >90% ee except for the case of cinnamaldehyde (**2.4i**). While enantiocontrol was reduced in this case, the ability of an α,β -unsaturated aldehydes to participate in the reaction is notable considering the propensity of Cu to react in conjugate addition type pathways with this class of electrophile.

Scheme 2.16. Enantioselective borylative aminoallylation employing the protonolysis workup.^[a]



^[a] Aldehyde **2.2** (0.200 mmol), **2.1** (1.05 eq), CuCl (5 mol%), ligand (6 mol%), NaO^tBu (1 equiv), B₂(pin)₂ (2 equiv); see the experimental methods section for details. Diastereomeric ratios (dr) were determined by ¹H NMR spectroscopy on the unpurified reaction mixture.

Finally, selective formation of the *anti*-diastereomer in the reaction was confirmed by comparison of **2.4i**, **2.4k**, **2.4n** and **2.4p** to the literature.⁸⁶ This is in contrast to reductive borylative allylation reactions

utilizing carbon-substituted allenes that afford the *syn*-diastereomer as the major isomer, as is discussed further in *Section III-G: Stereochemical model*.¹⁴⁸

D. Oxidation workup – Methyl ketone synthesis

While the described borylative aminoallylation followed by the protonation workup (**Scheme 2.6**) allows access to valuable products of a formal hydrogenative reductive coupling, arguably the power of the current transformation lies in the ability to functionalize the C-B bond present in **2.3** to a wide variety of other motifs using well-established organoborane chemistry.^{156–159} At the end of the 24-hour reaction period, prior to workup, the vinyl boronate intermediate **2.3** is the major product present; this gave the ability to further functionalize/derivatize to a diverse array of products via a simple change in the workup. Towards that end, subsequent oxidation of the C-B bond of **2.3** was next demonstrated to allow for additional heteroatom incorporation into the final products (**2.6**, **Table 2.6**).

The oxidative workup method was optimized as described in **Table 2.6**. Various methods to oxidize the C-B bond were examined; TMANO (entry 1) did not successfully oxidize the intermediate, and instead yielded the protonolysis product. Sodium perborate (entries 2 and 3) led to an approximate 1:2 ratio of protonation and oxidation products. The frontrunner was quickly identified as a workup with H₂O₂.

From here, methods varying the source of peroxide were explored. Organic peroxide sources, such as tert-butyl hydrogen peroxide (entry 4) and urea hydrogen peroxide (entry 5), did not successfully oxidize the intermediate to **2.6a**. Then, the use of increasing equivalents of hydrogen peroxide without pH 7 buffer was observed to generate the methyl ketone product **2.6a** in increasing degrees (compare entries 8, 9, 10, 11). The optimal workup method was then determined to be 20 equivalents of 30% H₂O₂ added to the crude reaction mixture directly after the 24-hour reaction period (entry 11). After 3 hours of stirring, the peroxide was quenched with the addition of 10% sodium thiosulfate solution.

With the optimal oxidation workup method in hand, the substrate scope of the reaction was explored (**Scheme 2.7**). Overall, the methyl ketone products could be obtained in equivalent yields and enantioselectivities compared to that obtained when employing a protonolysis workup. The standard

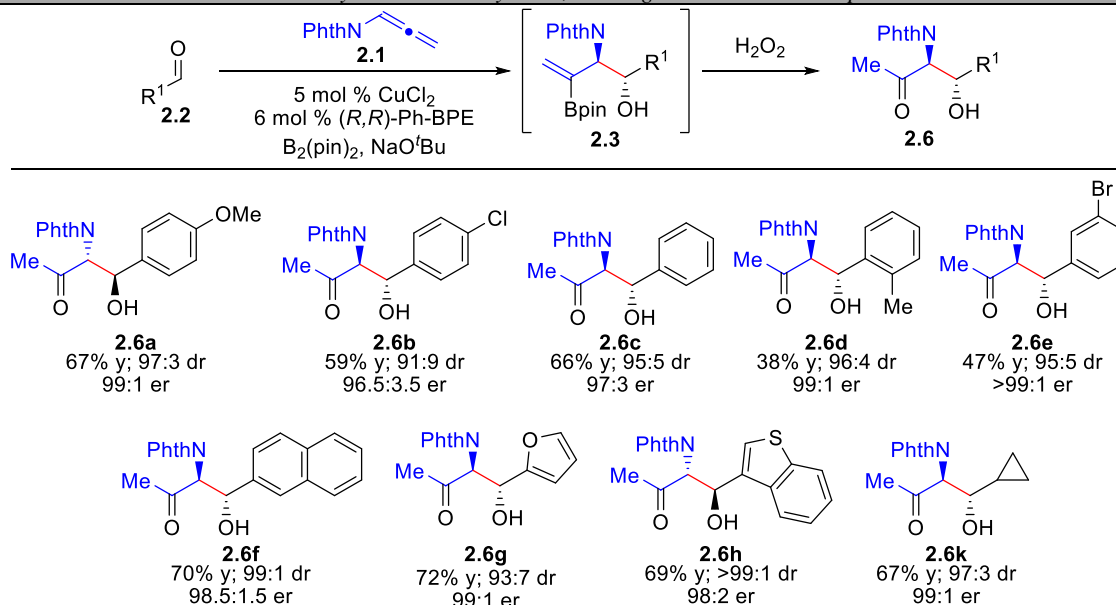
reaction with *p*-anisaldehyde **2.2a** was scaled up and ran at an 1.00 mmol scale to generate **2.6a** in 73% yield, with a 99:1 er.

Table 2.11. Oxidative workup optimization. ^[a]

Entry	Oxidation workup	% Yield 2.4a ^[b]	% Yield 2.6a ^[b]
1	Trimethylamine <i>N</i> -oxide (5 equiv), THF, 70 °C, 1 h	42	--
2	Sodium perborate (5 equiv)	24	43
3	Sodium perborate (5 equiv) with pH7 buffer	23	50
4	5 M TBHP in heptane (3 equiv)	12	10
5	Urea hydrogen peroxide (3 equiv)	10	16
6	30% H ₂ O ₂ (5 equiv), pH7 buffer	7	63
7	Concentrate, then 30% H ₂ O ₂ (5 equiv), pH7 buffer	22	52
8	2 equiv 30% H ₂ O ₂ workup, without buffer, 3 h	34	29
9	5 equiv 30% H ₂ O ₂ , without buffer, 3 h	34.5	47
10	10 equiv 30% H ₂ O ₂ , without buffer, 3 h	9	67
11	20 equiv 30% H₂O₂, without buffer, 3 h	1.5	69

^[a]Oxidation workup performed after GP-1 using 0.100 mmol of **2.2a**. ^[b]Determined by ¹H NMR spectroscopy on the unpurified reaction mixture using dimethylfumarate as standard.

Scheme 2.17. Enantioselective borylative aminoallylation, utilizing the oxidative workup. ^[a]



^[a] Performed using 0.200 mmol of aldehyde **2.2** (1 equiv); see the experimental methods section for details. Diastereomeric ratios (dr) were determined by ¹H NMR spectroscopy on the unpurified reaction mixture. Enantiomeric ratios were determined via chiral HPLC.

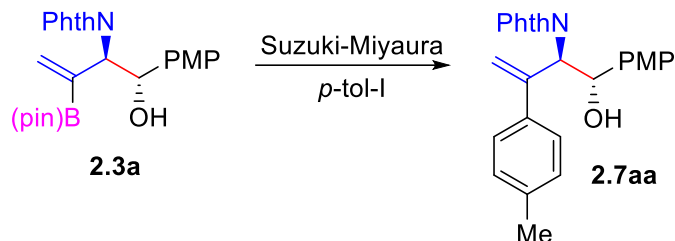
E. Suzuki-Miyaura Cross-coupling – 1,1-disubstituted olefin synthesis

Due to the synthetic power of the Suzuki-Miyaura cross-coupling reaction for the preparation of C-C bonds,¹⁶²⁻¹⁶⁴ we also examined the use of the vinyl boronate intermediate **2.3** in subsequent Pd-catalyzed cross-coupling reactions to generate further functionalized chiral 1,1-disubstituted olefins (**2.7**, **Table 2.7**).

Development of the optimized reaction conditions was particularly trying. The optimal ligand, base, and solvent were easily identified, **Table 2.7**, using the isolated vinyl boronate intermediate **2.3a** and 4-iodotoluene. The optimal base was identified as K₂CO₃ (entry 1) with higher yield of the Suzuki product generated, compared to KF (entry 2). A 4:1 ratio of organic solvent to water was examined for several solvent options. THF and IPA both gave low yields (entries 3 and 5). The Suzuki reaction was attempted using a 4:1 ratio of 50:50 MTBE/THF to water (2:2:1 MTBE/THF/H₂O) (entry 6), as the initial reaction is ran in 50:50 MTBE/THF, but the conversion to Suzuki product was unsatisfactory in this case. 1,4-Dioxane was identified as the choice solvent (entry 4). With the optimal solvent system for this reaction in hand, the optimal temperature and time of reaction was determined to be 50°C for 3 hours (entry 7), with a 90% yield of the Suzuki product **2.7a** generated from isolated vinyl boronate intermediate **2.3a**.

However, isolation of the vinyl boronate intermediate long term is not ideal due to the sensitivity of intermediate **2.3** to protonolysis during silica-gel chromatography, leading to heavy losses of the intermediate. Because of this, a one-pot telescoped process was next examined.

Regrettably, this optimized system failed during initial attempts (**Table 2.8**, entries 1, 2, and 3). Control experiments implied that leftover pinacol in the crude reaction mixture acted as a catalyst poison inhibiting the cross-coupling reaction. To circumvent this problem, the aminoallylation workup was modified to include a NaIO₄ treatment (**Table 2.8**, entries 4-7) to convert remaining pinacol to acetone, which is removed upon concentration.¹⁶⁵ Gratifyingly, this oxidative cleavage and removal of pinacol allowed for successful telescoping of the crude aminoallylation reaction into the cross-coupling reaction.

Table 2.12. Suzuki-Miyaura reaction optimization. ^[a]

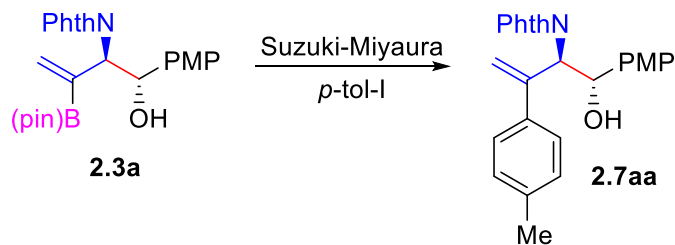
Entry	Temp, run time	Conditions	Yield 2.7aa ^[b]	Yield 2.4a ^[b]
1	60°C, 2 h	As listed below	74	18
2	60°C, 2 h	KF (2 equiv) as base	60	33
3	90°C, 2 h	IPA:Water 4:1	42	--
4	90°C, 2 h	Dioxane:Water 4:1	81	--
5	90°C, 2 h	THF:Water 4:1	39	38
6	55°C, 3 h	MTBE/THF:Water 4:1	25	75
7	50°C, 3 h	Dioxane:Water 4:1	90	--

^[a] Reactions ran using the isolated (chromatography on SiO₂) vinyl boronate intermediate **2.3a** from the 0.1 mmol scale reaction of **2.2a** and phthalimido-allene **2.1**. Workup following the reaction of GP-1 with **2.2a** at a 0.100 mmol scale. To the resultant residue was charged a stir-bar and the vial was taken into the glovebox. To the vial was charged Pd(OAc)₂ (0.003 mmol, 3 mol %), (AmPhos) (0.006 mmol, 6 mol %), K₂CO₃ (0.200 mmol, 2 equiv), aryl iodide (0.100 mmol, 1 equiv), and 0.5 mL of solvent.

^[b] Determined by ¹HNMR spectroscopy on the unpurified reaction mixture using dimethylfumarate as standard.

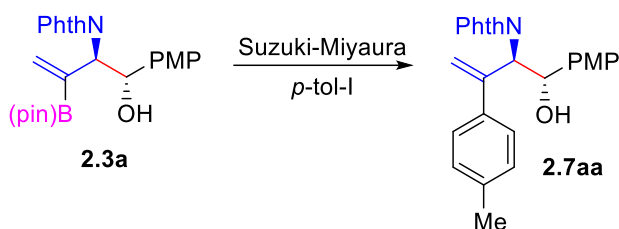
Once proper telescoping methods were identified, the cross-coupling reaction was further optimized, **Table 2.9**, via the examination of the palladium source and stoichiometry of the aryl halide. The preformed commercial catalyst (entry 3) was examined and compared to the catalyst/ligand that was allowed to stir and pre-complex (entry 6), and all reagents added at once (entry 5). The optimal method was determined to be GP-4 (see experimental methods), utilizing 5 mol% Pd(AmPhos)G3 and 5 mol% AmPhos.

Once optimized Suzuki reaction conditions were identified, three aldehydes that each performed well in the general reaction were chosen for cross-coupling with three chosen aryl halides, **Scheme 2.8**. The Suzuki-Miyaura cross-coupling reaction of crude vinyl boronate intermediates performed fairly well. Good overall yields could be obtained in the tandem process producing highly functionalized 1,1-disubstituted chiral products in excellent levels of stereocontrol that would be difficult to prepare by other means. An aryl bromide could also be successfully coupled in the developed protocol (**2.7aa**^b), with minimal modification.

Table 2.13. Suzuki-Miyaura telescoping process optimization. ^[a]

Entry	11a source	Yield 2.7aa ^[b]	Yield 2.4a ^[b]
1	Crude after citric acid workup (GP-1)	3	10
2	Crude – No workup	21	9
3	Crude – concentrated <i>in vacuo</i>	7	18
4	Crude after citric acid workup (GP-1) followed by treatment with 2 equiv NaIO ₄ (20 min), quench, extract, dry, and concentrated <i>in vacuo</i>	49	7
5	Crude after citric acid workup (GP-1) followed by treatment with 4 equiv NaIO ₄ (20 min), quench, extract, dry, and concentrated <i>in vacuo</i>	49	20
6	Crude after citric acid workup (GP-1) followed by treatment with 3 equiv NaIO ₄ (1 hour), quench, extract, dry, and concentrated <i>in vacuo</i>	47	8
7	Crude after citric acid workup (GP-1) followed by treatment with 5 equiv NaIO ₄ (20 min), quench, extract, dry, and concentrated <i>in vacuo</i>	46	8

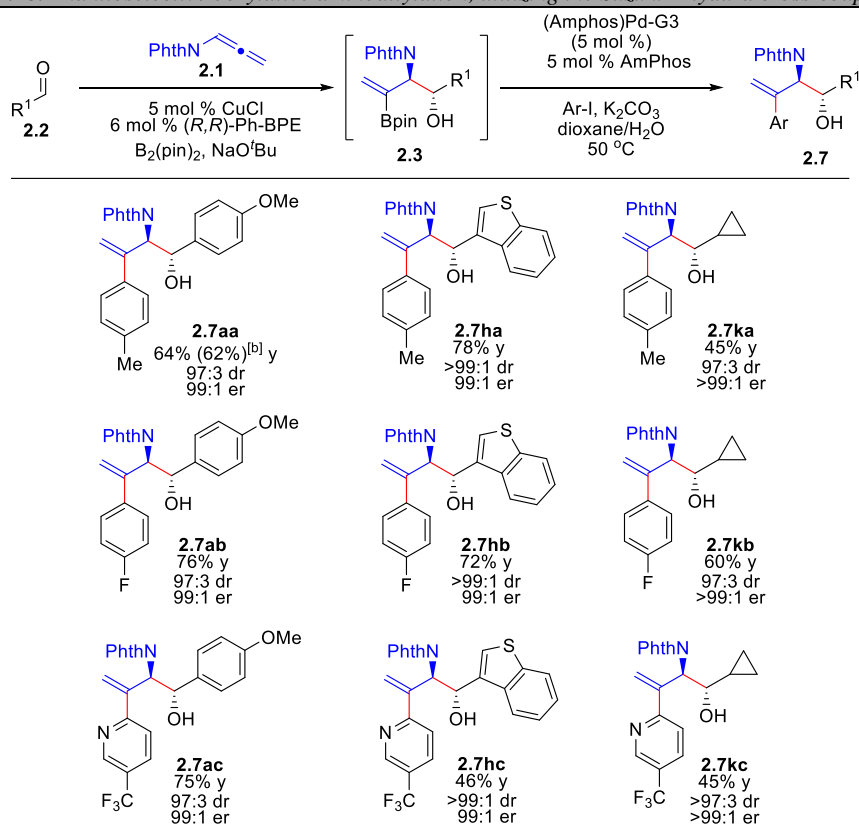
^[a]Reactions ran using the vinyl boronate intermediate **2.3a** from the 0.1 mmol scale reaction of **2.2a** and phthalimido-allene **2.1**. Workup following the reaction of GP-1 with **2.2a** at a 0.100 mmol scale. To the resultant residue was charged a stir-bar and the vial was taken into the glovebox. To the vial was charged Pd(OAc)₂ (0.003 mmol, 3 mol %), (AmPhos) (0.006 mmol, 6 mol %), K₂CO₃ (0.200 mmol, 2 equiv), aryl halide (0.100 mmol, 1 equiv), and 0.5 mL of 4:1 Dioxane/Water. The reaction was then heated at 50°C in an oil bath for 3 h. ^[b] Determined by ¹HNMR spectroscopy on the unpurified reaction mixture using dimethylfumarate as standard.

Table 2.14. Further optimization of the telescoped Suzuki-Miyaura reaction and Development of GP-4. ^[a]

Entry	Variance	Yield 13aa ^[b]	Yield 5a ^[b]
1	None (GP-4) ^[a]	64	--
2	1.3 eq 4-Iodo toluene	57	7
3	5mol% Pd(Amphos)G3, 5mol% Amphos	58	4
4	5 mol % Pd(OAc) ₂ , 2 eq 4-Iodo toluene	60	9
5	2.5 mol% Pd ₂ (dba) ₃ and 5 mol% Amphos - **Added all suzuki reactants to reaction at once**	--	25
6	2.5 mol% Pd ₂ (dba) ₃ and 5 mol% Amphos - **Added (pre-stirred ligand + Pd) to suzuki reactants**	62	15
7	5 mol % Pd ₂ (dba) ₃ as Pd source	78	3

^[a]Reactions ran using the vinyl boronate intermediate from the 0.1 mmol scale reaction of **2.2a** and phthalimido-allene **2.1**, 4-iodo toluene as the aryl halide. Workup following the reaction of GP-1 with **2.2a** at a 0.100 mmol scale, followed by citric acid workup 3 equiv NaIO₄ for 20 min. To the resultant residue was charged a stir-bar and the vial was taken into the glovebox. To the vial was charged (AmPhos)Pd-G3 (0.005 mmol, 5 mol %), (AmPhos) (0.005 mmol, 5 mol %), K₂CO₃ (0.200 mmol, 2 equiv), aryl halide (0.100 mmol, 1 equiv), and 0.5 mL of solvent, unless otherwise noted. ^[b]Determined by ¹HNMR spectroscopy on the unpurified reaction mixture using dimethylfumarate as standard.

Scheme 2.18. Enantioselective borylative aminoallylation, utilizing the Suzuki-Miyaura cross-coupling application.^[a]



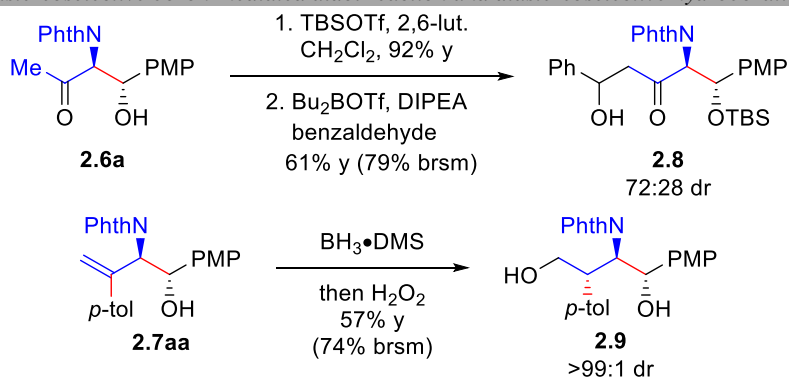
^[a] Performed using 0.200 mmol of aldehyde **2.2** (1 equiv); see the experimental methods section for details. Diastereomeric ratios (dr) were determined by ¹H NMR spectroscopy on the unpurified reaction mixture. Enantiomeric ratios were determined via chiral HPLC. ^[b] Cross-coupling reaction was performed using 4-bromotoluene at 70 °C for 3 h.

F. Synthetic Applications – Aldol and Hydroboration

The powerful synthetic potential of the methodology developed stems from its ability to access chiral aminoalcohol equivalents bearing additional functionality for further synthetic manipulations to arrive at heteroatom-rich complex chiral architectures quickly from readily available starting materials. To highlight this potential, the subsequent transformations described in **Scheme 2.9** were performed.

The oxidation product **2.6a** was first protected with TBSOTf, and subjected to a boron-mediated aldol reaction¹⁶⁶ with benzaldehyde to afford **2.8** in 79% yield brsm, with moderate stereocontrol (72:28 dr) at the newly formed stereocenter. Notably, this allows quick access to a stereodefined 1,3,5-*O*-2-*N*-substituted carbon framework in only three synthetic steps from allenamide **2.1**.

Scheme 2.19. Further synthetic application of the reductive coupling products via a diastereoselective boron-mediated aldol reaction and diastereoselective hydroboration.



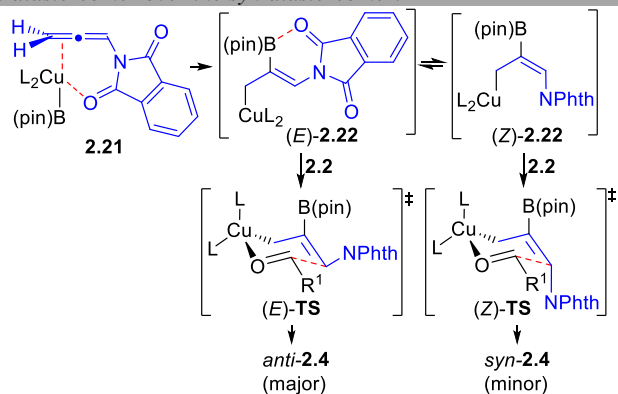
The Suzuki cross-coupling product **2.7aa** was further elaborated through a diastereoselective hydroboration to afford a single diastereomer of the 1,4-*O*-2-*N*-substituted carbon synthon **2.9** bearing three contiguous stereocenters.

G. Stereochemical Model

Finally, one intriguing feature of this borylative aminoallylation using the phthalimide-derived allenamide **2.1** was the selective formation of the anti-diastereomer of product. Previous reports of Cu-catalyzed borylative allylation reactions using *C*-based allenes with carbonyl electrophiles¹⁴⁸ preferentially gave the syn-diastereomer, even when using the same ligand ((*R*)-BINAP, **Table 2.1**, entry 2).

We propose that this is due to the carbonyl of the phthalimide-allene being able to coordinate to either the L_2Cu -catalyst or boron, directing the reaction through the (*E*)-**2.22** (**Scheme 2.10**).^{107,138,150} It is well-established that Cu-catalyzed reductive allylation reactions proceed through a six-membered Zimmerman-Traxler chair-like transition state.^{80–84,107,138,148,150,151,155} The product selectivity of these reactions are often controlled by Curtin-Hammett kinetics between rapidly equilibrating $\text{Cu}(\sigma\text{-allyl})$ complexes,^{83,84} meaning that the pathway with the lowest energy transition state is the preferred pathway to generate the major product.

Scheme 2.20. Stereochemical model for preferential generation of the anti-diastereomer over the syn-diastereomer.



For carbon-based allenes, it would be seen that the major syn-diastereomer of **2.4** is generated through (*Z*)-**2.22** via (*Z*)-**TS**.^{148,155} Borylcupration of allenes is proposed to occur at the more accessible, least sterically hindered terminal olefin of the allene, away from the R-group on the C-based allene to generate the C-based analog of (*Z*)-**2.22** selectively.^{148,155,167,168} This pathway is arguably more favorable due to the unfavorable sterics of the allene R-group and Bpin having a cis-relationship in (*E*)-**TS**.

In contrast, borylcupration may lead directly to (*E*)-**2.22** through an N-phthaloyl-directed intermediate **2.21**. From here, σ - π - σ equilibration may not be possible, or the interaction of the N-phthaloyl group with the vacant p-orbital of the B(pin) group of (*E*)-**2.22** facilitates the reaction through (*E*)-**TS** to afford the anti-diastereomer of **2.4** as the major product.

IV. Conclusions

In conclusion, we have developed a highly enantio- and diastereoselective Cu-catalyzed borylative reductive coupling method for the synthesis of aminoalcohols from alleneamides and aldehydes. After a long and tedious optimization process, rapid synthesis of highly functionalized chiral heteroatom-rich organic compounds was achieved using readily available starting materials. The Cu-catalyst system utilized is inexpensive and widely commercially available, and the reaction proceeds under ambient conditions to provide good yields and excellent stereoselectivity. Notably, access to a wide array of different dissonant chiral 1,2-aminoalcohol motif-containing products and diverse functionalities was achieved via CuB(pin)-catalyzed reductive coupling from the same intermediate/starting materials. Simple changes in the post-

reaction workup from the vinyl boronate intermediate **2.3** allows for access to the dissonant 1,2-aminoalcohol scaffold **2.4**, as well as the highly functionalized methyl ketone **2.6**, 1,1-disubstituted olefin suzuki products **2.7**, aldol **2.8**, and hydroboration products **2.9**. We anticipate the method here provided to serve as a platform for the use of cuproboration to access these dissonant aminoalcohol scaffolds and other densely functionalized molecules.

V. Experimental Procedures

A. General.

¹H NMR spectra were recorded on Bruker 600 MHz spectrometers. Chemical shifts are reported in ppm from tetramethylsilane with the solvent resonance as an internal standard (CDCl₃: 7.26 ppm). Data are reported as follows: chemical shift, integration, multiplicity (s = singlet, d = doublet, t = triplet, q = quartet, p = pentet, h = hextet, hept = heptet, br = broad, m = multiplet), and coupling constants (Hz). ¹³C NMR was recorded on a Bruker 600 MHz (151 MHz) instrument with complete proton decoupling. Chemical shifts are reported in ppm from tetramethylsilane with the solvent as the internal standard (CDCl₃: 77.0 ppm). Chiral HPLC analyses were performed on a Shimadzu Prominence i-series LC-2030C using chiral Daicel columns purchased from Chiral Technologies, Inc. Liquid chromatography was performed using forced flow (flash chromatography) on silica gel purchased from Silicycle. Thin layer chromatography (TLC) was performed on EMD silica gel F254 2.5x7.5 cm plates. Visualization was achieved using UV light, a 10% solution of phosphomolybdic acid in EtOH, or potassium permanganate in water followed by heating. HRMS was collected using a Jeol AccuTOF-DART™ mass spectrometer using DART source ionization. All reactions were conducted in oven or flame-dried glassware under an inert atmosphere of nitrogen or argon with magnetic stirring unless otherwise noted. Solvents were obtained from VWR as HPLC grade and transferred to septa-sealed bottles, degassed by Ar sparge, and analyzed by Karl-Fischer titration to ensure water content was ≤ 600 ppm. Allenamide **2.1** was prepared as described in the literature.⁸⁶ Aldehydes were purchased from Sigma Aldrich, TCI America, Alfa Aesar, or Oakwood Chemicals and used as received. All other materials were purchased from VWR, Sigma Aldrich, Combi-Blocks, Alfa-Aesar, or Strem Chemical Company and used as received.

B. Experimental Procedures

GP-1: Cu-catalyzed reductive borylative aminoallylation (Tables 2.1 -2.9):

In an Ar-filled glove-box, to a crimp cap vial with a magnetic stir-bar was charged copper(I) chloride (0.01mmol, 5 mol%), ligand (0.012 mmol, 6 mol%), NaO^tBu (0.200 mmol, 1 equiv), and solvent (1.3mL/0.200mmol aldehyde). The resulting mixture was allowed to stir for 1 h followed by addition of bis(pinacolato)diboron (0.400 mmol, 2 equiv). The obtained mixture was then allowed to stir for an additional 30 min prior to addition of allene **2.1** (0.210 mmol, 1.05 equiv) and aldehyde **2.2** (0.200 mmol, 1 equiv). The crimp cap vial was sealed and removed from the glovebox, and the reaction mixture was allowed to stir at room temperature for 24 hours. The crude solution was then worked up as described below to access the different products described.

GP-2: General protonolysis workup (Tables 2.1-2.5):

The Cu-catalyzed reductive borylative aminoallylation reaction mixture from GP-1 was quenched with the addition of 4 mL of aqueous citric acid and allowed to stir for 15 min. The reaction mixture was then extracted with CH₂Cl₂ (3x 5mL). The combined organic layers were then dried over anhydrous Na₂SO₄, filtered, and concentrated under reduced pressure. To the crude residue was then charged 0.5 mL of AcOH, and the resultant mixture allowed to stir for 30 min. To the mixture was then carefully added 7% aqueous sodium bicarbonate solution (gas evolution) followed by extraction with CH₂Cl₂ (3x 5mL). The combined organic layers were then dried over anhydrous Na₂SO₄, filtered, and concentrated under reduced pressure. Purification of the crude residue by flash column chromatography on silica gel afforded the desired product **2.4**.

GP-3: General oxidative workup with H₂O₂ (Table 2.6):

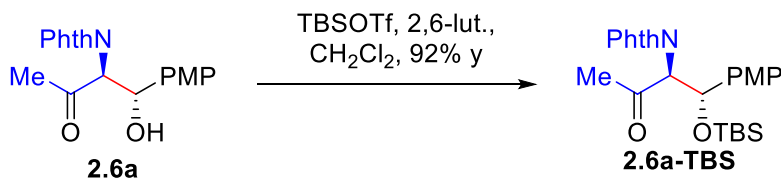
The Cu-catalyzed reductive borylative aminoallylation reaction mixture from GP-1 was oxidized by the addition of 20 equiv of 30% H₂O₂ and allowed to stir for 30 min. The resultant solution was then quenched with 10% Aq. sodium thiosulfate solution over ice (**EXOTHERMIC**), extracted with CH₂Cl₂ (3x 4mL), dried with Na₂SO₄, and concentrated under reduced pressure. The crude mixture was purified by flash silica gel column chromatography to afford the desired product **2.6**.

GP-4: General Suzuki-Miyaura reactions (Tables 2.7-2.9):

The Cu-catalyzed reductive borylative aminoallylation reaction mixture from GP-1 was quenched by the addition of 4 mL of aqueous 0.5M citric acid and 3 equiv NaIO₄ (oxidative cleavage of the remaining pinacol – catalyst poison – to acetone) and allowed to stir for 20 min. Saturated brine (3 mL) was added and the mixture was extracted with CH₂Cl₂ (3 x 4 mL). The combined organic layers were then dried with anhydrous Na₂SO₄, filtered, and concentrated into a 2-dram vial. The crude residue was then further dried *in vacuo* (~3 torr) for at least 1 h before performing the cross-coupling reaction.

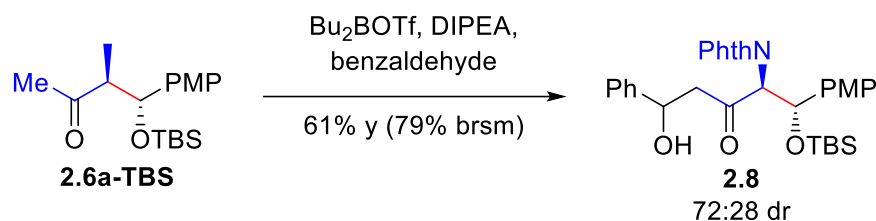
To the resultant residue was charged a stir-bar and the vial was taken into the glovebox. To the vial was charged (amPhos)Pd-G3 (0.010 mmol, 5mol%), (AmPhos) (0.010 mmol, 5mol%), K₂CO₃ (0.400mmol, 2 eq), aryl halide (0.200 mmol, 1 eq), and 1.0 mL of 1,4-Dioxane/Water (4/1 ratio). The reaction vial was then sealed, removed from glovebox and heated at 50 °C for 3 h with stirring in an oil bath. A color change from a yellow/brown to a dark black/purple was observed. After heating for 3 h, the reaction was allowed to cool to room temperature. Saturated brine (3mL) was added, and the mixture was extracted with CH₂Cl₂ (3 x 5 mL). The combined organic layers were dried with anhydrous Na₂SO₄, filtered, and concentrated *in vacuo*. The crude mixture was purified by flash column chromatography on silica gel to afford the desired product **2.7**.

Synthetic applications (Scheme 2.9):

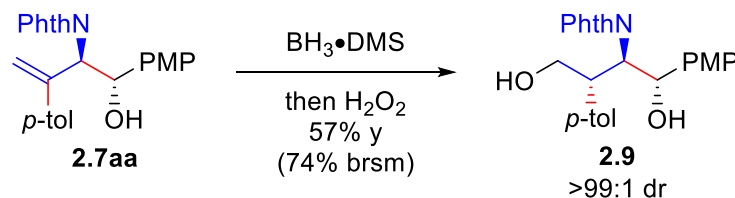


To a flame-dried round-bottom flask under inert atmosphere was charged **2.6a** (500mg, 1.47 mmol 1 equiv), CH₂Cl₂ (14 mL), and 2,6-lutidine (0.427 mL, 3.69 mmol, 2.5 equiv), under nitrogen. The reaction was cooled to -78 °C and TBSOTf (508μL, 2.21 mmol, 1.5 equiv) was added dropwise. The reaction was allowed to stir for 3 h. The reaction was quenched with the addition of 10% aqueous NaHCO₃ (10 mL). The layers were separated, and the aqueous layer was extracted with CH₂Cl₂ (3 x 10 mL). The combined organic

layers were dried over sodium sulfate and concentrated. The product was then isolated via column chromatography (0-40% EtOAc/Hexanes) to provide 613 mg (92%) of **2.6a-TBS** as a white foam. R_f = 0.30 (25% EtOAc/Hex). $^1\text{H NMR}$ (CDCl_3 , 600 MHz) δ : 7.67 (dd, J = 5.5 Hz, J = 3.5 Hz, 2H), 7.61 (dd, J = 5.5 Hz, J = 3.5 Hz, 2H), 7.17 (d, J = 8.8 Hz, 2H), 6.64 (d, J = 8.8 Hz, 2H), 5.66 (d, J = 8.8 Hz, 1H), 4.96 (d, J = 9.1 Hz, 1H), 3.64 (s, 3H), 2.31 (s, 3H), 0.82 (s, 9H), 0.08 (s, 3H), -0.27 (s, 3H) ppm. $^{13}\text{C NMR}$ (126 MHz, CDCl_3): δ 201.6, 167.2, 159.2, 134.0, 132.6, 131.2, 128.3, 123.3, 113.3, 71.6, 64.1, 55.0, 29.0, 25.7, 17.9, -4.5, -5.0. HRMS (DART) m/z calcd for $\text{C}_{25}\text{H}_{30}\text{NO}_4\text{Si}$ $[\text{M-OH}]^+$: 436.1939; Found $[\text{M-OH}]^+$: 436.1922.



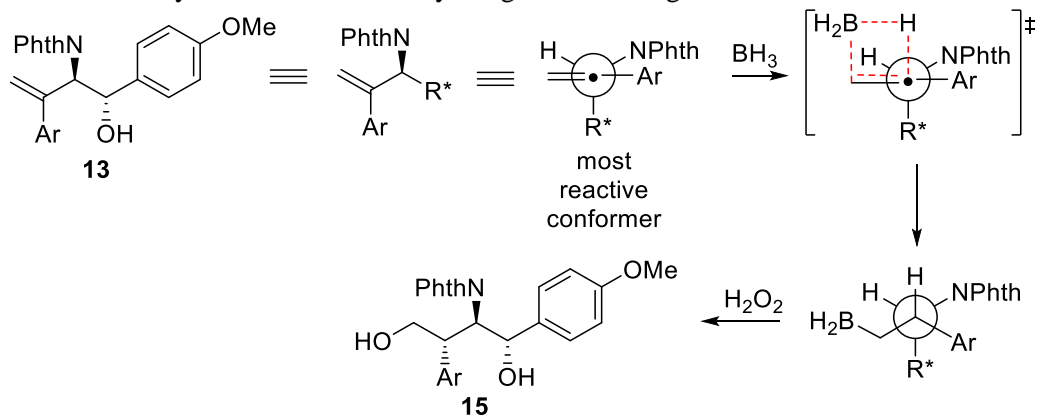
To a flame-dried round-bottom flask under inert atmosphere, was added **2.6a-TBS** (38.5mg, 0.085 mmol, 1 equiv), Et_2O (0.3 mL), $i\text{Pr}_2\text{Net}$ (21.1 μL , 0.121mmol, 1.4 equiv), and a stir bar. The solution was cooled to -78°C , and Bu_2BOTf (116 μL , 0.116 mmol, 1.4 equiv) was added dropwise. The reaction was allowed to stir and warm to room temperature for 30 minutes. The reaction mixture was then cooled to -78°C and 1.4 eq of a 1M solution of benzaldehyde (12.3 μL , 0.121 mmol) in Et_2O was slowly added dropwise. The mixture was allowed to warm to room temperature and stir for 3 h. The resulting solution was placed at 0°C and 0.2 mL of a 1:2 v/v solution of 30% $\text{H}_2\text{O}_2/\text{MeOH}$. The reaction was then allowed to warm to room temperature and stir for 1 hour. The solution was then diluted with Et_2O (1mL) and water (1 mL). The aqueous phase was extracted with Et_2O (3 x 3mL) and the combined organic layers were washed with sat. aqueous NaHCO_3 (3mL), followed by brine (3 mL), then dried over MgSO_4 and concentrated under reduced pressure. The product was then isolated via column chromatography (0-40% EtOAc/Hexanes) to provide 29.1 mg (61%, 79% brsm) of **2.8** as a white foam as a 72:28 mixture of diastereomers by $^1\text{H NMR}$. R_f = 0.26 (25% EtOAc/Hex.). $^1\text{H NMR}$ (C_6D_6 , 600 MHz) δ : 7.38 (d, J = 8.4 Hz, 2H), 7.36-7.25 (m, 4H), 7.07-7.01 (m, 2H), 7.00-6.94 (m, 1H), 6.65 (dd, J = 5.5 Hz, J = 3.2 Hz, 2H), 6.54 (d, J = 3.2 Hz, 2H), 6.10 (d, J = 8.2 Hz, 1H), 5.36 (d, J = 8.9 Hz, 1H), 5.20-5.17 (m, 1H), 3.11 (dd, J = 17 Hz, J = 10 Hz, 1H), 2.90 (dd, J = 17 Hz, J = 3.3 Hz, 1H), 0.91 (s, 9H), 0.20 (s, 3H), -0.12 (s, 3H) ppm. $^{13}\text{C NMR}$ (126 MHz, C_6D_6): δ 203.3, 167.3, 159.8, 143.7, 133.6, 131.5, 128.9, 128.47, 128.40, 127.5, 127.4, 125.9, 123.1, 113.7, 72.0, 70.4, 64.9, 54.3, 50.7, 26.0, 18.2, -4.3, -4.7. HRMS (DART) m/z calcd for $\text{C}_{32}\text{H}_{37}\text{NO}_6\text{Si}$ $[\text{M-OH}]^+$: 542.2357; Found $[\text{M-OH}]^+$: 542.2397.



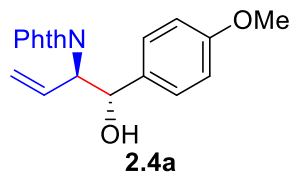
To a flame-dried round bottom flask under inert atmosphere was added **2.7aa** (32.0 mg, 0.072 mmol, 1 equiv) and anhydrous tetrahydrofuran (0.8 mL) with stirring. The reaction was cooled to 0°C and $\text{BH}_3\text{-Me}_2\text{S}$ in THF (2M) (21 μL , 3 equiv) was added dropwise. The reaction was allowed to stir at room temperature for 5 hours. After five hours, the reaction was cooled back to 0°C and a mixture of NaOH (2M) (0.2 mL) and H_2O_2 (33%) (0.1 mL) was added dropwise with stirring. The reaction was allowed to warm to room temperature and stir for 2 hours. The reaction was then quenched by the addition of 2 mL of sat. aq. $\text{Na}_2\text{S}_2\text{O}_3$. The resulting solution was extracted with EtOAc (3 x 4 mL). The combined organic layers were washed with 10 mL of brine. The mixture was dried over sodium sulfate, filtered, and concentrated

under reduced pressure. The residue was isolated via column chromatography on silica (0-60% EtOAc/hexanes)) to provide 19.1 mg (57%) of **2.9** as a white foam. Only a single diastereomer was observed by ¹HNMR spectroscopic analysis. $R_f = 0.09$ (25% EtOAc/hexanes).): ¹HNMR (CDCl₃, 600 MHz) δ : 7.57 (d, $J = 7.0$ Hz, 1H), 7.51 (t, $J = 7.0$ Hz, 1H), 7.48 (t, $J = 7.0$ Hz, 1H), 7.43 (d, $J = 7.7$ Hz, 1H), 7.29 (d, $J = 8.2$ Hz, 2H), 7.06 (d, $J = 8.6$ Hz, 2H), 6.90 (d, $J = 8.6$ Hz, 2H), 6.70 (d, $J = 8.6$ Hz, 2H), 5.46 (d, $J = 7.9$ Hz, 1H), 4.86 (dd, $J = 10.1$ Hz, $J = 7.9$ Hz, 1H), 4.02 (qd, $J = 11.9$ Hz, $J = 6.2$ Hz, 2H), 3.89 (ddd, $J = 10.8$ Hz, $J = 6.2$ Hz, $J = 4.7$ Hz, 1H), 3.66 (s, 3H), 2.13 (s, 3H) ppm. ¹³C NMR (126 MHz, CDCl₃): δ 166.8, 159.2, 137.1, 136.4, 133.5, 133.2, 129.0, 127.8, 127.7, 123.0, 122.5, 113.7, 75.0, 65.6, 58.9, 55.1, 49.4, 20.9. HRMS (DART) m/z calcd for C₂₆H₂₄NO₄ [M-OH]⁺: 414.1711; Found [M-OH]⁺: 414.1704.

Relative stereochemistry of **2.9** was tentatively assigned according to the Houk¹⁶⁹ model:



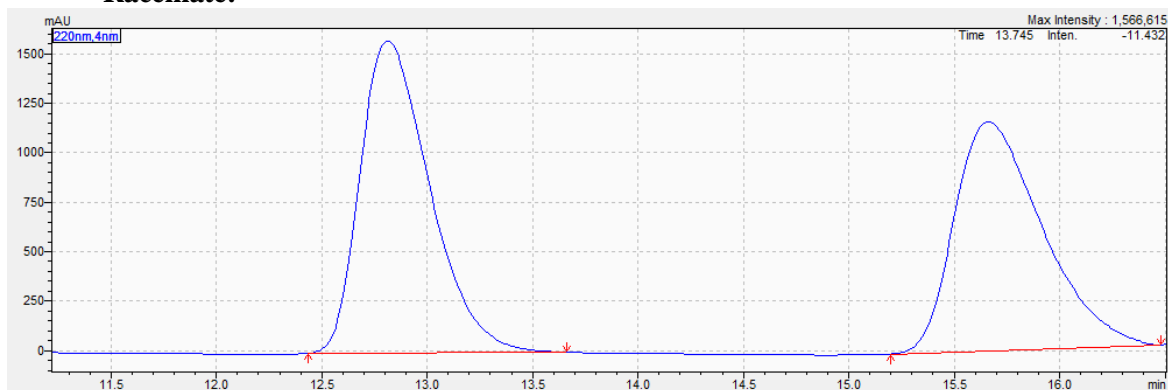
Reductive coupling product characterization data and HPLC traces



2-((1S,2R)-1-hydroxy-1-(4-methoxyphenyl)but-3-en-2-yl)isoindoline-1,3-dione (2.4a): According to the general protonation procedure (GP-1/GP-2) using (*R,R*)-Ph-BPE, the product was purified by silica gel chromatography (eluent: 0 – 40% EtOAc in hexanes) to provide 46.4 mg (72%) of **2.4a** as a clear oil as a single diastereomer, as a 97:3 mixture of enantiomers. Absolute and relative configuration was assigned by analogy to **2.4i**, **2.4k**, and **2.4n**. $R_f = 0.28$ (25% EtOAc/hexanes). $^1\text{H NMR}$ (CDCl_3 , 600 MHz) δ : 7.77 (dd, $J = 5.3$ Hz, $J = 3.2$ Hz, 2H), 7.68 (dd, $J = 5.3$ Hz, $J = 3.0$ Hz, 2H), 7.31 (d, $J = 8.6$ Hz, 2H), 6.78 (d, $J = 8.6$ Hz, 2H), 6.37 (ddd, $J = 17.5$ Hz, $J = 10.5$ Hz, $J = 7.7$ Hz, 1H), 5.33 (d, $J = 9.6$ Hz, 1H), 5.28 (d, $J = 17.5$ Hz, 1H), 5.26 (d, $J = 8.0$ Hz, 1H), 4.93 (t, $J = 7.3$ Hz, 1H), 3.73 (s, 3H), 3.13 (br s, 1H) ppm. $^{13}\text{C NMR}$ (126 MHz, CDCl_3): δ 167.9, 159.2, 134.0, 132.3, 131.7, 131.4, 127.7, 123.3, 120.0, 113.7, 73.3, 60.1, 55.1. HRMS (DART) m/z calcd for $\text{C}_{19}\text{H}_{16}\text{NO}_3$ $[\text{M-OH}]^+$: 306.1125; Found $[\text{M-OH}]^+$: 306.1135.

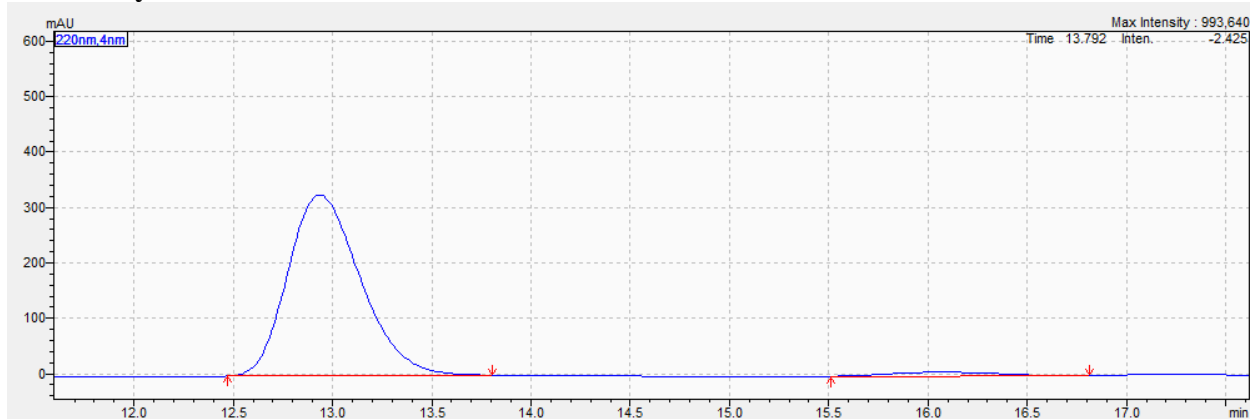
Chiral HPLC Analysis (Chiralpak OD-3 x 250 mm, heptane/isopropanol = 90/10, flow rate = 1.0 ml/min, $\lambda = 220$ nm) $t_R = 12.8$ (major), 15.6 (minor):

Racemate:

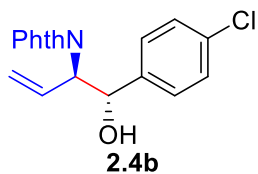


Ret. Time	Area%	Height	Conc.
12.813	51.984	1579480	0.000
15.661	48.016	1155960	0.000
	100.000	2735440	0.000

Asymmetric Reaction:



Ret. Time	Area%	Height	Conc.
12.935	96.810	326672	0.000
16.062	3.190	7070	0.000
	100.000	333743	0.000

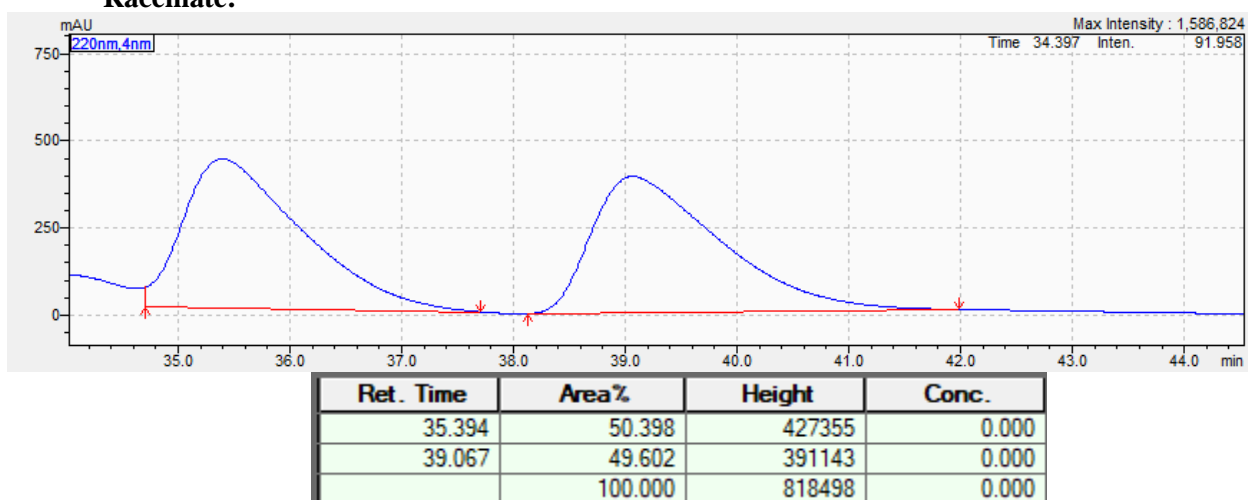


2-((1*S*,2*R*)-1-(4-chlorophenyl)-1-hydroxybut-3-en-2-yl)isoindoline-1,3-dione (2.4b): According to the general protonation procedure (GP-1/GP-2) using (*R,R*)-Ph-BPE, the product was purified by silica gel chromatography (eluent: 0 – 40% EtOAc in hexanes) to provide 46.8 mg (66%) of **2.4b** as a clear oil as a 91:9 mixture of diastereomers and the major diastereomer in a 98:2 mixture of enantiomers.

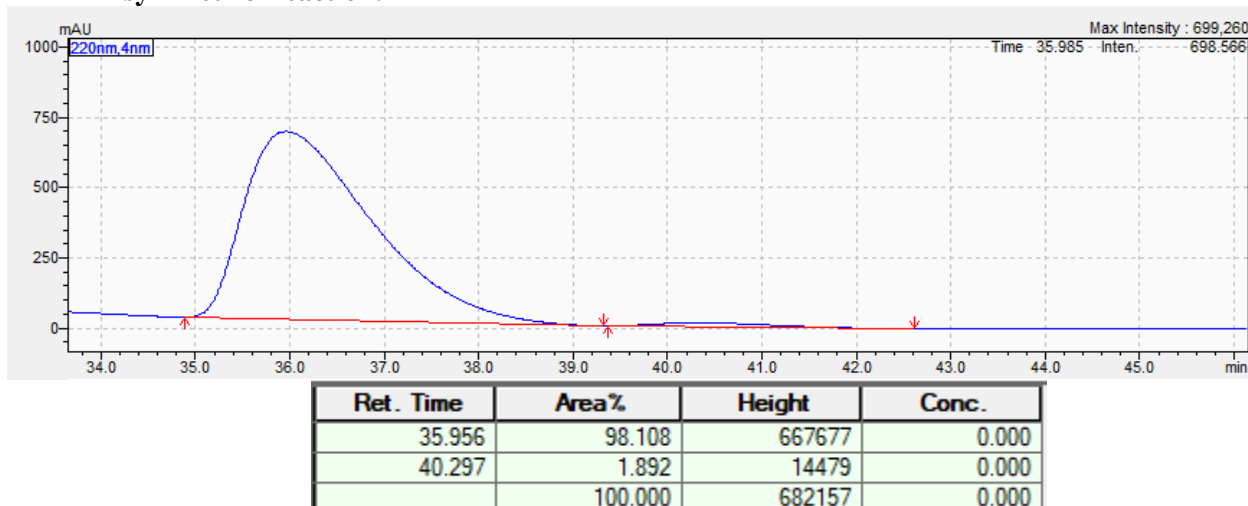
Absolute and relative configuration was assigned by analogy to **2.4i**, **2.4k**, and **2.4n**. $R_f = 0.67$ (10% EtOAc/CH₂Cl₂). ¹H NMR (CDCl₃, 600 MHz) δ : 7.79 (dd, $J = 5.3$ Hz, $J = 3.1$ Hz, 2H), 7.71 (dd, $J = 5.3$ Hz, $J = 3.1$ Hz, 2H), 7.34 (d, $J = 8.4$ Hz, 2H), 7.25 (d, $J = 8.4$ Hz, 2H), 6.32 (ddd, $J = 17.4$ Hz, $J = 10.3$ Hz, $J = 7.6$ Hz, 1H), 5.33 (d, $J = 10.2$ Hz, 1H), 5.27-5.22 (m, 2H), 4.91 (dd, $J = 7.3$ Hz, $J = 6.3$ Hz, 1H), 3.47 (br s, 1H) ppm. ¹³C NMR (126 MHz, CDCl₃): δ 168.1, 138.7, 134.2, 133.7, 131.4, 130.9, 128.5, 127.9, 123.5, 120.5, 73.37, 60.27. HRMS (DART) m/z calcd for C₁₈H₁₃ClNO₂ [M-OH]⁺: 310.0629; Found [M-OH]⁺: 310.0627.

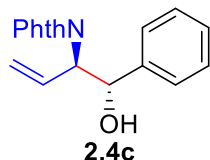
Chiral HPLC Analysis (Chiralpak IC-3 x 250 mm, heptane/isopropanol = 98/2, flow rate = 1.0 ml/min, $\lambda = 220$ nm) tR = 35.3 (major), 39.0 (minor):

Racemate:



Asymmetric Reaction:



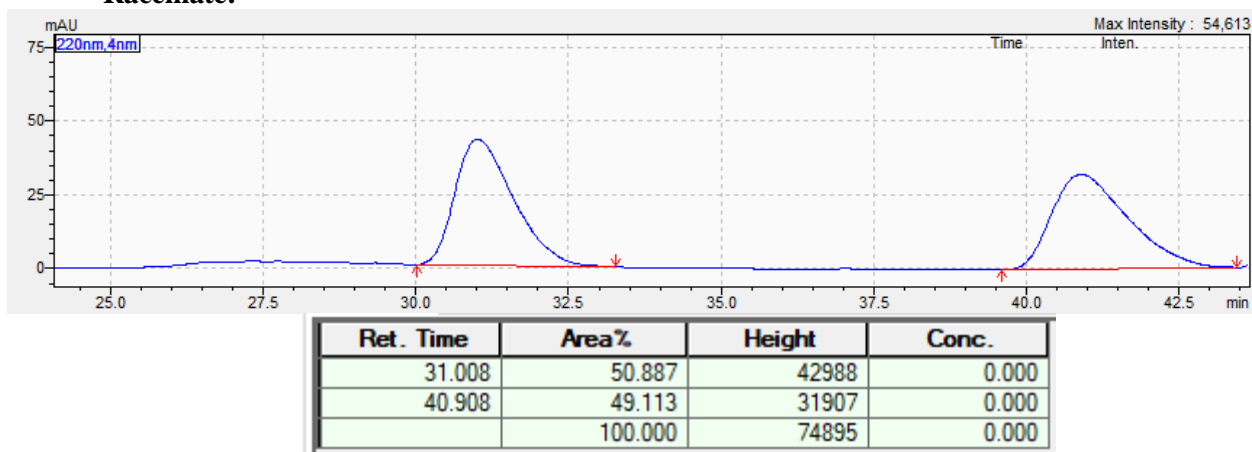


2-((1*S*,2*R*)-1-hydroxy-1-phenylbut-3-en-2-yl)isoindoline-1,3-dione (2.4c):

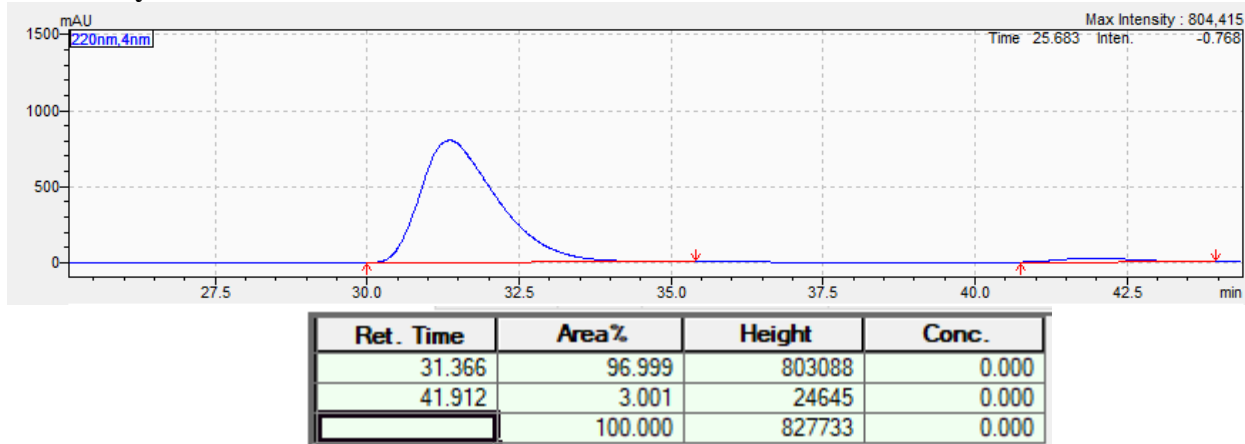
According to the general protonation procedure (GP-1/GP-2) using (*R,R*)-PhBPE, the product was purified by silica gel chromatography (eluent: 0 – 40% EtOAc in hexanes) to provide 36.8 mg (63%) of **2.4c** as a pale yellow oil as a 95:5 mixture of diastereomers and the major diastereomer in a 97:3 mixture of enantiomers. Absolute and relative configuration was assigned by analogy to **2.4i**, **2.4k**, and **2.4n**. $R_f = 0.30$ (25% EtOAc/hexanes). $^1\text{H NMR}$ (CDCl_3 , 600 MHz) δ : 7.78 (dd, $J = 5.8$ Hz, $J = 3.0$ Hz, 2H), 7.69 (dd, $J = 5.8$ Hz, $J = 3.0$ Hz, 2H), 7.39 (d, $J = 7.5$ Hz, 2H), 7.27 (t, $J = 7.5$ Hz, 2H), 7.21 (t, $J = 7.3$ Hz, 1H), 6.37 (ddd, $J = 17$ Hz, $J = 10$ Hz, $J = 5.3$ Hz, 1H), 5.33 (d, $J = 10$ Hz, 1H), 5.29 (d, $J = 6.6$ Hz, 1H), 5.26 (d, $J = 17$ Hz, 1H), 4.98 (t, $J = 7.1$ Hz, 1H), 3.39 (s, 1H) ppm. $^{13}\text{C NMR}$ (126 MHz, CDCl_3): δ 168.1, 140.2, 134.1, 131.4, 131.3, 128.3, 128.0, 126.5, 123.3, 120.0, 73.91, 60.31 ppm. HRMS (DART) m/z calcd for $\text{C}_{18}\text{H}_{14}\text{NO}_2$ $[\text{M-OH}]^+$: 276.1019; Found $[\text{M-OH}]^+$: 276.1025.

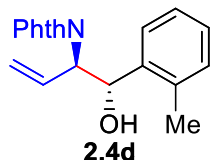
Chiral HPLC Analysis (Chiralpak OD-3 x 250 mm, heptane/isopropanol = 98/2, flow rate = 1.0 ml/min, $\lambda = 220$ nm) $t_R = 31.0$ (major), 40.9 (minor):

Racemate:



Asymmetric Reaction:



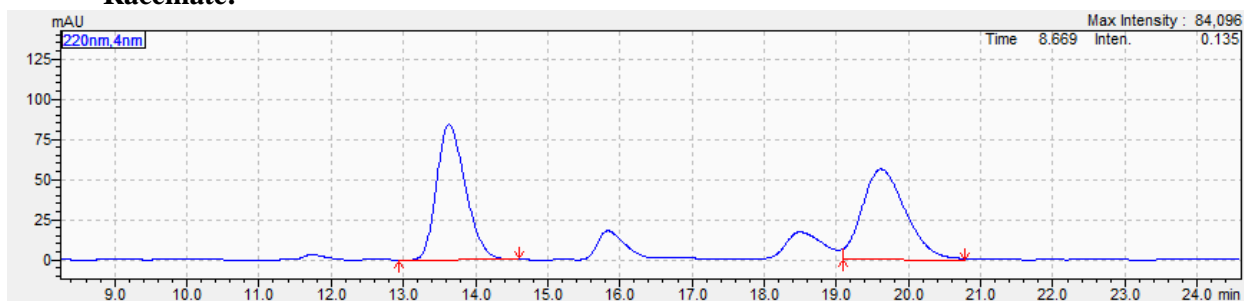


2-((1*S*,2*R*)-1-hydroxy-1-(*o*-tolyl)but-3-en-2-yl)isoindoline-1,3-dione (2.4d):

According to the general protonation procedure (GP-1/GP-2) using (*R,R*)-Ph-BPE, the product was purified by silica gel chromatography (eluent: 0 – 40% EtOAc in hexanes) to provide 27.3 mg (45%) of **2.4d** as a pale yellow oil as a >99:1 mixture of diastereomers and the major diastereomer in a 95:5 mixture of enantiomers. Absolute and relative configuration was assigned by analogy to **2.4i**, **2.4k**, and **2.4n**. R_f = 0.28 (25% EtOAc/hexanes). $^1\text{H NMR}$ (CDCl_3 , 600 MHz) δ : 7.84 (dd, $J = 5.3$ Hz, $J = 3.1$ Hz, 2H), 7.73 (dd, $J = 5.3$ Hz, $J = 3.1$ Hz, 2H), 7.59 (d, $J = 7.8$ Hz, 1H), 7.20 (t, $J = 7.0$ Hz, 1H), 7.16 (t, $J = 7.3$ Hz, 1H), 7.12 (d, $J = 8.1$ Hz, 1H), 6.33 (ddd, $J = 18$ Hz, $J = 10$ Hz, $J = 6.8$ Hz, 1H), 5.42 (dd, $J = 3.8$ Hz, $J = 1.5$ Hz, 1H), 5.28 (d, $J = 10.4$ Hz, 1H), 5.09 (d, $J = 17.3$ Hz, 1H), 5.03 (dd, $J = 5.7$ Hz, $J = 4.3$ Hz, 1H), 4.00 (br s, 1H), 2.34 (s, 3H) ppm. $^{13}\text{C NMR}$ (126 MHz, CDCl_3): δ 168.5, 138.2, 134.9, 134.3, 131.5, 130.4, 130.2, 127.7, 126.3, 125.9, 123.5, 119.4, 71.64, 58.78, 19.12 ppm. HRMS (DART) m/z calcd for $\text{C}_{19}\text{H}_{16}\text{NO}_2$ [M-OH] $^+$: 290.1176; Found [M-OH] $^+$: 290.1181.

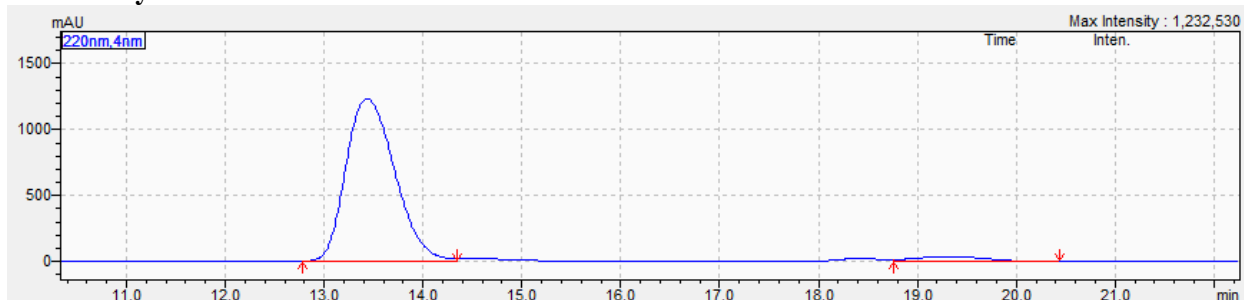
Chiral HPLC Analysis (Chiralpak OD-3 x 250 mm, heptane/isopropanol = 95:5, flow rate = 1.0 ml/min, $\lambda = 254$ nm) $t_R = 13.4$ (major), 19.3 (minor):

Racemate:

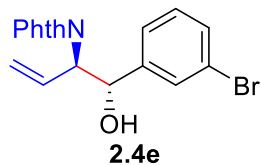


Ret. Time	Area%	Height	Conc.
13.633	49.894	84090	0.000
19.618	50.106	56077	0.000
	100.000	140167	0.000

Asymmetric Reaction:



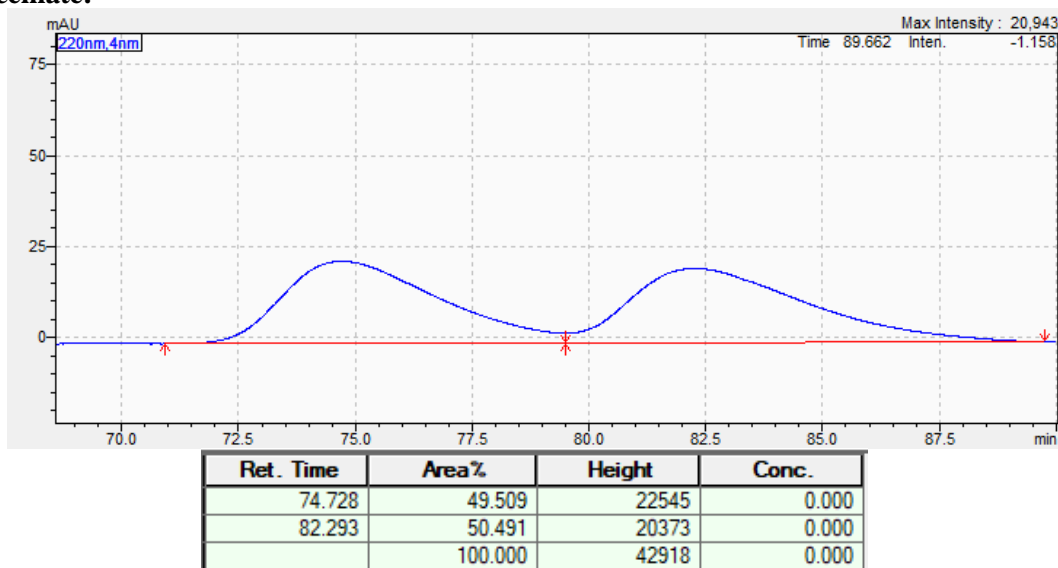
Ret. Time	Area%	Height	Conc.
13.437	95.389	1231721	0.000
19.299	4.611	40788	0.000
	100.000	1272509	0.000



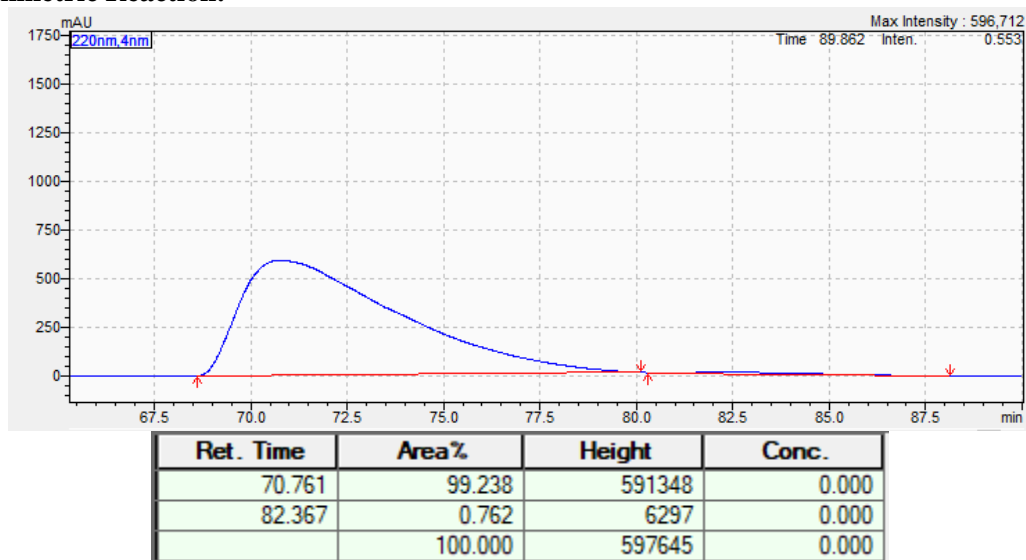
2-((1*S*,2*R*)-1-hydroxy-1-(*m*-bromophenyl)but-3-en-2-yl)isoindoline-1,3-dione (2.4e): According to the general protonation procedure (GP-1/GP-2) using (*R,R*)-Ph-BPE, the product was purified by silica gel chromatography (eluent: 0 – 40% EtOAc in hexanes) to provide 38.0 mg (51%) of **2.4e** as a pale yellow oil as a 95:5 mixture of diastereomers and the main diastereomer in a 99:1 mixture of enantiomers. Absolute and relative configuration was assigned by analogy to **2.4i**, **2.4k**, and **2.4n**. R_f = 0.28 (25% EtOAc/hexanes). ^1H NMR (CDCl_3 , 600 MHz) δ : 7.82 (dd, J = 5.3 Hz, J = 3.0 Hz, 2H), 7.72 (dd, J = 5.5 Hz, J = 3.0 Hz, 2H), 7.58 (s, 1H), 7.36 (d, J = 7.5 Hz, 1H), 7.33 (d, J = 8.8 Hz, 1H), 7.16 (t, J = 8.0 Hz, 1H), 6.30 (ddd, J = 17.1 Hz, J = 10.5 Hz, J = 7.3 Hz, 1H), 5.33 (d, J = 10.5 Hz, 1H), 5.23 (br s, 1H), 5.21 (d, J = 15.0 Hz, 1H), 4.93 (t, J = 7.4 Hz, 1H), 3.71 (s, 1H) ppm. ^{13}C NMR (126 MHz, CDCl_3): δ 168.2, 142.6, 134.3, 131.4, 131.1, 130.4, 129.9, 125.1, 123.5, 122.4, 120.4, 73.5, 60.4. HRMS (DART) m/z calcd for $\text{C}_{18}\text{H}_{13}\text{BrNO}_2$ $[\text{M}-\text{OH}]^+$: 354.0124; Found $[\text{M}-\text{OH}]^+$: 354.0111.

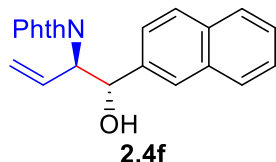
Chiral HPLC Analysis (Chiralpak OD-3 x 250 mm, heptane/isopropanol = 99/1, flow rate = 0.5 ml/min, λ = 254 nm) t_R = 70.6 (major), 82.3 (minor):

Racemate:



Asymmetric Reaction:

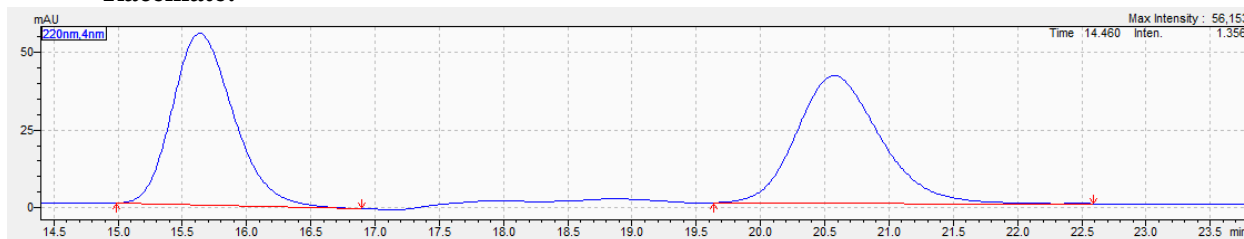




2-((1S,2R)-1-hydroxy-1-(naphthalen-2-yl)but-3-en-2-yl)isoindoline-1,3-dione (2.4f): According to the general protonation procedure (GP-1/GP-2) using (*R,R*)-Ph-BPE, the product was purified by silica gel chromatography (eluent: 0 – 40% EtOAc in hexanes) to provide 44.2 mg (65%) of **2.4f** as a thick glass as a >99:1 mixture of diastereomers and the major diastereomer in a 97.5:2.5 mixture of enantiomers. Absolute and relative configuration was assigned by analogy to **2.4i**, **2.4k**, and **2.4n**. $R_f = 0.69$ (10% EtOAc/ CH_2Cl_2). $^1\text{H NMR}$ (CDCl_3 , 600 MHz) δ : 7.87 (s, 1H), 7.74-7.80 (m, 5H), 7.67 (dd, $J = 5.3$ Hz, $J = 3.1$ Hz, 2H), 7.53 (dd, $J = 8.3$ Hz, $J = 1.5$ Hz, 1H), 7.42 (dd, $J = 6.0$ Hz, $J = 3.1$ Hz, 2H), 6.38 (ddd, $J = 17.0$ Hz, $J = 10.4$ Hz, $J = 7.3$ Hz, 1H), 5.46 (d, $J = 6.5$ Hz, 1H), 5.33 (d, $J = 10.7$ Hz, 1H), 5.25 (d, $J = 17.0$ Hz, 1H), 5.12 (t, $J = 7.0$ Hz, 1H), 3.59 (br s, 1H) ppm. $^{13}\text{C NMR}$ (126 MHz, CDCl_3): δ 168.2, 137.6, 134.1, 133.1, 133.0, 131.4, 131.1, 128.2, 128.0, 127.6, 126.0, 125.96, 125.93, 124.1, 123.4, 120.0, 74.1, 60.1. HRMS (DART) m/z calcd for $\text{C}_{22}\text{H}_{16}\text{NO}_2$ $[\text{M-OH}]^+$: 326.1187; Found $[\text{M-OH}]^+$: 326.1190.

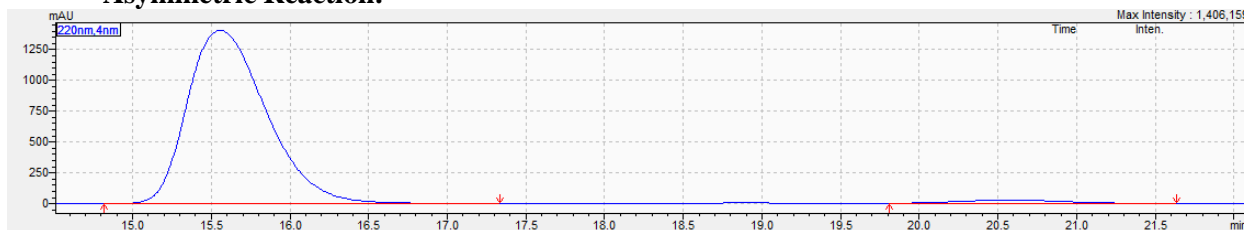
Chiral HPLC Analysis (Chiralpak OD-3 x 250 mm, heptane/isopropanol = 90/10, flow rate = 1.0 ml/min, $\lambda = 254$ nm) tR = 15.6 (major), 20.5 (minor):

Racemate:

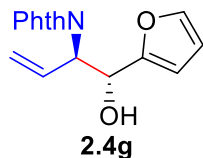


Ret. Time	Area%	Height	Conc.
15.636	49.929	55334	0.000
20.573	50.071	41047	0.000
	100.000	96381	0.000

Asymmetric Reaction:



Ret. Time	Area%	Height	Conc.
15.555	97.554	1404825	0.000
20.573	2.446	26926	0.000
	100.000	1431751	0.000

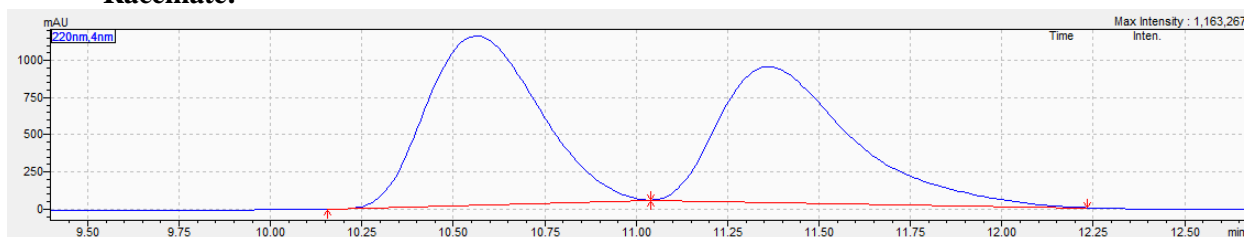


2-((1S,2R)-1-(furan-2-yl-1-hydroxy-but-3-en-2-yl)isoindoline-1,3-dione (2.4g):

According to the general protonation procedure (GP-1/GP-2) using (*R,R*)-Ph-BPE, the product was purified by silica gel chromatography (eluent: 0 – 40% EtOAc in hexanes) to provide 45.9 mg (65%) of **2.4g** as a white foam as a 92:8 mixture of diastereomers and the major diastereomer as a 98:2 mixture of enantiomers. Absolute and relative configuration was assigned by analogy to **2.4i**, **2.4k**, and **2.4n**. $R_f = 0.24$ (25% EtOAc/hexanes). $^1\text{H NMR}$ (CDCl_3 , 600 MHz) δ : 7.82 (dd, $J = 5.3$ Hz, $J = 3.1$ Hz, 2), 7.71 (dd, $J = 5.4$ Hz, $J = 3.1$ Hz, 2H), 7.33 (d, $J = 1.2$ Hz, 1H), 6.30 – 6.37 (m, 2H), 6.25 (dd, $J = 3.0$ Hz, $J = 1.7$ Hz, 1H), 5.35 (d, $J = 1.5$ Hz, 1H), 5.35 (d, $J = 6.2$ Hz, 1H), 5.29 (d, $J = 17.6$ Hz, 1H), 5.15 (t, $J = 7.1$ Hz, 1H), 3.35 (br s, 1H) ppm. $^{13}\text{C NMR}$ (126 MHz, CDCl_3): δ 168.0, 152.7, 142.4, 134.2, 131.5, 131.3, 123.4, 119.9, 110.2, 107.7, 68.05, 57.74. HRMS (DART) m/z calcd for $\text{C}_{16}\text{H}_{12}\text{NO}_3$ $[\text{M-OH}]^+$: 266.0823; Found $[\text{M-OH}]^+$: 266.0846.

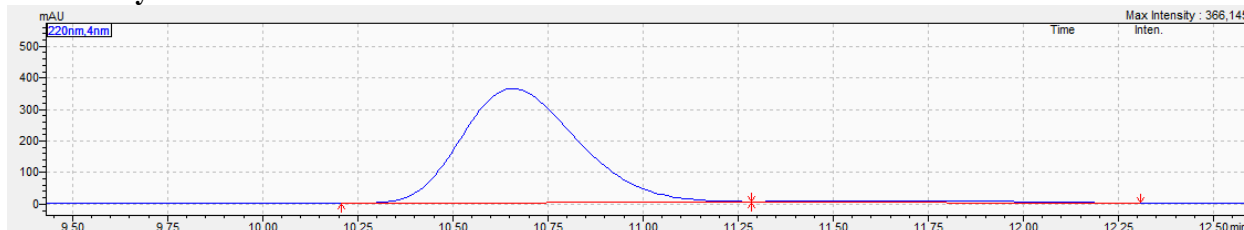
Chiral HPLC Analysis (Chiralpak OD-3 x 250 mm, heptane/isopropanol = 90/10, flow rate = 1.0 ml/min, $\lambda = 254$ nm) $t_R = 10.5$ (major), 11.4 (minor):

Racemate:

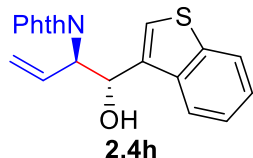


Ret. Time	Area%	Height	Conc.
10.564	51.515	1137842	0.000
11.361	48.485	909751	0.000
	100.000	2047593	0.000

Asymmetric Reaction:



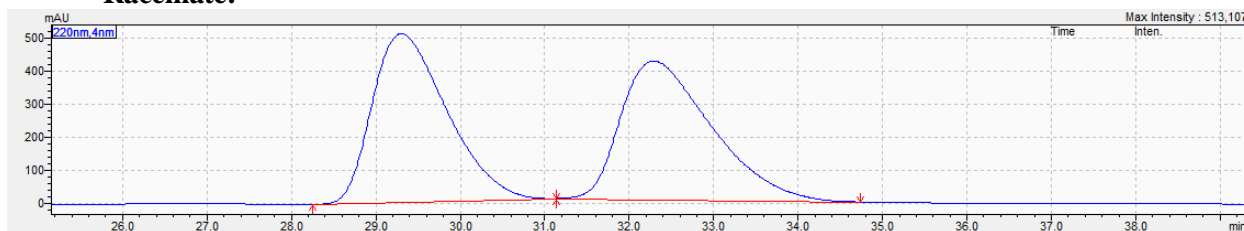
Ret. Time	Area%	Height	Conc.
10.657	98.049	361375	0.000
11.524	1.951	4324	0.000
	100.000	365700	0.000



2-((1S,2R)-1-(benzo[b]thiophen-3-yl)-1-hydroxybut-3-en-2-yl)isoindoline-1,3-dione (2.4h): According to the general protonation procedure (GP-1/GP-2) using (*R,R*)-Ph-BPE, the product was purified by silica gel chromatography (eluent: 0 – 40% EtOAc in hexanes) to provide 48.0 mg (69%) of **2.4h** as a yellow oil as a >99:1 mixture of diastereomers and the major diastereomer in a 99:1 mixture of enantiomers. Absolute and relative configuration was assigned by analogy to **2.4i**, **2.4k**, and **2.4n**. R_f = 0.24 (25% EtOAc/hexanes). $^1\text{H NMR}$ (CDCl_3 , 600 MHz) δ : 7.83 – 7.85 (m, 4H), 7.73 (dd, J = 5.4 Hz, J = 3.0 Hz, 2H), 7.58 (s, 1H), 7.39 (t, J = 7.4 Hz, 1H), 7.34 (t, J = 7.4 Hz, 1H), 6.35 (ddd, J = 17.1 Hz, J = 10.5 Hz, J = 6.6 Hz, 1H), 5.63 (d, J = 3.8 Hz, 1H), 5.30 (d overlapped with bs, J = 10.6 Hz, 2H), 5.10 (d, J = 17.1 Hz, 1H), 4.10 (br s, 1H) ppm. $^{13}\text{C NMR}$ (126 MHz, CDCl_3): δ 168.5, 140.8, 136.8, 135.1, 134.4, 131.5, 130.3, 124.4, 124.3, 124.2, 123.6, 122.9, 121.7, 119.7, 70.82, 58.48 ppm. HRMS (DART) m/z calcd for $\text{C}_{20}\text{H}_{14}\text{NO}_2\text{S}$ [M-OH] $^+$: 332.0751; Found [M-OH] $^+$: 332.0771.

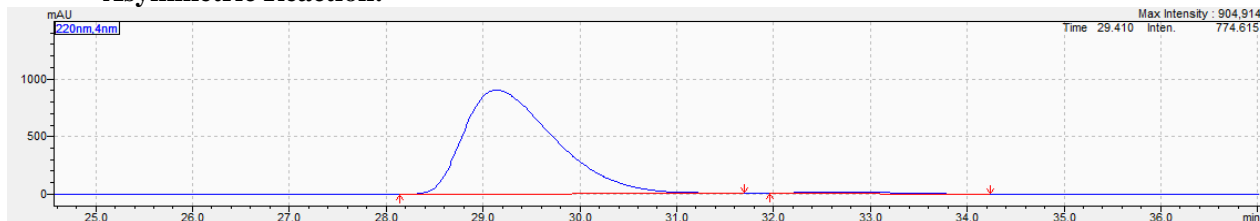
Chiral HPLC Analysis (Chiralpak OD-3 x 250 mm, heptane/isopropanol = 95/5, flow rate = 1.0 ml/min, λ = 254 nm) tR = 29.2 (major), 32.3 (minor):

Racemate:

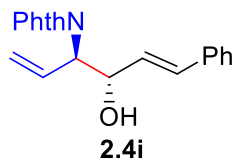


Ret. Time	Area%	Height	Conc.
29.299	49.970	508312	0.000
32.290	50.030	417354	0.000
	100.000	925666	0.000

Asymmetric Reaction:



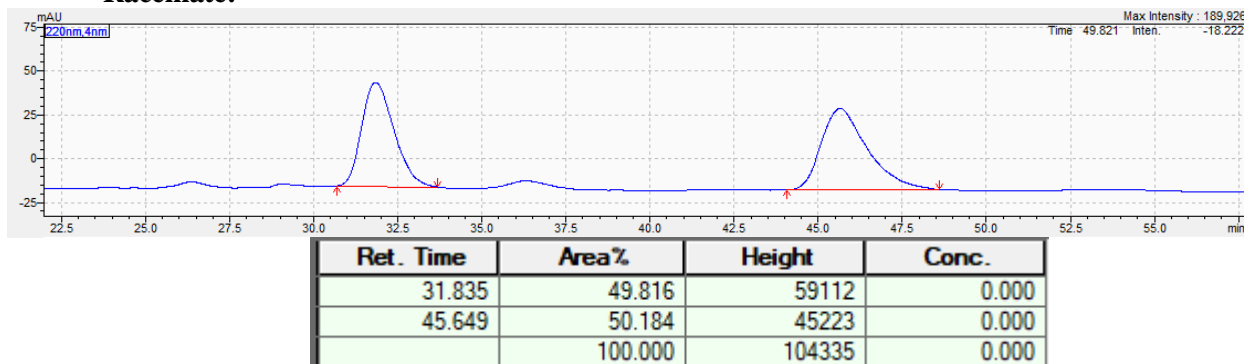
Ret. Time	Area%	Height	Conc.
29.142	98.721	902458	0.000
32.665	1.279	12290	0.000
	100.000	914748	0.000



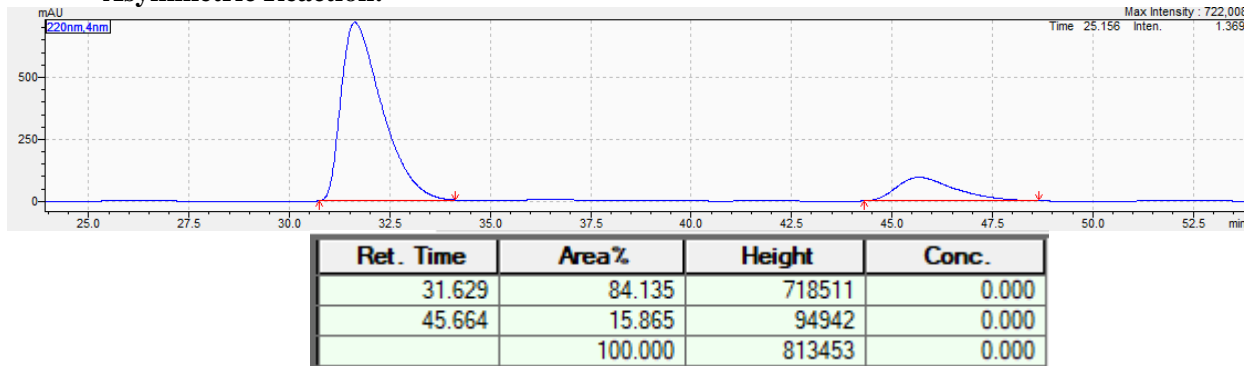
2-((3*R*,4*S*,*E*)-4-hydroxy-6-phenylhexa-1,5-dien-3-yl)isoindoline-1,3-dione (2.4i): According to the general protonation procedure (GP-1/GP-2) using (*R,R*)-Ph-BPE, the product was purified by silica gel chromatography (eluent: 0 – 40% EtOAc in hexanes) to provide 41.3 mg (62%) of **2.4i** as a pale yellow oil as a 90:10 mixture of diastereomers and the major diastereomer as an 84:16 mixture of enantiomers. $R_f = 0.39$ (25% EtOAc/hexanes). Spectral data matched that of the literature and confirmed the relative stereochemical configuration.^[1] Absolute configuration was confirmed by comparison of the chiral HPLC data to that reported in the literature.^[1]

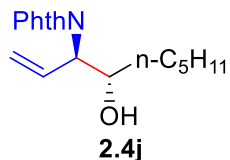
Chiral HPLC Analysis (Chiralpak OD-3 x 250 mm, heptane/isopropanol = 95/5, flow rate = 1.0 ml/min, $\lambda = 254$ nm) tR = 31.8 (major), 45.6 (minor); Lit.^[1] (OD-H Hexanes:IPA = 95:5, $\lambda = 230$ nm): tR = 47.5 (major), 68.2 (minor) min.

Racemate:



Asymmetric Reaction:

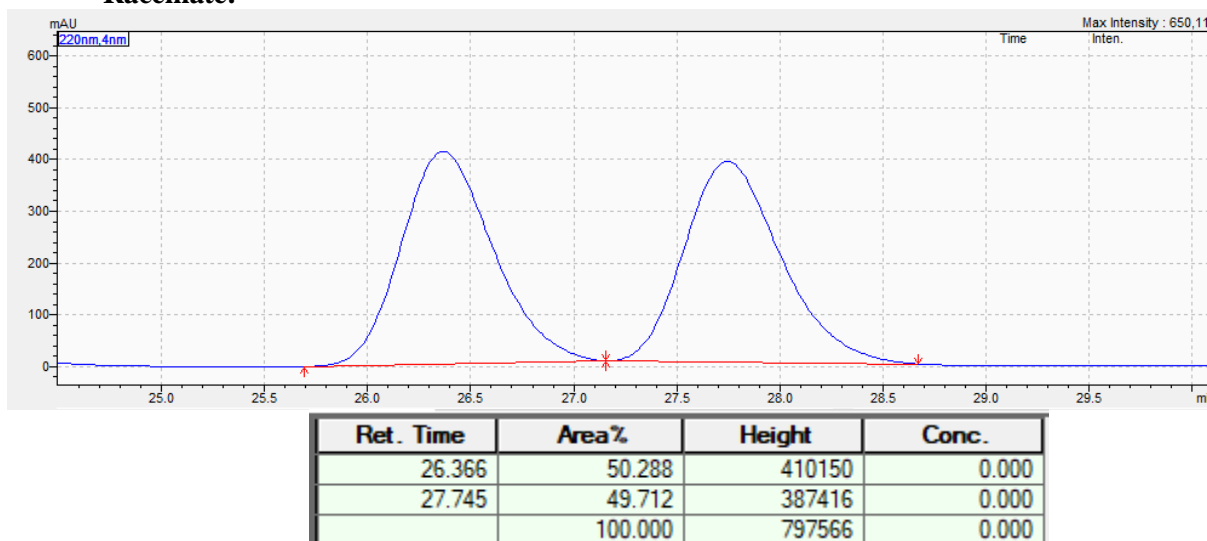




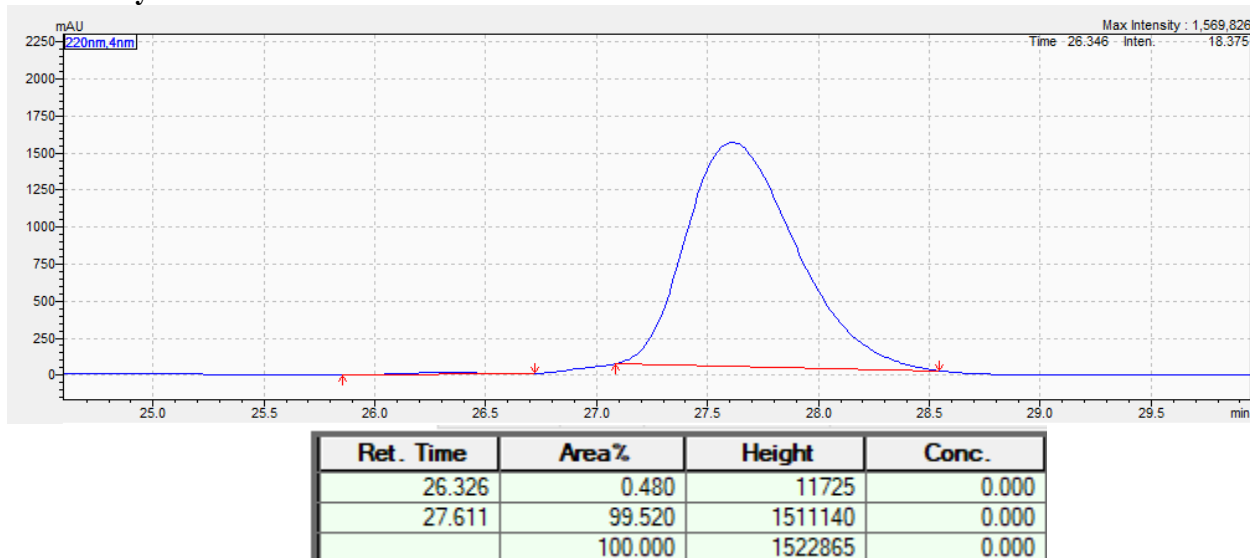
2-((3R,4S)-4-hydroxynon-1-en-3-yl)isoindoline-1,3-dione (2.4j): According to the general protonation procedure (GP-1/GP-2) using (*S,S*)-PhB-PE, the product was purified by silica gel chromatography (eluent: 0 – 40% EtOAc in hexanes) to provide 27.2 mg (48%) of **2.4j** as a pale yellow oil as a >99:1 mixture of diastereomers and the major diastereomer as a >97:3 mixture of enantiomers. Absolute and relative configuration was assigned by analogy to **2.4i**, **2.4k**, and **2.4n**. $R_f = 0.36$ (25% EtOAc/hexanes). $^1\text{H NMR}$ (CDCl_3 , 600 MHz) δ : 7.86 (dd, $J = 5.3$ Hz, $J = 3.0$ Hz, 2H), 7.74 (dd, $J = 5.4$ Hz, $J = 3.0$ Hz, 2H), 6.27 (ddd, $J = 17.5$ Hz, $J = 10.5$ Hz, $J = 8.0$ Hz, 1H), 5.31 (d, $J = 10$ Hz, 1H), 5.26 (d, $J = 16.5$ Hz, 1H), 4.70 (dd, $J = 7.7$ Hz, $J = 4.0$ Hz, 1H), 4.05 (dd, $J = 4.1$ Hz, $J = 2.5$ Hz, 1H), 3.69 (s, 1H), 3.60 (br s, 1H), 1.16–1.60 (m, 7H), 0.87 (t, $J = 7.0$ Hz, 3H) ppm. $^{13}\text{C NMR}$ (126 MHz, CDCl_3): δ 168.6, 134.2, 131.6, 131.1, 123.5, 119.8, 72.1, 59.3, 34.1, 31.6, 25.3, 22.5, 13.9. HRMS (DART) m/z calcd for $\text{C}_{17}\text{H}_{22}\text{NO}_3$ [$\text{M} + \text{H}$] $^+$: 288.1600; Found [$\text{M} + \text{H}$] $^+$: 288.1618.

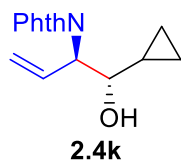
Chiral HPLC Analysis (Chiralpak AD-3 x 250 mm, heptane/isopropanol = 95/5, flow rate = 1.0 ml/min, $\lambda = 254$ nm) tR = 26.4 (minor), 27.5 (major):

Racemate:



Asymmetric Reaction:



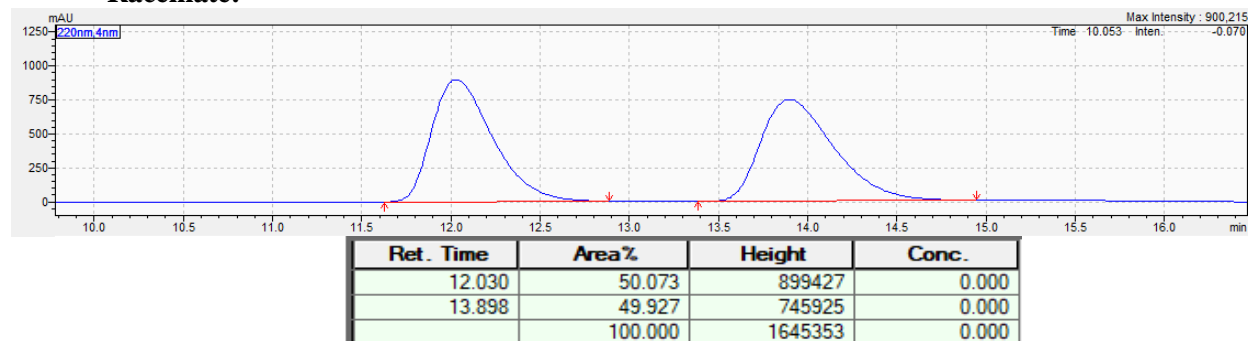


2-((1*S*,2*R*)-1-cyclopropyl-1-hydroxybut-3-en-2-yl)isoindoline-1,3-dione (2.4k):

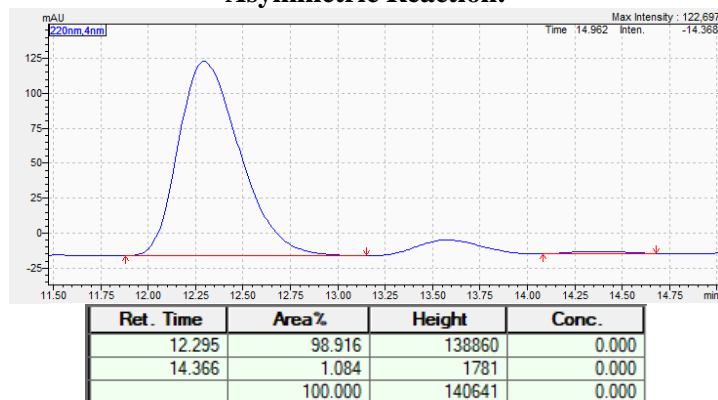
According to the general protonation procedure (GP-1/GP-2) using (*R,R*)-Ph-BPE, the product was purified by silica gel chromatography (eluent: 0 – 40% EtOAc in hexanes) to provide 31.5mg (60%) of **2.4k** as a pale yellow solid as a 97:3 mixture of diastereomers and the major diastereomer as a 99:1 mixture of enantiomers. $R_f = 0.21$ (25% EtOAc/hexanes). Spectral data matched that of the literature and confirmed the relative stereochemical configuration.^[1] Absolute configuration was confirmed by comparison of the chiral HPLC data to that reported in the literature.^[1]

Chiral HPLC Analysis (Chiralpak OD-3 x 250 mm, heptane/isopropanol = 95/5, flow rate = 1.0 ml/min, $\lambda = 254$ nm) $t_R = 12.0$ (major), 13.8 (minor); Lit.^[1] (OD-H Hexanes:IPA = 95:5, $\lambda = 230$ nm): $t_R = 15.1$ (major), 18.3 (minor) min.

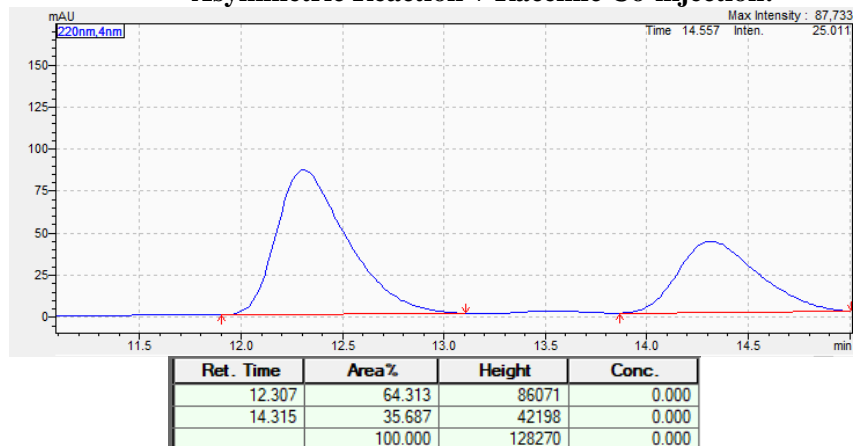
Racemate:

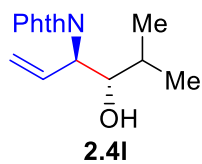


Asymmetric Reaction:



Asymmetric Reaction + Racemic Co-injection:

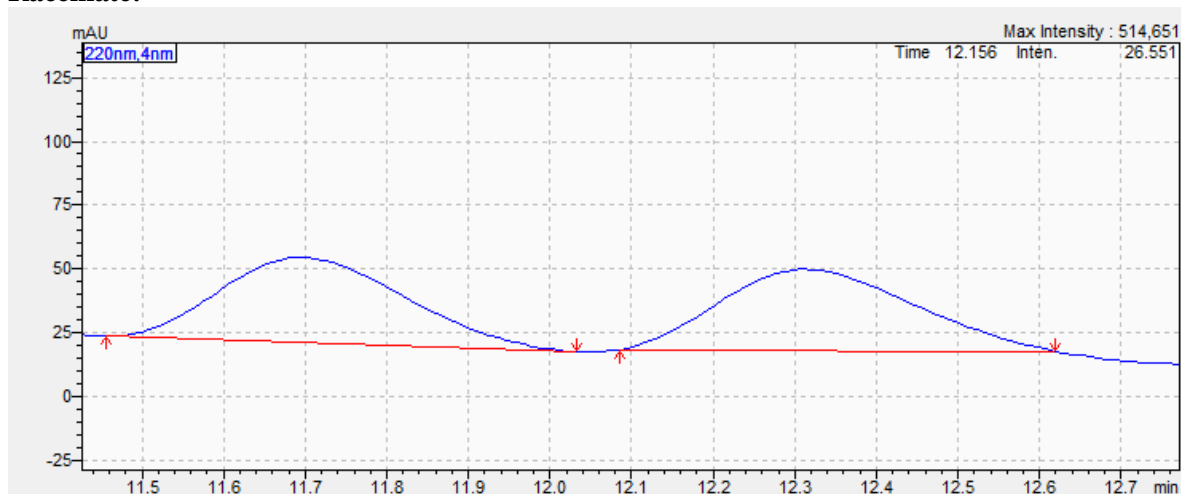




2-((3R,4S)-4-hydroxy-5-methylhex-1-en-3-yl)isoindoline-1,3-dione (2.4I): According to the general protonation procedure (GP-1/GP-2) using (*R,R*)-PhBPE, the product was purified by silica gel chromatography (eluent: 0 – 40% EtOAc in hexanes) to provide 27.9 mg (54%) of **2.4I** as a yellow oil as a 80:20 mixture of diastereomers and >99:1 mixture of enantiomers. Absolute and relative configuration was assigned by analogy to **2.4i**, **2.4k**, and **2.4n**. $R_f = 0.62$ (10% EtOAc/ CH_2Cl_2). $^1\text{H NMR}$ (CDCl_3 , 600 MHz) δ : 7.84 (dd, $J = 5.5$ Hz, $J = 3.1$ Hz, 2H), 7.73 (dd, $J = 5.5$ Hz, $J = 3.1$ Hz, 2H), 6.28 (ddd, $J = 17.7$ Hz, $J = 10.4$ Hz, $J = 7.6$ Hz, 1H), 5.29 (dt, $J = 10.4$ Hz, $J = 1.0$ Hz, 1H), 5.26 (dt, $J = 17.0$ Hz, $J = 1.0$ Hz, 1H), 4.86 (dd, $J = 7.5$ Hz, $J = 5.1$ Hz, 1H), 3.87 (t, $J = 5.5$ Hz, 1H), 3.16 (br s, 1H), 1.74 (hex, $J = 6.6$ Hz, 1H), 1.01 (d, $J = 6.6$ Hz, 3H), 0.98 ($J = 6.6$ Hz, 3H) ppm. $^{13}\text{C NMR}$ (126 MHz, CDCl_3): δ 168.4, 134.2, 132.0, 131.7, 123.5, 119.6, 76.77, 30.40, 19.80, 16.75. HRMS (DART) m/z calcd for $\text{C}_{15}\text{H}_{18}\text{NO}_3$ [$\text{M} + \text{H}$] $^+$: 260.1287; Found [$\text{M} + \text{H}$] $^+$: 260.1281.

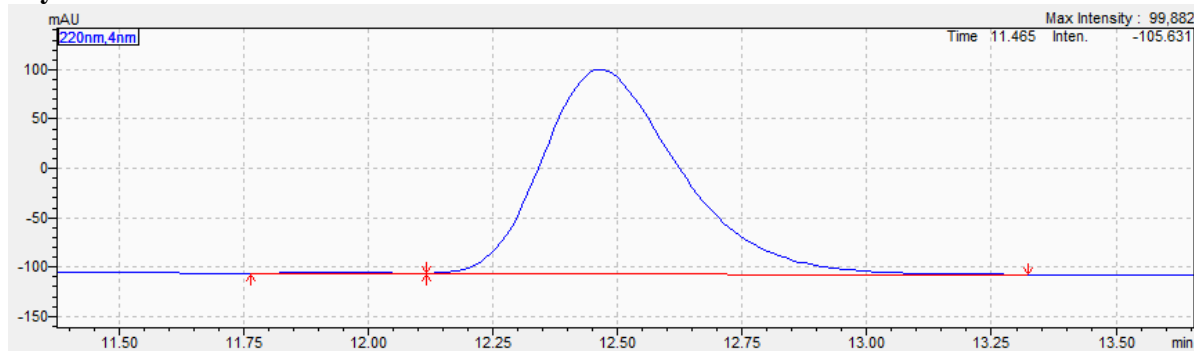
Chiral HPLC Analysis (Chiralpak AD-3 x 250 mm, heptane/isopropanol = 90/10, flow rate = 1.0 ml/min, $\lambda = 220$ nm) $t_R = 11.9$ (major), 12.4 (minor):

Racemate:

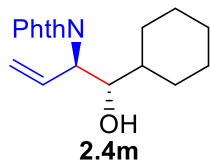


Ret. Time	Area%	Height	Conc.
11.695	50.290	33445	0.000
12.313	49.710	31754	0.000
	100.000	65199	0.000

Asymmetric Reaction:



Ret. Time	Area%	Height	Conc.
11.948	0.165	631	0.000
12.465	99.835	206534	0.000
	100.000	207165	0.000

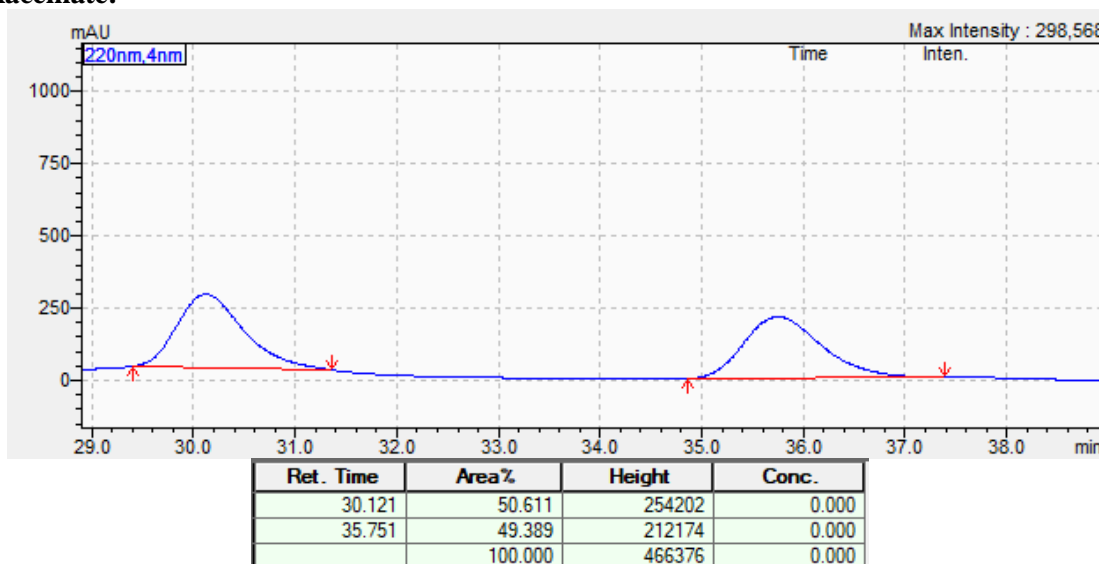


2-((1S,2R)-1-cyclohexyl-1-hydroxybut-3-en-2-yl)isoindoline-1,3-dione (2.4m):

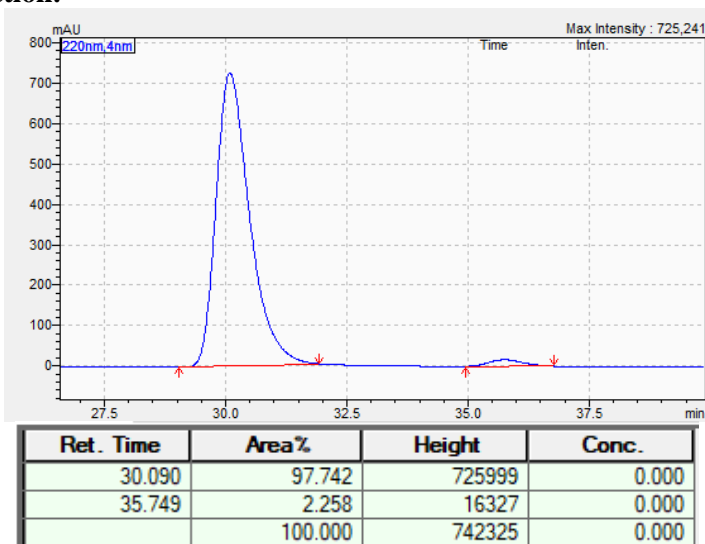
According to the general protonation procedure (GP-1/GP-2) using (*R,R*)-Ph-BPE, the product was purified by silica gel chromatography (eluent: 0 – 40% EtOAc in hexanes) to provide 34.9 mg (57%) of **2.4m** as a yellow oil as a >99:1 mixture of diastereomers and the major diastereomer as a 98:2 mixture of enantiomers. Absolute and relative configuration was assigned by analogy to **2.4i**, **2.4k**, and **2.4n**. $R_f = 0.30$ (25% EtOAc/hexanes). $^1\text{H NMR}$ (CDCl_3 , 600 MHz) δ : 7.85 (dd, $J = 5.5$ Hz, $J = 3.1$ Hz, 2H), 7.74 (dd, $J = 5.5$ Hz, $J = 3.1$ Hz, 2H), 6.28 (ddd, $J = 17.8$ Hz, $J = 10.4$ Hz, $J = 7.4$ Hz, 1H), 5.29 (d, $J = 10.5$ Hz, 1H), 5.24 (d, $J = 17.6$ Hz, 1H), 4.93 (dd, $J = 7.3$ Hz, $J = 4.5$ Hz, 1H), 3.83 (dd, $J = 5.9$ Hz, $J = 4.6$ Hz, 1H), 3.35 (br s, 1H), 1.94 (d, $J = 13.3$ Hz, 1H), 1.78-1.70 (m, 2H), 1.63 (d, $J = 10.3$ Hz, 1H), 1.46-1.37 (m, 1H), 1.3-1.0 (m, 5H), 0.90 – 0.74 (m, 1H) ppm. $^{13}\text{C NMR}$ (126 MHz, CDCl_3): δ 168.5, 134.2, 131.8, 131.7, 123.5, 119.4, 76.07, 56.34, 40.34, 29.92, 27.33, 26.31, 26.23, 25.97. HRMS (DART) m/z calcd for $\text{C}_{18}\text{H}_{22}\text{NO}_3$ $[\text{M} + \text{H}]^+$: 300.1600; Found $[\text{M} + \text{H}]^+$: 300.1601.

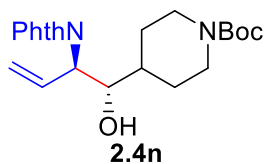
Chiral HPLC Analysis (Chiralpak AD-3 x 250 mm, heptane/isopropanol = 95/5, flow rate = 1.0 ml/min, $\lambda = 254$ nm) $t_R = 30.1$ (major), 35.7 (minor):

Racemate:



Asymmetric Reaction:

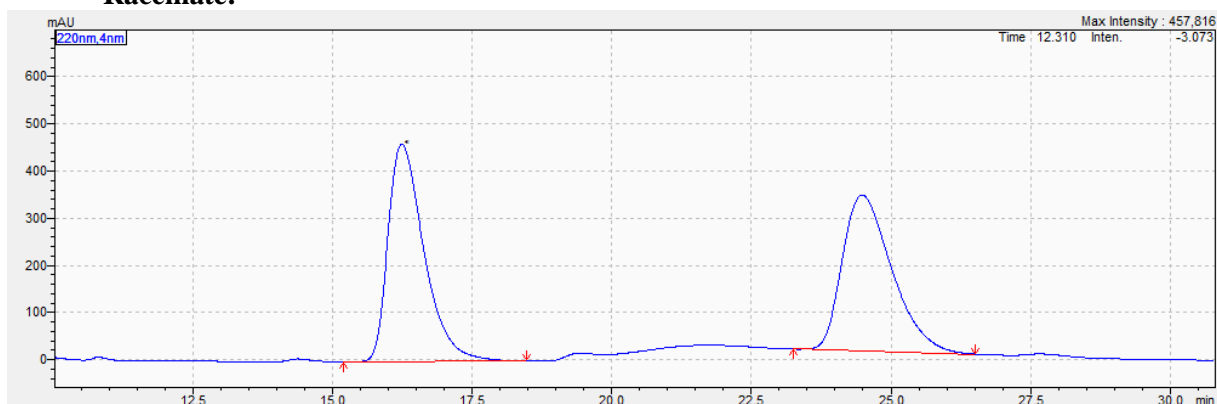




tert-butyl 4-((1S,2R)-2-(1,3-dioxoisindolin-2-yl)-1-hydroxybut-3-en-1-yl)piperidine-1-carboxylate (2.4n): According to the general protonation procedure (GP-1/GP-2) using (*R,R*)-PhBPE, the product was purified by silica gel chromatography (eluent: 0 – 40% EtOAc in hexanes) to provide 39.5 mg (49%) of **2.4n** as a pale yellow oil as a 95:5 mixture of diastereomers and 98.5:1.5 mixture of enantiomers. $R_f = 0.11$ (25% EtOAc/hexanes). Spectral data matched that of the literature and confirmed the relative stereochemical configuration.^[1] Absolute configuration was confirmed by comparison of the chiral HPLC data to that reported in the literature.^[1]

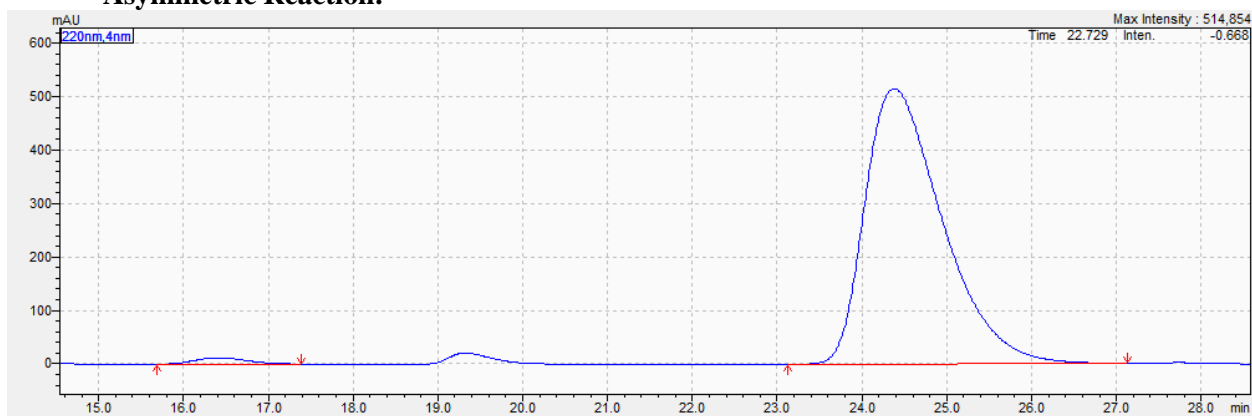
Chiral HPLC Analysis (Chiralpak OD-3 x 250 mm, heptane/isopropanol = 95/5, flow rate = 1.0 ml/min, $\lambda = 220$ nm) tR = 16.2 (minor), 24.4 (major); Lit.^[1] (OD-H Hexanes:IPA = 93:7, $\lambda = 230$ nm): tR = 29.2 (minor), 44.1 (major) min.

Racemate:

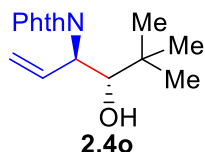


Ret. Time	Area%	Height	Conc.
16.244	50.290	461516	50.290
24.481	49.710	331256	49.710
	100.000	792772	100.000

Asymmetric Reaction:



Ret. Time	Area%	Height	Conc.
16.408	1.568	12064	0.000
24.380	98.432	515227	0.000
	100.000	527291	0.000

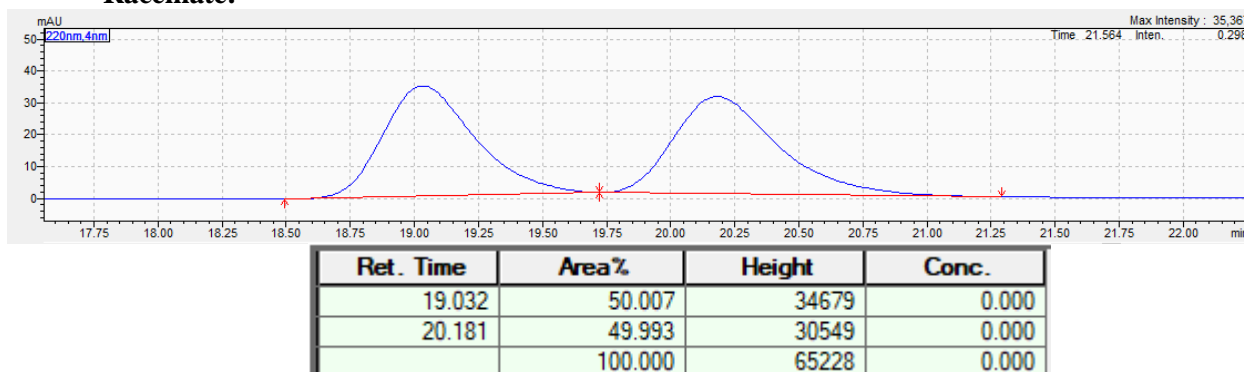


2-((3R,4S)-4-hydroxy-5,5-dimethylhex-1-en-3-yl)isoindoline-1,3-dione (2.4o):

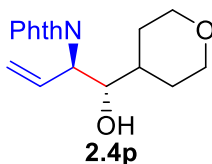
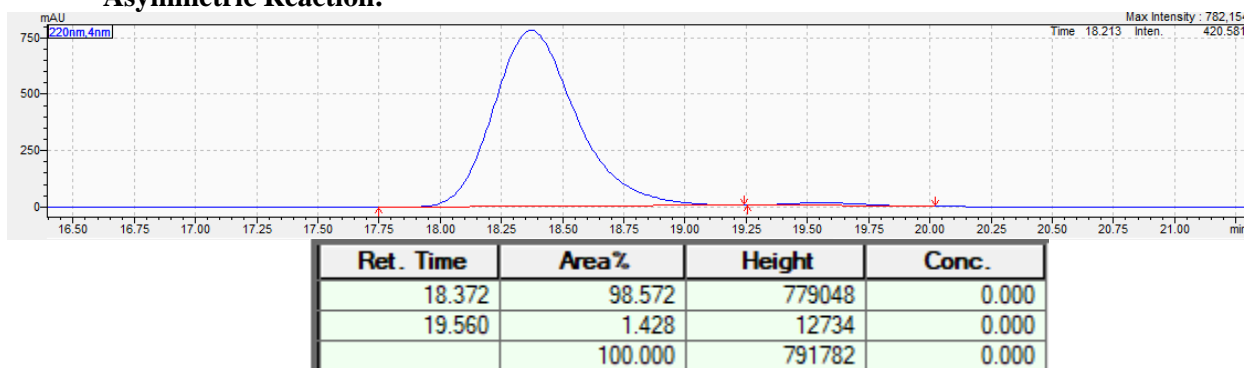
According to the general protonation procedure (GP-1/GP-2) using (*R,R*)-PhBPE, the product was purified by silica gel chromatography (eluent: 0 – 40% EtOAc in hexanes) to provide 30.9 mg (57%) of **2.4o** as a pale yellow oil as a >99:1 mixture of diastereomers and the major diastereomer as a 98.5:1.5 mixture of enantiomers. Absolute and relative configuration was assigned by analogy to **2.4i**, **2.4k**, and **2.4n**. $R_f = 0.40$ (25% EtOAc/hexanes). $^1\text{H NMR}$ (CDCl_3 , 600 MHz) δ : 7.86 (dd, $J = 5.5$ Hz, $J = 3.1$ Hz, 2H), 7.74 (dd, $J = 5.5$ Hz, $J = 3.1$ Hz, 2H), 6.31 (ddd, $J = 17.4$ Hz, $J = 10.4$ Hz, $J = 7.6$ Hz, 1H), 5.22 (d, $J = 10$ Hz, 1H), 5.15 (d, $J = 17.5$ Hz, 1H), 5.10 (dd, $J = 7.0$ Hz, $J = 1.0$ Hz, 1H), 3.80 (br s, 1H), 3.60 (s, 1H), 1.01 (s, 9H) ppm. $^{13}\text{C NMR}$ (126 MHz, CDCl_3): δ 168.5, 134.2, 132.6, 131.7, 123.5, 118.17, 80.6, 54.7, 35.1, 26.4. HRMS (DART) m/z calcd for $\text{C}_{16}\text{H}_{20}\text{NO}_3$ $[\text{M} + \text{H}]^+$: 274.1443; Found $[\text{M} + \text{H}]^+$: 274.1458.

Chiral HPLC Analysis (Chiralpak AD-3 x 250 mm, heptane/isopropanol = 98/2, flow rate = 1.0 ml/min, $\lambda = 254$ nm) $t_R = 19.0$ (major), 20.1 (minor):

Racemate:



Asymmetric Reaction:

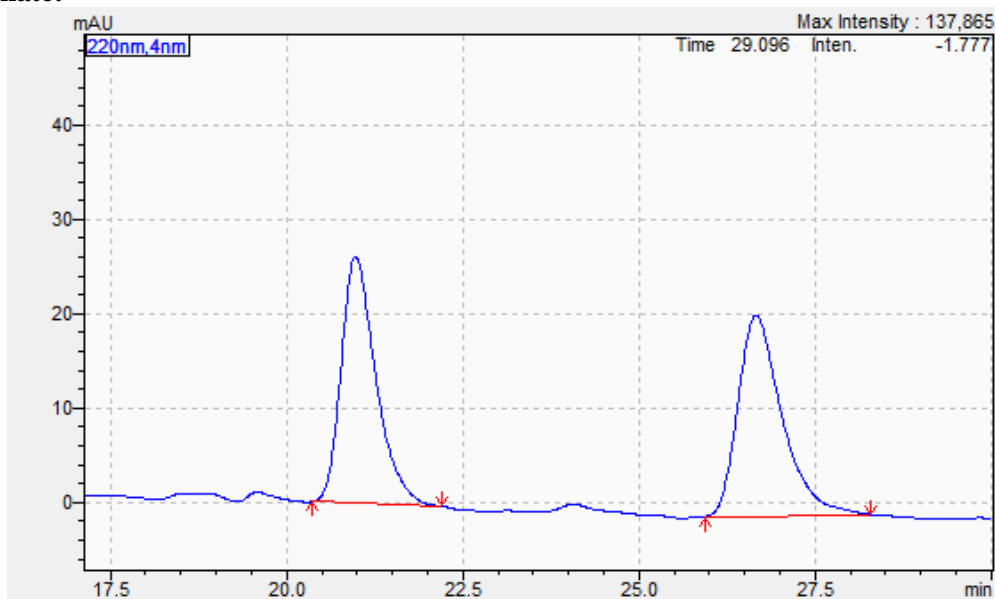


2-((1S,2R)-1-hydroxy-1-(tetrahydro-2H-pyran-4-yl)but-3-en-2-yl)isoindoline-1,3-dione (2.4p):

According to the general protonation procedure, the product was purified by silica gel chromatography (eluent: 0 – 40% EtOAc in hexanes) to provide 54% of **2.4p** as a clear glass as a 66:34 mixture of diastereomers and 96:4 mixture of enantiomers. Spectra of isolated compound matched known literature (Ref -Krische). HRMS (DART) m/z calcd for $\text{C}_{17}\text{H}_{20}\text{NO}_4$ $[\text{M} + \text{H}]^+$: 302.1392; Found $[\text{M} + \text{H}]^+$: 302.1400.

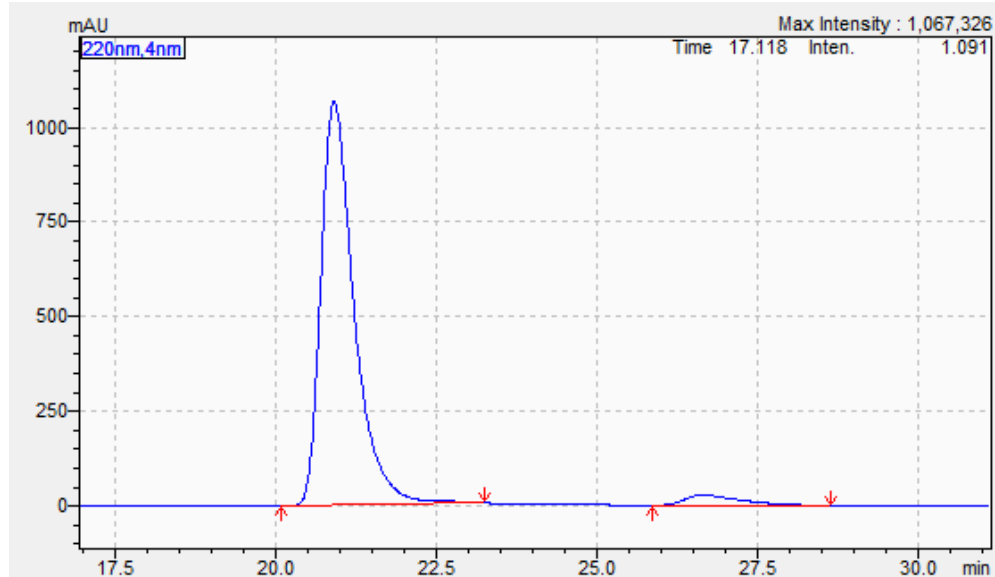
Chiral HPLC Analysis (Chiralpak AD-3 x 250 mm, heptane/isopropanol = 90/10, flow rate = 1.0 ml/min, $\lambda = 254 \text{ nm}$) tR = 20.9 (major), 26.6(minor):

Racemate:



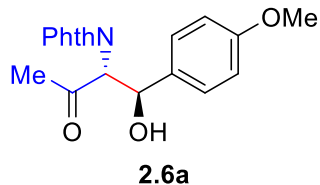
Ret. Time	Area%	Height	Conc.
20.977	49.248	26143	0.000
26.665	50.752	21250	0.000
	100.000	47393	0.000

Asymmetric Reaction:



Ret. Time	Area%	Height	Conc.
20.913	95.877	1063934	0.000
26.654	4.123	27674	0.000
	100.000	1091608	0.000

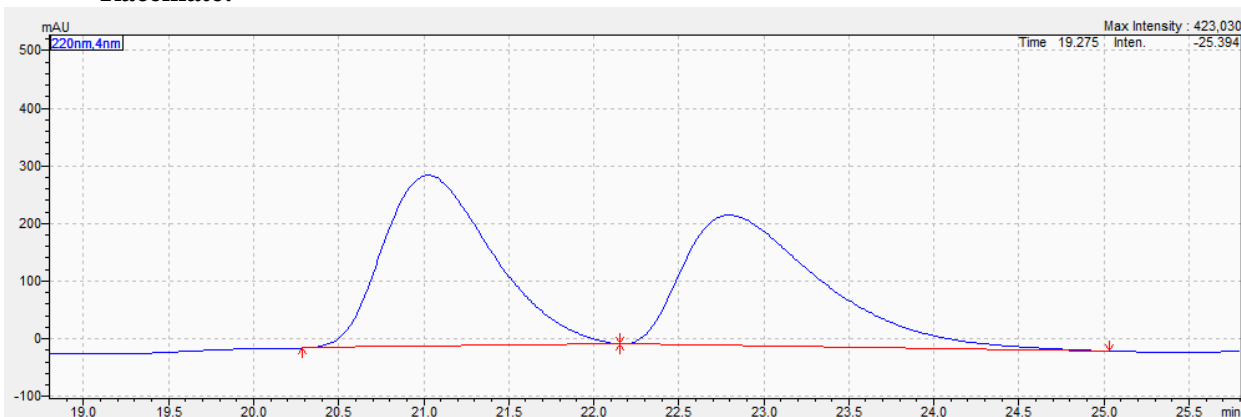
Oxidation Products



2-((1*S*,2*S*)-1-hydroxy-1-(4-methoxyphenyl)-3-oxobutan-2-yl)isoindoline-1,3-dione (2.6a): According to the general oxidation procedure (GP-1/GP-3) using (*S,S*)-Ph-BPE, the product was purified by silica gel chromatography (eluent: 0 – 40% EtOAc in hexanes) to provide 48.1 mg (67%) of **2.6a** as a thick glass as a 97:3 mixture of diastereomers and the major diastereomer in a 99:1 mixture of enantiomers. Upon scaling this reaction to 1.00 mmol, the product **2.6a** was isolated as 252.4 mg (73.2%). $R_f = 0.10$ (25% EtOAc/hexanes). $^1\text{H NMR}$ (CDCl_3 , 600 MHz) δ : 7.78 (dd, $J = 5.5$ Hz, $J = 3.1$ Hz, 2H), 7.71 (dd, $J = 5.5$ Hz, $J = 3.1$ Hz, 2H), 7.26 (d, $J = 8.6$ Hz, 2H), 6.74 (d, $J = 8.6$ Hz, 2H), 5.45 (d, $J = 7.4$ Hz, 1H), 4.93 (d, $J = 7.4$ Hz, 1H), 4.16 (br s, 1H), 3.71 (s, 3H), 2.14 (s, 3H) ppm. $^{13}\text{C NMR}$ (126 MHz, CDCl_3): δ 204.9, 167.4, 159.3, 134.4, 131.2, 131.0, 127.7, 123.6, 113.6, 71.5, 63.9, 55.1, 27.9. HRMS (DART) m/z calcd for $\text{C}_{19}\text{H}_{18}\text{NO}_5$ $[\text{M} + \text{H}]^+$: 340.1185; Found $[\text{M} + \text{H}]^+$: 340.1179.

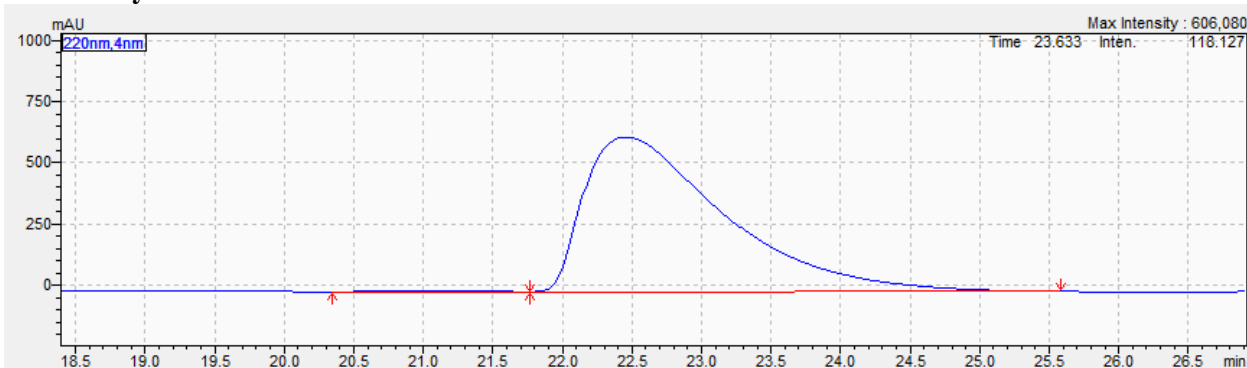
Chiral HPLC Analysis (Chiralpak OD-3 x 250 mm, heptane/isopropanol = 90:10, flow rate = 1.0 ml/min, $\lambda = 220$ nm) $t_R = 21.0$ (minor), 22.7 (major):

Racemate:

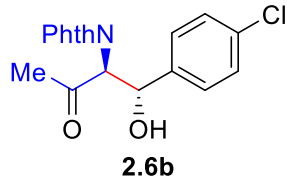


Ret. Time	Area%	Height	Conc.
21.024	51.013	296550	0.000
22.794	48.987	226012	0.000
	100.000	522562	0.000

Asymmetric Reaction:



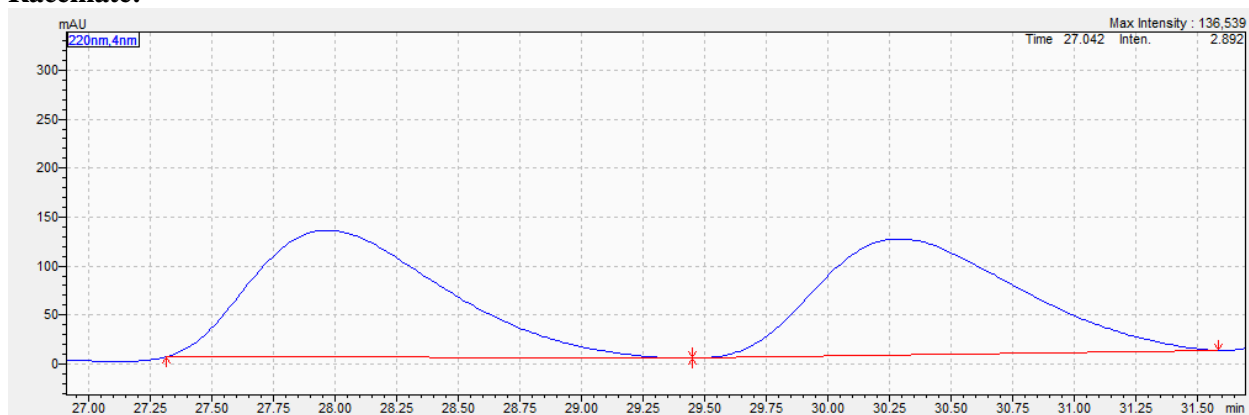
Ret. Time	Area%	Height	Conc.
21.126	0.458	4482	0.000
22.459	99.542	631497	0.000
	100.000	635979	0.000



2-((1S,2S)-1-(4-chlorophenyl)-1-hydroxy-3-oxobutan-2-yl)isoindoline-1,3-dione (2.6b): According to the general oxidation procedure (GP-1/GP-3) using (*R,R*)-Ph-BPE, the product was purified by silica gel chromatography (eluent: 0 – 40% EtOAc in hexanes) to provide 40.8 mg (59%) of **2.6b** as a white foam as a 91:9 mixture of diastereomers and the major diastereomer in a 96.5:3.5 mixture of enantiomers. $R_f = 0.19$ (25% EtOAc/hexanes). $^1\text{H NMR}$ (CDCl_3 , 600 MHz) δ : 7.80 (dd, $J = 5.5$ Hz, $J = 3.0$ Hz, 2H), 7.74 (dd, $J = 5.5$ Hz, $J = 3.0$ Hz, 2H), 7.28 (d, $J = 8.5$ Hz, 2H), 7.19 (d, $J = 8.5$ Hz, 2H), 5.47 (dd, $J = 7.0$ Hz, $J = 2.5$ Hz, 1H), 4.90 (d, $J = 7.8$ Hz, 1H), 4.25 (d, $J = 2.5$ Hz, 1H), 2.12 (s, 3H) ppm. $^{13}\text{C NMR}$ (126 MHz, CDCl_3): δ 204.6, 168.7, 137.5, 134.6, 131.1, 128.5, 128.0, 123.8, 71.4, 63.8, 27.8. HRMS (DART) m/z calcd for $\text{C}_{18}\text{H}_{15}\text{ClNO}_4$ [$\text{M} + \text{H}$] $^+$: 344.0690; Found [$\text{M} + \text{H}$] $^+$: 344.0717.

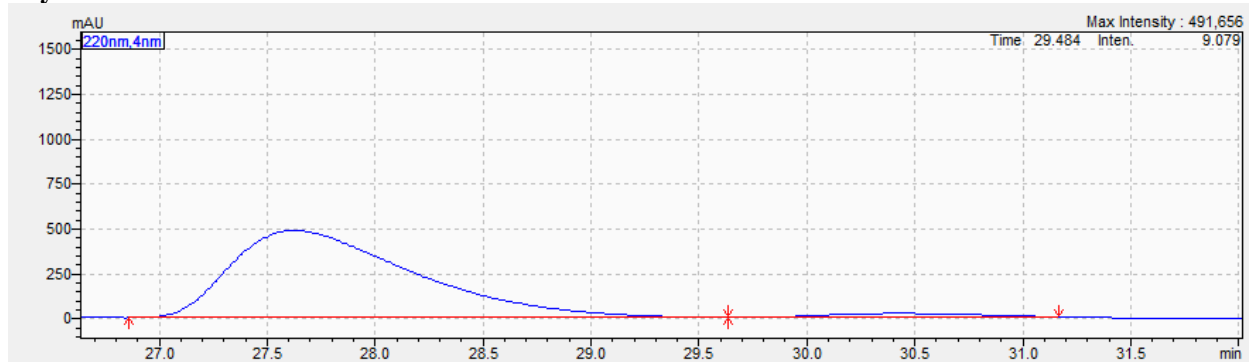
Chiral HPLC Analysis (Chiralpak OD-3 x 250 mm, heptane/isopropanol = 95/5, flow rate = 1.0 ml/min, $\lambda = 220$ nm) tR = 27.9 (major), 30.2 (minor):

Racemate:

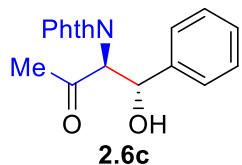


Ret. Time	Area%	Height	Conc.
27.968	51.039	129853	0.000
30.287	48.961	118908	0.000
	100.000	248761	0.000

Asymmetric Reaction:



Ret. Time	Area%	Height	Conc.
27.627	96.614	485561	0.000
30.428	3.386	20873	0.000
	100.000	506434	0.000



2-((1S,2S)-1-hydroxy-3-oxo-1-phenylbutan-2-yl)isoindoline-1,3-dione (2.6c):

According to the general oxidation procedure (GP-1/GP-3) using (*R,R*)-Ph-BPE, the product was purified by silica gel chromatography (eluent: 0 – 40% EtOAc in hexanes) to provide 41.1mg (66%) of **2.6c** as a yellow oil as a 95:5 mixture of diastereomers and the major diastereomer in a 97:3 mixture of enantiomers. $R_f = 0.20$ (25% EtOAc/hexanes). $^1\text{H NMR}$ (CDCl_3 , 600 MHz) δ : 7.78 (dd, $J = 5.6$ Hz, $J = 3.0$ Hz, 2H), 7.71 (dd, $J = 5.6$ Hz, $J = 3.0$ Hz, 2H), 7.34 (d, $J = 7.4$ Hz, 2H), 7.22 (t, $J = 7.4$ Hz, 2H), 7.18 (t, $J = 7.3$ Hz, 1H), 5.48 (dd, $J = 6.7$ Hz, $J = 2.3$ Hz, 1H), 4.97 (d, $J = 6.7$ Hz, 1H), 4.26 (d, $J = 2.4$ Hz, 1H), 2.12 (s, 3H) ppm. $^{13}\text{C NMR}$ (126 MHz, CDCl_3): δ 204.6, 167.5, 134.4, 129.3, 128.9, 128.29, 128.22, 126.4, 123.9, 123.6, 71.8, 64.0, 27.9. HRMS (DART) m/z calcd for $\text{C}_{18}\text{H}_{16}\text{NO}_4$ $[\text{M} + \text{H}]^+$: 310.1079; Found $[\text{M} + \text{H}]^+$: 310.1108.

For this reaction, a portion of the crude mixture was exposed to AcOH/protonation workup (GP-2) to convert to **2.4c** to analyze the enantioselectivity of the reaction.

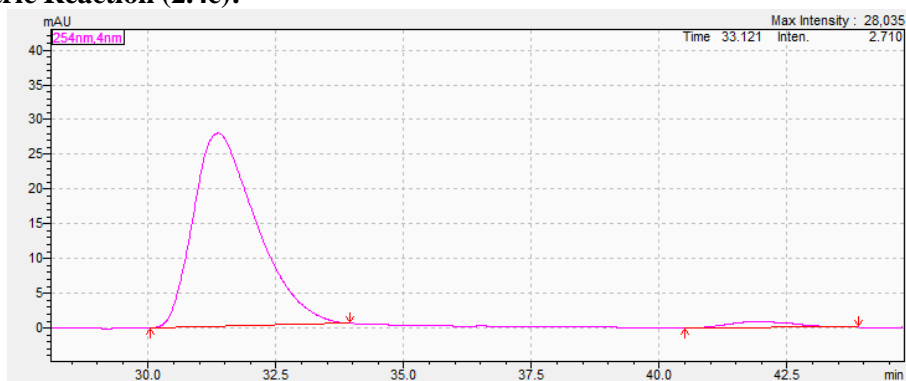
Chiral HPLC Analysis (Chiralpak OD-3 x 250 mm, heptane/isopropanol = 98:2, flow rate = 1.0 ml/min, $\lambda = 254$ nm) $t_R = 30.94$ (major), 40.68 (minor):

Racemate (2.4c):

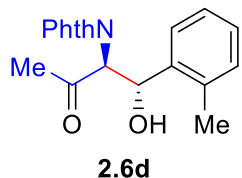


Ret. Time	Area%	Height	Conc.
30.949	50.029	4462	0.000
40.688	49.971	3213	0.000
	100.000	7675	0.000

Asymmetric Reaction (2.4c):



Ret. Time	Area%	Height	Conc.
31.372	96.824	27810	0.000
41.895	3.176	884	0.000
	100.000	28694	0.000

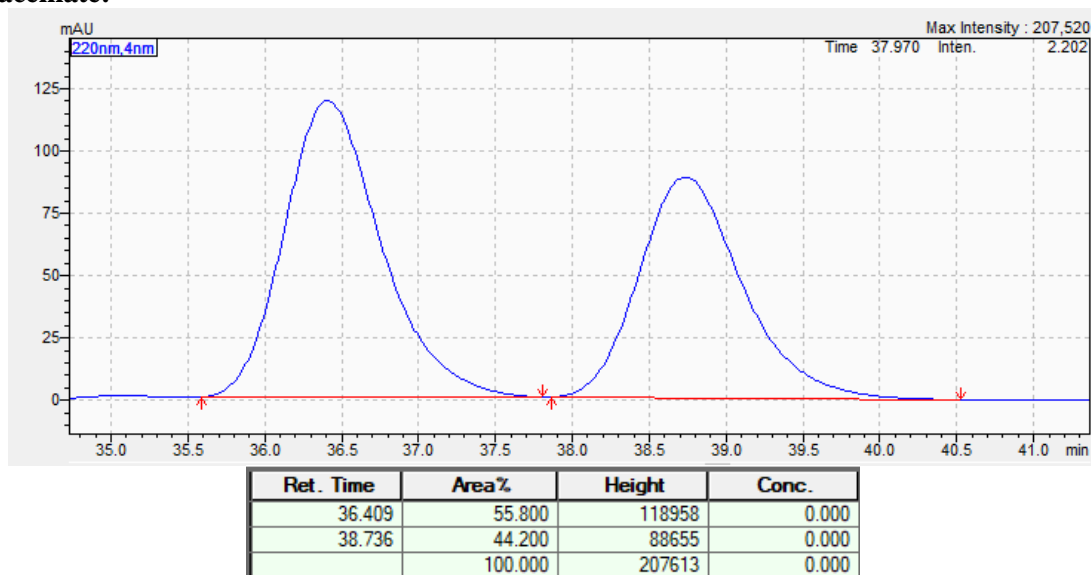


2-((1S,2S)-1-hydroxy-3-oxo-1-(o-tolyl)butan-2-yl)isoindoline-1,3-dione (2.6d):

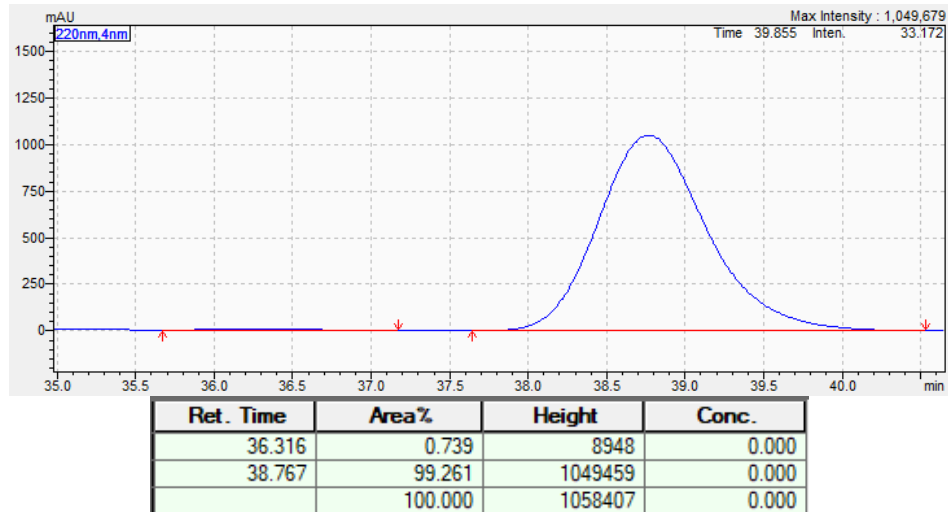
According to the general oxidation procedure (GP-1/GP-3) using (*R,R*)-Ph-BPE, the product was purified by silica gel chromatography (eluent: 0 – 40% EtOAc in hexanes) to provide 24.0 mg (38%) of **2.6d** as a pale yellow oil as a 96:4 mixture of diastereomers and the major diastereomer in a 99:1 mixture of enantiomers. $R_f = 0.20$ (25% EtOAc/hexanes). $^1\text{H NMR}$ (CDCl_3 , 600 MHz) δ : 7.81 (dd, $J = 5.6$ Hz, $J = 3.5$ Hz, 2H), 7.72 (dd, $J = 5.6$ Hz, $J = 3.5$ Hz, 2H), 7.54 (d, $J = 7.8$ Hz, 1H), 7.20 (t, $J = 7.0$ Hz, 1H), 7.16 (t, $J = 7.3$ Hz, 1H), 7.12 (d, $J = 8.1$ Hz, 1H), 7.06 (d, $J = 7.5$ Hz, 1H), 5.65 (dd, $J = 5.6$ Hz, $J = 2.8$ Hz, 1H), 5.10 (d, $J = 5.6$ Hz, $J = 1.5$ Hz, 1H), 4.38 (d, $J = 2.6$ Hz, 1H), 2.30 (s, 3H), 2.14 (s, 3H) ppm. $^{13}\text{C NMR}$ (126 MHz, CDCl_3): δ 203.8, 167.8, 137.0, 135.4, 134.5, 131.3, 130.7, 128.0, 126.9, 123.7, 69.9, 63.8, 28.2, 19.2. HRMS (DART) m/z calcd for $\text{C}_{19}\text{H}_{16}\text{NO}_3$ $[\text{M}-\text{OH}]^+$: 306.1136; Found $[\text{M}-\text{OH}]^+$: 306.1145.

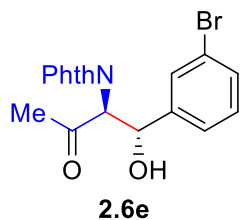
Chiral HPLC Analysis (Chiralpak AD-3 x 250 mm, heptane/isopropanol = 90/10, flow rate = 1.0 ml/min, $\lambda = 220$ nm) $t_R = 36.4$ (major), 38.7 (minor):

Racemate:



Asymmetric Reaction:



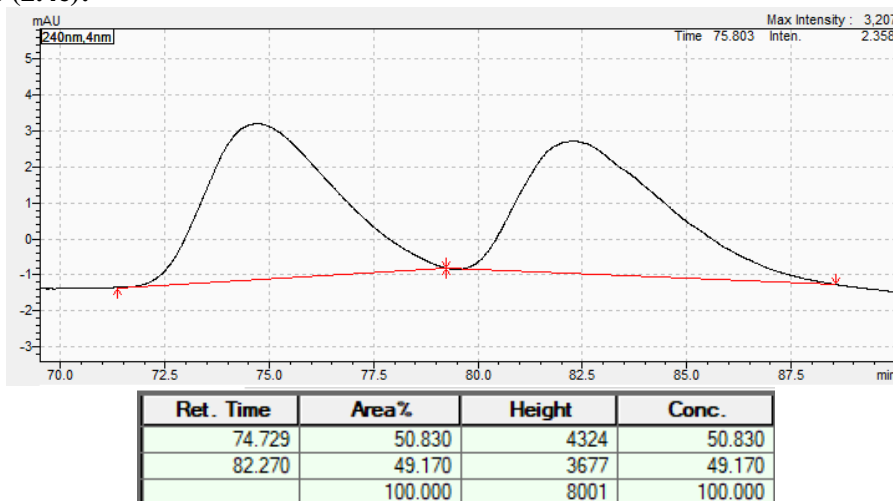


2-((1*S*,2*S*)-1-(3-bromophenyl)-1-hydroxy-3-oxobutan-2-yl)isoindoline-1,3-dione (2.6e): According to the general oxidation procedure (GP-1/GP-3) using (*R,R*)-PhBPE, the product was purified by silica gel chromatography (eluent: 0 – 5% EtOAc in DCM) to provide 36.3 mg (47%) of **2.6e** as a yellow oil as a 95:5 mixture of diastereomers and the main diastereomer in a 99:1 mixture of enantiomers. $R_f = 0.18$ (25% EtOAc/hexanes). $^1\text{H NMR}$ (CDCl_3 , 600 MHz) δ : 7.81 (dd, $J = 5.4$ Hz, $J = 3.1$ Hz, 2H), 7.74 (dd, $J = 5.4$ Hz, $J = 3.1$ Hz, 2H), 7.48 (s, 1H), 7.31 (d, $J = 8.0$ Hz, 1H), 7.28 (d, $J = 7.4$ Hz, 1H), 7.10 (t, $J = 8.0$ Hz, 1H), 5.43 (dd, $J = 6.8$ Hz, $J = 2.4$ Hz, 1H), 4.90 (d, $J = 7.0$ Hz, 1H), 4.33 (d, $J = 2.7$ Hz, 1H), 2.12 (s, 3H) ppm. $^{13}\text{C NMR}$ (126 MHz, CDCl_3): δ 204.2, 167.5, 14.3, 134.6, 131.3, 131.1, 129.9, 129.7, 125.0, 123.8, 122.4, 71.4, 64.0, 27.9. HRMS (DART) m/z calcd for $\text{C}_{18}\text{H}_{15}\text{BrNO}_4$ [$\text{M} + \text{H}$] $^+$: 388.0184; Found [$\text{M} + \text{H}$] $^+$: 388.0213.

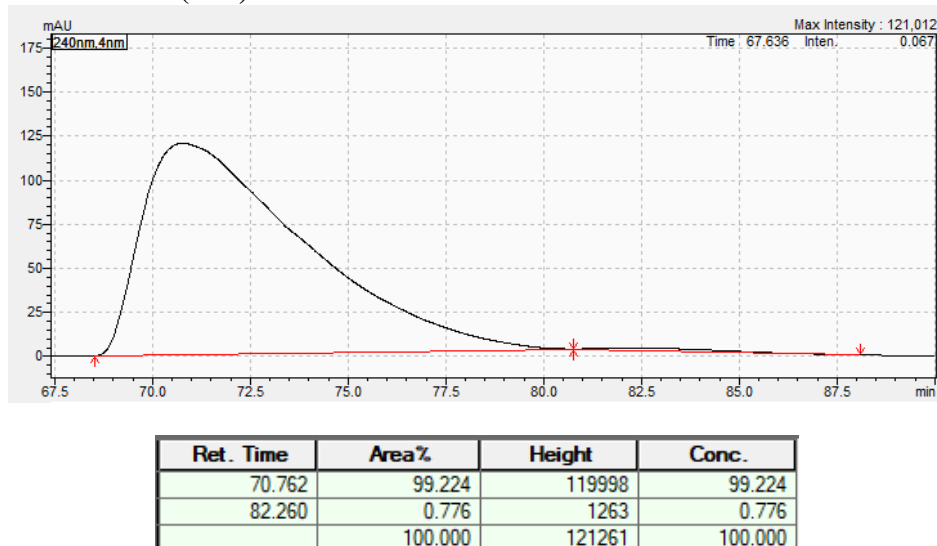
For this reaction, a portion of the crude mixture was exposed to AcOH/protonation workup (GP-2) to convert to **2.4e** to analyze the enantioselectivity of the reaction.

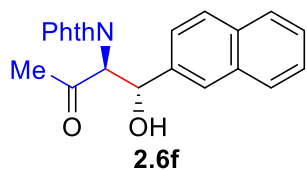
Chiral HPLC Analysis (Chiralpak AD-3 x 250 mm, heptane/isopropanol = 99/1, flow rate = 0.5 ml/min, $\lambda = 240\text{nm}$) $t_R = 74.7$ (major), 82.2 (minor):

Racemate (2.4e):



Asymmetric Reaction (2.4e):

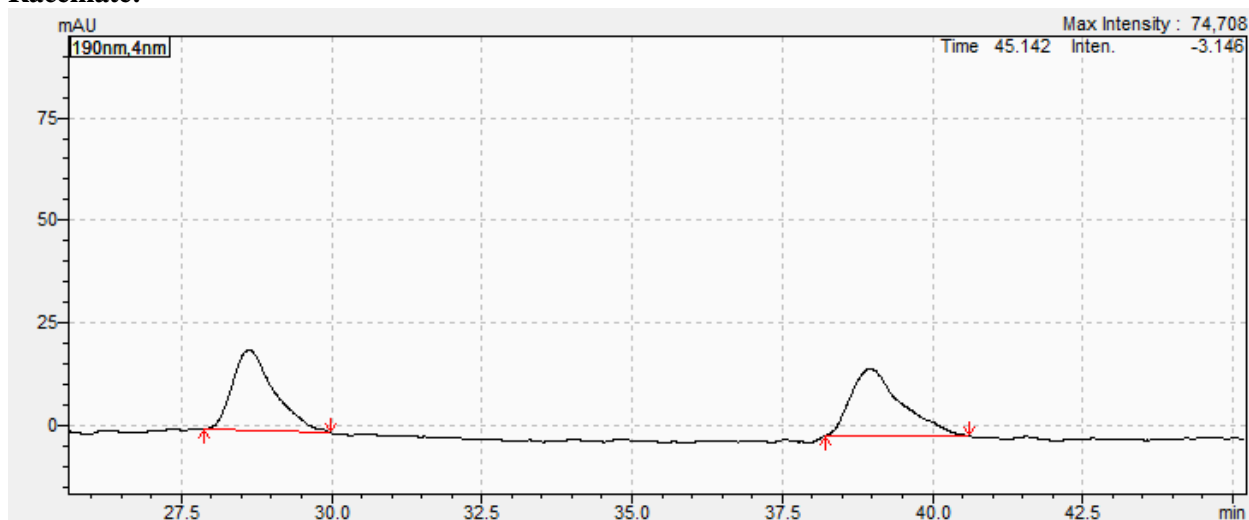




2-((1*S*,2*S*)-1-hydroxy-1-(naphthalen-2-yl)-3-oxobutan-2-yl)isoindoline-1,3-dione (2.6f): According to the general oxidation procedure (GP-1/GP-3), the product was purified by silica gel chromatography (eluent: 0 – 40% EtOAc in hexanes) to provide 52.1mg (70%) of **2.6f** as a yellow solid as a 99:1 mixture of diastereomers and the major diastereomer in a 98.5:1.5 mixture of enantiomers. $R_f = 0.20$ (25% EtOAc/hexanes). $^1\text{H NMR}$ (CDCl_3 , 600 MHz) δ : 7.81 (s, 1H), 7.79-7.73 (m, 4H), 7.71 (d, $J = 7.7$ Hz, 1H), 7.67 (dd, $J = 5.2$ Hz, $J = 3.1$ Hz, 2H), 7.51 (d, $J = 8.5$ Hz, 1H), 7.44-7.38 (m, 2H), 5.67 (dd, $J = 6.3$ Hz, $J = 1.8$ Hz, 1H), 5.14 (d, $J = 6.5$ Hz, 1H), 4.43 (d, $J = 2.4$ Hz, 1H), 2.13 (s, 3H) ppm. $^{13}\text{C NMR}$ (126 MHz, CDCl_3): δ 204.2, 167.6, 136.4, 134.4, 133.1, 132.9, 131.2, 128.3, 128.0, 127.6, 126.13, 126.10, 125.9, 123.9, 123.7, 72.2, 64.3, 28.1. HRMS (DART) m/z calcd for $\text{C}_{22}\text{H}_{16}\text{NO}_3$ $[\text{M} - \text{OH}]^+$: 342.1136; Found $[\text{M} - \text{OH}]^+$: 342.1138.

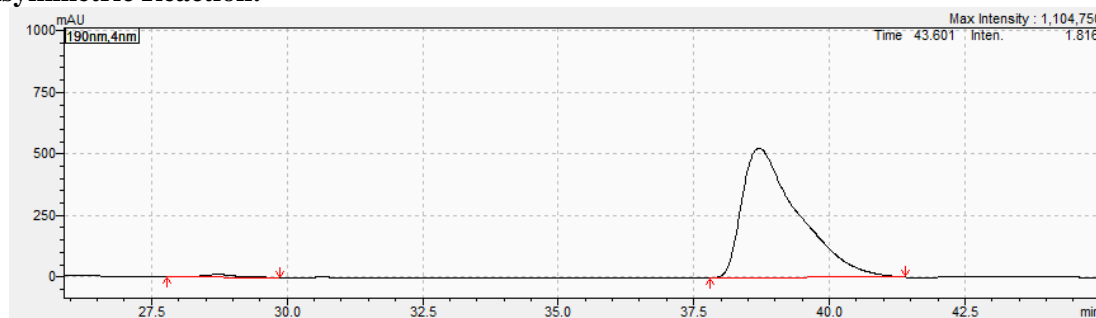
Chiral HPLC Analysis (Chiralpak IC-3 x 250 mm, heptane/isopropanol = 90/10, flow rate = 1.0 ml/min, $\lambda = 190$ nm) $t_R = 28.6$ (major), 38.9 (minor):

Racemate:

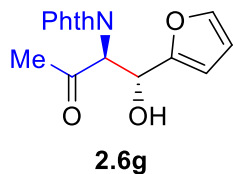


Ret. Time	Area%	Height	Conc.
28.624	49.894	19622	49.894
38.968	50.106	16350	50.106
	100.000	35973	100.000

Asymmetric Reaction:



Ret. Time	Area%	Height	Conc.
28.741	1.392	12118	1.392
38.702	98.608	526965	98.608
	100.000	539083	100.000



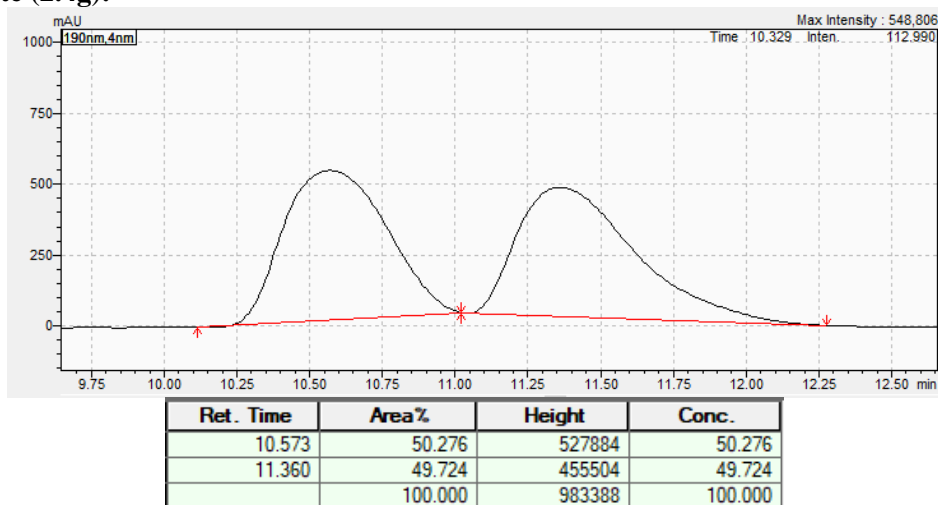
2-((1S,2S)-1-cyclopropyl-1-hydroxy-3-oxobutan-2-yl)isoindoline-1,3-dione (2.6g):

According to the general oxidation procedure (GP-1/GP-3) using (*R,R*)-Ph-BPE, the product was purified by silica gel chromatography (eluent: 0 – 40% EtOAc in hexanes) to provide 43.3mg (72%) of **2.6g** as a white foam as a single diastereomer and the major diastereomer as a 99:1 mixture of enantiomers. $R_f = 0.17$ (25% EtOAc/hexanes). $^1\text{H NMR}$ (CDCl_3 , 600 MHz) δ : 7.85 (dd, $J = 5.5$ Hz, $J = 3.0$ Hz, 2H), 7.75 (dd, $J = 5.5$ Hz, $J = 3.0$ Hz, 2H), 7.31 (dd, $J = 1.8$ Hz, $J = 0.8$ Hz, 1H), 6.35 (dt, $J = 3.2$ Hz, $J = 0.7$ Hz, 1H), 6.26 (dd, $J = 3.2$ Hz, $J = 1.8$ Hz, 1H), 5.51 (dd, $J = 5.6$ Hz, $J = 2.6$ Hz, 1H), 5.23 (d, $J = 5.8$ Hz, 1H), 4.42 (d, $J = 3.1$ Hz, 1H), 2.12 (s, 3H) ppm. $^{13}\text{C NMR}$ (126 MHz, CDCl_3): δ 203.2, 167.7, 151.8, 142.5, 134.5, 131.3, 123.7, 110.5, 108.1, 67.0, 62.5, 27.7. HRMS (DART) m/z calcd for $\text{C}_{16}\text{H}_{12}\text{NO}_4$ [M-OH] $^+$: 282.0772; Found [M-OH] $^+$: 282.0762.

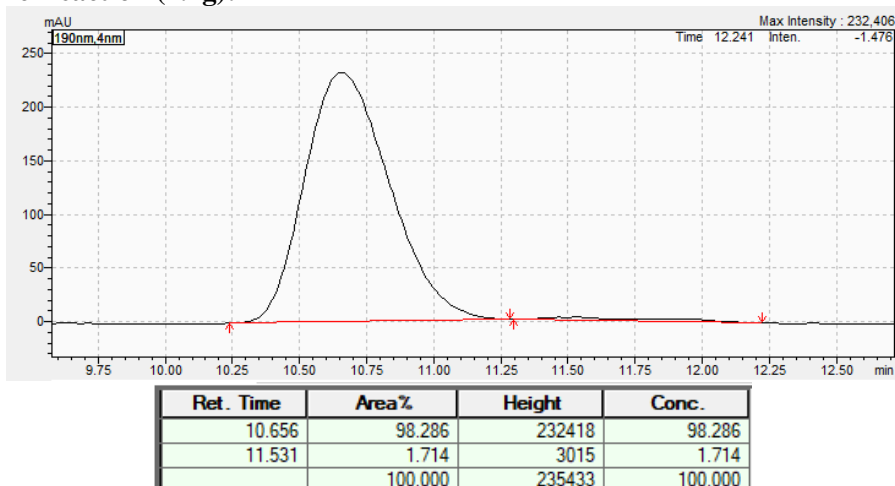
For this reaction, a portion of the crude mixture was exposed to AcOH/protonation workup (GP-2) to convert to **2.4g** to analyze the enantioselectivity.

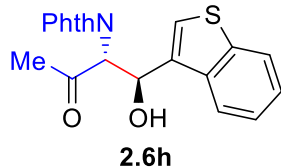
Chiral HPLC Analysis (Chiralpak OD-3 x 250 mm, heptane/isopropanol = 90/10, flow rate = 1.0 ml/min, $\lambda = 190$ nm) tR = 10.65 (major), 11.53 (minor):

Racemate (2.4g):



Asymmetric Reaction (2.4g):

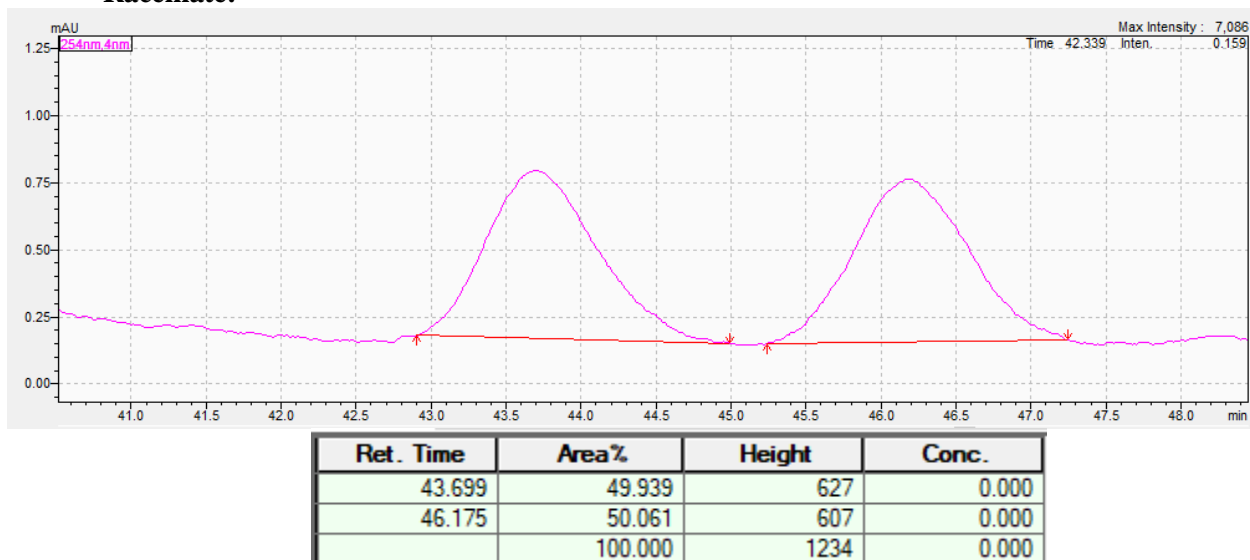




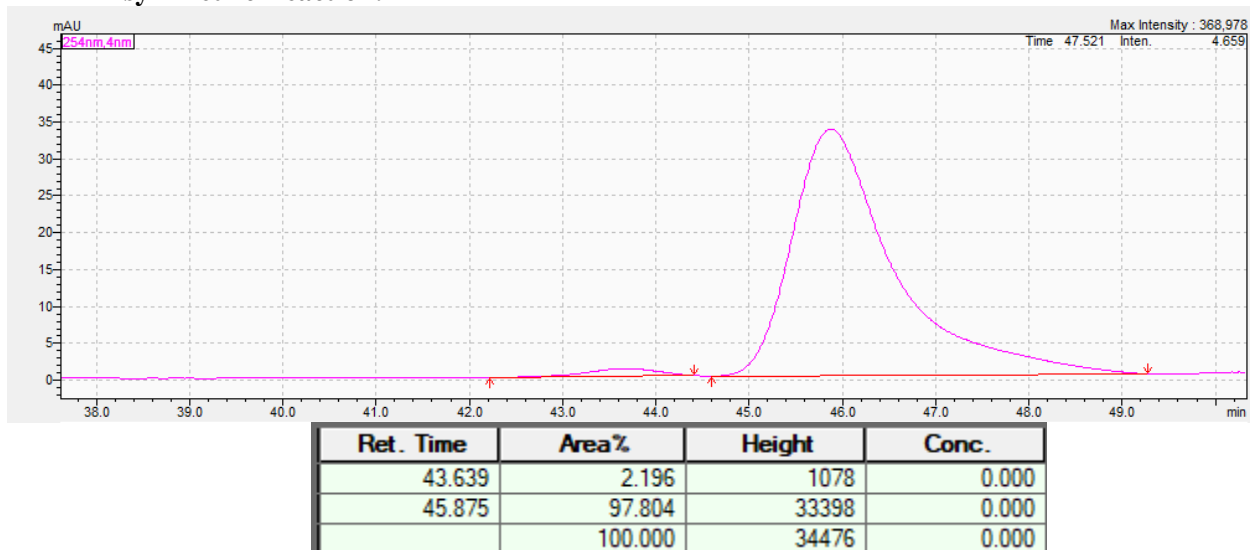
2-((1S,2S)-1-(benzo[b]thiophen-3-yl)-1-hydroxy-3-oxobutan-2-yl)isoindoline-1,3-dione (2.6h): According to the general oxidation procedure (GP-1/GP-3) using (*S,S*)-PhBPE, the product was purified by silica gel chromatography (eluent: 0 – 30% EtOAc in hexanes) to provide 50.7 mg (69%) of **2.6h** as a white foam as a >99:1 mixture of diastereomers and the major diastereomer in a 98:2 mixture of enantiomers. $R_f = 0.20$ (25% EtOAc/hexanes). $^1\text{H NMR}$ (CDCl_3 , 600 MHz) δ : 7.77 - 7.81 (m, 4H), 7.71 (dd, $J = 5.3$ Hz, $J = 3.3$ Hz, 2H), 7.57 (s, 1H), 7.33 (t, $J = 7.8$ Hz, 1H), 7.29 (t, $J = 7.8$ Hz, 1H), 7.81 (dd, $J = 5.3$ Hz, $J = 2.5$ Hz, 1H), 5.32 (d, $J = 5.3$ Hz, 1H), 4.64 (d, $J = 2.8$ Hz, 1H), 2.14 (s, 3H) ppm. $^{13}\text{C NMR}$ (126 MHz, CDCl_3): δ 203.2, 167.9, 140.7, 136.6, 134.5, 134.2, 131.3, 124.8, 124.5, 124.3, 123.7, 122.9, 121.9, 69.0, 63.7, 28.3 ppm. HRMS (DART) m/z calcd for $\text{C}_{20}\text{H}_{14}\text{NO}_3\text{S}$ $[\text{M-OH}]^+$: 348.0689; Found $[\text{M-OH}]^+$: 348.0674.

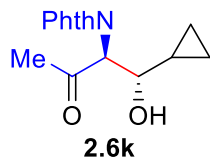
Chiral HPLC Analysis (Chiralpak AD-3 x 250 mm, heptane/isopropanol = 90/10, flow rate = 1.0 ml/min, $\lambda = 254$ nm) $t_R = 43.63$ (minor), 46.18 (major):

Racemate:



Asymmetric Reaction:





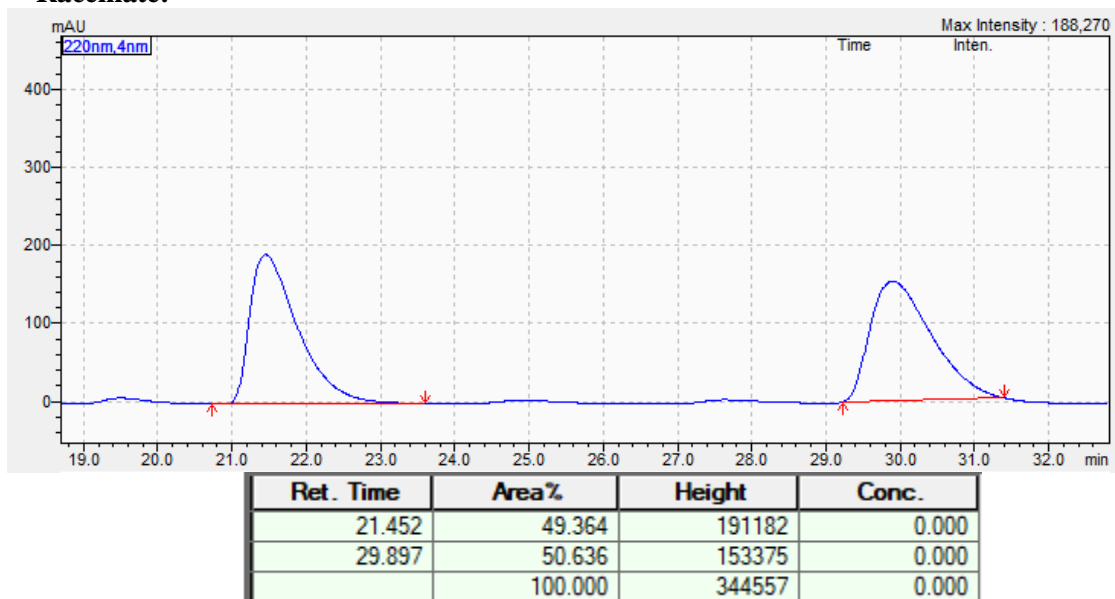
2-((1S,2S)-1-cyclopropyl-1-hydroxy-3-oxobutan-2-yl)isoindoline-1,3-dione (2.6k):

According to the general oxidation procedure (GP-1/GP-3) using (*R,R*)-Ph-BPE, the product was purified by silica gel chromatography (eluent: 0 – 40% EtOAc in hexanes) to provide 37.4mg (67%) of **2.6k** as a clear oil as a single diastereomer and the major diastereomer as a 99:1 mixture of enantiomers. $R_f = 0.14$ (25% EtOAc/hexanes).

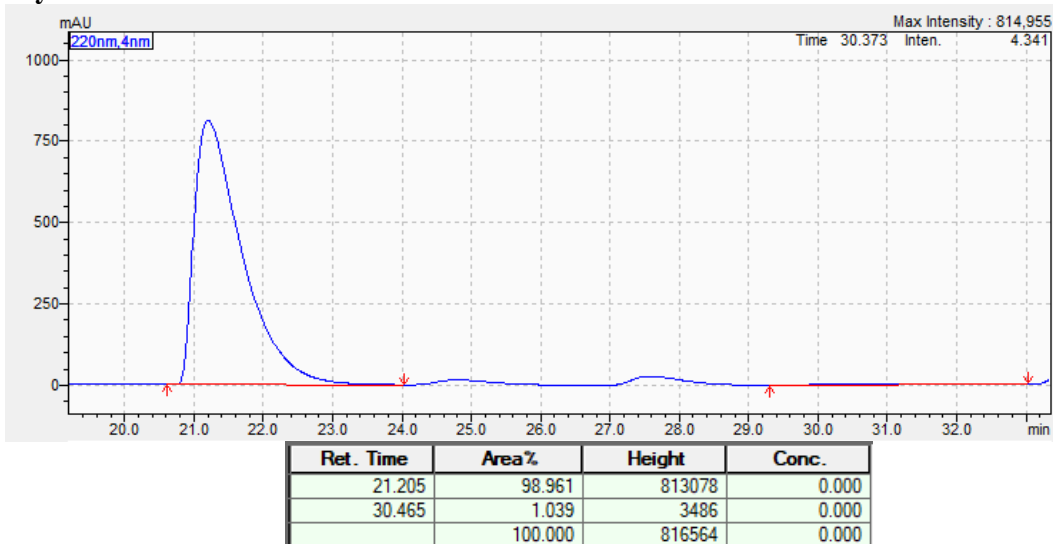
$^1\text{H NMR}$ (CDCl_3 , 600 MHz) δ : 7.91 (dd, $J = 5.7\text{ Hz}$, $J = 3.2\text{ Hz}$, 2H), 7.80 (dd, $J = 5.7\text{ Hz}$, $J = 3.2\text{ Hz}$, 2H), 4.79 (d, $J = 6.7\text{ Hz}$, 1H), 3.79 (d, $J = 3.8\text{ Hz}$, 1H), 3.63 (ddd, $J = 10.2\text{ Hz}$, $J = 7.4\text{ Hz}$, $J = 2.5\text{ Hz}$, 1H), 2.23 (s, 3H), 1.00-0.91 (m, 1H), 0.58-0.47 (m, 1H), 0.43-0.34 (m, 1H), 0.31-0.22 (m, 1H), 0.1-0.03 (m, 1H) ppm. $^{13}\text{C NMR}$ (126 MHz, CDCl_3): δ 205.1, 167.9, 134.6, 131.5, 123.8, 74.1, 63.0, 27.5, 14.4, 2.37, 2.32. HRMS (DART) m/z calcd for $\text{C}_{15}\text{H}_{16}\text{NO}_4$ $[\text{M} + \text{H}]^+$: 274.1079; Found $[\text{M} + \text{H}]^+$: 274.1071.

Chiral HPLC Analysis (Chiralpak OD-3 x 250 mm, heptane/isopropanol = 95/5, flow rate = 1.0 ml/min, $\lambda = 220\text{ nm}$) $t_R = 21.4$ (major), 29.8 (minor):

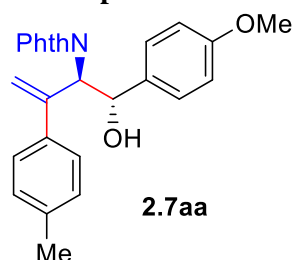
Racemate:



Asymmetric Reaction:



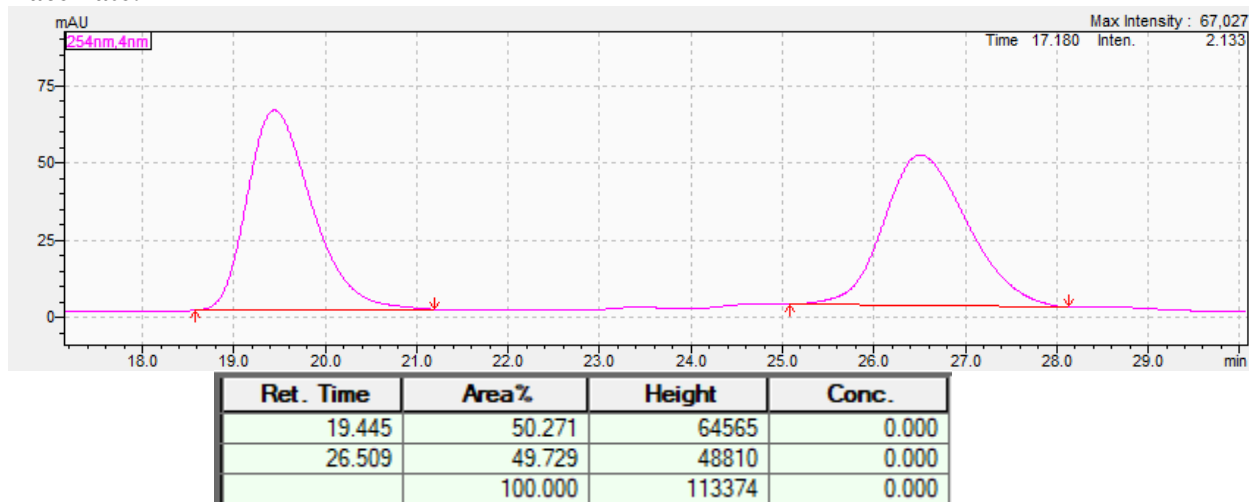
Suzuki products



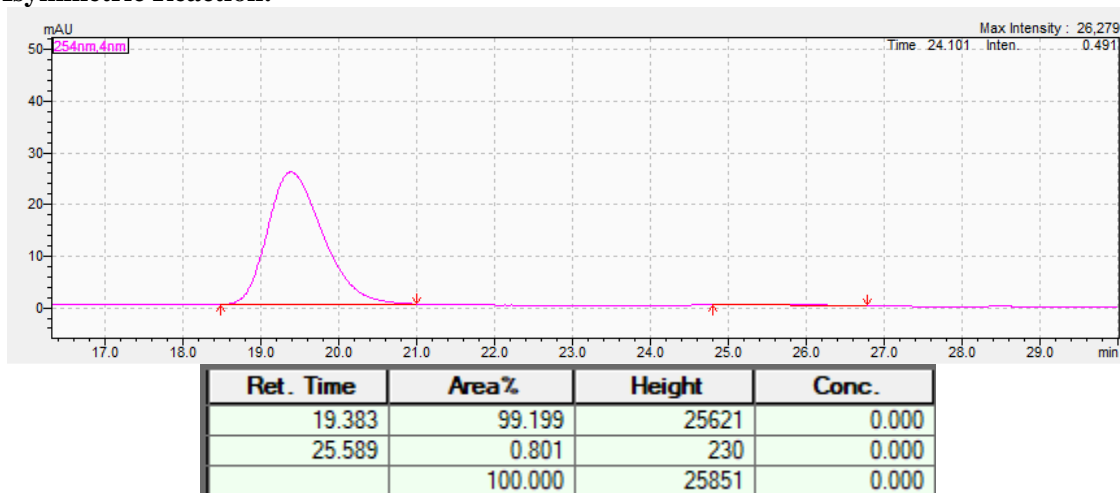
2-((1*S*,2*R*)-1-hydroxy-1-(4-methoxyphenyl)-3-(*p*-tolyl)but-3-en-2-yl)isoindoline-1,3-dione (13aa**):** According to the General Suzuki-Miyaura procedure (GP-1/GP-4) using (*S,S*)-PhBPE, the product was purified by silica gel chromatography (eluent: 0 – 40% EtOAc in hexanes) to provide 53.1 mg (64%) of **13aa** as a pale red/pink foam as a 97:3 mixture of diastereomers and the major diastereomer as an 99:1 mixture of enantiomers. Absolute and relative configuration was assigned by analogy to **5i**, **5k**, and **5n**. $R_f = 0.10$ (25% EtOAc/hexanes). $^1\text{H NMR}$ (CDCl_3 , 600 MHz) δ : 7.63 (dd, $J = 5.2$ Hz, $J = 2.8$ Hz, 2H), 7.58 (dd, $J = 5.3$ Hz, $J = 2.9$ Hz, 2H), 7.35 (d, $J = 8.2$ Hz, 2H), 7.32 (d, $J = 8.2$ Hz, 2H), 7.06 (d, $J = 7.3$ Hz, 2H), 6.71 (d, $J = 8.5$ Hz, 2H), 5.90 (s, 1H), 5.75 (d, $J = 9.1$ Hz, 1H), 5.69 (s, 1H), 5.49 (d, $J = 8.8$ Hz, 1H), 3.69 (s, 3H), 2.59 (br s, 1H), 2.28 (s, 3H) ppm. $^{13}\text{C NMR}$ (126 MHz, CDCl_3): δ 167.6, 159.3, 144.3, 137.6, 137.5, 133.7, 132.3, 131.2, 128.9, 127.9, 126.6, 123.0, 116.9, 113.6, 72.55, 58.24, 55.09, 21.03 ppm. HRMS (DART) m/z calcd for $\text{C}_{26}\text{H}_{22}\text{NO}_3$ $[\text{M}-\text{OH}]^+$: 396.1605; Found $[\text{M}-\text{OH}]^+$: 396.1580.

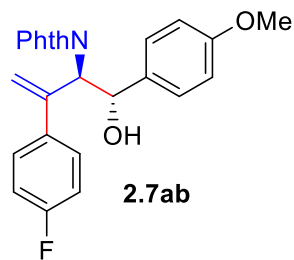
Chiral HPLC Analysis (Chiralpak IC-3 x 250 mm, heptane/isopropanol = 90/10, flow rate = 1.0 ml/min, $\lambda = 220$ nm) $t_R = 19.44$ (major), 26.50 (minor):

Racemate:



Asymmetric Reaction:

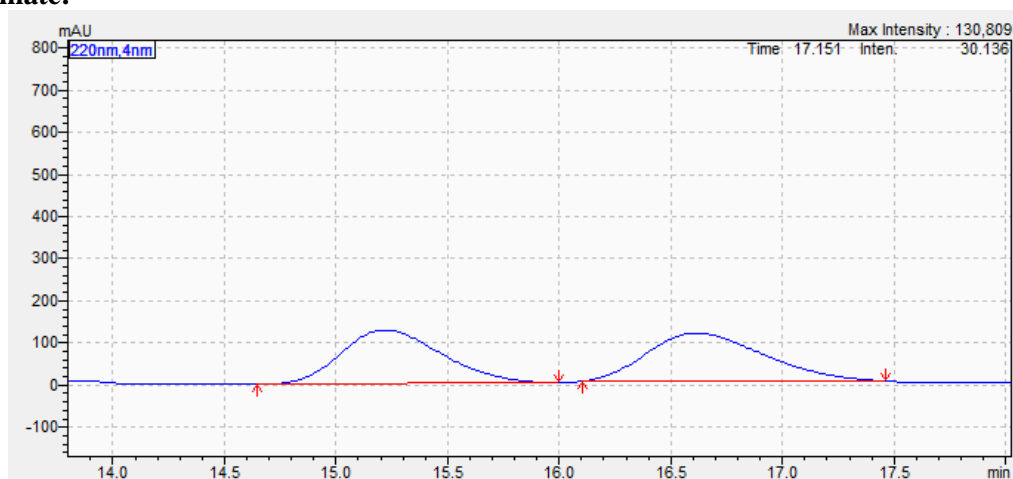




2-((1*S*,2*R*)-3-(4-fluorophenyl)-1-hydroxy-1-(4-methoxyphenyl)but-3-en-2-yl)isoindoline-1,3-dione (13ab**):** According to the General Suzuki-Miyaura procedure (GP-1/GP-4) using (*S,S*)-Ph-BPE, the product was purified by silica gel chromatography (eluent: 0 – 40% EtOAc in hexanes) to provide 65.3mg (76%) of **13ab** as a pale red/pink foam as a 97:3 mixture of diastereomers and the major diastereomer as an 99:1 mixture of enantiomers. Absolute and relative configuration was assigned by analogy to **5i**, **5k**, and **5n**. $R_f = 0.17$ (25% EtOAc/hexanes). $^1\text{H NMR}$ (CDCl_3 , 600 MHz) δ : 7.63-7.66 (m, 2H), 7.58-7.60 (m, 2H), 7.39 (dd, $J = 9.1$ Hz, $J = 6.2$ Hz, 2H), 7.30 (d, $J = 9.1$ Hz, 1H), 6.93 (t, $J = 8.3$ Hz, 2H), 6.71 (d, $J = 8.6$ Hz, 2H), 5.89 (s, 1H), 5.72 (d, $J = 8.4$ Hz, 1H), 5.62 (s, 1H), 5.45 (d, $J = 8.4$ Hz, 1H), 3.68 (s, 3H), 2.69 (br s, 1H) ppm. $^{13}\text{C NMR}$ (126 MHz, CDCl_3): δ 167.7, 162.3 (d, $J = 245.8$ Hz), 159.3, 143.7, 136.7 (d, $J = 3.4$ Hz), 133.9, 132.3, 131.1, 128.5 (d, $J = 7.6$ Hz), 127.8, 123.1, 117.5, 115.0 (d, $J = 22.0$ Hz), 113.7, 72.6, 58.5, 55.1 ppm. $^{19}\text{F NMR}$ (CDCl_3 , 565 MHz) δ : -114.74 ppm. HRMS (DART) m/z calcd for $\text{C}_{25}\text{H}_{19}\text{FNO}_3$ $[\text{M}-\text{OH}]^+$: 400.1354; Found $[\text{M}-\text{OH}]^+$: 400.1376.

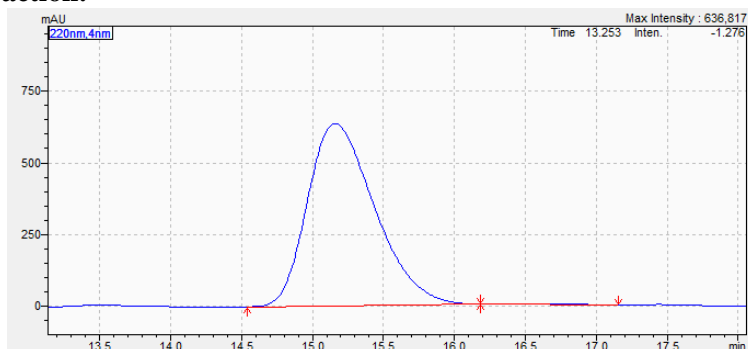
Chiral HPLC Analysis (Chiralpak OD-3 x 250 mm, heptane/isopropanol = 90/10, flow rate = 1.0 ml/min, $\lambda = 220$ nm) tR = 15.21 (major), 16.61 (minor):

Racemate:

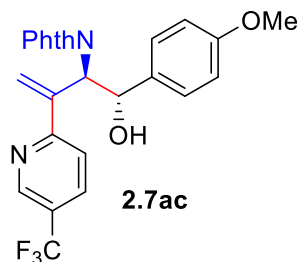


Ret. Time	Area%	Height	Conc.
15.219	49.046	127446	0.000
16.615	50.954	113903	0.000
	100.000	241349	0.000

Asymmetric Reaction:



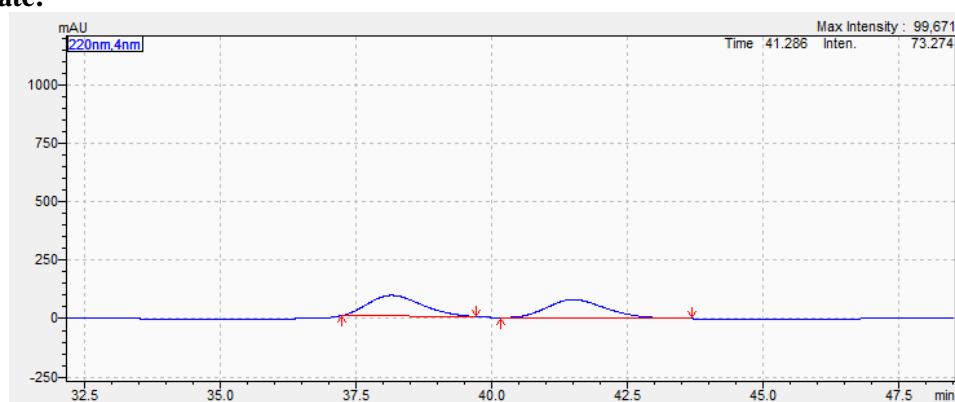
Ret. Time	Area%	Height	Conc.
15.161	99.655	634789	0.000
16.403	0.345	2247	0.000
	100.000	637036	0.000



2-((1*S*,2*R*)-1-hydroxy-1-(4-methoxyphenyl)-3-(5-(trifluoromethyl) pyridin-2-yl)but-3-en-2-yl)isoindoline-1,3-dione (13ac**):** According to the General Suzuki-Miyaura procedure (GP-1/GP-4) using (*S,S*)-PhBPE, the product was purified by silica gel chromatography (eluent: 0 – 20% EtOAc in CH₂Cl₂) to provide 78.6 mg (75%) of **13ac** as a off-white foam as a single diastereomer and the major diastereomer as an 99:1 mixture of enantiomers. Absolute and relative configuration was assigned by analogy to **5i**, **5k**, and **5n**. *R_f* = 0.12 (25% EtOAc/hexanes). ¹HNMR (CDCl₃, 600 MHz) δ : 8.81 (s, 1H), 7.92 (d, *J* = 8.0 Hz, 1H), 7.69 (dd, *J* = 6.7 Hz, *J* = 4.0 Hz, 2H), 7.67-7.62 (m, 2H), 7.59 (d, *J* = 8.6 Hz, 1H), 7.30 (d, *J* = 8.3 Hz, 2H), 6.71 (d, *J* = 8.3 Hz, 2H), 6.14 (s, 1H), 5.99 (s, 1H), 5.78 (d, *J* = 8.8 Hz, 1H), 5.68 (dd, *J* = 8.6 Hz, *J* = 3.0 Hz, 1H), 4.74 (d, *J* = 3.0 Hz, 1H), 3.70 (s, 3H) ppm. ¹³C NMR (126 MHz, CDCl₃): δ 167.8, 159.2, 144.5, 134.1, 134.0, 132.7, 131.3, 127.9, 127.8, 123.9, 123.2, 121.4, 113.7, 113.6, 72.0, 58.3, 55.1. ¹⁹F NMR (CDCl₃, 561 MHz) δ : -63.36 ppm. HRMS (DART) *m/z* calcd for C₂₅H₁₈F₃N₂O₃ [M-OH]⁺: 451.1275; Found [M-OH]⁺: 451.1292.

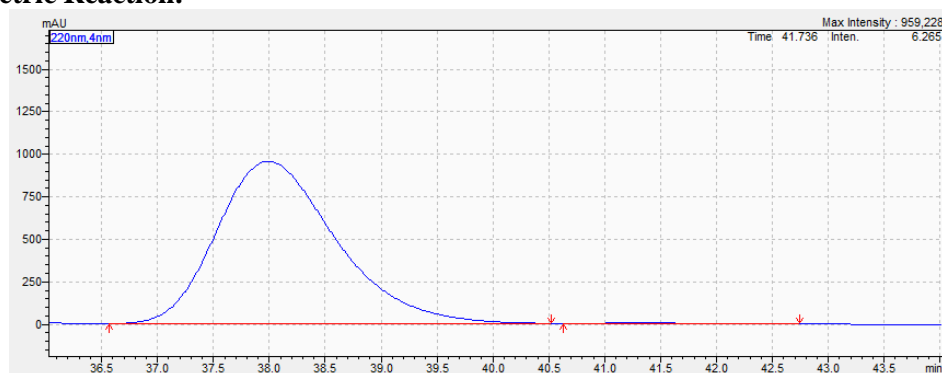
Chiral HPLC Analysis (Chiralpak AD-3 x 250 mm, heptane/isopropanol = 80/20, flow rate = 1.0 ml/min, λ = 220 nm) t_R = 38.1 (major), 41.5 (minor):

Racemate:

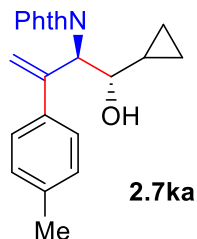


Ret. Time	Area%	Height	Conc.
38.163	50.528	88221	0.000
41.507	49.472	78645	0.000
	100.000	166865	0.000

Asymmetric Reaction:



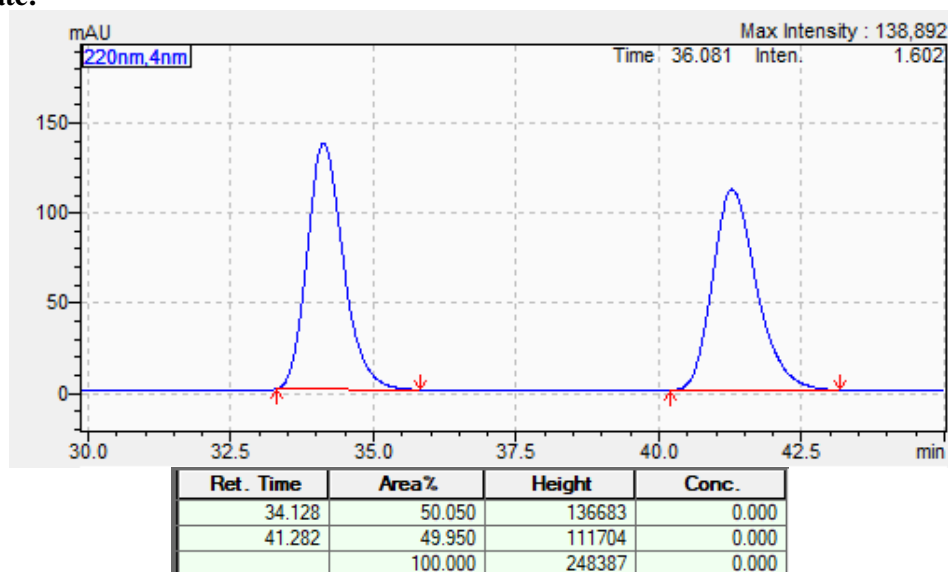
Ret. Time	Area%	Height	Conc.
37.992	99.675	954733	0.000
41.328	0.325	3831	0.000
	100.000	958564	0.000



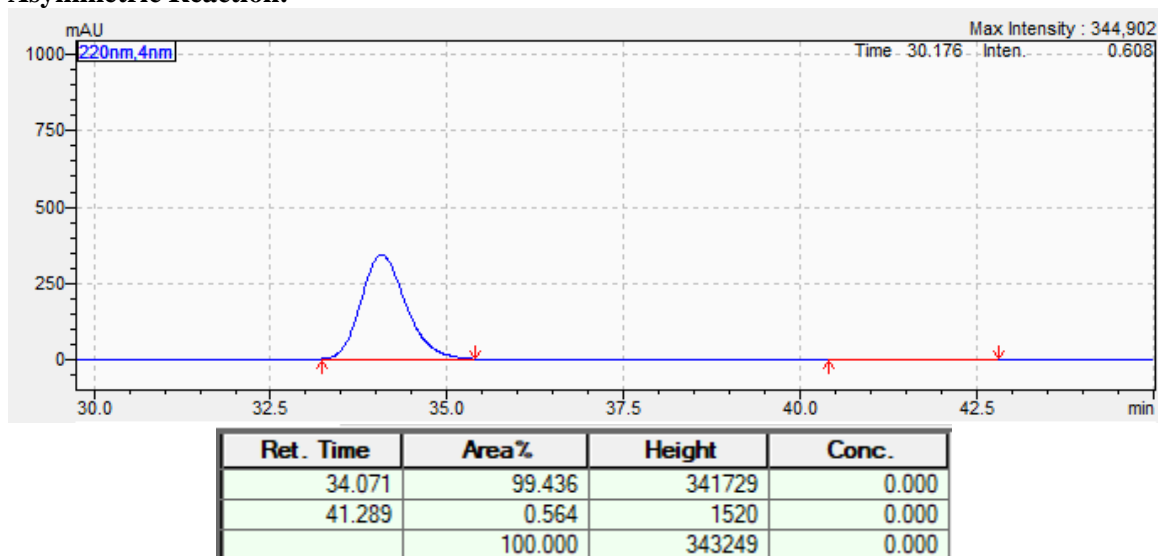
2-((1*S*,2*R*)-1-cyclopropyl-1-hydroxy-3-(*p*-tolyl)but-3-en-2-yl)isoindoline-1,3-dione (2.7ka): According to the General Suzuki-Miyaura procedure (GP-1/GP-4) using (*S,S*)-Ph-BPE, the product was purified by silica gel chromatography (eluent: 0 – 40% EtOAc in hexanes) to provide 30.5 mg (45%) of **2.7ka** as a pale red/pink foam as a 97:3 mixture of diastereomers and the major diastereomer as a >99:1 mixture of enantiomers. $R_f = 0.23$ (25% EtOAc/hexanes). $^1\text{H NMR}$ (CDCl_3 , 600 MHz) δ : 7.76 – 7.80 (m, 2H), 7.66 – 7.69 (m, 2H), 7.37 (d, $J = 7.7$ Hz, 2H), 7.08 (d, $J = 7.7$ Hz, 2H), 5.61 (s, 2H), 5.44 (d, $J = 7.2$ Hz, 1H), 3.81 (t, $J = 8.0$ Hz, 1H), 2.78 (br s, 1H), 2.28 (s, 3H), 0.88 – 0.91 (m, 1H), 0.45 – 0.50 (m, 1H), 0.34 – 0.38 (m, 1H), 0.22 – 0.27 (m, 1H), 0.17 – 0.20 (m, 1H) ppm. $^{13}\text{C NMR}$ (126 MHz, CDCl_3): δ 168.4, 143.6, 137.6, 137.5, 134.2, 134.0, 131.4, 128.9, 126.6, 123.3, 116.5, 75.02, 57.99, 21.04, 15.56, 2.62, 2.47. HRMS (DART) m/z calcd for $\text{C}_{22}\text{H}_{20}\text{NO}_2$ [M-OH] $^+$: 330.1500; Found [M-OH] $^+$: 330.1499.

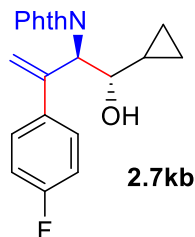
Chiral HPLC Analysis (Chiralpak AD-3 x 250 mm, heptane/isopropanol = 90/10, flow rate = 1.0 ml/min, $\lambda = 220\text{nm}$) $t_R = 34.12$ (major), 41.28 (minor):

Racemate:



Asymmetric Reaction:

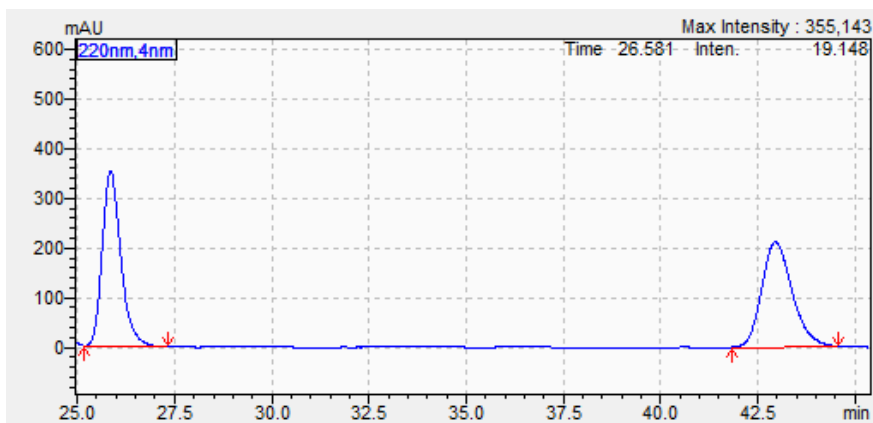




2-((1S,2R)-1-cyclopropyl-3-(4-fluorophenyl)-1-hydroxybut-3-en-2-yl)isoindoline-1,3-dione (2.7kb): According to the General Suzuki-Miyaura procedure (GP-1/GP-4) using (*S,S*)-PhBPE, the product was purified by silica gel chromatography (eluent: 0 – 40% EtOAc in hexanes) to provide 42.4 mg (60%) of **2.7kb** as a pale red/pink foam as a 97/3 mixture of diastereomers and the major diastereomer as an 99:1 mixture of enantiomers. $R_f = 0.27$ (25% EtOAc/hexanes). $^1\text{H NMR}$ (CDCl_3 , 600 MHz) δ : 7.79 (dd, $J = 4.9$ Hz, $J = 3.0$ Hz, 2H), 7.70 (dd, $J = 4.9$ Hz, $J = 3.0$ Hz, 2H), 7.44 (dd, $J = 8.6$ Hz, $J = 5.1$ Hz, 2H), 6.96 (dd, $J = 9.1$ Hz, $J = 8.3$ Hz, 2H), 5.63 (s, 1H), 5.57 (s, 1H), 5.39 (d, $J = 6.7$ Hz, 1H), 3.79 (dd, $J = 8.3$ Hz, $J = 7.2$ Hz, 1H), 2.82 (br s, 1H), 0.91-0.83 (m, 1H), 0.51-0.47 (m, 1H), 0.39-0.32 (m, 1H), 0.30-0.22 (m, 1H), 0.22-0.15 (m, 1H) ppm. $^{13}\text{C NMR}$ (126 MHz, CDCl_3): δ 168.4, 162.4 (d, $J = 247.4$ Hz), 143.0, 136.7 (d, $J = 3.5$ Hz), 134.1, 131.3, 128.5 (d, $J = 7.7$ Hz), 123.3, 117.3, 115.1 (d, $J = 21.1$ Hz), 75.0, 58.2, 15.7, 2.6, 2.5. $^{19}\text{F NMR}$ (CDCl_3 , 561 MHz) δ : -114.52 ppm. H HRMS (DART) m/z calcd for $\text{C}_{21}\text{H}_{17}\text{FNO}_2$ [M-OH] $^+$: 334.1249; Found [M-OH] $^+$: 334.1265.

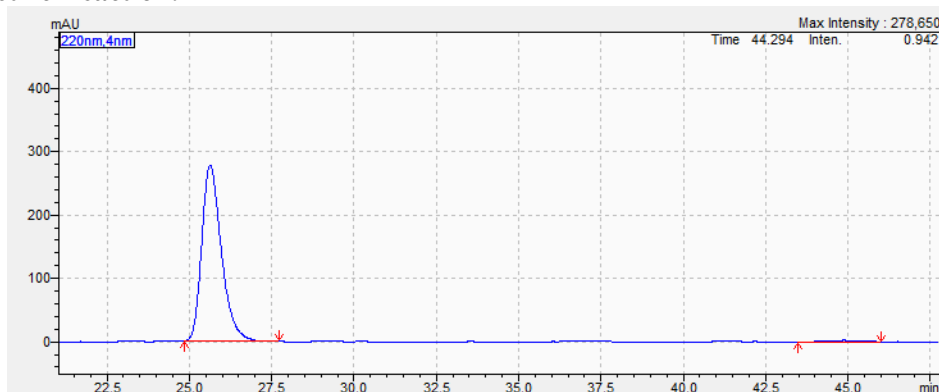
Chiral HPLC Analysis (Chiralpak AD-3 x 250 mm, heptane/isopropanol = 90/10, flow rate = 1.0 ml/min, $\lambda = 220$ nm) tR = 25.85 (major), 42.95 (minor):

Racemate:

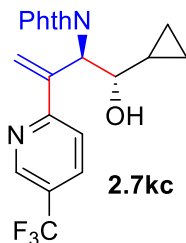


Ret. Time	Area%	Height	Conc.
25.856	50.442	352477	0.000
42.956	49.558	211419	0.000
	100.000	563896	0.000

Asymmetric Reaction:



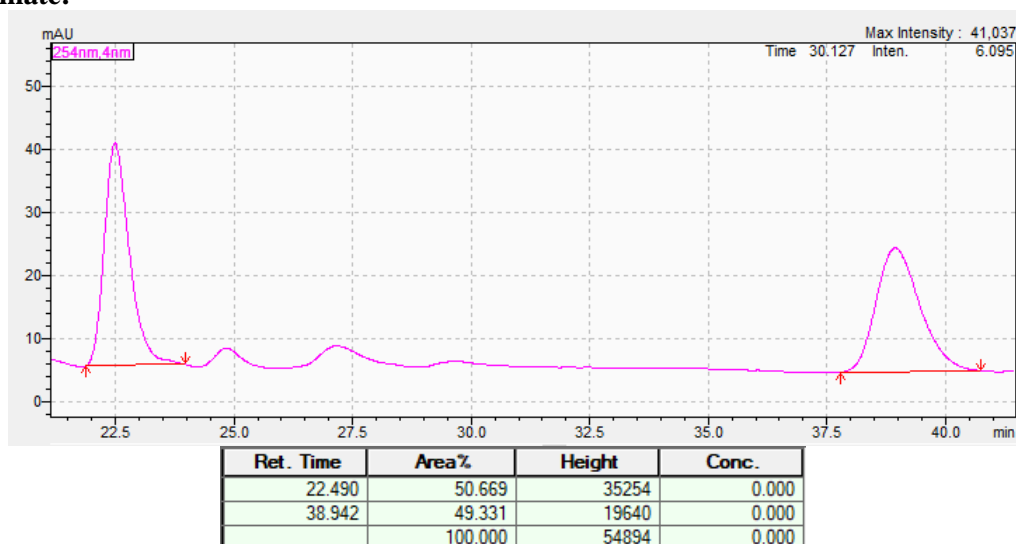
Ret. Time	Area%	Height	Conc.
25.634	98.920	277608	0.000
44.873	1.080	2207	0.000
	100.000	279815	0.000



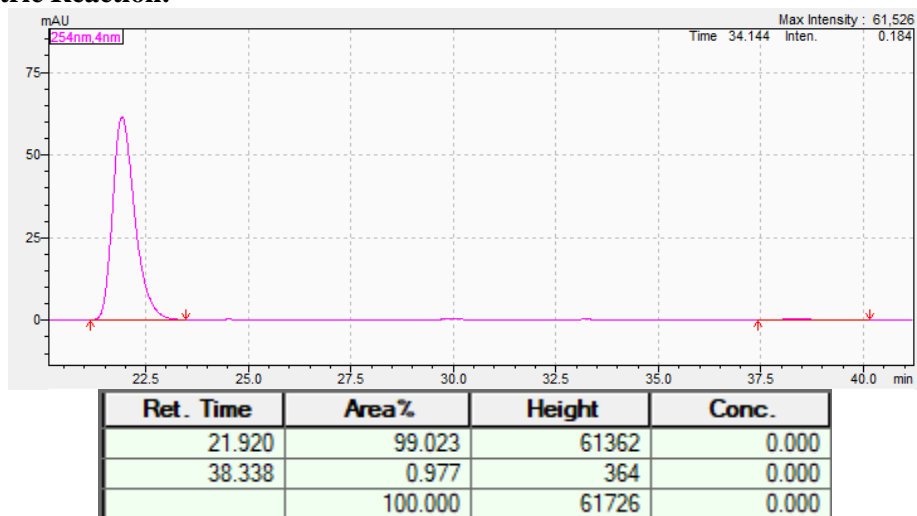
2-((1*S*,2*R*)-1-cyclopropyl-1-hydroxy-3-(5-(trifluoromethyl)pyridin-2-yl)but-3-en-2-yl)isoindoline-1,3-dione (2.7kc): According to the General Suzuki-Miyaura procedure (GP-1/GP-4) using (*S,S*)-PhBPE, the product was purified by silica gel chromatography (eluent: 0 – 40% EtOAc in hexanes) to provide 23.1 mg (45%) of **2.7kc** as a white foam as a >97:3 mixture of diastereomers and the major diastereomer as an 99:1 mixture of enantiomers. $R_f = 0.14$ (25% EtOAc/hexanes). $^1\text{H NMR}$ (CDCl_3 , 600 MHz) δ : 8.80 (dd, $J = 1.6$ Hz, $J = 0.8$ Hz, 1H), 7.90 (dd, $J = 8.5$ Hz, $J = 2.5$ Hz, 1H), 7.81 (dd, $J = 5.5$ Hz, $J = 3.0$ Hz, 2H), 7.71 (dd, $J = 5.5$ Hz, $J = 3.0$ Hz, 2H), 7.60 (d, $J = 8.0$ Hz, 1H), 6.03 (d, $J = 0.6$ Hz, 1H), 5.98 (s, 1H), 5.69 (dd, 8.6, 0.6, 1H), 4.08 (d, $J = 3.7$ Hz, 1H), 3.93 (td, $J = 8.7$ Hz, $J = 3.5$ Hz, 1H), 1.01-0.92 (m, 1H), 0.50-0.42 (m, 1H), 0.41-0.35 (m, 1H), 0.32-0.25 (m, 1H), 0.20-0.14 (m, 1H) ppm. $^{13}\text{C NMR}$ (126 MHz, CDCl_3): δ 168.3, 161.8, 145.3 (q, $J = 4.0$ Hz), 143.8, 134.17, 134.14 (q, $J = 4.0$ Hz), 131.6, 124.0, 123.47 (q, $J = 273.0$ Hz), 123.40, 121.4, 73.4, 57.5, 15.3, 2.6, 1.6. $^{19}\text{F NMR}$ (CDCl_3 , 561 MHz) δ : -62.35 ppm. HRMS (DART) m/z calcd for $\text{C}_{21}\text{H}_{18}\text{F}_3\text{N}_2\text{O}_3$ $[\text{M}+\text{H}]^+$: 403.1270; Found $[\text{M}+\text{H}]^+$: 403.1250.

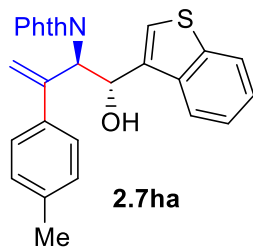
Chiral HPLC Analysis (Chiralpak AD-3 x 250 mm, heptane/isopropanol = 90/10, flow rate = 1.0 ml/min, $\lambda = 220$ nm) $t_R = 21.9$ (major), 38.3 (minor):

Racemate:



Asymmetric Reaction:

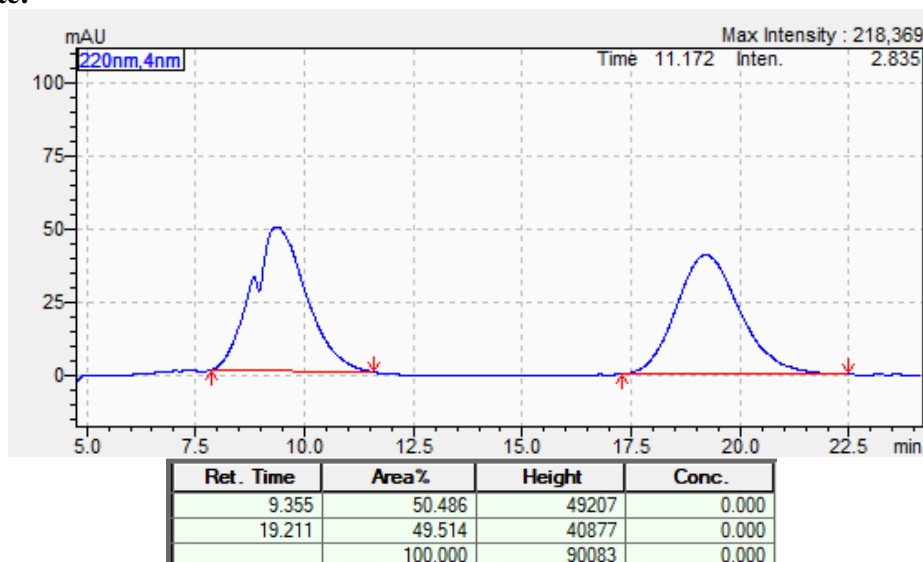




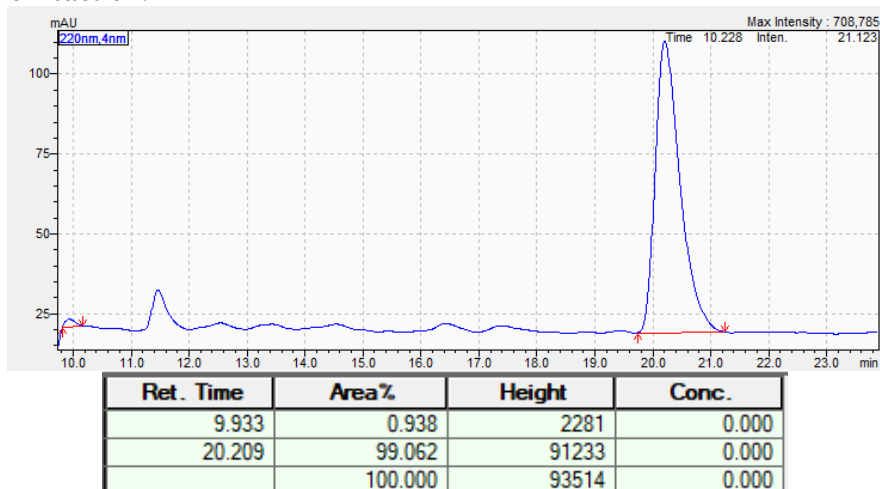
2-((1S,2R)-1-(benzo[b]thiophen-3-yl)-1-hydroxy-3-(p-tolyl)but-3-en-2-yl)-isoindoline-1,3-dione (2.7ha): According to the General Suzuki-Miyaura procedure (GP-1/GP-4) using (*S,S*)-PhBPE, the product was purified by silica gel chromatography (eluent: 0 – 20% EtOAc in CH₂Cl₂) to provide 68.6 mg (78%) of **2.7ha** as a white foam as a single diastereomer and the major diastereomer as an 99:1 mixture of enantiomers. *R_f* = 0.77 (10% EtOAc/CH₂Cl₂). ¹HNMR (CDCl₃, 600 MHz) δ: 7.90 (d, *J* = 8.0 Hz, 1H), 7.73 (d, *J* = 8.0 Hz, 1H), 7.71 (dd, *J* = 5.3 Hz, *J* = 3.0 Hz, 2H), 7.63 (dd, *J* = 5.3 Hz, *J* = 3.2 Hz, 2H), 7.36 (t, *J* = 7.5 Hz, 1H), 7.30 (s, 1H), 7.28 (t, *J* = 7.5 Hz, 1H), 7.19 (d, *J* = 8.3 Hz, 2H), 6.95 (d, *J* = 7.8 Hz, 2H), 6.02 (dd, *J* = 6.5 Hz, *J* = 2.5 Hz, 1H), 5.91 (d, *J* = 6.2 Hz, 1H), 5.68 (s, 1H), 5.58 (s, 1H), 3.69 (s, 1H), 3.59 (d, *J* = 2.1 Hz, 1H), 2.24 (s, 3H) ppm. ¹³C NMR (126 MHz, CDCl₃): δ 168.2, 144.0, 140.5, 137.5, 137.4, 136.8, 134.9, 134.1, 133.4, 131.3, 128.8, 126.5, 124.6, 124.2, 124.1, 123.4, 122.7, 121.9, 116.6, 69.6, 57.7, 21.0. HRMS (DART) *m/z* calcd for C₂₇H₂₀NO₂S [M-OH]⁺: 422.1220; Found [M-OH]⁺: 422.1257.

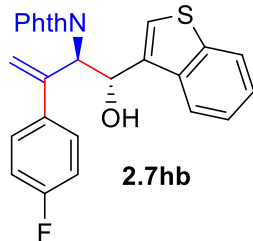
Chiral HPLC Analysis (Chiralpak AD-3 x 250 mm, heptane/isopropanol = 90/10, flow rate = 1.0 ml/min, λ = 220nm) tR = 9.35 (minor), 19.21 (major):

Racemate:



Asymmetric Reaction:

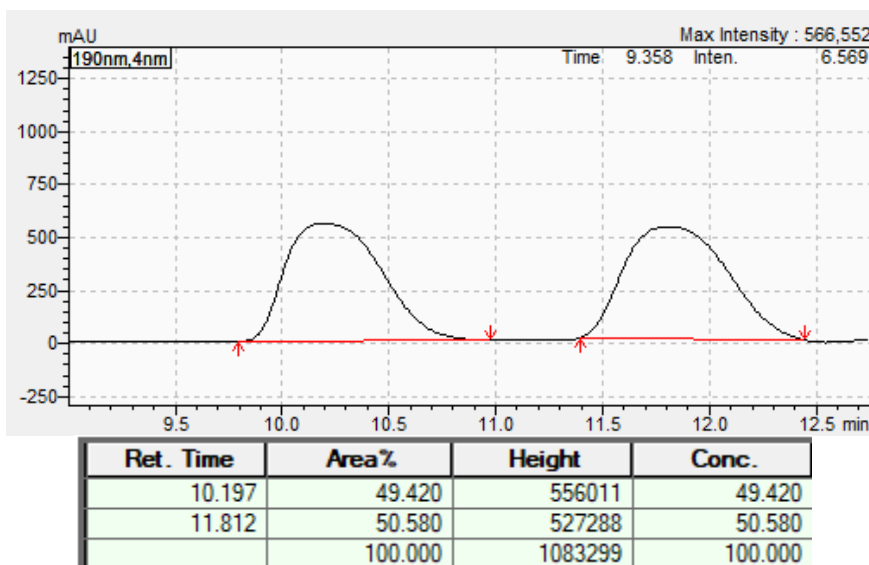




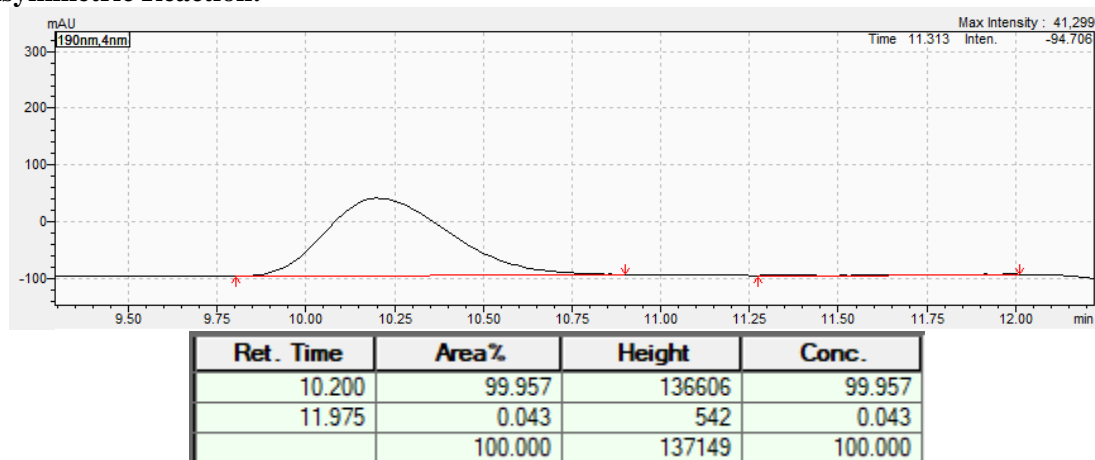
2-((1S,2R)-1-(benzo[b]thiophen-3-yl)-3-(4-fluorophenyl)-1-hydroxybut-3-en-2-yl)isoindoline-1,3-dione (2.7hb): According to the General Suzuki-Miyaura procedure (GP-1/GP-4) using (*S,S*)-PhBPE, the product was purified by silica gel chromatography (eluent: 0 – 40% EtOAc in hexanes) to provide 63.5 mg (72%) of **2.7hb** as a pale red/pink foam as a single diastereomer and the major diastereomer as an 99:1 mixture of enantiomers. $R_f = 0.26$ (25% EtOAc/hexanes). $^1\text{H NMR}$ (CDCl_3 , 600 MHz) δ : 7.84 (d, $J = 8.0$ Hz, 1H), 7.78-7.72 (m, 3H), 7.68 (dd, $J = 5.3$ Hz, $J = 2.8$ Hz, 2H), 7.37 (dd, $J = 8.1$ Hz, $J = 7.1$ Hz, 1H), 7.29 (dd, $J = 8.1$ Hz, $J = 7.1$ Hz, 1H), 7.27 (s, 1H), 7.22 (dd, $J = 8.5$ Hz, $J = 5.5$ Hz, 2H), 6.80 (t, $J = 8.7$ Hz, 2H), 5.95 (d, $J = 5.5$ Hz, 1H), 5.89 (d, $J = 5.5$ Hz, 1H), 5.62 (s, 1H), 5.51 (s, 1H), 3.90 (br s, 1H) ppm. $^{13}\text{C NMR}$ (126 MHz, CDCl_3): δ 168.3, 162.2 (d, $J = 249.9$ Hz), 143.2, 140.5, 136.58 (d, $J = 3.0$ Hz), 136.54, 134.8, 134.24, 131.19, 128.4 (d, $J = 8.2$ Hz), 124.5, 124.2, 124.1, 123.4, 122.8, 121.7, 117.2, 114.9, 114.7, 69.6, 58.0. $^{19}\text{F NMR}$ (CDCl_3 , 565 MHz) δ : -114.64 ppm. HRMS (DART) m/z calcd for $\text{C}_{26}\text{H}_{17}\text{FNO}_2\text{S}$ $[\text{M}-\text{OH}]^+$: 426.0970; Found $[\text{M}-\text{OH}]^+$: 426.0987.

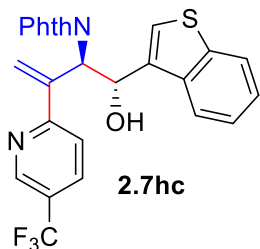
Chiral HPLC Analysis (Chiralpak IC-3 x 250 mm, heptane/isopropanol = 90/10, flow rate = 1.0 ml/min, $\lambda = 190$ nm) tR = 10.19 (major), 11.81 (minor):

Racemate:



Asymmetric Reaction:

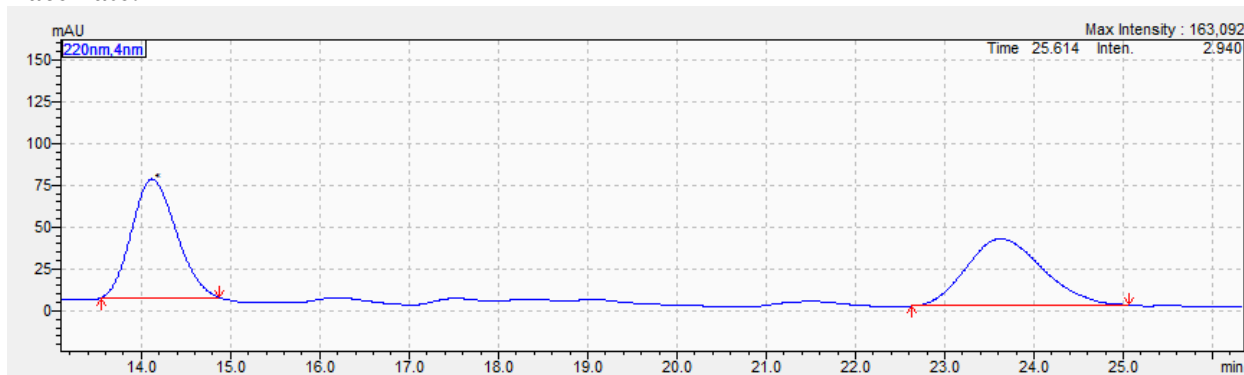




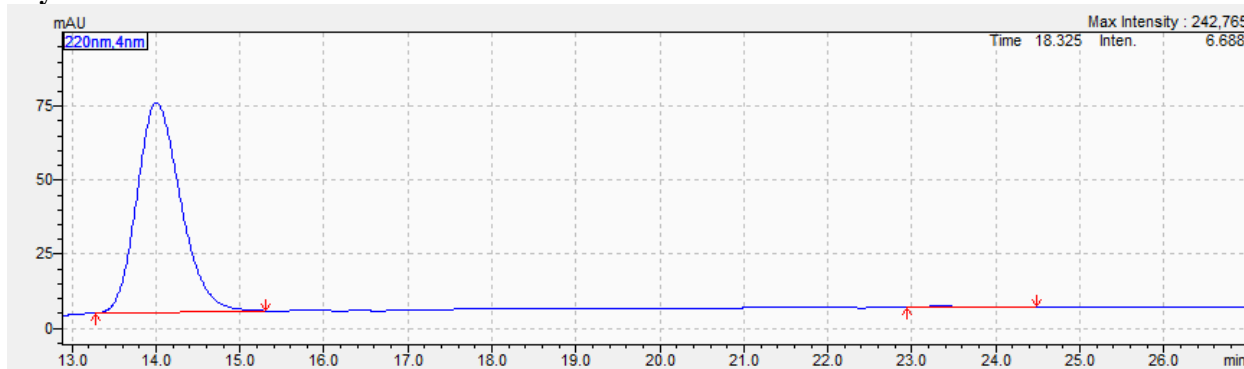
2-((1S,2R)-1-(benzo[b]thiophen-3-yl)-1-hydroxy-3-(5-(trifluoromethyl)pyridin-2-yl)but-3-en-2-yl)isoindoline-1,3-dione (2.7hc): According to the General Suzuki-Miyaura procedure (GP-1/GP-4) using (*S,S*)-PhBPE, the product was purified by silica gel chromatography (eluent: 0 – 40% EtOAc in hexanes) to provide 44.5mg (46%) of **2.7hc** as a pale red/pink foam as a >99:1 mixture of diastereomers and the major diastereomer as an 99:1 mixture of enantiomers. Absolute and relative configuration was assigned by analogy to **2.4i**, **2.4k**, and **2.4n**. $R_f = 0.24$ (25% EtOAc/hexanes). $^1\text{H NMR}$ (CDCl_3 , 600 MHz) δ : 8.66 (br s, 1H), 7.97 (d, $J = 7.7$ Hz, 1H), 7.87 (dd, $J = 8.5$ Hz, $J = 2$ Hz, 1H), 7.76-7.71 (m, 3H), 7.66 (dd, $J = 5.5$ Hz, $J = 3.5$ Hz, 2H), 7.53 (d, $J = 8.0$ Hz, 1H), 7.36 (t, $J = 7.6$ Hz, 1H), 7.33 (s, 1H), 7.29 (t, $J = 7.6$ Hz, 1H), 6.25 (d, $J = 7.0$ Hz, 1H), 6.05 (d, $J = 7.0$ Hz, 1H), 5.99 (s, 1H), 5.92 (s, 1H) ppm. $^{13}\text{C NMR}$ (126 MHz, CDCl_3): δ 168.2, 161.6, 145.0 (q, $J = 3.7$ Hz), 144.1, 140.5, 137.1, 135.3, 134.1, 134.0 (q, $J = 3.7$ Hz), 131.3, 124.3, 124.2, 124.1, 123.5, 123.4, 123.2 (q, $J = 273.0$ Hz), 122.6, 122.2, 121.4, 68.56, 57.51. $^{19}\text{F NMR}$ (CDCl_3 , 565 MHz) δ : -62.43 ppm. HRMS (DART) m/z calcd for $\text{C}_{26}\text{H}_{18}\text{F}_3\text{N}_2\text{O}_3\text{S}$ $[\text{M}+\text{H}]^+$: 495.0990; Found $[\text{M}+\text{H}]^+$: 495.1001.

Chiral HPLC Analysis (Chiralpak IC-3 x 250 mm, heptane/isopropanol = 90/10, flow rate = 1.0 ml/min, $\lambda = 220$ nm) $t_R = 14.12$ (major), 23.60 (minor):

Racemate:



Asymmetric Reaction:



CHAPTER 3

Mechanistic Investigation into the Suzuki-Miyaura Cross-Couplings of Electron-Deficient Systems

I. Introduction

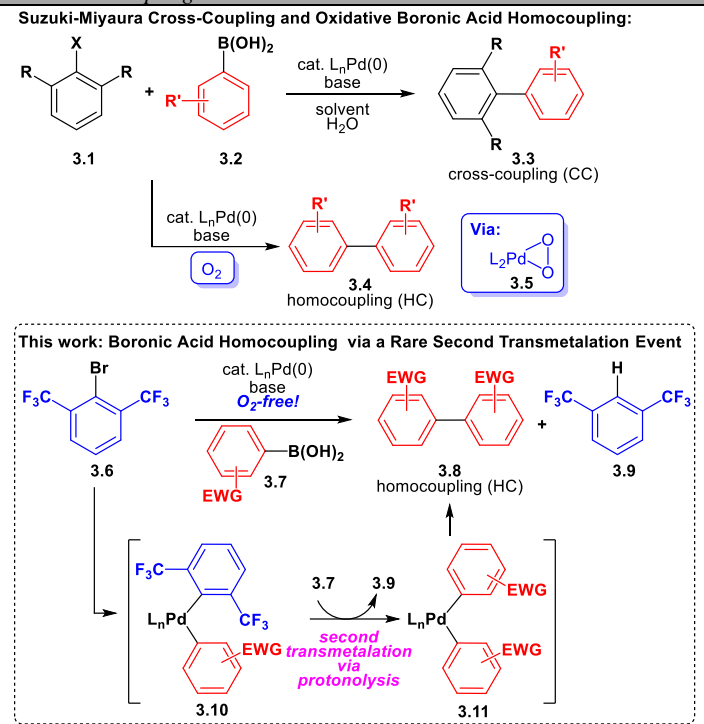
The Suzuki-Miyaura cross-coupling reaction is a widely utilized method for generating biaryl organic molecules.^{162,164,170,171} The palladium-catalyzed reaction couples an aryl halide with an aryl boronic acid, forming a sp^2 - sp^2 C-C bond between two aromatic rings. This method is extensively used in industrial applications¹⁷²⁻¹⁷⁴ for the synthesis of biaryl compounds of biological significance, due to the reaction's mild conditions, cheap and readily available starting materials, and the water tolerance of the reaction.¹⁷⁵ Reductive elimination, the final step of the Suzuki-Miyaura cross-coupling catalytic cycle, is sensitive to the electronics and sterics of the two fragments being coupled, with electron-deficient systems being increasingly slow to react.¹⁷⁶ This poses an issue and roadblock to accessing these electron-deficient biaryl products.

During an effort to prepare a Schreiner's thiourea¹⁷⁷ analog within a covalent organic framework (COF) for investigations in heterogeneous catalysis applications, we sought the formation of the required electron-poor biaryl linker for COF formation using a Suzuki-Miyaura cross-coupling reaction. Surprisingly, initial efforts using 4-Bromo-3,5-bis(trifluoromethyl)aniline as the aryl halide yielded exclusively boronic acid homocoupling rather than the desired cross-coupling product. Further study of this process revealed that this homocoupling process occurred by a unique mechanism specific to the electron-deficient aryl halide coupling partner employed in the reaction. While traditional generation of boronic acid homocoupling products occurs through the presence of oxygen in the reaction,¹⁷⁸⁻¹⁸² this was not the cause for homocoupling observed in this example, as rigorous oxygen exclusion was performed. Through reaction optimization, mechanistic studies, and stoichiometric analyses, a novel mechanism for the generation of boronic acid homo-coupling product in the Suzuki-Miyaura cross-coupling reaction of electron-deficient systems was discovered and is herein described.

Study of the cross-coupling reactions using a 2,6-bis(trifluoromethyl)-substituted aryl halide with aryl boronic acids (**Scheme 3.1**) was evaluated as a model system and found to suffer from substantial

amounts of boronic acid homo-coupling by-product formation along with dehalogenation. Study of the catalyst enabled improvement in the amounts of cross-coupling products formed and identified a new mechanism for homocoupling in these systems. Homocoupling formation in this process likely occurs through a rare protonolysis/second transmetalation event rather than the well-established mechanism requiring the involvement of O_2 . The scope of this

Scheme 3.1. Suzuki-Miyaura Cross-coupling and competitive boronic acid homocoupling.



boronic acid homocoupling reaction was investigated and shown to predominate with electron-deficient aryl boronic acids. Finally, good yield of cross-coupling could be obtained by switching the ligand.

II. Background

A. Heterogeneous vs. Homogeneous Catalysis

Catalysis can broadly be defined as the method of increasing the rate of reaction by the use of a catalyst.⁴² There are two main categories of catalysis in organic synthesis: homogeneous and heterogeneous. The two are named based on their differentiating factor: the phase of the catalyst. In homogeneous catalysis, the catalyst is in solution with the reactants (*i.e.*, same phase). On the other hand, heterogeneous catalysis utilizes a solid-phase insoluble catalyst that remains in a different phase from the reactants throughout the reaction and does not become consumed in the process.

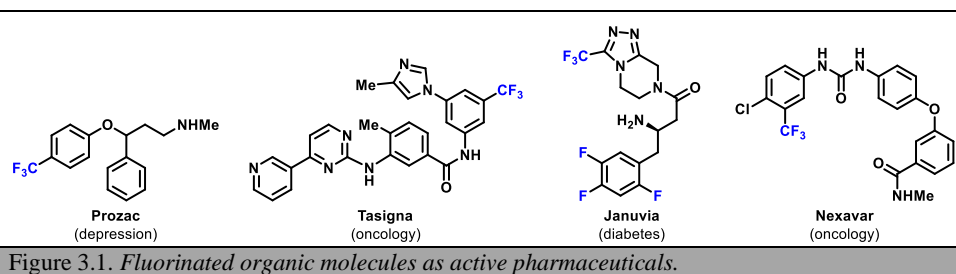
In recent years, heterogeneous catalysis has become the preferred method of catalysis in the pharmaceutical industry if good yield and selectivity can be obtained.¹⁸³ Benefits of heterogeneous catalysis include the ability to recover the catalyst from the reaction using simple filtration, as well as the ability to

recycle the catalyst.¹⁸⁴ Transition metal catalysts are quite expensive, and this recyclability leads to a substantially lower cost of reaction and improves the reaction's overall sustainability and contribution to environmental protection.¹⁸³ As a result, the need to generate heterogeneous catalysts for industrial applications is apparent.

B. Covalent-Organic Frameworks (COFs)

In recent years, covalent-organic frameworks (COFs) have risen in popularity immensely. First reported by Yaghi in 2005,¹⁸⁵ COFs are highly porous, crystalline carbon-based scaffolds used for a variety of different applications, including gas storage and separation, small molecule adsorption, heterogeneous catalysis, and drug delivery.¹⁸⁶ Unlike metal-organic frameworks (MOFs), which are carbon-based scaffolds linked together by a metal cation, COFs lack that metal center and instead are held together by strong covalent bonds, leading to lower density and high thermal stability.¹⁸⁷ Some notable aspects of COFs include their ability to self-heal or self-correct.^{188,189} Their innate ability to come together to form large uniform patterns helps them withstand harsh reaction conditions, including acidic, basic, oxidative, and reductive conditions.¹⁸⁶ One commonly employed method to form a COF involves the polymerization condensation of aldehyde-containing fragments with amine-containing linkers through generation of an imine bond.¹⁹⁰

C. Fluorinated Pharmaceuticals



Fluorinated organic molecules, such as those in **Figure 3.1**, are used extensively in medicinal chemistry and the pharmaceutical industry due to the unique properties that arise with the incorporation of the C-F bond into the active pharmaceutical ingredients (API). For example, incorporation of a fluorine

into a molecule can increase both lipophilicity and metabolic stability.^{130,191–194} Lipophilicity is the molecule's ability to dissolve in fats, which plays a significant role in the absorption, distribution, metabolism, excretion, and toxicity of the drug.¹⁹⁵ The incorporation of fluorine into a drug also changes the molecule's polarity, which then improves the bioavailability.¹⁹⁶

As mentioned, C-F functionalized drugs are more metabolically stable than their non-fluorinated counterparts. This is because the carbon-fluorine bond is not found in nature. Instead, fluorine is found in nature in the form of minerals such as CaF₂, known as Fluorite.¹⁹⁷ The human body, therefore, does not have efficient mechanisms of processing or metabolizing the C-F bond, increasing the drug's half-life in the body.^{130,191–194,196}

The importance of organofluorine compounds and their beneficial pharmacological effects on drug metabolism leads to the need to develop more practical methods of synthesizing these fluorine-containing molecules. The Suzuki-Miyaura cross-coupling reaction lends itself as a practical and useful method for generating fluorinated biaryl compounds and accessing potentially useful therapeutics.

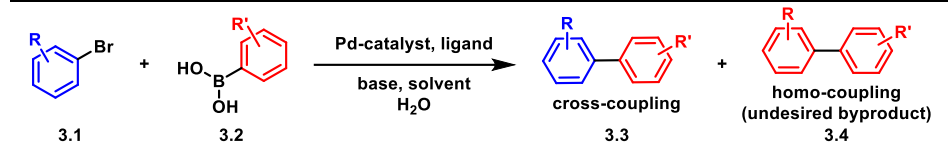
D. Suzuki-Miyaura Cross-Coupling

i. History

Awarded the Nobel Prize in Chemistry in 2010, the Suzuki-Miyaura cross-coupling reaction is one of the most powerful and widely utilized methods for generating important biaryl compounds both in industrial and academic settings.^{162,164,170,171}

First reported^{198–200} in 1979 by Akira Suzuki and Norio Miyaura, the Suzuki-Miyaura cross-coupling reaction is defined as the palladium-catalyzed cross-coupling reaction between organoboron compounds and organic halides or triflates (**Scheme 3.2**).¹⁶² This reaction must take place in the presence of a base and water.¹⁷⁵ Some advantages of this reaction include its mild reaction conditions as well as the wide commercial availability and stability of the required starting materials.

Scheme 3.2. The overall reaction of the standard Suzuki-Miyaura Cross-coupling reaction.

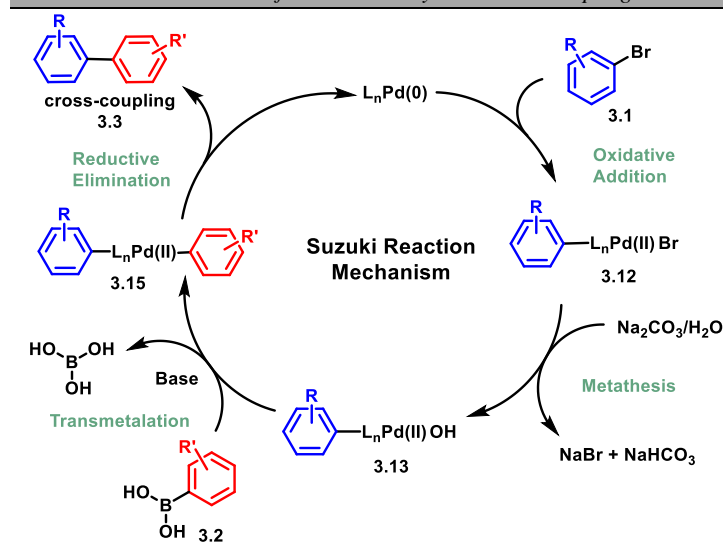


Research developments in this area over the last 50 years have led to an in-depth understanding of the mechanism that has allowed for the identification of widely applicable and efficient Pd-catalysts^{163,201–211} that can operate with low catalyst loadings, even in the ppm range, making the reactions suitable for scale-up.^{172–174} Many reviews have been published over the years, describing the versatility of the reaction and the various developments to date.²¹²

ii. Mechanism

The mechanism of the Suzuki-Miyaura Cross-coupling reaction, provided in **Scheme 3.3**, is analogous to that of other transition-metal cross-coupling reactions. Beginning with Pd(0), **(1)** oxidative addition of an organic halide forms the Pd(II) complex **3.12**. Next, **(2)** metathesis, or exchange of the anion attached to palladium for the anion of the base occurs, followed by **(3)** transmetalation between Pd(II)OH complex **3.13** and the organoborate **3.14**. Finally, **(4)** reductive elimination of the two R groups of **3.15** generates the cross-coupling product **3.3** and regenerates Pd(0), restarting the catalytic cycle.

Scheme 3.3. Mechanism of the Suzuki-Miyaura Cross-coupling reaction.



There are two transmetalation mechanisms that likely depend on the specific conditions of the respective reactions. Transmetalation with Pd(OH) species **3.13** uses the free boronic acid **3.2**, as confirmed by Hartwig.²¹³ The other transmetalation process as proposed by Miyaura²¹⁴ includes the use of base and water to generate a charged borate species (not shown), which can then transmetallate with Pd-X species **3.12** directly to form **3.15**. In this reaction, the base is essential for generating the borate **3.14** needed for transmetalation with Pd(II), and metathesis to generate the Pd(II)-OH intermediate **3.13**. Each step of the mechanism is affected by various aspects of the reaction and can significantly affect the yield, rate, and selectivity.

iii. Factors that govern Oxidative Addition

Oxidative addition is governed by the strength of the C-X bond of the aryl halide, typically reacting in the order of I>Br>OTf>>Cl, with iodo- compounds reacting the fastest.¹⁷⁶ The weaker the C-X bond, the easier it is for palladium to insert itself into the bond. Additionally, the electronics of the aryl halide **3.1** affects the rate of oxidative addition. Electron-withdrawing groups on the aryl halide increases the rate, while electron-donating groups make it more challenging, and thus reduce the rate.^{175,215} The ligand can also affect the rate of oxidative addition, with more electron-donating ligands facilitating this step.

iv. Factors that govern Transmetalation

Suzuki cross-coupling reactions require water and base to facilitate the transmetalation step in the mechanism. This is most likely due to the formation of the “borate” **3.14**, or the formation of a Pd(OH) species **3.13**, which may then facilitate transmetalation.^{214,216} Transmetalation is also facilitated by the use of an electron-rich aryl boronate species.¹⁷⁶

v. Factors that govern Reductive Elimination

Reductive elimination is traditionally the last step of the cross-coupling mechanism. It is governed by the electronics of the system, as well as the sterics and electronics of the ligand/Pd complex.¹⁷⁵ In this system, reductive elimination is facilitated when the two coupling partners have complementary electronics – one electron-rich and one electron-deficient; this is referred to as matched electronics.²¹⁷ However, when

the two fragments are similar in electronics, the reactivities of the two fragments hinder the process, and this hindrance leads to the classification of this system as mismatched.

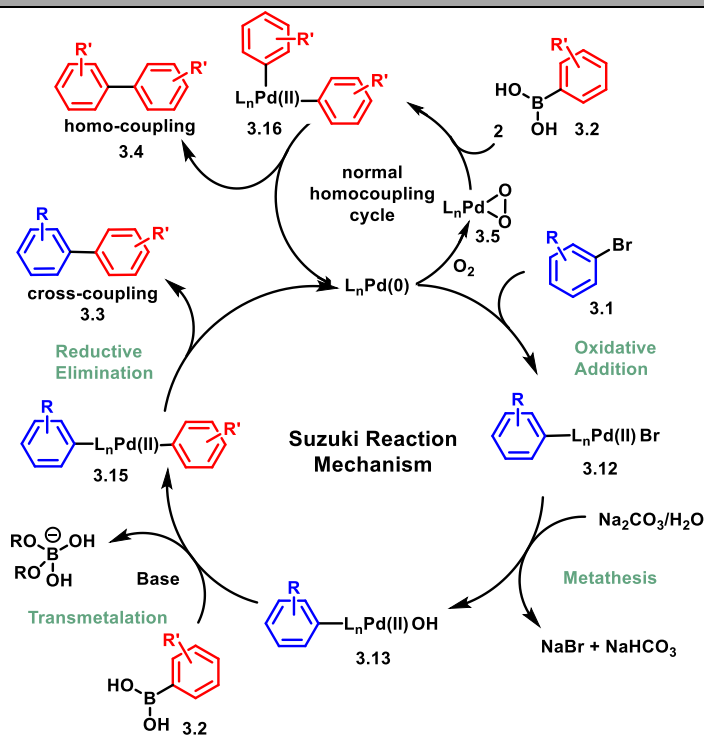
As the two fragments are brought together in complex **3.15**, the bite angle of the ligand used will affect reductive elimination, with larger bite angles forcing the fragments closer together, facilitating reductive elimination. Because the metal accepts electrons in this step, electron-withdrawing ligands that lower the electron density around the metal center, speed up reductive elimination. The main cross-coupling catalytic cycle is largely influenced by the organic ligand used with the Pd-catalyst, and reaction outcomes and product distributions can often be controlled by modifying the ligand employed.

While the cross-coupling products are desired, homo-coupling of the boronic acid is often an unwanted side product that leads to poor cross-coupling yields and the need to separate these impurities from the desired products. Other side products that can be generated include the dehalogenation of the aryl halide, and protodeboration of the boronic acid.^{218–220} To generate desired yields of the cross-coupling product, the pathways that lead to these undesired products need to be mitigated and thus avoided.

E. Typical homocoupling mechanism with O₂

Traditionally, the homocoupling product of Suzuki-Miyaura coupling reactions is believed to occur as a by-product from the presence of oxygen in the reaction (**Scheme 3.4**). Detailed mechanistic investigations known in the literature^{178–182} shows that the presence of O₂ leads to a Pd(peroxo) species **3.5** that can undergo two sequential transmetalation processes to generate complex **3.16**. After double transmetalation, reductive elimination results in the homocoupling product **3.4** and generates Pd(0), restarting the catalytic cycle. Because homocoupling is known to occur from the presence of oxygen, strategic avoidance of oxygen is essential to avoid the generation of this by-product. As a result, special precaution and rigorous exclusion of O₂ should be performed to avoid this unwanted pathway and generation of this undesired product.

Scheme 3.4. Traditional homocoupling mechanism in the Suzuki-Miyaura cross-coupling reaction.



F. Electron-deficient coupling and why it is inherently difficult

As discussed previously with the mechanism, reductive elimination is governed by the electronics of the two fragments to be coupled. The rate of reductive elimination is greatly reduced when attempting to couple two fragments that are similar in electronics. Bonds are formed naturally between one fragment that is electron-rich and another that is – to some extent – electron-poor. However, when attempting to bring together two electron-deficient fragments, there is not enough electron density to readily form a bond, making the rate of reductive elimination very slow.¹⁷⁶

III. Experimental design and Reaction development

A. Initial Plan and Troubleshooting; Early Attempts

Initially, this project began with our desire to generate a derivative of Schreiner's thiourea organocatalyst (**3.17**, **Figure 3.2**) for use in asymmetric catalysis. Schreiner's thiourea catalyst was first published by Peter Schreiner in 2002¹⁷⁷ and has primarily been used in organic synthesis as a hydrogen-bond donor in the activation of carbonyls, imines, nitroolefins, and more.²²¹ The molecule works to catalyze reactions by activating the carbonyl via non-covalent interactions, demonstrated in **Figure 3.2**, for use in a variety of organocatalytic transformations.²²²

Schreiner's catalyst **3.17**, along with various analogs containing the 3,5-bis(trifluoromethyl)aniline group, works well in this purpose, due to the extreme electron-withdrawing ability of the CF₃-groups, which increases the catalyst's overall polarity, acidity, and π - π interactions.²²² The electron-withdrawing nature of the electron-deficient aryl CF₃-groups leads to a highly active nitrogen hydrogen-bond donor species, which is very efficient in the organocatalytic activation of carbonyls.

We sought to incorporate Schreiner's H-bond donor catalyst into a solid support for heterogeneous catalysis applications using COF technology. Our proposed plan was to utilize aniline **3.19** bearing an aromatic aldehyde substituent so that after formation of the thiourea, a covalent-organic framework could be produced using the polymerization condensation of the aldehyde motif with various amine linkers (**Scheme 3.5**). We envisioned that the scaffold required to generate the COF **3.20** could be formed via a thiocarbamate coupling/synthesis using thiocarbonyl diimidazole (TCDI) from biaryl **3.19**. Biaryl **3.19** could be formed via the widely applicable Suzuki-Miyaura cross-coupling reaction, as previously discussed, between the aryl boronic acid **3.2** and aryl halide **3.18**.

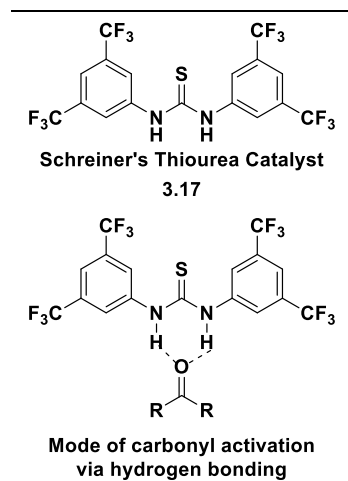
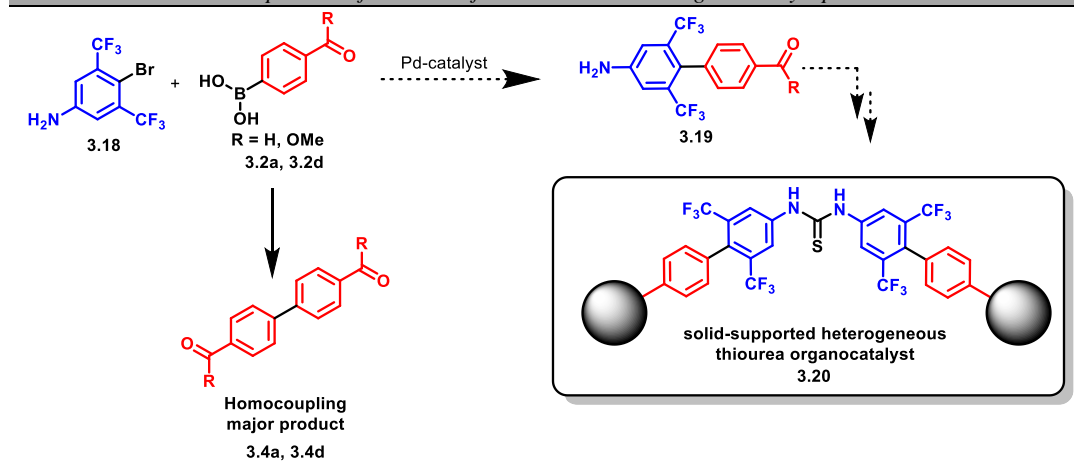


Figure 3.2. Schreiner's Thiourea catalyst and the carbonyl activation via hydrogen bonding.

Scheme 3.5. Initial attempts at the formation of the thiourea-based organocatalyst precursors.



Initial attempts at the cross-coupling reaction in **Scheme 3.5** were unsuccessful, and instead, the major products observed were the boronic acid homo-coupling product **3.4** and the protodehalogenation product **3.9**. The poor efficiency at affording the desired cross-coupling product under typical Suzuki-Miyaura reaction conditions was hypothesized to be due to the electron-deficient nature of both coupling partners caused by inhibition of the rate of reductive elimination by the strong electron-withdrawing nature of the two coupling aryl fragments (*vide supra*).¹⁷⁶ As a result, homocoupling may compete. While the typical mechanism for the generation of homo-coupling product is due to the presence of O₂ in the reaction,^{178–182} high quantities of homocoupling product generation was still observed, even with the rigorous exclusion of O₂. Furthermore, it was somewhat surprising that the reaction cleanly afforded only the boronic acid coupling product **3.4a** and protodehalogenation product **3.9** that implied an alternative mechanism for homocoupling may be operable leading to the formation of **3.9**. To probe this idea and to find a system that would allow us to obtain the desired cross-coupling product needed to form the COF, an optimization study was performed on a model system using aryl bromide **3.6** to avoid any effects of the aniline-moiety (**Table 3.1**).

Initial studies began with a ligand survey to determine the highest performing ligand in the reaction. Surprisingly, the use of (dppf)PdCl₂, a commonly employed ligand for Suzuki-Miyaura cross-coupling reactions, led to substantial homocoupling product generation (**Table 3.1**, entry 1).

Monophosphine ligands in general performed poorly in this reaction (compare entries 2-7). Bisphosphine ligands were examined due to their bite angle which is known to help facilitate the reductive coupling step by forcing the two fragments closer together. The bite angle of the bis(phosphine) ligand, however, did not seem to have a presiding effect on the reaction selectivity (**Table 3.1**, entries 8-11). On the other hand, XantPhos (entry 12) yielded high cross-coupling product. This may have occurred due to the facilitation of the reductive coupling step via the particularly wide bite angle of XantPhos.²²³ Buchwald's SPhos ligand (entry 14) also yielded high cross-coupling product generation, most likely also due to the bite angle effect.

Table 3.1. Ligand survey for the Suzuki-Miyaura Cross-Coupling reaction of the electron-deficient system.

Entry	Ligand	% CC ^b	% HC ^c	% DesBr ^b
1	dppf ^d	17	78	65
2	PPh ₃	56	15	10
3	P(<i>o</i> -tol) ₃	5	60	71
4	P(C ₆ F ₅) ₃	< 5	14	12
5	PCy ₃	< 5	61	64
6	P(<i>t</i> -Bu) ₃	44	9	7
7	P(<i>n</i> -Bu) ₃	< 5	67	60
8	dppm ^e	8	42	38
9	dppe ^e	< 5	9	5
10	dppp ^e	2	6	2
11	dppb ^e	6	6	2
12	Xantphos ^e	82	7	7
13	XPhos	20	68	62
14	SPhos	93	10	6

^aArylBr **3.6** (0.325 mmol), ArB(OH)₂ **3.21** (0.650 mmol), Na₂CO₃ (0.650 mmol), Pd(OAc)₂ (3 mol %), ligand (6 mol %), 1,4-dioxane (0.7 mL), H₂O (0.25 mL).

^bYield determined by ¹⁹FNMR spectroscopic analysis of the unpurified reaction mixture using α,α,α -trifluorotoluene as standard. ^cYield determined by ¹HNMR spectroscopic analysis of the unpurified reaction mixture using dimethyl fumarate as standard. ^d3 mol % (dppf)PdCl₂ used as catalyst. ^e3 mol % of ligand used.

Completion of the ligand survey in **Table 3.1** showed that Buchwald's SPhos ligand (entry 14) afforded high yields of the desired cross-coupling product **3.22**. We also noticed that regardless of the ligand used, near equal amounts of homo-coupling **3.23** and protodehalogenation product **3.9** were generated for each reaction, leading us to believe they may be connected mechanistically, rather than through the traditional route of homo-coupling arising from the presence of O₂ in the reaction.

In an effort to further discount the homocoupling product formation by the presence of oxygen in the system, additional experiments were performed. First, performing the reaction under an inert atmosphere in an argon-filled glovebox with degassed solvent still led to no improvements providing boronic acid homocoupling product **3.23** as the major product. Second, a control experiment utilizing (dppf)PdCl₂ as a catalyst in the absence of aryl halide **3.6** was conducted and only trace amounts of homocoupling product **3.23** was obtained. This second result implies that aryl halide **3.6** is indeed required for boronic acid homocoupling product **3.23** to be formed and taken together, the standard O₂-induced homocoupling mechanism is unlikely in this system.

B. Homocoupling

During the initial ligand optimization for this system, similar amounts of boronic acid homocoupling (**3.23**) and protodehalogenation product **3.9** were generated, regardless of which ligand was utilized. Based on these results, and the control experiments discussed above discounting O₂-involvement, we hypothesized that the boronic acid homocoupling and protodehalogenation were linked mechanistically. As a result, we proposed a mechanism resulting through a rare second transmetalation pathway,^{224,225} that was previously unknown in Suzuki-Miyaura cross-coupling, that can compete when the cross-coupling reductive elimination rate is significantly slow (See section D). Since the observed boronic acid homocoupling process in this system appeared to proceed through a unique mechanism, we decided to analyze the substrate scope of this homocoupling reaction (**Scheme 3.6**) to determine its generality and gain further insights into the possible reaction mechanism. The reaction scope with respect to the effect of the

boronic acid fragment on the efficiency of boronic acid homocoupling *vs* cross-coupling was investigated by employing electronically and sterically different boronic acids with (dppf)PdCl₂ as the catalyst. Because (dppf)PdCl₂ yielded high boronic acid homo-coupling product in the standard reaction, the results obtained by varying the boronic acid reactant should directly reflect the effect of the electronics and sterics of the boronic acid on the reaction's homocoupling/cross-coupling generation ratio. In general, electron-deficient boronic acids favored the formation of the boronic acid homocoupling product over the cross-coupling product. Trends are highlighted below and are consistent with boronic acid homocoupling over cross-coupling selectivity for coupling partners with expected slow cross-coupling reductive elimination rates.

i. Electronic effect

Fluorine and other halogens, when employed as aryl substituents, behave as mild deactivating groups. As fluorine is electronegative and pulls electron density out of the ring, the substitution pattern affects the reactivity in the corresponding positions across the ring.^{42,226} When 4-fluorophenyl boronic acid **3.2h** was employed, equal amounts of homocoupling and cross-coupling were obtained, however, when the 3-fluorophenyl derivative **3.2i** was used, homocoupling increased. This result demonstrates a key electronic effect, as the *p*-fluoro substituent's electron-donating ability by resonance decreases the amount of homocoupling generated. The *m*-fluoro substituent lacks this resonance effect, and therefore is strictly electron-withdrawing in nature, generating major homocoupling product. Protection of the aldehyde functional group as a 1,3-dioxolane (**3.2m**) led to a reduction in the ratio of homocoupling to cross-coupling product. This is another example of the electronic effects of this reaction. The destruction of the conjugation in the system that occurs when replacing the aldehyde with the dioxolane results in the reduction of the electron-withdrawing ability and thus allows for the increase in the rate of reductive elimination to form the cross-coupling product.

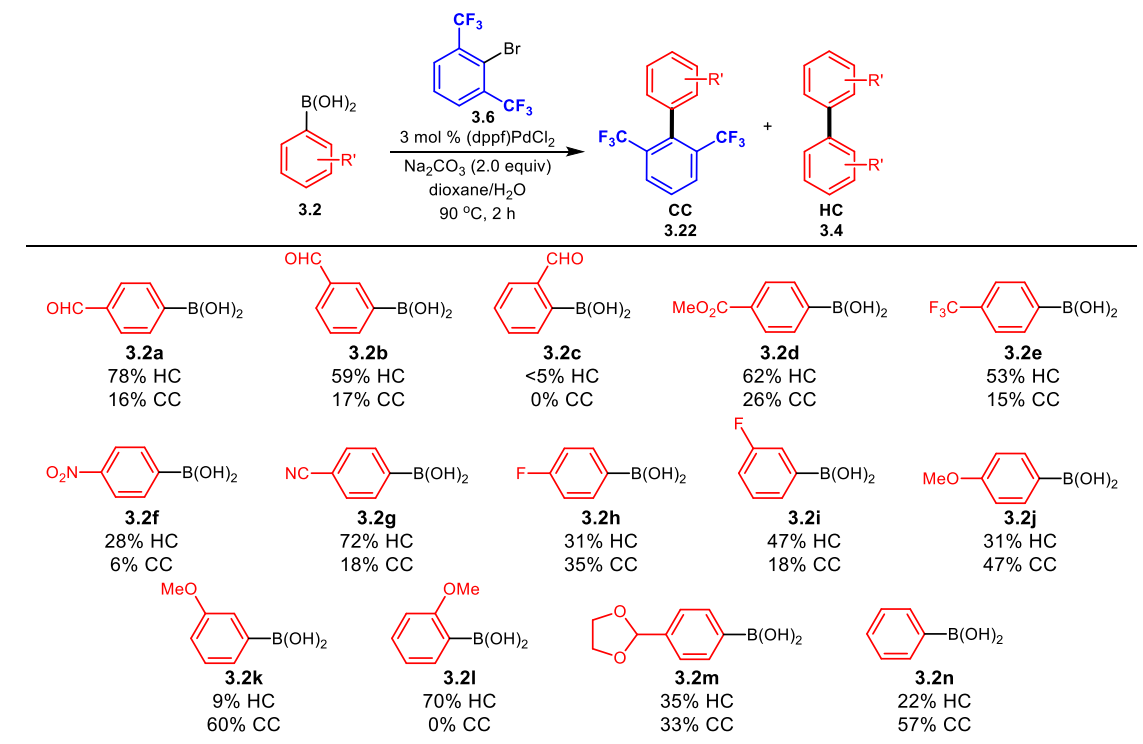
When electron-donating substituents (**3.2j,k**), or a simple phenyl ring was utilized (**3.2n**), cross-coupling was the major product. This is due to the increased ease of bringing together and coupling two

fragments with matched electronics. It is much easier to couple an electron-rich and an electron-deficient group than to couple two highly electron-deficient groups. Therefore, more electron-rich arenes led to an increase in the rate of reductive elimination, leading to higher cross-coupling generation.

ii. *Steric effect*

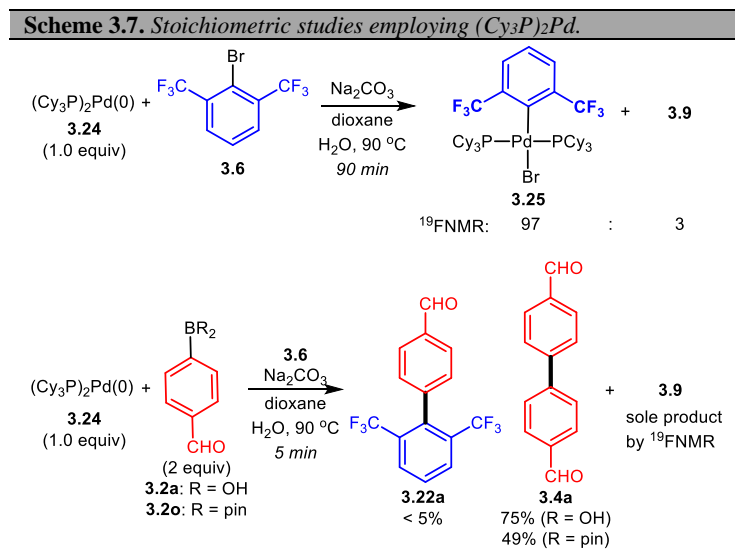
Boronic acids containing an *ortho*-substituent were either not tolerated, (**3.2c**, **Scheme 3.6**) or solely generated homocoupling product (**3.2i**). The cross-coupling product generated in this system is already sterically hindered – containing two *ortho*-substituents from the aryl halide fragment **3.6**. Therefore, attempting to incorporate a third *ortho*-group in the biaryl cross-coupling product produced with an *ortho*-substituted aryl boronic acid will be highly unfavorable, which is observed with the low tolerance/cross-coupling ability with this system and *ortho*-substituted boronic acids.

Scheme 3.6. Boronic acid homocoupling reaction scope employing 3.6.



C. Stoichiometric studies to ensure and propose an anaerobic mechanism

To further determine a possible mechanism for boronic acid homocoupling and protodehalogenation product generation without the presence of O₂, stoichiometric studies (**Scheme 3.7**) were performed.



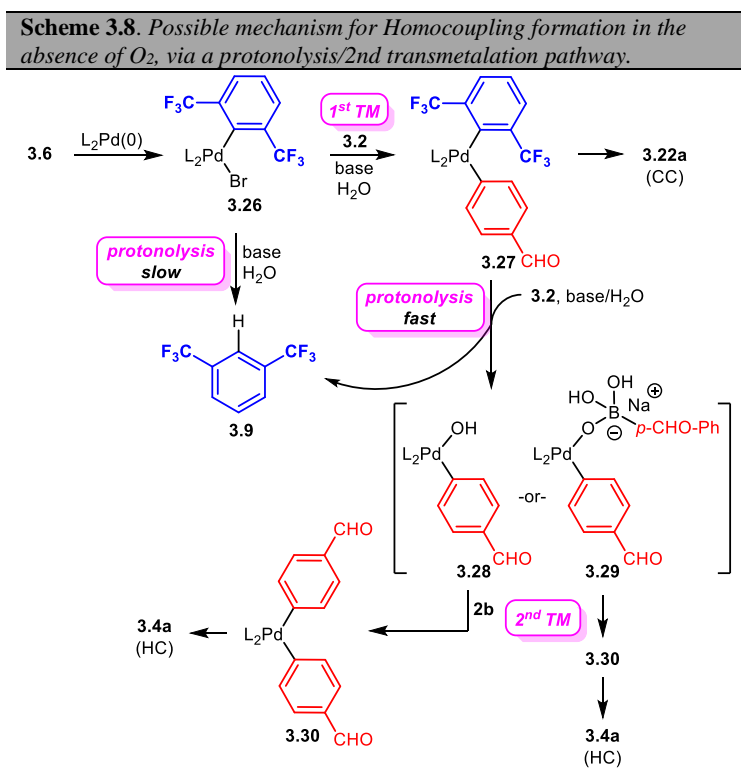
One possibility for homo-coupling product generation is the direct protodepalladation of the bis(trifluoromethyl)aryl fragment from the oxidative addition Pd complex **3.25**. To examine this possible route, the reaction of aryl bromide **3.6** in the absence of a boronic acid coupling partner, with preformed catalyst (Cy₃P)₂Pd(0), as PCy₃ generated high levels of homocoupling, was investigated. After 90 minutes of heating at 90°C, a 97:3 ratio (by ¹⁹FNMR spectroscopy) of oxidative addition complex **3.25** and protodehalogenation product **3.9** was observed. This result confirmed that the oxidative addition step occurs successfully, but without the boronic acid coupling partner, the protodehalogenation product is only generated in small quantities. In stark contrast, when this same reaction was repeated in the presence of aryl boronic acid **3.2a**, complete conversion of aryl bromide **3.6** to the protodehalogenation product was observed by ¹⁹FNMR spectroscopy after just 5 minutes of heating, affording 75% yield of boronic acid homocoupling product by NMR, with only traces of cross-coupling product **3.22**. No other fluorine products were present by ¹⁹FNMR spectroscopy. This builds off the previous reaction, showing that the

protodehalogenation product is not formed without the boronic acid coupling partner, but as soon as the boronic acid fragment is added, the reaction is incredibly fast and generates high boronic acid homocoupling product. Repeating this reaction using the aryl pinacol boronate ester **3.20** gave complete conversion of the aryl bromide **3.6** to protodehalogenation product **3.9** after only 5 minutes of heating, with minimal cross-coupling generated. The boronate ester, however, generated homocoupling to a lower extent (49% yield by NMR) than the boronic acid, with unreacted aryl boronate still present.

D. Mechanistic insight and proposed pathway

A possible mechanism to account for all these results is a second transmetalation pathway.^{224,225} This would require Pd-C protonolysis²²⁷ to occur to enable aryl boronic acid transmetalation (**Scheme 3.4**). Homocoupling product formation of the organometallic coupling partner through a second transmetalation is well established for Negishi²²⁴ and Kumada²²⁵ coupling reactions. In these examples, the second transmetalation occurs via a direct aryl-aryl exchange that prevails when the reductive elimination proves to be slow. However, this pathway is not possible in Suzuki-Miyaura reactions, since transmetalation between palladium and aryl boron is well-established to require a Pd-O-B interaction;^{213,214,216,228-236} therefore, palladium is not expected to undergo direct aryl-aryl exchange with boronic acids. Alternatively, protonolysis of the more sterically hindered 2,6-bis(trifluoromethyl)phenyl fragment of **3.27** generates **3.9** directly and provides **3.28** or **3.29**, potentially competent intermediates^{213,214,216,228-236} for a second transmetalation with **3.2** to lead to homocoupling product **3.4** via **3.30**. This is a surprising result, as Pd-C bonds are relatively inert to protonolysis.²²⁷ This pathway seems to be unique to this 2,6-bis(trifluoromethyl) substitution. Furthermore, the boronate derivative is required since minimal formation of dehalogenation product **3.9** was observed in the absence of boronic acid but was quickly generated in the presence of boronate derivatives (**Scheme 3.7**). Protonolysis of the Pd complex **3.27** may occur directly by the boronic acid to afford **3.29**,²²⁸ or could simply be facilitated by the presence of the second aryl group of complex **3.27** that gets introduced after the first transmetalation. Because both boronic acid **3.2a** and boronate ester **3.20** provided fast dehalogenation of **3.27** (**Scheme 3.7**), the second scenario seems more

likely. Additionally, the rate of transmetalation of aryl pinacol boronates is lower than the corresponding boronic acid in Suzuki-Miyaura cross-coupling reactions.²²⁸ Because of this, use of boronate **3.2o** in place of boronic acid **3.2a** should lead to a reduced rate of homocoupling formation in the stoichiometric reactions in **Scheme 3.7** if a second transmetalation is operating. The presence of unreacted boronate **3.2o**, and reduced yield of **3.4a**, when employing the boronate over boronic acid is fully consistent with this argument.

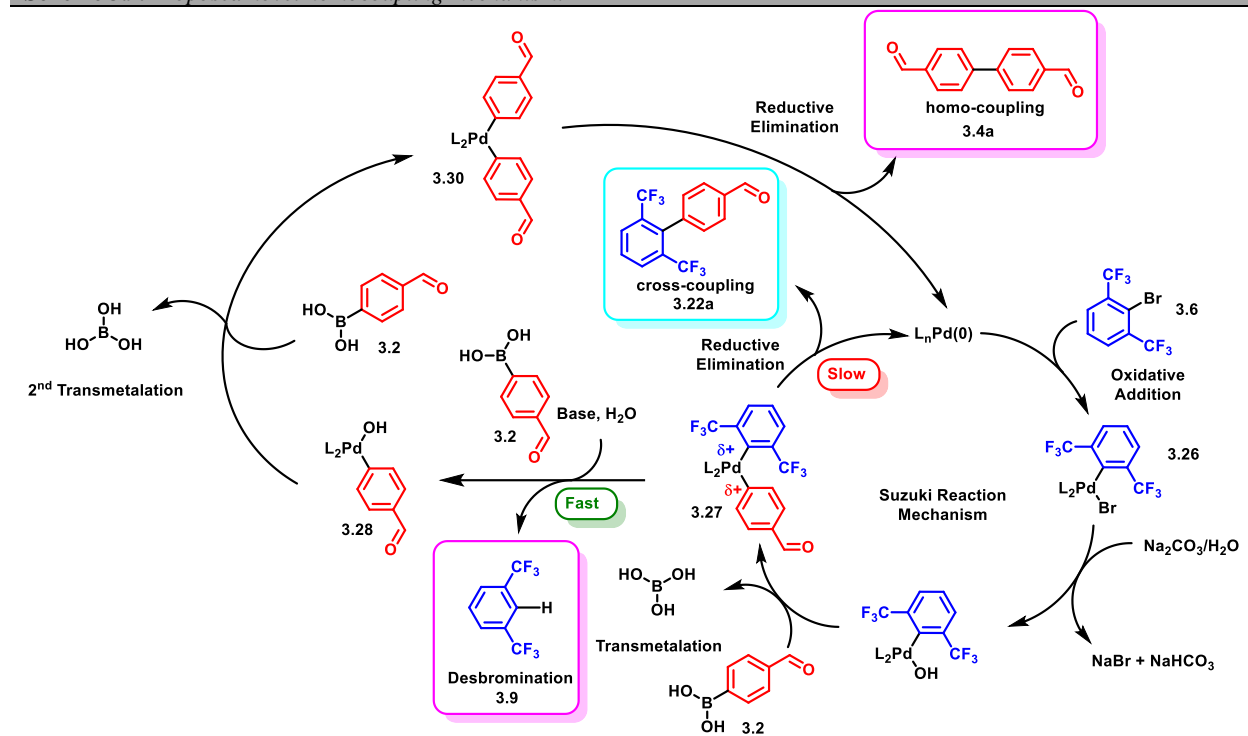


Based on the proposed mechanism in **Scheme 3.8**, the ratio of cross-coupling to boronic acid homocoupling product would be dictated by the rate of reductive elimination of **3.27** versus the outlined homocoupling pathway. When the reductive elimination of **3.27** is slow, (for example, when the boronic acid employed is more electron-deficient), homo-coupling **3.4a** product should dominate.^{224,225} The results obtained from the reaction investigation of **3.6** with boronic acids of variable structure when using (dppf)PdCl₂ as catalyst (**Scheme 3.6**) further support this proposal.

Because of the high electron-withdrawing ability of the CF₃-groups, reductive elimination from complex **3.27** to generate the cross-coupling product would be increasingly slow when electron-deficient

boronic acids are employed (e.g. **3.2a-g,i**). This is due to the polarity mismatch in forming C-C bonds between two electropositive carbon atoms. In addition to the electronics discussed previously, a steric effect is present that inhibits cross-coupling due to the bis(*ortho*) arrangement of the 2,6-disubstitution pattern of the CF₃-groups. Because of this steric prevention of reductive elimination, the protonolysis followed by second transmetalation can compete, leading to the preferential boronic acid homocoupling **3.4**. In contrast, electron-rich boronic acids (e.g. **3.2h,j,k**) should increase the rate of reductive elimination from the respective analogs of the unsymmetric L_nPd(Ar) Ar' complex of **3.27**, by minimizing the polarity mismatch and lead to increased amounts of cross-coupling products, as was observed (Scheme **3.6**). Finally, an electron-rich, but sterically-hindered boronic acid (e.g. **3.2l**), presumably would favor homocoupling due to sterics.

Scheme 3.9. Proposed novel homocoupling mechanism.



Overall, the formation of boronic acid homocoupling by-products in the Suzuki-Miyaura cross-coupling reaction of fluorinated arene **3.6** appears to be a result of the unique properties of this compound that is produced by the high electron-withdrawing ability and the steric effect of the 2,6-disubstitution

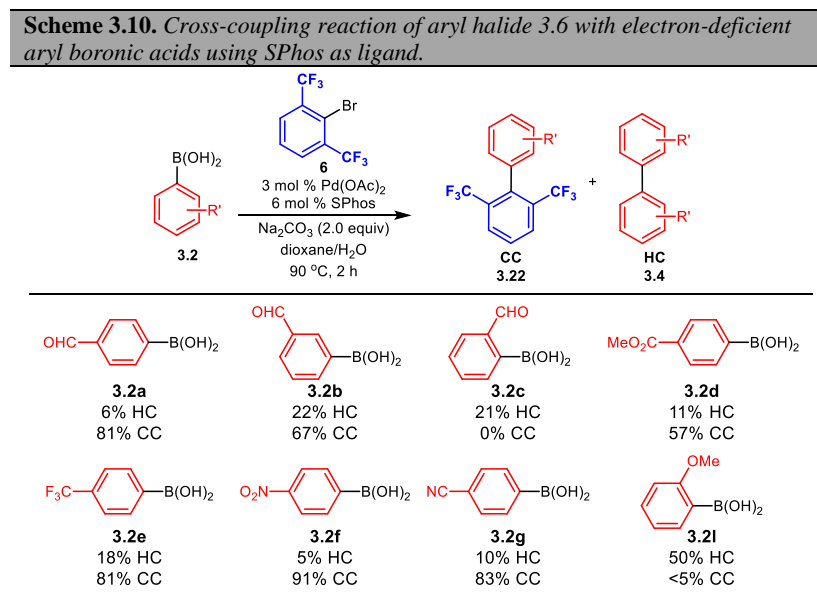
pattern of the two CF₃-mioeties leading to a surprisingly quick and easy protonolysis event enabling a second transmetalation to be possible. This problem is exacerbated when electron-deficient aryl boronic acid partners are employed in the reaction.

The unique ability of intermediates, including **3.27**, to undergo protonolysis of the 2,6-bis(trifluoromethyl)aryl group warrants further investigation and is likely not facilitated by retro-CMD²²⁷ enabled by the presence of HCO₃⁻, as control experiments utilizing other bases, such as NaOH or KF, failed to afford an improvement in cross-coupling selectivity, *see experimental information Table 3.S1*.

High selectivity for boronic acid homocoupling using other aryl bromide partners, other than **3.6**, has not been identified. For example, preliminary studies using perfluorinated bromobenzene and boronic acid **3.2a**, or 2-bromo-1,3-dimethoxybenzene with boronic acid **3.2i**, afforded the respective cross-coupling as the major product.

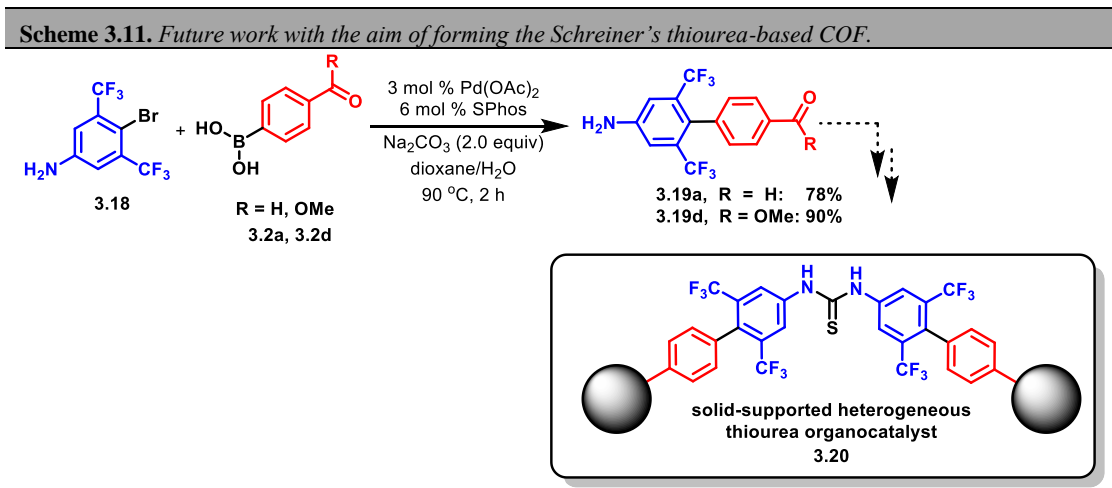
E. Cross coupling

Finally, conditions to successfully generate the cross-coupling product were determined. Use of Buchwald's SPhos ligand²³⁷ with the standard reaction was identified as optimal ligand for cross-coupling production. The substrate scope for the reaction of the electron-deficient aryl halide with electron-deficient aryl boronic acids was further evaluated, as they were found to be difficult to couple (**Scheme 3.10**).



The cross-coupling conditions worked well for most of the electron-deficient aryl boronic acids examined. However, *ortho*-substituted aryl boronic acids did not perform well, generating solely low homocoupling product yield. This was likely due to destabilizing steric effects related to forging a hindered biaryl axis (*vide supra*).^{238–247}

F. Future Work



Future directions in this project aims to optimize the reaction using the 4-Bromo-3,5-bis(trifluoromethyl) aniline **3.18** as the aryl halide to form the biaryl **3.19**. Then the next steps would be to make the COF **3.20** from the biaryl **3.19** in **Scheme 3.11**. Efforts thus far have led to decent yields of **3.19a** and **3.19d**, however, the thiourea coupling attempts to date have not been fruitful.

G. Project SEED – Bre’shon Dunson

This project spanned most of my first two years of graduate school. During the summer of 2019, my first summer of research, I had the pleasure of mentoring Bre’shon Dunson, a local Richmond public high school student, in the lab through ACS Project SEED. Throughout the summer that he was with us, he learned how to set up Suzuki cross-coupling reactions, workup them up, and isolate products via column chromatography.

He was able to complete a good portion of the SPhos cross-coupling substrate table reactions and isolated them via column chromatography. At the end of his summer with us, as a part of Project SEED, Bre'shon prepared a research summary and presented his research progress via poster presentation to the other Project SEED participants and mentors. He was a pleasure to have in the lab and his energy was contagious.

IV. Conclusions

In conclusion, we discovered and a novel mechanism for electron-deficient boronic acid homocoupling that occurs under anaerobic conditions in Suzuki-Miyaura cross-coupling reactions. This homocoupling pathway is unique to the 2,6-bis(trifluoromethyl)substitution of the aryl halide **3.6**, that slows the rate of reductive elimination leading to cross-coupling when electron-deficient boronic acids are employed. This electronic effect is consistent with the fact that electron-rich boronic acids gave more cross-coupling product under the same conditions. Instead, the Pd cross-coupling complex **3.27** can undergo fast protonolysis that then enables a second transmetalation. To the best of our knowledge, this represents the first evidence of a second transmetalation process in Suzuki-Miyaura cross-coupling reactions, and we've observed this pathway to be unique to the highly electron-deficient 2,6-bis(trifluoromethyl)-substitution of the aryl halide. Finally, cross-coupling using electron-deficient boronic acids could be improved by employing SPhos as the ligand in the Suzuki-Miyaura cross-coupling reaction.

Because of the significance of the Suzuki-Miyaura cross-coupling reaction and fluorinated organic compounds, the discovery of this novel homocoupling pathway and optimization of the cross-coupling reaction described, is vital to the future of the development of Suzuki-Miyaura cross-coupling reactions with fluorine-containing arene partners. These results can also lend useful alternative mechanisms for boronic acid homo-coupling product generation in Suzuki-Miyaura cross-coupling reactions where the rate of traditional reductive elimination may be slow, such in the case of coupling fragments with multiple ortho-substitutions.²³⁸⁻²⁴⁸

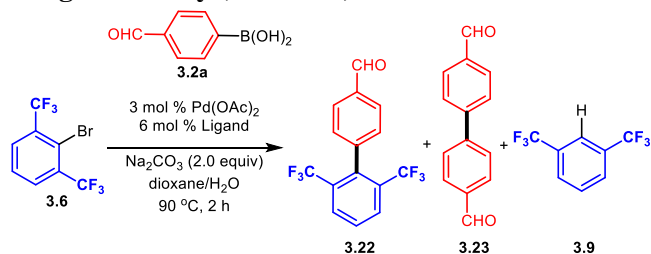
V. Experimental Procedures

A. General.

^1H NMR spectra were recorded on Bruker 600 MHz spectrometers. Chemical shifts are reported in ppm from tetramethylsilane with the solvent resonance as an internal standard (CDCl_3 : 7.26 ppm, C_6D_6 : 7.15 ppm). Data are reported as follows: chemical shift, integration, multiplicity (s = singlet, d = doublet, t = triplet, q = quartet, p = pentet, h = hextet, hept = heptet, br = broad, m = multiplet), and coupling constants (Hz). ^{13}C NMR was recorded on a Bruker 600 MHz (151 MHz) instrument with complete proton decoupling. Chemical shifts are reported in ppm from tetramethylsilane with the solvent as the internal standard (CDCl_3 : 77.0 ppm, C_6D_6 : 128.4 ppm). ^{19}F NMR was recorded on a Bruker 600 MHz (565 MHz) instrument with complete proton decoupling and ^{31}P NMR was recorded on a Bruker 600 MHz (243 MHz) instrument with complete proton decoupling with shifts reported relative to 85% H_3PO_4 . Liquid chromatography was performed using forced flow (flash chromatography) on silica gel purchased from Silicycle. Thin layer chromatography (TLC) was performed on glass-backed 250 μm silica gel F254 plates purchased from Silicycle / EMD silica gel F254 2.5x7.5 cm plates. Visualization was achieved using UV light, a 10% solution of phosphomolybdic acid in EtOH, or potassium permanganate in water, followed by heating. HRMS was collected using a Jeol AccuTOFDARTTM mass spectrometer using DART source ionization. All reactions were conducted in oven- or flame-dried glassware under an inert atmosphere of nitrogen or argon with magnetic stirring unless otherwise noted. Solvents were obtained from VWR as HPLC grade and transferred to septa-sealed bottles, degassed by Ar sparge, and analyzed by Karl-Fischer titration to ensure water content was < 600 ppm. Aryl halides and Aryl boronic acids were purchased from Sigma Aldrich, TCI America, Alfa Aesar, or Oakwood Chemicals and used as received. All other materials were purchased from VWR, Sigma Aldrich, Combi-Blocks, Alfa-Aesar, or Strem Chemical Company and used as received.

B. Experimental Procedures

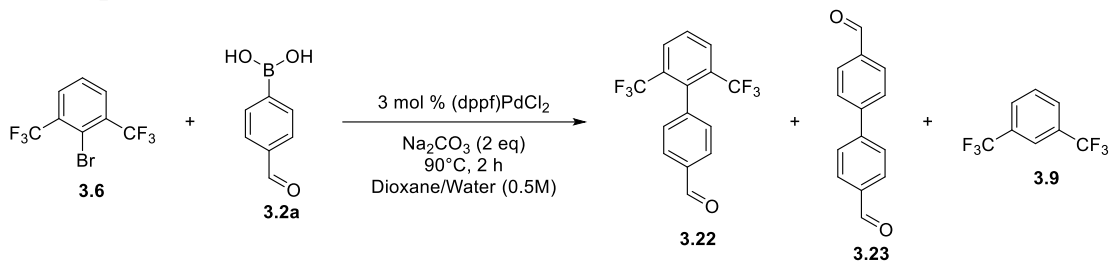
General procedure for the ligand survey (Table 3.1):



To a 20 mL crimp-cap vial with stir-bar was charged 95.7 mg (0.327 mmol) of 2-bromo-1,3-bis(trifluoromethyl)benzene, 97.9 mg (0.653 mmol) of (4-formylphenyl)boronic acid, 69.2 mg (0.653 mmol) of sodium carbonate, 2.20 mg (0.010 mmol) of $\text{Pd}(\text{OAc})_2$, and 0.020 mmol of ligand. The vial was then sealed with a crimp-cap septum, and made inert under nitrogen. To the vial was charged degassed 1,4-dioxane (0.7 mL) and degassed water (0.25 mL). The vial was then immersed in an oil bath at 90°C for two hours. To vial was allowed to cool to room temperature, then was charged water followed by extraction with DCM (2x4mL). The combined organics were charged with 60.0 μL (0.488 mmol) of $\square, \square, \square$ -trifluorotoluene as an added standard, and an aliquot was diluted in CDCl_3 for analysis by ^{19}F NMR spectroscopy to determine the yield of **3.22** and **3.9**. The combined organic layers were dried with Na_2SO_4 and concentrated *in vacuo*. To the crude residue was charged dimethylfumarate (10 – 15 mg), and the

mixture was diluted in ~0.5 mL of CDCl₃. Further dilution of an aliquot and analysis by NMR was used to determine the yield of **3.23**.

Additional Optimization data.^a



Entry	Base	% Yield 3.22 ^b	% Yield 3.4a ^b	% Yield 3.9 ^b
1	Na ₂ CO ₃	16.7	77.9	65.2
2	NaOH	2.8	20.9	32.1
3	KF	2.3	15.5	22.7

^aReactions performed as described in the general ligand survey procedure. ^bDetermined by quantitative ¹HNMR and ¹⁹FNMR spectroscopic analysis on the unpurified reaction mixture using dimethylfumarate and α,α,α -trifluorotoluene as standard, respectively.

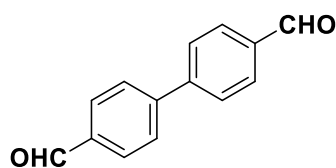
General HC procedure employing (dppf)PdCl₂ as catalyst (Scheme 3.6):

To a 20 mL crimp-cap vial with stir-bar was charged 95.7 mg (0.327 mmol) of 2-bromo-1,3-bis(trifluoromethyl)benzene, 97.9 mg (0.653 mmol) of (4-formylphenyl)boronic acid, 69.2 mg (0.653 mmol) of sodium carbonate, and 6.64 mg (0.010 mmol) of (dppf)PdCl₂. The vial was then sealed with a crimp-cap septum, and made inert under nitrogen. To the vial was charged degassed 1,4-dioxane (0.7 mL) and degassed water (0.25 mL). The vial was then immersed in an oil bath at 90°C for two hours. To vial was allowed to cool to room temperature, and water was then charged, followed by extraction with CH₂Cl₂ (2x4mL). The combined organic layers were dried with Na₂SO₄ and concentrated *in vacuo*. The homo-coupling and cross-coupling products, if present, were then isolated via silica gel column chromatography.

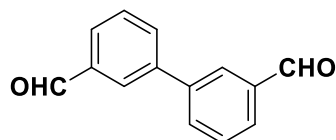
General CC procedure employing SPhos/Pd(OAc)₂ as catalyst (Scheme 3.10):

To a 20 mL crimp-cap vial with stir-bar was charged 95.7 mg (0.327 mmol) of 2-Br-1,3-bis(trifluoromethyl)benzene, 97.9 mg (0.653 mmol) of (4-formylphenyl)boronic acid, 69.2 mg (0.653 mmol) of sodium carbonate, 2.2 mg (0.010 mmol) of Pd(OAc)₂, and 8.3 mg (0.020 mmol) of SPhos. The vial was then sealed with a crimp-cap septum, and made inert under nitrogen. To the vial was charged degassed 1,4-dioxane (0.7 mL) and degassed water (0.25 mL). The vial was then immersed in an oil bath at 90°C for two hours. To vial was allowed to cool to room temperature, then was charged water followed by extraction with DCM (2x4mL). The combined organic layers were dried with Na₂SO₄ and concentrated *in vacuo*. The homo-coupling, if present, and cross-coupling products were then isolated via silica gel column chromatography.

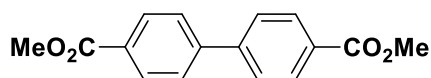
1. Analytical data for the reaction using (dppf)PdCl₂:



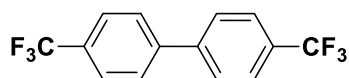
[1,1'-biphenyl]-4,4'-dicarbaldehyde (3.4a): According to the HC general procedure, the product was purified by silica gel chromatography (eluent: 0-25% EtOAc in hexanes) to provide 53.2 mg (77.9%) of [1,1'-biphenyl]-4,4'-dicarbaldehyde as a white solid. $R_f = 0.26$ (25% EtOAc/hexanes). ¹HNMR (CDCl₃, 600 MHz) δ : 10.09 (s, 2H), 8.00 (d, $J = 8$ Hz, 4H), 7.80 (d, $J = 8$ Hz, 4H) ppm. ¹³C NMR (150 MHz, CDCl₃) δ : 191.7, 145.5, 135.9, 130.4, 128.0 ppm. HRMS (DART) m/z calcd for C₁₄H₁₀O₂ [M + H]⁺: 211.0759; Found [M+H]⁺: 211.0788.



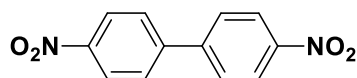
[1,1'-biphenyl]-3,3'-dicarbaldehyde (3.4b): According to the HC general procedure, the product was purified by silica gel chromatography (eluent: 0-25% EtOAc in hexanes) to provide 40.5 mg (59.3%) of [1,1'-biphenyl]-3,3'-dicarbaldehyde as a white solid. $R_f = 0.45$ (25% EtOAc/hexanes). ¹HNMR (CDCl₃, 600 MHz) δ : 10.12 (s, 2H), 8.15 (s, 2H), 7.92 (td, $J = 6$ Hz, $J = 1$ Hz, 4H), 7.67 (t, $J = 8$ Hz, 2H) ppm. ¹³C NMR (150 MHz, CDCl₃) δ : 192.0, 140.6, 137.0, 132.9, 129.8, 129.4, 127.9. HRMS (DART) m/z calcd for C₁₄H₁₀O₂ [M + H]⁺: 211.0759; Found [M+H]⁺: 211.0762.



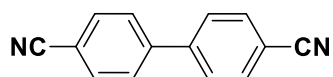
[1,1'-biphenyl]-4,4'-dimethylester (3.4d): According to the HC general procedure, the product was purified by silica gel chromatography (eluent: 0-25% EtOAc in hexanes) to provide 47.5 mg (53.2%) of [1,1'-biphenyl]-4,4'-dimethylester as a white solid. $R_f = 0.37$ (25% EtOAc/hexanes). ¹HNMR (CDCl₃, 600 MHz) δ : 8.12 (d, $J = 7.6$ Hz, 4H), 7.69 (d, $J = 7.6$ Hz, 4H) ppm. ¹³C NMR (150 MHz, CDCl₃) δ : 166.8, 144.3, 130.2, 129.7, 127.2, 52.2. HRMS (DART) m/z calcd for C₁₆H₁₄O₄ [M + H]⁺: 271.0970; Found [M+H]⁺: 271.0958.



4,4'-bis(trifluoromethyl)-1,1'-biphenyl (3.4e): According to the HC, the product was purified by silica gel chromatography (eluent: 0-5% EtOAc in hexanes) to provide 74.5 mg of an inseparable mixture of the homo-coupling product, **14e** (69.1 wt%, 52.7% yield) and the cross-coupling product, **13e** (24.4 wt%, 15.1% yield), as a white solid. $R_f = 0.86$ (25% EtOAc/hexanes). ¹HNMR (CDCl₃, 600 MHz) δ : 7.73 (d, $J = 8$ Hz, 4H), 7.70 (d, $J = 8$ Hz, 4H) ppm. ¹³C NMR (150 MHz, CDCl₃) δ : 143.2, 130.3 (q, $J = 33$ Hz), 127.6, 125.9 (q, $J = 4$ Hz), 124.0 (q, $J = 270$ Hz). ¹⁹F NMR (565 MHz, CDCl₃) δ : -62.84 ppm. HRMS (DART) m/z calcd for C₁₄H₈F₆ [M + H]⁺: 290.0530; Found [M+H]⁺: 290.0559.

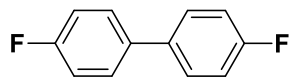


4,4'-dinitro-1,1'-biphenyl (3.4f): According to the HC general procedure, the product was purified by silica gel chromatography (eluent: 0-25% EtOAc in hexanes) to provide 22.8 mg (27.8%) of 4,4'-dinitro-1,1'-biphenyl as a white solid. $R_f = 0.43$ (25% EtOAc/hexanes). ¹HNMR (CDCl₃, 600 MHz) δ : 8.36 (d, $J = 9$ Hz, 4H), 7.78 (d, $J = 9$ Hz, 4H) ppm. ¹³C NMR (150 MHz, CDCl₃) δ : 148.0, 145.0, 128.3, 124.4 ppm. HRMS (DART) m/z calcd for C₁₂H₈N₂O₄ [M + H]⁺: 245.0562; Found [M+H]⁺: 245.0575.

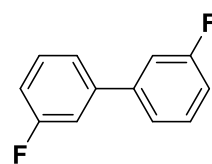


[1,1'-biphenyl]-4,4'-dicyanide (3.4g): According to the HC general procedure, the product was purified by silica gel chromatography (eluent: 0-25% EtOAc in hexanes) to provide 49.4 mg (71.9%) of [1,1'-biphenyl]-4,4'-dicyanide as a white solid. $R_f = 0.40$ (25% EtOAc/hexanes). ¹HNMR (CDCl₃, 600 MHz) δ : 7.78 (d, J

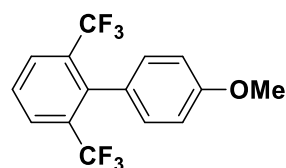
= 8 Hz, 4H), 7.69 (d, $J = 8$ Hz, 4H) ppm. ^{13}C NMR (150 MHz, CDCl_3) δ : 143.4, 132.8, 127.8, 118.3, 112.3. HRMS (DART) m/z calcd for $\text{C}_{14}\text{H}_8\text{O}_2$ [$\text{M} + \text{H}$] $^+$: 205.0766; Found [$\text{M} + \text{H}$] $^+$: 205.0785.



4,4'-difluoro-1,1'-biphenyl (3.4h): According to the HC general procedure, the product was purified by silica gel chromatography (eluent: 0-25% EtOAc in hexanes) to provide 62.0 mg of a 50/50 inseparable mixture of **3.4h**, (31.52 wt%, 30.6% yield) and the cross-coupling product, **3.22h**, (58.2 wt%, 34.9% yield), as a white solid. $R_f = 0.73$ (25% EtOAc/hexanes). ^1H NMR (CDCl_3 , 600 MHz) δ : 7.49 (dd, $J = 8$ Hz, $J = 6$ Hz, 4H), 7.12 (t, $J = 8$ Hz, 4H) ppm. ^{13}C NMR (150 MHz, CDCl_3) δ : 162.3, 136.4, 128.7, 115.8. ^{19}F NMR (565 MHz, CDCl_3): δ -116.01 ppm. HRMS (DART) m/z calcd for $\text{C}_{12}\text{H}_8\text{F}_2$ [$\text{M} + \text{H}$] $^+$: 190.0594; Found [$\text{M} + \text{H}$] $^+$: 190.0622. Cross-coupling (**3.22h**): ^1H NMR (CDCl_3 , 600 MHz) δ : 7.95 (d, $J = 8$ Hz, 2H), 7.62 (t, $J = 8$ Hz, 1 H), 7.22 (dd, $J = 8$ Hz, $J = 5$ Hz, 2H), 7.08 (t, $J = 8$ Hz, 2H) ppm. ^{13}C NMR (150 MHz, CDCl_3) δ : 162.6, 139.4, 131.8 (d, $J = 8$ Hz), 131.5 (q, $J = 29$ Hz), 129.3 (q, $J = 5$ Hz), 128.4, 128.0, 123.1 (q, $J = 275$ Hz), 114.1. ^{19}F NMR (565 MHz, CDCl_3) δ : -57.61, -113.73 ppm.

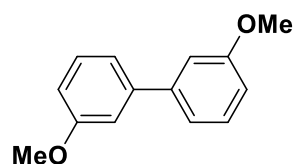


3,3'-difluoro-1,1'-biphenyl (3.4i): According to the HC general procedure, the product was purified by silica gel chromatography (eluent: 0-5% EtOAc in hexanes) to provide 54.2 mg of an inseparable mixture of the homo-coupling product, **14i** (55.0 wt%, 46.7% yield) and the cross-coupling product, **13i** (35.0 wt%, 18.3% yield), as a white solid. $R_f = 0.83$ (25% EtOAc/hexanes). ^1H NMR (CDCl_3 , 600 MHz) δ : 7.41 (td, $J = 8$ Hz, $J = 6$ Hz, 2H), 7.35 (d, $J = 8$ Hz, 2H), 7.27 (dt, $J = 10$ Hz, $J = 2$ Hz, 2H), 7.07 (td, $J = 8$ Hz, $J = 2$ Hz, 2H) ppm. ^{13}C NMR (150 MHz, CDCl_3) δ : 163.1 (d, 245 Hz), 142.1 (dd, $J = 8$ Hz, $J = 2$ Hz), 130.4 (d, $J = 9$ Hz), 122.7 (d, $J = 2$ Hz), 114.6 (d, $J = 22$ Hz), 114.0 (d, $J = 22$ Hz). ^{19}F NMR (565 MHz, CDCl_3) δ : -112.9 ppm. HRMS (DART) m/z calcd for $\text{C}_{12}\text{H}_8\text{F}_2$ [$\text{M} + \text{H}$] $^+$: 190.0594; Found [$\text{M} + \text{H}$] $^+$: 190.0613. Cross-coupling (**13i**): ^1H NMR (CDCl_3 , 600 MHz) δ : 7.96 (d, $J = 9$ Hz, 2H), 7.64 (t, $J = 8$ Hz, 1H), 7.35 (m, 1H), 7.13 (td, $J = 8$ Hz, $J = 2$ Hz, 1H), 7.04 (d, $J = 8$ Hz, 1H), 6.99 (d, $J = 9$ Hz, 1H). ^{13}C NMR (150 MHz, CDCl_3) δ : 161.5 (d, $J = 245$ Hz), 138.7, 135.8 (d, $J = 8$ Hz), 131.2 (q, $J = 30$ Hz), 129.3 (q, $J = 6$ Hz), 128.5 (d, $J = 9$ Hz), 128.3, 125.9 (d, $J = 2$ Hz), 123.1 (q, $J = 275$ Hz), 117.3 (d, $J = 23$ Hz), 115.4 (d, $J = 23$ Hz). ^{19}F NMR (565 MHz, CDCl_3) δ : -57.51, -114.1 ppm.



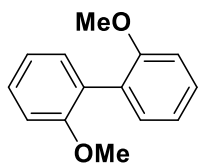
4'-methoxy-2,6-bis(trifluoromethyl)-1,1'-biphenyl (3.22j): According to the HC general procedure, the product was purified by silica gel chromatography (eluent: 0-25% EtOAc in hexanes) to provide 49.9 mg (47.0%) of 4'-methoxy-2,6-bis(trifluoromethyl)-1,1'-biphenyl as a white solid. $R_f = 0.60$ (25% EtOAc/hexanes). ^1H NMR (CDCl_3 , 600 MHz) δ : 8.93 (d, $J = 8$ Hz, 2H), 7.59 (t, $J = 8$ Hz, 1H), 7.15 (d, $J = 7.15$ Hz, 2H), 6.90 (d, $J = 8$ Hz, 2H), 3.86 (s, 3H) ppm. ^{13}C NMR (150 MHz, CDCl_3) δ : 159.5, 140.4, 131.6 (q, $J = 28$ Hz), 131.0, 129.1 (q, $J = 5$ Hz), 127.7, 126.0, 123.4 (q, $J = 275$ Hz), 112.3, 55.12. ^{19}F NMR (565 MHz, CDCl_3) δ : -57.62 ppm. HRMS (DART) m/z calcd for $\text{C}_{15}\text{H}_{10}\text{F}_6\text{O}$ [$\text{M} + \text{H}$] $^+$: 321.0714; Found [$\text{M} + \text{H}$] $^+$: 321.0732.

3,3'-dimethoxy-1,1'-biphenyl (3.4k): According to the HC general procedure, the product was purified by silica gel chromatography (eluent: 0-25% EtOAc in hexanes) to provide 62.9 mg of an inseparable mixture of the homo-coupling product, **3.4k** (57 wt%, 49.8% yield) and the cross-coupling product, **3.22k** (49 wt%, 28.9% yield), as a clear oil. $R_f = 0.53$ (25% EtOAc/hexanes). ^1H NMR (CDCl_3 , 600 MHz) δ : 7.95

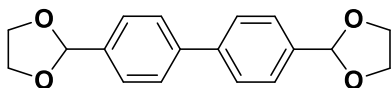


(d, $J = 8$ Hz, 2H), 7.35 (t, $J = 8$ Hz, 2H), 7.20 (s, 2H), 7.18 (d, $J = 8$ Hz, 2H), 3.87 (s, 6H) ppm. ^{13}C NMR (150 MHz, CDCl_3) δ : 159.9, 142.6, 129.7, 119.7, 112.9, 112.8, 55.32. HRMS (DART) m/z calcd for $\text{C}_{15}\text{H}_{10}\text{F}_6\text{O}$ [$\text{M} + \text{H}$] $^+$: 321.0714; Found [$\text{M} + \text{H}$] $^+$: 321.0714. Cross-coupling (**3.22k**): ^1H NMR (CDCl_3 , 600 MHz) δ : 7.95 (d, $J = 8$ Hz, 2H), 7.61 (t, $J = 8$ Hz, 1H), 7.31 (td, $J = 8$ Hz, $J = 2$ Hz, 1H), 6.98 (d, $J = 8$ Hz, 1H), 6.87 (d, $J = 8$ Hz, 1H), 6.83 (s, 1H), 3.82 (s, 3H) ppm. ^{13}C NMR (150 MHz, CDCl_3) δ : 158.2, 140.1, 135.1, 131.2 (q, $J = 30$ Hz), 129.2 (q, $J = 5$ Hz), 127.9 (d, $J = 8$ Hz), 123.4 (q, $J = 275$ Hz), 122.6, 115.9, 113.8, 55.26. ^{19}F NMR (565 MHz, CDCl_3) δ : -57.54 ppm.

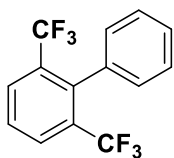
2,2'-dimethoxy-1,1'-biphenyl (3.4l): According to the HC general procedure, the product was purified by silica gel chromatography (eluent: 0-25% EtOAc in hexanes) to provide 49.9 mg (69.6%) of 2,2'-dimethoxy-1,1'-biphenyl as a white solid. $R_f = 0.53$ (25% EtOAc/hexanes). ^1H NMR (CDCl_3 , 600 MHz) δ : 7.33 (ddd, $J = 8$ Hz, $J = 2$ Hz, $J = 0.8$ Hz, 2H), 7.25 (dd, $J = 7$ Hz, $J = 2$ Hz, 2H), 7.00 (td, $J = 7$ Hz, $J = 1$ Hz, 2H), 6.98 (dd, $J = 8$ Hz, $J = 0.8$ Hz, 2H), 3.78 (s, 6H) ppm. ^{13}C NMR (150 MHz, CDCl_3) δ : 156.9, 131.4, 128.5, 127.7, 120.2, 111.0, 55.63. HRMS (DART) m/z calcd for $\text{C}_{14}\text{H}_{14}\text{O}_2$ [$\text{M} + \text{H}$] $^+$: 215.1072; Found [$\text{M} + \text{H}$] $^+$: 215.1077.



4,4'-di(1,3-dioxolan-2-yl)-1,1'-biphenyl (3.4m): According to the HC general procedure, the product was purified by silica gel chromatography (eluent: 0-25% EtOAc in hexanes) to provide 35.5 mg (35.4%) of 4,4'-di(1,3-dioxolan-2-yl)-1,1'-biphenyl as a white solid. $R_f = 0.42$ (25% EtOAc/hexanes). ^1H NMR (CDCl_3 , 600 MHz) δ : 7.60 (d, $J = 8$ Hz, 4H), 7.55 (d, $J = 8$ Hz, 4H), 5.87 (s, 2H), 4.19-4.12 (m, 4H), 4.10-4.03 (m, 4H) ppm. ^{13}C NMR (150 MHz, CDCl_3) δ : 141.6, 137.0, 127.2, 126.8, 103.5, 65.32. HRMS (DART) m/z calcd for $\text{C}_{18}\text{H}_{18}\text{O}_4$ [$\text{M} + \text{H}$] $^+$: 329.1205; Found [$\text{M} + \text{H}$] $^+$: 298.1227.

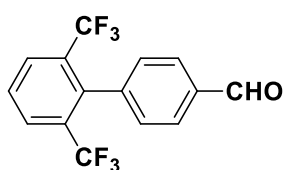


2',6'-bis(trifluoromethyl)-1,1'-biphenyl (3.3n): According to the HC general procedure, the product was purified by silica gel chromatography (eluent: 0-20% EtOAc in hexanes) to provide 55.7 mg (57.1%) of 2',6'-bis(trifluoromethyl)-1,1'-biphenyl as a white solid. $R_f = 0.69$ (25% EtOAc/hexanes). ^1H NMR (CDCl_3 , 600 MHz) δ : 7.95 (d, $J = 7$ Hz, 2H), 7.61 (t, $J = 8$ Hz, 1H), 7.46-7.34 (m, 3H), 7.25 (d, $J = 8$ Hz, 2H) ppm. ^{13}C NMR (150 MHz, CDCl_3) δ : 140.3, 133.9, 131.2 (q, $J = 29.6$ Hz), 129.9, 129.1 (q, $J = 5$ Hz), 128.2, 127.8, 126.8, 123.3 (q, $J = 273$ Hz). ^{19}F NMR (565 MHz, CDCl_3) δ : -57.50 ppm. HRMS (DART) m/z calcd for $\text{C}_{14}\text{H}_8\text{F}_6$ [$\text{M} + \text{H}$] $^+$: 290.0530; Found [$\text{M} + \text{H}$] $^+$: 290.0559.

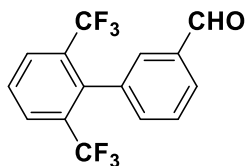


Analytical data for the reaction using SPhos/Pd(OAc) $_2$:

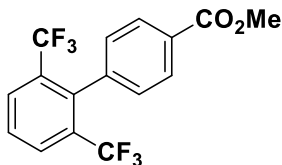
2',6'-bis(trifluoromethyl)-[1,1'-biphenyl]-4-carbaldehyde (3.22a): According to the CC general procedure, the product was purified by silica gel chromatography (eluent: 0-25% EtOAc in hexanes) to provide 84.6 mg (80.7%) of 2',6'-bis(trifluoromethyl)-[1,1'-biphenyl]-4-carbaldehyde as a white solid. $R_f = 0.59$ (25% EtOAc/hexanes). ^1H NMR (CDCl_3 , 600 MHz) δ : 10.09 (s, 1H), 7.99 (d, $J = 8$ Hz, 2H), 7.91 (d, $J = 8$ Hz, 2H), 7.68 (t, $J = 8$ Hz, 1H), 7.45 (d, $J = 8$ Hz, 2H) ppm. ^{13}C NMR (150 MHz, CDCl_3) δ : 191.8, 140.3, 138.7, 136.1, 130.9 (q, $J = 30$ Hz), 130.8, 129.4 (q, $J = 5$ Hz), 128.5, 128.2, 123.1 (q, $J = 275$ Hz). ^{19}F NMR (565 MHz, CDCl_3) δ : -57.46 ppm. HRMS (DART) m/z calcd for $\text{C}_{15}\text{H}_8\text{F}_6\text{O}$ [$\text{M} + \text{H}$] $^+$: 319.0558; Found [$\text{M} + \text{H}$] $^+$: 319.0578.



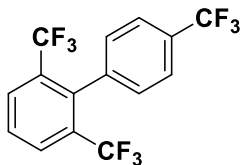
2',6'-bis(trifluoromethyl)-[1,1'-biphenyl]-3-carbaldehyde (3.22b): According to the CC general procedure, the product was purified by silica gel chromatography (eluent: 0-25% EtOAc in hexanes) to provide 69.6 mg (67.3%) of 2',6'-bis(trifluoromethyl)-[1,1'-biphenyl]-3-carbaldehyde as a white solid. $R_f = 0.57$ (25% EtOAc/hexanes). $^1\text{H NMR}$ (CDCl_3 , 600 MHz) δ : 10.05 (s, 1H), 7.99 (d, $J = 8$ Hz, 2H), 7.97 (d, $J = 8$ Hz, 1H), 7.78 (s, 1H), 7.68 (t, $J = 8$ Hz, 1H), 7.58 (t, $J = 8$ Hz, 1H), 7.54 (d, $J = 8$ Hz, 1H) ppm. $^{13}\text{C NMR}$ (150 MHz, CDCl_3) δ : 191.7, 138.6, 135.7, 135.3, 135.0, 131.3 (q, $J = 29$ Hz), 131.3, 129.6, 129.3 (q, $J = 5$ Hz), 128.5, 127.8, 123.1 (q, $J = 274$ Hz). $^{19}\text{F NMR}$ (565 MHz, CDCl_3) δ : -57.36 ppm. HRMS (DART) m/z calcd for $\text{C}_{15}\text{H}_8\text{F}_6\text{O}$ $[\text{M} + \text{H}]^+$: 319.0558; Found $[\text{M} + \text{H}]^+$: 319.0574.



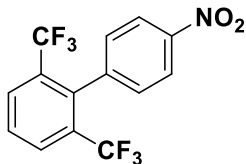
2',6'-bis(trifluoromethyl)-[1,1'-biphenyl]-4-methyl ester (3.22d): According to the CC general procedure, the product was purified by silica gel chromatography (eluent: 0-25% EtOAc in hexanes) to provide 65.8 mg (57.4%) of 2',6'-bis(trifluoromethyl)-[1,1'-biphenyl]-4-methyl ester as a white solid. $R_f = 0.61$ (25% EtOAc/hexanes). $^1\text{H NMR}$ (CDCl_3 , 600 MHz) δ : 8.07 (d, $J = 8$ Hz, 2H), 7.97 (d, $J = 8$ Hz, 2H), 7.65 (t, $J = 8$ Hz, 1H), 7.34 (d, $J = 8$ Hz, 2H), 3.95 (s, 3H) ppm. $^{13}\text{C NMR}$ (150 MHz, CDCl_3) δ : 166.7, 139.1, 138.7, 131.0 (q, $J = 29$ Hz), 130.2, 130.1, 129.3 (q, $J = 5$ Hz), 128.3, 128.2, 123.0 (q, $J = 274$ Hz), 52.17. $^{19}\text{F NMR}$ (565 MHz, CDCl_3) δ : -57.37 ppm. HRMS (DART) m/z calcd for $\text{C}_{16}\text{H}_{10}\text{F}_6\text{O}_2$ $[\text{M} + \text{H}]^+$: 3349.0663; Found $[\text{M} + \text{H}]^+$: 349.0653.

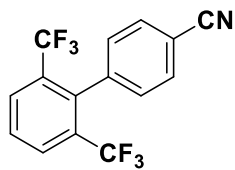


2,4',6-tris(trifluoromethyl)-1,1'-biphenyl (3.22e): According to the CC general procedure, the product was purified by silica gel chromatography (eluent: 0-5% EtOAc in hexanes) to provide 116.9 mg of an inseparable mixture of the homo-coupling product, **3.4e** (15 wt%, 18% yield) and the cross-coupling product, **3.22e** (82.3 wt%, 80.8% yield), as a white solid. $R_f = 0.86$ (25% EtOAc/hexanes). $^1\text{H NMR}$ (CDCl_3 , 600 MHz) δ : 7.98 (d, $J = 8$ Hz, 2H), 7.75-7.64 (m, 3H), 7.39 (d, $J = 8$ Hz, 2H) ppm. $^{13}\text{C NMR}$ (150 MHz, CDCl_3) δ : 138.7, 137.7, 131.1 (q, $J = 27$ Hz), 130.7 (q, $J = 33$ Hz), 130.4, 129.3 (q, $J = 5$ Hz), 128.5, 124.0 (q, $J = 273$ Hz), 124.0 (q, $J = 4$ Hz), 123.0 (q, $J = 275$ Hz), 122.2. $^{19}\text{F NMR}$ (565 MHz, CDCl_3) δ : -57.43, -62.71 ppm. HRMS (DART) m/z calcd for $\text{C}_{15}\text{H}_7\text{F}_9$ $[\text{M} + \text{H}]^+$: 358.0404; Found $[\text{M} + \text{H}]^+$: 358.0440.



4'-nitro-2,6-bis(trifluoromethyl)-1,1'-biphenyl (3.22f): According to the CC general procedure, the product was purified by silica gel chromatography (eluent: 0-10% EtOAc in hexanes) to provide 101.9 mg (90.5%) of 4'-nitro-2,6-bis(trifluoromethyl)-1,1'-biphenyl as a white solid. $R_f = 0.46$ (25% EtOAc/hexanes). $^1\text{H NMR}$ (CDCl_3 , 600 MHz) δ : 8.27 (d, $J = 8$ Hz, 2H), 8.00 (d, $J = 8$ Hz, 2H), 7.71 (t, $J = 8$ Hz, 1H), 7.46 (d, $J = 8$ Hz, 2H) ppm. $^{13}\text{C NMR}$ (150 MHz, CDCl_3) δ : 148.0, 140.8, 137.6, 131.2, 130.9 (q, $J = 30$ Hz), 129.5 (q, $J = 5$ Hz), 129.0, 122.9 (q, $J = 275$ Hz), 122.2. $^{19}\text{F NMR}$ (565 MHz, CDCl_3) δ : -57.36 ppm. HRMS (DART) m/z calcd for $\text{C}_{14}\text{H}_7\text{F}_6\text{NO}_2$ $[\text{M} + \text{H}]^+$: 336.0459; Found $[\text{M} + \text{H}]^+$: 336.0475.

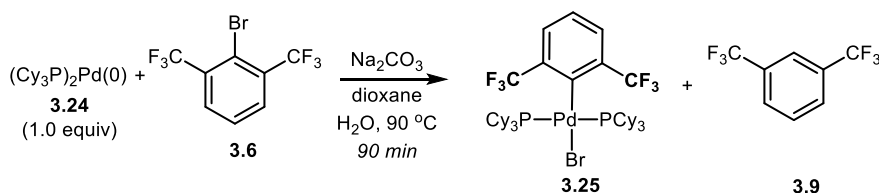




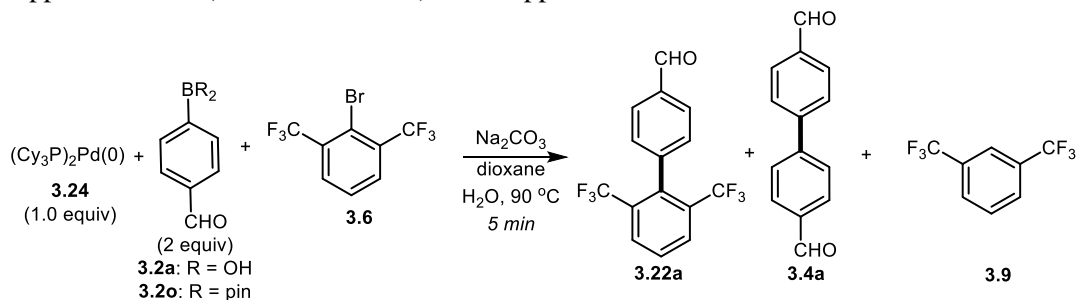
2',6'-bis(trifluoromethyl)-[1,1'-biphenyl]-4-carbonitrile (3.22g): According to the CC general procedure, the product was purified by silica gel chromatography (eluent: 0-25% EtOAc in hexanes) to provide 87.5 mg (82.6%) of 2',6'-bis(trifluoromethyl)-[1,1'-biphenyl]-4-carbonitrile as a white solid. $R_f = 0.57$ (25% EtOAc/hexanes).

$^1\text{H NMR}$ (CDCl_3 , 600 MHz) δ : 7.99 (d, $J = 8$ Hz, 2H), 7.70 (m, 3H), 7.39 (d, $J = 8$ Hz, 2H) ppm. $^{13}\text{C NMR}$ (150 MHz, CDCl_3) δ : 138.8, 137.9, 130.9 (q, $J = 29.6$ Hz), 130.8, 129.4 (q, $J = 5.6$ Hz), 128.8, 122.9 (q, $J = 273$ Hz), 118.4, 112.6. $^{19}\text{F NMR}$ (565 MHz, CDCl_3) δ : -57.37 ppm. HRMS (DART) m/z calcd for $\text{C}_{15}\text{H}_7\text{F}_6\text{N}$ [$\text{M} + \text{H}$] $^+$: 316.0561; Found [$\text{M} + \text{H}$] $^+$: 316.0562.

Stoichiometric Studies (Scheme 3.7):



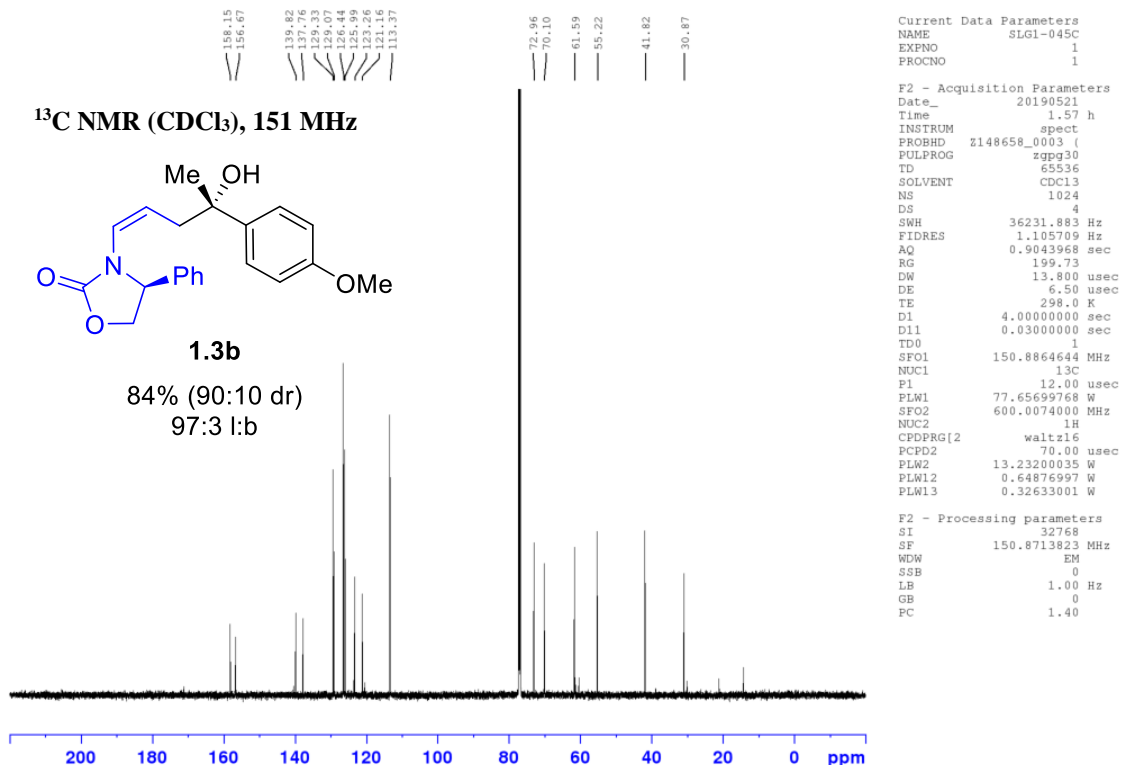
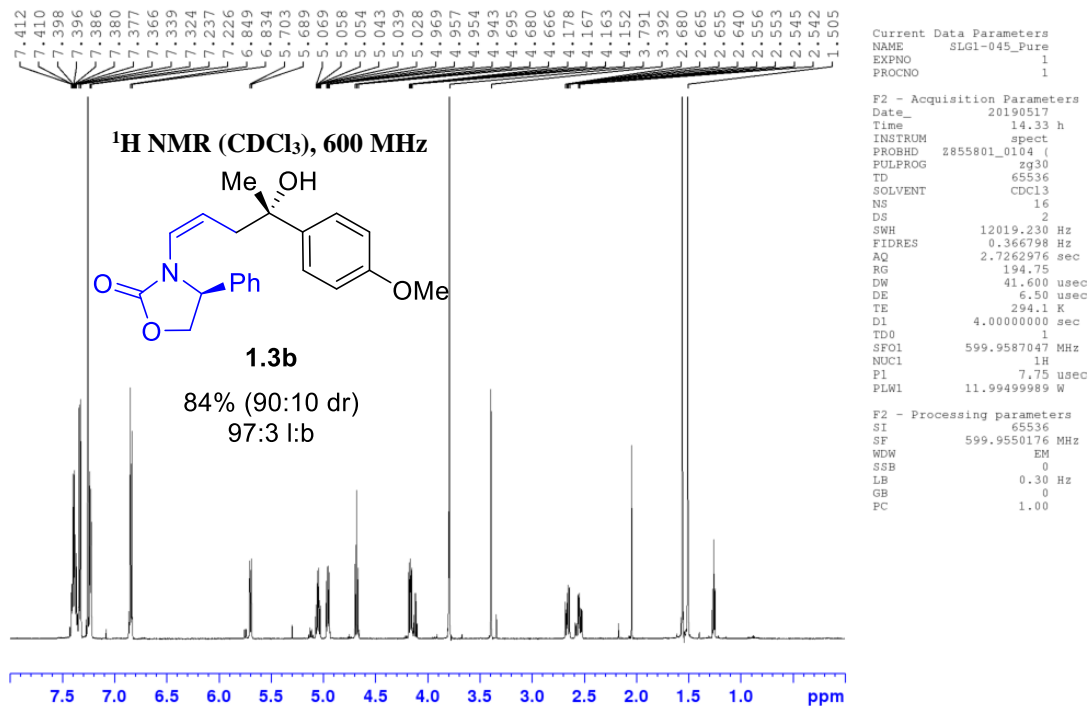
To a microwave vial with magnetic stir bar was charged 10.0 mg (0.0341 mmol) of arene **3.6** and 7.2 mg (0.068 mmol) of Na_2CO_3 . The vial was then taken into a glove-box under an Ar atmosphere and 22.8 mg (0.0341 mmol) of $(\text{Cy}_3\text{P})_2\text{Pd}$ **3.24** was charged. The vial was sealed with a crimp-cap septum and removed from the glove-box. Degassed dioxane (0.25 mL) and water (0.07 mL) were charged and the vial was inserted into an oil bath preheated to 90°C . Aliquots were taken and analyzed by $^{19}\text{F NMR}$ spectroscopy. After 90 min, the vial was removed and cooled to rt. To the white slurry was then charged 2 mL of MTBE and the solid was collected by filtration and washed with water (2x2mL), IPA (2x1mL), and MTBE (2x1mL). After further drying *in vacuo* 18.3 mg (56%) of complex **3.25** was obtained as a white solid contaminated with a small impurity. Note that a control experiment performed in the same manner but without the addition of Na_2CO_3 and water provided the same product implying the material is not the Pd-OH complex. $^1\text{H NMR}$ (CDCl_3 , 600 MHz) δ : 7.55 (d, $J = 7.7$ Hz, 2H), 7.21 (t, $J = 7.7$ Hz, 1H), 1.0 – 2.23 (m, 66 H) ppm. $^{13}\text{C NMR}$ (150 MHz, CDCl_3) δ : 146.4 (m), 139.2 (q, $J = 28.0$ Hz), 129.9, 124.8 (q, $J = 272$ Hz), 123.7, 35.78 (t, $J = 8.2$ Hz), 30.36, 27.82 (t, $J = 4.9$ Hz), 26.33 ppm. $^{19}\text{F NMR}$ (565 MHz, CDCl_3) δ : -54.5 ppm. $^{31}\text{P NMR}$ (243 MHz, CDCl_3) δ : 18.1 ppm.



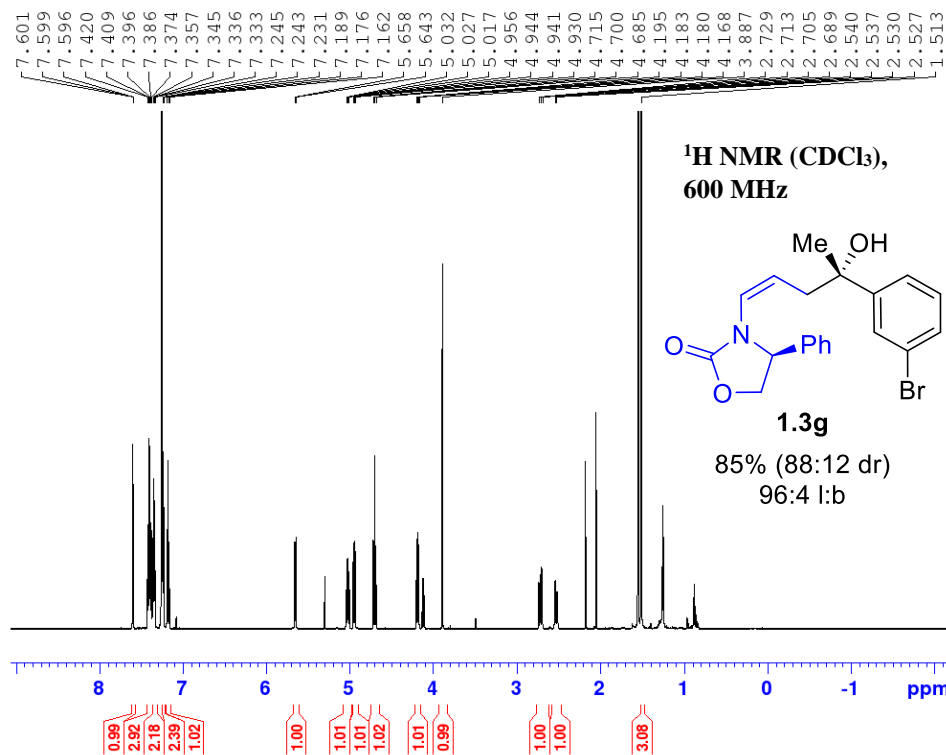
To a microwave vial with magnetic stir bar was charged 10.0 mg (0.0341 mmol) of arene **3.6**, aryl boron derivative **3.2** (0.068 mmol), and 7.2 mg (0.068 mmol) of Na_2CO_3 . The vial was then taken into a glove-box under an Ar atmosphere and 22.8 mg (0.0341 mmol) of $(\text{Cy}_3\text{P})_2\text{Pd}$ **3.24** was charged. The vial was sealed with a crimp-cap septum and removed from the glove-box. Degassed dioxane (0.25 mL) and water (0.07 mL) were charged, and the vial was inserted into an oil bath preheated to 90°C . After 5 min, the vial was removed and cooled quickly to rt in an ice bath. An aliquot was taken and dissolved in CDCl_3 and analyzed by $^{19}\text{F NMR}$ spectroscopy. To the mixture was then charged 2 mL of water followed by extraction with CH_2Cl_2 (2x2mL). The combined organics were dried with Na_2SO_4 and concentrated. The yield was then determined by quantitative $^1\text{H NMR}$ spectroscopy using dimethyl fumarate as the analytical standard.

Appendix A1. Select NMR Spectra from Chapter 1

i. Linear-selective with chiral auxiliary



SLG1-046
 Pure Isolated Product
 PROTON CDC13 {C:\Bruker\TopSpin3.5p17} Sieber 2

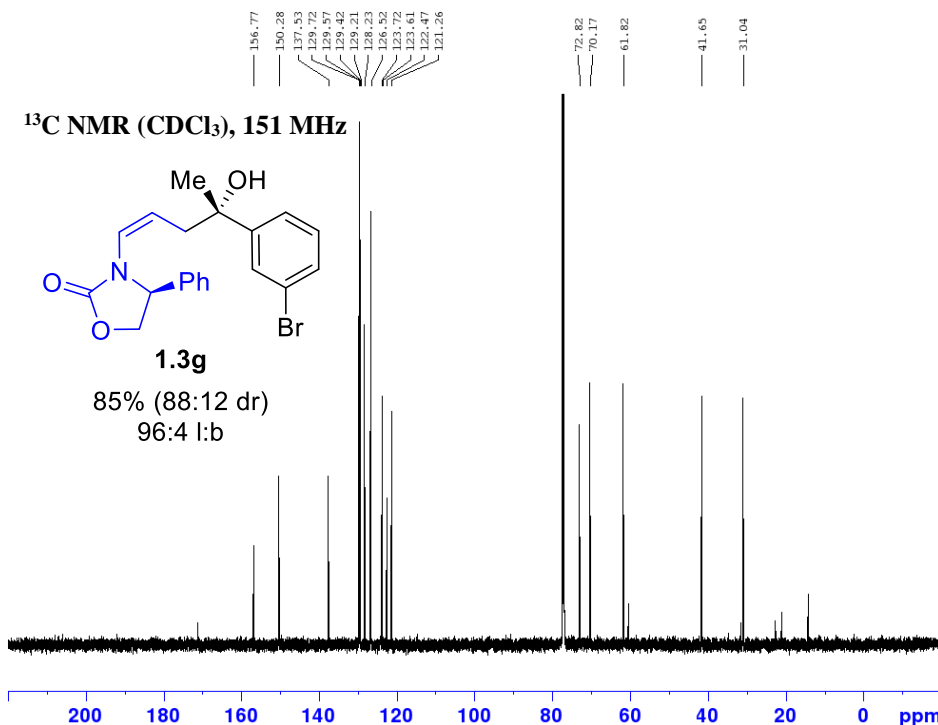


Current Data Parameters
 NAME SLG1-046_Pure_Isolated
 EXPNO 1
 PROCNO 1

F2 - Acquisition Parameters
 Date_ 20190519
 Time 0.27 h
 INSTRUM spect
 PROBHD Z855801_0104 (
 PULPROG zg30
 TD 65536
 SOLVENT CDC13
 NS 16
 DS 2
 SWH 12019.230 Hz
 FIDRES 0.366798 Hz
 AQ 2.7262976 sec
 RG 194.75
 DW 41.600 usec
 DE 6.50 usec
 TE 294.8 K
 D1 4.0000000 sec
 TD0 1
 SFO1 599.9587047 MHz
 NUC1 1H
 P1 7.75 usec
 PLW1 11.99499989 W

F2 - Processing parameters
 SI 65536
 SF 599.9550183 MHz
 WDW EM
 SSB 0
 LB 0.30 Hz
 GB 0
 PC 1.00

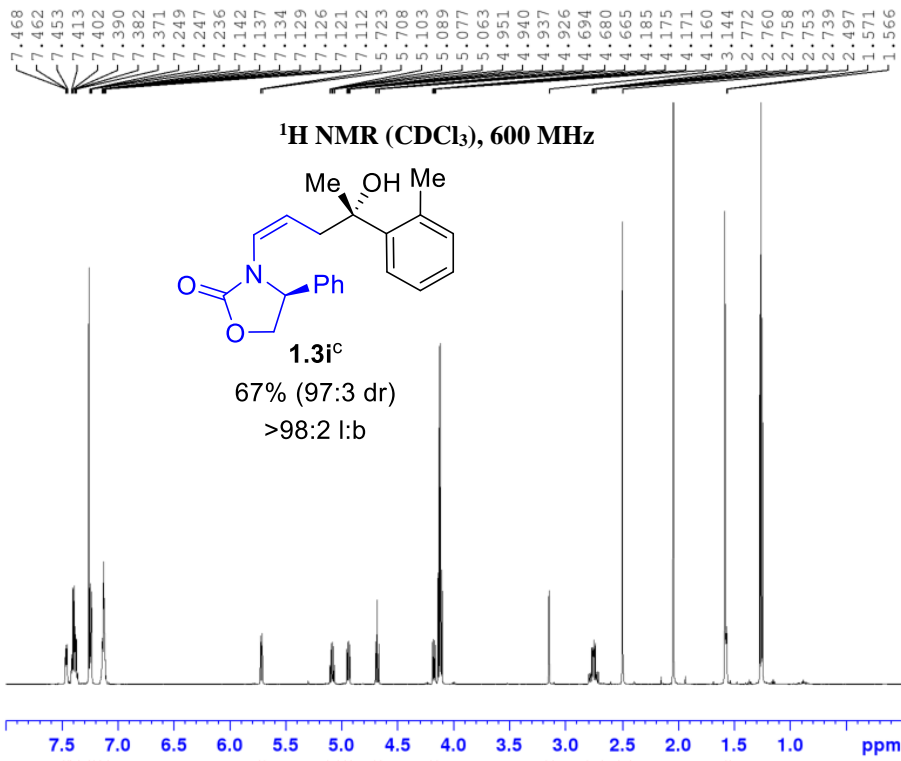
SLG1-046
 Carbon
 C13CPD CDC13 {C:\Bruker\TopSpin3.5p17} Sieber 8



Current Data Parameters
 NAME SLG1-046C
 EXPNO 1
 PROCNO 1

F2 - Acquisition Parameters
 Date_ 20190521
 Time 3.26 h
 INSTRUM spect
 PROBHD Z148658_0003 (
 PULPROG zgpg30
 TD 65536
 SOLVENT CDC13
 NS 1024
 DS 4
 SWH 36231.883 Hz
 FIDRES 1.105709 Hz
 AQ 0.9043968 sec
 RG 199.73
 DW 13.800 usec
 DE 6.50 usec
 TE 298.0 K
 D1 4.0000000 sec
 D11 0.03000000 sec
 TD0 1
 SFO1 150.8864644 MHz
 NUC1 13C
 P1 12.00 usec
 PLW1 77.65699768 W
 SFO2 600.0074000 MHz
 NUC2 1H
 CPDPRG2 waltz16
 PCPD2 70.00 usec
 PLW2 13.23200035 W
 PLW12 0.64876997 W
 PLW13 0.32633001 W

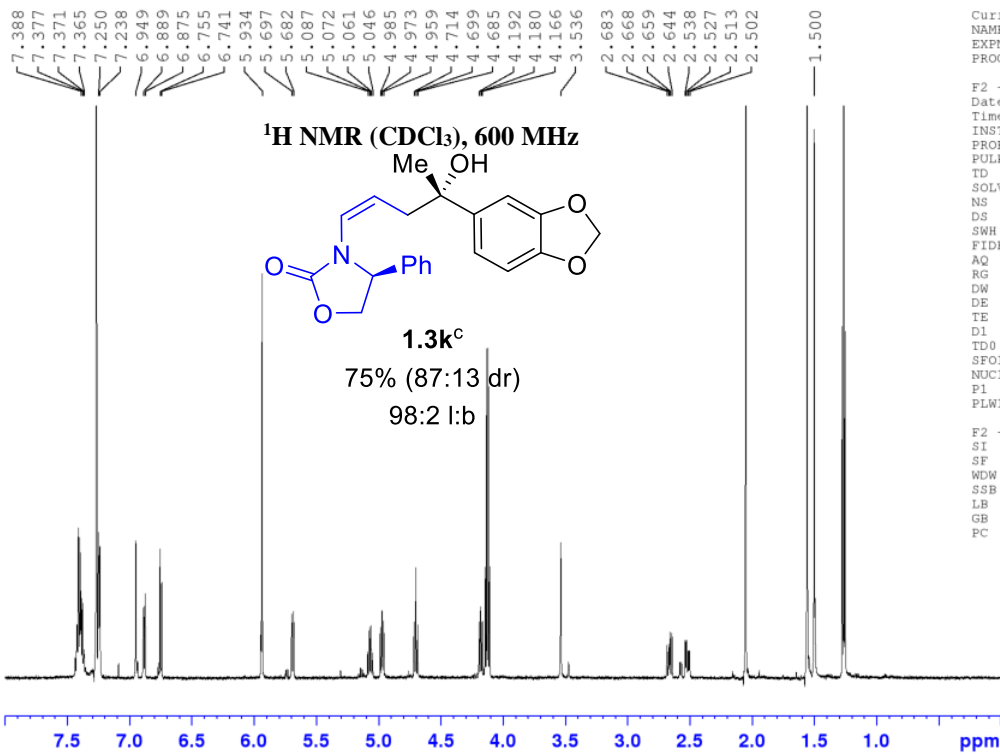
F2 - Processing parameters
 SI 32768
 SF 150.8713776 MHz
 WDW EM
 SSB 0
 LB 1.00 Hz
 GB 0
 PC 1.40



Current Data Parameters
 NAME SLG1-059_Fourth
 EXPNO 1
 PROCNO 1

F2 - Acquisition Parameters
 Date_ 20190601
 Time 21.07 h
 INSTRUM spect
 PROBHD Z148658_0003 (
 PULPROG zg30
 TD 65536
 SOLVENT CDCl3
 NS 16
 DS 2
 SWH 12019.230 Hz
 FIDRES 0.366798 Hz
 AQ 2.7262976 sec
 RG 199.73
 DW 41.600 usec
 DE 6.50 usec
 TE 294.5 K
 D1 4.0000000 sec
 TD0 1
 SFO1 600.0087050 MHz
 NUC1 1H
 P1 15.50 usec
 PLW1 13.23200035 W

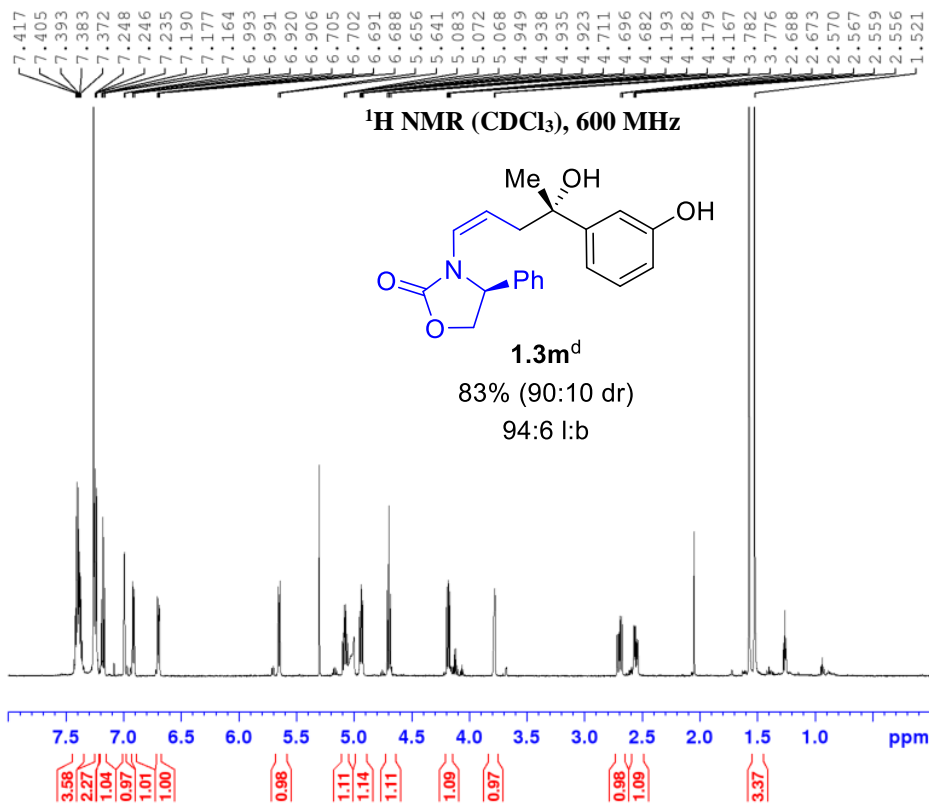
F2 - Processing parameters
 SI 65536
 SF 600.0050161 MHz
 WDW EM
 SSB 0
 LB 0.30 Hz
 GB 0
 PC 1.00



Current Data Parameters
 NAME SLG1-060_4
 EXPNO 1
 PROCNO 1

F2 - Acquisition Parameters
 Date_ 20190613
 Time 17.42 h
 INSTRUM spect
 PROBHD Z148658_0003 (
 PULPROG zg30
 TD 65536
 SOLVENT CDCl3
 NS 16
 DS 2
 SWH 12019.230 Hz
 FIDRES 0.366798 Hz
 AQ 2.7262976 sec
 RG 199.73
 DW 41.600 usec
 DE 6.50 usec
 TE 293.7 K
 D1 4.0000000 sec
 TD0 1
 SFO1 600.0087050 MHz
 NUC1 1H
 P1 15.50 usec
 PLW1 13.23200035 W

F2 - Processing parameters
 SI 65536
 SF 600.0050128 MHz
 WDW EM
 SSB 0
 LB 0.30 Hz
 GB 0
 PC 1.00



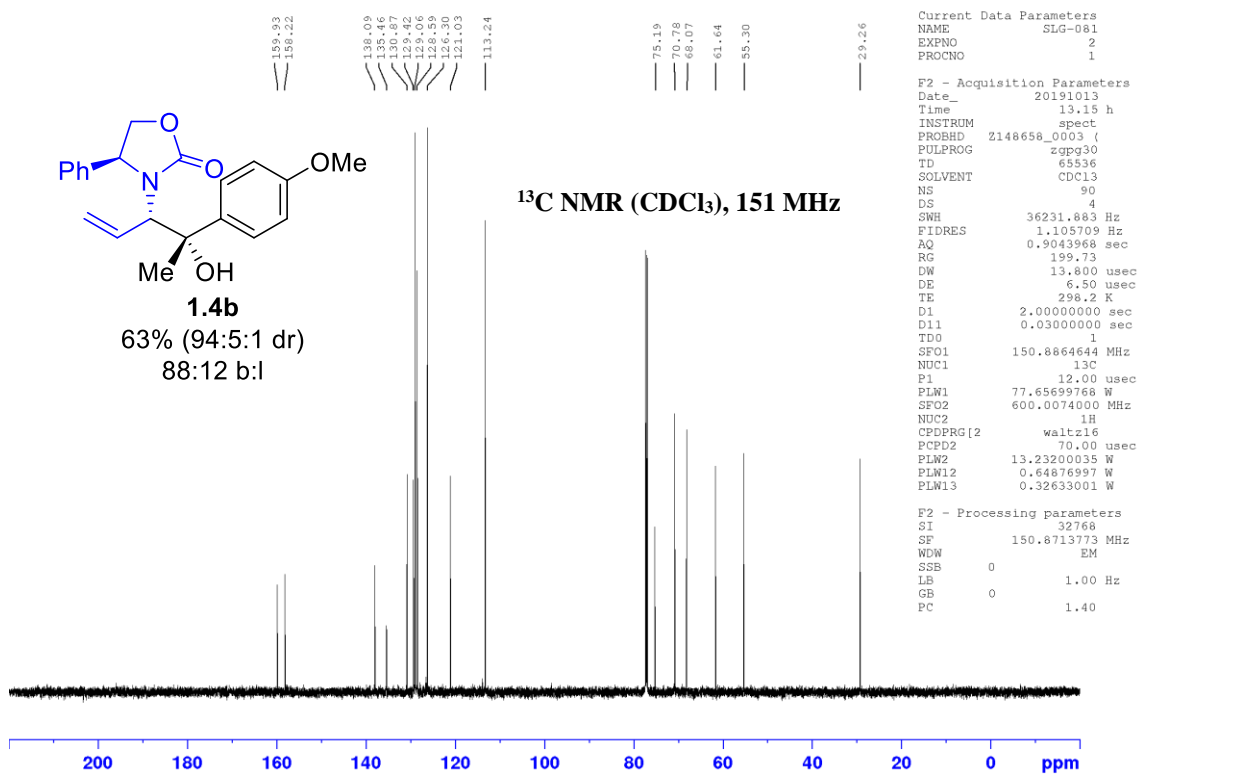
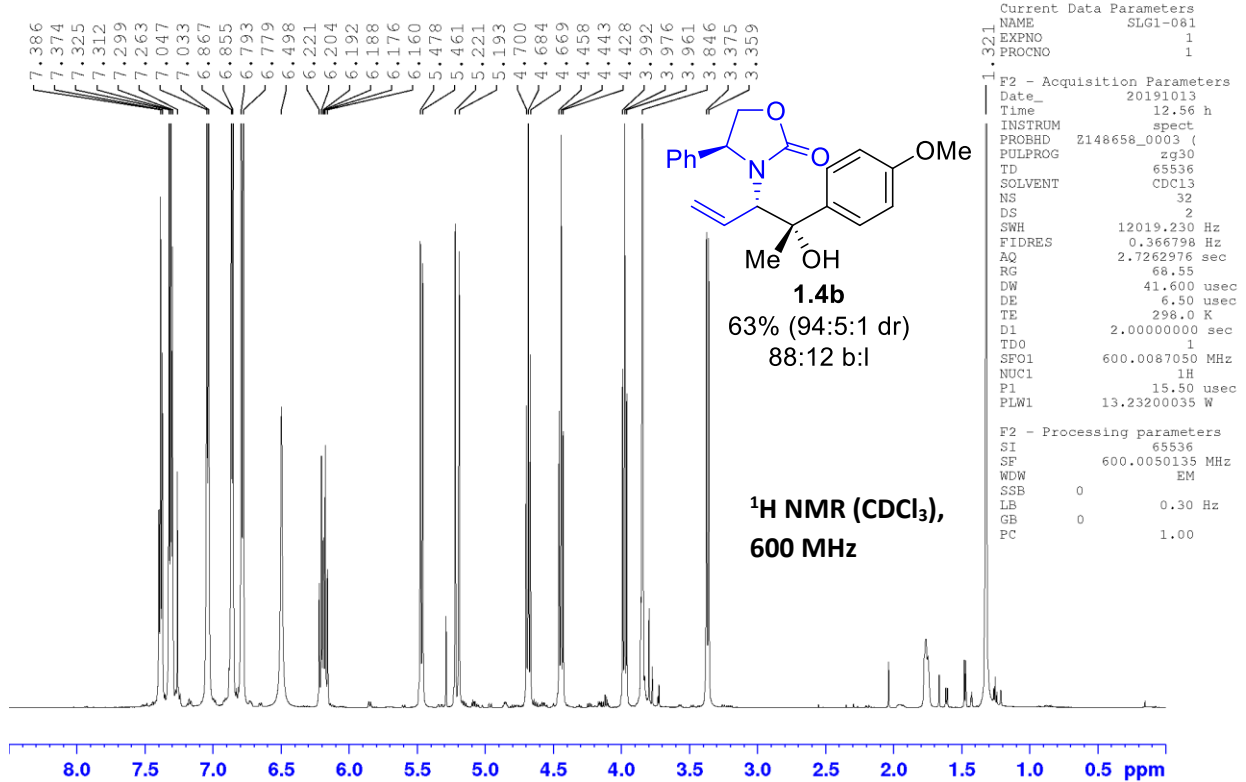
Current Data Parameters
NAME SLG1-085_Column
EXFNO 1
PROCNO 1

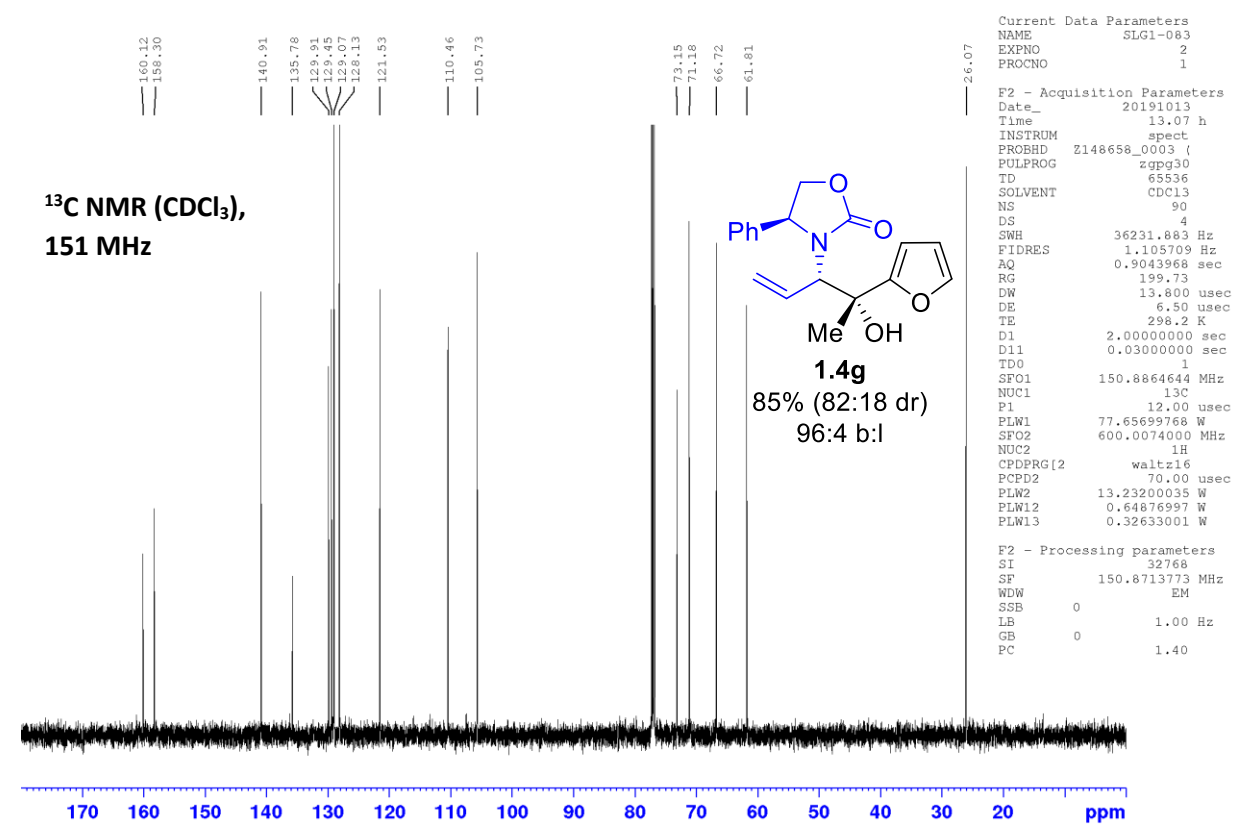
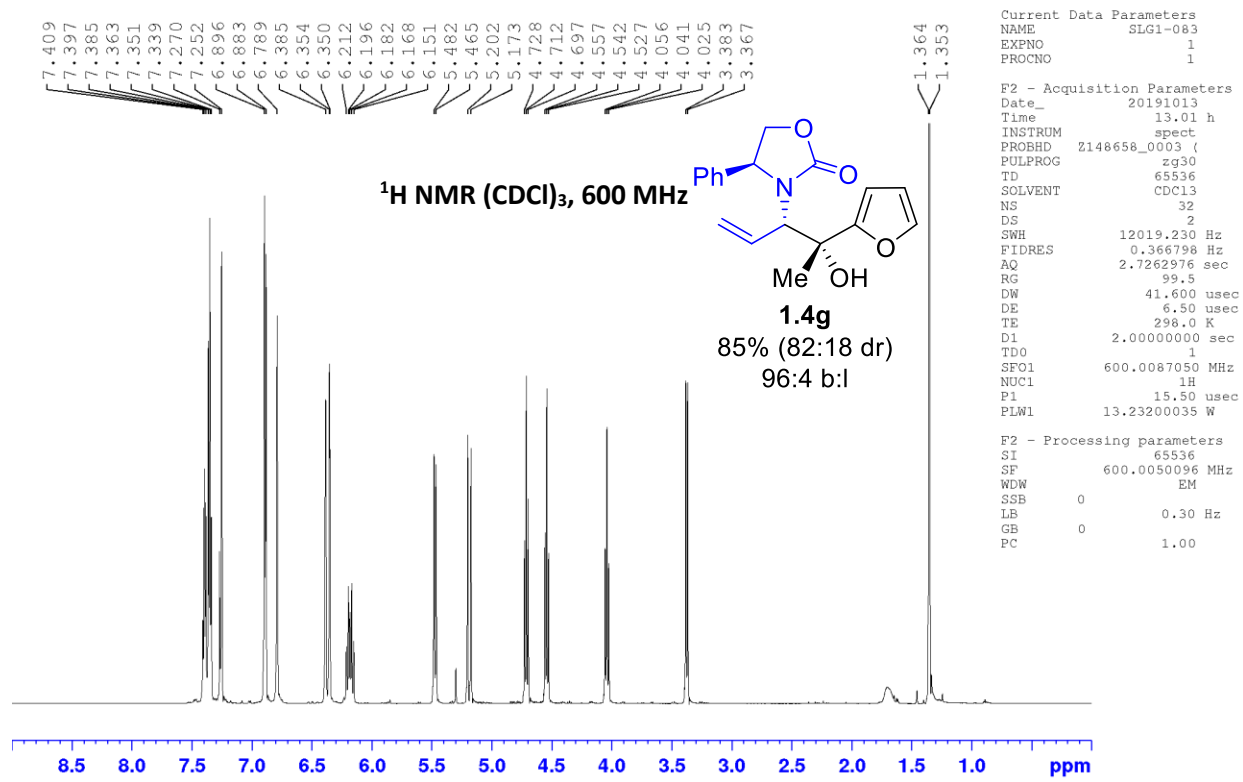
F2 - Acquisition Parameters
Date_ 20190709
Time 15.16
INSTRUM spect
PROBHD 5 mm PATXI 1H/
PULPROG zg30
TD 65536
SOLVENT cdcl3
NS 16
DS 2
SWH 12019.230 Hz
FIDRES 0.183399 Hz
AQ 2.7262976 sec
RG 194.75
DW 41.600 usec
DE 6.50 usec
TE 293.3 K
D1 4.00000000 sec
TD0 1

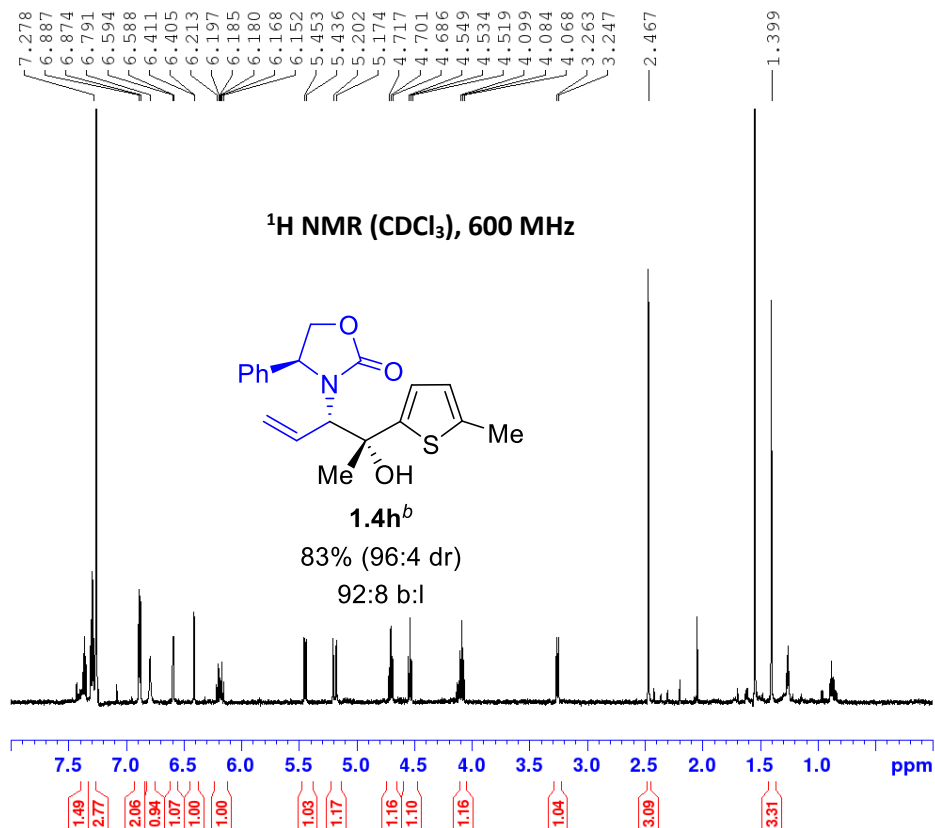
==== CHANNEL f1 =====
SFO1 599.9587050 MHz
NUC1 1H
P1 7.75 usec
PLW1 11.99499989 W

F2 - Processing parameters
SI 65536
SF 599.9550167 MHz
WDW EM
SSB 0
LB 0.30 Hz
GB 0
PC 1.00

ii. Branched-selective



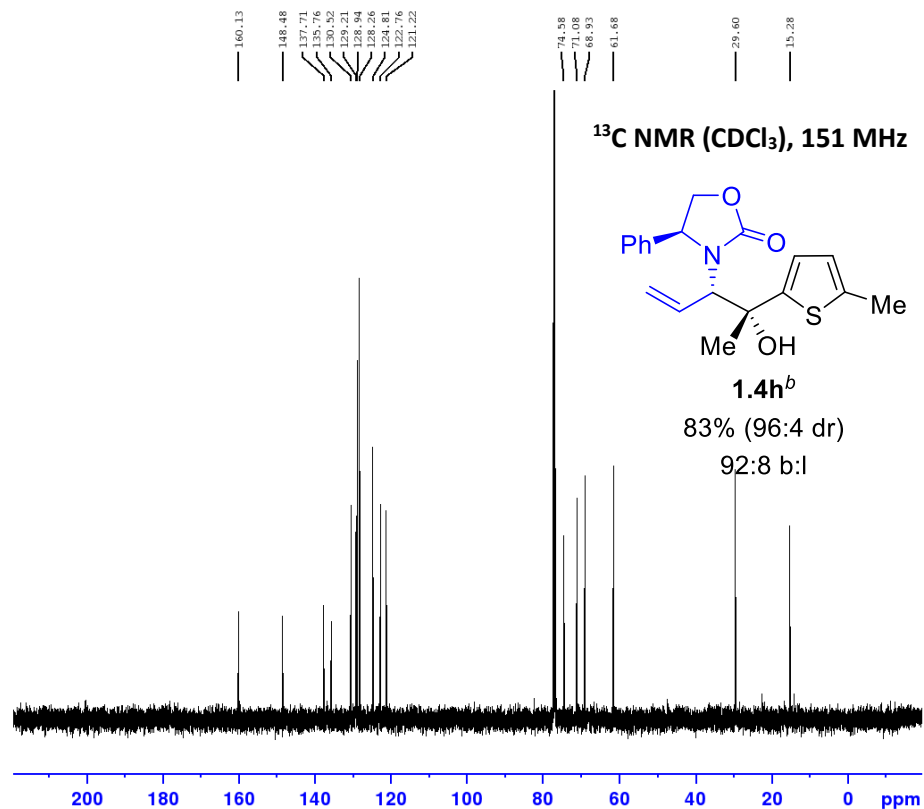




Current Data Parameters
 NAME SLG1-072_2
 EXPNO 1
 PROCNO 1

F2 - Acquisition Parameters
 Date_ 20190620
 Time 16.48 h
 INSTRUM spect
 PROBHD Z148658_0003 (
 PULPROG zg30
 TD 65536
 SOLVENT CDCl3
 NS 16
 DS 2
 SWH 12019.230 Hz
 FIDRES 0.366798 Hz
 AQ 2.7262976 sec
 RG 199.73
 DW 41.600 usec
 DE 6.50 usec
 TE 293.5 K
 D1 4.0000000 sec
 TDO 1
 SFO1 600.0087050 MHz
 NUC1 1H
 P1 15.50 usec
 PLW1 13.23200035 W

F2 - Processing parameters
 SI 65536
 SF 600.0050178 MHz
 WDW EM
 SSB 0
 LB 0.30 Hz
 GB 0
 PC 1.00



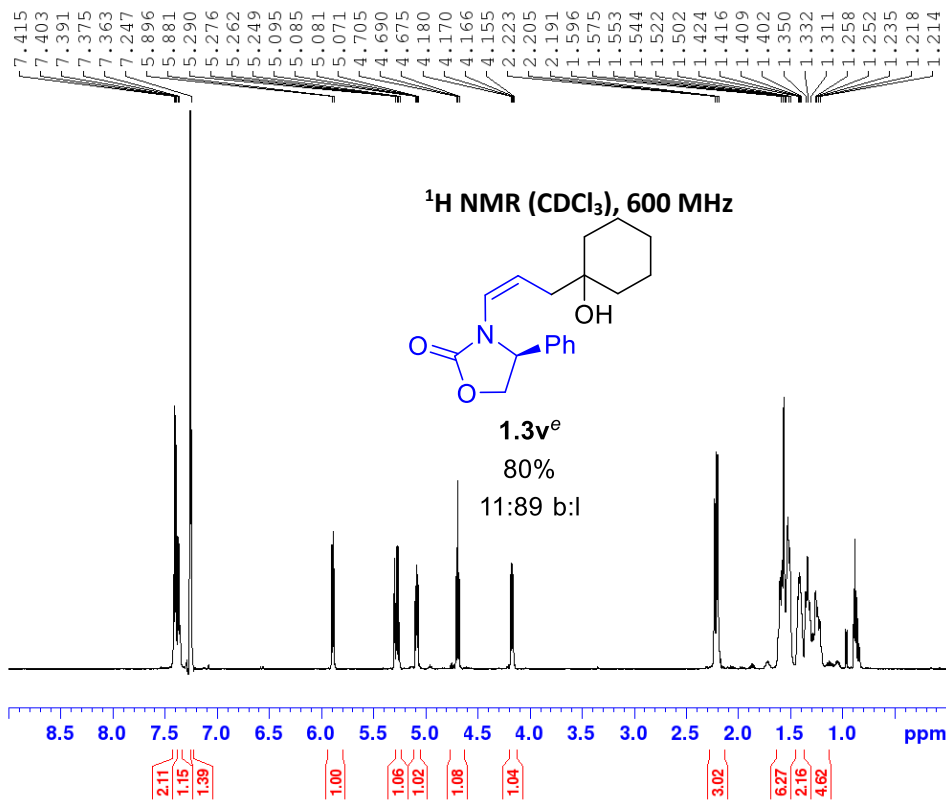
Current Data Parameters
 NAME SLG1-072_2c13
 EXPNO 1
 PROCNO 1

F2 - Acquisition Parameters
 Date_ 20190620
 Time 18.40
 INSTRUM spect
 PROBHD 5 mm PATXI 1H/
 PULPROG zgpg30
 TD 65536
 SOLVENT CDCl3
 NS 96
 DS 4
 SWH 36057.691 Hz
 FIDRES 0.550197 Hz
 AQ 0.9087659 sec
 RG 194.75
 DW 13.867 usec
 DE 6.50 usec
 TE 294.1 K
 D1 2.0000000 sec
 D11 0.03000000 sec
 TDO 1

===== CHANNEL f1 =====
 SFO1 150.8738899 MHz
 NUC1 13C
 P1 11.40 usec
 PLW1 176.19999695 W

===== CHANNEL f2 =====
 SFO2 599.9573998 MHz
 NUC2 1H
 CPDPRG2 waltz16
 PCPD2 70.00 usec
 PLW2 11.99499989 W
 PLW12 0.14703000 W
 PLW13 0.07204500 W

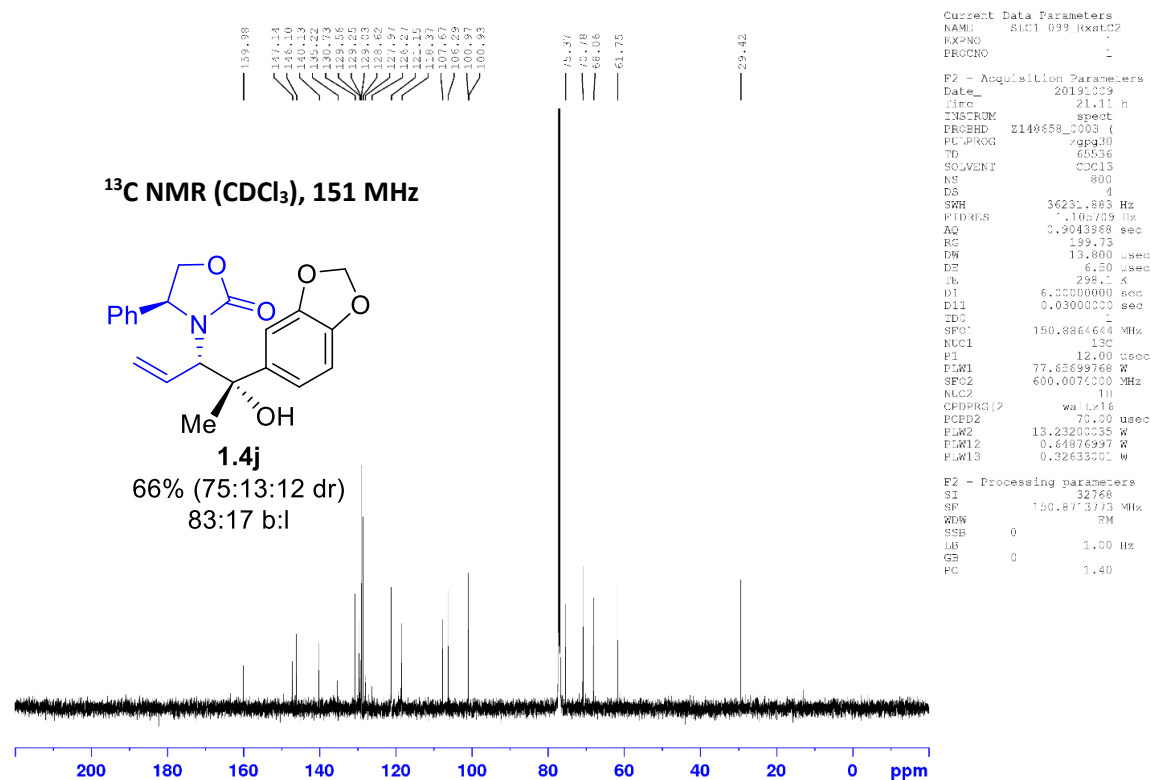
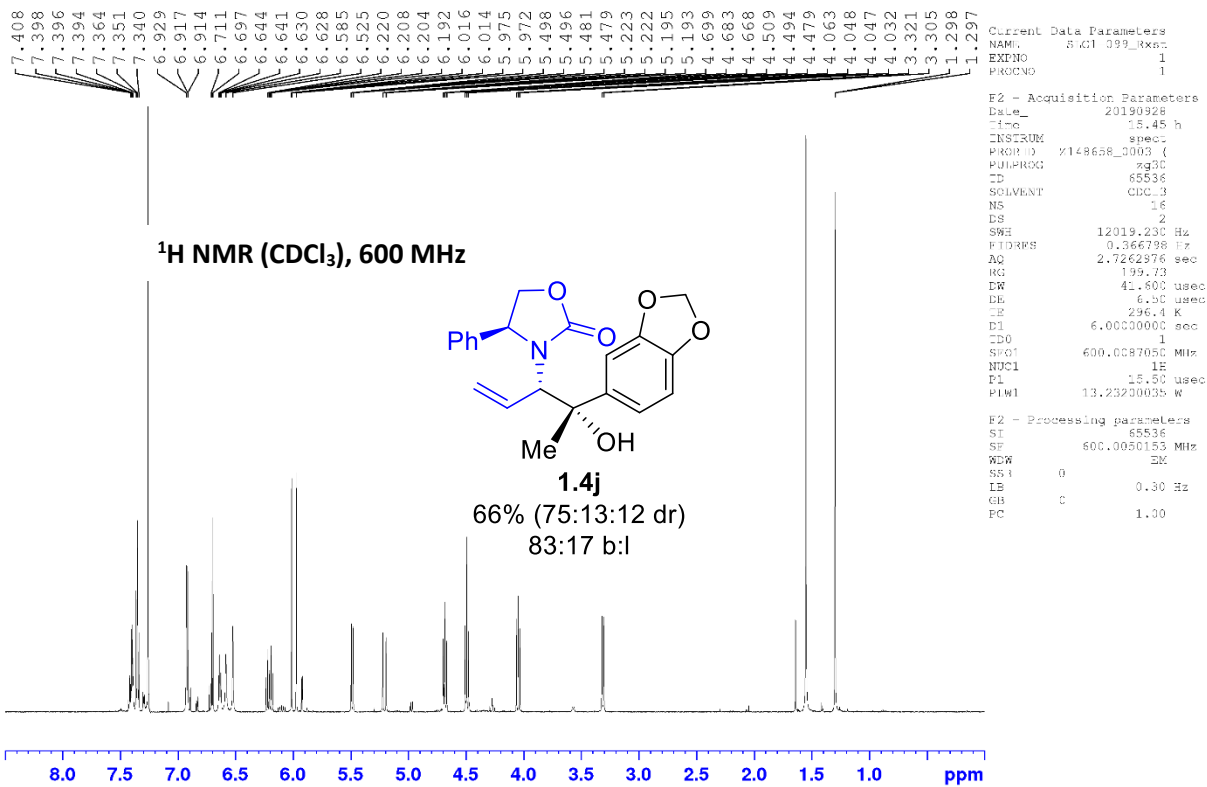
F2 - Processing parameters
 SI 32768
 SF 150.8588147 MHz
 WDW EM
 SSB 0
 LB 1.00 Hz
 GB 0
 PC 1.40

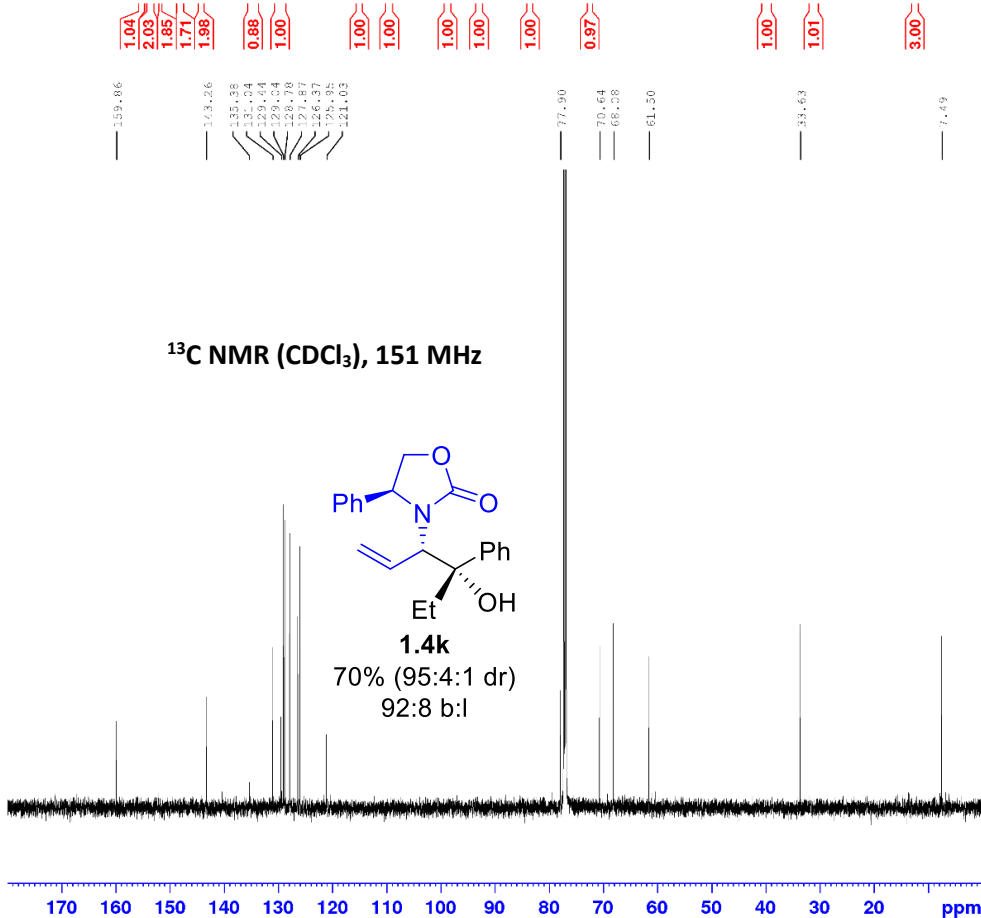
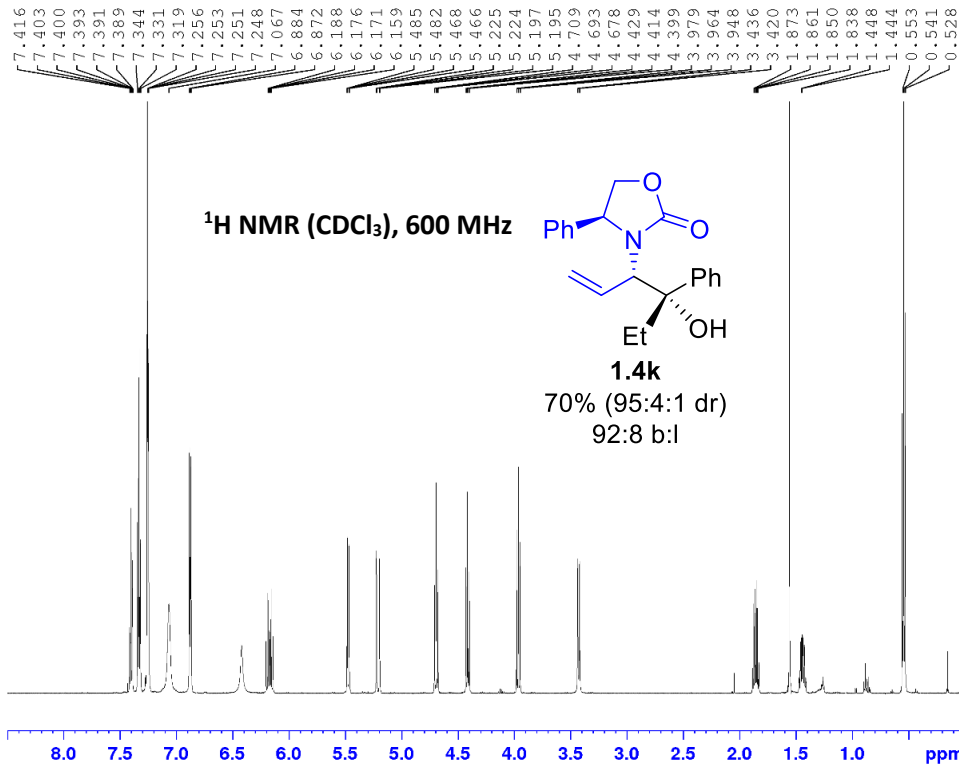


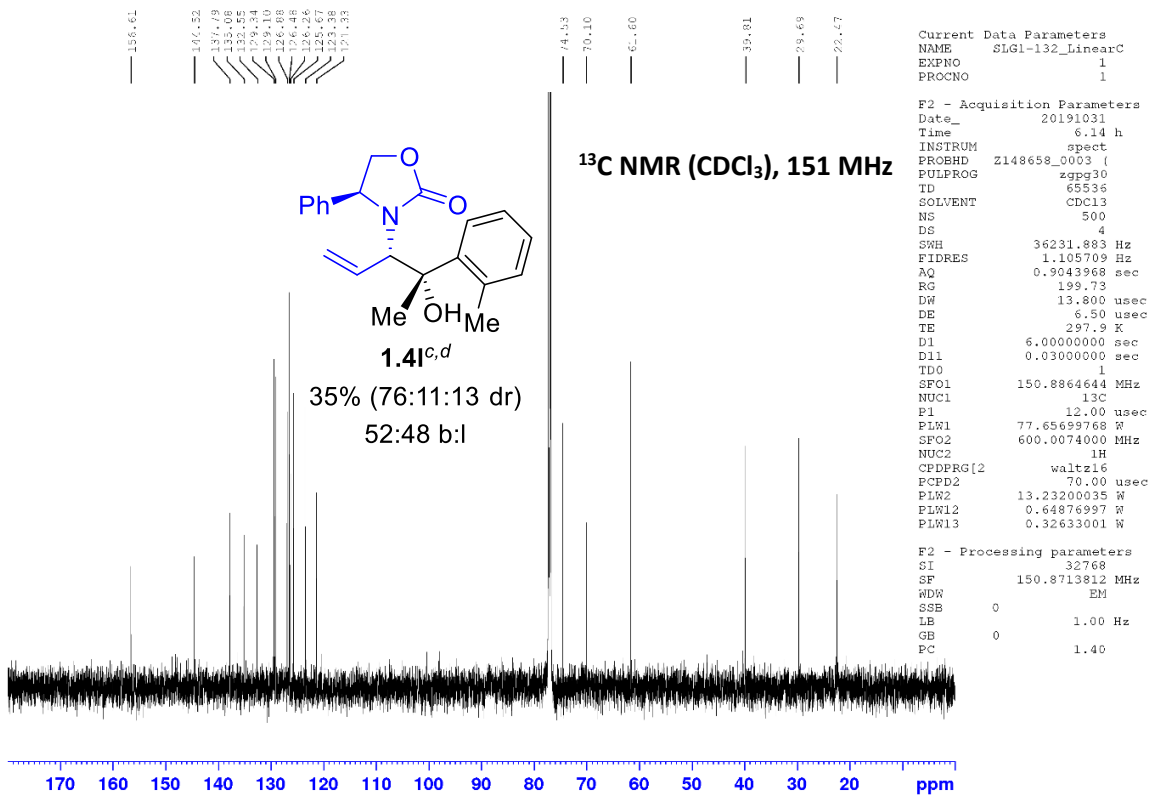
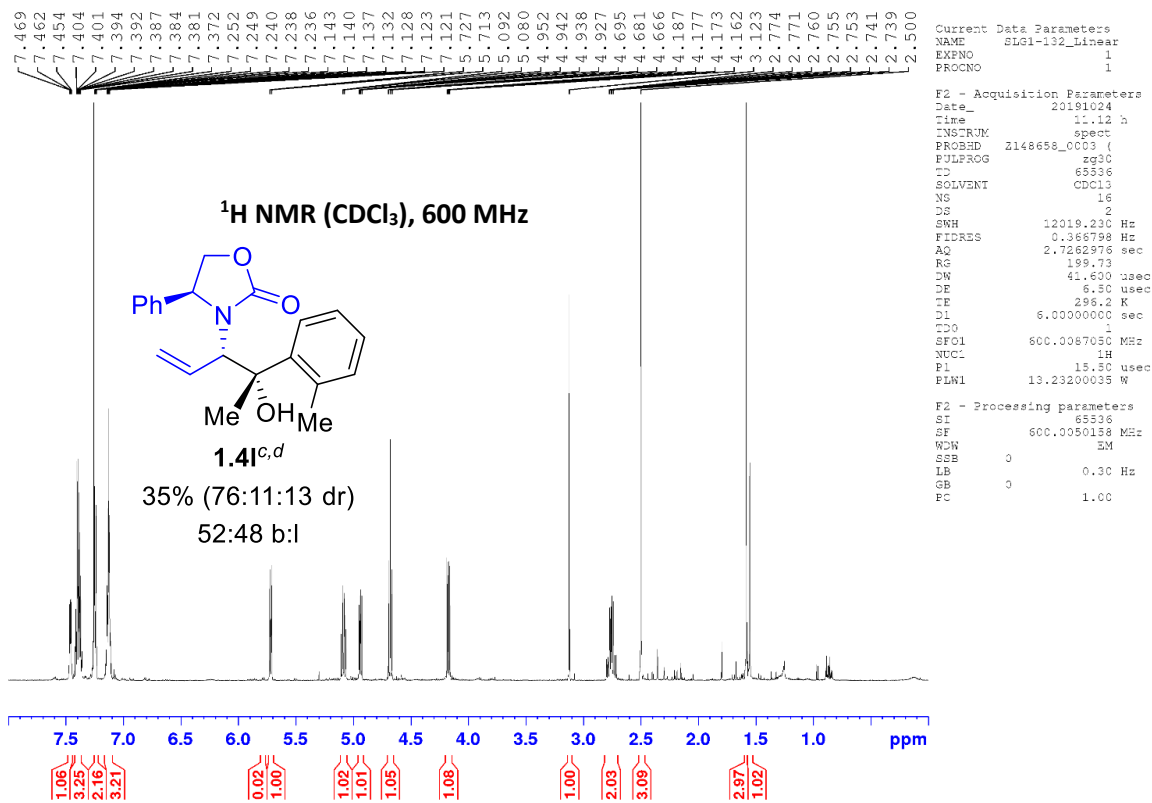
Current Data Parameters
 NAME SLGI-058
 EXPNO 1
 PROCNO 1

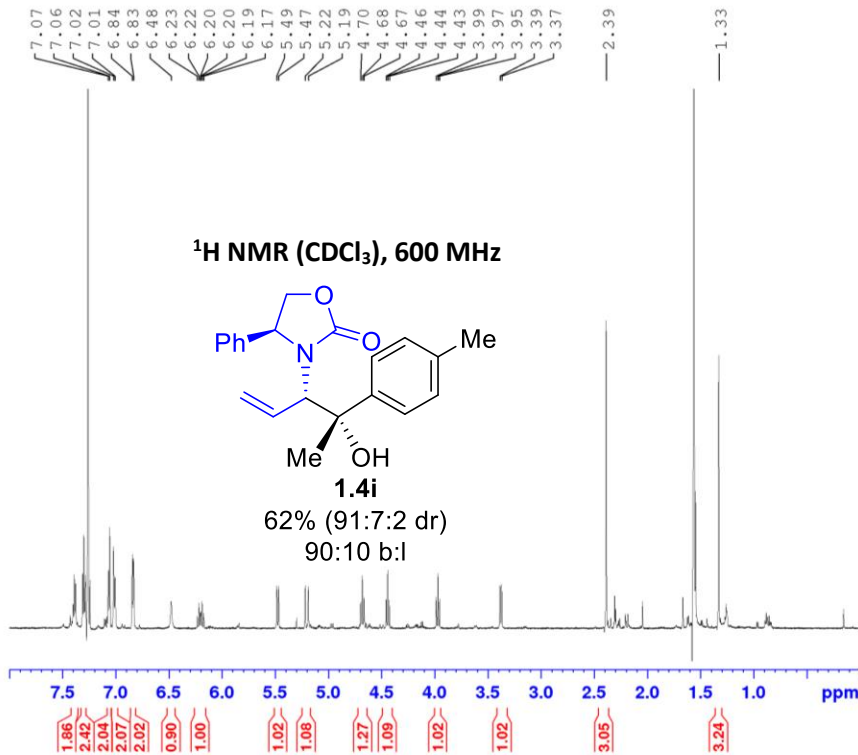
F2 - Acquisition Parameters
 Date_ 20190621
 Time 18.11 h
 INSTRUM spect
 PROBHD Z855801_0104 ()
 PULPROG zg30
 TD 65536
 SOLVENT CDCl3
 NS 16
 DS 2
 SWH 12019.230 Hz
 FIDRES 0.366798 Hz
 AQ 2.7262976 sec
 RG 194.75
 DW 41.600 usec
 DE 6.50 usec
 TE 293.6 K
 D1 4.0000000 sec
 TD0 1
 SF01 599.9587047 MHz
 NUC1 1H
 P1 7.75 usec
 PLW1 11.99499989 W

F2 - Processing parameters
 SI 65536
 SF 599.9550183 MHz
 NDW 0
 SSB 0
 LB 0.30 Hz
 GB 0
 PC 1.00









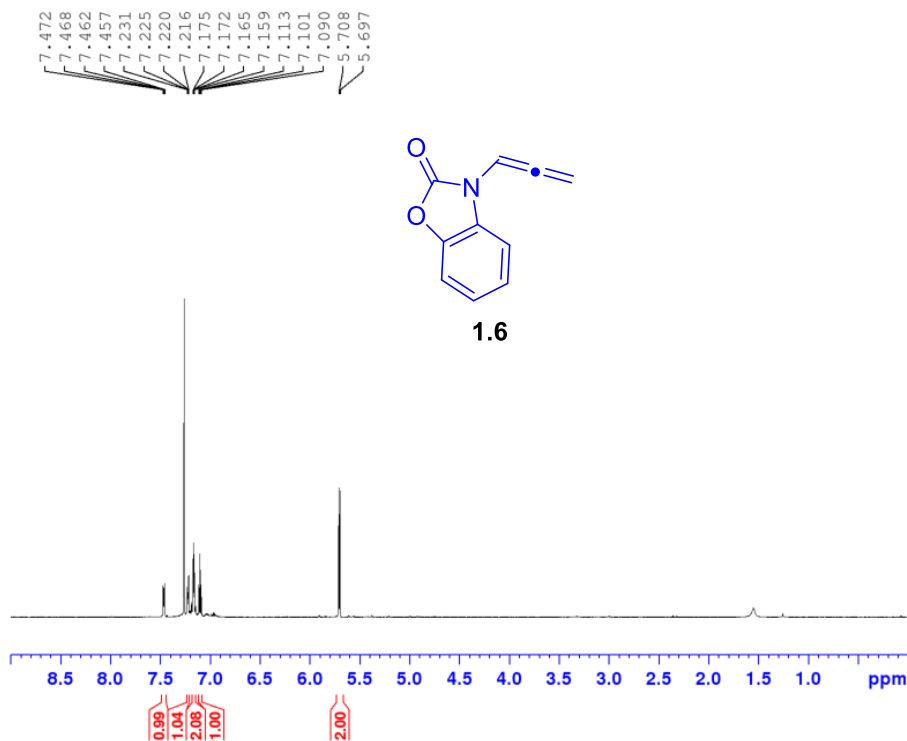
Current Data Parameters
NAME SLG1-102_SS
EXPNO 1
PROCNO 1

F2 - Acquisition Parameters
Date_ 20190816
Time 12.37 h
INSTRUM spect
PROBHD Z855801_0104 ()
PULPROG zg30
TD 65536
SOLVENT CDCl3
NS 16
DS 2
SWH 12019.230 Hz
FIDRES 0.366798 Hz
AQ 2.7262976 sec
RG 194.75
DW 41.600 usec
DE 6.50 usec
TE 296.1 K
D1 4.00000000 sec
TD0 1
SFO1 599.9587047 MHz
NUC1 1H
P1 7.75 usec
PLW1 11.99499989 W

F2 - Processing parameters
SI 65536
SF 599.9550156 MHz
WDW EM
SSB 0
LB 0.30 Hz
GB 0
PC 1.00

iii. Fused Phenyl NMR data:

Fused Phenyl Allene
 SLG2-054-1
 PROTON CDC13 {D:\nmrdata} Sieber 2

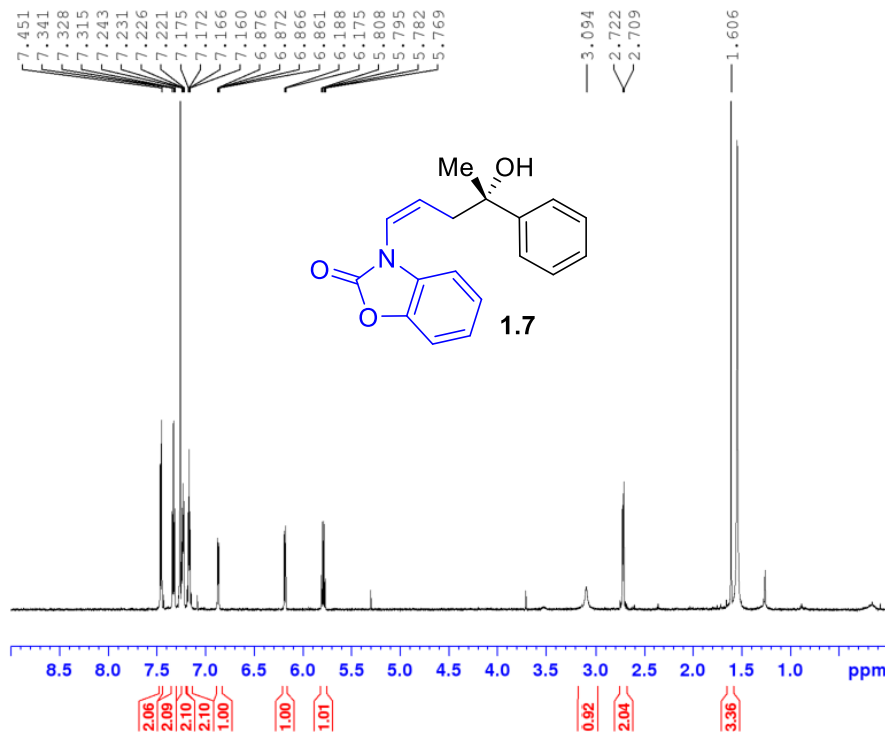


Current Data Parameters
 NAME SLG3-095
 EXPNO 2
 PROCNO 1

F2 - Acquisition Parameters
 Date_ 20220720
 Time 9.26 h
 INSTRUM spect
 PROBHD z148658_0003 (
 PULPROG zg30
 TD 65536
 SOLVENT CDCl3
 NS 16
 DS 2
 SWH 12019.230 Hz
 FIDRES 0.366798 Hz
 AQ 2.7262976 sec
 RG 199.73
 DW 41.600 usec
 DE 10.33 usec
 TE 298.1 K
 D1 4.00000000 sec
 TD0 1
 SFO1 600.0087050 MHz
 NUC1 1H
 P0 5.17 usec
 P1 15.50 usec
 PLW1 13.23200035 W

F2 - Processing parameters
 SI 65536
 SF 600.0050153 MHz
 WDW EM
 SSB 0
 LB 0.30 Hz
 GB 0
 PC 1.00

Linear product with Fused Phenyl allene and Acetophenone
 SLG3-095a-col
 PROTON CDC13 {D:\nmrdata} Sieber 7

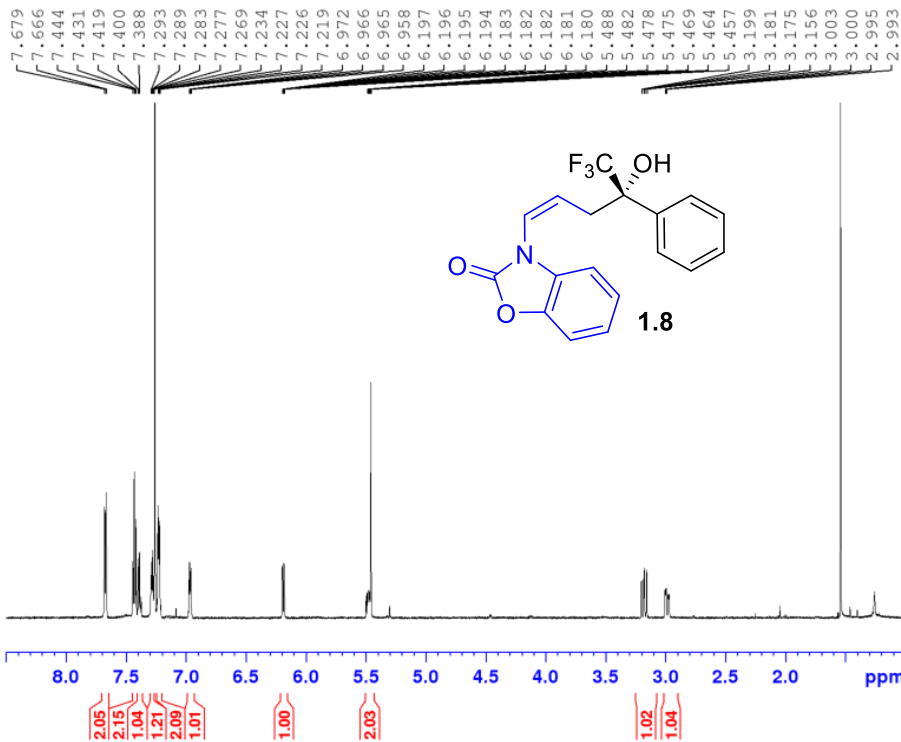


Current Data Parameters
 NAME SLG3-095
 EXPNO 16
 PROCNO 1

F2 - Acquisition Parameters
 Date_ 20220803
 Time 16.53 h
 INSTRUM spect
 PROBHD z148658_0003 (
 PULPROG zg30
 TD 65536
 SOLVENT CDCl3
 NS 16
 DS 2
 SWH 12019.230 Hz
 FIDRES 0.366798 Hz
 AQ 2.7262976 sec
 RG 199.73
 DW 41.600 usec
 DE 10.33 usec
 TE 298.1 K
 D1 4.00000000 sec
 TD0 1
 SFO1 600.0087050 MHz
 NUC1 1H
 P0 5.17 usec
 P1 15.50 usec
 PLW1 13.23200035 W

F2 - Processing parameters
 SI 65536
 SF 600.0050155 MHz
 WDW EM
 SSB 0
 LB 0.30 Hz
 GB 0
 PC 1.00

Linear CF3 product
 PROTON CDC13 {C:\Bruker\TopSpin3.5pl7} Sieber 1

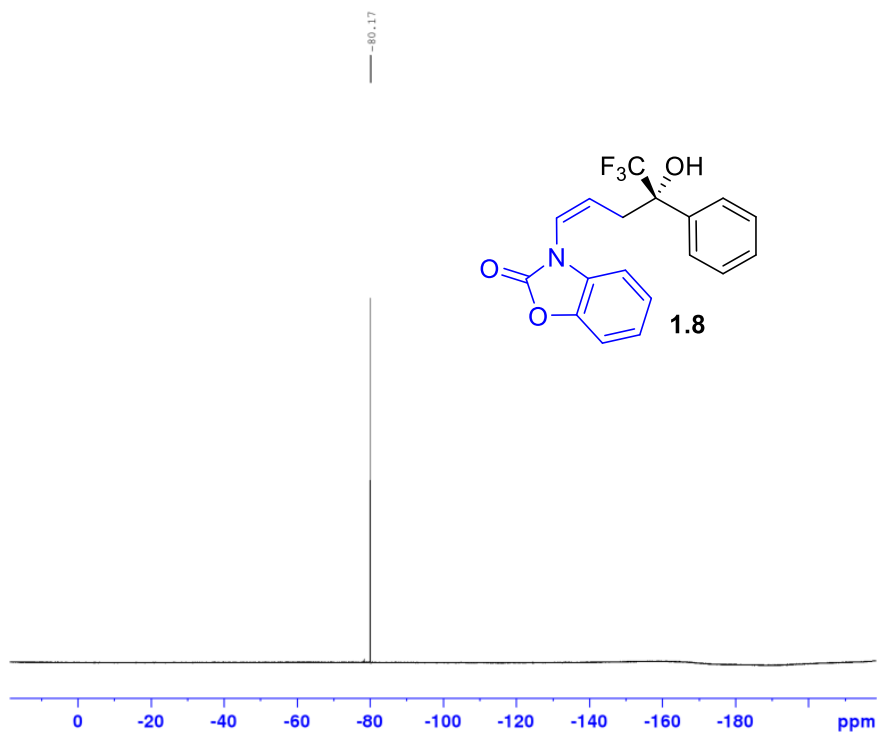


Current Data Parameters
 NAME SLG1-189-2
 EXPNO 1
 PROCNO 1

F2 - Acquisition Parameters
 Date_ 20200206
 Time 11.23 h
 INSTRUM spect
 PROBHD Z148658_0003 (
 PULPROG zg30
 TD 65536
 SOLVENT CDCl3
 NS 16
 DS 2
 SWH 12019.230 Hz
 FIDRES 0.366798 Hz
 AQ 2.7262976 sec
 RG 199.73
 DW 41.600 usec
 DE 6.50 usec
 TE 296.3 K
 D1 6.00000000 sec
 TD0 1
 SFO1 600.0087050 MHz
 NUC1 1H
 P1 15.50 usec
 PLW1 13.23200035 W

F2 - Processing parameters
 SI 65536
 SF 600.0050158 MHz
 WDW EM
 SSB 0
 LB 0.30 Hz
 GB 0
 PC 1.00

Linear CF3 product 1.8, 19FNMR
 F19CPD_vcu CDC13 {C:\Bruker\TopSpin3.5pl7} Sieber 1

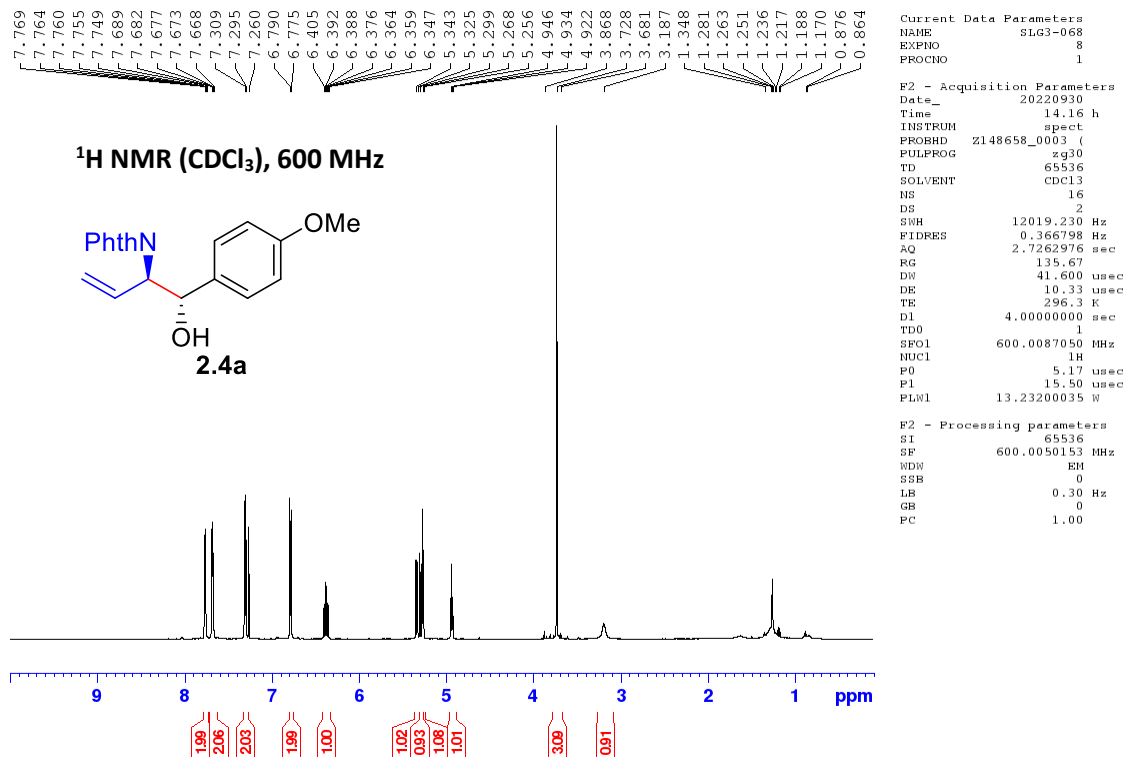


Current Data Parameters
 NAME SLG1-189-2F
 EXPNO 1
 PROCNO 1

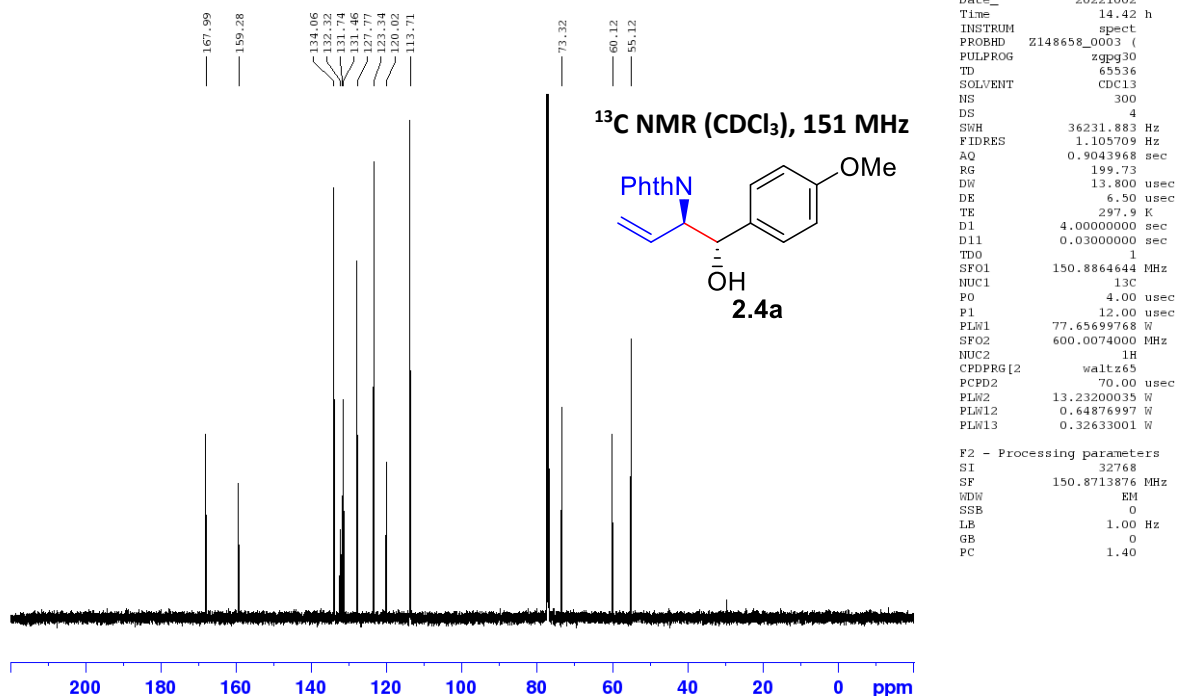
F2 - Acquisition Parameters
 Date_ 20200206
 Time 11.28 h
 INSTRUM spect
 PROBHD Z148658_0003 (
 PULPROG zgfhgqr.2
 TD 131072
 SOLVENT CDCl3
 NS 16
 DS 4
 SWH 133928.578 Hz
 FIDRES 2.043588 Hz
 AQ 0.4893355 sec
 RG 199.73
 DW 3.733 usec
 DE 6.50 usec
 TE 296.4 K
 D1 10.00000000 sec
 D11 0.03000000 sec
 D12 0.00002000 sec
 TD0 1
 SFO1 564.5123141 MHz
 NUC1 19F
 P1 15.00 usec
 PLW1 26.76399994 W
 SFO2 600.0074000 MHz
 NUC2 1H
 CPOPRG[2] waltz16
 PCPD2 70.00 usec
 PLW2 13.23200035 W
 PLW12 0.64876997 W

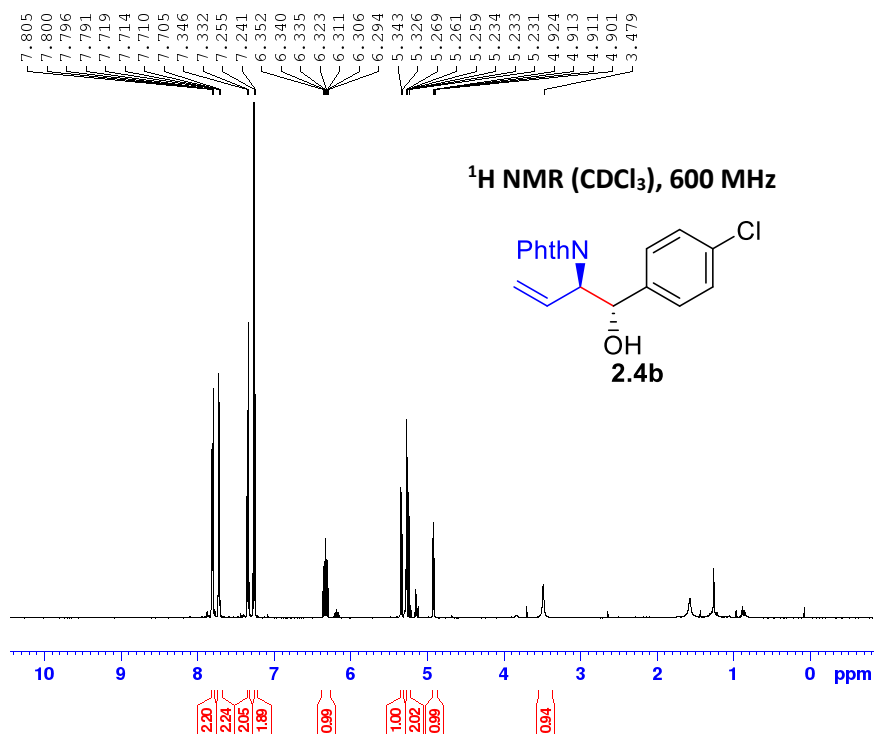
F2 - Processing parameters
 SI 65536
 SF 564.5687710 MHz
 WDW EM
 SSB 0
 LB 0.30 Hz
 GB 0
 PC 1.00

Appendix A2. Select NMR Spectra from Chapter 2



SLG3-068a-col
 13CNMR
 C13CPD CDC13 {D:\nmrdata} Sieber 2



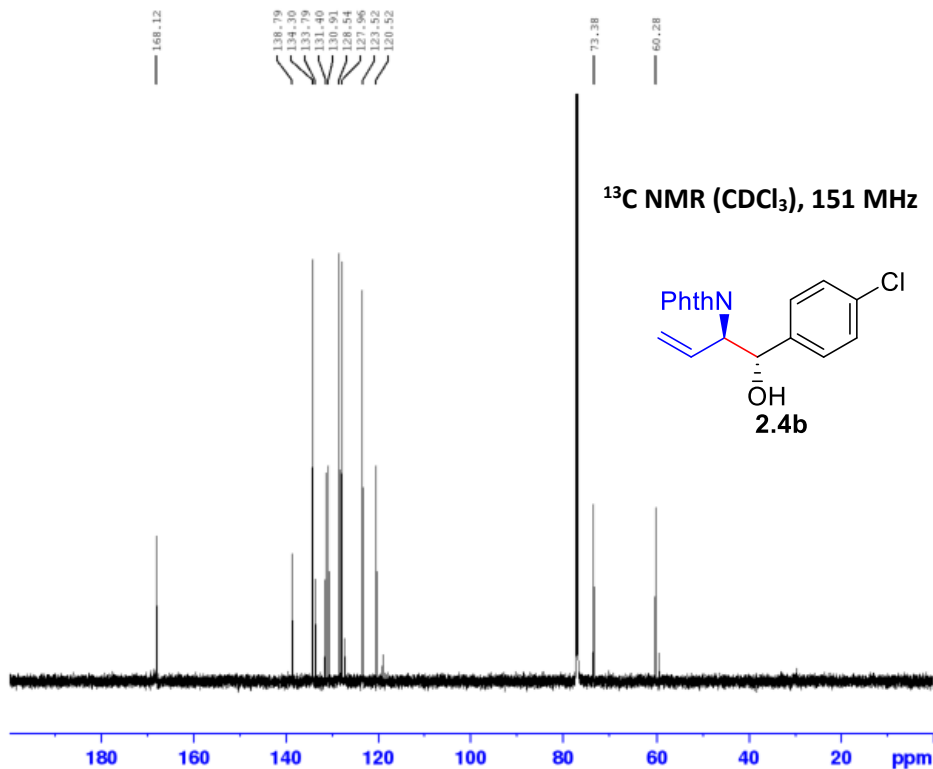


Current Data Parameters
 NAME SIG3-068
 EXPNO 14
 PROCNO 1

F2 - Acquisition Parameters
 Date_ 20221008
 Time 19.53 h
 INSTRUM spect
 PROBHD Z148658_0003 ()
 PULPROG zg30
 TD 65536
 SOLVENT CDCl3
 NS 16
 DS 2
 SWH 12019.230 Hz
 FIDRES 0.386798 Hz
 AQ 2.7262976 sec
 RG 199.73
 DW 41.600 usec
 DE 10.33 usec
 TE 296.5 K
 D1 4.00000000 sec
 TD0 1
 SF01 600.0087050 MHz
 NUC1 1H
 P0 5.17 usec
 P1 15.50 usec
 PLW1 13.23200035 W

F2 - Processing parameters
 SI 65536
 SF 600.0050168 MHz
 WDW EM
 SSB 0
 LB 0.30 Hz
 GB 0
 PC 1.00

SIG3-068b-col
 C13CPD CDCl3 (D:\nmrdata) Sieber 1



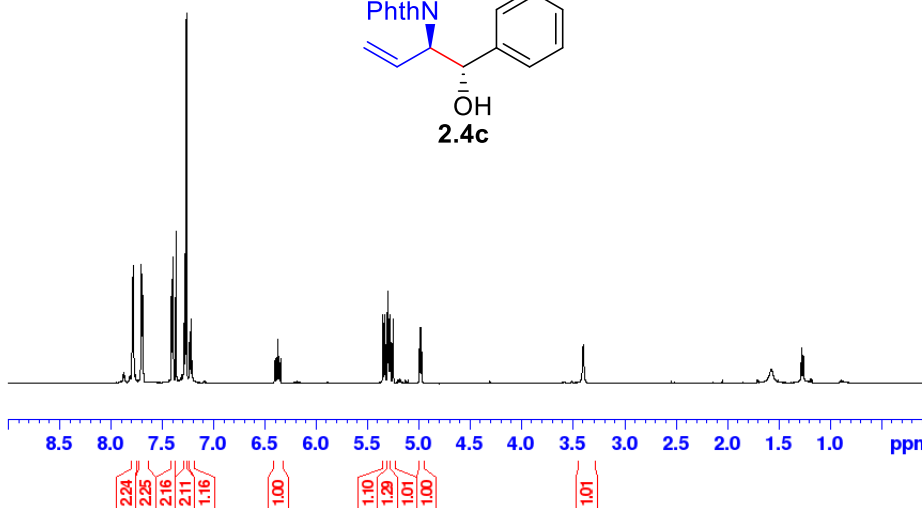
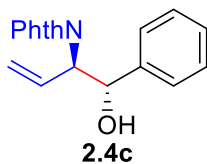
Current Data Parameters
 NAME SIG3-068
 EXPNO 15
 PROCNO 1

F2 - Acquisition Parameters
 Date_ 20221009
 Time 1.13 h
 INSTRUM spect
 PROBHD Z148658_0003 ()
 PULPROG zgpg30
 TD 65536
 SOLVENT CDCl3
 NS 300
 DS 4
 SWH 36231.883 Hz
 FIDRES 1.105709 Hz
 AQ 0.9043968 sec
 RG 199.73
 DW 13.800 usec
 DE 6.50 usec
 TE 297.8 K
 D1 6.00000000 sec
 D11 0.03000000 sec
 TD0 1
 SF01 150.8864644 MHz
 NUC1 13C
 P0 4.00 usec
 P1 12.00 usec
 PLW1 77.65699768 W
 SF02 600.0074000 MHz
 NUC2 1H
 CPDPRG2 waltz65
 PCPD2 70.00 usec
 PLW2 13.23200035 W
 PLW12 0.64876997 W
 PLW13 0.32633001 W

F2 - Processing parameters
 SI 32768
 SF 150.8713827 MHz
 WDW EM
 SSB 0
 LB 1.00 Hz
 GB 0
 PC 1.40

7.697
7.692
7.688
7.683
7.402
7.390
7.283
7.271
7.225
7.213
7.200
6.398
6.386
6.381
6.369
6.357
6.352
6.340
5.341
5.324
5.297
5.283
5.271
5.242
4.985
4.974
4.962
3.388

¹H NMR (CDCl₃), 600 MHz



Current Data Parameters
NAME SLG3-034
EXPNO 13
PROCNO 1

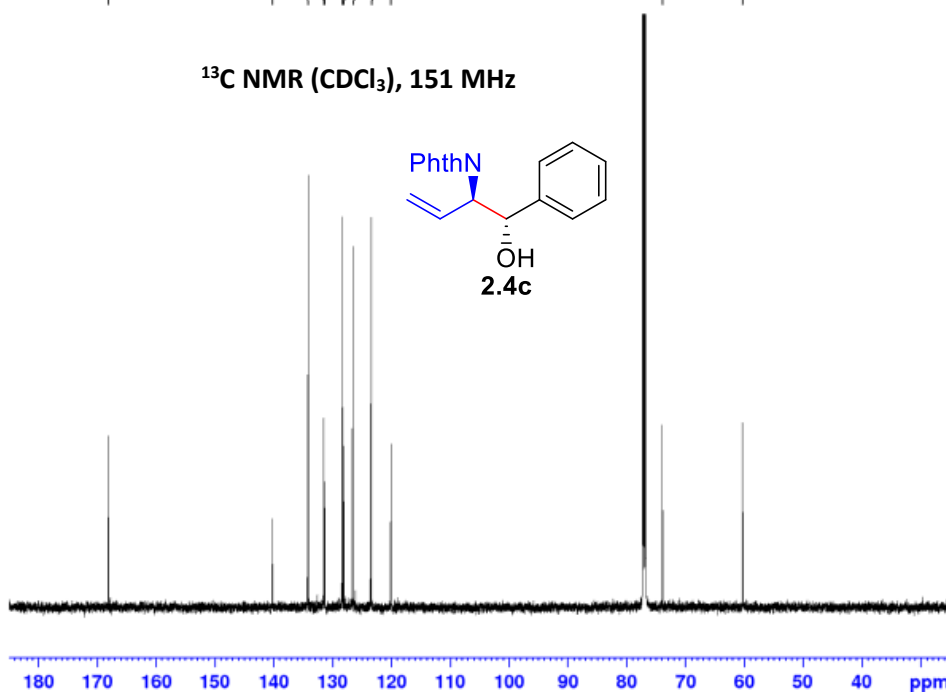
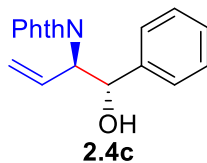
F2 - Acquisition Parameters
Date_ 20221102
Time 17.35 h
INSTRUM spect
PROBHD Z148658_0003 (
PULPROG zg30
TD 65536
SOLVENT CDCl3
NS 16
DS 2
SWH 12019.230 Hz
FIDRES 0.366798 Hz
AQ 2.7262976 sec
RG 199.73
DW 41.600 usec
DE 10.33 usec
TE 296.2 K
D1 4.0000000 sec
TD0 1
SF01 600.0087050 MHz
NUC1 1H
P0 5.17 usec
P1 15.50 usec
PLW1 13.23200035 W

F2 - Processing parameters
SI 65536
SF 600.0050166 MHz
WDW EM
SSB 0
LB 0.30 Hz
GB 0
PC 1.00

SLG3-034a-col-13CNMR
C13CPD CDC13 {D:\nmrdata} Sieber 23

168.10
140.24
134.14
131.47
131.32
128.34
126.53
123.38
120.07
73.92
60.32

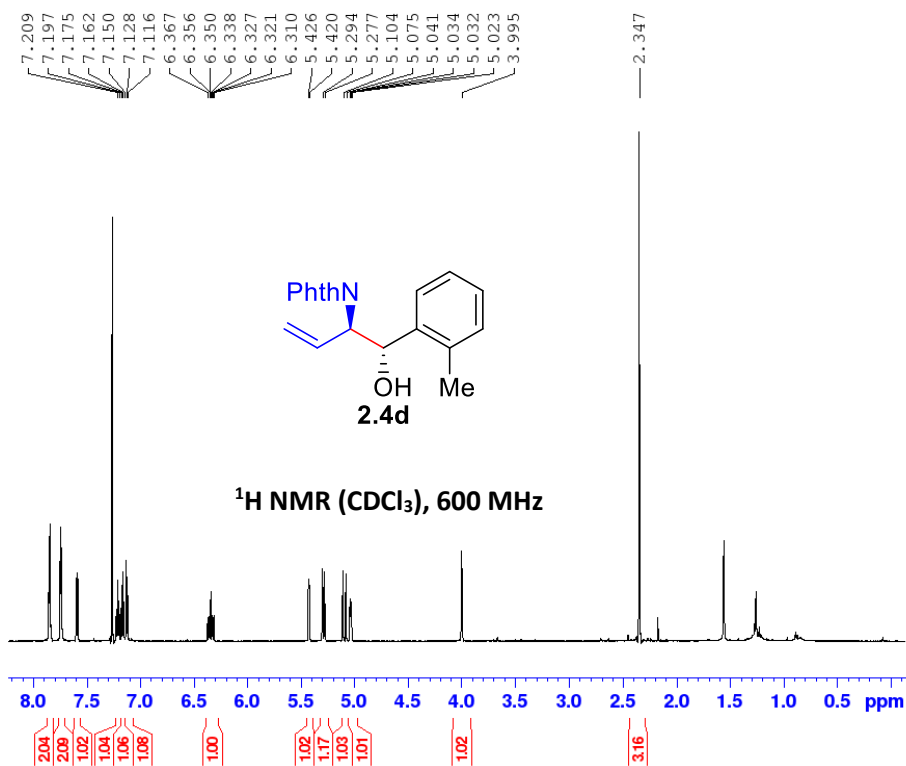
¹³C NMR (CDCl₃), 151 MHz



Current Data Parameters
NAME SLG3-034
EXPNO 17
PROCNO 1

F2 - Acquisition Parameters
Date_ 20220526
Time 0.18 h
INSTRUM spect
PROBHD Z148658_0003 (
PULPROG zgpg30
TD 65536
SOLVENT CDCl3
NS 1024
DS 4
SWH 36231.883 Hz
FIDRES 1.105709 Hz
AQ 0.9043968 sec
RG 199.73
DW 13.800 usec
DE 6.50 usec
TE 297.9 K
D1 6.0000000 sec
D11 0.03000000 sec
TD0 1
SF01 150.8864644 MHz
NUC1 13C
P0 4.00 usec
P1 12.00 usec
PLW1 77.65699768 W
SF02 600.0074000 MHz
NUC2 1H
CFDPRG[2] waltz65
PCPD2 70.00 usec
PLW2 13.23200035 W
PLW12 0.64876997 W
PLW13 0.32633001 W

F2 - Processing parameters
SI 32768
SF 150.8713842 MHz
WDW EM
SSB 0
LB 1.00 Hz
GB 0
PC 1.40

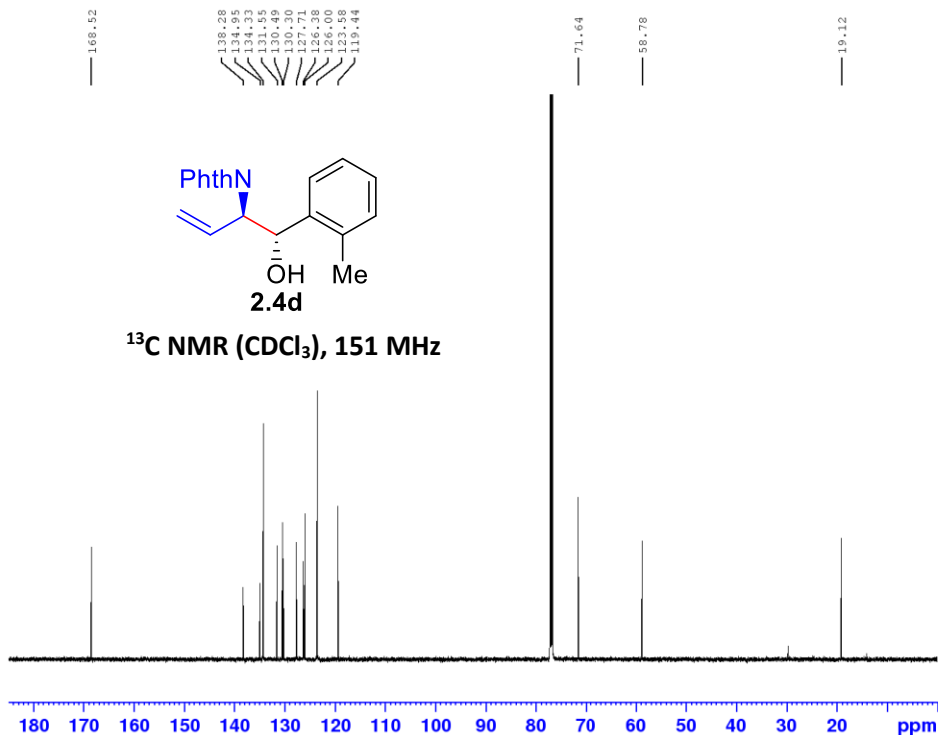


Current Data Parameters
 NAME SLG3-034_2
 EXPNO 6
 PROCNO 1

F2 - Acquisition Parameters
 Date_ 20220503
 Time 16.46 h
 INSTRUM spect
 PROBHD Z148658_0003 (
 PULPROG zg30
 TD 65536
 SOLVENT CDCl3
 NS 16
 DS 2
 SWH 12019.230 Hz
 FIDRES 0.366798 Hz
 AQ 2.7262976 sec
 RG 199.73
 DW 41.600 usec
 DE 10.33 usec
 TE 296.1 K
 D1 4.0000000 sec
 TD0 1
 SFO1 600.0087050 MHz
 NUC1 1H
 P0 5.17 usec
 P1 15.50 usec
 PLW1 13.23200035 W

F2 - Processing parameters
 SI 65536
 SF 600.0050158 MHz
 NDNW EM
 SSB 0
 LB 0.30 Hz
 GB 0
 PC 1.00

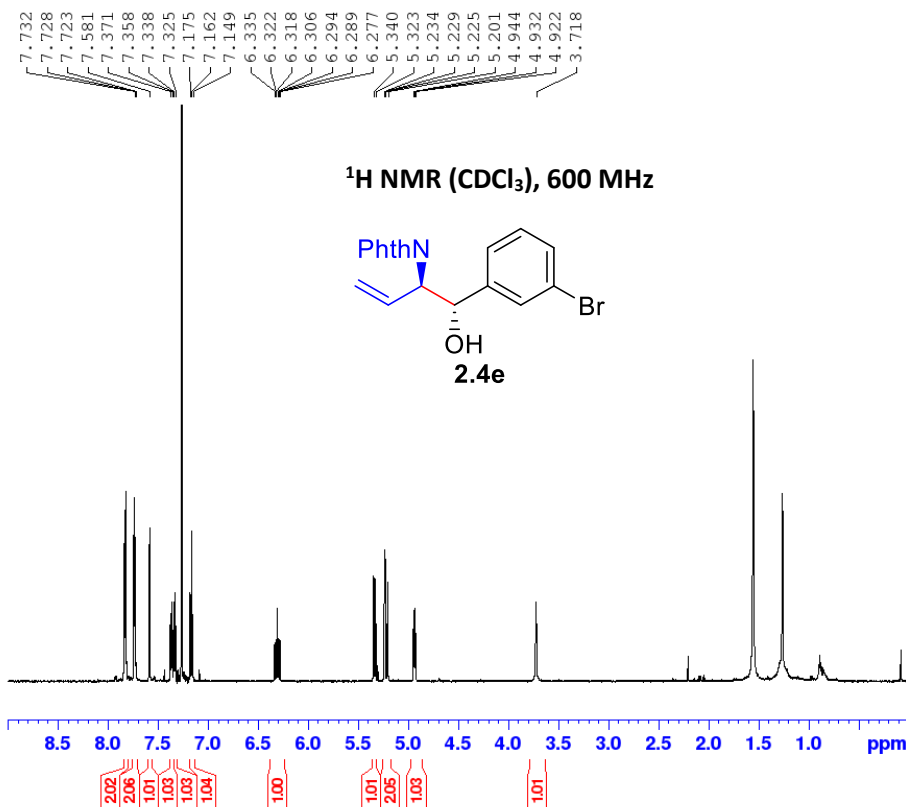
SLG3-034b-col-13CNMR
 C13CPD CDCl3 {D:\nmrdata} Sieber 21



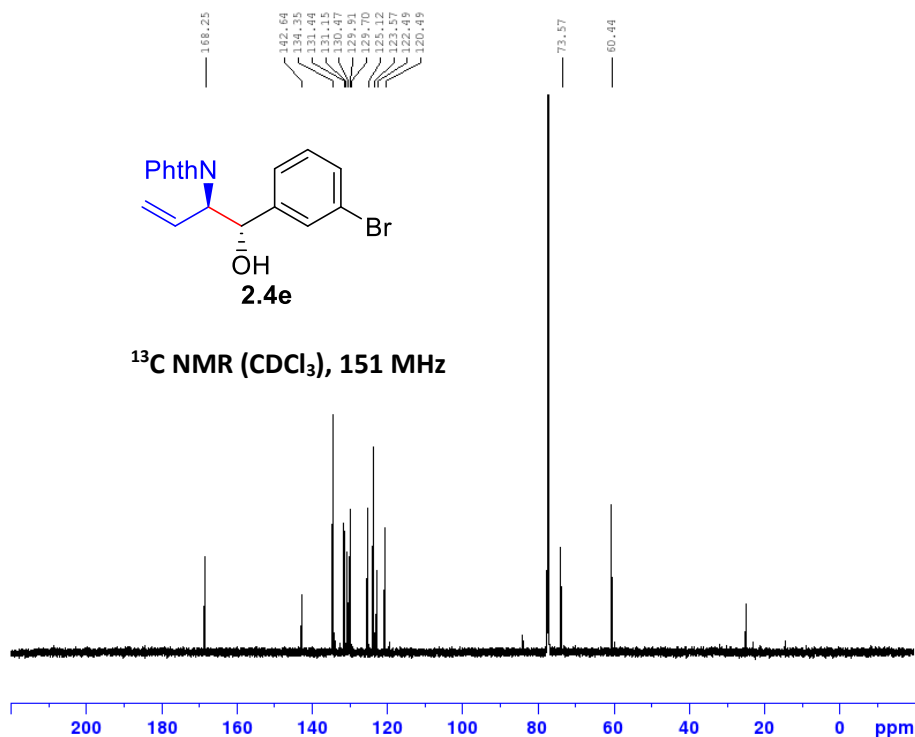
Current Data Parameters
 NAME SLG3-034
 EXPNO 19
 PROCNO 1

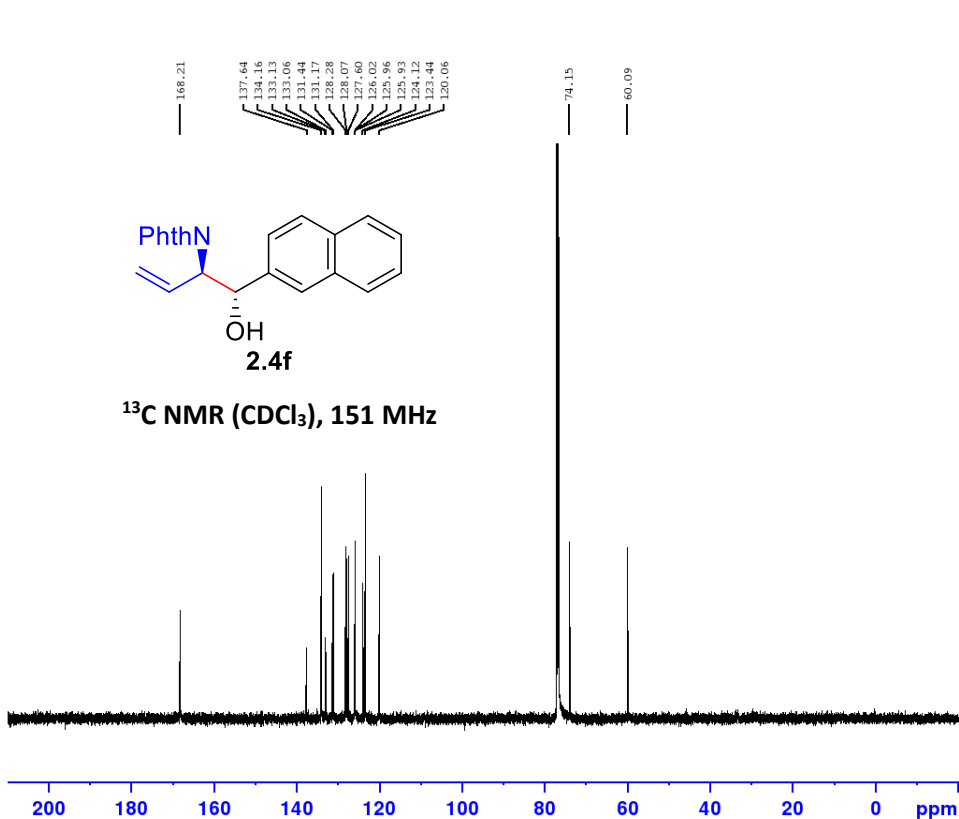
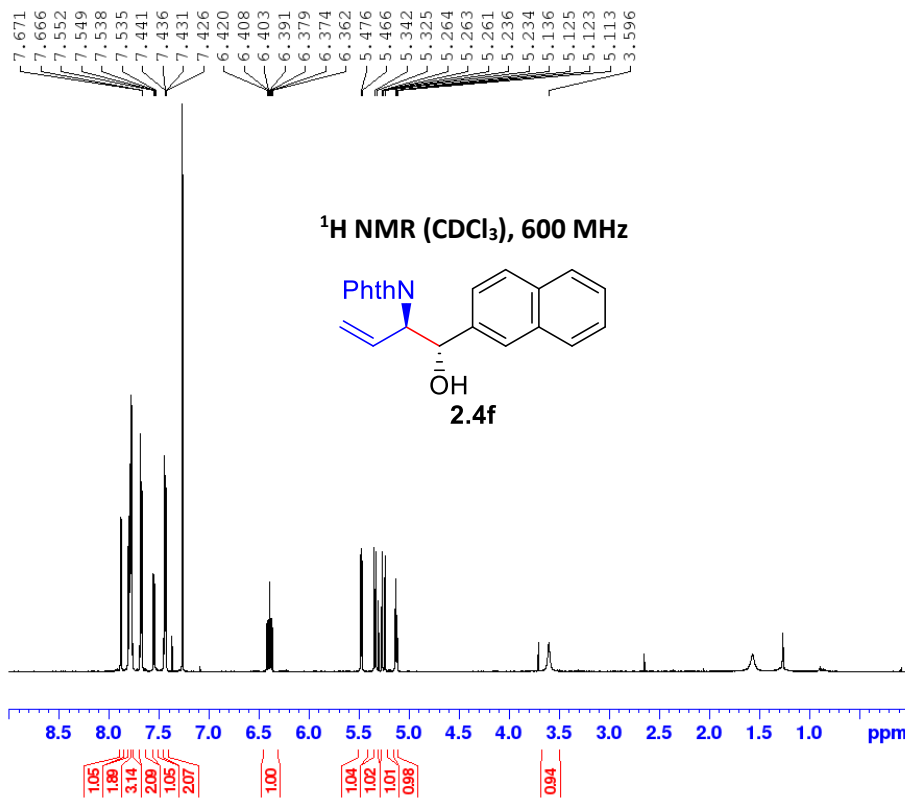
F2 - Acquisition Parameters
 Date_ 20220526
 Time 22.09 h
 INSTRUM spect
 PROBHD Z148658_0003 (
 PULPROG zgpg30
 TD 65536
 SOLVENT CDCl3
 NS 1024
 DS 4
 SWH 36231.883 Hz
 FIDRES 1.105709 Hz
 AQ 0.9043968 sec
 RG 199.73
 DW 13.800 usec
 DE 6.50 usec
 TE 297.8 K
 D1 6.0000000 sec
 D11 0.03000000 sec
 TD0 1
 SFO1 150.8864644 MHz
 NUC1 13C
 P0 4.00 usec
 P1 12.00 usec
 PLW1 77.65699768 W
 SFO2 600.0074000 MHz
 NUC2 1H
 CPDPRG[2] waltz65
 PCPD2 70.00 usec
 PLW2 13.23200035 W
 PLW12 0.64876997 W
 PLW13 0.32633001 W

F2 - Processing parameters
 SI 32768
 SF 150.8713828 MHz
 NDNW EM
 SSB 0
 LB 1.00 Hz
 GB 0
 PC 1.40

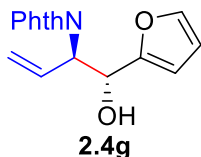


SLG3-034c-recol
C13CPD CDC13 {D:\nmrdata} Sieber 2

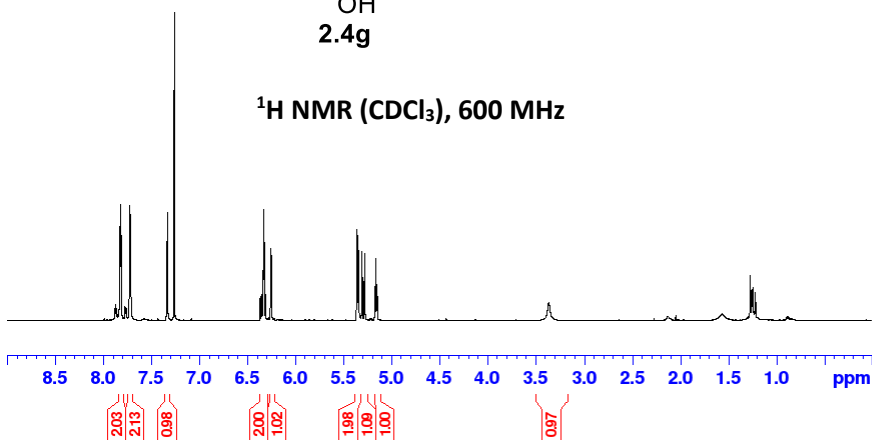




7.818
7.813
7.724
7.719
7.715
7.710
7.328
6.364
6.352
6.347
6.335
6.328
6.323
6.306
6.254
6.252
6.250
6.247
5.355
5.353
5.345
5.335
5.302
5.273
5.167
5.155
5.144
3.355



¹H NMR (CDCl₃), 600 MHz



Current Data Parameters
NAME SLG3-038
EXPNO 10
PROCNO 1

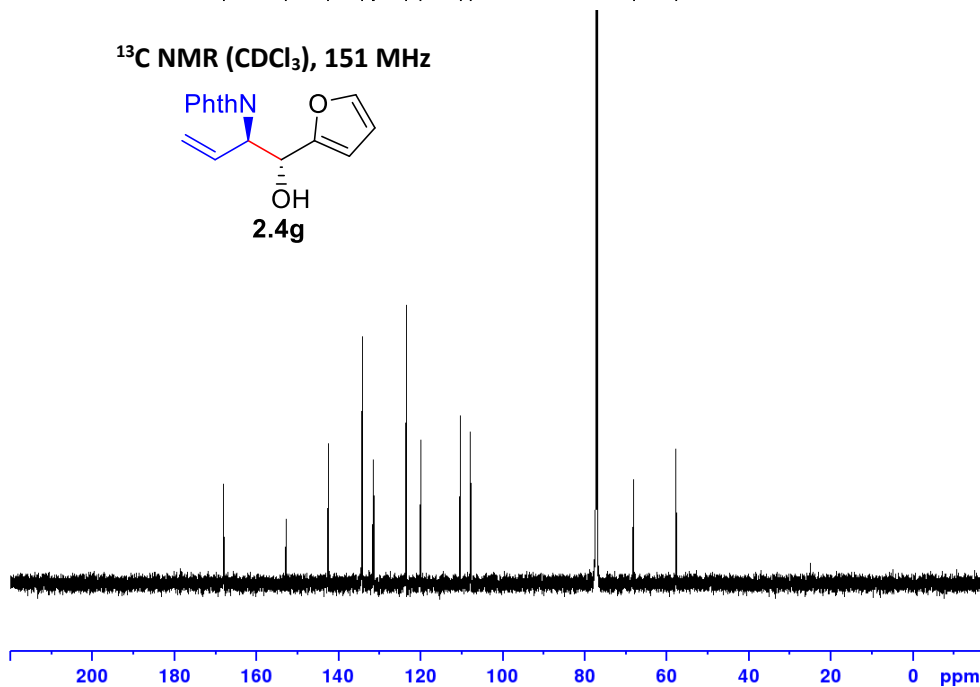
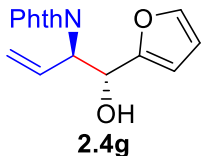
F2 - Acquisition Parameters
Date_ 20211214
Time 14.39 h
INSTRUM spect
PROBHD Z855801_0104 ()
PULPROG zg30
TD 65536
SOLVENT CDCl3
NS 16
DS 2
SWH 12019.230 Hz
FIDRES 0.366798 Hz
AQ 2.7262976 sec
RG 194.75
DN 41.600 usec
DE 6.50 usec
TE 296.5 K
D1 4.0000000 sec
TD0 1
SF01 599.9587047 MHz
NUC1 1H
P1 7.75 usec
PLW1 11.99499989 W

F2 - Processing parameters
SI 65536
SF 599.9550173 MHz
WDW EM
SSB 0
LB 0.30 Hz
GB 0
PC 1.00

SLG3-038e-col-13C
C13CPD CDCl3 (D:\nmrdata) Sieber 4

168.00
152.79
142.47
134.23
131.52
131.34
123.49
115.98
110.26
107.76
68.05
57.74

¹³C NMR (CDCl₃), 151 MHz

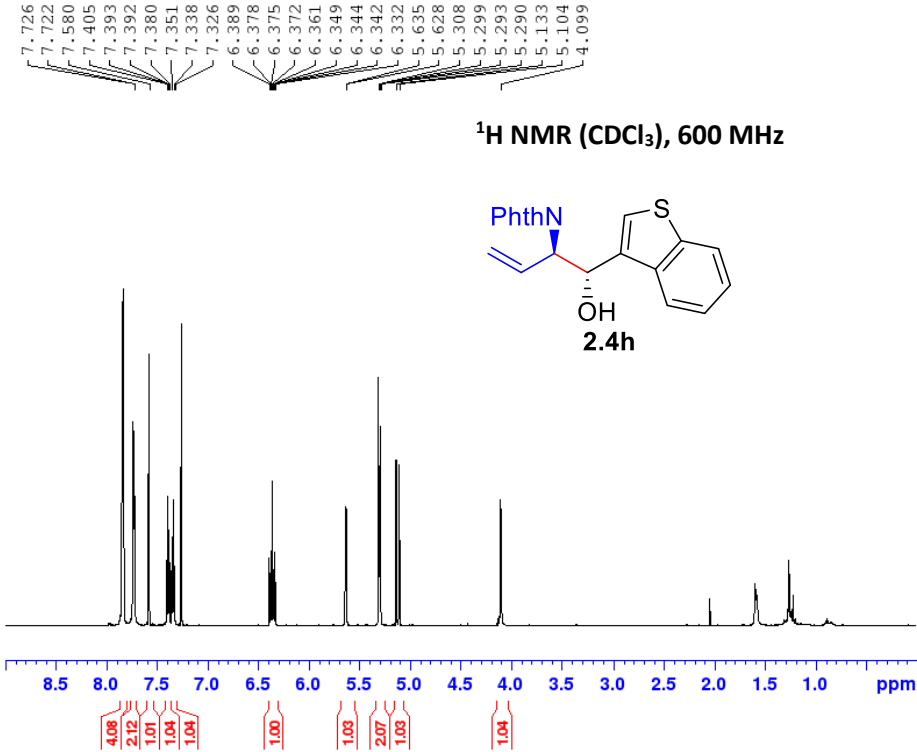


Current Data Parameters
NAME SLG3-038_2
EXPNO 7
PROCNO 1

F2 - Acquisition Parameters
Date_ 20220503
Time 22.09 h
INSTRUM spect
PROBHD z148658_0003 ()
PULPROG zgpg30
TD 65536
SOLVENT CDCl3
NS 300
DS 4
SWH 36231.883 Hz
FIDRES 1.105709 Hz
AQ 0.9043968 sec
RG 199.73
DN 13.800 usec
DE 6.50 usec
TE 298.0 K
D1 6.0000000 sec
D11 0.0300000 sec
TD0 1
SF01 150.8864644 MHz
NUC1 13C
P0 4.00 usec
P1 12.00 usec
PLW1 77.65699768 W
SF02 600.0074000 MHz
NUC2 1H
CPDPRG2 waltz65
PCPD2 70.00 usec
PLW2 13.23200035 W
PLW12 0.64876997 W
PLW13 0.32633001 W

F2 - Processing parameters
SI 32768
SF 150.8713820 MHz
WDW EM
SSB 0
LB 1.00 Hz
GB 0
PC 1.40

SLG3-001b-1
 PROTON CDC13 {C:\Bruker\TopSpin3.5pl7} Sieber 3

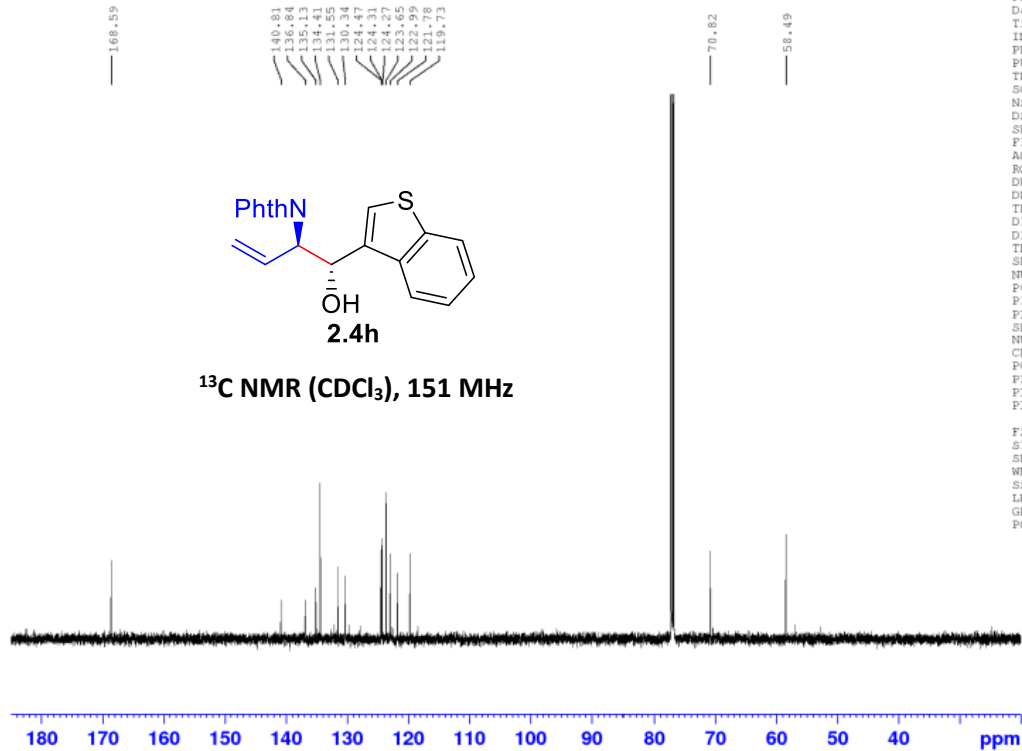


Current Data Parameters
 NAME SLG3-001
 EXPNO 3
 PROCNO 1

F2 - Acquisition Parameters
 Date_ 20210920
 Time 14.54 h
 INSTRUM spect
 PROBHD Z855801_0104 ()
 PULPROG zg30
 TD 65536
 SOLVENT CDC13
 NS 16
 DS 2
 SWH 12019.230 Hz
 FIDRES 0.366798 Hz
 AQ 2.7262976 sec
 RG 140.87
 DW 41.600 usec
 DE 6.50 usec
 TE 298.0 K
 D1 4.00000000 sec
 TDO 1
 SFO1 599.9587047 MHz
 NUC1 1H
 F1 7.75 usec
 PLW1 11.99499989 W

F2 - Processing parameters
 SI 65536
 SF 599.9550158 MHz
 WDW EM
 SSB 0
 LB 0.30 Hz
 GB 0
 PC 1.00

SLG3-001b-1
 13CNMR
 C13CPD CDC13 {D:\nmrdata} Sieber 4

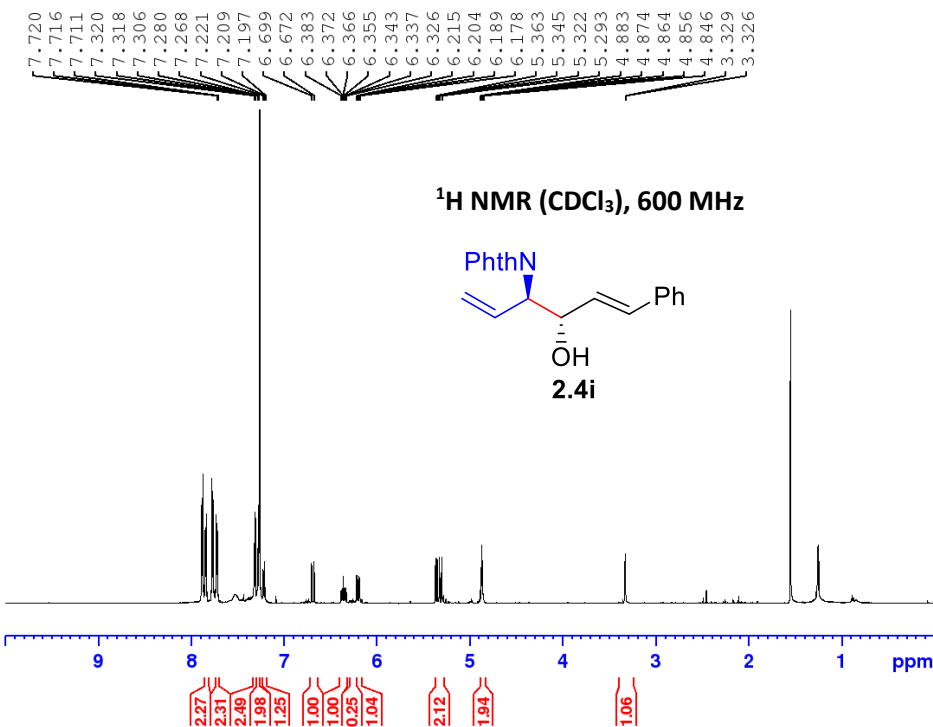


Current Data Parameters
 NAME SLG3-001
 EXPNO 14
 PROCNO 1

F2 - Acquisition Parameters
 Date_ 20220513
 Time 14.20 h
 INSTRUM spect
 PROBHD z148658_0003 ()
 PULPROG zgpg30
 TD 65536
 SOLVENT CDC13
 NS 100
 DS 4
 SWH 36231.883 Hz
 FIDRES 1.105709 Hz
 AQ 0.9043968 sec
 RG 199.73
 DW 13.800 usec
 DE 6.50 usec
 TE 297.5 K
 D1 6.00000000 sec
 D11 0.03000000 sec
 TDO 1
 SFO1 150.8864644 MHz
 NUC1 13C
 F0 4.00 usec
 F1 12.00 usec
 PLW1 77.65699768 W
 SFO2 600.0074000 MHz
 NUC2 1H
 CPDPRG2 waltz65
 PCPD2 70.00 usec
 PLW2 13.23200035 W
 PLW12 0.64876997 W
 PLW13 0.32633001 W

F2 - Processing parameters
 SI 32768
 SF 150.8713773 MHz
 WDW EM
 SSB 0
 LB 1.00 Hz
 GB 0
 PC 1.40

SLG3-006-1
 PROTON CDC13 {C:\Bruker\TopSpin3.5pl7} Sieber 12

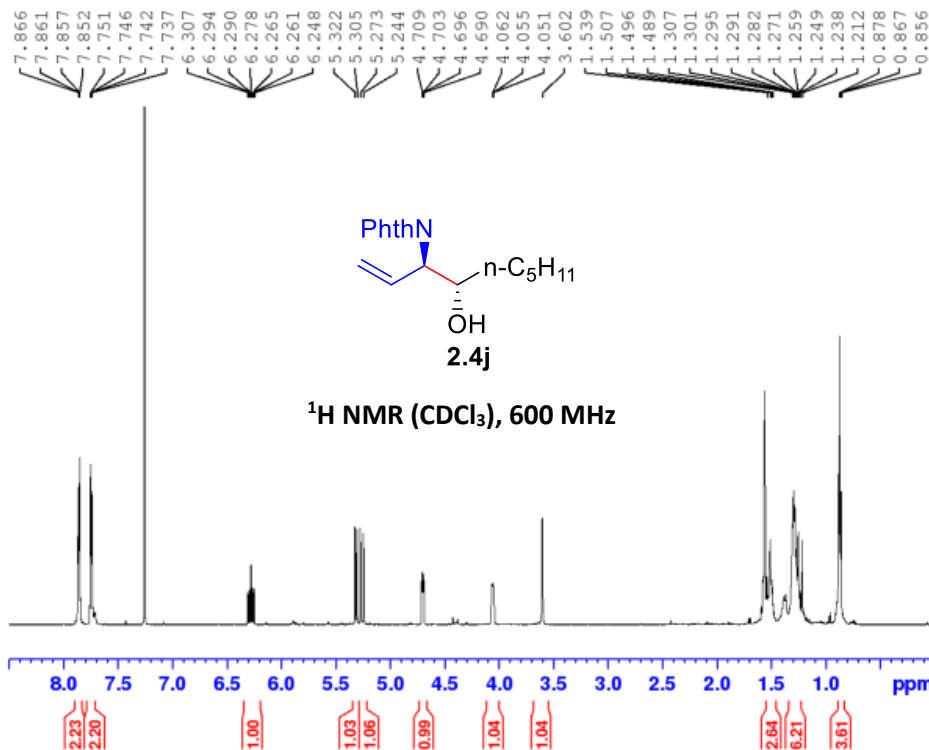


Current Data Parameters
 NAME SLG3-006
 EXPNO 2
 PROCNO 1

F2 - Acquisition Parameters
 Date_ 20210930
 Time 16.12 h
 INSTRUM spect
 PROBHD Z855801_0104 ((
 PULPROG zg30
 ID 65536
 SOLVENT CDC13
 NS 16
 DS 2
 SWH 12019.230 Hz
 FIDRES 0.366798 Hz
 AQ 2.7262976 sec
 RG 194.75
 DW 41.600 usec
 DE 6.50 usec
 TE 298.0 K
 D1 4.0000000 sec
 TD0 1
 SFO1 599.9587047 MHz
 NUC1 1H
 P1 7.75 usec
 PLW1 11.99499989 W

F2 - Processing parameters
 SI 65536
 SF 599.9550160 MHz
 WDM EM
 SSB 0
 LB 0.30 Hz
 GB 0
 PC 1.00

SLG3-057c-col
 PROTON CDC13 {D:\nmrdata} Sieber 1

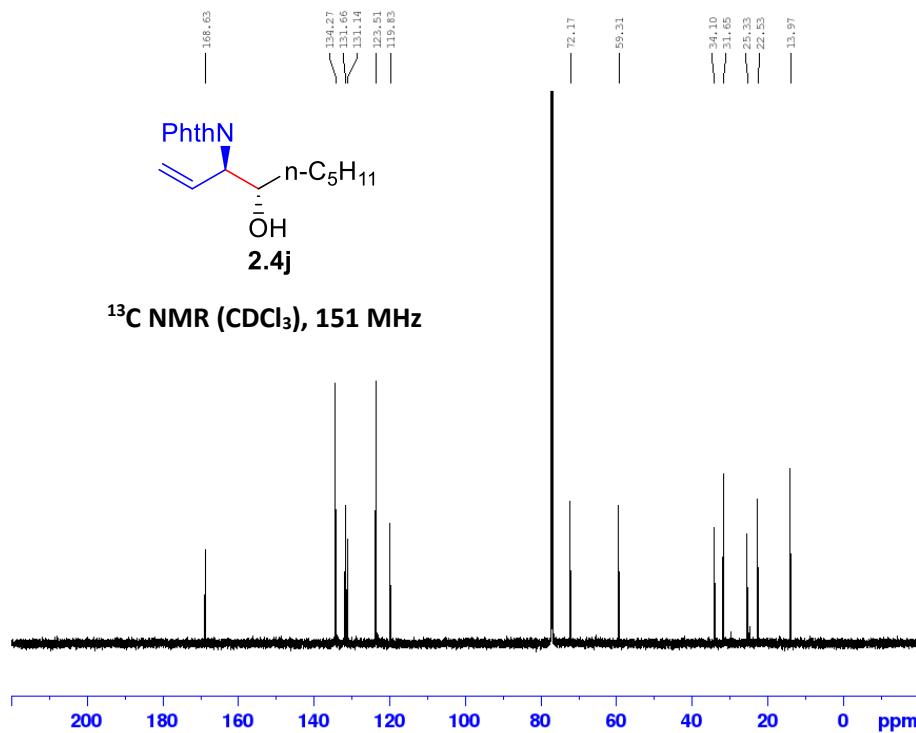


Current Data Parameters
 NAME SLG3-057
 EXPNO 4
 PROCNO 1

F2 - Acquisition Parameters
 Date_ 20220506
 Time 17.22 h
 INSTRUM spect
 PROBHD Z148658_0003 ((
 PULPROG zg30
 ID 65536
 SOLVENT CDC13
 NS 16
 DS 2
 SWH 12019.230 Hz
 FIDRES 0.366798 Hz
 AQ 2.7262976 sec
 RG 199.73
 DW 41.600 usec
 DE 10.33 usec
 TE 296.3 K
 D1 4.0000000 sec
 TD0 1
 SFO1 600.0087050 MHz
 NUC1 1H
 PD 5.17 usec
 P1 15.50 usec
 PLW1 13.23200035 W

F2 - Processing parameters
 SI 65536
 SF 600.0050175 MHz
 WDM EM
 SSB 0
 LB 0.30 Hz
 GB 0
 PC 1.00

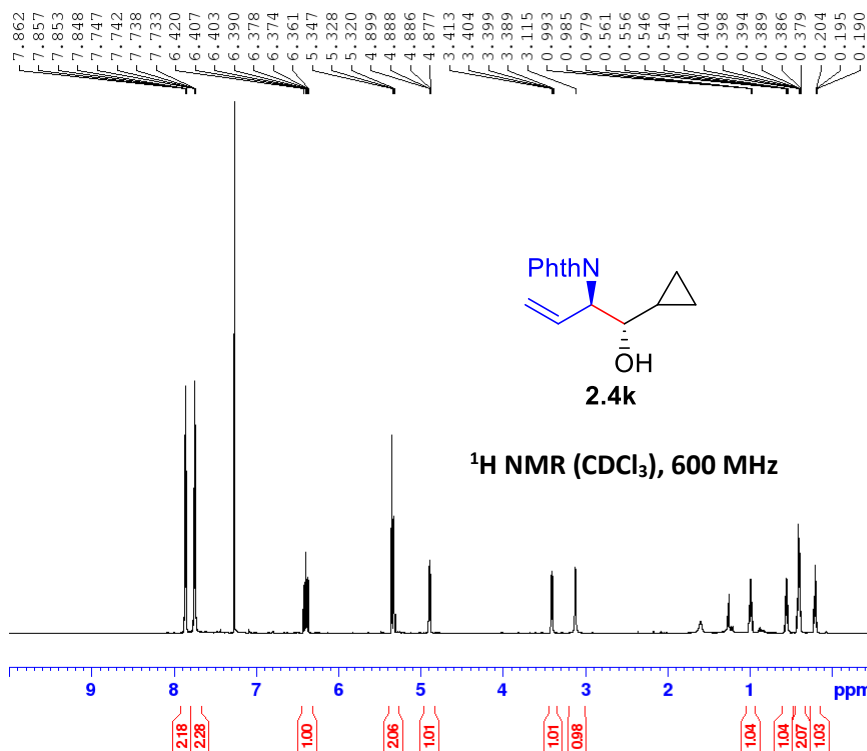
SLG3-057c-col
 C13CPD CDC13 {D:\nmrdata} Sieber 7



Current Data Parameters
 NAME SLG3-057
 EXPNO 6
 PROCNO 1

F2 - Acquisition Parameters
 Date_ 20221022
 Time 12.42 h
 INSTRUM spect
 PROBHD Z148658_0003 (
 PULPROG zgpg30
 TD 65536
 SOLVENT CDC13
 NS 400
 DS 4
 SWH 36231.883 Hz
 FIDRES 1.105709 Hz
 AQ 0.9043968 sec
 RG 199.73
 DW 13.800 usec
 DE 6.50 usec
 TE 297.9 K
 D1 6.0000000 sec
 D11 0.0300000 sec
 TDO 1
 SFO1 150.8864644 MHz
 NUC1 13C
 P0 4.00 usec
 P1 12.00 usec
 PLW1 77.65699768 W
 SFO2 600.0074000 MHz
 NUC2 1H
 CPDPRG2 waltz65
 PCPD2 70.00 usec
 PLW2 13.23200035 W
 PLW12 0.64876997 W
 PLW13 0.32633001 W

F2 - Processing parameters
 SI 32768
 SF 150.8713850 MHz
 NDM 0
 SSB 0
 LB 1.00 Hz
 GB 0
 PC 1.40

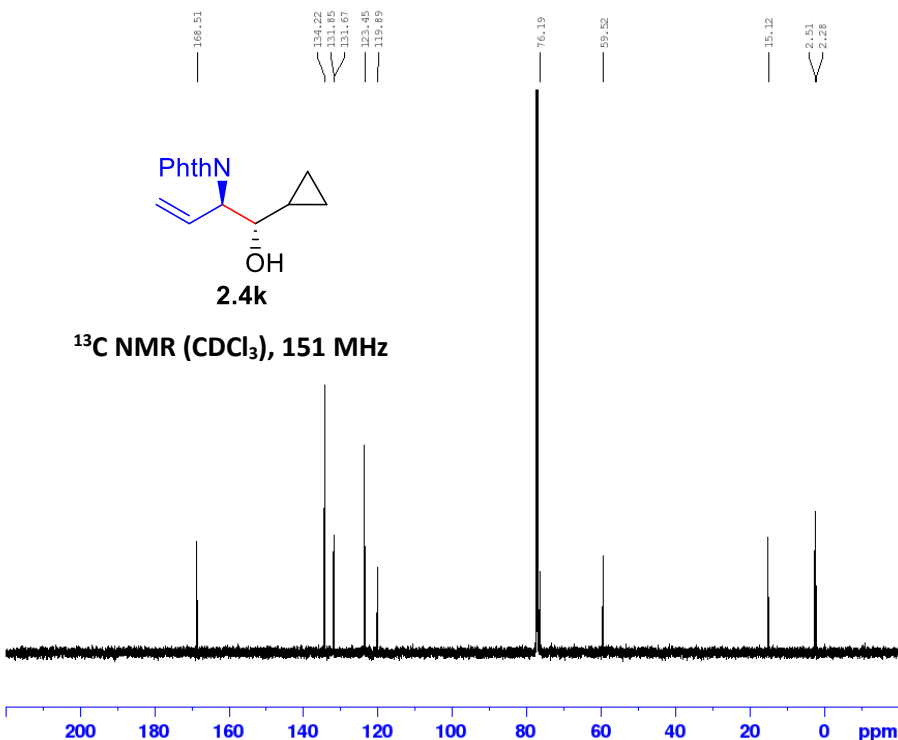


Current Data Parameters
 NAME SLG3-041_2
 EXPNO 1
 PROCNO 1

F2 - Acquisition Parameters
 Date_ 20221023
 Time 9.29 h
 INSTRUM spect
 PROBHD Z148658_0003 (
 PULPROG zg30
 TD 65536
 SOLVENT CDC13
 NS 16
 DS 2
 SWH 12019.230 Hz
 FIDRES 0.366798 Hz
 AQ 2.7262976 sec
 RG 199.73
 DW 41.600 usec
 DE 10.33 usec
 TE 296.3 K
 D1 4.0000000 sec
 TDO 1
 SFO1 600.0087050 MHz
 NUC1 1H
 P0 5.17 usec
 P1 15.50 usec
 PLW1 13.23200035 W

F2 - Processing parameters
 SI 65536
 SF 600.0050160 MHz
 NDM 0
 SSB 0
 LB 0.30 Hz
 GB 0
 PC 1.00

SLG3-041c-col
 C13CPD CDC13 {D:\nmrdata} Sieber 5

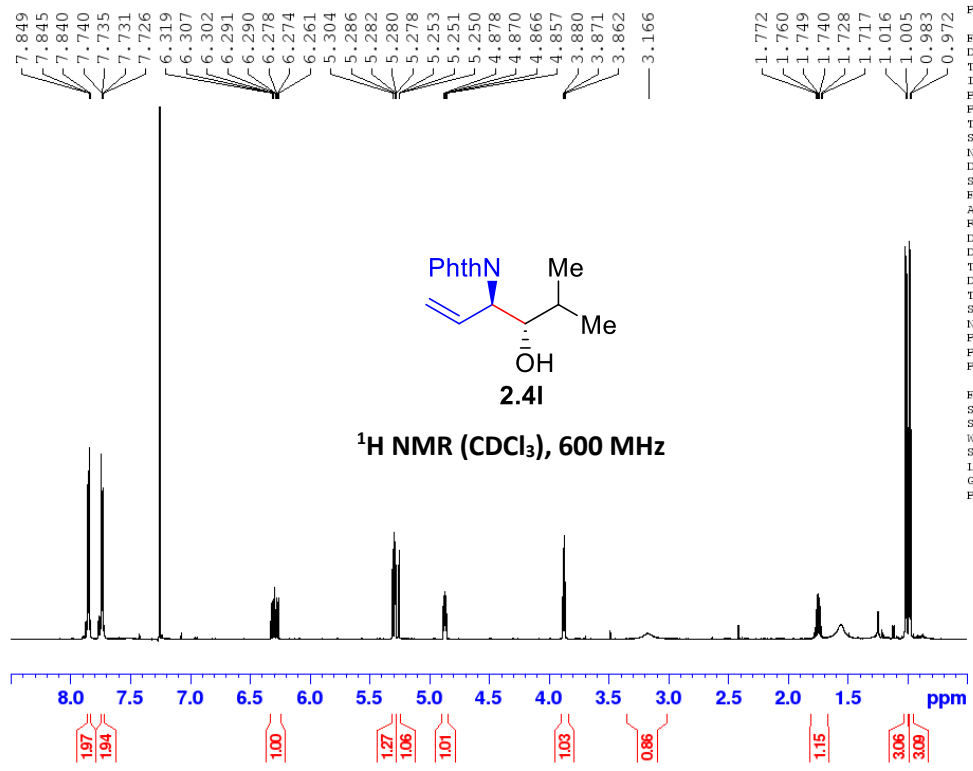


Current Data Parameters
 NAME SLG3-041_2
 EXPNO 2
 PROCNO 1

F2 - Acquisition Parameters
 Date_ 20221022
 Time 11.51 h
 INSTRUM spect
 PROBHD Z148658_0003 (
 PULPROG zgpg30
 TD 65536
 SOLVENT CDCl3
 NS 400
 DS 4
 SWH 36231.883 Hz
 FIDRES 1.105709 Hz
 AQ 0.9043968 sec
 RG 199.73
 DW 13.800 usec
 DE 6.50 usec
 TE 297.9 K
 D1 6.0000000 sec
 D11 0.0300000 sec
 TD0 1
 SFO1 150.8864644 MHz
 NUC1 13C
 P0 4.00 usec
 P1 12.00 usec
 PLW1 77.65699768 W
 SFO2 600.0074000 MHz
 NUC2 1H
 CPDPRG2 waltz65
 PCPD2 70.00 usec
 PLW2 13.23200035 W
 PLW12 0.64876997 W
 PLW13 0.32633001 W

F2 - Processing parameters
 SI 32768
 SF 150.8713835 MHz
 WDW EM
 SSB 0
 LB 1.00 Hz
 GB 0
 PC 1.40

SLG3-038c-col
 PROTON CDC13 {D:\nmrdata} Sieber 8

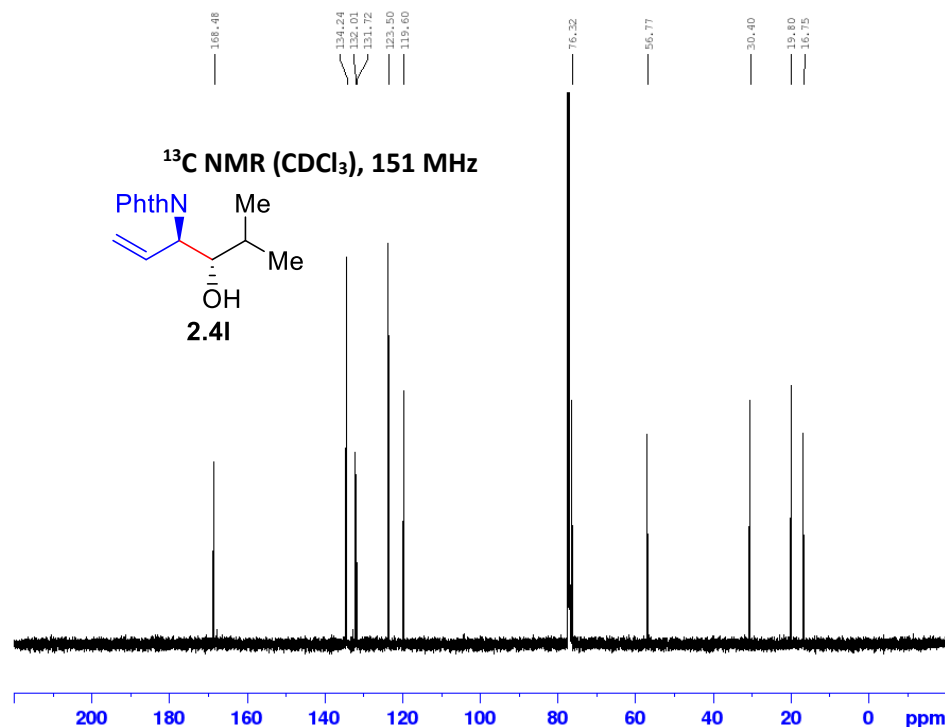


Current Data Parameters
 NAME SLG3-038_2
 EXPNO 6
 PROCNO 1

F2 - Acquisition Parameters
 Date_ 20221008
 Time 21.35 h
 INSTRUM spect
 PROBHD Z148658_0003 (
 PULPROG zg30
 TD 65536
 SOLVENT CDCl3
 NS 16
 DS 2
 SWH 12019.230 Hz
 FIDRES 0.366798 Hz
 AQ 2.7262976 sec
 RG 199.73
 DW 41.600 usec
 DE 10.33 usec
 TE 296.4 K
 D1 4.0000000 sec
 TD0 1
 SFO1 600.0087050 MHz
 NUC1 1H
 P0 5.17 usec
 P1 15.50 usec
 PLW1 13.23200035 W

F2 - Processing parameters
 SI 65536
 SF 600.0050210 MHz
 WDW EM
 SSB 0
 LB 0.30 Hz
 GB 0
 PC 1.00

SLG3-038c-col
 13CNMR
 C13CPD CDC13 {D:\nmrdata} Sieber 8

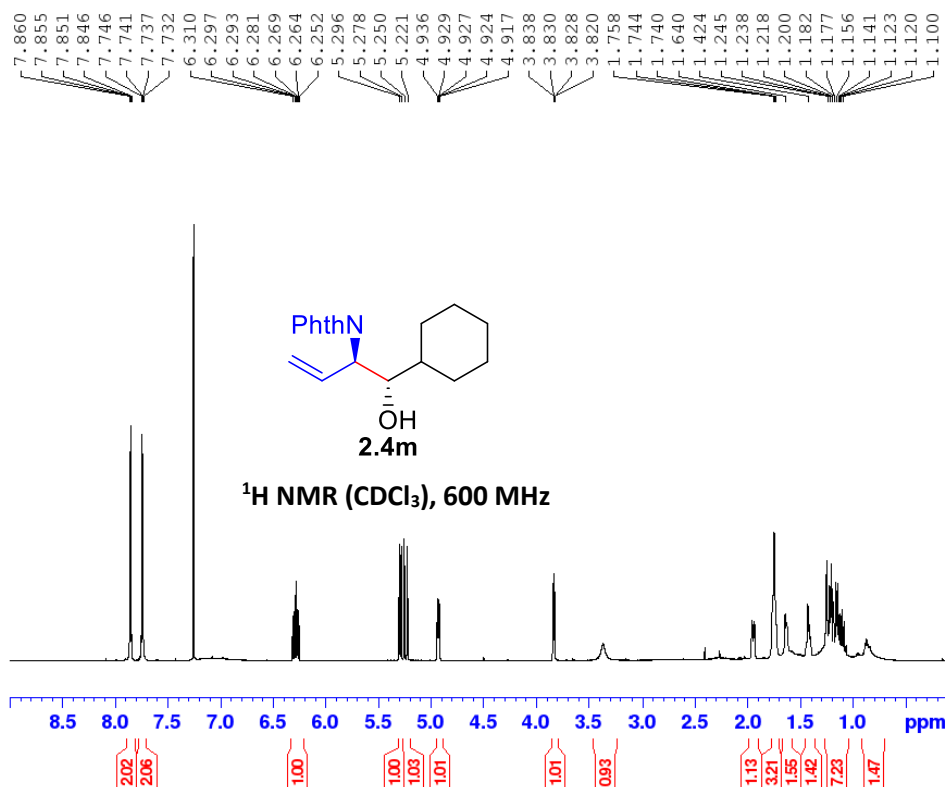


Current Data Parameters
 NAME SLG3-038_2
 EXPNO 8
 PROCNO 1

F2 - Acquisition Parameters
 Date_ 20221009
 Time_ 13.54 h
 INSTRUM spect
 PROBHD Z148658_0003 (
 PULPROG zgpg30
 TD 65536
 SOLVENT CDCl3
 NS 1024
 DS 4
 SNH 36231.883 Hz
 FIDRES 1.105709 Hz
 AQ 0.9043968 sec
 RG 199.73
 DW 13.800 usec
 DE 6.50 usec
 TE 298.2 K
 D1 4.0000000 sec
 D11 0.0300000 sec
 TD0 1
 SFO1 150.8864644 MHz
 NUC1 13C
 P0 4.00 usec
 P1 12.00 usec
 PLW1 77.65699768 W
 SFO2 600.0074000 MHz
 NUC2 1H
 CPDPRG2 waltz65
 PCPD2 70.00 usec
 PLW2 13.23200035 W
 PLW12 0.64876997 W
 PLW13 0.32633001 W

F2 - Processing parameters
 SI 32768
 SF 150.8713819 MHz
 WDN EH
 SSB 0
 LB 1.00 Hz
 GB 0
 PC 1.40

SLG3-034d-col
 PROTON CDC13 {D:\nmrdata} Sieber 2

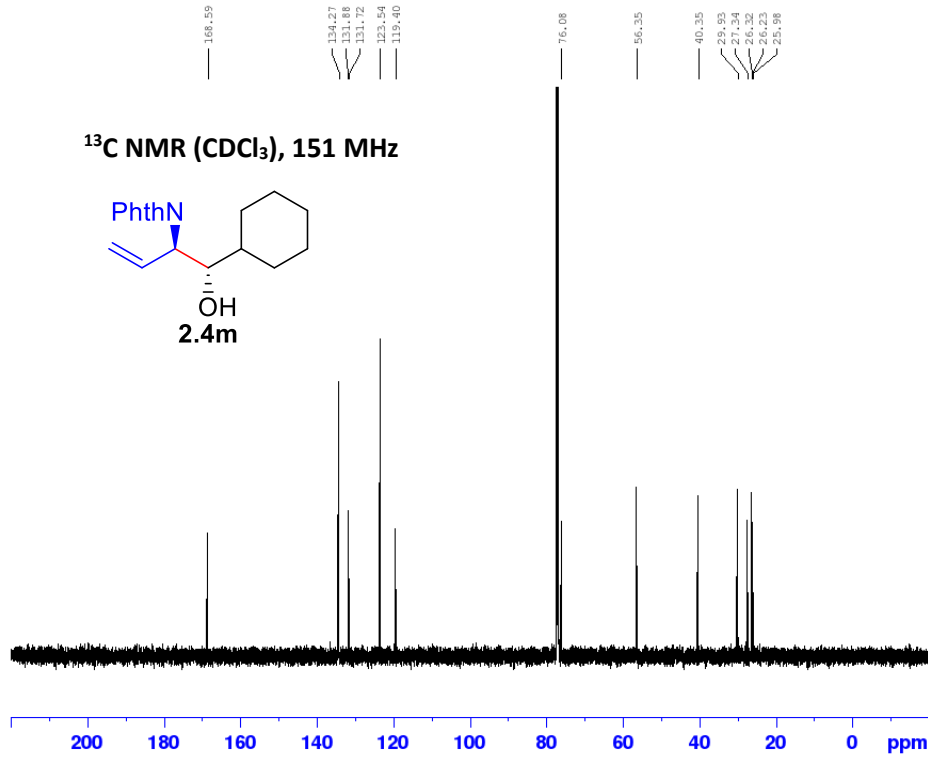


Current Data Parameters
 NAME SLG3-034_2
 EXPNO 11
 PROCNO 1

F2 - Acquisition Parameters
 Date_ 20221008
 Time_ 19.58 h
 INSTRUM spect
 PROBHD Z148658_0003 (
 PULPROG zg30
 TD 65536
 SOLVENT CDCl3
 NS 16
 DS 2
 SNH 12019.230 Hz
 FIDRES 0.366798 Hz
 AQ 2.7262976 sec
 RG 199.73
 DW 41.600 usec
 DE 10.33 usec
 TE 296.5 K
 D1 4.0000000 sec
 TD0 1
 SFO1 600.0087050 MHz
 NUC1 1H
 P0 5.17 usec
 P1 15.50 usec
 PLW1 13.23200035 W

F2 - Processing parameters
 SI 65536
 SF 600.0050196 MHz
 WDN EH
 SSB 0
 LB 0.30 Hz
 GB 0
 PC 1.00

SLG3-034d-col
 C13CPD CDCl3 {D:\nmrdata} Sieber 2

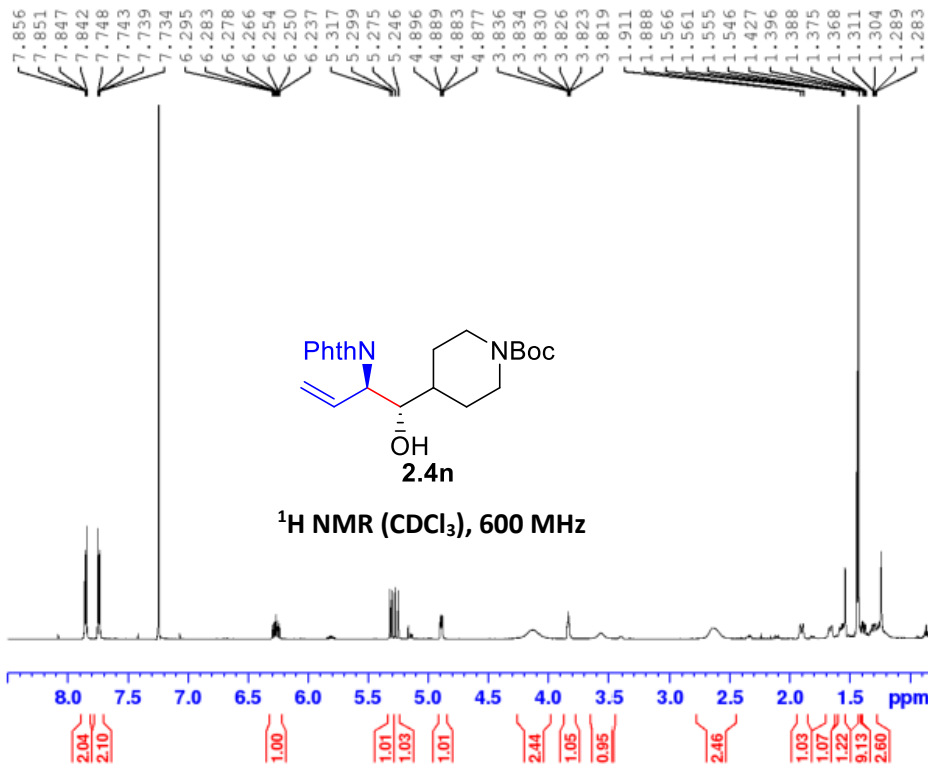


Current Data Parameters
 NAME SLG3-034_2
 EXPNO 12
 PROCNO 1

F2 - Acquisition Parameters
 Date_ 20221009
 Time 1.58 h
 INSTRUM spect
 PROBHD Z148658_0003 (
 PULPROG zgpg30
 TD 65536
 SOLVENT cdcl3
 NS 300
 DS 4
 SWH 36231.883 Hz
 FIDRES 1.105709 Hz
 AQ 0.9043968 sec
 RG 199.73
 DW 13.800 usec
 DE 6.50 usec
 TE 297.8 K
 D1 6.0000000 sec
 D11 0.0300000 sec
 TD0 1
 SFO1 150.8864644 MHz
 NUC1 13C
 P0 4.00 usec
 P1 12.00 usec
 PLW1 77.65699768 W
 SFO2 600.0074000 MHz
 NUC2 1H
 CPMRG2 waltz65
 PCPD2 70.00 usec
 PLW2 13.23200035 W
 PLW12 0.64876997 W
 PLW13 0.32633001 W

F2 - Processing parameters
 SI 32768
 SF 150.8713805 MHz
 WDW EM
 SSB 0
 LB 1.00 Hz
 GB 0
 PC 1.40

SLG3-040e-2
 PROTON CDCl3 {D:\nmrdata} Sieber 5

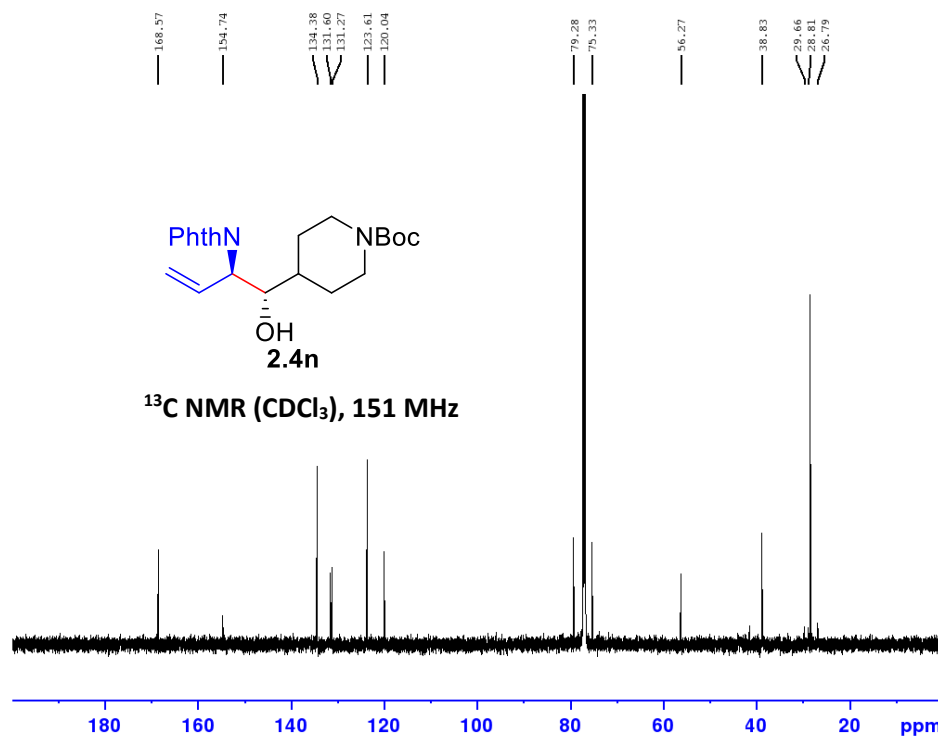


Current Data Parameters
 NAME SLG3-040_2
 EXPNO 10
 PROCNO 1

F2 - Acquisition Parameters
 Date_ 20221019
 Time 17.39 h
 INSTRUM spect
 PROBHD Z148658_0003 (
 PULPROG zg30
 TD 65536
 SOLVENT cdcl3
 NS 16
 DS 2
 SWH 12019.230 Hz
 FIDRES 0.366798 Hz
 AQ 2.7262976 sec
 RG 199.73
 DW 41.600 usec
 DE 10.33 usec
 TE 296.4 K
 D1 4.0000000 sec
 TD0 1
 SFO1 600.0087050 MHz
 NUC1 1H
 P0 5.17 usec
 P1 15.50 usec
 PLW1 13.23200035 W

F2 - Processing parameters
 SI 65536
 SF 600.0050254 MHz
 WDW EM
 SSB 0
 LB 0.30 Hz
 GB 0
 PC 1.00

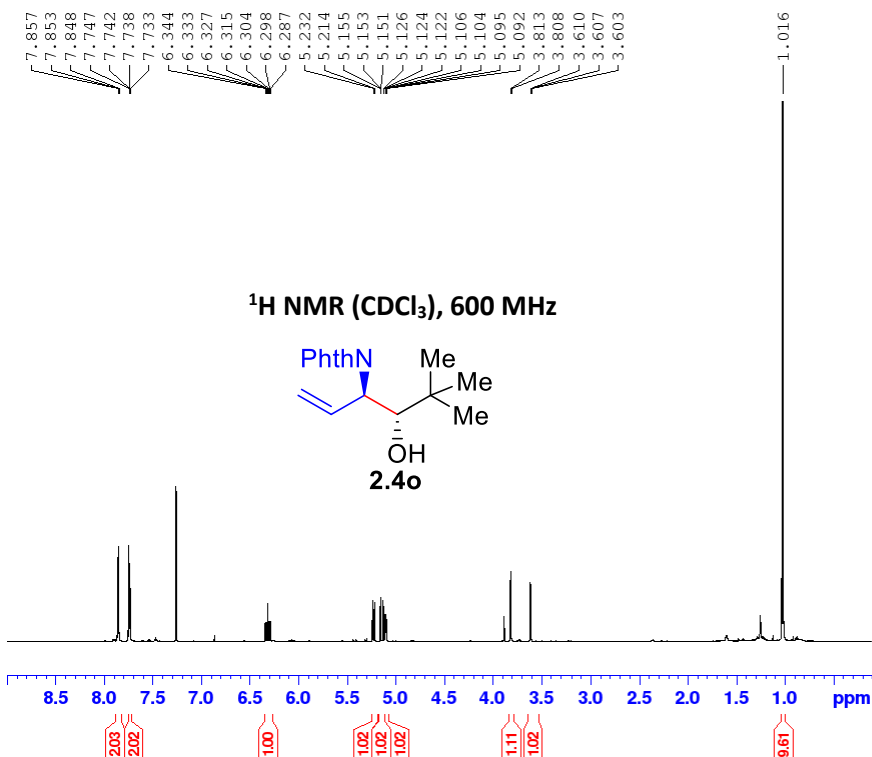
SLG3-040e-2-col
 C13CPD CDC13 {D:\nmrdata} Sieber 4



Current Data Parameters
 NAME SLG3-040_3
 EXPNO 14
 PROCNO 1

F2 - Acquisition Parameters
 Date_ 20221022
 Time 21.24 h
 INSTRUM spect
 PROBHD Z148658_0003 (
 PULPROG zgpg30
 TD 65536
 SOLVENT CDC13
 NS 1200
 DS 4
 SWH 36231.883 Hz
 FIDRES 1.105709 Hz
 AQ 0.9043968 sec
 RG 199.73
 DW 13.800 usec
 DE 6.50 usec
 TE 297.9 K
 D1 6.00000000 sec
 D11 0.03000000 sec
 TDO 1
 SFO1 150.8864644 MHz
 NUC1 13C
 P0 4.00 usec
 P1 12.00 usec
 PLW1 77.65699768 W
 SFO2 600.0074000 MHz
 NUC2 1H
 CPDPRG2 waltz65
 PCPD2 70.00 usec
 PLW2 13.23200035 W
 PLW12 0.64876997 W
 PLW13 0.32633001 W

F2 - Processing parameters
 SI 32768
 SF 150.8713844 MHz
 WDW EM
 SSB 0
 LB 1.00 Hz
 GB 0
 PC 1.40

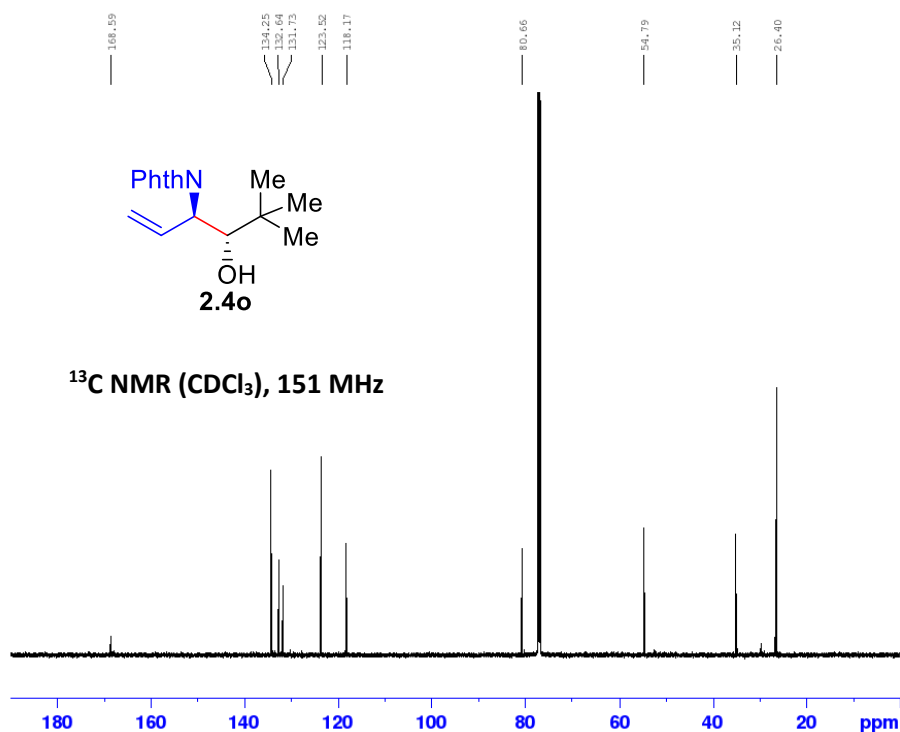


Current Data Parameters
 NAME SLG3-038_3
 EXPNO 3
 PROCNO 1

F2 - Acquisition Parameters
 Date_ 20221023
 Time 9.18 h
 INSTRUM spect
 PROBHD Z148658_0003 (
 PULPROG zg30
 TD 65536
 SOLVENT CDC13
 NS 16
 DS 2
 SWH 12019.230 Hz
 FIDRES 0.366798 Hz
 AQ 2.7262976 sec
 RG 176.24
 DW 41.600 usec
 DE 10.33 usec
 TE 296.3 K
 D1 4.00000000 sec
 TDO 1
 SFO1 600.0087050 MHz
 NUC1 1H
 P0 5.17 usec
 P1 15.50 usec
 PLW1 13.23200035 W

F2 - Processing parameters
 SI 65536
 SF 600.0050171 MHz
 WDW EM
 SSB 0
 LB 0.30 Hz
 GB 0
 PC 1.00

SLG3-038d-1
 C13CPD CDC13 {D:\nmrdata} Sieber 3

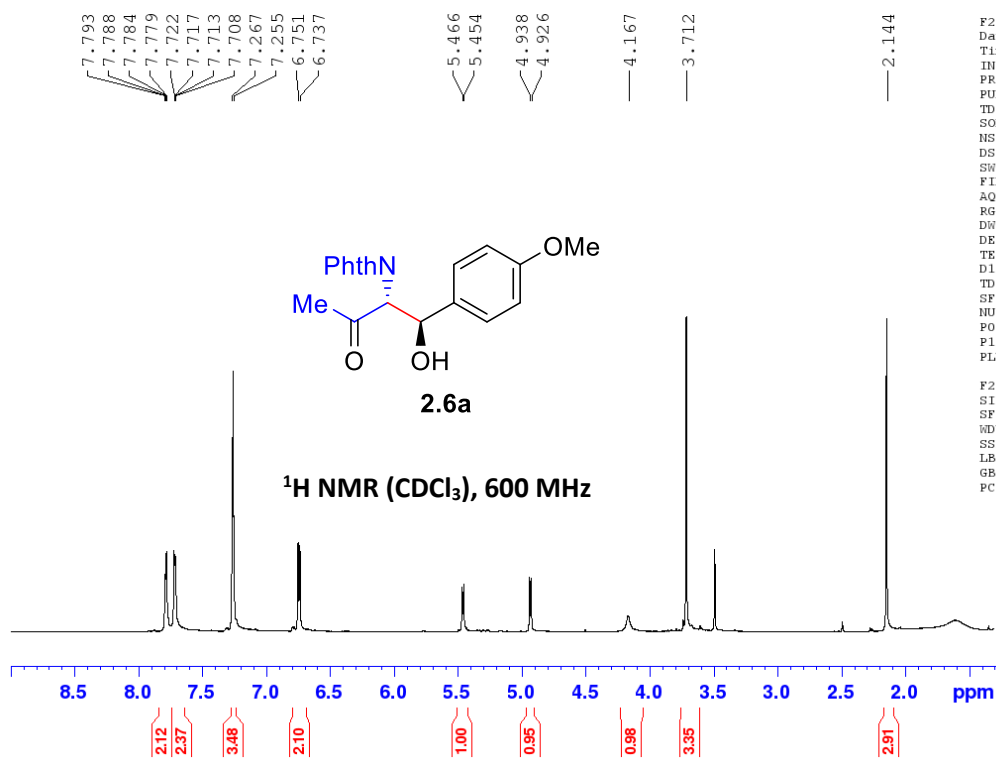


Current Data Parameters
 NAME SLG3-038_3
 EXPNO 4
 PROCNO 1

F2 - Acquisition Parameters
 Date_ 20221022
 Time 3.56 h
 INSTRUM spect
 PROBHD Z148658_0003 ()
 PULPROG zgpg30
 TD 65536
 SOLVENT CDC13
 NS 1024
 DS 4
 SWH 36231.883 Hz
 FIDRES 1.105709 Hz
 AQ 0.9043968 sec
 RG 199.73
 DN 13.800 usec
 DE 6.50 usec
 TE 297.9 K
 D1 6.0000000 sec
 D11 0.0300000 sec
 TDO 1
 SFO1 150.8864644 MHz
 NUC1 13C
 P0 4.00 usec
 P1 12.00 usec
 PLW1 77.65699768 W
 SFO2 600.0074000 MHz
 NUC2 1H
 CPDPRG2 waltz65
 PCPD2 70.00 usec
 PLW2 13.23200035 W
 PLW12 0.64876997 W
 PLW13 0.32633001 W

F2 - Processing parameters
 SI 32768
 SF 150.8713848 MHz
 NDNW EM
 SSB 0
 LB 1.00 Hz
 GB 0
 PC 1.40

SLG3-110-co1
 Hivac
 PROTON CDC13 D:\ Sieber 1

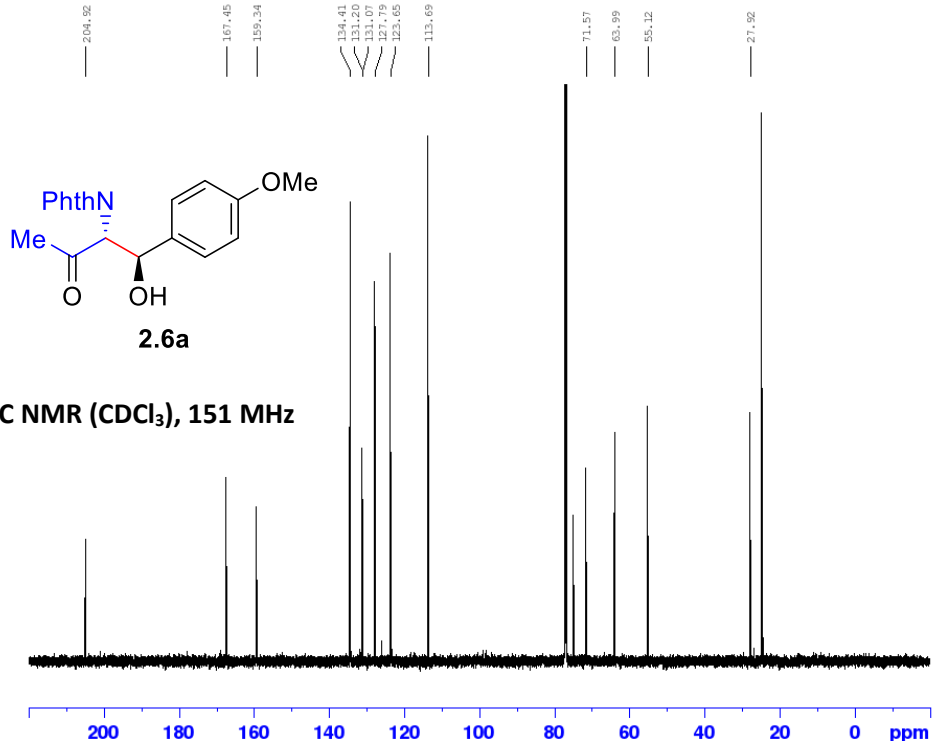


Current Data Parameters
 NAME SLG3-110
 EXPNO 3
 PROCNO 1

F2 - Acquisition Parameters
 Date_ 20220918
 Time 10.49 h
 INSTRUM spect
 PROBHD Z855801_0104 ()
 PULPROG zg30
 TD 65536
 SOLVENT CDC13
 NS 16
 DS 2
 SWH 12019.230 Hz
 FIDRES 0.366798 Hz
 AQ 2.7262976 sec
 RG 194.75
 DN 41.600 usec
 DE 11.65 usec
 TE 296.2 K
 D1 4.0000000 sec
 TDO 1
 SFO1 599.9587047 MHz
 NUC1 1H
 P0 2.58 usec
 P1 7.75 usec
 PLW1 11.99499989 W

F2 - Processing parameters
 SI 65536
 SF 599.9550155 MHz
 NDNW EM
 SSB 0
 LB 0.30 Hz
 GB 0
 PC 1.00

SLG3-110-col
 C13CPD CDC13 {D:\nmrdata} Sieber 10

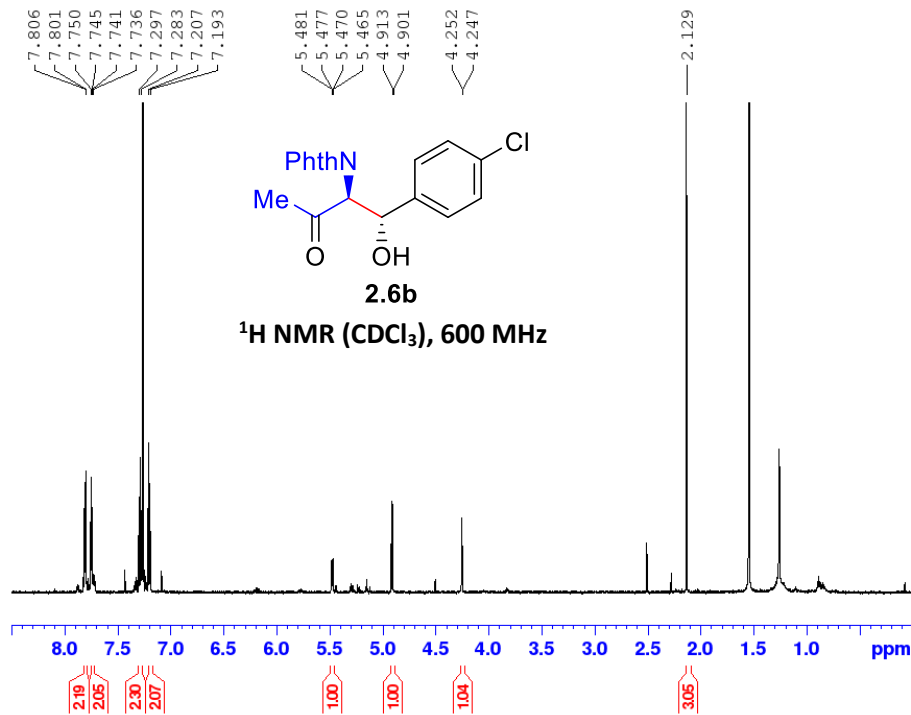


Current Data Parameters
 NAME SLG3-110_2
 EXPNO 2
 PROCNO 1

F2 - Acquisition Parameters
 Date_ 20221021
 Time 23.49 h
 INSTRUM spect
 PROBHD Z148658_0003 (
 PULPROG zgpg30
 TD 65536
 SOLVENT CDC13
 NS 300
 DS 4
 SWH 36231.883 Hz
 FIDRES 1.105709 Hz
 AQ 0.9043968 sec
 RG 199.73
 DW 13.800 usec
 DE 6.50 usec
 TE 297.8 K
 D1 6.00000000 sec
 D11 0.03000000 sec
 TD0 1
 SFO1 150.8864644 MHz
 NUC1 13C
 P0 4.00 usec
 P1 12.00 usec
 PLW1 77.65699768 W
 SFO2 600.0074000 MHz
 NUC2 1H
 CPOPRG[2] waltz55
 PCPD2 70.00 usec
 PLW2 13.23200035 W
 PLW12 0.64876997 W
 PLW13 0.32633001 W

F2 - Processing parameters
 SI 32768
 SF 150.8713872 MHz
 WDN EM
 SSB 0
 LB 1.00 Hz
 GB 0
 PC 1.40

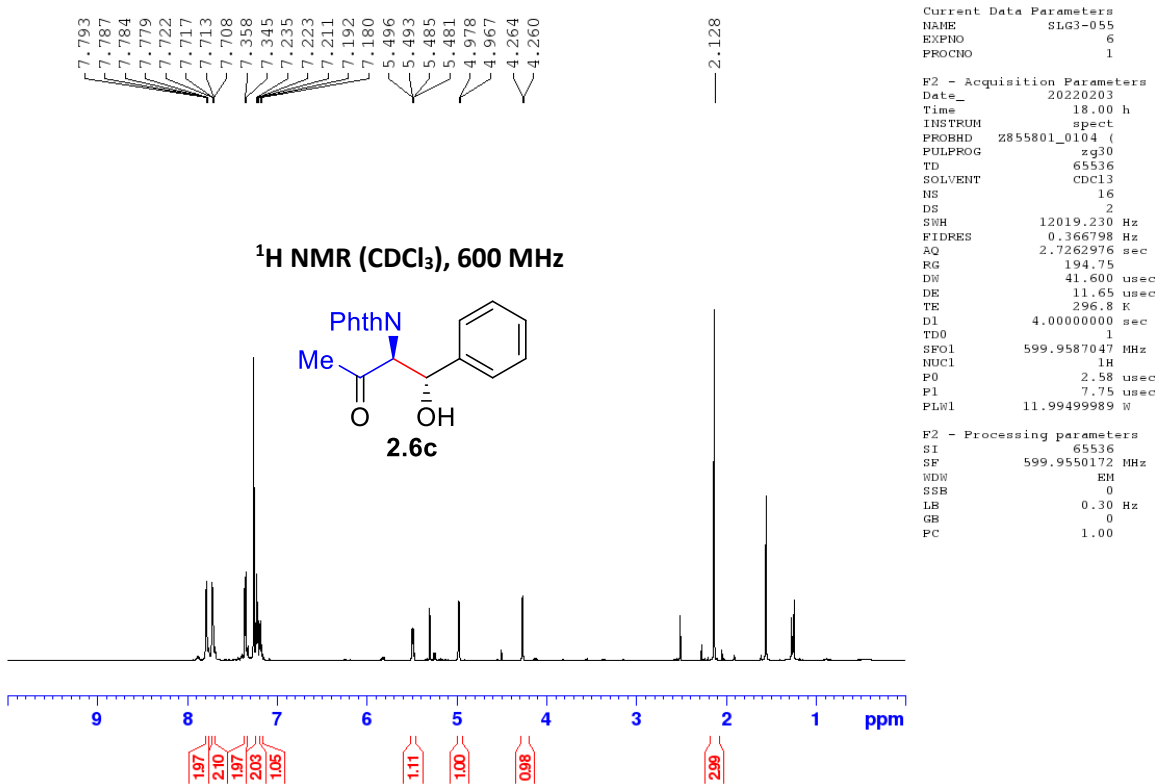
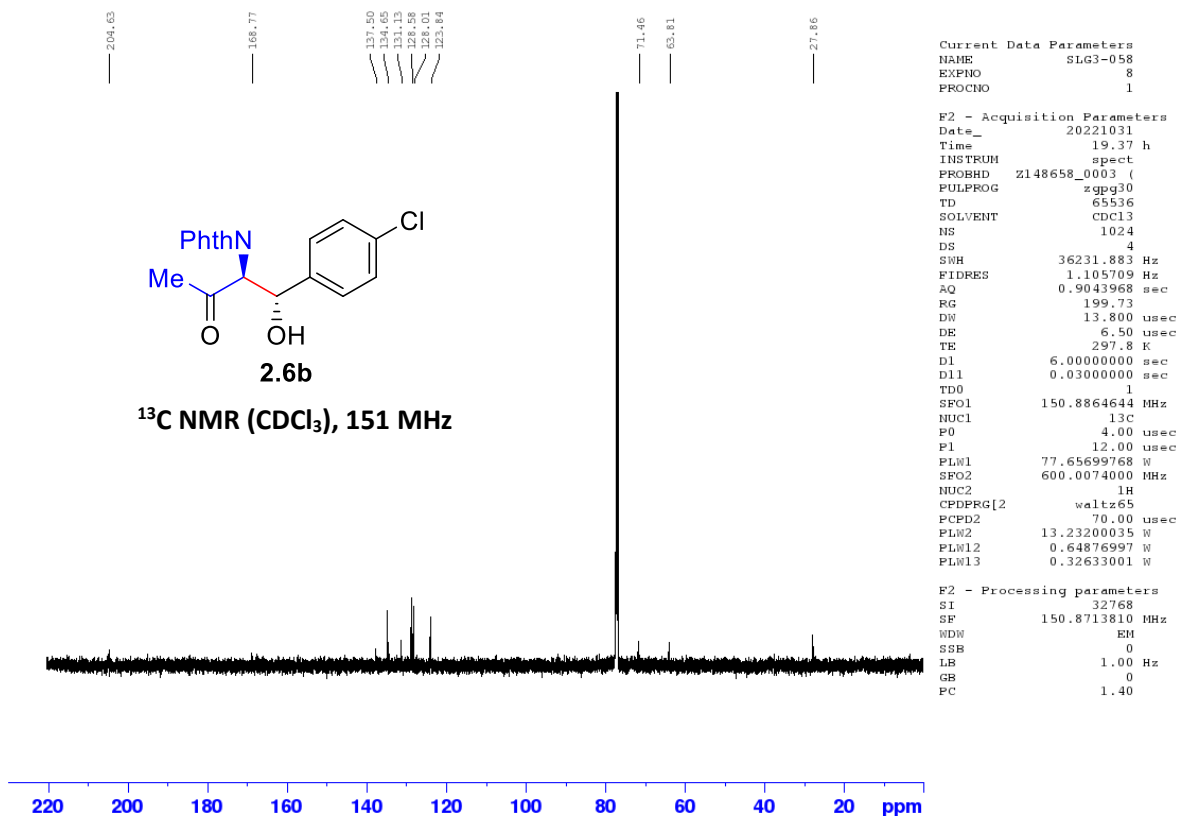
SLG3-058a-col-hivac
 PROTON CDC13 {D:\nmrdata} Sieber 11

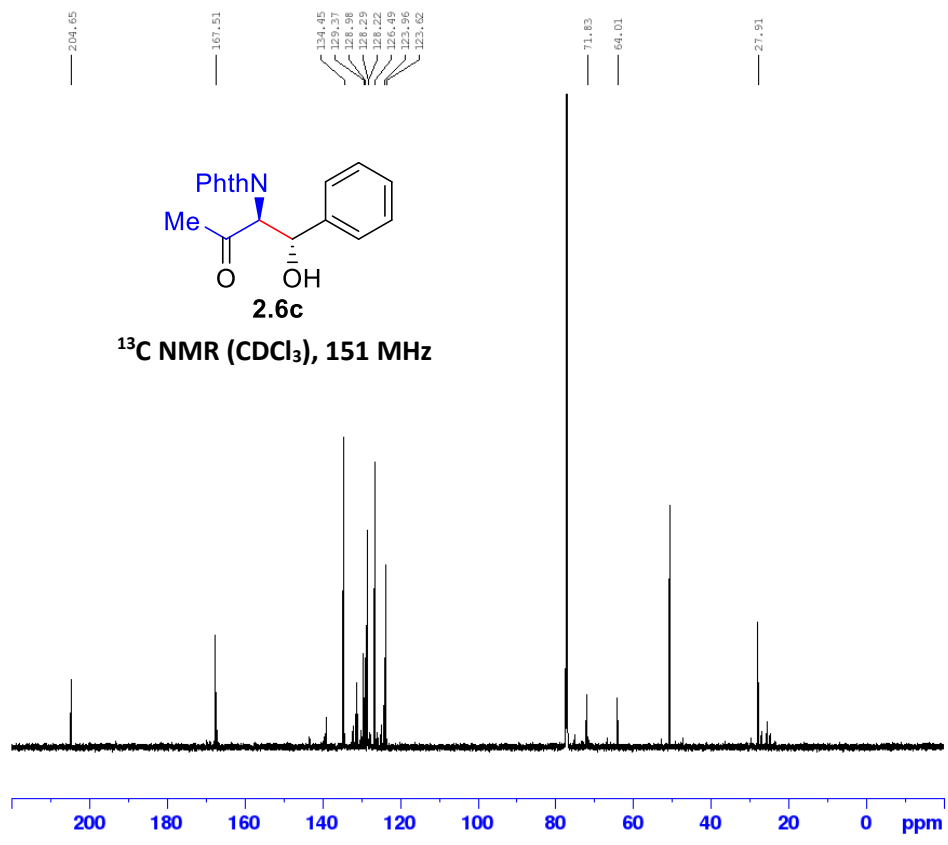


Current Data Parameters
 NAME SLG3-058
 EXPNO 10
 PROCNO 1

F2 - Acquisition Parameters
 Date_ 20221101
 Time 17.20 h
 INSTRUM spect
 PROBHD Z148658_0003 (
 PULPROG zg30
 TD 65536
 SOLVENT CDC13
 NS 15
 DS 2
 SWH 12019.230 Hz
 FIDRES 0.366798 Hz
 AQ 2.7262976 sec
 RG 199.73
 DW 41.600 usec
 DE 10.33 usec
 TE 296.2 K
 D1 4.00000000 sec
 TD0 1
 SFO1 600.0087050 MHz
 NUC1 1H
 P0 5.17 usec
 P1 15.50 usec
 PLW1 13.23200035 W

F2 - Processing parameters
 SI 65536
 SF 600.0050159 MHz
 WDN EM
 SSB 0
 LB 0.30 Hz
 GB 0
 PC 1.00





```

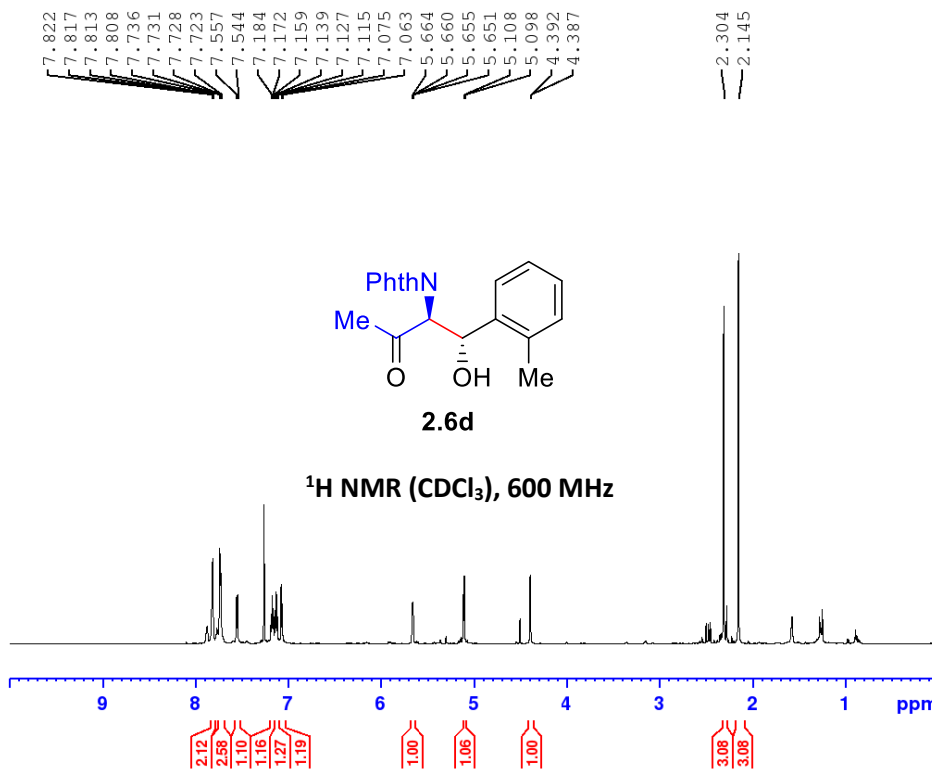
Current Data Parameters
NAME      SLG3-055_2
EXPNO     5
PROCNO    1

F2 - Acquisition Parameters
Date_     20221021
Time_     0.23 h
INSTRUM   spect
PROBHD    Z148658_0003 (
PULPROG   zgpg30
TD         65536
SOLVENT   CDCl3
NS         1024
DS         4
SWH        36231.883 Hz
FIDRES     1.105709 Hz
AQ         0.9043968 sec
RG         199.73
DN         13.800 usec
DE         6.50 usec
TE         297.9 K
D1         6.0000000 sec
D11        0.0300000 sec
TD0        1
SFO1       150.8864644 MHz
NUC1       13C
P0         4.00 usec
P1         12.00 usec
PLW1       77.65699768 W
SFO2       600.0074000 MHz
NUC2       1H
PCPDPRG2   waltz65
PCPD2      70.00 usec
PLW2       13.23200035 W
PLW12      0.64876997 W
PLW13      0.32633001 W

F2 - Processing parameters
SI         32768
SF         150.8713876 MHz
NDW        EH
SSB        0
LB         1.00 Hz
GB         0
PC         1.40

```

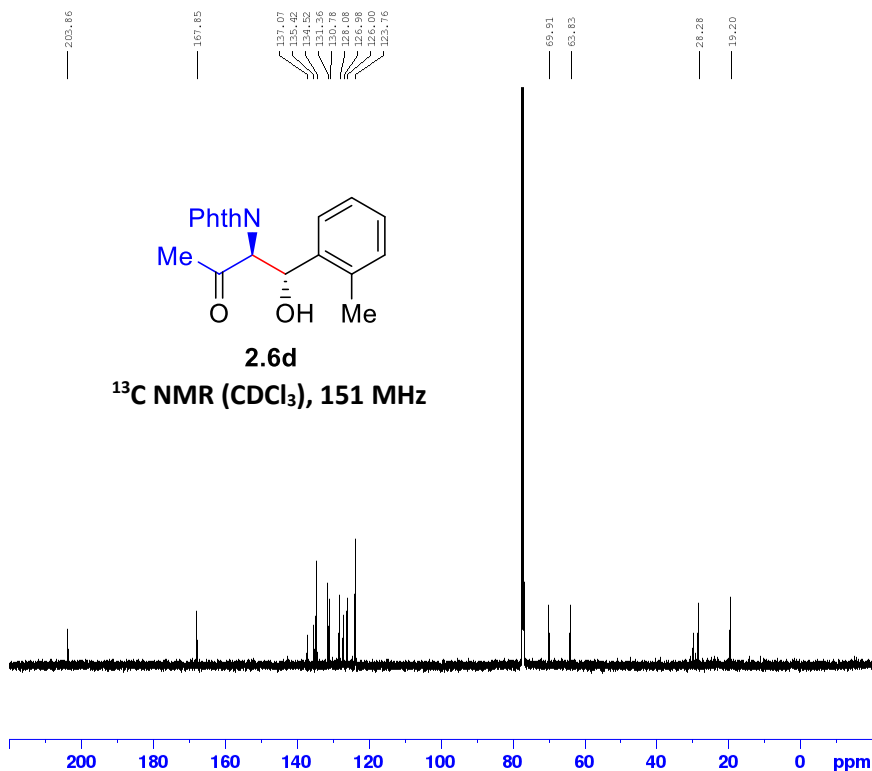
SLG3-055b-2
 PROTON CDC13 {C:\Bruker\TopSpin3.6.2} Sieber 4



Current Data Parameters
 NAME SLG3-055
 EXPNO 8
 PROCNO 1

F2 - Acquisition Parameters
 Date_ 20220203
 Time 18.10 h
 INSTRUM spect
 PROBHD Z855801_0104 (
 PULPROG zg30
 TD 65536
 SOLVENT CDC13
 NS 16
 DS 2
 SWH 12019.230 Hz
 FIDRES 0.366798 Hz
 AQ 2.7262976 sec
 RG 154.29
 DW 41.600 usec
 DE 11.65 usec
 TE 296.7 K
 D1 4.00000000 sec
 TD0 1
 SFO1 599.9587047 MHz
 NUC1 1H
 P0 2.58 usec
 p1 7.75 usec
 PLW1 11.99499989 W

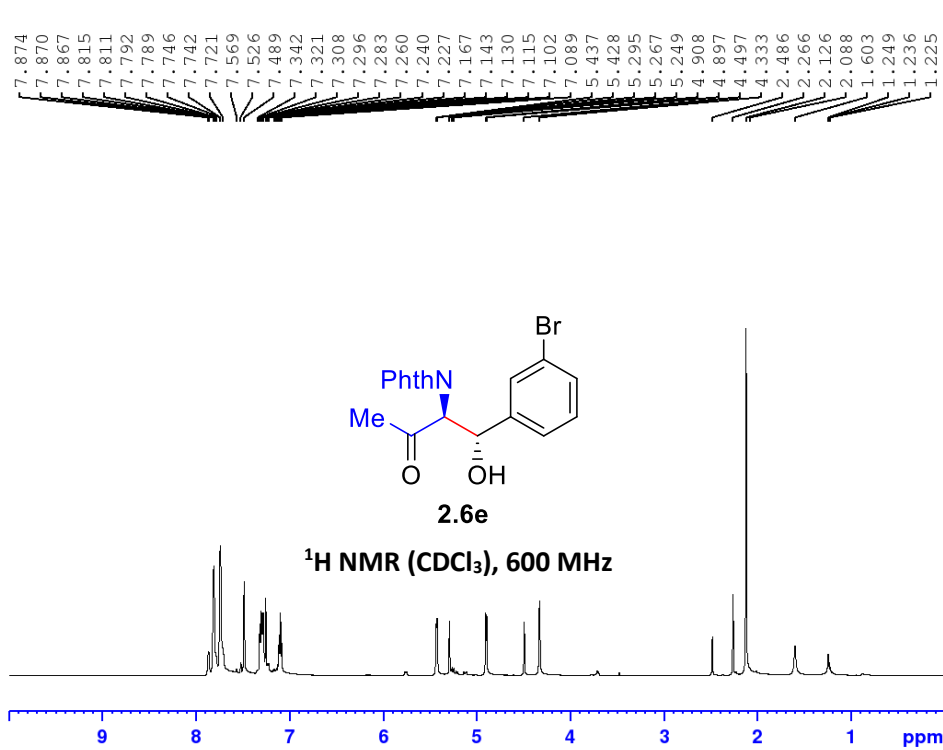
F2 - Processing parameters
 SI 65536
 SF 599.9550155 MHz
 WDW EM
 SSB 0
 LB 0.30 Hz
 GB 0
 PC 1.00



Current Data Parameters
 NAME SLG3-070
 EXPNO 23
 PROCNO 1

F2 - Acquisition Parameters
 Date_ 20221028
 Time 21.16 h
 INSTRUM spect
 PROBHD Z148658_0003 (
 PULPROG zgpg30
 TD 65536
 SOLVENT CDC13
 NS 1200
 DS 4
 SWH 36231.883 Hz
 FIDRES 1.105709 Hz
 AQ 0.9043968 sec
 RG 199.73
 DW 13.800 usec
 DE 6.50 usec
 TE 297.8 K
 D1 6.00000000 sec
 D11 0.03000000 sec
 TD0 1
 SFO1 150.8864644 MHz
 NUC1 13C
 P0 4.00 usec
 p1 12.00 usec
 PLW1 77.65699768 W
 SFO2 600.0074000 MHz
 NUC2 1H
 CPDPRG[2] waltz65
 PCPD2 70.00 usec
 PLW2 13.23200035 W
 PLW12 0.64876997 W
 PLW13 0.32633001 W

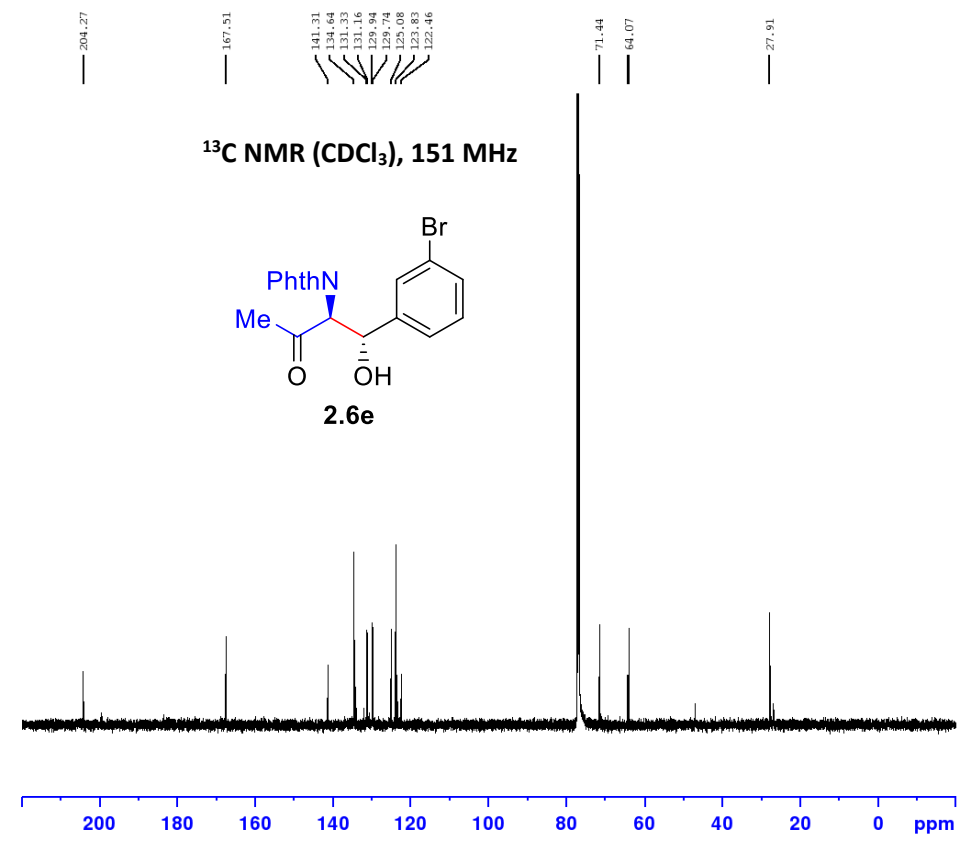
F2 - Processing parameters
 SI 32768
 SF 150.8713795 MHz
 WDW EM
 SSB 0
 LB 1.00 Hz
 GB 0
 PC 1.40



Current Data Parameters
NAME SLG3-123
EXPNO 3
PROCNO 1

F2 - Acquisition Parameters
Date_ 20221105
Time 20.38 h
INSTRUM spect
PROBHD Z855801_0104 (
PULPROG zg30
TD 65536
SOLVENT CDCl3
NS 16
DS 2
SWH 12019.230 Hz
FIDRES 0.366798 Hz
AQ 2.7262976 sec
RG 125.31
DW 41.600 usec
DE 11.65 usec
TE 296.5 K
D1 4.00000000 sec
D10 1
SF01 599.9587047 MHz
NUC1 1H
P0 2.58 usec
P1 7.75 usec
PLW1 11.99499989 W

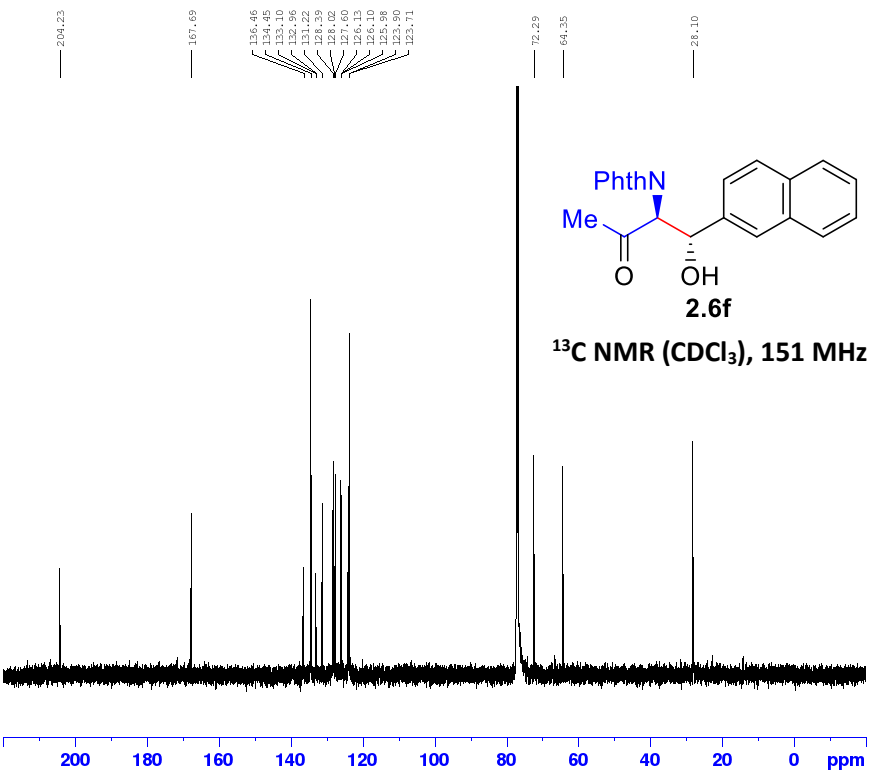
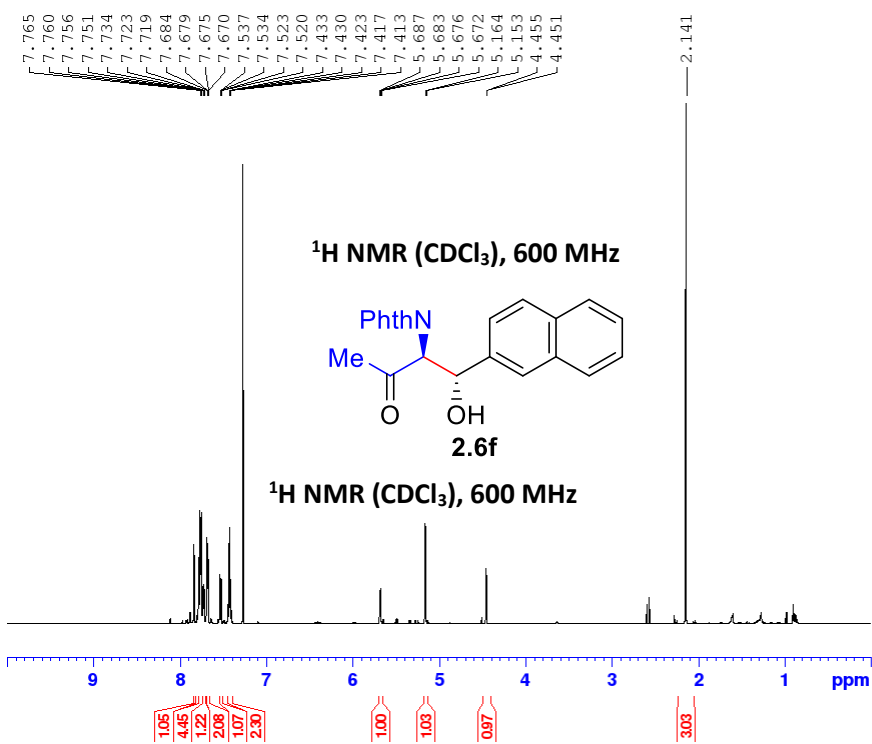
F2 - Processing parameters
SI 65536
SF 599.9550165 MHz
WDW EM
SSB 0
LB 0.30 Hz
GB 0
PC 1.00

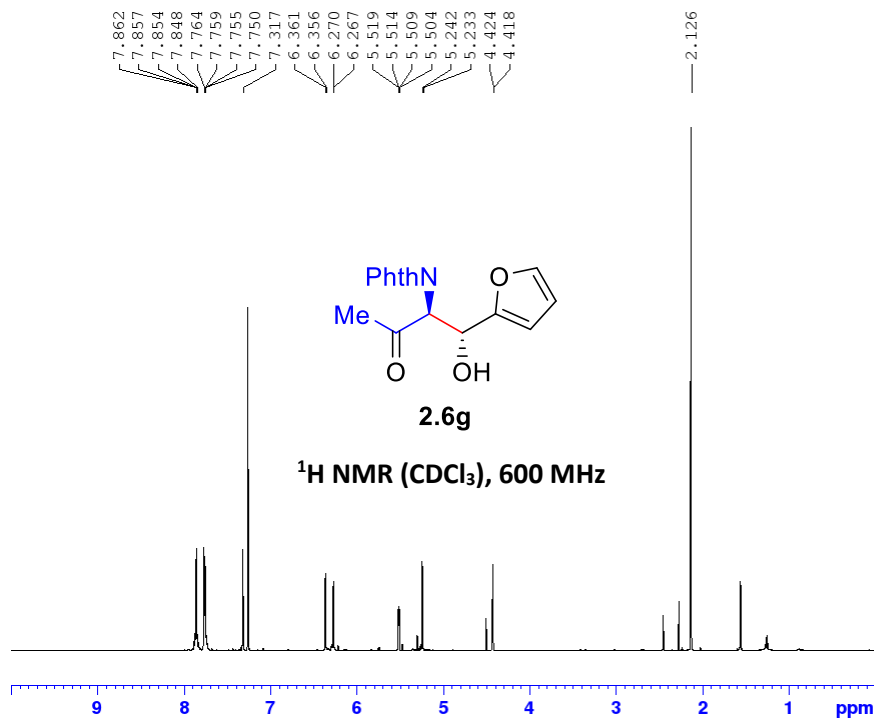


Current Data Parameters
NAME SLG3-123
EXPNO 4
PROCNO 1

F2 - Acquisition Parameters
Date_ 20221105
Time 23.10 h
INSTRUM spect
PROBHD Z855801_0104 (
PULPROG zgpg30
TD 65536
SOLVENT CDCl3
NS 800
DS 4
SWH 36231.883 Hz
FIDRES 1.105709 Hz
AQ 0.9043968 sec
RG 194.75
DW 13.800 usec
DE 6.50 usec
TE 297.8 K
D1 6.00000000 sec
D11 0.03000000 sec
D10 1
SF01 150.8738906 MHz
NUC1 13C
P0 3.80 usec
P1 11.40 usec
PLW1 176.19999695 W
SFO2 599.9573998 MHz
NUC2 1H
CPDPRG2 waltz65
PCPD2 70.00 usec
PLW2 11.99499989 W
PLW12 0.14703000 W
PLW13 0.07395500 W

F2 - Processing parameters
SI 32768
SF 150.8588103 MHz
WDW EM
SSB 0
LB 1.00 Hz
GB 0
PC 1.40





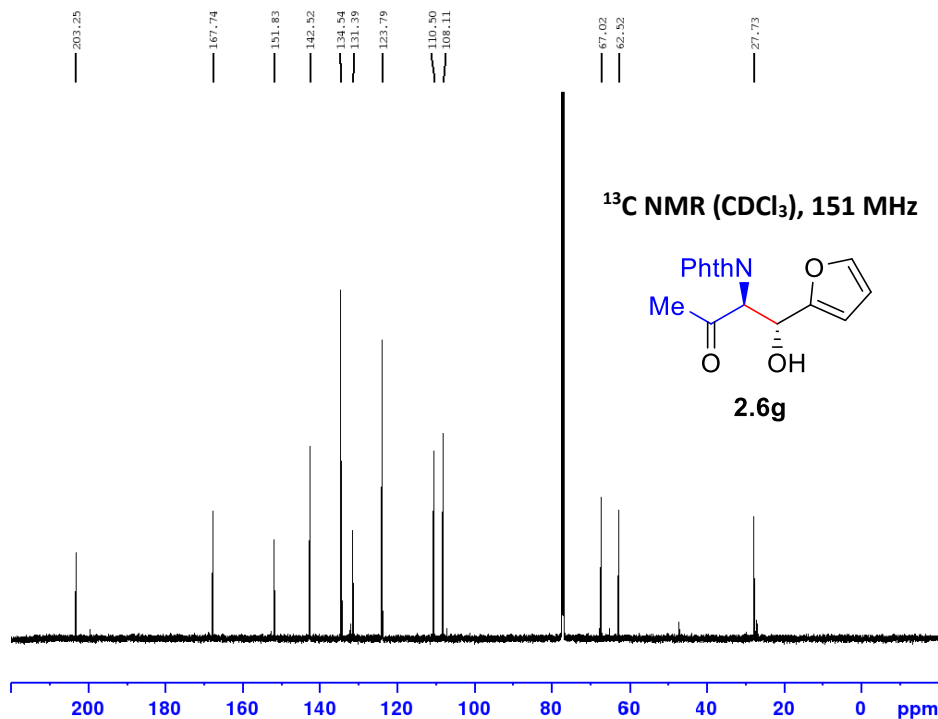
```

Current Data Parameters
NAME      SLG3-070
EXPNO    10
PROCNO    1

F2 - Acquisition Parameters
Date_    20220531
Time     9.23 h
INSTRUM  spect
PROBHD   Z148658_0003 (
PULPROG  zg30
TD       65536
SOLVENT  CDCl3
NS       16
DS       2
SWH      12019.230 Hz
FIDRES   0.366798 Hz
AQ       2.7262976 sec
RG       199.73
DW       41.600 usec
DE       10.33 usec
TE       296.3 K
D1       4.00000000 sec
TD0      1
SF01     600.0087050 MHz
NUC1     1H
P0       5.17 usec
P1       15.50 usec
PLW1     13.23200035 W

F2 - Processing parameters
SI       65536
SF       600.0050172 MHz
WDW      EM
SSB      0
LB       0.30 Hz
GB       0
PC       1.00
  
```

SLG3-070a-col
C13CPD CDCl3 {D:\nmrdata} Sieber 8

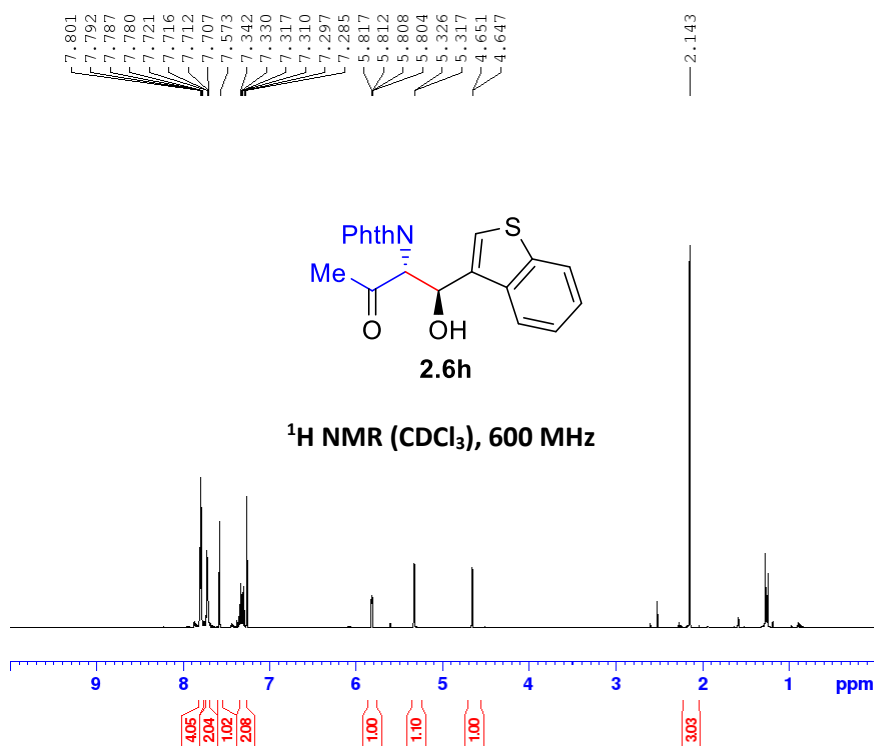


```

Current Data Parameters
NAME      SLG3-070_2
EXPNO    2
PROCNO    1

F2 - Acquisition Parameters
Date_    20221021
Time     23.10 h
INSTRUM  spect
PROBHD   Z148658_0003 (
PULPROG  zgpg30
TD       65536
SOLVENT  CDCl3
NS       1024
DS       4
SWH      36231.883 Hz
FIDRES   1.105709 Hz
AQ       0.9043968 sec
RG       199.73
DW       13.800 usec
DE       6.50 usec
TE       298.0 K
D1       6.00000000 sec
D11      0.03000000 sec
TD0      1
SF01     150.8864644 MHz
NUC1     13C
P0       4.00 usec
P1       12.00 usec
PLW1     77.65699768 W
SFO2     600.0074000 MHz
NUC2     1H
CPDPRG2  waltz65
PCPD2    70.00 usec
PLM2     13.23200035 W
PLM12    0.64876997 W
PLM13    0.32633001 W

F2 - Processing parameters
SI       32768
SF       150.8713833 MHz
WDW      EM
SSB      0
LB       1.00 Hz
GB       0
PC       1.40
  
```



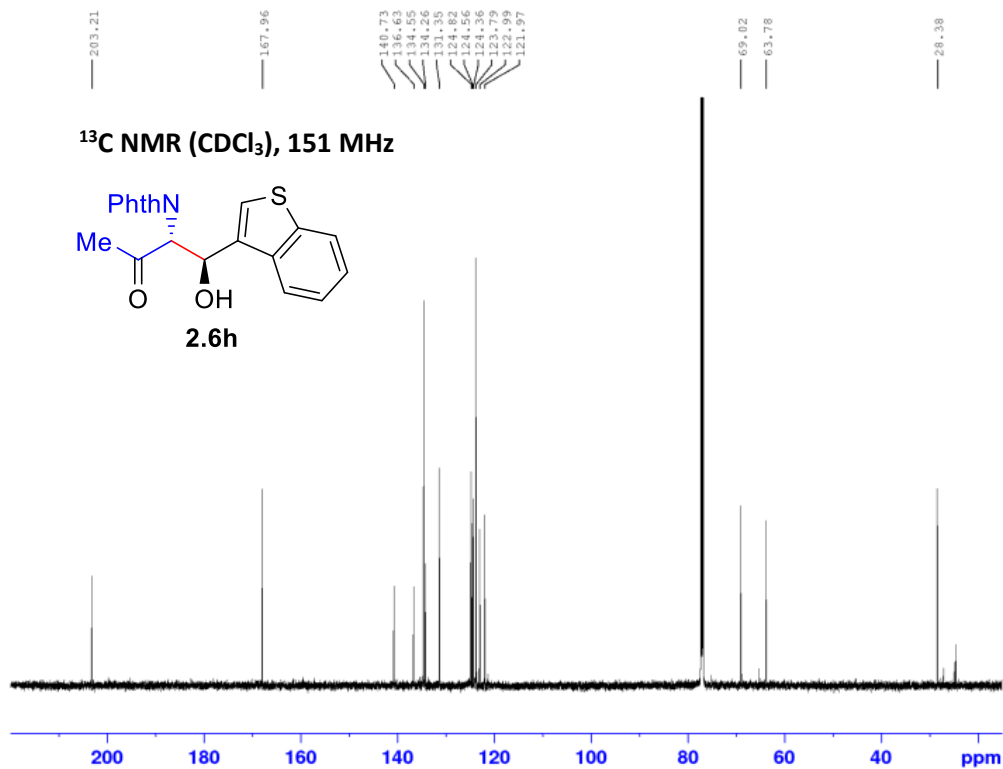
```

Current Data Parameters
NAME      SLG3-053_2
EXPNO    1
PROCNO   1

F2 - Acquisition Parameters
Date_    20220512
Time     17.23 h
INSTRUM  spect
PROBHD   Z148658_0003 (
PULPROG  zg30
TD        65536
SOLVENT  CDCl3
NS        16
DS        2
SINH      12019.230 Hz
FIDRES    0.366798 Hz
AQ        2.7262976 sec
RG        199.73
DN        41.600 usec
DE        10.33 usec
TE        296.4 K
D1        4.0000000 sec
TD0       1
SF01      600.0087050 MHz
NUC1      1H
P0        5.17 usec
P1        15.50 usec
PLW1      13.23200035 W

F2 - Processing parameters
SI        65536
SF        600.0050163 MHz
WDW       EM
SSB       0
LB        0.30 Hz
GB        0
PC        1.00
  
```

SLG3-053b-coll13CNMR
C13CPD CDCl3 {D:\nmrdata} Sieber 4

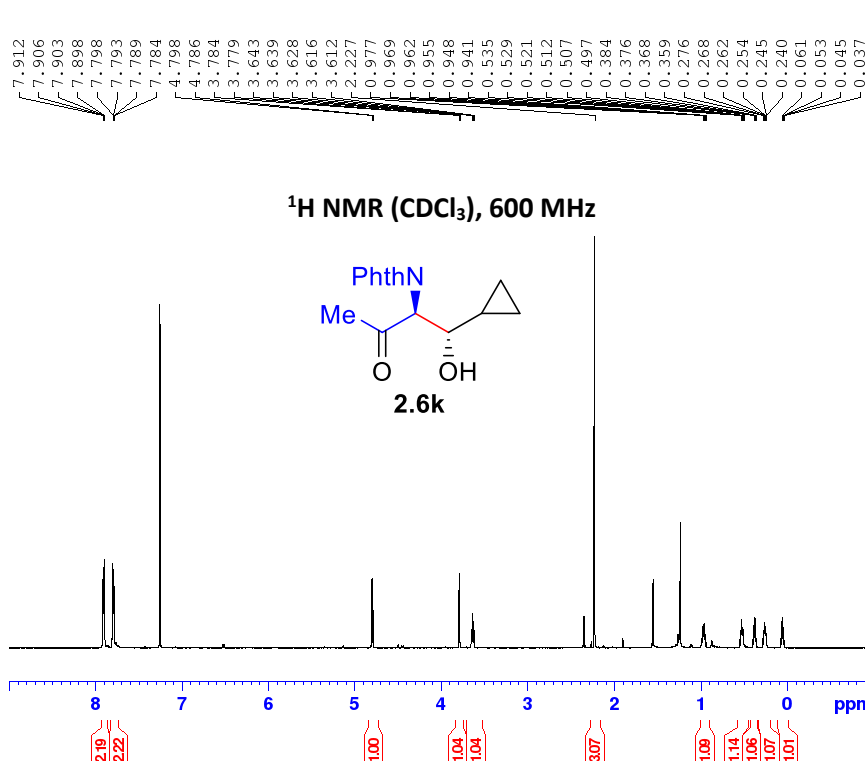


```

Current Data Parameters
NAME      SLG3-053_2
EXPNO    2
PROCNO   1

F2 - Acquisition Parameters
Date_    20220513
Time     0.06 h
INSTRUM  spect
PROBHD   Z148658_0003 (
PULPROG  zgpg30
TD        65536
SOLVENT  CDCl3
NS        1024
DS        4
SINH      36231.883 Hz
FIDRES    1.105709 Hz
AQ        0.9043968 sec
RG        199.73
DN        12.800 usec
DE        6.50 usec
TE        297.8 K
D1        6.0000000 sec
D11       0.03000000 sec
TD0       1
SF01      150.8846444 MHz
NUC1      13C
P0        4.00 usec
P1        12.00 usec
PLW1      77.65699768 W
SF02      600.0074000 MHz
NUC2      1H
CPDPRG2  waltz16
PCPD2     70.00 usec
PLW2     13.23200035 W
PLW12    0.64876997 W
PLW13    0.32633001 W

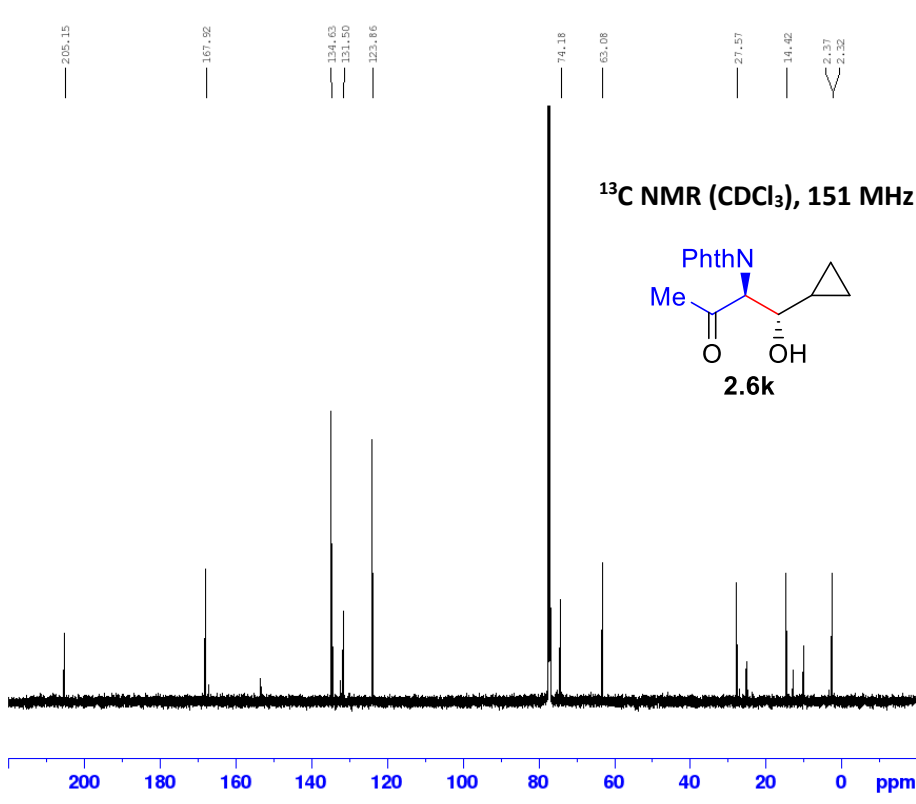
F2 - Processing parameters
SI        32768
SF        150.8713773 MHz
WDW       EM
SSB       0
LB        1.00 Hz
GB        0
PC        1.40
  
```



Current Data Parameters
 NAME SLG3-070
 EXPNO 11
 PROCNO 1

F2 - Acquisition Parameters
 Date_ 20220531
 Time 9.29 h
 INSTRUM spect
 PROBHD Z148658_0003 ()
 PULPROG zg30
 TD 65536
 SOLVENT CDCl3
 NS 16
 DS 2
 SWH 12019.230 Hz
 FIDRES 0.366798 Hz
 AQ 2.7262976 sec
 RG 199.73
 DW 41.600 usec
 DE 10.33 usec
 TE 296.3 K
 D1 4.0000000 sec
 TD0 1
 SFO1 600.0087050 MHz
 NUC1 1H
 P0 5.17 usec
 P1 15.50 usec
 PLW1 13.23200035 W

F2 - Processing parameters
 SI 65536
 SF 600.0050209 MHz
 WDM EM
 SSB 0
 LB 0.30 Hz
 GB 0
 PC 1.00

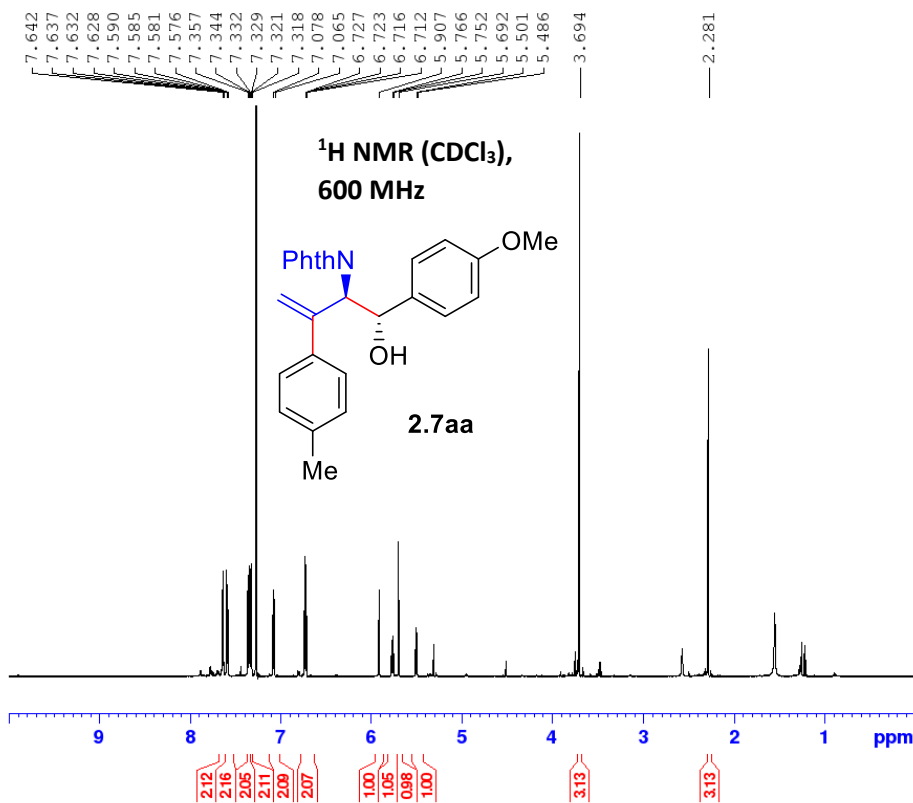


Current Data Parameters
 NAME SLG3-070
 EXPNO 21
 PROCNO 1

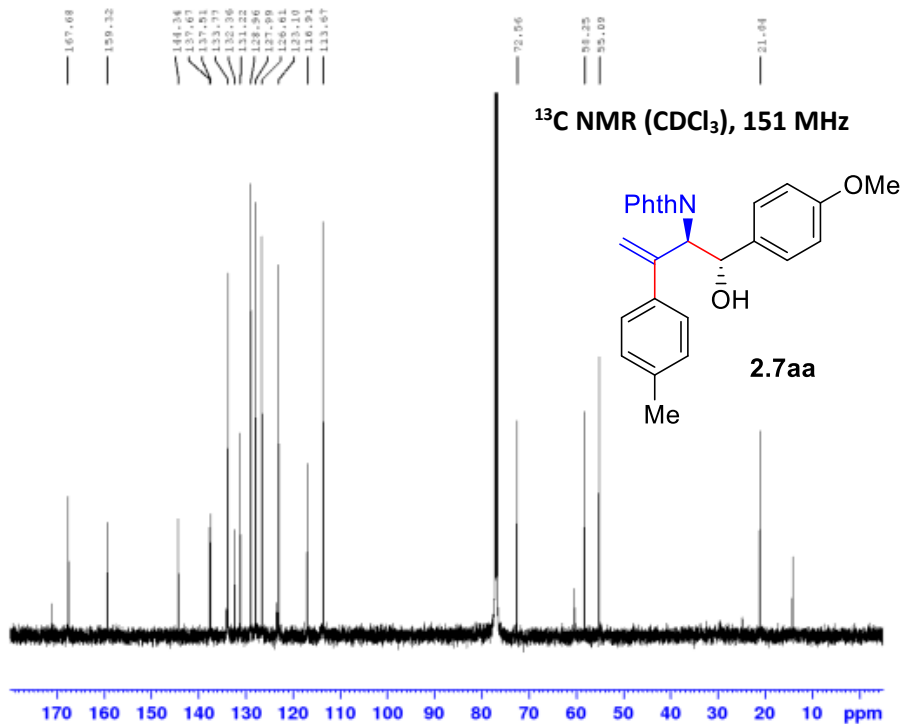
F2 - Acquisition Parameters
 Date_ 20221028
 Time 18.53 h
 INSTRUM spect
 PROBHD Z148658_0003 ()
 PULPROG zgpg30
 TD 65536
 SOLVENT CDCl3
 NS 1200
 DS 4
 SWH 36231.883 Hz
 FIDRES 1.105709 Hz
 AQ 0.9043968 sec
 RG 199.73
 DW 13.800 usec
 DE 6.50 usec
 TE 297.9 K
 D1 6.0000000 sec
 D11 0.0300000 sec
 TD0 1
 SFO1 150.8864644 MHz
 NUC1 13C
 P0 4.00 usec
 P1 12.00 usec
 PLW1 77.65699768 W
 SFO2 600.0074000 MHz
 NUC2 1H
 CPDPRG[2] waltz65
 PCPD2 70.00 usec
 PLW2 13.23200035 W
 PLW12 0.64876997 W
 PLW13 0.32633001 W

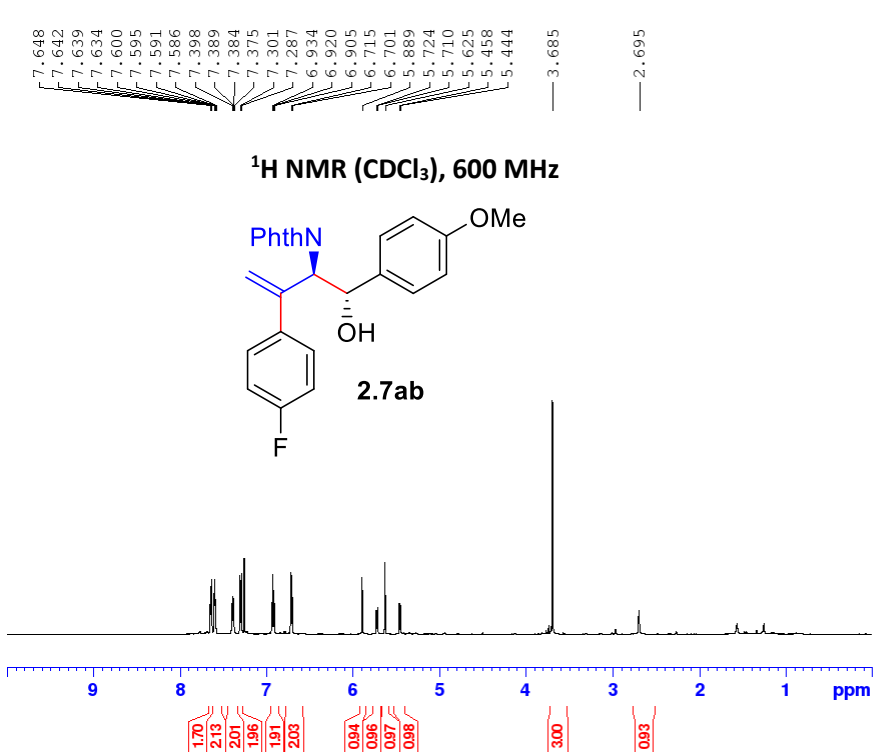
F2 - Processing parameters
 SI 32768
 SF 150.8713805 MHz
 WDM EM
 SSB 0
 LB 1.00 Hz
 GB 0
 PC 1.40

Suzuki Products



SLG3-091a-col-13C
C13CPD CDC13 D:\ Sieber 5

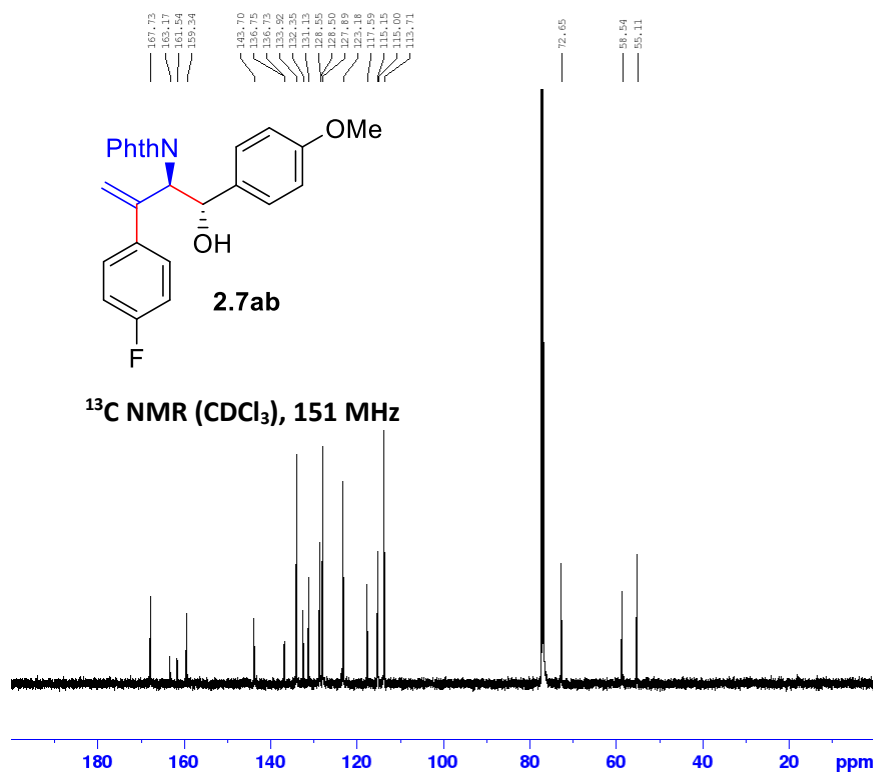




Current Data Parameters
NAME SLG3-089
EXPNO 7
PROCNO 1

F2 - Acquisition Parameters
Date_ 20220816
Time 16.01 h
INSTRUM spect
PROBHD Z855801_0104 (
PULPROG zg30
TD 65536
SOLVENT CDCl3
NS 16
DS 2
SWH 12019.230 Hz
FIDRES 0.366798 Hz
AQ 2.7262976 sec
RG 154.29
DM 41.600 usec
DE 11.65 usec
TE 298.1 K
D1 4.00000000 sec
TD0 1
SFO1 599.9587047 MHz
NUC1 1H
P0 2.58 usec
P1 7.75 usec
PLW1 11.99499989 W

F2 - Processing parameters
SI 65536
SF 599.9550191 MHz
WDW EM
SSB 0
LB 0.30 Hz
GB 0
PC 1.00

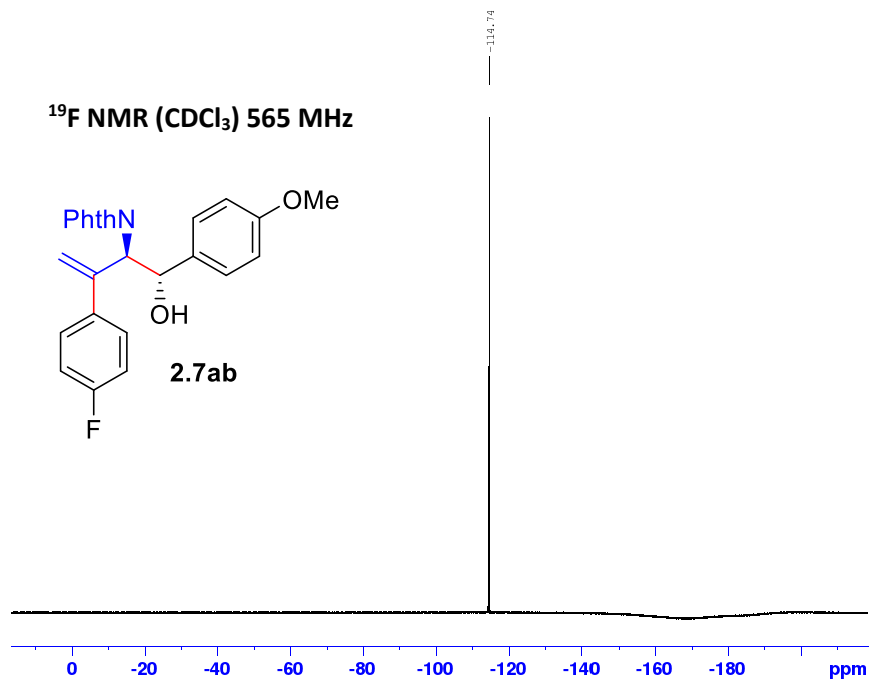


Current Data Parameters
NAME SLG3-089
EXPNO 9
PROCNO 1

F2 - Acquisition Parameters
Date_ 20220819
Time 0.22 h
INSTRUM spect
PROBHD Z855801_0104 (
PULPROG zgpg30
TD 65536
SOLVENT CDCl3
NS 400
DS 4
SWH 36231.883 Hz
FIDRES 1.105709 Hz
AQ 0.9043968 sec
RG 194.75
DM 13.800 usec
DE 6.50 usec
TE 298.1 K
D1 6.00000000 sec
D11 0.03000000 sec
TD0 1
SFO1 150.8738906 MHz
NUC1 13C
P0 3.80 usec
P1 11.40 usec
PLW1 176.19999695 W
SFO2 599.9573998 MHz
NUC2 1H
CPDPRG[2] waltz65
PCPD2 70.00 usec
PLW2 11.99499989 W
PLW12 0.14703000 W
PLW13 0.07395500 W

F2 - Processing parameters
SI 32768
SF 150.8588130 MHz
WDW EM
SSB 0
LB 1.00 Hz
GB 0
PC 1.40

SLG3-089c-col-F
F19CPD_vcu CDC13 {D:\nmrdata} Sieber 1

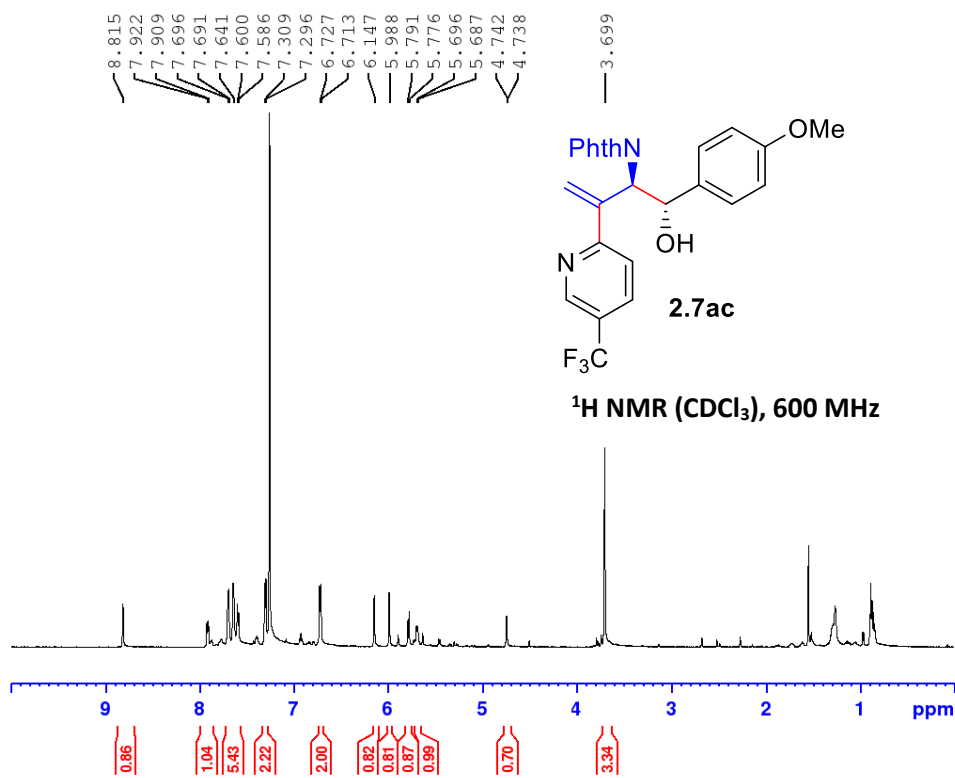


```
Current Data Parameters
NAME          SLG3-089_2
EXPNO         7
PROCNO        1

F2 - Acquisition Parameters
Date_         20221029
Time          5.28 h
INSTRUM       spect
PROBHD        Z148658_0003 (
PULPROG       zgfhigqn.2
TD            131072
SOLVENT       CDCl3
NS            16
DS            4
SWH           133928.578 Hz
FIDRES        2.043588 Hz
AQ            0.4893355 sec
RG            199.73
DM            3.733 usec
DE            6.50 usec
TE            296.4 K
D1            10.0000000 sec
D11           0.03000000 sec
D12           0.00002000 sec
TD0           1
SFO1          564.5123141 MHz
NUC1          19F
P1            15.00 usec
PLW1          26.76399994 W
SFO2          600.0074000 MHz
NUC2          1H
CPDPRG[2]    waltz16
PCPD2        70.00 usec
PLW2          13.23200035 W
PLW12         0.64876997 W

F2 - Processing parameters
SI            65536
SF            564.5687710 MHz
WDW           EM
SSB           0
LB            0.30 Hz
GB            0
PC            1.00
```

SLG3-089b-col-3
PROTON CDC13 D:\\ Sieber 13

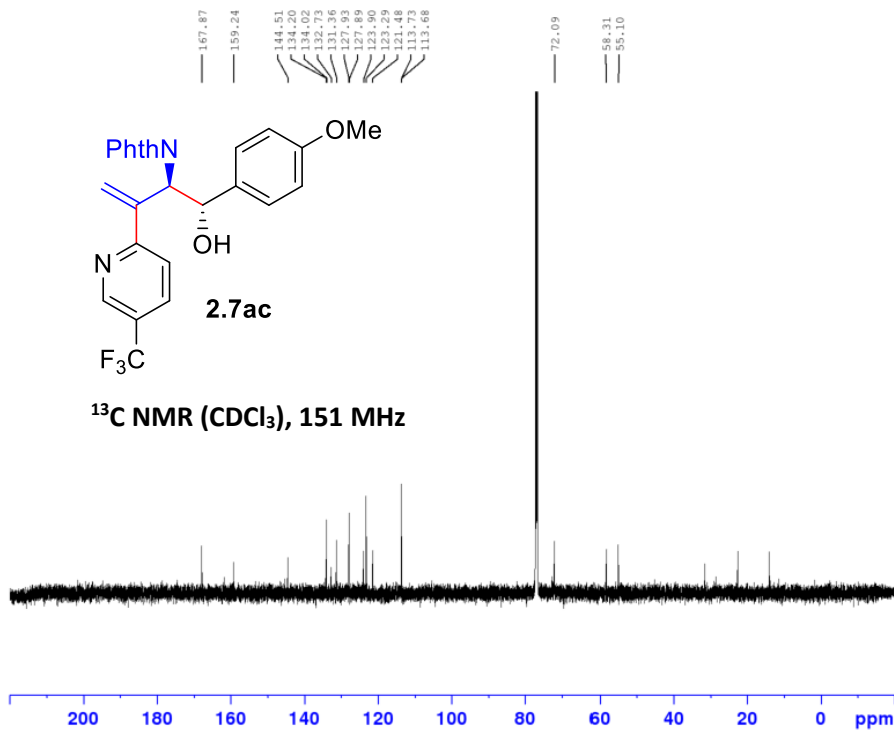


```
Current Data Parameters
NAME          SLG3-089
EXPNO         11
PROCNO        1

F2 - Acquisition Parameters
Date_         20221021
Time          16.04 h
INSTRUM       spect
PROBHD        z855801_0104 (
PULPROG       zg30
TD            65536
SOLVENT       CDCl3
NS            16
DS            2
SWH           12019.230 Hz
FIDRES        0.366798 Hz
AQ            2.7262976 sec
RG            194.75
DM            41.600 usec
DE            11.65 usec
TE            296.6 K
D1            4.00000000 sec
TD0           1
SFO1          599.9587047 MHz
NUC1          1H
P0            2.58 usec
P1            7.75 usec
PLW1          11.99499989 W

F2 - Processing parameters
SI            65536
SF            599.9550169 MHz
WDW           EM
SSB           0
LB            0.30 Hz
GB            0
PC            1.00
```

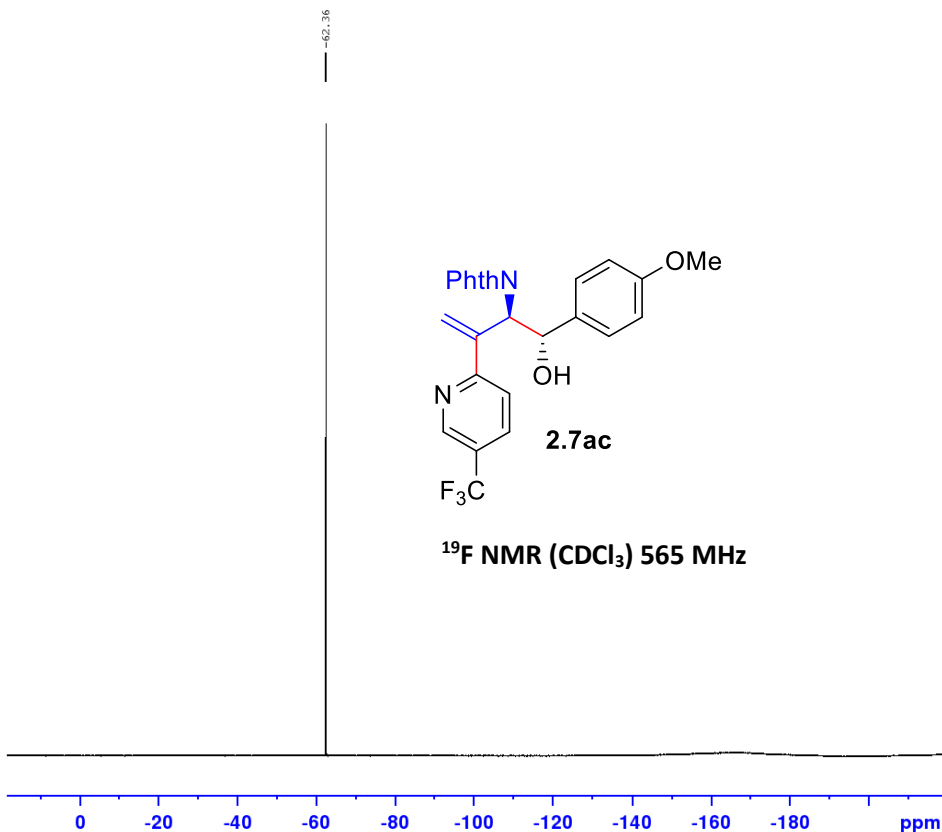
SLG3-089b-col-2
 C13CPD CDCl3 {D:\nmrdata} Sieber 1



Current Data Parameters
 NAME SLG3-089_2
 EXPNO 3
 PROCNO 1

F2 - Acquisition Parameters
 Date_ 20221023
 Time 21.06 h
 INSTRUM spect
 PROBHD Z148658_0003 (
 PULPROG zgpg30
 TD 65536
 SOLVENT CDCl3
 NS 1200
 DS 4
 SWH 36231.883 Hz
 FIDRES 1.105709 Hz
 AQ 0.9043968 sec
 RG 199.73
 DW 13.800 usec
 DE 6.50 usec
 TE 297.8 K
 D1 6.0000000 sec
 D11 0.0300000 sec
 TD0 1
 SF01 150.8864644 MHz
 NUC1 13C
 P0 4.00 usec
 P1 12.00 usec
 PLW1 77.65699768 W
 SFO2 600.0074000 MHz
 NUC2 1H
 CPDPRG[2] waltz65
 PCPD2 70.00 usec
 PLW2 13.23200035 W
 PLW12 0.64876997 W
 PLW13 0.32633001 W

F2 - Processing parameters
 SI 32768
 SF 150.8713821 MHz
 WDW EM
 SSB 0
 LB 1.00 Hz
 GB 0
 PC 1.40

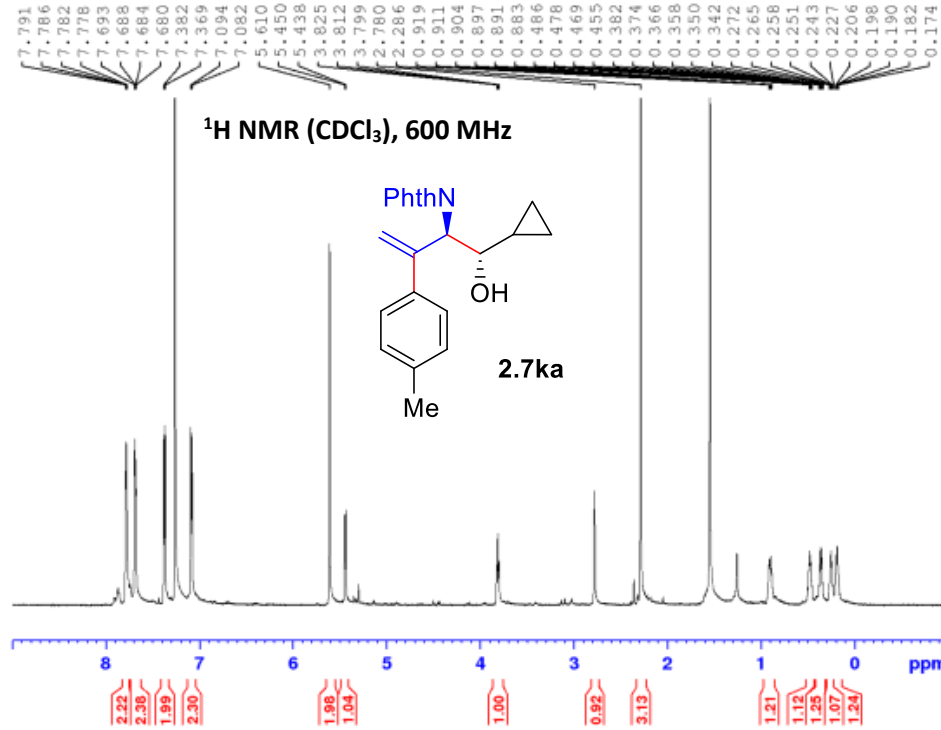


Current Data Parameters
 NAME SLG3-092
 EXPNO 10
 PROCNO 1

F2 - Acquisition Parameters
 Date_ 20221102
 Time 8.34 h
 INSTRUM spect
 PROBHD Z148658_0003 (
 PULPROG zgfhigqn.2
 TD 131072
 SOLVENT cdcl3
 NS 16
 DS 4
 SWH 133928.578 Hz
 FIDRES 2.043588 Hz
 AQ 0.4893355 sec
 RG 199.73
 DW 3.733 usec
 DE 6.50 usec
 TE 296.7 K
 D1 10.0000000 sec
 D11 0.0300000 sec
 D12 0.0000200 sec
 TD0 1
 SF01 564.5123141 MHz
 NUC1 19F
 P1 15.00 usec
 PLW1 26.76399994 W
 SFO2 600.0074000 MHz
 NUC2 1H
 CPDPRG[2] waltz16
 PCPD2 70.00 usec
 PLW2 13.23200035 W
 PLW12 0.64876997 W

F2 - Processing parameters
 SI 65536
 SF 564.5687710 MHz
 WDW EM
 SSB 0
 LB 0.30 Hz
 GB 0
 PC 1.00

SLG3-091c-col
 PROTON CDCl3 D:\ Sieber 3

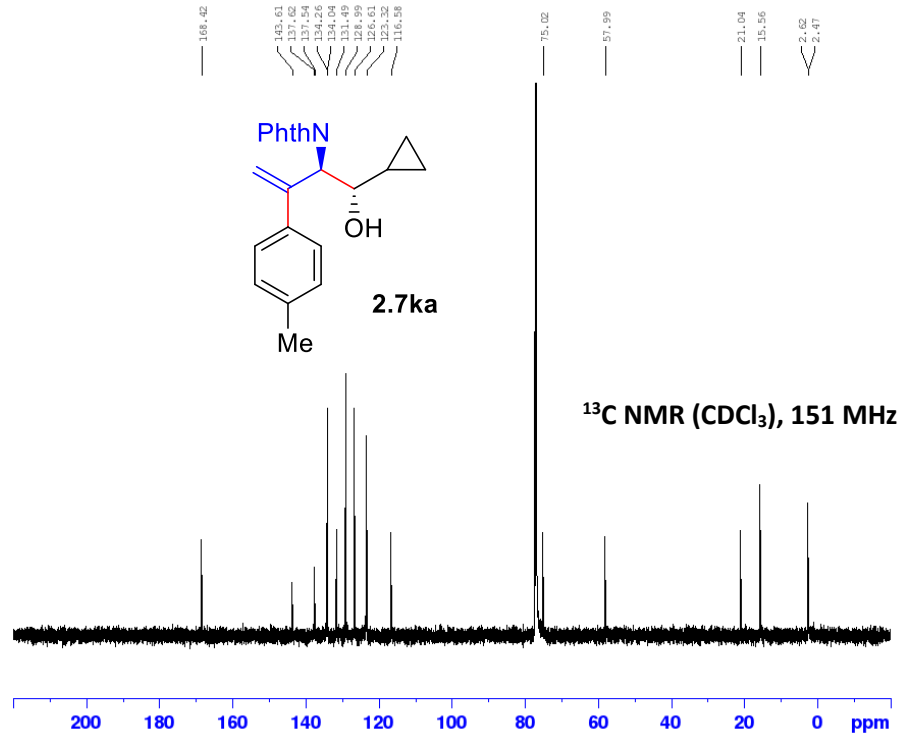


Current Data Parameters
 NAME SLG3-091
 EXPNO 8
 PROCNO 1

F2 - Acquisition Parameters
 Date_ 20220819
 Time 11.18 h
 INSTRUM spect
 PROBHD Z855801_0104
 PULPROG zg30
 TD 65536
 SOLVENT CDCl3
 NS 16
 DS 2
 SWH 12019.250 Hz
 FIDRES 0.366798 Hz
 AQ 2.7262976 sec
 RG 194.75
 DW 41.660 usec
 DE 11.65 usec
 TE 298.1 K
 D1 4.00000000 sec
 TDO 1
 SFO1 599.9587047 MHz
 NUC1 1H
 P0 2.58 usec
 P1 7.75 usec
 PLW1 11.99499989 W

F2 - Processing parameters
 SI 65536
 SF 599.958151 MHz
 WDW EM
 SSB 0
 LB 0.30 Hz
 GB 0
 PC 1.00

SLG3-091c-13CNMR
 C13CPD CDCl3 D:\ Sieber 9



Current Data Parameters
 NAME SLG3-091
 EXPNO 11
 PROCNO 1

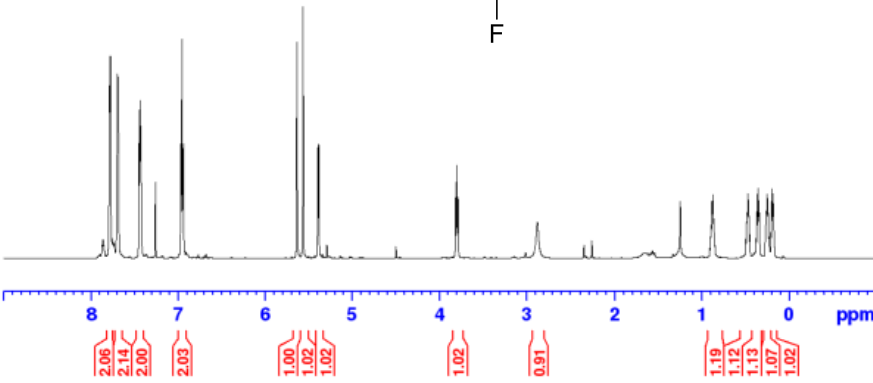
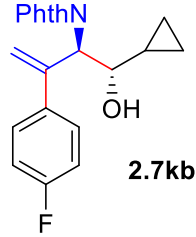
F2 - Acquisition Parameters
 Date_ 20220905
 Time 22.20 h
 INSTRUM spect
 PROBHD Z855801_0104
 PULPROG zgpg30
 TD 65536
 SOLVENT CDCl3
 NS 400
 DS 4
 SWH 36231.883 Hz
 FIDRES 1.105709 Hz
 AQ 0.9043968 sec
 RG 194.75
 DW 13.800 usec
 DE 6.50 usec
 TE 297.5 K
 D1 6.00000000 sec
 D11 0.03000000 sec
 TDO 1
 SFO1 150.8738906 MHz
 NUC1 13C
 P0 3.80 usec
 P1 11.40 usec
 PLW1 176.19999695 W
 SFO2 599.9573998 MHz
 NUC2 1H
 CPDPRG2 waltz65
 ECPD2 70.00 usec
 PLW2 11.99499989 W
 PLW12 0.14703000 W
 PLW13 0.07395500 W

F2 - Processing parameters
 SI 32768
 SF 150.8588144 MHz
 WDW EM
 SSB 0
 LB 1.00 Hz
 GB 0
 PC 1.40

SLG3-091d-col-1HNMR
 PROTON CDCl3 D:\\ Sieber 1

7.787
7.782
7.778
7.773
7.695
7.590
7.686
7.681
7.444
7.434
7.429
7.420
6.964
6.950
6.935
5.629
5.561
5.391
5.379
3.807
3.794
3.781
0.881
0.874
0.867
0.859
0.481
0.475
0.467
0.459
0.454
0.363
0.355
0.347
0.339
0.259
0.251
0.245
0.237
0.232
0.194
0.186
0.178
0.170

¹H NMR (CDCl₃), 600 MHz

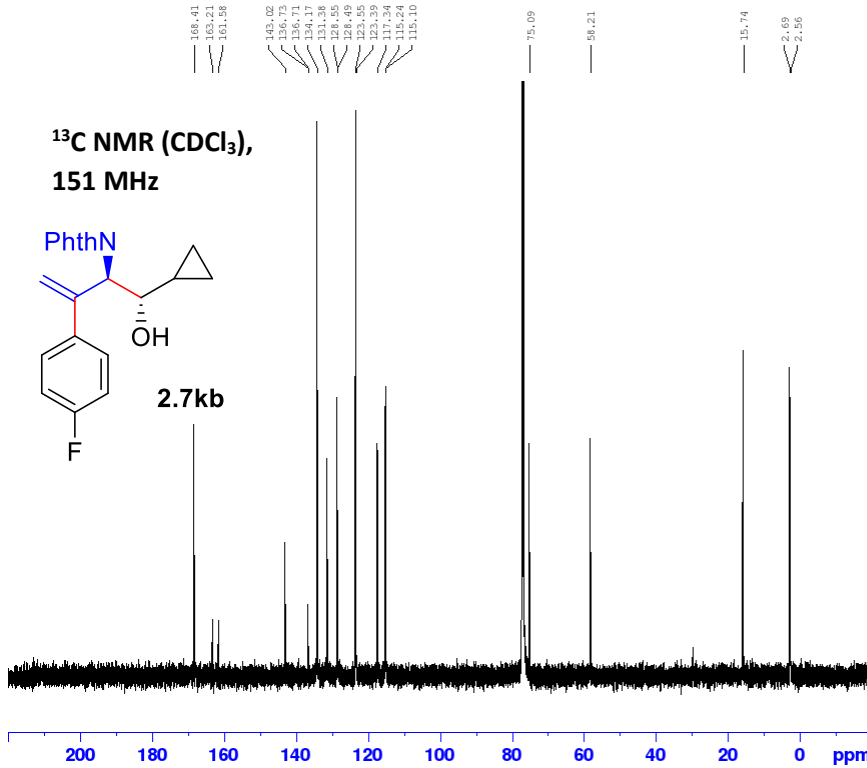
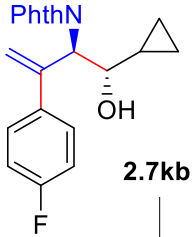


Current Data Parameters
 NAME SLG3-091
 EXPRO 13
 PROCNO 1

F2 - Acquisition Parameters
 Date_ 20220912
 Time 15.43 h
 INSTRUM spect
 PROBHD Z855801_0104 ()
 PULPROG zg30
 TD 65536
 SOLVENT CDCl3
 NS 16
 DS 2
 SWH 12019.230 Hz
 FIDRES 0.366798 Hz
 AQ 2.7262976 sec
 RG 71.41
 DW 41.600 usec
 DE 11.65 usec
 TE 297.9 K
 D1 4.00000000 sec
 TD0 1
 SFO1 599.9587047 MHz
 NUC1 1H
 P0 2.58 usec
 P1 7.75 usec
 PLW1 11.99499989 W

F2 - Processing parameters
 SI 65536
 SF 599.9550186 MHz
 WDW EM
 SSB 0
 LB 0.30 Hz
 GB 0
 PC 1.00

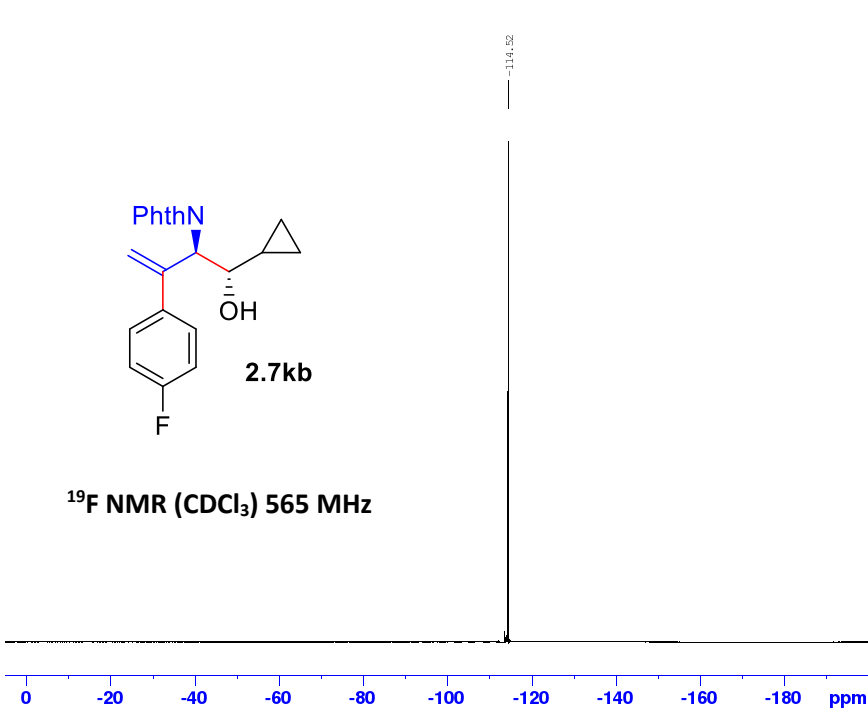
¹³C NMR (CDCl₃),
 151 MHz



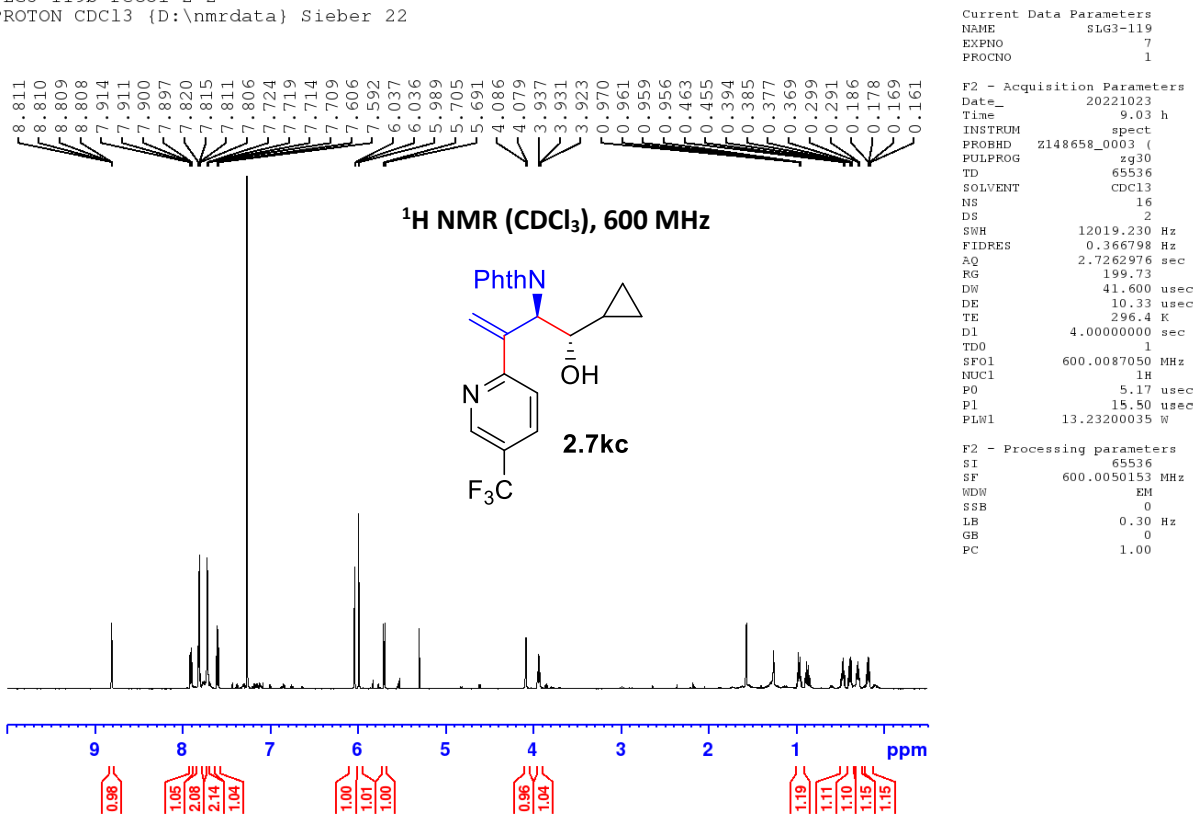
Current Data Parameters
 NAME SLG3-091
 EXPRO 14
 PROCNO 1

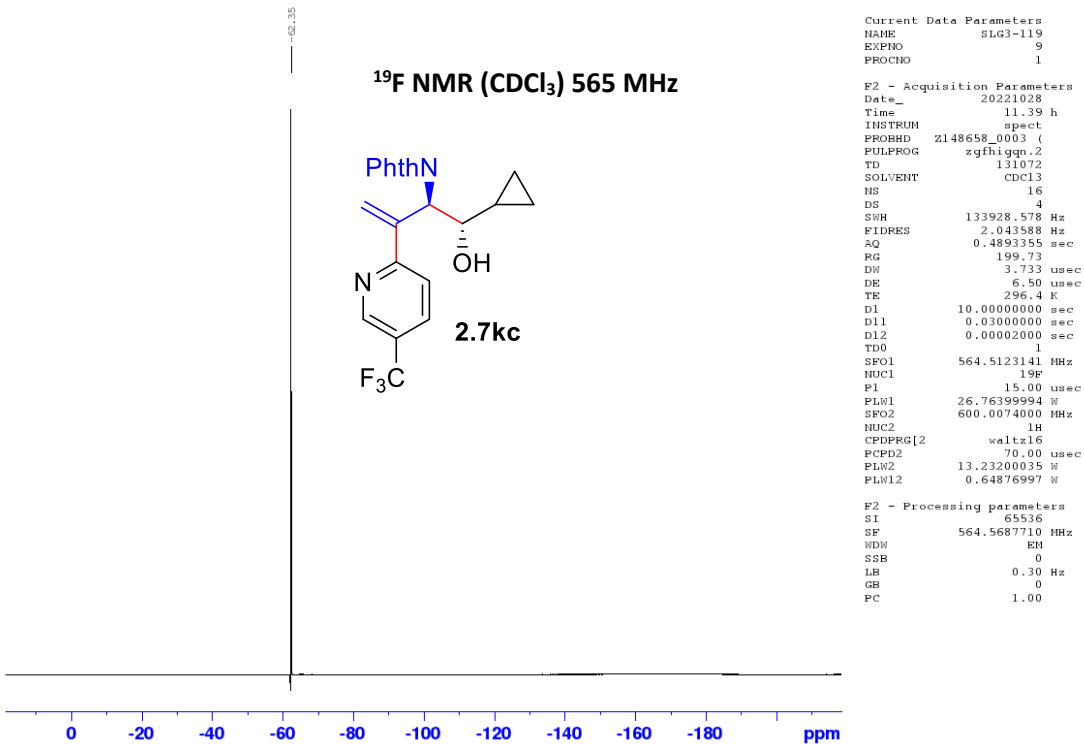
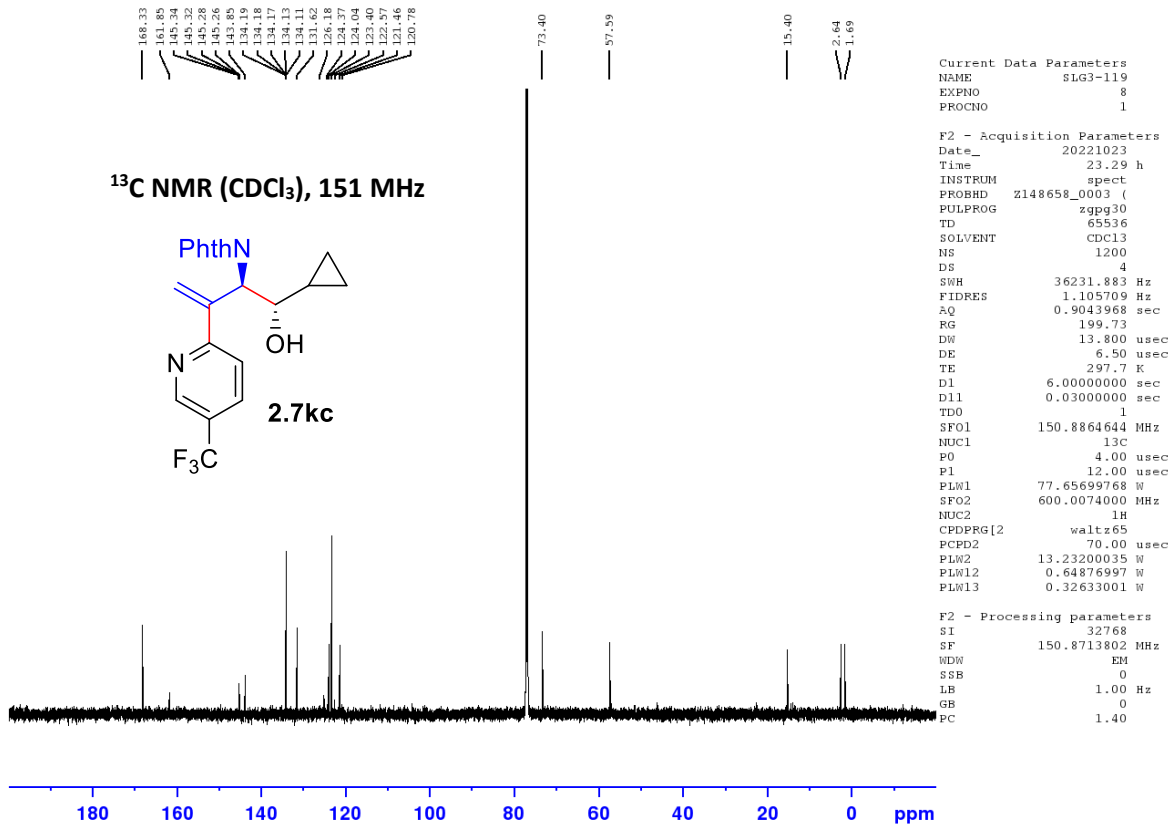
F2 - Acquisition Parameters
 Date_ 20220912
 Time 21.30 h
 INSTRUM spect
 PROBHD Z855801_0104 ()
 PULPROG zgpg30
 TD 65536
 SOLVENT CDCl3
 NS 400
 DS 4
 SWH 36231.883 Hz
 FIDRES 1.105709 Hz
 AQ 0.9043968 sec
 RG 194.75
 DW 13.800 usec
 DE 6.50 usec
 TE 297.3 K
 D1 6.00000000 sec
 D11 0.03000000 sec
 TD0 1
 SFO1 150.8738906 MHz
 NUC1 13C
 P0 3.80 usec
 P1 11.40 usec
 PLW1 176.19999695 W
 SFO2 599.9573998 MHz
 NUC2 1H
 CPDPRG2 waltz65
 PCPD2 70.00 usec
 PLW2 11.99499989 W
 PLW12 0.14703000 W
 PLW13 0.07395500 W

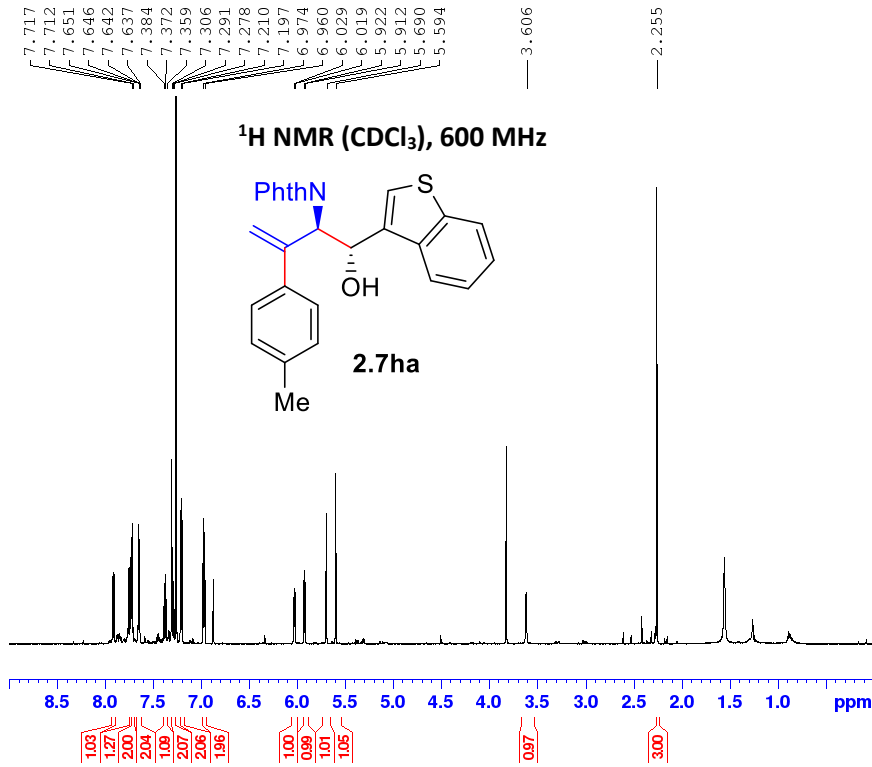
F2 - Processing parameters
 SI 32768
 SF 150.8588124 MHz
 WDW EM
 SSB 0
 LB 1.00 Hz
 GB 0
 PC 1.40



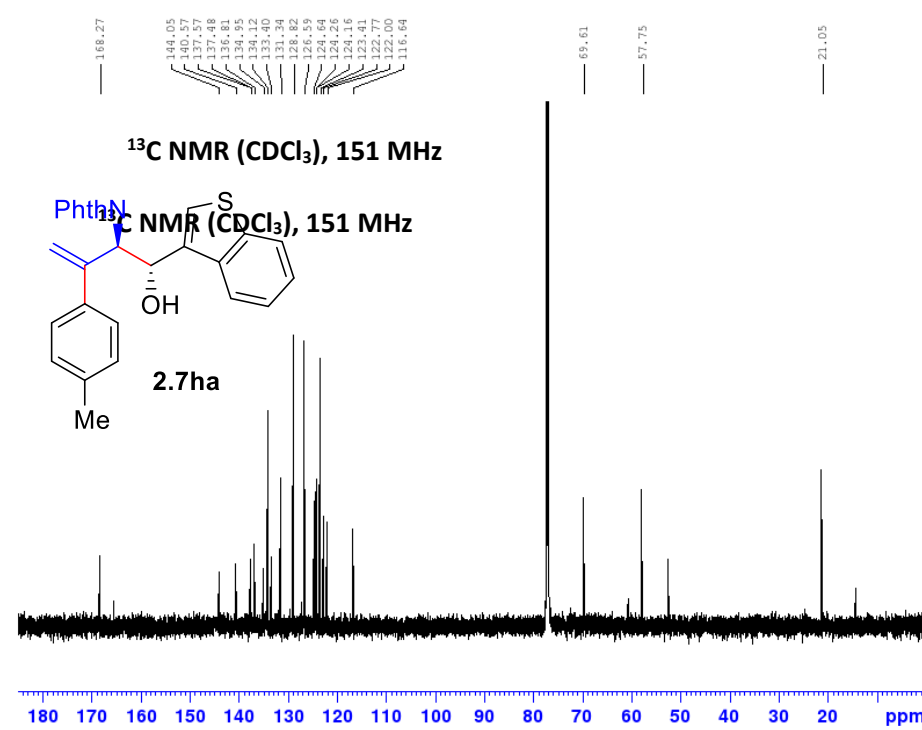
SLG3-119b-recol-2-2
 PROTON CDCl3 {D:\nmrdata} Sieber 22







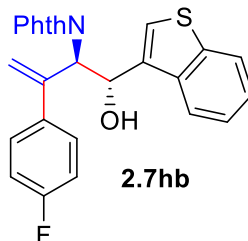
SLG3-096a-col-2
 C13CPD CDCl3 {D:\nmrdata} Sieber 3



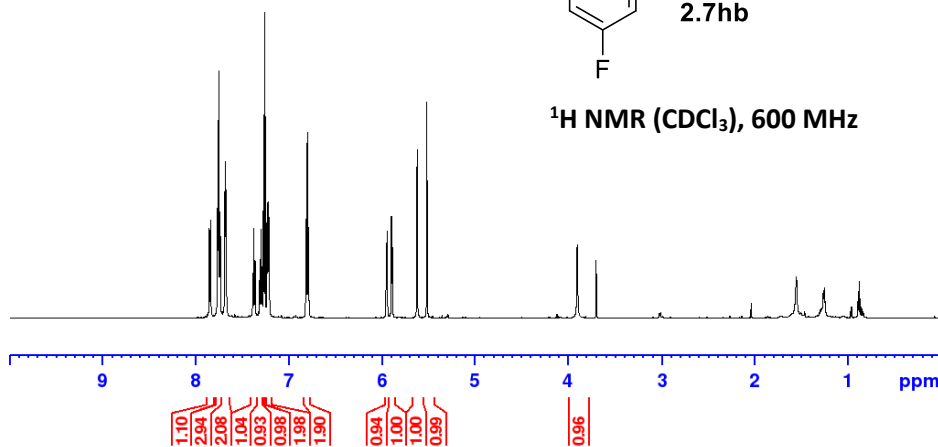
7.763
7.759
7.754
7.741
7.688
7.683
7.679
7.674
7.390
7.378
7.365
7.312
7.300
7.287
7.272
7.237
7.228
7.223
7.214
6.818
6.804
6.790
5.955
5.946
5.900
5.891
5.623
5.519
3.902

Current Data Parameters
NAME SLG3-096
EXPNO 13
PROCNO 1

F2 - Acquisition Parameters
Date_ 20220816
Time 15.38 h
INSTRUM spect
PROBHD z855801_0104 ((
PULPROG zg30
TD 65536
SOLVENT CDCl3
NS 16
DS 2
SWH 12019.230 Hz
FIDRES 0.366798 Hz
AQ 2.7262976 sec
RG 172.91
DW 41.600 usec
DE 11.65 usec
TE 298.1 K
D1 4.0000000 sec
TD0 1
SFO1 599.9587047 MHz
NUC1 1H
P0 2.58 usec
P1 7.75 usec
PLW1 11.99499989 W



¹H NMR (CDCl₃), 600 MHz

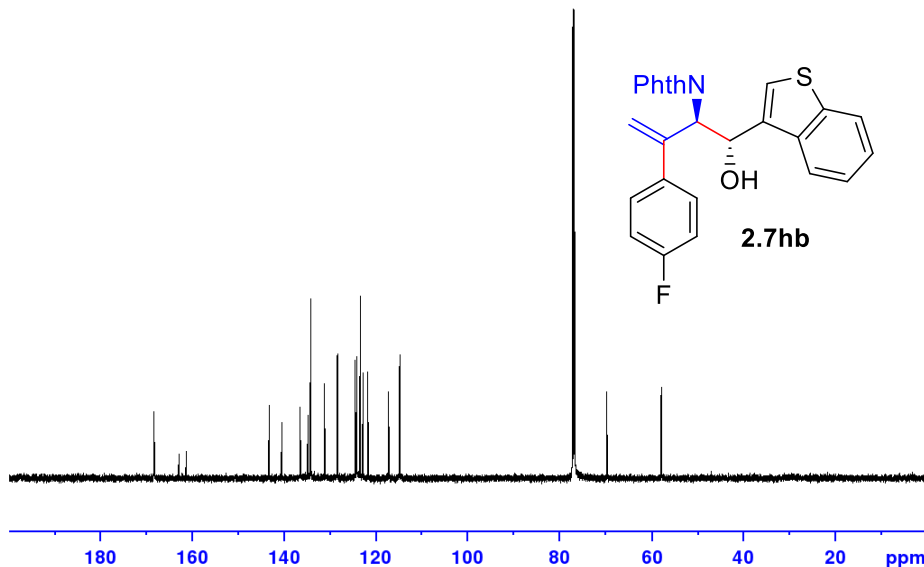
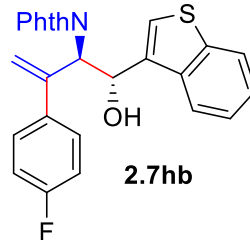


F2 - Processing parameters
SI 65536
SF 599.9550164 MHz
WDW EM
SSB 0
LB 0.30 Hz
GB 0
PC 1.00

168.36
163.02
161.38
143.29
140.96
136.97
136.57
136.55
134.89
134.25
131.20
128.43
124.58
124.48
124.26
124.17
123.47
122.83
122.83
121.76
117.22
116.62
114.78

69.69
98.01

¹³C NMR (CDCl₃), 151 MHz

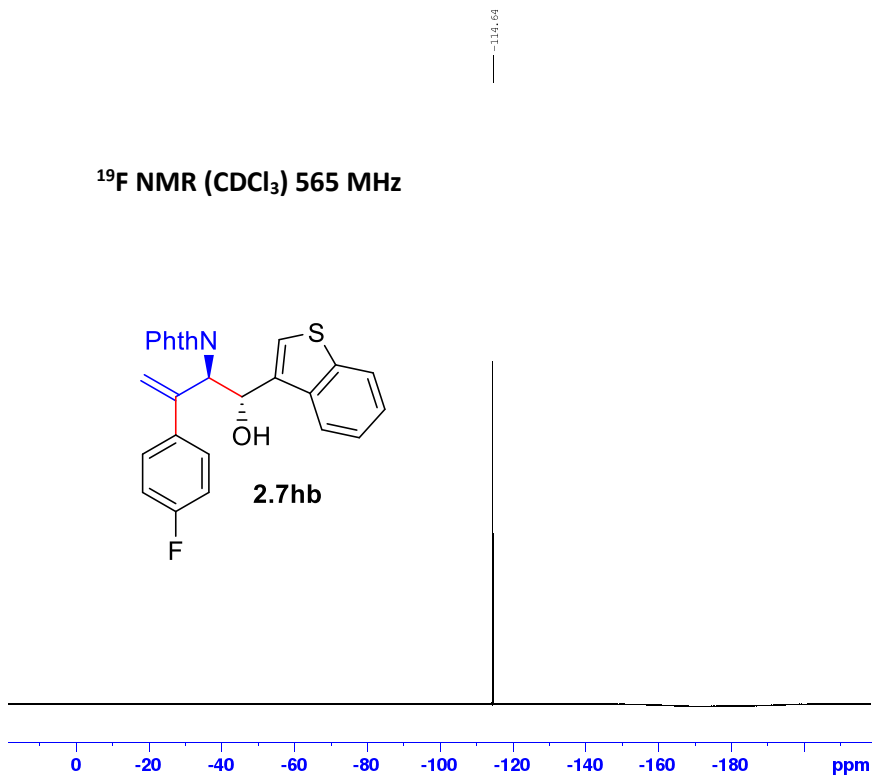


Current Data Parameters
NAME SLG3-096
EXPNO 17
PROCNO 1

F2 - Acquisition Parameters
Date_ 20220818
Time 21.20 h
INSTRUM spect
PROBHD z855801_0104 ((
PULPROG zgpg30
TD 65536
SOLVENT CDCl3
NS 400
DS 4
SWH 36231.883 Hz
FIDRES 1.105709 Hz
AQ 0.9043968 sec
RG 194.75
DW 13.800 usec
DE 6.50 usec
TE 298.1 K
D1 6.0000000 sec
D11 0.0300000 sec
TD0 1
SFO1 150.8738906 MHz
NUC1 13C
P0 3.80 usec
P1 11.40 usec
PLW1 176.19999695 W
SFO2 599.9573998 MHz
NUC2 1H
CPDPRG[2] waltz65
PCPD2 70.00 usec
PLW2 11.99499989 W
PLW12 0.14703000 W
PLW13 0.07395500 W

F2 - Processing parameters
SI 32768
SF 150.8588159 MHz
WDW EM
SSB 0
LB 1.00 Hz
GB 0
PC 1.40

¹⁹F NMR (CDCl₃) 565 MHz

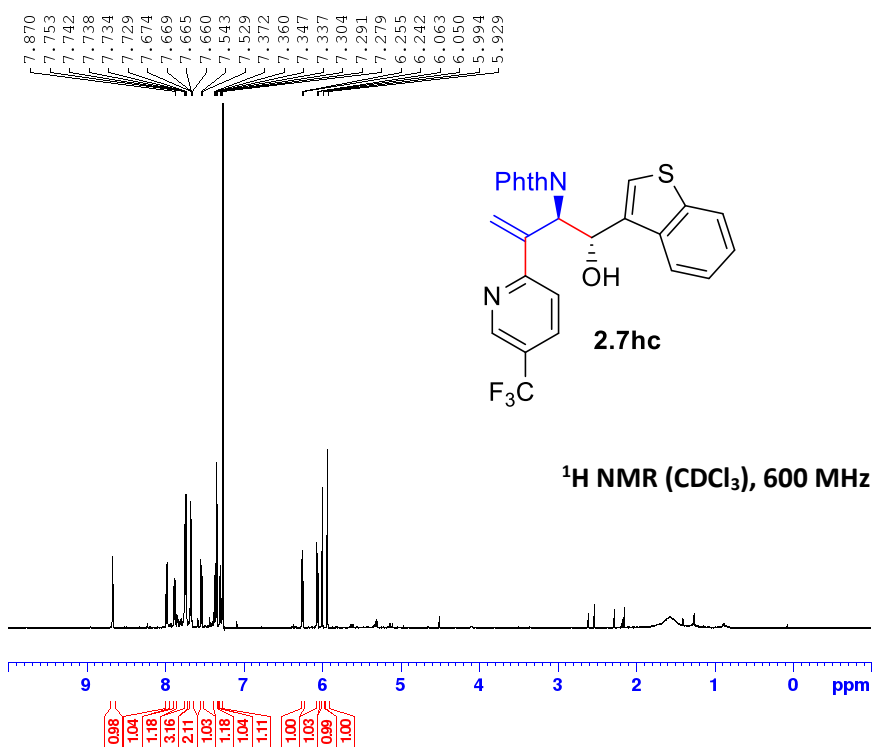


```

Current Data Parameters
NAME      SLG3-096_2
EXPNO    14
PROCNO   1

F2 - Acquisition Parameters
Date_    20221028
Time     11.50 h
INSTRUM  spect
PROBHD   Z148658_0003 (
PULPROG  zgfhigpn.2
TD       131072
SOLVENT  CDCl3
NS       16
DS       4
SWH      133928.578 Hz
FIDRES   2.043588 Hz
AQ       0.4893355 sec
RG       199.73
DW       3.733 usec
DE       6.50 usec
TE       296.4 K
D1       10.00000000 sec
D11      0.03000000 sec
D12      0.00002000 sec
TD0      1
SF01     564.5123141 MHz
NUC1     19F
P1       15.00 usec
PLW1     26.76399994 W
SF02     600.0074000 MHz
NUC2     1H
CPDPRG2  waltz16
PCPD2    70.00 usec
PLW2     13.23200035 W
PLW12    0.64876997 W

F2 - Processing parameters
SI       65536
SF       564.5687710 MHz
WDW      EM
SSB      0
LB       0.30 Hz
GB       0
PC       1.00
    
```

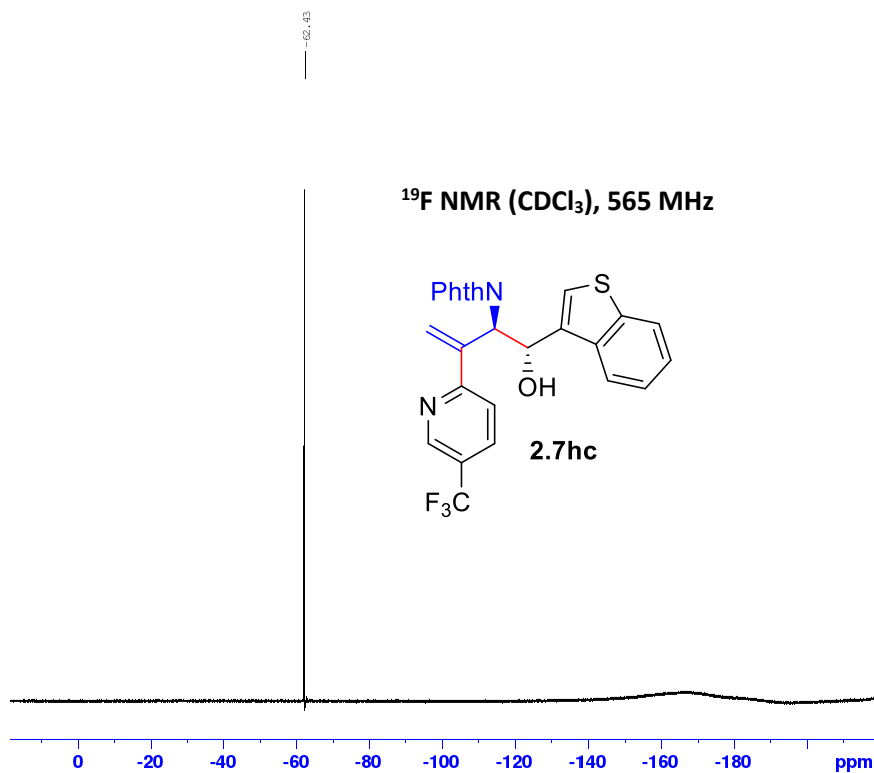
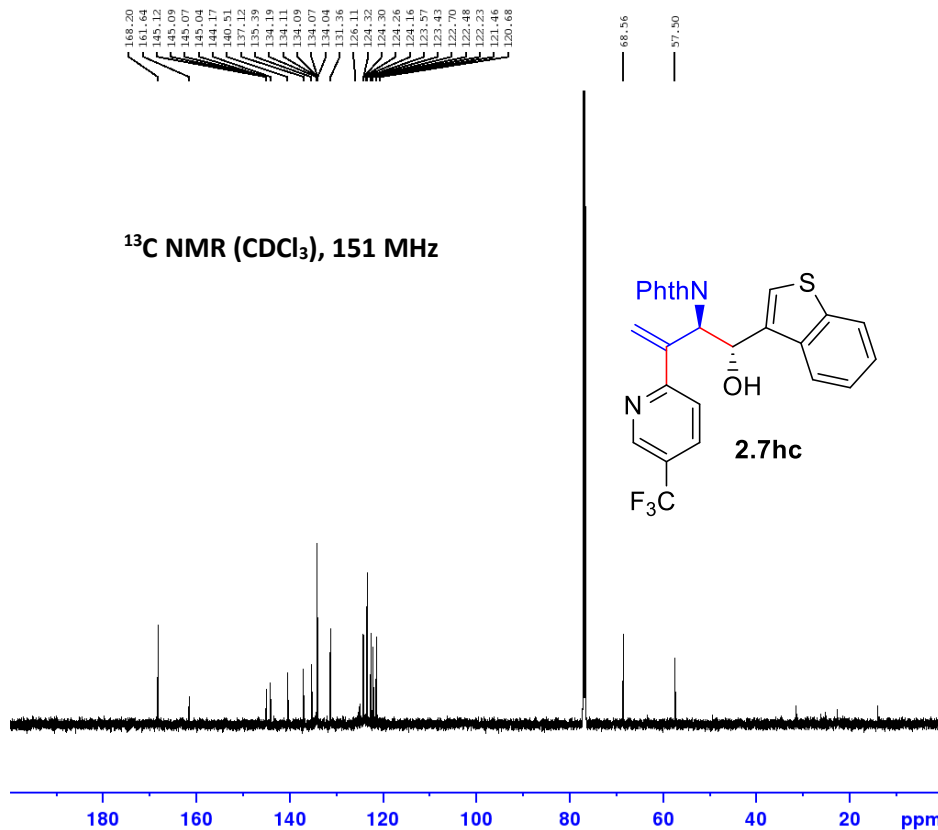


```

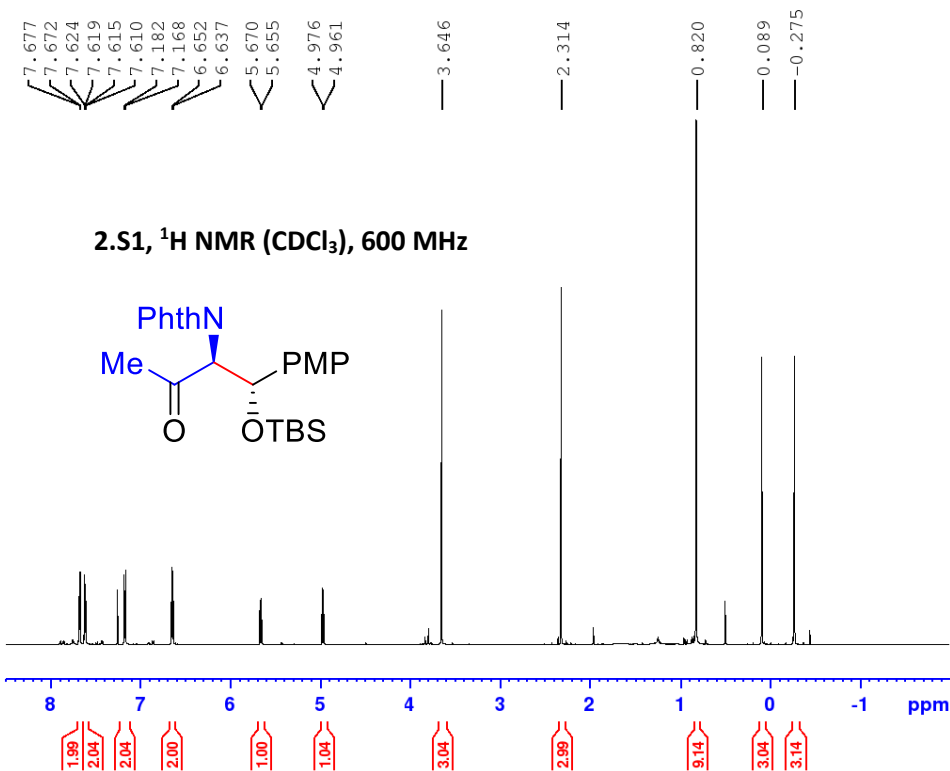
Current Data Parameters
NAME      SLG3-096_2
EXPNO    19
PROCNO   1

F2 - Acquisition Parameters
Date_    20221103
Time     17.57 h
INSTRUM  spect
PROBHD   Z148658_0003 (
PULPROG  zg30
TD       65536
SOLVENT  CDCl3
NS       16
DS       2
SWH      12019.230 Hz
FIDRES   0.366798 Hz
AQ       2.7262976 sec
RG       199.73
DW       41.600 usec
DE       10.33 usec
TE       296.5 K
D1       4.00000000 sec
TD0      1
SF01     600.0087050 MHz
NUC1     1H
P1       5.17 usec
P2       15.50 usec
PLW1     13.23200035 W

F2 - Processing parameters
SI       65536
SF       600.0050159 MHz
WDW      EM
SSB      0
LB       0.30 Hz
GB       0
PC       1.00
    
```



SLG3-051-3
 hivac
 PROTON CDC13 {D:\nmrdata} Sieber 23

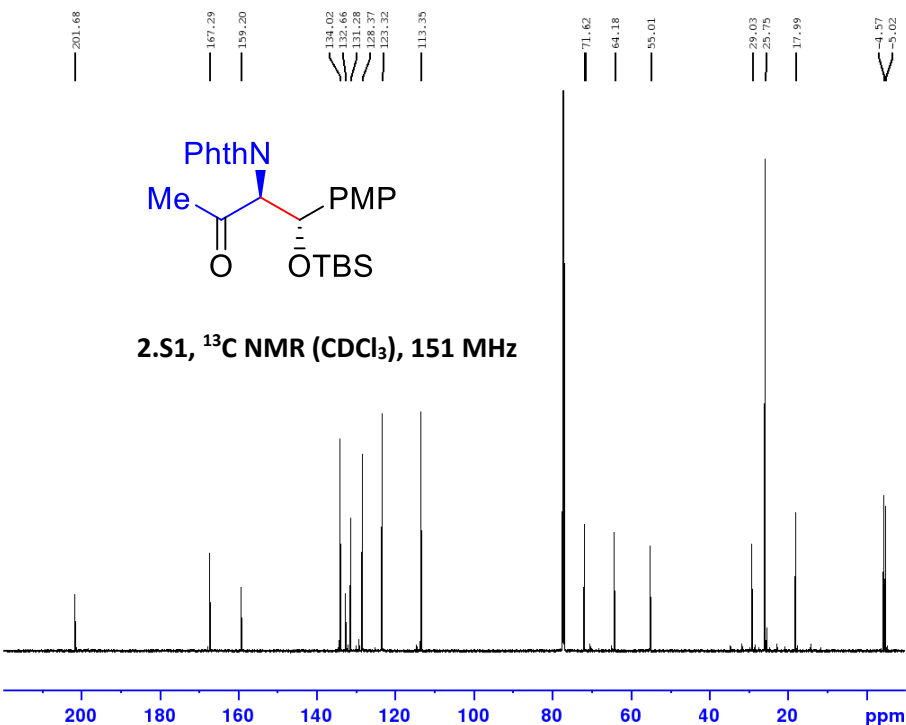


Current Data Parameters
 NAME SLG3-051_2
 EXPNO 3
 PROCNO 1

F2 - Acquisition Parameters
 Date_ 20221023
 Time 8.58 h
 INSTRUM spect
 PROBHD Z148658_0003 (
 PULPROG zg30
 TD 65536
 SOLVENT CDCl3
 NS 16
 DS 2
 SWH 12019.230 Hz
 FIDRES 0.366798 Hz
 AQ 2.7262976 sec
 RG 68.55
 DW 41.600 usec
 DE 10.33 usec
 TE 296.4 K
 D1 4.00000000 sec
 TD0 1
 SFO1 600.0087050 MHz
 NUC1 1H
 P0 5.17 usec
 P1 15.50 usec
 PLW1 13.23200035 W

F2 - Processing parameters
 SI 65536
 SF 600.0050177 MHz
 WDW EM
 SSB 0
 LB 0.30 Hz
 GB 0
 PC 1.00

SLG3-051-3
 hivac
 C13CPD CDC13 {D:\nmrdata} Sieber 23

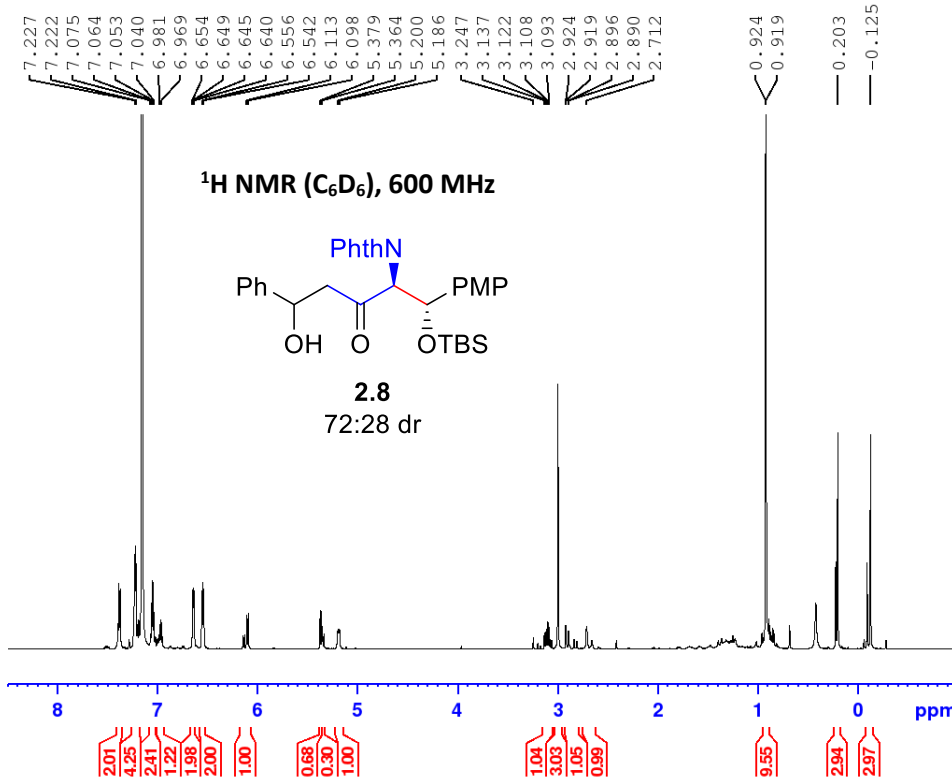


Current Data Parameters
 NAME SLG3-051
 EXPNO 6
 PROCNO 1

F2 - Acquisition Parameters
 Date_ 20221023
 Time 8.42 h
 INSTRUM spect
 PROBHD Z148658_0003 (
 PULPROG zgpg30
 TD 65536
 SOLVENT CDCl3
 NS 1024
 DS 4
 SWH 36231.883 Hz
 FIDRES 1.105709 Hz
 AQ 0.9043968 sec
 RG 199.73
 DW 13.800 usec
 DE 6.50 usec
 TE 297.9 K
 D1 6.00000000 sec
 D11 0.03000000 sec
 TD0 1
 SFO1 150.8864644 MHz
 NUC1 13C
 P0 4.00 usec
 P1 12.00 usec
 PLW1 77.65699768 W
 SFO2 600.0074000 MHz
 NUC2 1H
 CPDPRG2 waltz65
 PCPD2 70.00 usec
 PLW2 13.23200035 W
 PLW12 0.64876997 W
 PLW13 0.32633001 W

F2 - Processing parameters
 SI 32768
 SF 150.8713831 MHz
 WDW EM
 SSB 0
 LB 1.00 Hz
 GB 0
 PC 1.40

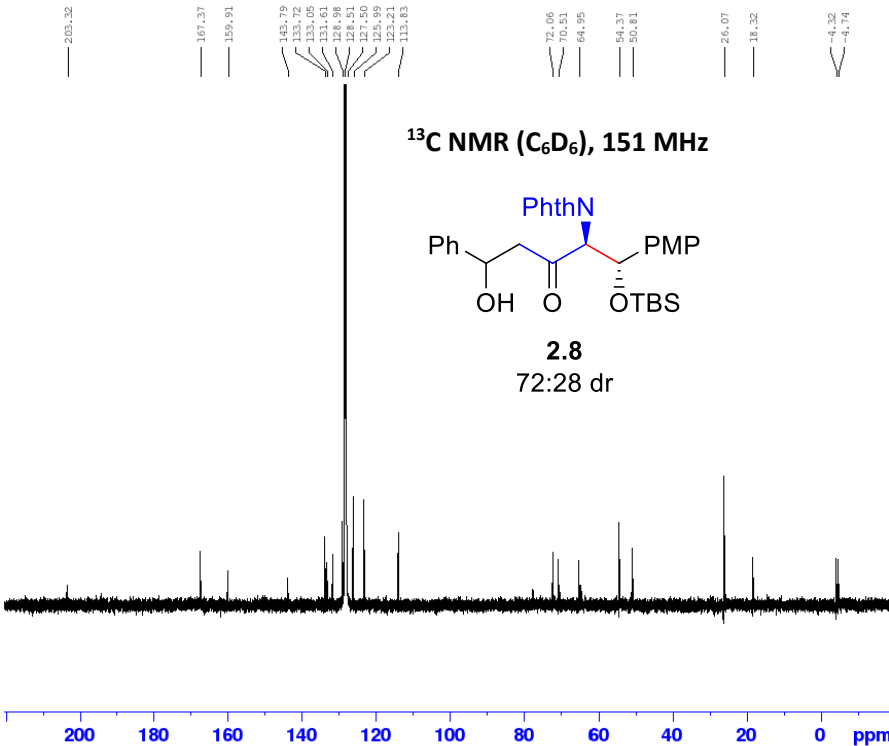
SLG3-054-3-d6benzene
 PROTON C6D6 {C:\Bruker\TopSpin3.5p17} Sieber 1



Current Data Parameters
 NAME SLG3-054_2
 EXPNO 1
 PROCNO 1

F2 - Acquisition Parameters
 Date_ 20220126
 Time 9.51 h
 INSTRUM spect
 PROBHD Z855801_0104 (
 PULPROG zg30
 TD 65536
 SOLVENT C6D6
 NS 16
 DS 2
 SWH 12019.230 Hz
 FIDRES 0.366798 Hz
 AQ 2.7262976 sec
 RG 172.91
 DW 41.600 usec
 DE 6.50 usec
 TE 296.3 K
 D1 4.00000000 sec
 TD0 1
 SFO1 599.9587047 MHz
 NUC1 1H
 P1 7.75 usec
 PLW1 11.99499989 W

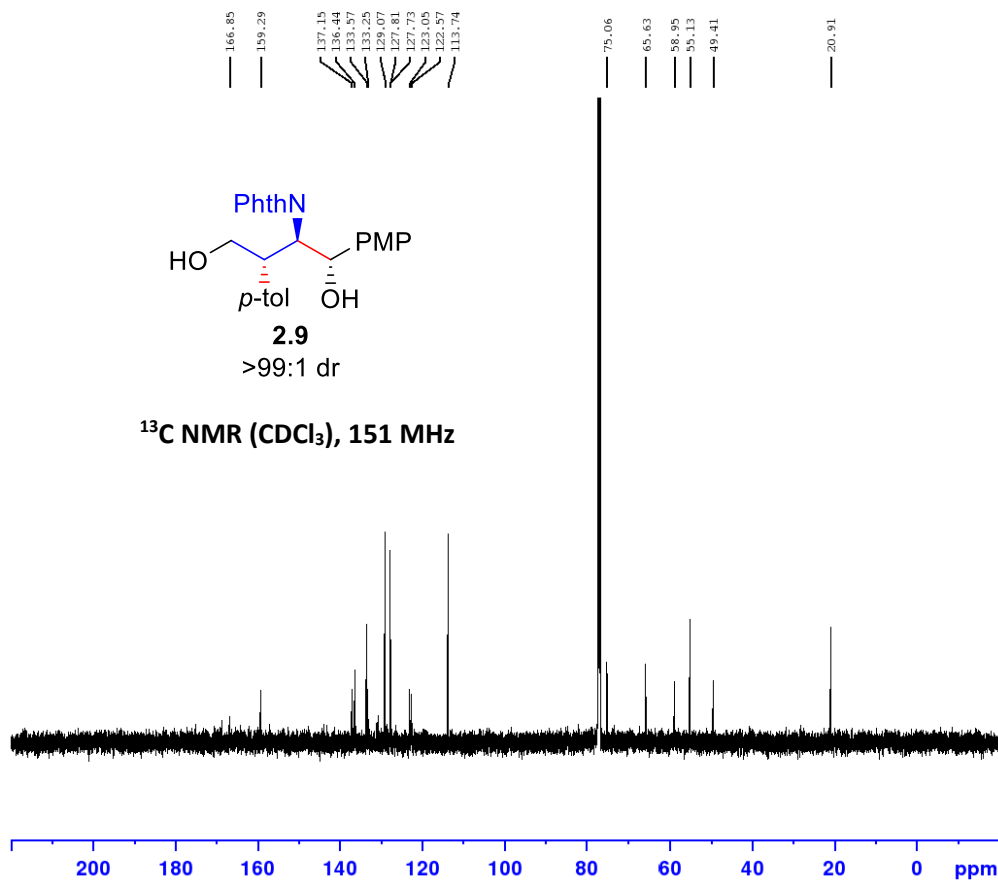
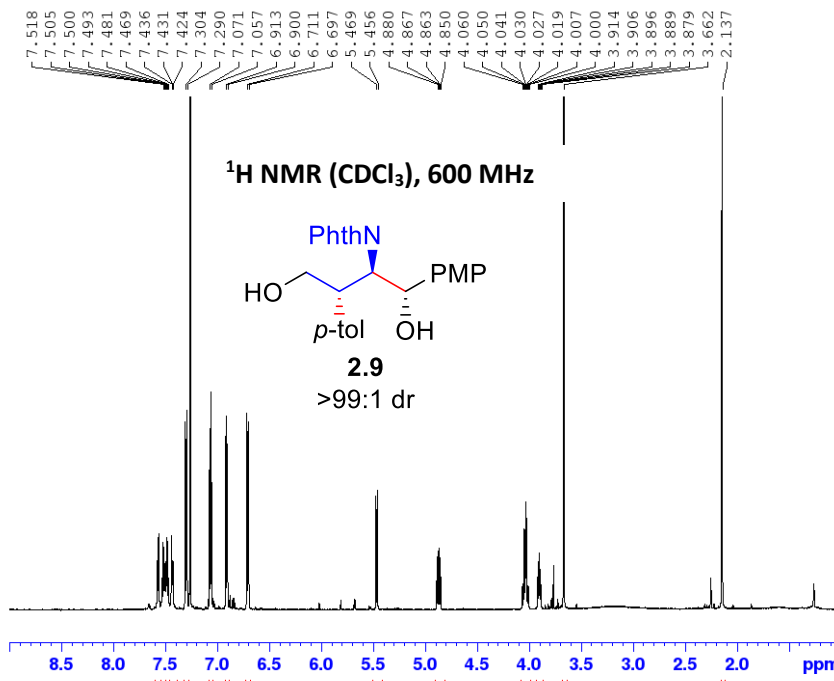
F2 - Processing parameters
 SI 65536
 SF 599.9549967 MHz
 NDM EM
 SSB 0
 LB 0.30 Hz
 GB 0
 PC 1.00



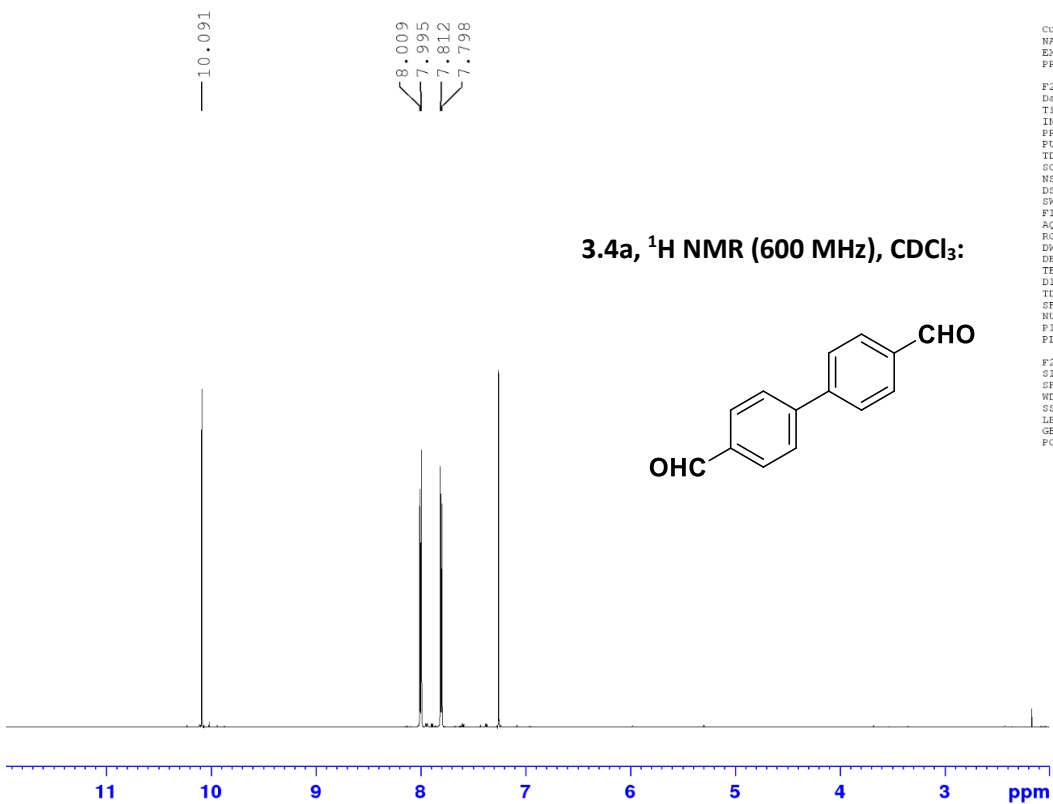
Current Data Parameters
 NAME SLG3-054_2
 EXPNO 5
 PROCNO 1

F2 - Acquisition Parameters
 Date_ 20221028
 Time 16.30 h
 INSTRUM spect
 PROBHD Z148658_0003 (
 PULPROG zgpg30
 TD 65536
 SOLVENT C6D6
 NS 1200
 DS 4
 SWH 36231.883 Hz
 FIDRES 1.105709 Hz
 AQ 0.9043968 sec
 RG 199.73
 DW 13.800 usec
 DE 6.50 usec
 TE 297.9 K
 D1 6.00000000 sec
 D11 0.03000000 sec
 TD0 1
 SFO1 150.8864644 MHz
 NUC1 13C
 P0 4.00 usec
 P1 12.00 usec
 PLW1 77.65699768 W
 SFO2 600.0074000 MHz
 NUC2 1H
 CPDPRG2 waltz65
 PCPD2 70.00 usec
 PLW2 13.23200035 W
 PLW12 0.64876997 W
 PLW13 0.32633001 W

F2 - Processing parameters
 SI 32768
 SF 150.8713251 MHz
 NDM EM
 SSB 0
 LB 1.00 Hz
 GB 0
 PC 1.40



Appendix A3. Select NMR data for Chapter 3

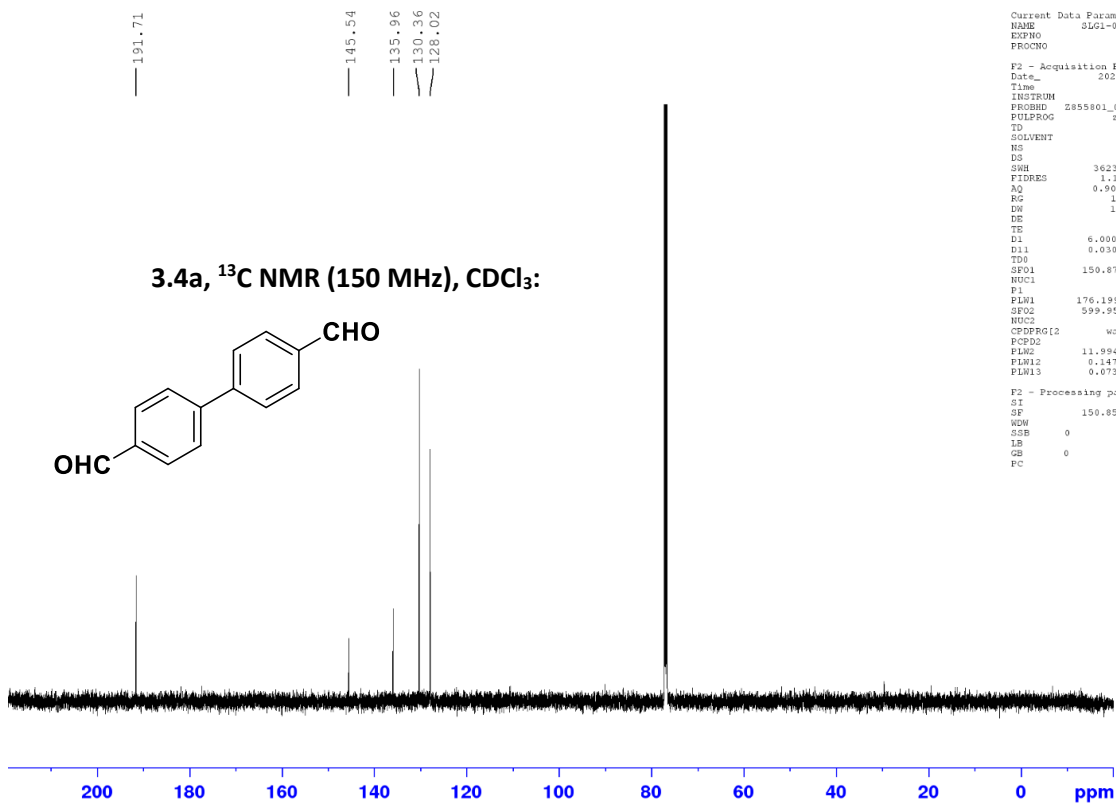


```

Current Data Parameters
NAME      SLG1-021-2-1H
EXPNO    1
PROCNO   1

F2 - Acquisition Parameters
Date_    20200309
Time     17.09 h
INSTRUM  spect
PROBHD   zgpg30
PULPROG  zg30
TD       65536
SOLVENT  CDCl3
NS       16
DS       2
SWH      12019.230 Hz
FIDRES   0.366798 Hz
AQ       2.7262976 sec
RG       194.75
DE       41.600 usec
TE       296.3 K
D1       6.00000000 sec
TDO      1
SF01     599.9587047 MHz
NUC1     1H
P1       7.75 usec
PLW1     11.99499989 W

F2 - Processing Parameters
SI       65536
SF       599.9550162 MHz
WDW      EM
SSB      0
LB       0.30 Hz
GB       0
PC       1.00
    
```

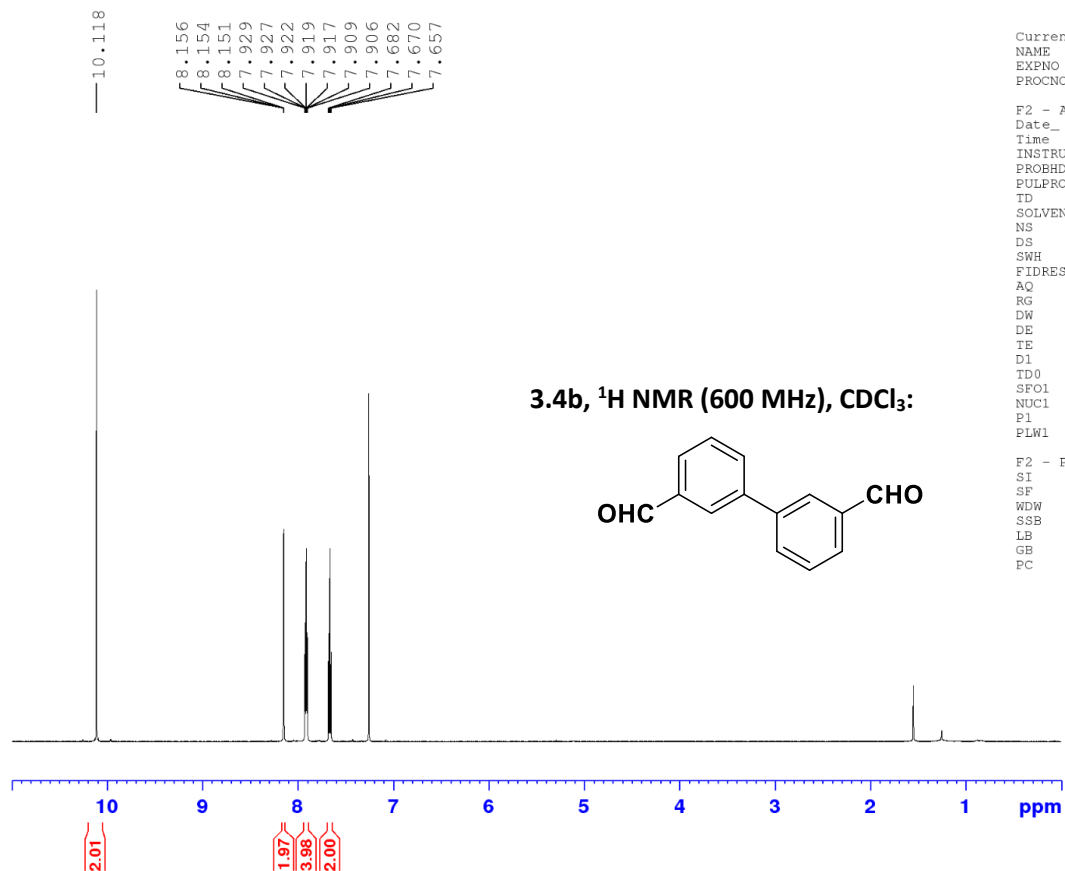


```

Current Data Parameters
NAME      SLG1-021-2C
EXPNO    1
PROCNO   1

F2 - Acquisition Parameters
Date_    20200310
Time     0.48 h
INSTRUM  spect
PROBHD   zgpg30
PULPROG  zgpg30
TD       65536
SOLVENT  CDCl3
NS       660
DS       4
SWH      36231.883 Hz
FIDRES   1.108709 Hz
AQ       0.9043968 sec
RG       194.75
DE       13.800 usec
TE       296.7 K
D1       6.00000000 sec
D11      0.03000000 sec
TDO      1
SF01     150.8738906 MHz
NUC1     13C
P1       11.40 usec
PLW1     176.19999695 W
SF02     599.9573998 MHz
NUC2     1H
CPDPRG2  waltz16
FCPD2    70.00 usec
PLM2     11.99499989 W
PLW12    0.14703000 W
PLW13    0.07395500 W

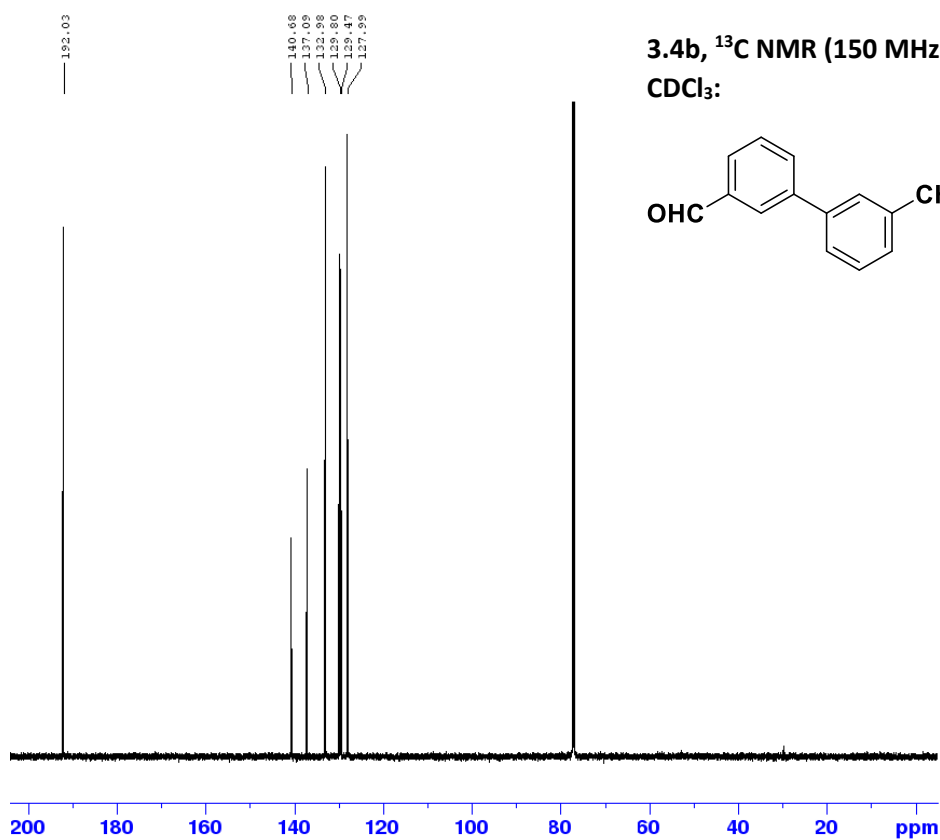
F2 - Processing Parameters
SI       32768
SF       150.8588101 MHz
WDW      EM
SSB      0
LB       1.00 Hz
GB       0
PC       1.40
    
```



Current Data Parameters
 NAME SLG2-019_02-hivac
 EXPNO 1
 PROCNO 1

F2 - Acquisition Parameters
 Date_ 20200617
 Time 21.18 h
 INSTRUM spect
 PROBHD Z148658_0003 (65536)
 PULPROG zg30
 TD 65536
 SOLVENT CDCl3
 NS 16
 DS 2
 SWH 12019.230 Hz
 FIDRES 0.366798 Hz
 AQ 2.7262976 sec
 RG 199.73
 DW 41.600 usec
 DE 6.50 usec
 TE 296.0 K
 D1 4.0000000 sec
 TD0 1
 SFO1 600.0087050 MHz
 NUC1 1H
 P1 15.50 usec
 PLW1 13.2320035 W

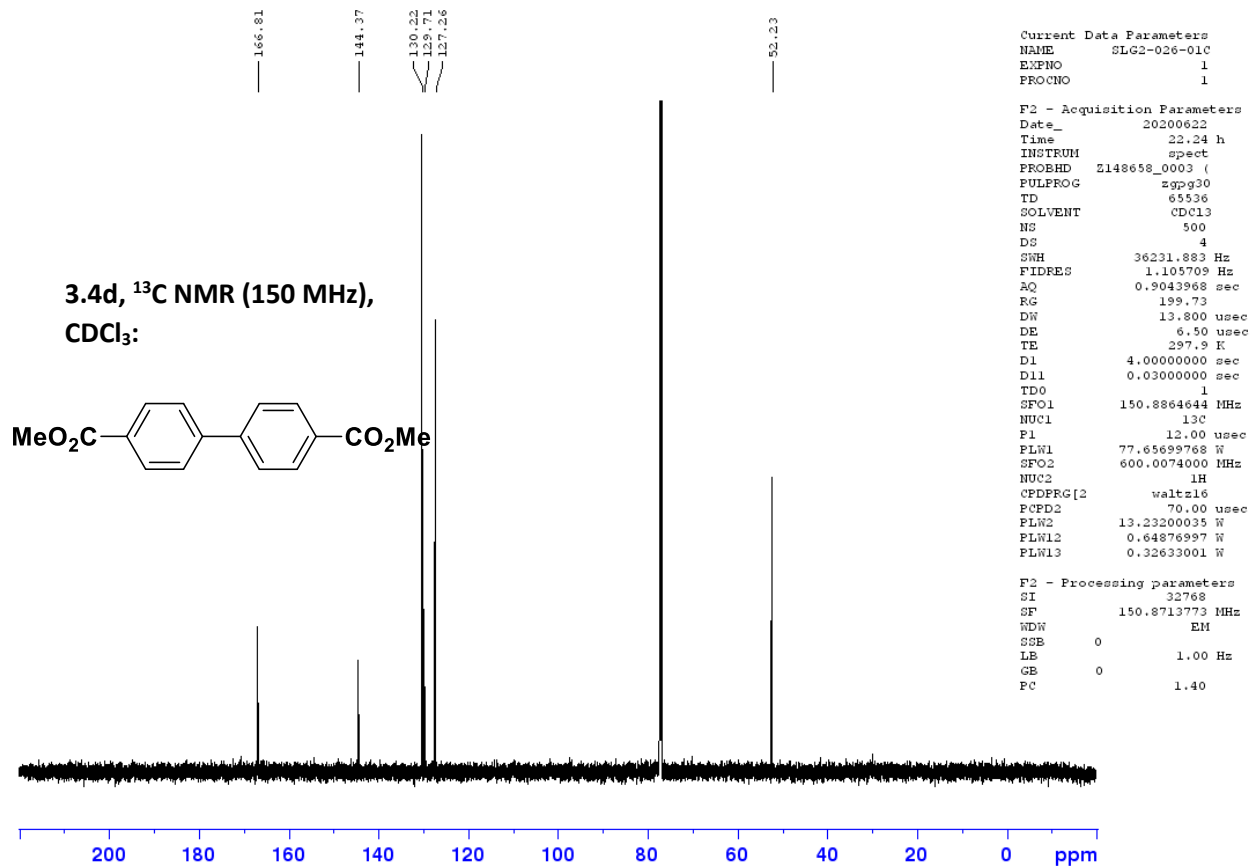
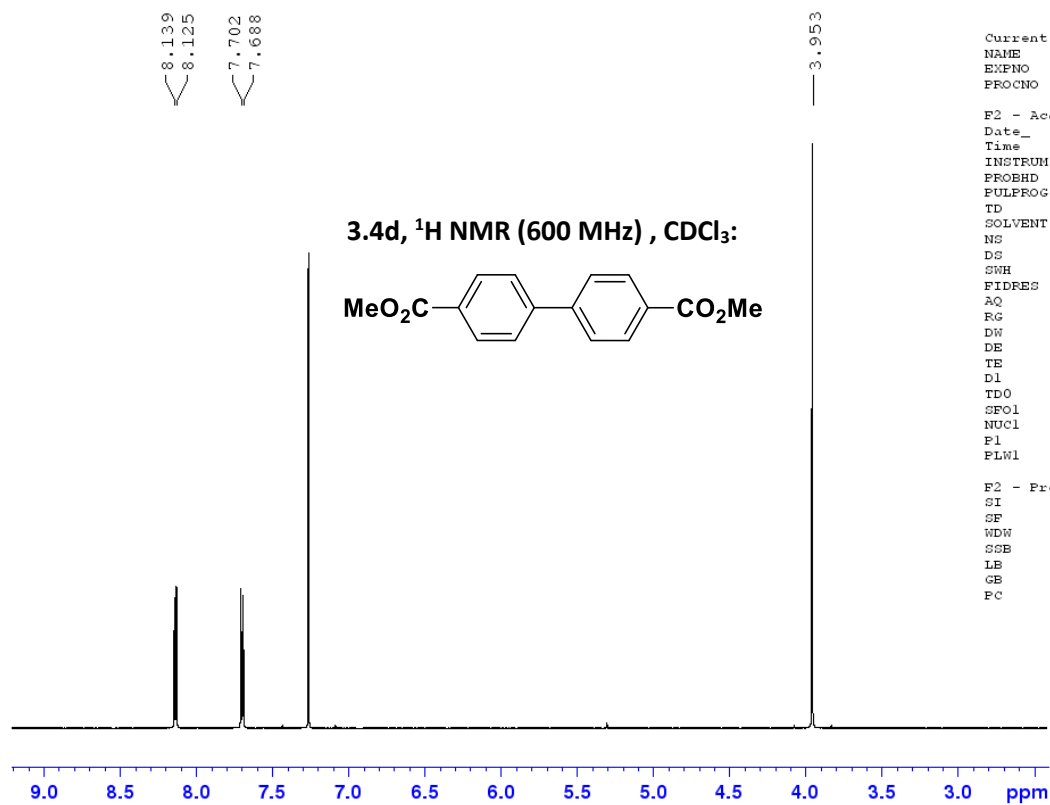
F2 - Processing parameters
 SI 65536
 SF 600.0050155 MHz
 WDW EM
 SSB 0
 LB 0.30 Hz
 GB 0
 PC 1.00

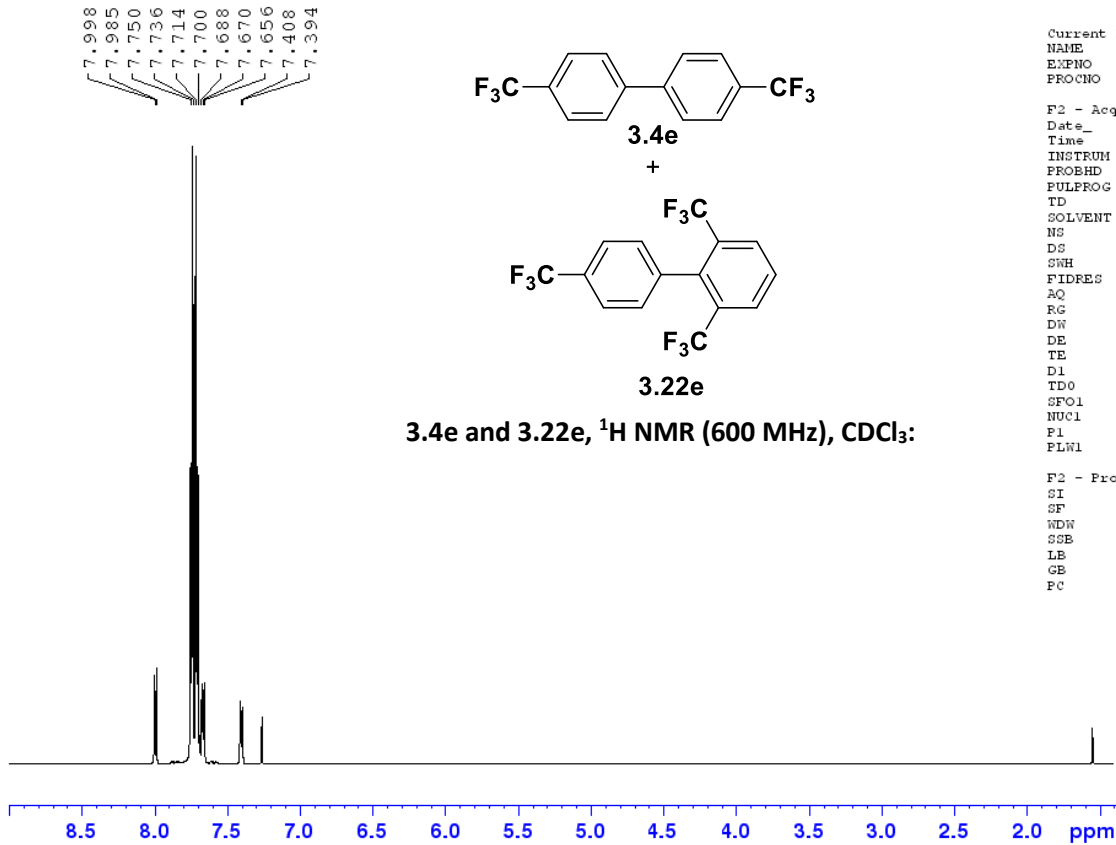


Current Data Parameters
 NAME SLG2-019_02-hivac_13C
 EXPNO 1
 PROCNO 1

F2 - Acquisition Parameters
 Date_ 20200617
 Time 22.01 h
 INSTRUM spect
 PROBHD Z148658_0003 (65536)
 PULPROG zgpg30
 TD 65536
 SOLVENT CDCl3
 NS 300
 DS 4
 SWH 36231.883 Hz
 FIDRES 1.105709 Hz
 AQ 0.9043968 sec
 RG 199.73
 DW 13.800 usec
 DE 6.50 usec
 TE 297.7 K
 D1 4.0000000 sec
 D11 0.0300000 sec
 TD0 1
 SFO1 150.8864644 MHz
 NUC1 13C
 P1 12.00 usec
 PLW1 77.65699768 W
 SFO2 600.0074000 MHz
 NUC2 1H
 CPDPRG2 waltz16
 PCPD2 70.00 usec
 PLW2 13.2320035 W
 PLW12 0.64876997 W
 PLW13 0.32633001 W

F2 - Processing parameters
 SI 32768
 SF 150.8713773 MHz
 WDW EM
 SSB 0
 LB 1.00 Hz
 GB 0
 PC 1.40



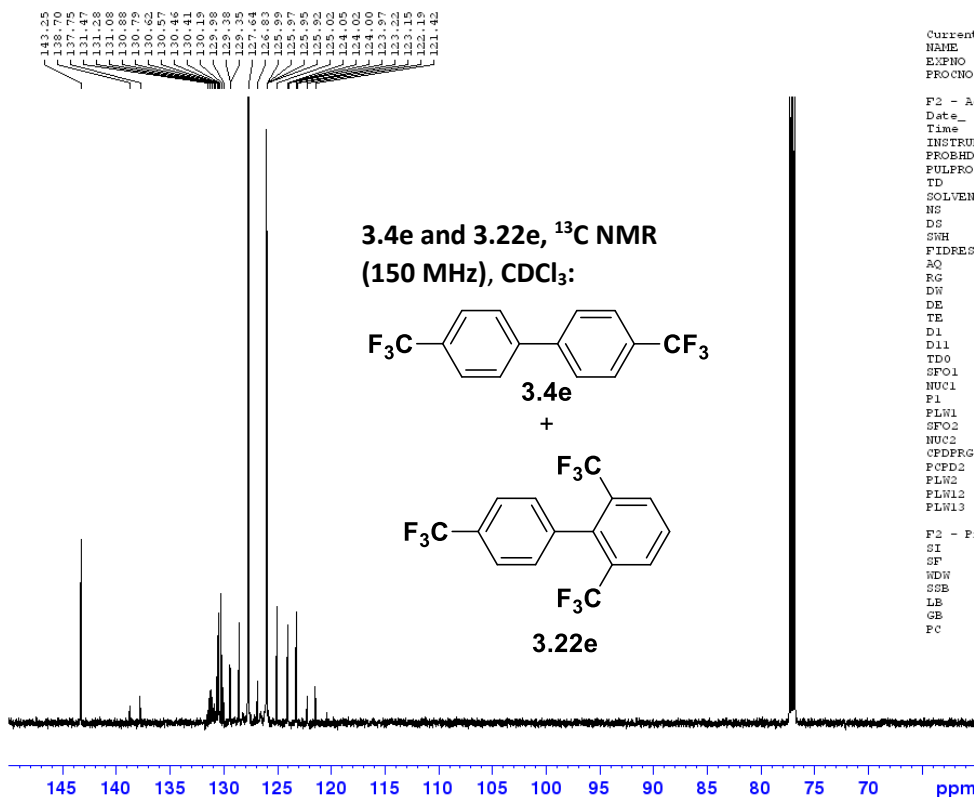


```

Current Data Parameters
NAME      SLG2-036a_1
EXPNO    1
PROCNO   1

F2 - Acquisition Parameters
Date_    20200707
Time     2.38 h
INSTRUM  spect
PROBHD   Z855801_0104 (
PULPROG  zg30
TD        65536
SOLVENT  CDCl3
NS        16
DS        2
SWH       12019.230 Hz
FIDRES    0.366798 Hz
AQ        2.7262976 sec
RG        78.28
DW        41.600 usec
DE        6.50 usec
TE        296.2 K
D1        4.00000000 sec
TDO       1
SFO1     599.9587047 MHz
NUC1      1H
P1        7.75 usec
PLW1     11.99499989 W

F2 - Processing parameters
SI        65536
SF        599.9551210 MHz
WDW       EM
SSB       0
LB        0.30 Hz
GB        0
PC        1.00
  
```



```

Current Data Parameters
NAME      SLG2-036a_1C
EXPNO    1
PROCNO   1

F2 - Acquisition Parameters
Date_    20200707
Time     3.30 h
INSTRUM  spect
PROBHD   Z855801_0104 (
PULPROG  zgpg30
TD        65536
SOLVENT  CDCl3
NS        600
DS        4
SWH       36231.883 Hz
FIDRES    1.105709 Hz
AQ        0.9043968 sec
RG        194.75
DW        13.800 usec
DE        6.50 usec
TE        296.6 K
D1        4.00000000 sec
D11      0.03000000 sec
TDO       1
SFO1     150.8738906 MHz
NUC1      13C
P1        11.40 usec
PLW1     176.19999695 W
SFO2     599.9573998 MHz
NUC2      1H
CPDPRG2  waltz16
PCPD2    70.00 usec
PLW2     11.99499989 W
PLW12    0.14703000 W
PLW13    0.07395500 W

F2 - Processing parameters
SI        32768
SF        150.8588050 MHz
WDW       EM
SSB       0
LB        1.00 Hz
GB        0
PC        1.40
  
```

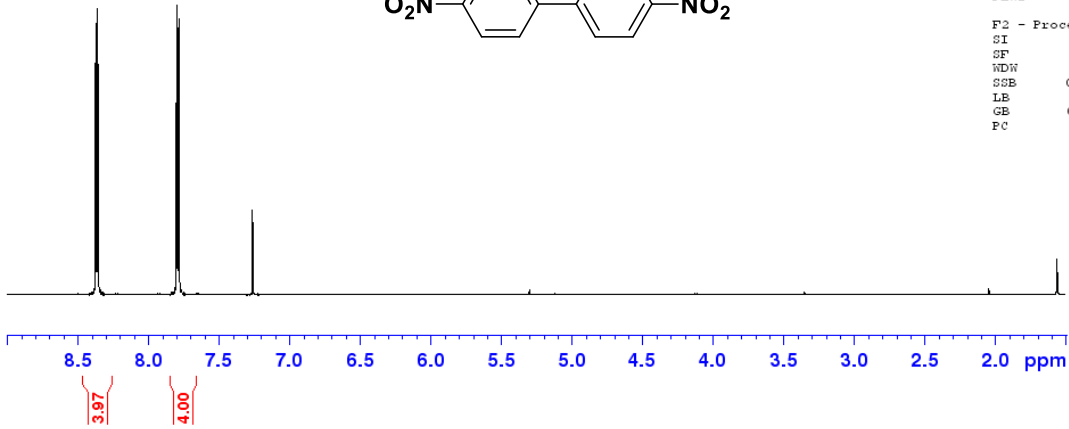
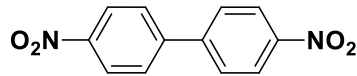

8.370
8.356
7.797
7.782

Current Data Parameters
 NAME SLG2-034a-2
 EXPNO 1
 PROCNO 1

F2 - Acquisition Parameters
 Date_ 20200702
 Time 0.22 h
 INSTRUM spect
 PROBHD Z855801_0104 (
 PULPROG zg30
 TD 65536
 SOLVENT CDCl3
 NS 16
 DS 2
 SWH 12019.230 Hz
 FIDRES 0.366798 Hz
 AQ 2.7262976 sec
 RG 194.75
 DN 41.600 usec
 DE 6.50 usec
 TE 295.9 K
 D1 4.00000000 sec
 TDO 1
 SFO1 599.9587047 MHz
 NUC1 1H
 FL1 7.75 usec
 PLW1 11.99499989 W

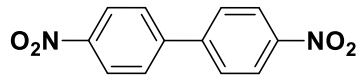
F2 - Processing parameters
 SI 65536
 SF 599.9550163 MHz
 WDN EM
 SSB 0
 LB 0.30 Hz
 GB 0
 PC 1.00

3.4f, ¹H NMR (600 MHz), CDCl₃:



148.07
145.00
128.36
124.41

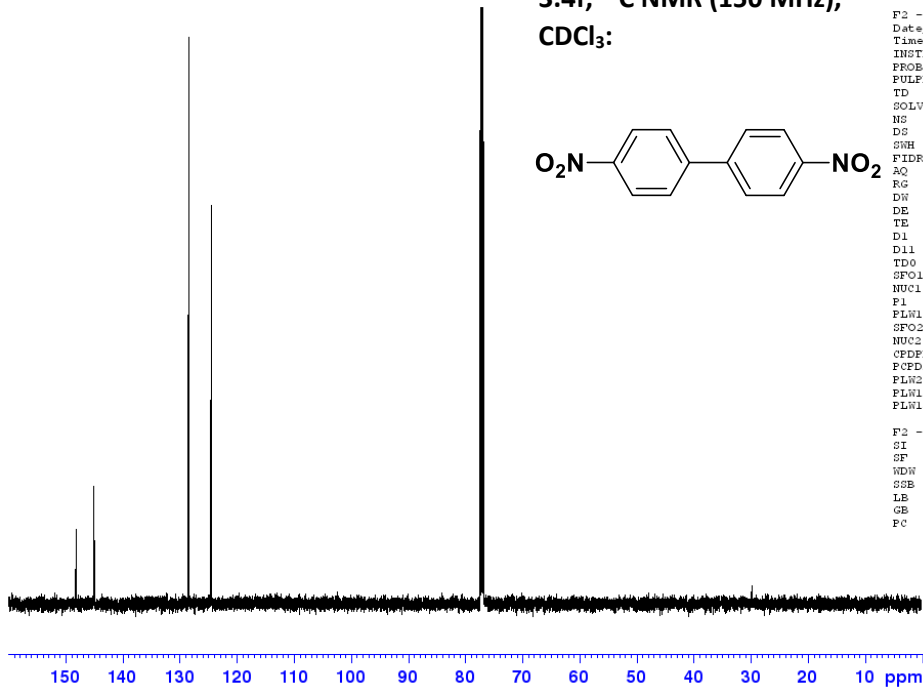
3.4f, ¹³C NMR (150 MHz),
CDCl₃:

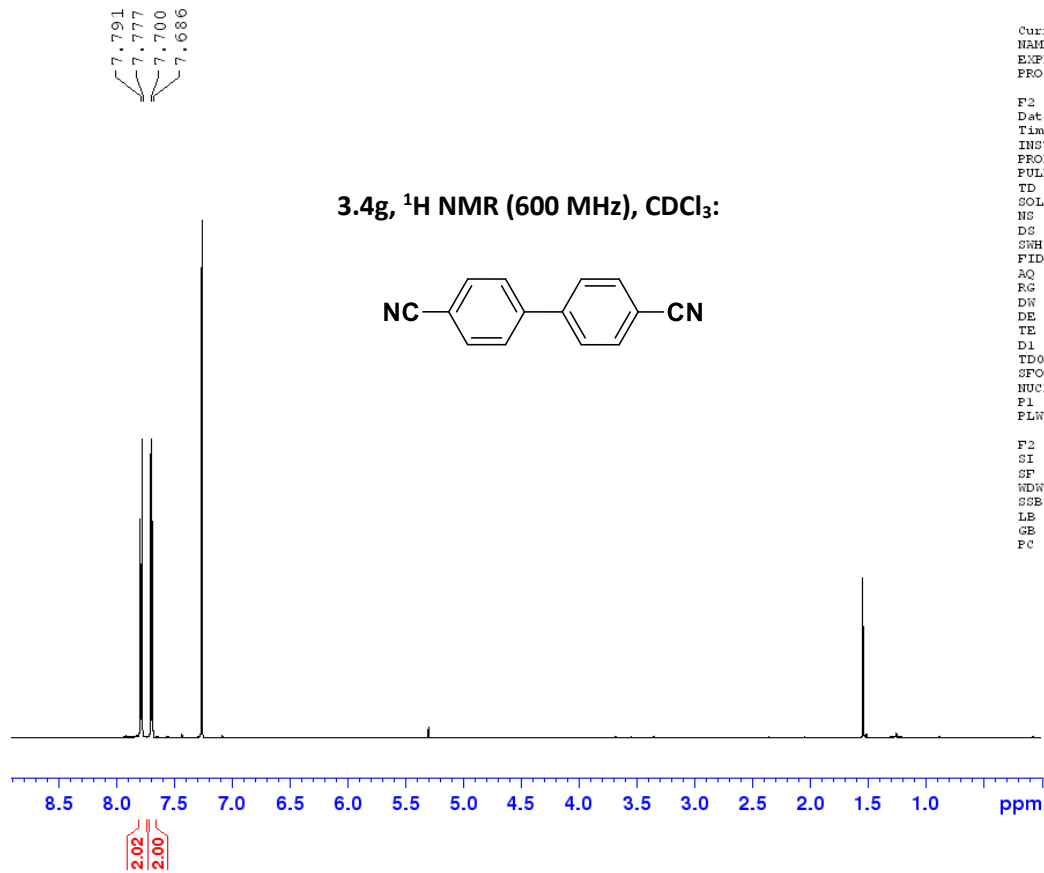


Current Data Parameters
 NAME SLG2-034a-2C
 EXPNO 1
 PROCNO 1

F2 - Acquisition Parameters
 Date_ 20200702
 Time 1.03 h
 INSTRUM spect
 PROBHD Z855801_0104 (
 PULPROG zgpg30
 TD 65536
 SOLVENT CDCl3
 NS 200
 DS 4
 SWH 36231.883 Hz
 FIDRES 1.105709 Hz
 AQ 0.9043968 sec
 RG 194.75
 DN 13.800 usec
 DE 6.50 usec
 TE 296.3 K
 D1 4.00000000 sec
 D11 0.03000000 sec
 TDO 1
 SFO1 150.8738906 MHz
 NUC1 13C
 FL1 11.40 usec
 SFO2 599.9573998 MHz
 NUC2 1H
 CPDPRG2 waltz16
 PCPD2 70.00 usec
 PLW2 11.99499989 W
 PLW12 0.14703000 W
 PLW13 0.07395500 W

F2 - Processing parameters
 SI 32768
 SF 150.8588050 MHz
 WDN EM
 SSB 0
 LB 1.00 Hz
 GB 0
 PC 1.40

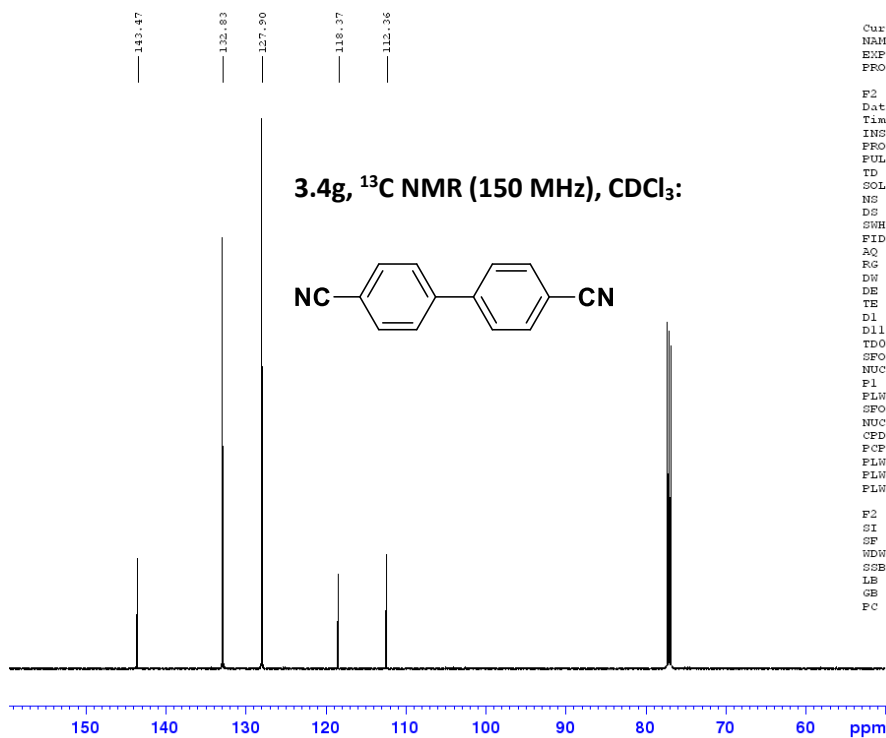




Current Data Parameters
NAME BAD1-005-3hivac
EXPNO 1
PROCNO 1

F2 - Acquisition Parameters
Date_ 20200619
Time 0.47 h
INSTRUM spect
PROBHD Z148658_0003 ()
PULPROG zg30
TD 65536
SOLVENT CDCl3
NS 16
DS 2
SWH 12019.230 Hz
FIDRES 0.366798 Hz
AQ 2.7262976 sec
RG 199.73
DN 41.600 usec
DE 6.50 usec
TE 296.2 K
D1 4.00000000 sec
TDO 1
SFO1 600.0087050 MHz
NUC1 1H
P1 15.50 usec
PLW1 13.23200035 W

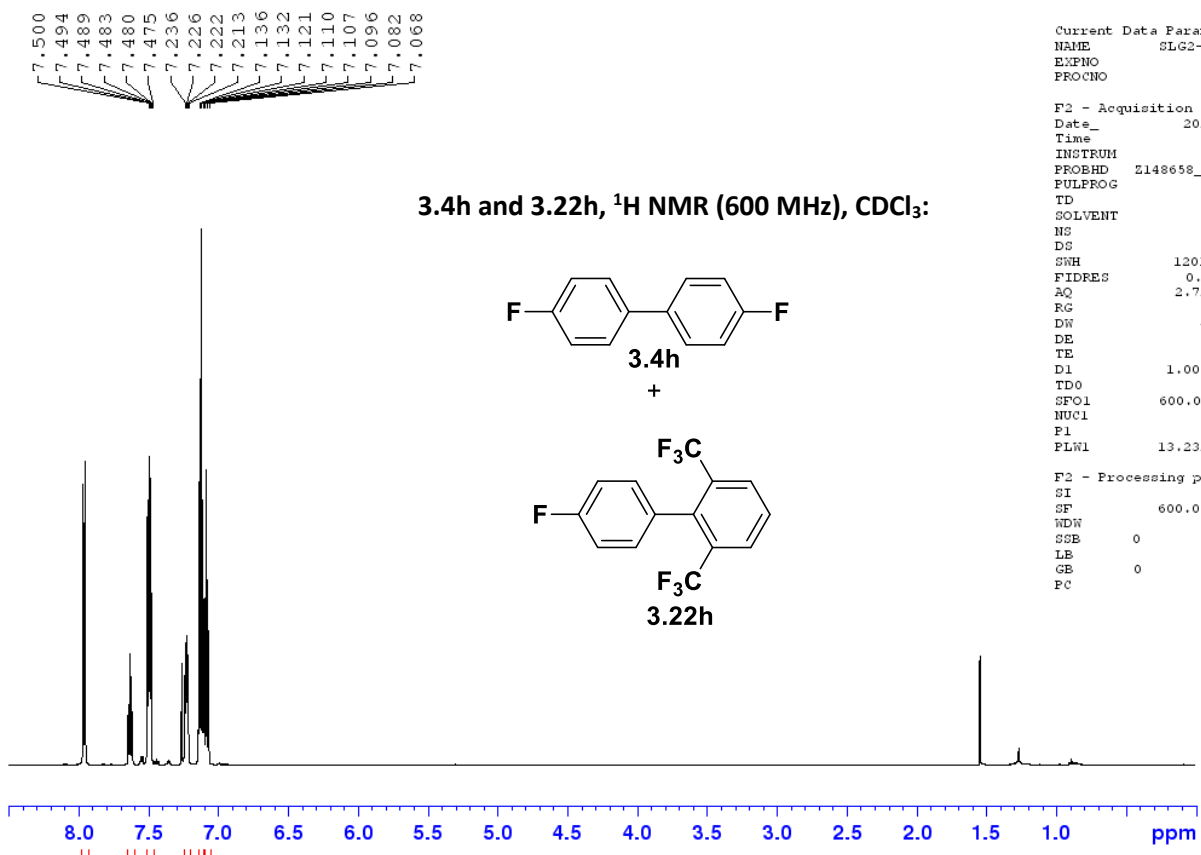
F2 - Processing parameters
SI 65536
SF 600.0050159 MHz
WDW EM
SSB 0
LB 0.30 Hz
GB 0
FC 1.00



Current Data Parameters
NAME BAD1-005-3hivac-13C
EXPNO 1
PROCNO 1

F2 - Acquisition Parameters
Date_ 20200619
Time 1.51 h
INSTRUM spect
PROBHD Z148658_0003 ()
PULPROG zgpg30
TD 65536
SOLVENT CDCl3
NS 500
DS 4
SWH 36231.883 Hz
FIDRES 1.105709 Hz
AQ 0.9043968 sec
RG 199.73
DN 13.800 usec
DE 6.50 usec
TE 298.0 K
D1 4.00000000 sec
D11 0.03000000 sec
TDO 1
SFO1 150.8864644 MHz
NUC1 13C
P1 12.00 usec
PLW1 77.65699768 W
SFO2 600.0074000 MHz
NUC2 1H
CPDPRG2 waltz16
PCPD2 70.00 usec
PLM2 13.23200035 W
PLM12 0.64876997 W
PLM13 0.32633001 W

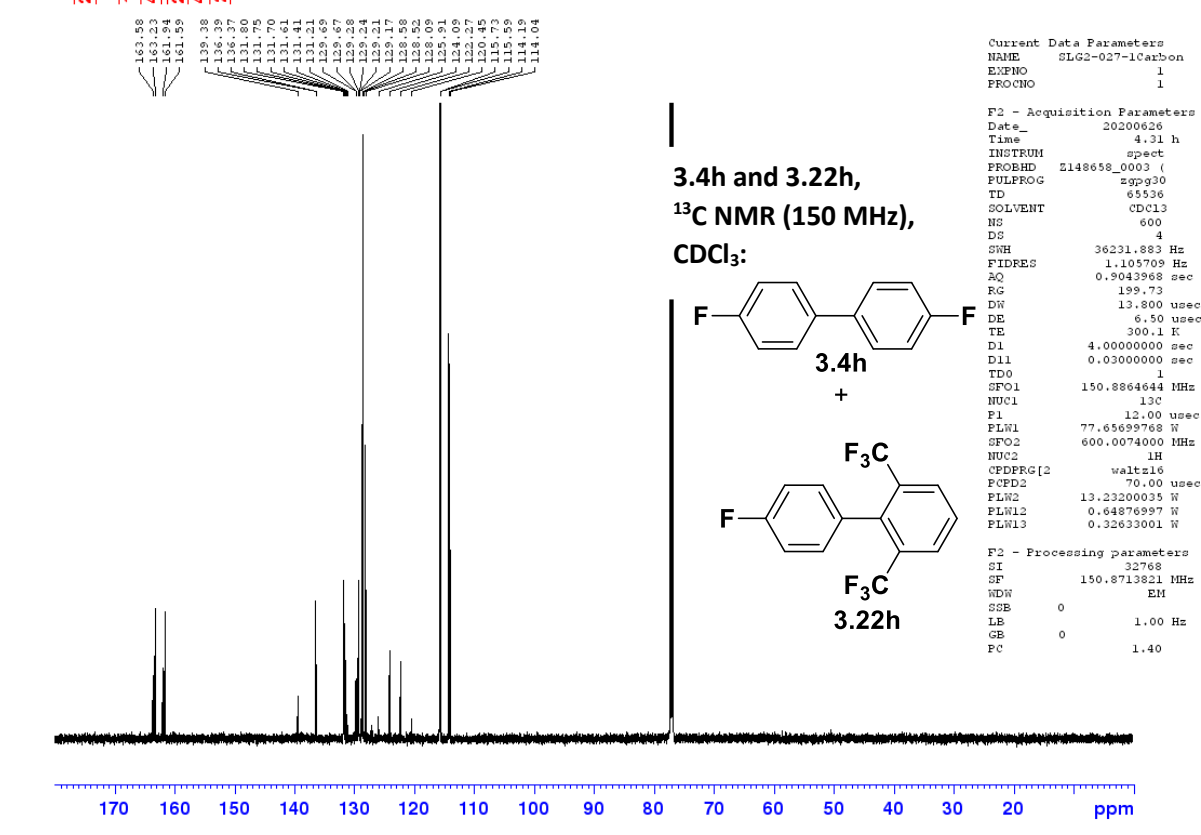
F2 - Processing parameters
SI 32768
SF 150.8713879 MHz
WDW EM
SSB 0
LB 1.00 Hz
GB 0
FC 1.40



Current Data Parameters
 NAME SLG2-027-1C
 EXPNO 1
 PROCNO 1

F2 - Acquisition Parameters
 Date_ 20200626
 Time 1.47 h
 INSTRUM spect
 PROBHD E148658_0003 (
 PULPROG zg30
 TD 65536
 SOLVENT CDCl3
 NS 16
 DS 2
 SWH 12019.230 Hz
 FIDRES 0.366798 Hz
 AQ 2.7262976 sec
 RG 176.24
 DW 41.600 usec
 DE 6.50 usec
 TE 298.6 K
 D1 1.00000000 sec
 TD0 1
 SFO1 600.0087050 MHz
 NUC1 1H
 P1 15.50 usec
 PLW1 13.23200035 W

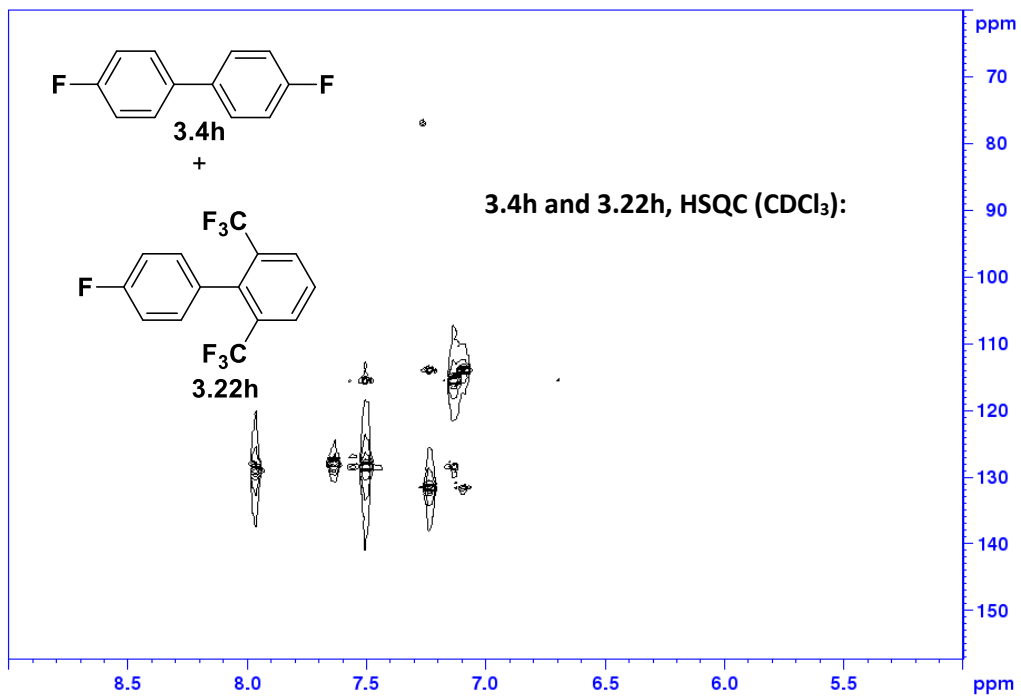
F2 - Processing parameters
 SI 65536
 SF 600.0050169 MHz
 WDW EM
 SSB 0
 LE 0.30 Hz
 GE 0
 PC 1.00



Current Data Parameters
 NAME SLG2-027-1Carbon
 EXPNO 1
 PROCNO 1

F2 - Acquisition Parameters
 Date_ 20200626
 Time 4.31 h
 INSTRUM spect
 PROBHD E148658_0003 (
 PULPROG zgpg30
 TD 65536
 SOLVENT CDCl3
 NS 600
 DS 4
 SWH 36231.883 Hz
 FIDRES 1.105709 Hz
 AQ 0.9043968 sec
 RG 199.73
 DW 13.800 usec
 DE 6.50 usec
 TE 300.1 K
 D1 4.00000000 sec
 D11 0.03000000 sec
 TD0 1
 SFO1 150.8864644 MHz
 NUC1 13C
 P1 12.00 usec
 PLW1 77.65699768 W
 SFO2 600.0074000 MHz
 NUC2 1H
 CPDPRG2 waltz16
 PCPD2 70.00 usec
 PLW2 13.23200035 W
 PLW12 0.64876997 W
 PLW13 0.32633001 W

F2 - Processing parameters
 SI 32768
 SF 150.8713821 MHz
 WDW EM
 SSB 0
 LE 1.00 Hz
 GE 0
 PC 1.40



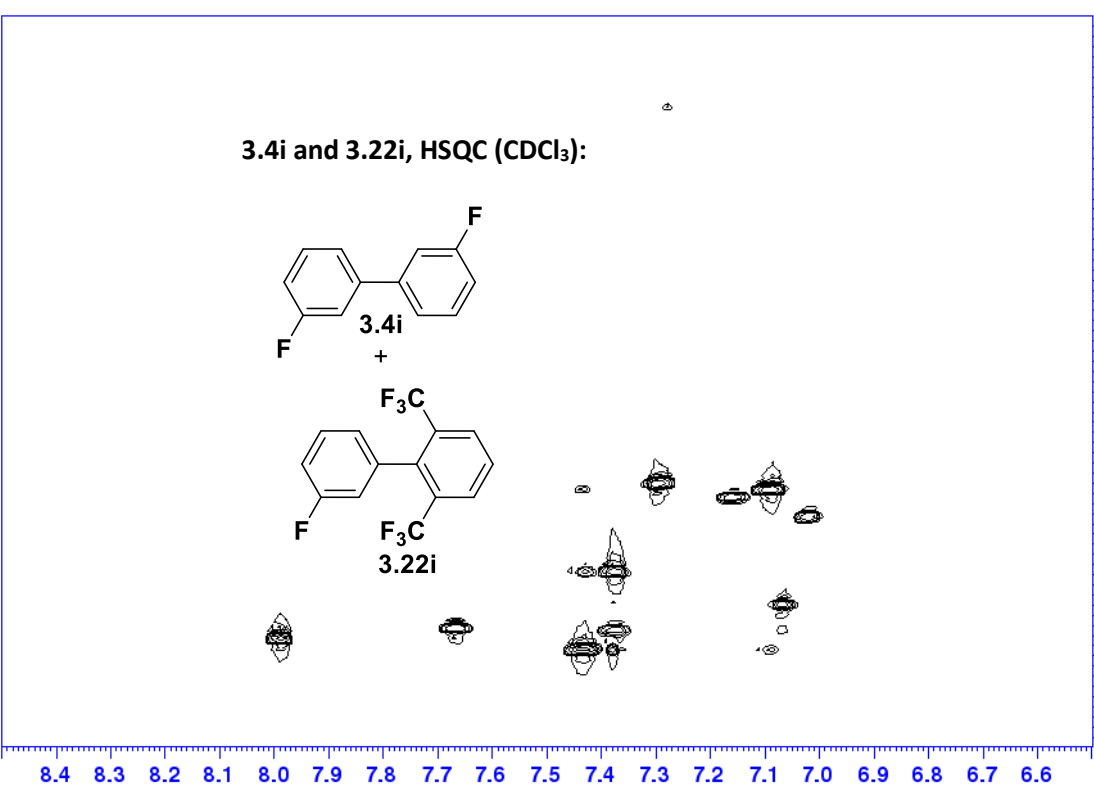
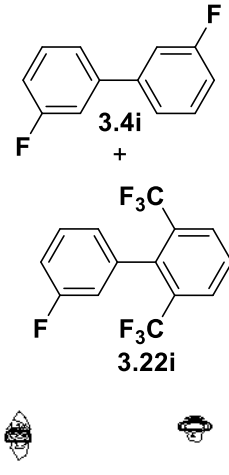
3.4h and 3.22h, HSQC (CDCl₃):

```

Current Data Parameters
NAME      0502-02-10
EXPNO    1
PROCNO   1
F2 - Acquisition Parameters
Date_    20200424
Time     1:51 h
INSTRUM  spect
PROBHD   5mmQNP1H3
PULPROG  zgpg30
TD        65536
SOLVENT  CDCl3
NS        4
DS        2
SFO      752.1300 MHz
FIDRES   0.1310700 J/Hz
AQ       199.73
RG        48.000
DE        6.50 uHz
TE        299.2 K
CHFT2    145.0000000
CHFT1    -0.0000000
DQ        0.0000000 J/Hz
DE2       4.0000000 J/Hz
D4         0.00172414 J/Hz
D11        0.03000000 J/Hz
D12        0.00020000 J/Hz
D24        0.00244100 J/Hz
D28        0.00041200 J/Hz
HMQ       0.00000040 J/Hz
TEMR      4
SFO2     400.0071200 MHz
NUC1      1H
P1         15.50 uHz
P2         31.00 uHz
P3         1000.00 uHz
P4         13.2200000 U
SFO3     150.8228224 MHz
NUC2      13C
CPDPRG2   gmgp
P14        12.00 uHz
P15        500.00 uHz
P16        2000.00 uHz
P17        1750.00 uHz
P18        40.00 uHz
P19        0 U
P20        77.0000000 U
P21        3.10450042 U
SFO4     0 J/Hz
SFO5     17.05400044 U
SFO6     0.000
SFO7     17.05400044 U
SFO8     0 J/Hz
SFO9     150.8228224 U
SFO10     0.000
SFO11     4.00000000 U
SFO12     50.00 uHz
SFO13     100.00 uHz
SFO14     20.00 uHz
SFO15     11.00 uHz
SFO16     100.00 uHz
SFO17     5.00 uHz
P10       1000.00 uHz
P11       600.00 uHz
F2 - Processing parameters
TD        65536
SFO1     752.1300 MHz
FIDRES   0.1310700 MHz
AQ       199.73
RG        48.000
DE        6.50 uHz
TE        299.2 K
SFO2     400.0071200 MHz
NUC1      1H
P1         15.50 uHz
P2         31.00 uHz
P3         1000.00 uHz
P4         13.2200000 U
SFO3     150.8228224 MHz
NUC2      13C
CPDPRG2   gmgp
P14        12.00 uHz
P15        500.00 uHz
P16        2000.00 uHz
P17        1750.00 uHz
P18        40.00 uHz
P19        0 U
P20        77.0000000 U
P21        3.10450042 U
SFO4     0 J/Hz
SFO5     17.05400044 U
SFO6     0.000
SFO7     17.05400044 U
SFO8     0 J/Hz
SFO9     150.8228224 U
SFO10     0.000
SFO11     4.00000000 U
SFO12     50.00 uHz
SFO13     100.00 uHz
SFO14     20.00 uHz
SFO15     11.00 uHz
SFO16     100.00 uHz
SFO17     5.00 uHz
P10       1000.00 uHz
P11       600.00 uHz

```


3.4i and 3.22i, HSQC (CDCl₃):



ppm

70

80

90

100

110

120

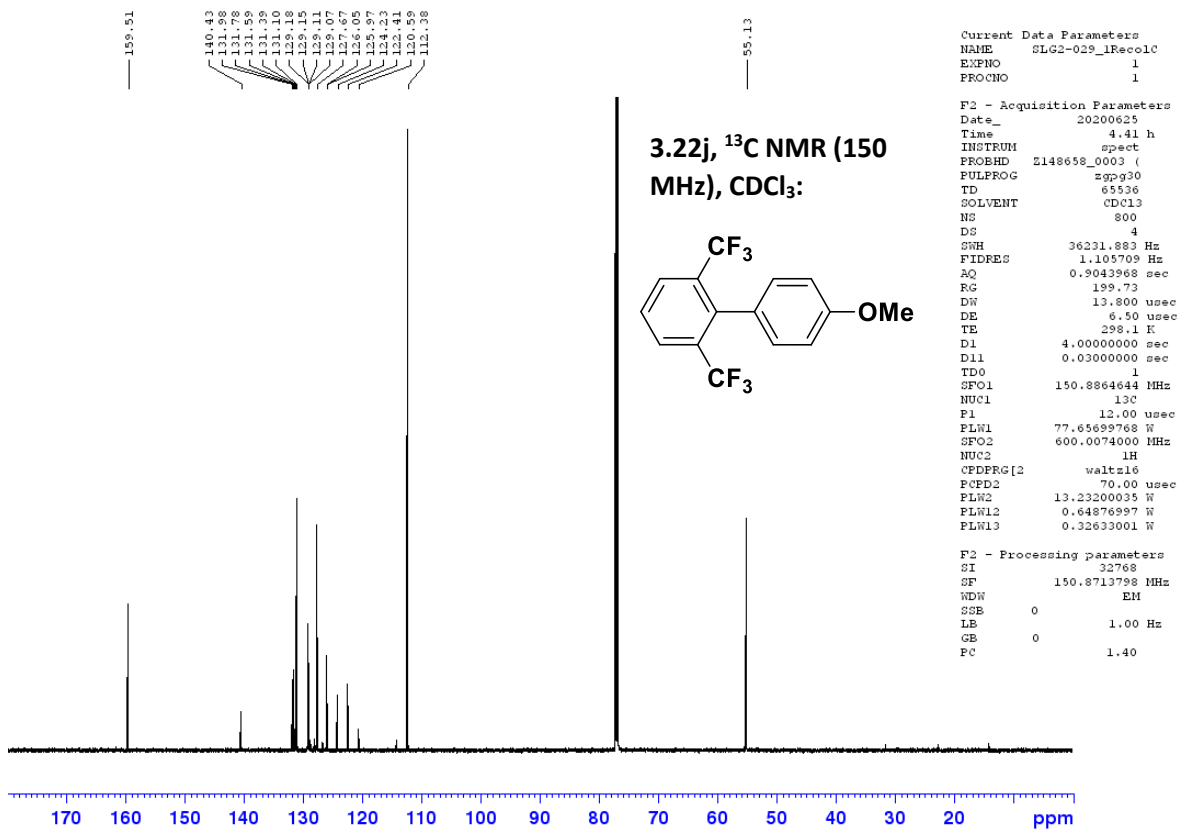
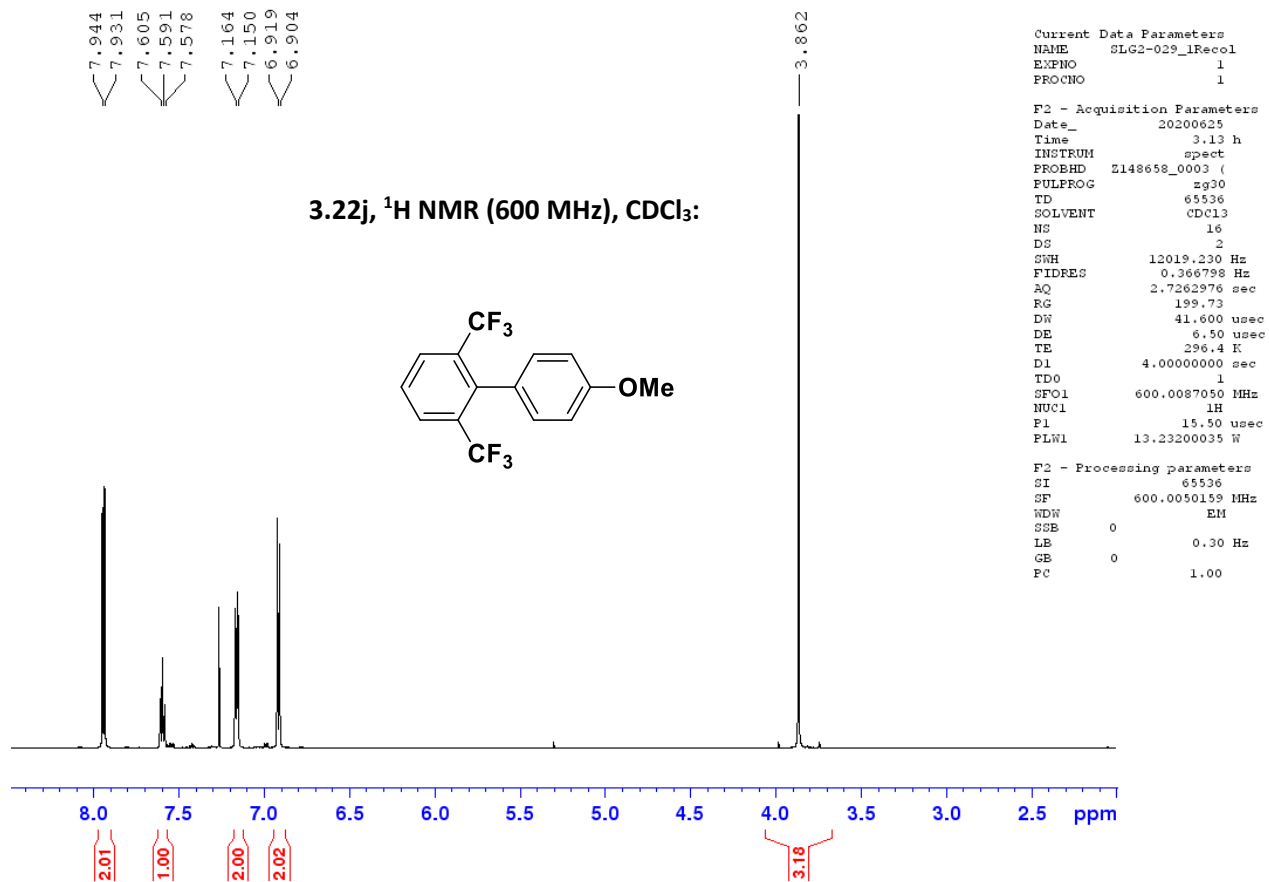
130

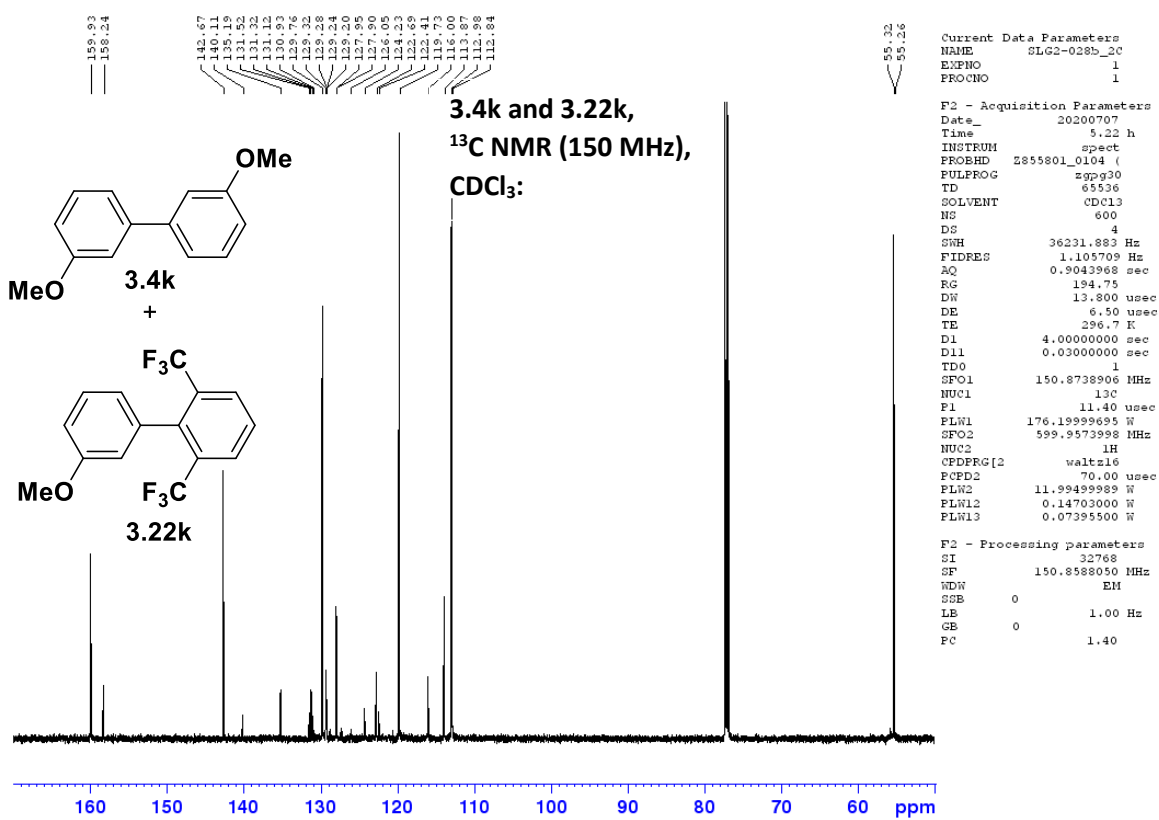
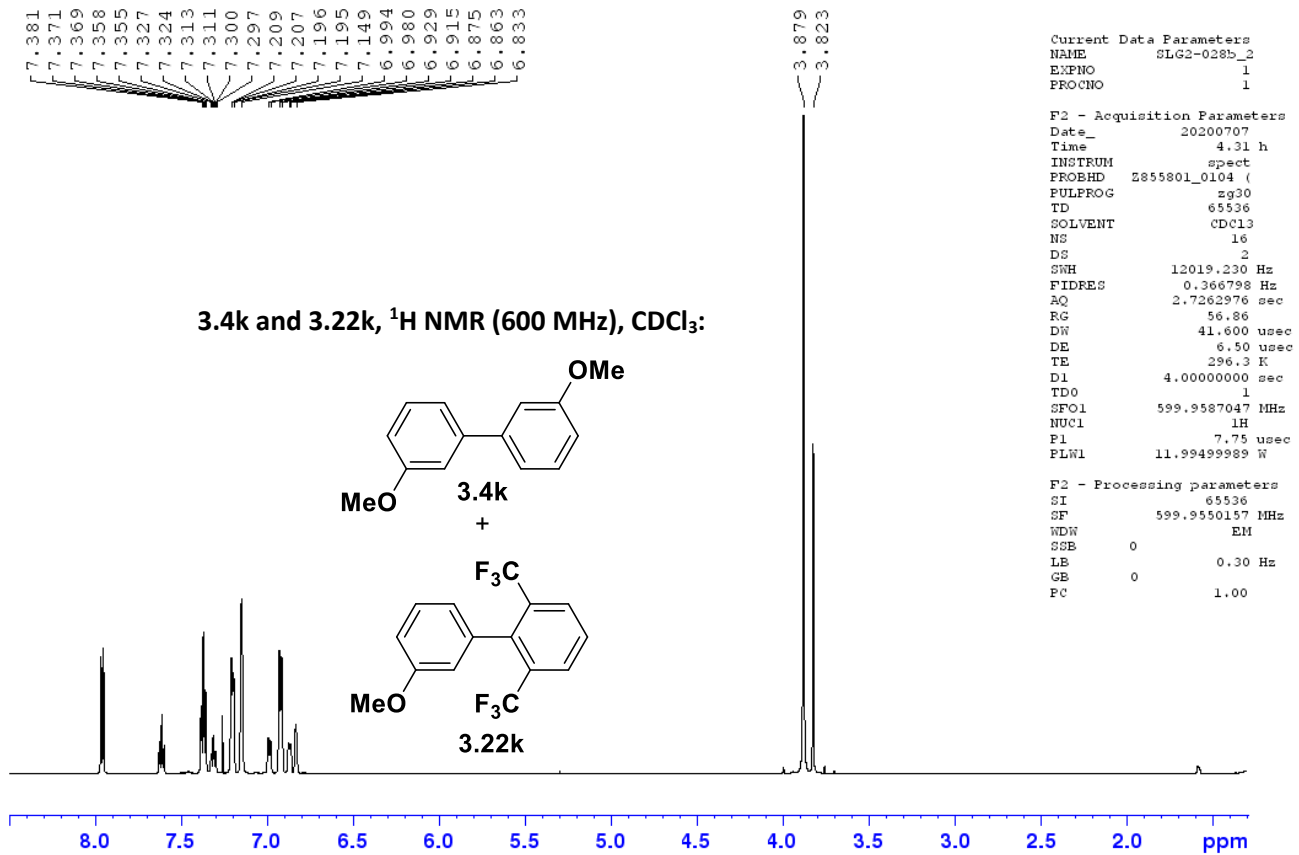
ppm

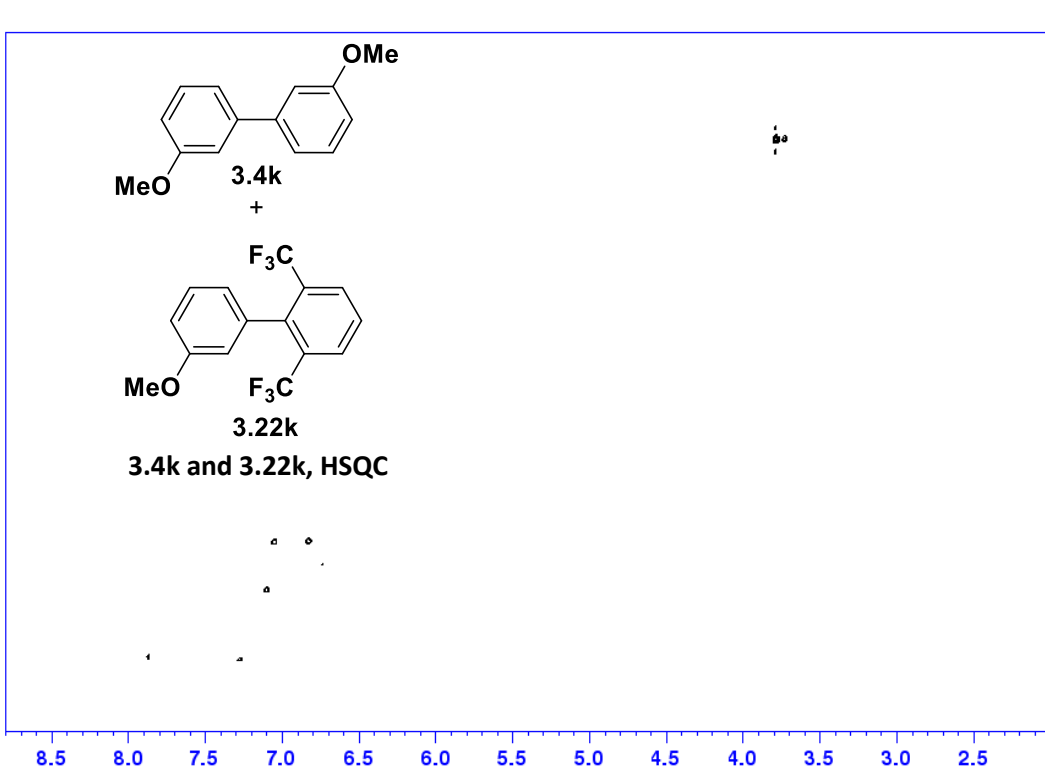
```

Current Data Parameters
NAME      0102-021-10
EXPNO     2
PROCNO    1

F2 - Acquisition Parameters
Date_     20200226
Time      3:07 h
INSTRUM   spect
PROBHD    zgpg300
PULPROG   zgpg300
TD         65536
SOLVENT    CDCl3
DS         4
DE         21
DPR       5312.500 Hz
FIDRES    7.422355 Hz
AQ        0.1310720 sec
RG         199.72
DE         64.0000 usec
DE         6.50 usec
TE        299.2 K
CHFT3     145.0000000
CHFT1*    -0.1000000
DO        0.0000000 usec
D1        1.500000000 usec
D4        0.00172414 usec
D11       0.02000000 usec
D16       0.00020000 usec
D21       0.00248500 usec
D24       0.00051200 usec
DHO       0.00002010 usec
TEMR      1
DPO1      600.0073200 MHz
NUC1       13
P1         15.50 usec
P2         51.00 usec
P25        1000.00 usec
P31        13.23200035 H
P32        150.35200035 H
P33        130
P34        130
P35        130
P36        130
P37        130
P38        130
P39        130
P40        130
P41        130
P42        130
P43        130
P44        130
P45        130
P46        130
P47        130
P48        130
P49        130
P50        130
P51        130
P52        130
P53        130
P54        130
P55        130
P56        130
P57        130
P58        130
P59        130
P60        130
P61        130
P62        130
P63        130
P64        130
P65        130
P66        130
P67        130
P68        130
P69        130
P70        130
P71        130
P72        130
P73        130
P74        130
P75        130
P76        130
P77        130
P78        130
P79        130
P80        130
P81        130
P82        130
P83        130
P84        130
P85        130
P86        130
P87        130
P88        130
P89        130
P90        130
P91        130
P92        130
P93        130
P94        130
P95        130
P96        130
P97        130
P98        130
P99        130
P100       130
P101       130
P102       130
P103       130
P104       130
P105       130
P106       130
P107       130
P108       130
P109       130
P110       130
P111       130
P112       130
P113       130
P114       130
P115       130
P116       130
P117       130
P118       130
P119       130
P120       130
P121       130
P122       130
P123       130
P124       130
P125       130
P126       130
P127       130
P128       130
P129       130
P130       130
P131       130
P132       130
P133       130
P134       130
P135       130
P136       130
P137       130
P138       130
P139       130
P140       130
P141       130
P142       130
P143       130
P144       130
P145       130
P146       130
P147       130
P148       130
P149       130
P150       130
P151       130
P152       130
P153       130
P154       130
P155       130
P156       130
P157       130
P158       130
P159       130
P160       130
P161       130
P162       130
P163       130
P164       130
P165       130
P166       130
P167       130
P168       130
P169       130
P170       130
P171       130
P172       130
P173       130
P174       130
P175       130
P176       130
P177       130
P178       130
P179       130
P180       130
P181       130
P182       130
P183       130
P184       130
P185       130
P186       130
P187       130
P188       130
P189       130
P190       130
P191       130
P192       130
P193       130
P194       130
P195       130
P196       130
P197       130
P198       130
P199       130
P200       130
P201       130
P202       130
P203       130
P204       130
P205       130
P206       130
P207       130
P208       130
P209       130
P210       130
P211       130
P212       130
P213       130
P214       130
P215       130
P216       130
P217       130
P218       130
P219       130
P220       130
P221       130
P222       130
P223       130
P224       130
P225       130
P226       130
P227       130
P228       130
P229       130
P230       130
P231       130
P232       130
P233       130
P234       130
P235       130
P236       130
P237       130
P238       130
P239       130
P240       130
P241       130
P242       130
P243       130
P244       130
P245       130
P246       130
P247       130
P248       130
P249       130
P250       130
P251       130
P252       130
P253       130
P254       130
P255       130
P256       130
P257       130
P258       130
P259       130
P260       130
P261       130
P262       130
P263       130
P264       130
P265       130
P266       130
P267       130
P268       130
P269       130
P270       130
P271       130
P272       130
P273       130
P274       130
P275       130
P276       130
P277       130
P278       130
P279       130
P280       130
P281       130
P282       130
P283       130
P284       130
P285       130
P286       130
P287       130
P288       130
P289       130
P290       130
P291       130
P292       130
P293       130
P294       130
P295       130
P296       130
P297       130
P298       130
P299       130
P300       130
P301       130
P302       130
P303       130
P304       130
P305       130
P306       130
P307       130
P308       130
P309       130
P310       130
P311       130
P312       130
P313       130
P314       130
P315       130
P316       130
P317       130
P318       130
P319       130
P320       130
P321       130
P322       130
P323       130
P324       130
P325       130
P326       130
P327       130
P328       130
P329       130
P330       130
P331       130
P332       130
P333       130
P334       130
P335       130
P336       130
P337       130
P338       130
P339       130
P340       130
P341       130
P342       130
P343       130
P344       130
P345       130
P346       130
P347       130
P348       130
P349       130
P350       130
P351       130
P352       130
P353       130
P354       130
P355       130
P356       130
P357       130
P358       130
P359       130
P360       130
P361       130
P362       130
P363       130
P364       130
P365       130
P366       130
P367       130
P368       130
P369       130
P370       130
P371       130
P372       130
P373       130
P374       130
P375       130
P376       130
P377       130
P378       130
P379       130
P380       130
P381       130
P382       130
P383       130
P384       130
P385       130
P386       130
P387       130
P388       130
P389       130
P390       130
P391       130
P392       130
P393       130
P394       130
P395       130
P396       130
P397       130
P398       130
P399       130
P400       130
P401       130
P402       130
P403       130
P404       130
P405       130
P406       130
P407       130
P408       130
P409       130
P410       130
P411       130
P412       130
P413       130
P414       130
P415       130
P416       130
P417       130
P418       130
P419       130
P420       130
P421       130
P422       130
P423       130
P424       130
P425       130
P426       130
P427       130
P428       130
P429       130
P430       130
P431       130
P432       130
P433       130
P434       130
P435       130
P436       130
P437       130
P438       130
P439       130
P440       130
P441       130
P442       130
P443       130
P444       130
P445       130
P446       130
P447       130
P448       130
P449       130
P450       130
P451       130
P452       130
P453       130
P454       130
P455       130
P456       130
P457       130
P458       130
P459       130
P460       130
P461       130
P462       130
P463       130
P464       130
P465       130
P466       130
P467       130
P468       130
P469       130
P470       130
P471       130
P472       130
P473       130
P474       130
P475       130
P476       130
P477       130
P478       130
P479       130
P480       130
P481       130
P482       130
P483       130
P484       130
P485       130
P486       130
P487       130
P488       130
P489       130
P490       130
P491       130
P492       130
P493       130
P494       130
P495       130
P496       130
P497       130
P498       130
P499       130
P500       130
P501       130
P502       130
P503       130
P504       130
P505       130
P506       130
P507       130
P508       130
P509       130
P510       130
P511       130
P512       130
P513       130
P514       130
P515       130
P516       130
P517       130
P518       130
P519       130
P520       130
P521       130
P522       130
P523       130
P524       130
P525       130
P526       130
P527       130
P528       130
P529       130
P530       130
P531       130
P532       130
P533       130
P534       130
P535       130
P536       130
P537       130
P538       130
P539       130
P540       130
P541       130
P542       130
P543       130
P544       130
P545       130
P546       130
P547       130
P548       130
P549       130
P550       130
P551       130
P552       130
P553       130
P554       130
P555       130
P556       130
P557       130
P558       130
P559       130
P560       130
P561       130
P562       130
P563       130
P564       130
P565       130
P566       130
P567       130
P568       130
P569       130
P570       130
P571       130
P572       130
P573       130
P574       130
P575       130
P576       130
P577       130
P578       130
P579       130
P580       130
P581       130
P582       130
P583       130
P584       130
P585       130
P586       130
P587       130
P588       130
P589       130
P590       130
P591       130
P592       130
P593       130
P594       130
P595       130
P596       130
P597       130
P598       130
P599       130
P600       130
P601       130
P602       130
P603       130
P604       130
P605       130
P606       130
P607       130
P608       130
P609       130
P610       130
P611       130
P612       130
P613       130
P614       130
P615       130
P616       130
P617       130
P618       130
P619       130
P620       130
P621       130
P622       130
P623       130
P624       130
P625       130
P626       130
P627       130
P628       130
P629       130
P630       130
P631       130
P632       130
P633       130
P634       130
P635       130
P636       130
P637       130
P638       130
P639       130
P640       130
P641       130
P642       130
P643       130
P644       130
P645       130
P646       130
P647       130
P648       130
P649       130
P650       130
P651       130
P652       130
P653       130
P654       130
P655       130
P656       130
P657       130
P658       130
P659       130
P660       130
P661       130
P662       130
P663       130
P664       130
P665       130
P666       130
P667       130
P668       130
P669       130
P670       130
P671       130
P672       130
P673       130
P674       130
P675       130
P676       130
P677       130
P678       130
P679       130
P680       130
P681       130
P682       130
P683       130
P684       130
P685       130
P686       130
P687       130
P688       130
P689       130
P690       130
P691       130
P692       130
P693       130
P694       130
P695       130
P696       130
P697       130
P698       130
P699       130
P700       130
P701       130
P702       130
P703       130
P704       130
P705       130
P706       130
P707       130
P708       130
P709       130
P710       130
P711       130
P712       130
P713       130
P714       130
P715       130
P716       130
P717       130
P718       130
P719       130
P720       130
P721       130
P722       130
P723       130
P724       130
P725       130
P726       130
P727       130
P728       130
P729       130
P730       130
P731       130
P732       130
P733       130
P734       130
P735       130
P736       130
P737       130
P738       130
P739       130
P740       130
P741       130
P742       130
P743       130
P744       130
P745       130
P746       130
P747       130
P748       130
P749       130
P750       130
P751       130
P752       130
P753       130
P754       130
P755       130
P756       130
P757       130
P758       130
P759       130
P760       130
P761       130
P762       130
P763       130
P764       130
P765       130
P766       130
P767       130
P768       130
P769       130
P770       130
P771       130
P772       130
P773       130
P774       130
P775       130
P776       130
P777       130
P778       130
P779       130
P780       130
P781       130
P782       130
P783       130
P784       130
P785       130
P786       130
P787       130
P788       130
P789       130
P790       130
P791       130
P792       130
P793       130
P794       130
P795       130
P796       130
P797       130
P798       130
P799       130
P800       130
P801       130
P802       130
P803       130
P804       130
P805       130
P806       130
P807       130
P808       130
P809       130
P810       130
P811       130
P812       130
P813       130
P814       130
P815       130
P816       130
P817       130
P818       130
P819       130
P820       130
P821       130
P822       130
P823       130
P824       130
P825       130
P826       130
P827       130
P828       130
P829       130
P830       130
P831       130
P832       130
P833       130
P834       130
P835       130
P836       130
P837       130
P838       130
P839       130
P840       130
P841       130
P842       130
P843       130
P844       130
P845       130
P846       130
P847       130
P848       130
P849       130
P850       130
P851       130
P852       130
P853       130
P854       130
P855       130
P856       130
P857       130
P858       130
P859       130
P860       130
P861       130
P862       130
P863       130
P864       130
P865       130
P866       130
P867       130
P868       130
P869       130
P870       130
P871       130
P872       130
P873       130
P874       130
P875       130
P876       130
P877       130
P878       130
P879       130
P880       130
P881       130
P882       130
P883       130
P884       130
P885       130
P886       130
P887       130
P888       130
P889       130
P890       130
P891       130
P892       130
P893       130
P894       130
P895       130
P896       130
P897       130
P898       130
P899       130
P900       130
P901       130
P902       130
P903       130
P904       130
P905       130
P906       130
P907       130
P908       130
P909       130
P910       130
P911       130
P912       130
P913       130
P914       130
P915       130
P916       130
P917       130
P918       130
P919       130
P920       130
P921       130
P922       130
P923       130
P924       130
P925       130
P926       130
P927       130
P928       130
P929       130
P930       130
P931       130
P932       130
P933       130
P934       130
P935       130
P936       130
P937       130
P938       130
P939       130
P940       130
P941       130
P942       130
P943       130
P944       130
P945       130
P946       130
P947       130
P948       130
P949       130
P950       130
P951       130
P952       130
P953       130
P954       130
P955       130
P956       130
P957       130
P958       130
P959       130
P960       130
P961       130
P962       130
P963       130
P964       130
P965       130
P966       130
P967       130
P968       130
P969       130
P970       130
P971       130
P972       130
P973       130
P974       130
P975       130
P976       130
P977       130
P978       130
P979       130
P980       130
P981       130
P982       130
P983       130
P984       130
P985       130
P986       130
P987       130
P988       130
P989       130
P990       130
P991       130
P992       130
P993       130
P994       130
P995       130
P996       130
P997       130
P998       130
P999       130
P1000      130
    
```

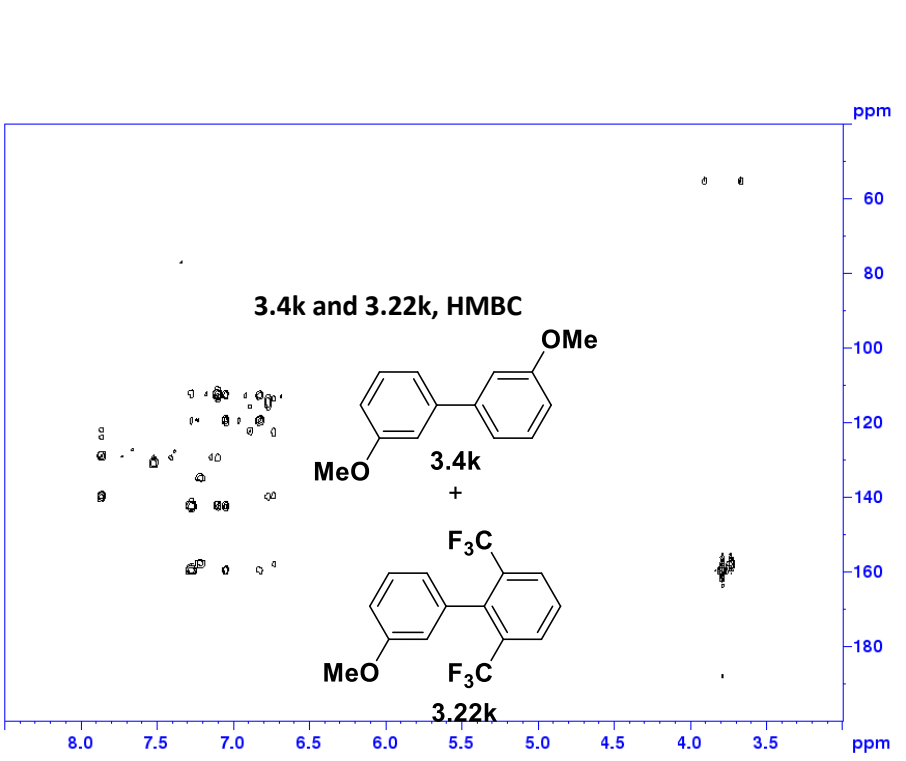






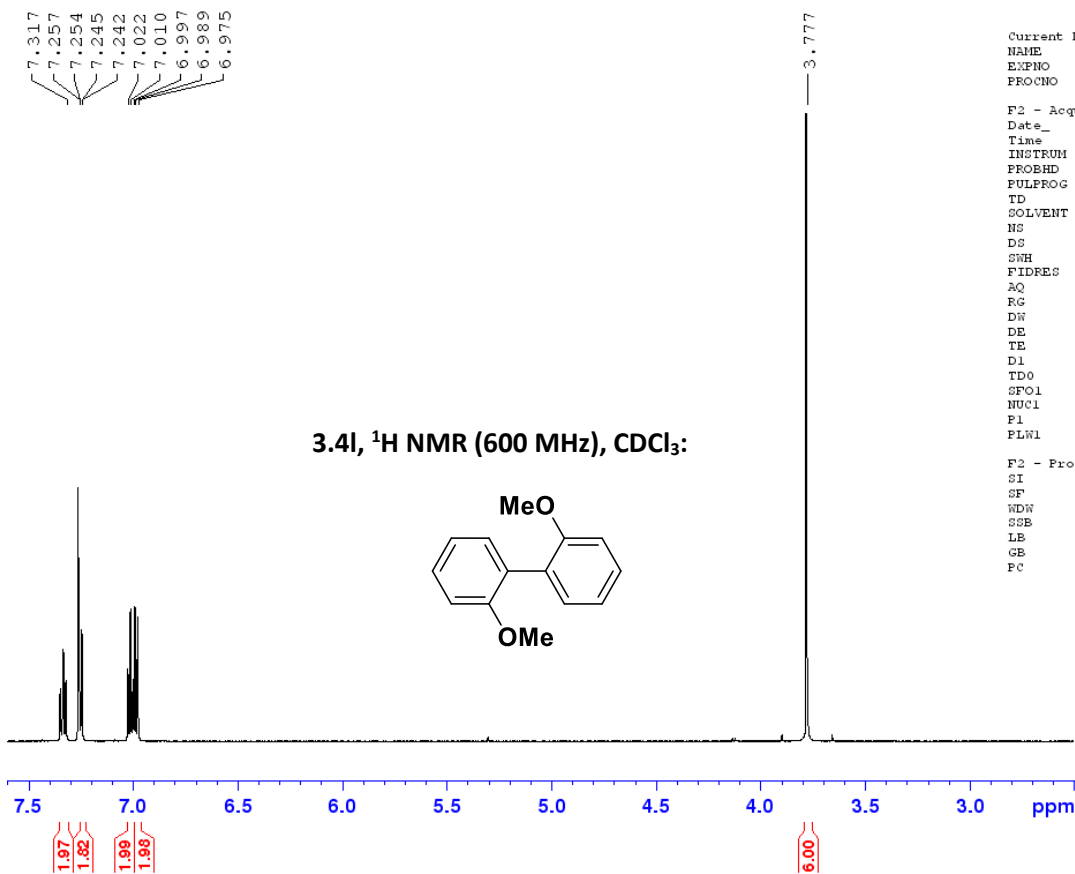
Current Data Parameters
NAME jds-1g-023b-2
EXPNO 1
PROCNO 1

F2 - Acquisition Parameters
Date_ 20200714
Time 20:45 k
INSTRUM spect
PROBHD 5mmBBO-1H/13C
PULPROG zgpg30
TD 65536
SOLVENT CDCl3
NS 2
DS 4
SWH 5424.782 Hz
FIDRES 10.414810 Hz
AQ 0.0928098 sec
RG 194.75
DQ 52.000 usec
DE 6.50 usec
TE 296.2 K
CMT12 145.0000000
D0 0.00000200 sec
D1 1.47122802 sec
D2 0.00172814 sec
D3 0.00000000 sec
D4 0.00020000 sec
D5 0.00020000 sec
D6 0.00020000 sec
D7 0.00020000 sec
D8 0.00020000 sec
D9 0.00020000 sec
D10 0.00020000 sec
D11 0.00020000 sec
D12 0.00020000 sec
D13 0.00020000 sec
D14 0.00020000 sec
D15 0.00020000 sec
D16 0.00020000 sec
D17 0.00020000 sec
D18 0.00020000 sec
D19 0.00020000 sec
D20 0.00020000 sec
D21 0.00020000 sec
D22 0.00020000 sec
D23 0.00020000 sec
D24 0.00020000 sec
D25 0.00020000 sec
D26 0.00020000 sec
D27 0.00020000 sec
D28 0.00020000 sec
D29 0.00020000 sec
D30 0.00020000 sec
D31 0.00020000 sec
D32 0.00020000 sec
D33 0.00020000 sec
D34 0.00020000 sec
D35 0.00020000 sec
D36 0.00020000 sec
D37 0.00020000 sec
D38 0.00020000 sec
D39 0.00020000 sec
D40 0.00020000 sec
D41 0.00020000 sec
D42 0.00020000 sec
D43 0.00020000 sec
D44 0.00020000 sec
D45 0.00020000 sec
D46 0.00020000 sec
D47 0.00020000 sec
D48 0.00020000 sec
D49 0.00020000 sec
D50 0.00020000 sec
D51 0.00020000 sec
D52 0.00020000 sec
D53 0.00020000 sec
D54 0.00020000 sec
D55 0.00020000 sec
D56 0.00020000 sec
D57 0.00020000 sec
D58 0.00020000 sec
D59 0.00020000 sec
D60 0.00020000 sec
D61 0.00020000 sec
D62 0.00020000 sec
D63 0.00020000 sec
D64 0.00020000 sec
D65 0.00020000 sec
D66 0.00020000 sec
D67 0.00020000 sec
D68 0.00020000 sec
D69 0.00020000 sec
D70 0.00020000 sec
D71 0.00020000 sec
D72 0.00020000 sec
D73 0.00020000 sec
D74 0.00020000 sec
D75 0.00020000 sec
D76 0.00020000 sec
D77 0.00020000 sec
D78 0.00020000 sec
D79 0.00020000 sec
D80 0.00020000 sec
D81 0.00020000 sec
D82 0.00020000 sec
D83 0.00020000 sec
D84 0.00020000 sec
D85 0.00020000 sec
D86 0.00020000 sec
D87 0.00020000 sec
D88 0.00020000 sec
D89 0.00020000 sec
D90 0.00020000 sec
D91 0.00020000 sec
D92 0.00020000 sec
D93 0.00020000 sec
D94 0.00020000 sec
D95 0.00020000 sec
D96 0.00020000 sec
D97 0.00020000 sec
D98 0.00020000 sec
D99 0.00020000 sec
D100 0.00020000 sec



Current Data Parameters
NAME jds-1g-023b-2
EXPNO 1
PROCNO 1

F2 - Acquisition Parameters
Date_ 20200714
Time 21:05 h
INSTRUM spect
PROBHD 5mmBBO-1H/13C
PULPROG zgpg30
TD 65536
SOLVENT CDCl3
NS 2
DS 4
SWH 5424.782 Hz
FIDRES 10.414810 Hz
AQ 0.0928098 sec
RG 194.75
DQ 52.000 usec
DE 6.50 usec
TE 296.2 K
CMT12 145.0000000
D0 0.00000200 sec
D1 1.47122802 sec
D2 0.00172814 sec
D3 0.00000000 sec
D4 0.00020000 sec
D5 0.00020000 sec
D6 0.00020000 sec
D7 0.00020000 sec
D8 0.00020000 sec
D9 0.00020000 sec
D10 0.00020000 sec
D11 0.00020000 sec
D12 0.00020000 sec
D13 0.00020000 sec
D14 0.00020000 sec
D15 0.00020000 sec
D16 0.00020000 sec
D17 0.00020000 sec
D18 0.00020000 sec
D19 0.00020000 sec
D20 0.00020000 sec
D21 0.00020000 sec
D22 0.00020000 sec
D23 0.00020000 sec
D24 0.00020000 sec
D25 0.00020000 sec
D26 0.00020000 sec
D27 0.00020000 sec
D28 0.00020000 sec
D29 0.00020000 sec
D30 0.00020000 sec
D31 0.00020000 sec
D32 0.00020000 sec
D33 0.00020000 sec
D34 0.00020000 sec
D35 0.00020000 sec
D36 0.00020000 sec
D37 0.00020000 sec
D38 0.00020000 sec
D39 0.00020000 sec
D40 0.00020000 sec
D41 0.00020000 sec
D42 0.00020000 sec
D43 0.00020000 sec
D44 0.00020000 sec
D45 0.00020000 sec
D46 0.00020000 sec
D47 0.00020000 sec
D48 0.00020000 sec
D49 0.00020000 sec
D50 0.00020000 sec
D51 0.00020000 sec
D52 0.00020000 sec
D53 0.00020000 sec
D54 0.00020000 sec
D55 0.00020000 sec
D56 0.00020000 sec
D57 0.00020000 sec
D58 0.00020000 sec
D59 0.00020000 sec
D60 0.00020000 sec
D61 0.00020000 sec
D62 0.00020000 sec
D63 0.00020000 sec
D64 0.00020000 sec
D65 0.00020000 sec
D66 0.00020000 sec
D67 0.00020000 sec
D68 0.00020000 sec
D69 0.00020000 sec
D70 0.00020000 sec
D71 0.00020000 sec
D72 0.00020000 sec
D73 0.00020000 sec
D74 0.00020000 sec
D75 0.00020000 sec
D76 0.00020000 sec
D77 0.00020000 sec
D78 0.00020000 sec
D79 0.00020000 sec
D80 0.00020000 sec
D81 0.00020000 sec
D82 0.00020000 sec
D83 0.00020000 sec
D84 0.00020000 sec
D85 0.00020000 sec
D86 0.00020000 sec
D87 0.00020000 sec
D88 0.00020000 sec
D89 0.00020000 sec
D90 0.00020000 sec
D91 0.00020000 sec
D92 0.00020000 sec
D93 0.00020000 sec
D94 0.00020000 sec
D95 0.00020000 sec
D96 0.00020000 sec
D97 0.00020000 sec
D98 0.00020000 sec
D99 0.00020000 sec
D100 0.00020000 sec

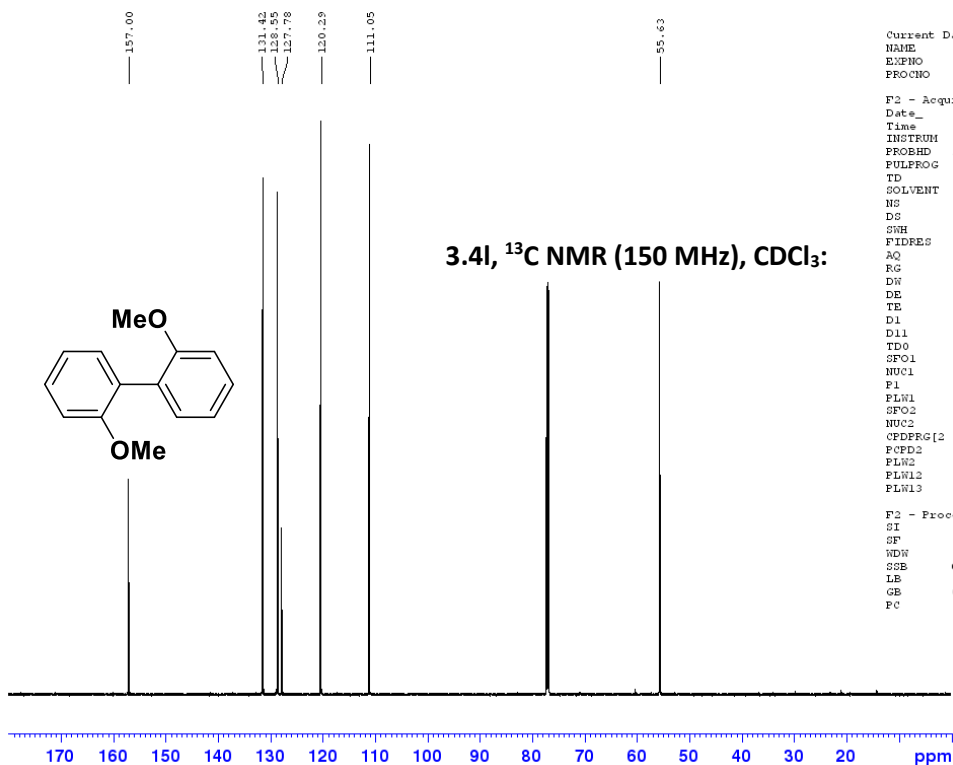


```

Current Data Parameters
NAME      SLG2-030-1
EXPNO    1
PROCNO   1

F2 - Acquisition Parameters
Date_    20200625
Time     0.36 h
INSTRUM  spect
PROBHD   E148658_0003 (
PULPROG  zg30
TD       65536
SOLVENT  CDCl3
NS       16
DS       2
SWH      12019.230 Hz
FIDRES   0.366798 Hz
AQ       2.7262976 sec
RG       199.73
DN       41.600 usec
DE       6.50 usec
TE       296.2 K
D1       4.00000000 sec
TD0      1
SFO1     600.0087050 MHz
NUC1     1H
P1       15.50 usec
PLW1     13.23200035 W

F2 - Processing parameters
SI       65536
SF       600.0050156 MHz
WDW      EM
SSB      0
LB       0.30 Hz
GB       0
PC       1.00
  
```

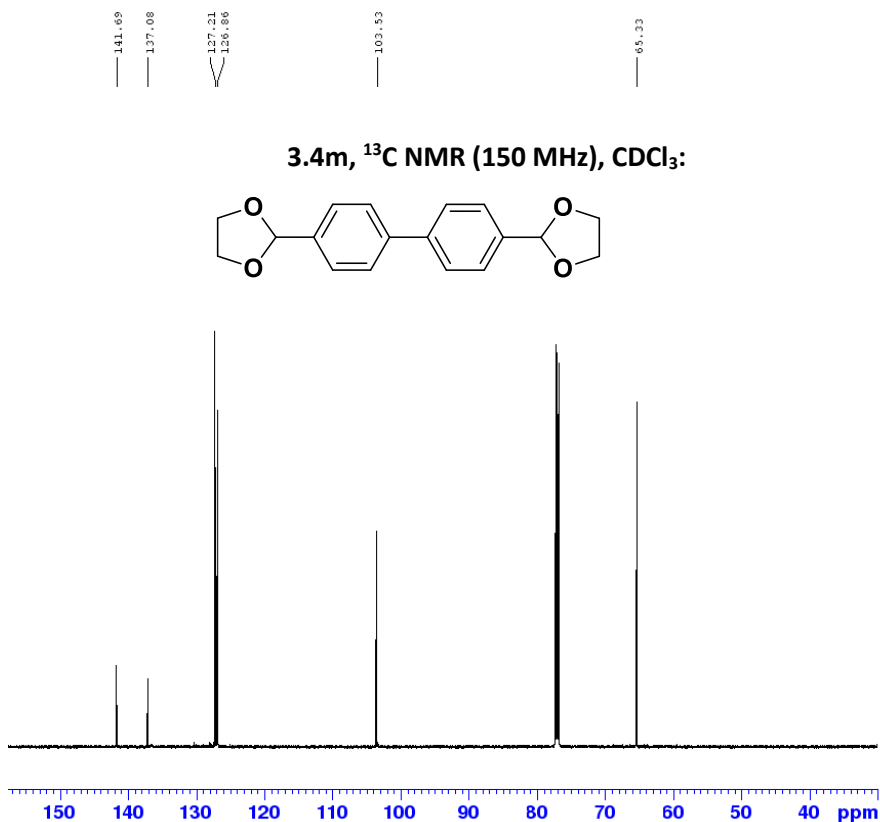
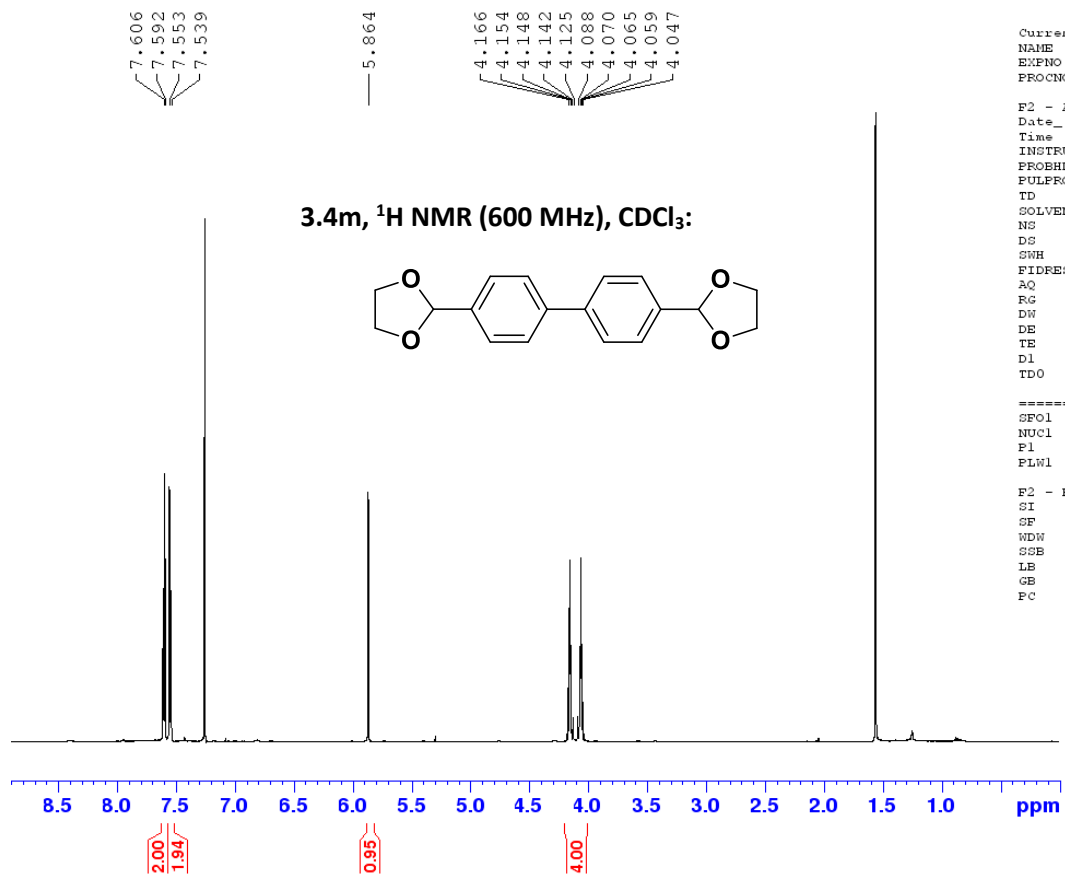


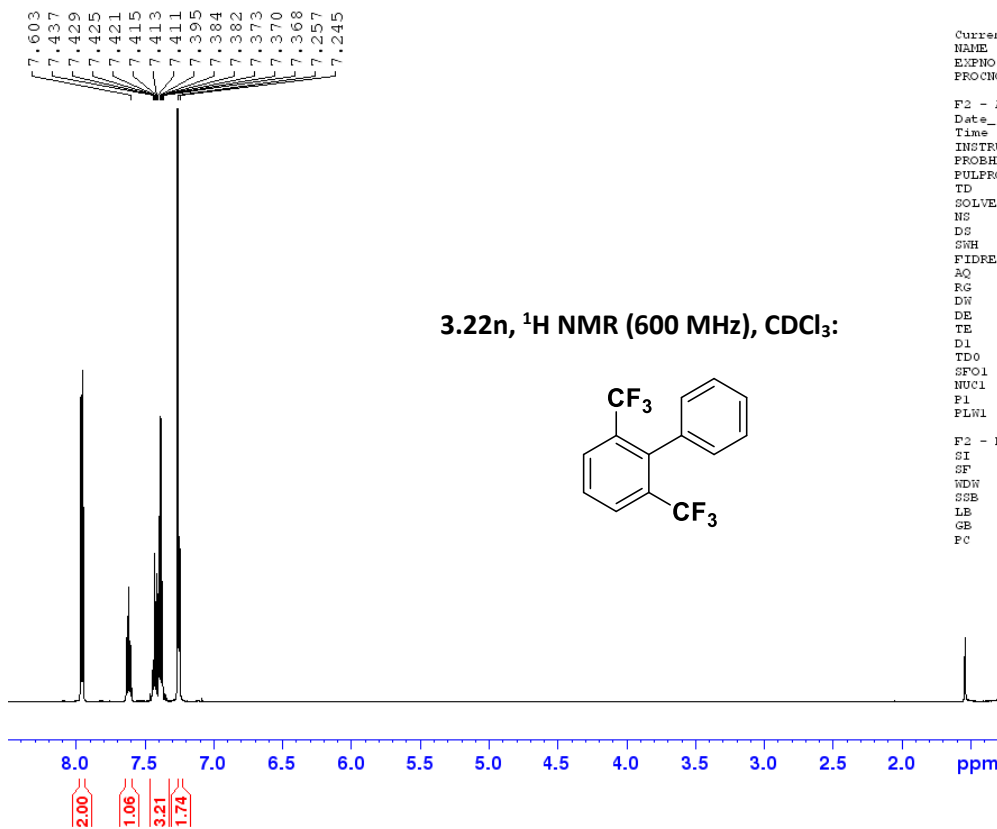
```

Current Data Parameters
NAME      SLG2-030-1C
EXPNO    1
PROCNO   1

F2 - Acquisition Parameters
Date_    20200625
Time     1.55 h
INSTRUM  spect
PROBHD   E148658_0003 (
PULPROG  zgpg30
TD       65536
SOLVENT  CDCl3
NS       600
DS       4
SWH      36231.883 Hz
FIDRES   1.103709 Hz
AQ       0.9043968 sec
RG       199.73
DN       13.800 usec
DE       6.50 usec
TE       298.0 K
D1       4.00000000 sec
D11      0.03000000 sec
TD0      1
SFO1     150.8864644 MHz
NUC1     13C
P1       12.00 usec
PLW1     77.65699768 W
SFO2     600.0074000 MHz
NUC2     1H
CFDPRG2  waltz16
PCPD2    70.00 usec
PLW2     13.23200035 W
PLW12    0.64876997 W
PLW13    0.32633001 W

F2 - Processing parameters
SI       32768
SF       150.8713932 MHz
WDW      EM
SSB      0
LB       1.00 Hz
GB       0
PC       1.40
  
```

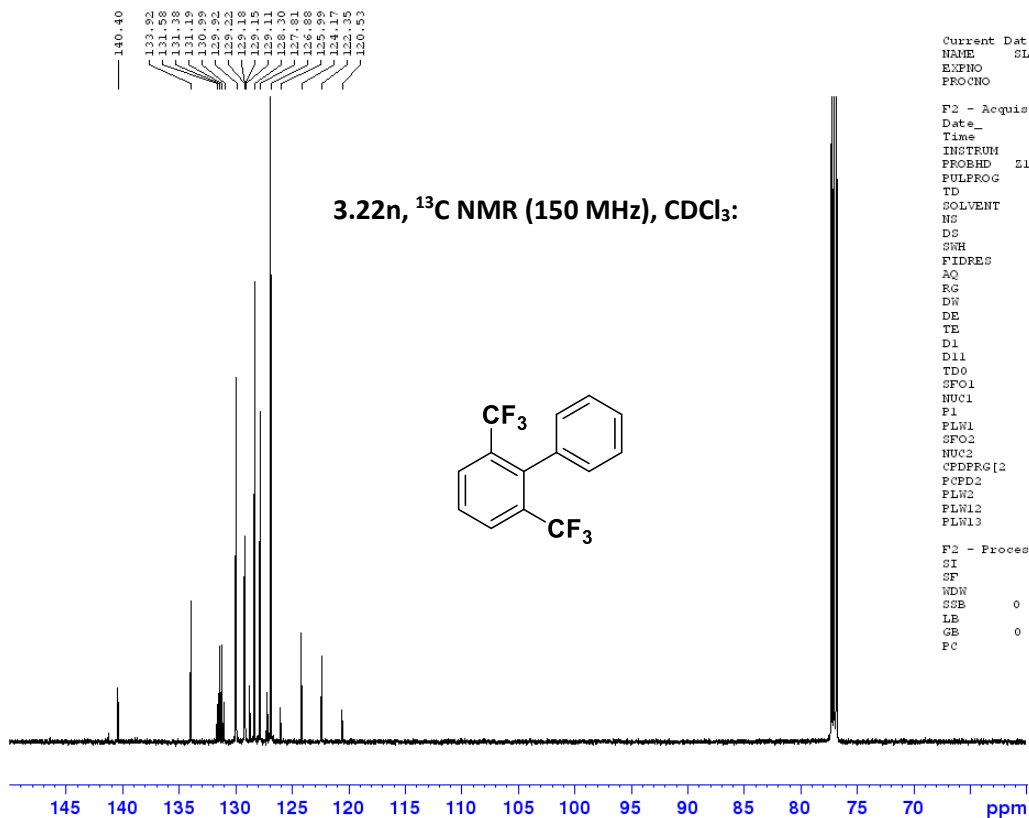




Current Data Parameters
NAME SLG2-011_Col
EXPNO 1
PROCNO 1

F2 - Acquisition Parameters
Date_ 20200616
Time 23.55 h
INSTRUM spect
PROBHD E148658_0003 (
PULPROG zg30
TD 65536
SOLVENT CDCl3
NS 16
DS 2
SWH 12019.230 Hz
FIDRES 0.366798 Hz
AQ 2.7262976 sec
RG 199.73
DN 41.600 usec
DE 6.50 usec
TE 296.1 K
D1 4.00000000 sec
TD0 1
SFO1 600.0087050 MHz
NUC1 1H
P1 15.50 usec
PLW1 13.23200035 W

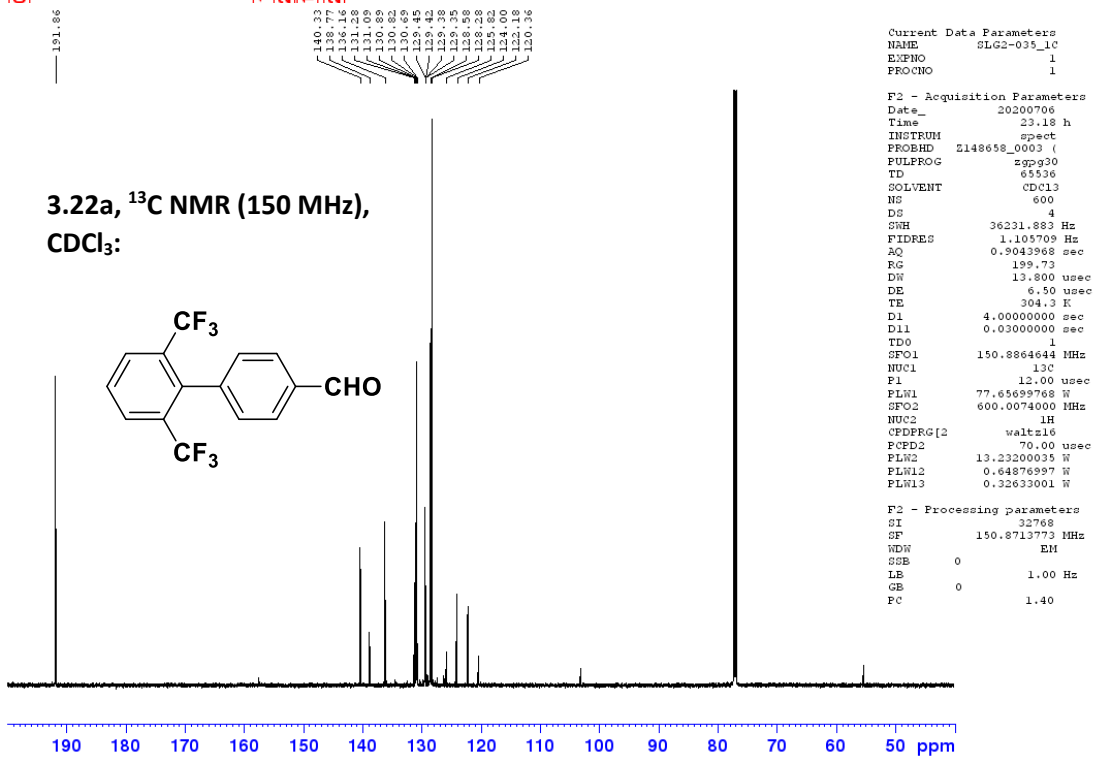
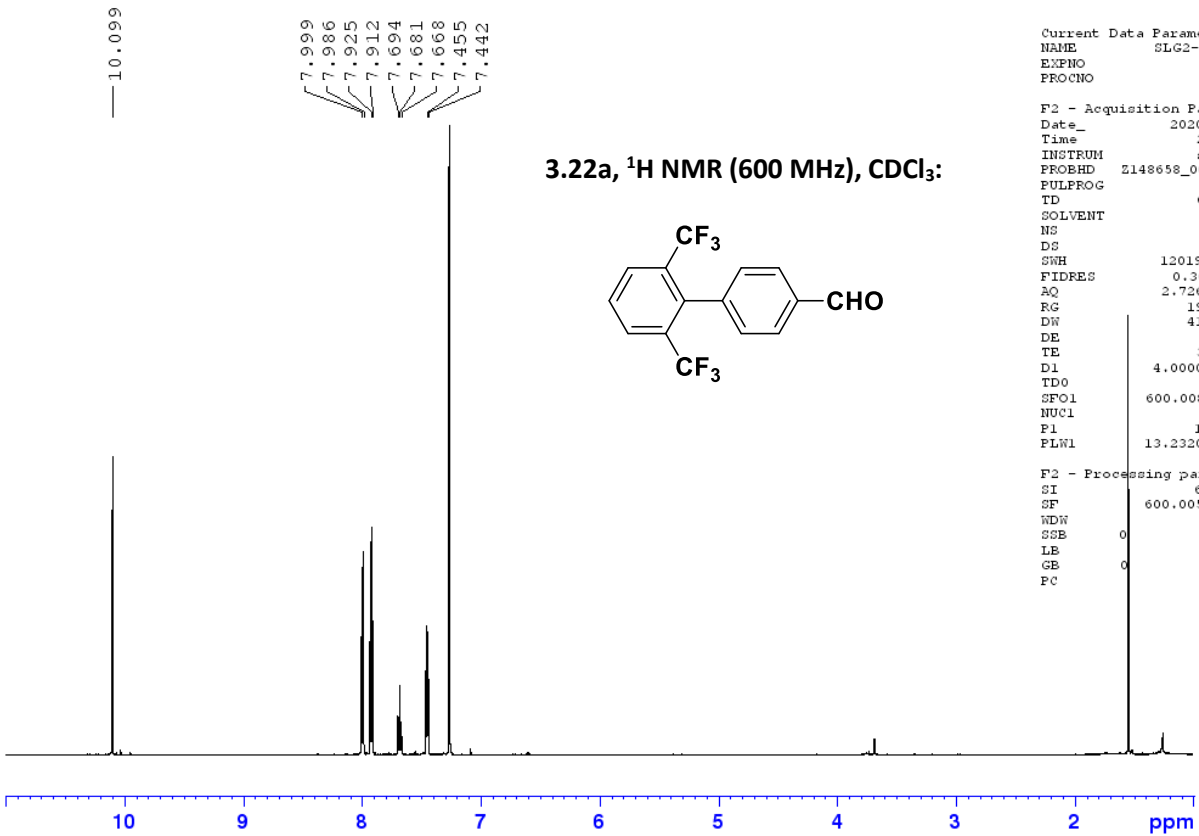
F2 - Processing parameters
SI 65536
SF 600.0050161 MHz
WDW EM
SSE 0
LB 0.30 Hz
GB 0
PC 1.00

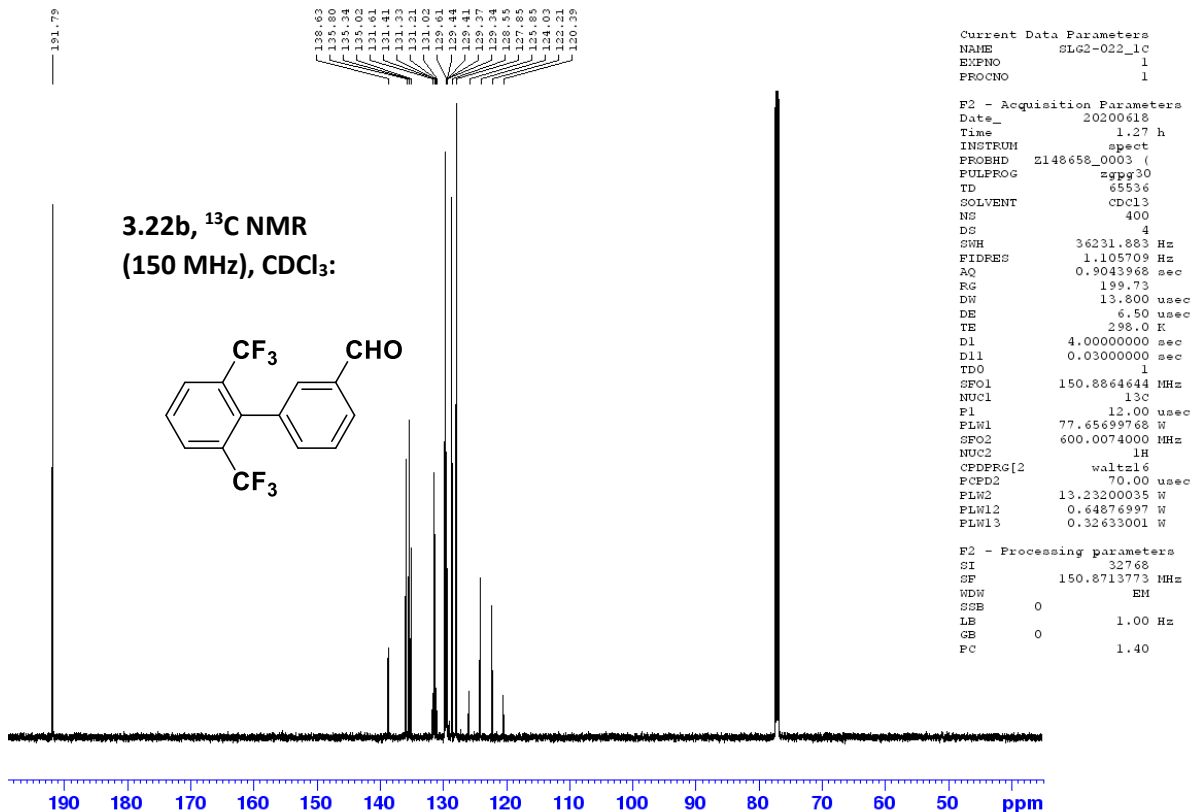
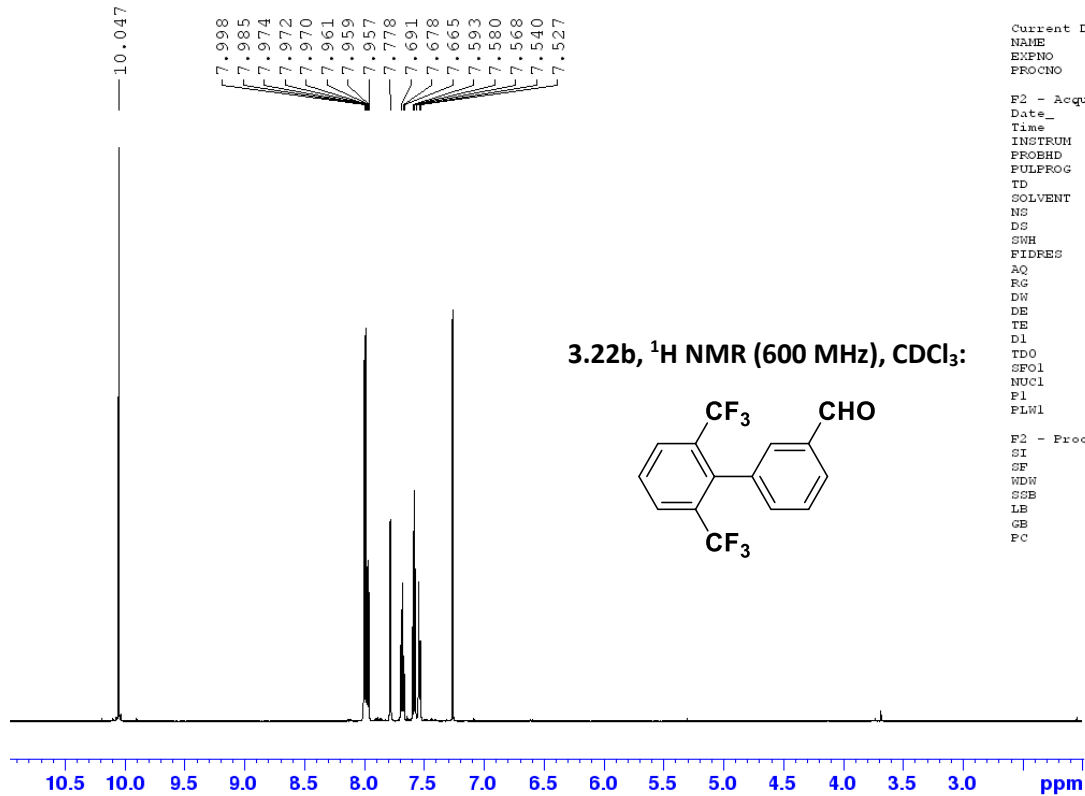


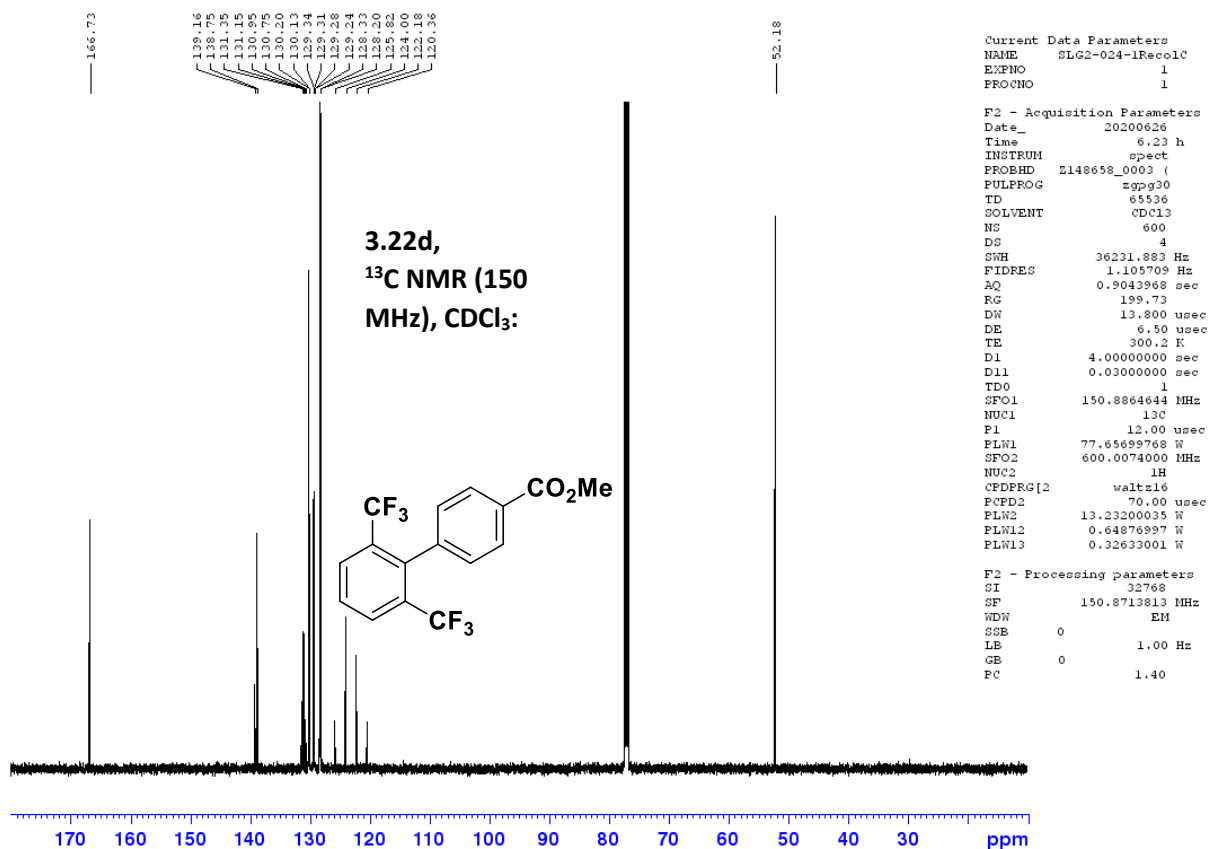
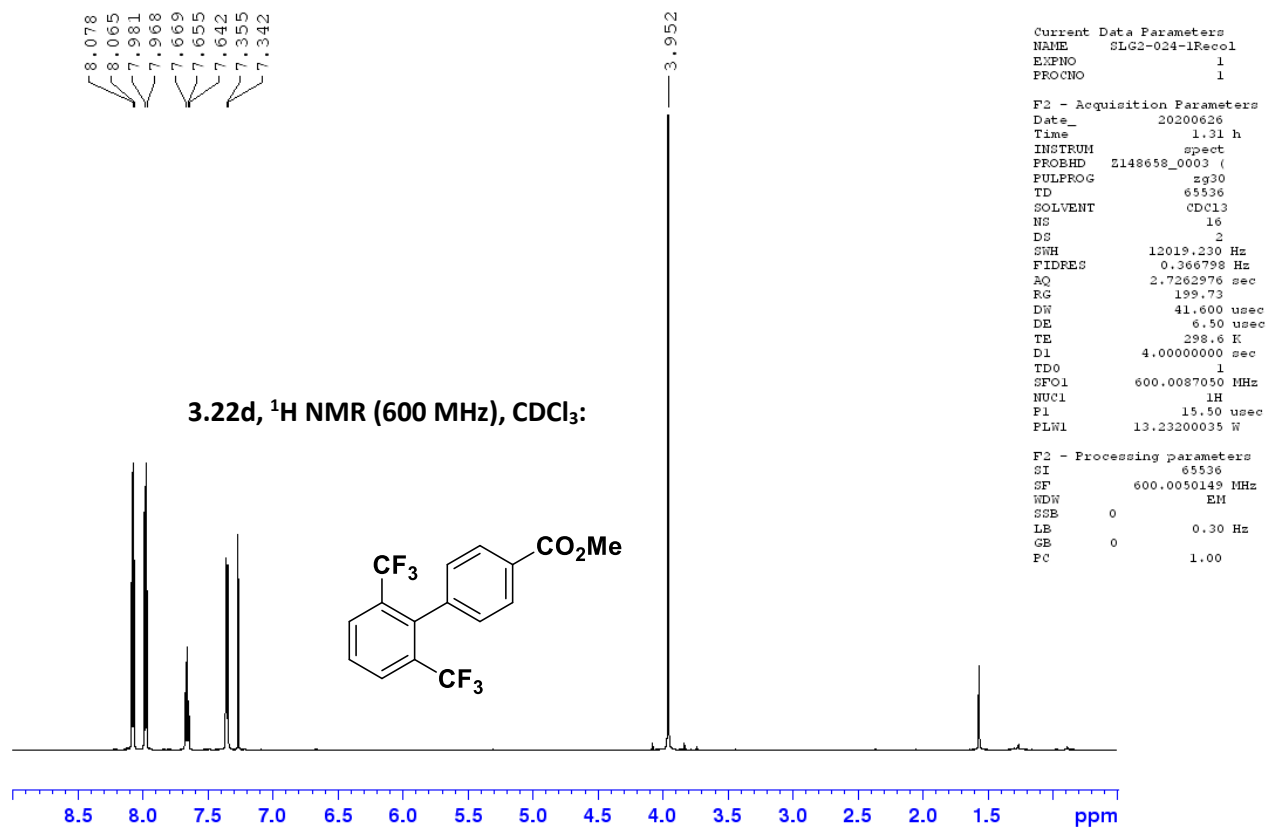
Current Data Parameters
NAME SLG2-011_Col_13C
EXPNO 1
PROCNO 1

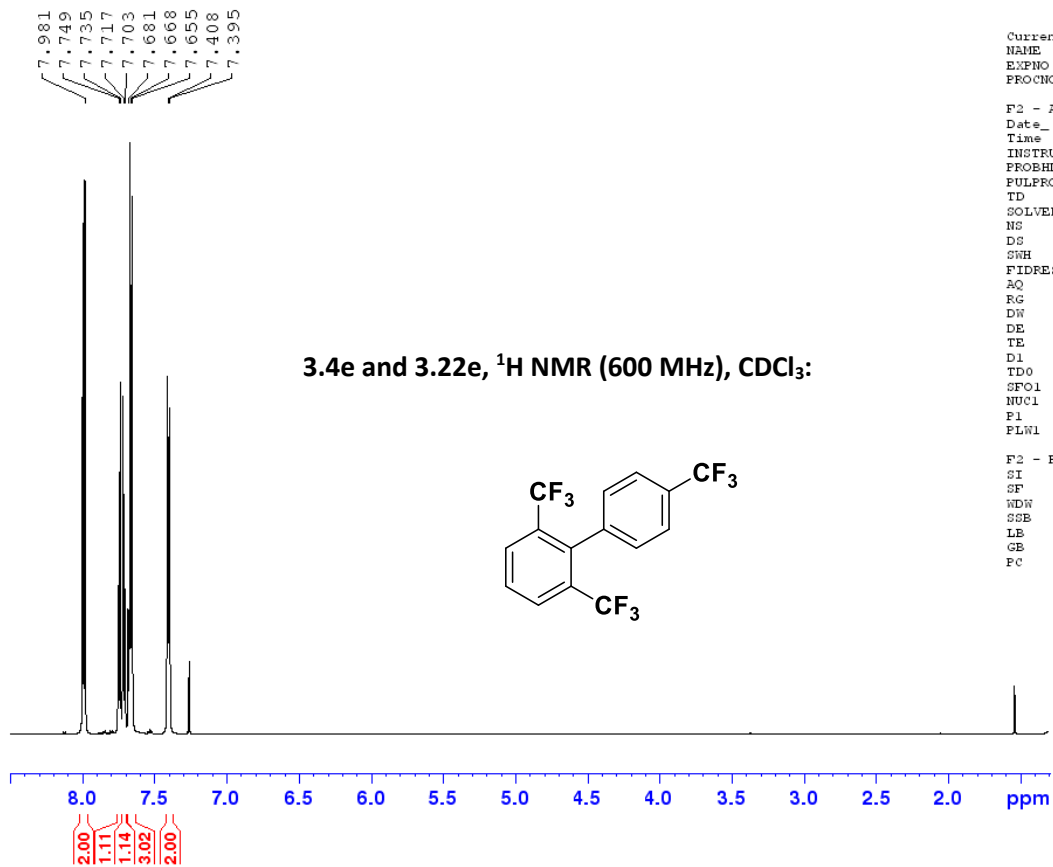
F2 - Acquisition Parameters
Date_ 20200617
Time 3.27 h
INSTRUM spect
PROBHD E148658_0003 (
PULPROG zgpg30
TD 65536
SOLVENT CDCl3
NS 1024
DS 4
SWH 36231.883 Hz
FIDRES 1.105709 Hz
AQ 0.9043968 sec
RG 199.73
DN 13.800 usec
DE 6.50 usec
TE 298.3 K
D1 4.00000000 sec
D11 0.03000000 sec
TD0 1
SFO1 150.8864644 MHz
NUC1 13C
P1 12.00 usec
PLH1 77.65699768 W
SFO2 600.0074000 MHz
NUC2 1H
CPDPRG2 waltz16
PCPD2 70.00 usec
PLW2 13.23200035 W
PLW12 0.64876997 W
PLW13 0.32633001 W

F2 - Processing parameters
SI 32768
SF 150.8713816 MHz
WDW EM
SSE 0
LB 1.00 Hz
GB 0
PC 1.40







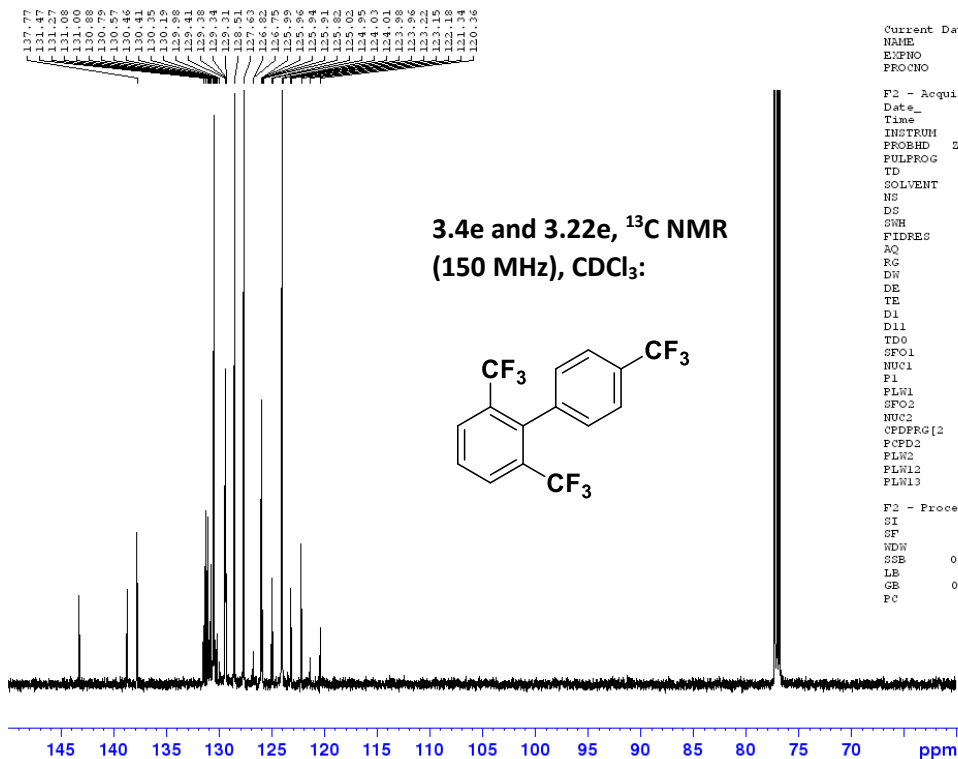


```

Current Data Parameters
NAME      SLG2-036b_1
EXPNO    1
PROCNO   1

F2 - Acquisition Parameters
Date_    20200707
Time     3.35 h
INSTRUM  spect
PROBHD   Z855801_0104 (
PULPROG  zg30
TD       65536
SOLVENT  CDCl3
NS       16
DS       2
SWH      12019.230 Hz
FIDRES   0.366798 Hz
AQ       2.7262976 sec
RG       78.28
DW       41.600 usec
DE       6.50 usec
TE       296.3 K
D1       4.00000000 sec
TD0      1
SFO1     599.9587047 MHz
NUC1     1H
F1       7.75 usec
PLWL     11.99499989 W

F2 - Processing parameters
SI       65536
SF       599.9550163 MHz
WDW      EM
SSB      0
LB       0.30 Hz
GB       0
PC       1.00
  
```

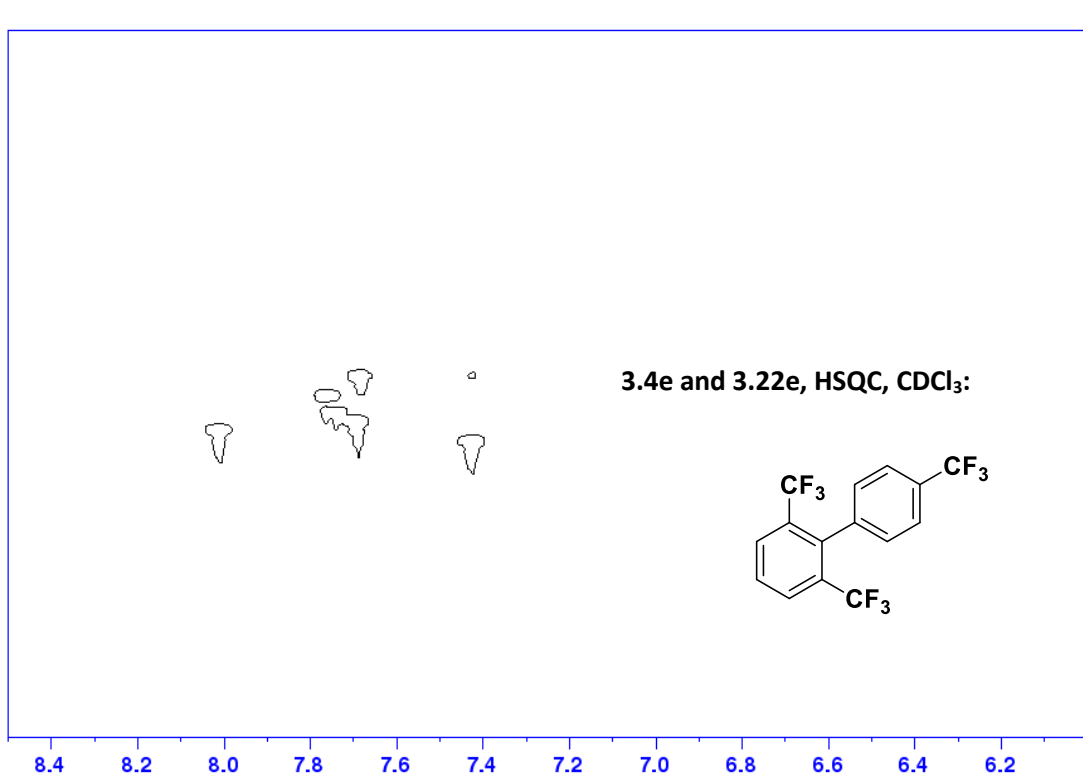


```

Current Data Parameters
NAME      SLG2-036b_1C
EXPNO    1
PROCNO   1

F2 - Acquisition Parameters
Date_    20200707
Time     4.26 h
INSTRUM  spect
PROBHD   Z855801_0104 (
PULPROG  zgpg30
TD       65536
SOLVENT  CDCl3
NS       600
DS       4
SWH      36231.883 Hz
FIDRES   1.105709 Hz
AQ       0.9043968 sec
RG       194.75
DW       13.800 usec
DE       6.50 usec
TE       296.7 K
D1       4.00000000 sec
D11      0.03000000 sec
TD0      1
SFO1     150.8738906 MHz
NUC1     13C
F1       11.40 usec
PLW1     176.19999695 W
SFO2     599.9573998 MHz
NUC2     1H
CPDPRG2  waltz16
PCPD2    70.00 usec
PLW2     11.99499989 W
PLW12    0.14703000 W
PLW13    0.07395500 W

F2 - Processing parameters
SI       32768
SF       150.8588050 MHz
WDW      EM
SSB      0
LB       1.00 Hz
GB       0
PC       1.40
  
```

```

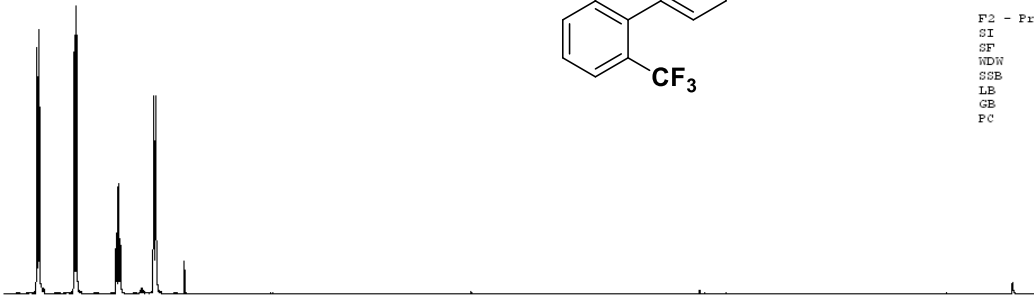
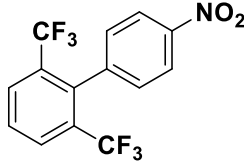
Current Data Parameters
NAME 0122-036b-1H2DQ
EXPNO 2
PROCNO 1

F2 - Acquisition Parameters
Date_ 20200707
Time 22:34 h
INSTRUM spect
PROBHD 145552_0003 (
PULPROG zgpg30
TD 3284
SOLVENT CDCl3
NS 4
DS 2
SWH 7212.500 Hz
FIDRES 7.423295 Hz
AQ 0.1210720 sec
RG 191.72
DE 44.000 usec
TE 303.2 K
NUC1 145.0000000
NUC2 1
CHFT2 185.0000000
CHFT1 -0.5000000
D0 0.00000300 sec
D1 1.50000000 sec
D4 0.00172414 sec
D11 0.00000000 sec
D14 0.00020000 sec
D21 0.00344500 sec
D34 0.00004200 sec
IH0 0.00002010 sec
IH1 1
TEMR 600.0075200 MHz
FID1 18
F1 15.50 usec
F2 31.00 usec
F3 1000.00 usec
F4 12.22500025 Hz
SF2 150.8329256 MHz
NUC1 13C
CPDPRG2 gmg4
F5 12.00 usec
F14 500.00 usec
F14 2000.00 usec
F21 1730.00 usec
F2D2 60.00 usec
F2D 0 Hz
F2D2 77.5658765 Hz
F2D12 0.10630012 Hz
GPHH[2] Csp40.0.5.20.1
GFOA1 0.500
GFOFPD0 0 Hz
GPHH[7] Csp40.0.0.0.4
GFOA7 0.500
GFOFPD7 0 Hz
GPHH[10] Csp40.0.0.11.2
GFOA10 0.500
GFOFPD10 0 Hz
GPHH[14] Csp40.0.0.0.0
GPHH[1] CHDQ10.100
GPHH[2] CHDQ10.100
GPHH[3] CHDQ10.100
GPHH[4] CHDQ10.100
GPHH[5] CHDQ10.100
GPHH[6] CHDQ10.100
GPHH[8] CHDQ10.100
GPHH[9] CHDQ10.100
GPHH[11] CHDQ10.100
GPHH[12] CHDQ10.100
GPHH[13] CHDQ10.100
GPHH[15] CHDQ10.100
GPHH[16] CHDQ10.100
GPHH[17] CHDQ10.100
GPHH[18] CHDQ10.100
F1 - Acquisition parameters
TD 256
SF 150.8327 MHz
FIDRES 194.240750 Hz
DE 104.267 ppm
F2HODR EchoAntiScho

F2 - Processing parameters
SI 1024
SF 600.000000 MHz
DS 2
DE 44.00 usec
TE 303.2 K
TEMR 600.0075200 MHz
FIDRES 194.240750 Hz
DE 104.267 ppm
F2HODR EchoAntiScho
  
```

8.270
8.255
8.014
8.000
7.727
7.713
7.700
7.470
7.456

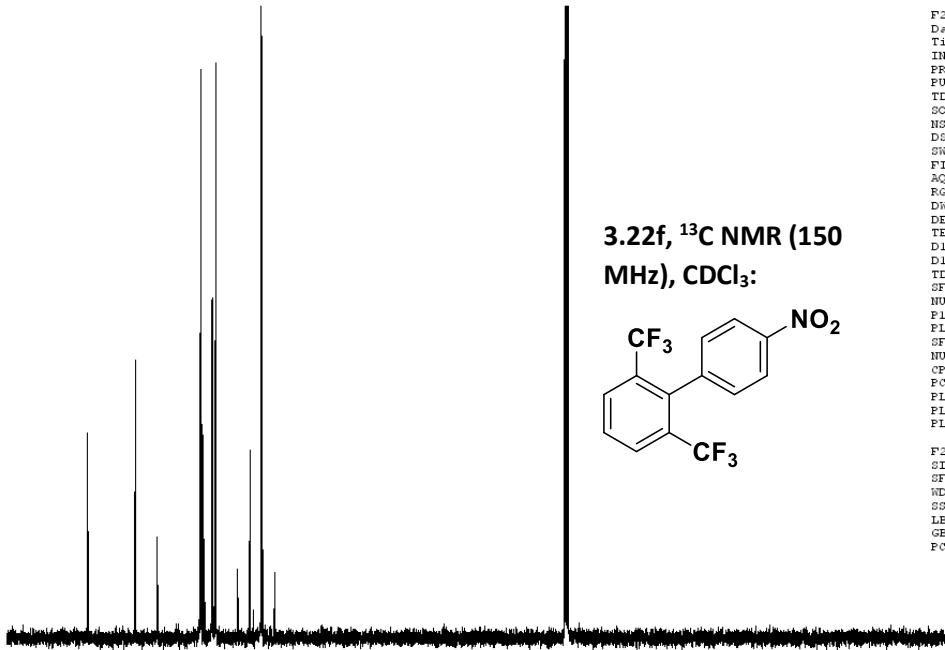
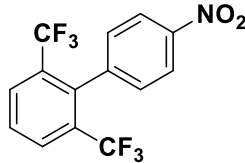
3.22f, ¹H NMR (600 MHz), CDCl₃:



8.0 7.5 7.0 6.5 6.0 5.5 5.0 4.5 4.0 3.5 3.0 2.5 2.0 ppm

148.01
140.86
137.67
131.21
131.21
130.86
130.86
130.67
129.57
129.54
129.54
129.50
129.01
128.73
125.73
123.91
122.26
122.26
120.29

3.22f, ¹³C NMR (150 MHz), CDCl₃:



150 140 130 120 110 100 90 80 70 60 50 40 30 ppm

Current Data Parameters
NAME SLG2-034b-1
EXPNO 1
PROCNO 1

F2 - Acquisition Parameters
Date_ 20200702
Time 0.27 h
INSTRUM spect
PROBHD Z855801_0104 ()
PULPROG zg30
TD 65536
SOLVENT CDCl3
NS 16
DS 2
SWH 12019.230 Hz
FIDRES 0.366798 Hz
AQ 2.7262976 sec
RG 89.24
DW 41.600 usec
DE 6.50 usec
TE 295.9 K
D1 4.0000000 sec
TD0 1
SFO1 599.9587047 MHz
NUC1 1H
P1 7.75 usec
PLW1 11.99499989 W

F2 - Processing parameters
SI 65536
SF 599.9550155 MHz
WDW EM
SSB 0
LB 0.30 Hz
GB 0
PC 1.00

Current Data Parameters
NAME SLG2-034b-1C
EXPNO 1
PROCNO 1

F2 - Acquisition Parameters
Date_ 20200702
Time 1.24 h
INSTRUM spect
PROBHD Z855801_0104 ()
PULPROG zgpg30
TD 65536
SOLVENT CDCl3
NS 200
DS 4
SWH 36231.883 Hz
FIDRES 1.105709 Hz
AQ 0.904398 sec
RG 194.75
DW 13.800 usec
DE 6.50 usec
TE 296.3 K
D1 4.0000000 sec
D11 0.0300000 sec
TD0 1
SFO1 150.8738906 MHz
NUC1 13C
P1 11.40 usec
PLW1 176.19999695 W
SFO2 599.9573998 MHz
NUC2 1H
CFPRG[2] waltz16
PCPD2 70.00 usec
PLW2 11.99499989 W
PLW12 0.14703000 W
PLW13 0.07395500 W

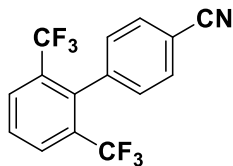
F2 - Processing parameters
SI 32768
SF 150.8588050 MHz
WDW EM
SSB 0
LB 1.00 Hz
GB 0
PC 1.40

8.003
7.989
7.708
7.705
7.697
7.694
7.683
7.398
7.385

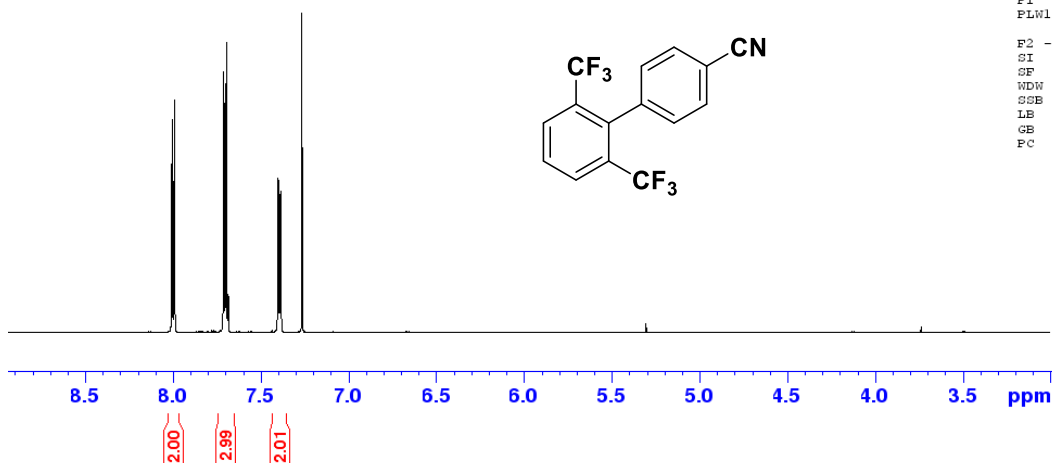
Current Data Parameters
NAME BAD1-014-1
EXPNO 1
PROCNO 1

F2 - Acquisition Parameters
Date_ 20200303
Time 10.43 h
INSTRUM spect
PROBHD Z148658_0003 ()
PULPROG zg30
TD 65536
SOLVENT CDCl3
NS 16
DS 2
SWH 12019.230 Hz
FIDRES 0.366798 Hz
AQ 2.7262976 sec
RG 199.73
DW 41.600 usec
DE 6.50 usec
TE 296.6 K
D1 6.00000000 sec
TDO 1
SFO1 600.0087050 MHz
NUC1 1H
P1 15.50 usec
PLW1 13.23200035 W

3.22g, ¹H NMR (600 MHz), CDCl₃:



F2 - Processing parameters
SI 65536
SF 600.0050137 MHz
WDW EM
SSE 0
LB 0.30 Hz
GB 0
FC 1.00

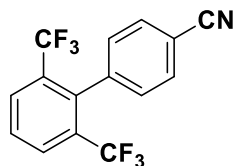


138.89
137.87
130.93
130.83
129.49
129.42
129.38
128.83
125.70
123.88
122.06
120.24
118.42
112.63

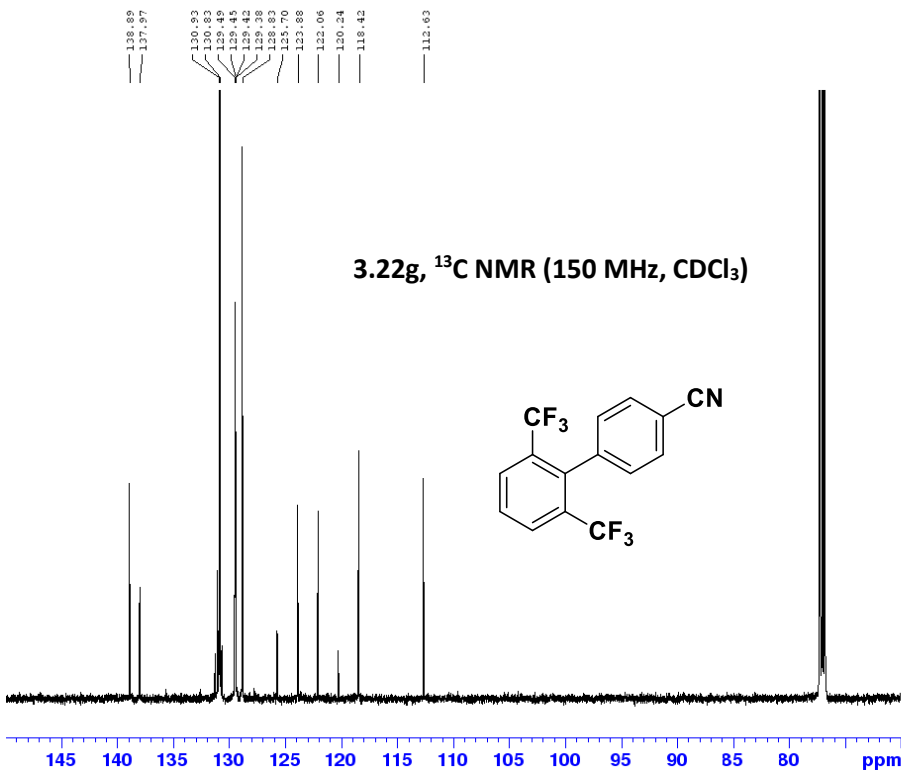
Current Data Parameters
NAME BAD1-014-01-13
EXPNO 1
PROCNO 1

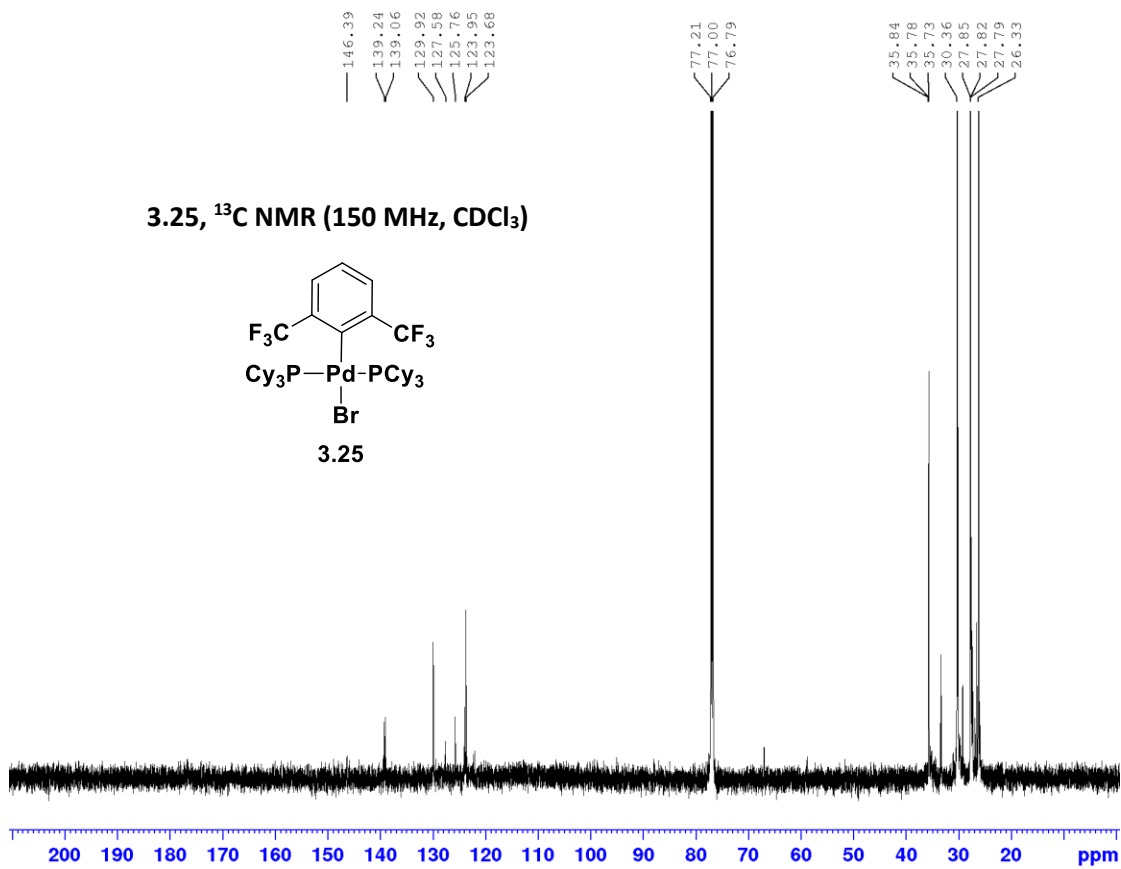
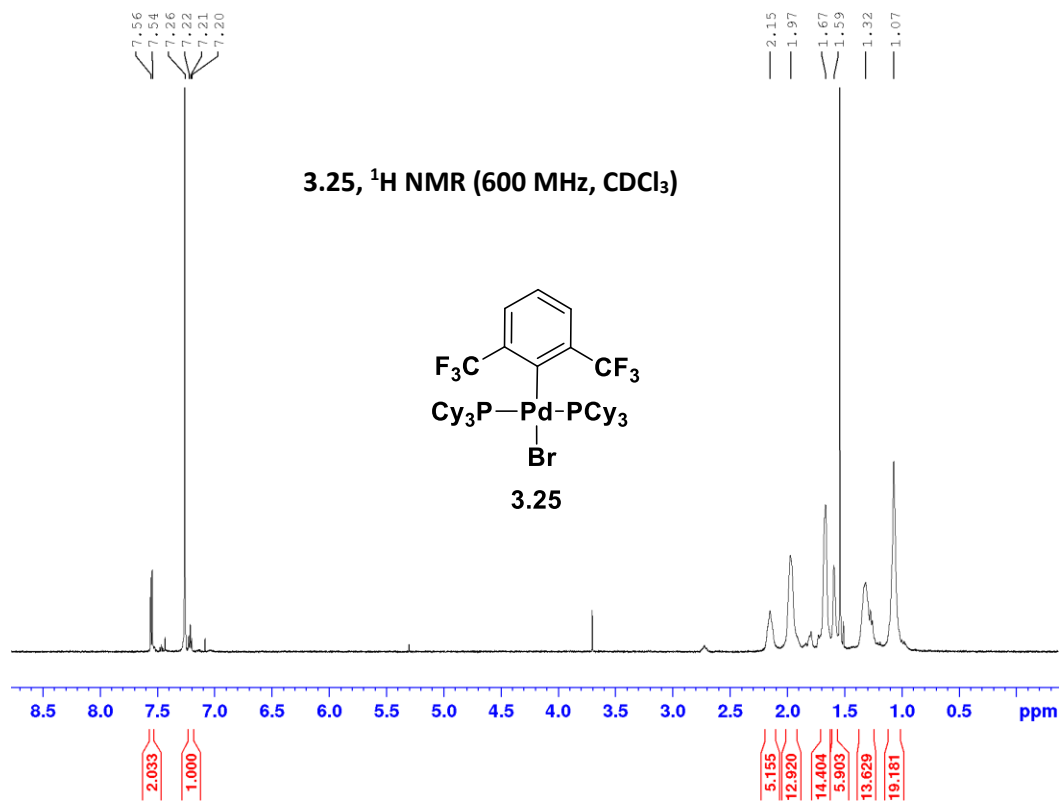
F2 - Acquisition Parameters
Date_ 20200615
Time 23.46 h
INSTRUM spect
PROBHD Z148658_0003 ()
PULPROG zgpg30
TD 65536
SOLVENT CDCl3
NS 1024
DS 4
SWH 36231.883 Hz
FIDRES 1.105709 Hz
AQ 0.9043968 sec
RG 199.73
DW 13.800 usec
DE 6.50 usec
TE 298.0 K
D1 4.00000000 sec
D11 0.03000000 sec
TDO 1
SFO1 150.8864644 MHz
NUC1 13C
P1 12.00 usec
PLW1 77.65699768 W
SFO2 600.0074000 MHz
NUC2 1H
CPDPRG2 waltz16
PCPD2 70.00 usec
PLW2 13.23200035 W
PLW12 0.64876997 W
PLW13 0.32633001 W

3.22g, ¹³C NMR (150 MHz), CDCl₃



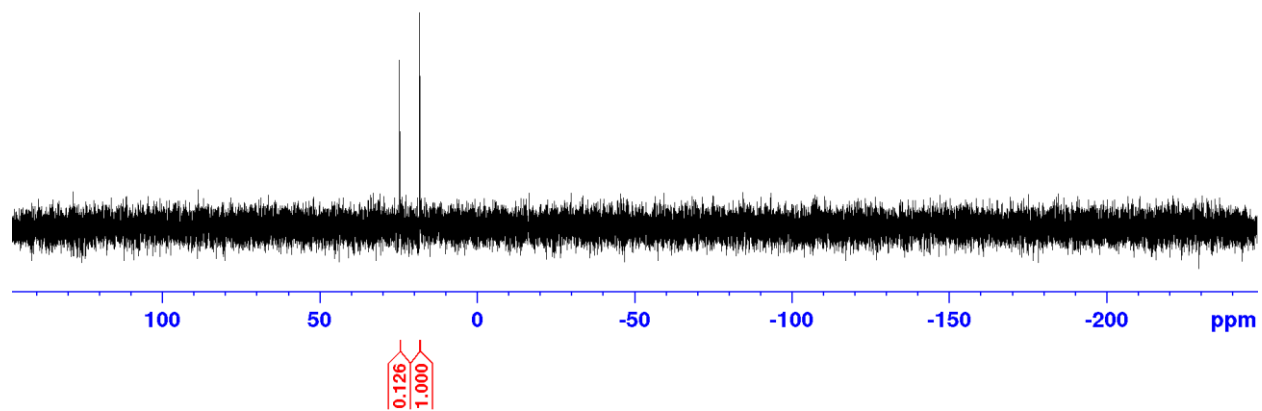
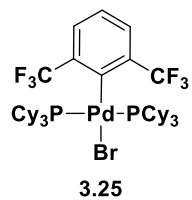
F2 - Processing parameters
SI 32768
SF 150.8713835 MHz
WDW EM
SSE 0
LB 1.00 Hz
GB 0
FC 1.40





— 24.52
— 18.15

3.25, ^{31}P NMR (243 MHz, CDCl_3)



REFERENCES

- (1) Iwatsuki, M.; Nishihara-Tsukashima, A.; Ishiyama, A.; Namatame, M.; Watanabe, Y.; Handasah, S.; Pranamuda, H.; Marwoto, B.; Matsumoto, A.; Takahashi, Y.; Otaguro, K.; Omura, S. Jogyamycin, a New Antiprotozoal Aminocyclopentitol Antibiotic, Produced by *Streptomyces* Sp. a-WM-JG-16.2. *J Antibiot (Tokyo)* **2012**, *65* (3), 169–171. <https://doi.org/10.1038/JA.2011.136>.
- (2) Hartwig, W.; Born, L. Diastereoselective and Enantioselective Total Synthesis of the Hepatoprotective Agent Clausenamamide. *J Org Chem* **1987**, *52* (19), 4352–4358. <https://doi.org/10.1021/jo00228a037>.
- (3) Davison, E. K.; Sperry, J. Natural Products with Heteroatom-Rich Ring Systems. *J Nat Prod* **2017**, *80* (11), 3060–3079. <https://doi.org/10.1021/acs.jnatprod.7b00575>.
- (4) Gupta, P.; Mahajan, N. Biocatalytic Approaches towards the Stereoselective Synthesis of Vicinal Amino Alcohols. *New Journal of Chemistry* **2018**, *42* (15), 12296–12327. <https://doi.org/10.1039/C8NJ00485D>.
- (5) Wetzel, S.; Schuffenhauer, A.; Roggo, S.; Ertl, P.; Waldmann, H. Cheminformatic Analysis of Natural Products and Their Chemical Space. *Chimia (Aarau)* **2007**, *61* (6), 355–360. <https://doi.org/10.2533/chimia.2007.355>.
- (6) Sehl, T.; Maugeri, Z.; Rother, D. Multi-Step Synthesis Strategies towards 1,2-Amino Alcohols with Special Emphasis on Phenylpropanolamines. *J Mol Catal B Enzym* **2015**, *114*, 65–71. <https://doi.org/10.1016/j.molcatb.2014.12.005>.
- (7) Mushtaq, S.; Abbasi, B. H.; Uzair, B.; Abbasi, R. Natural Products as Reservoirs of Novel Therapeutic Agents. *EXCLI J* **2018**, *17*, 420–451. <https://doi.org/10.17179/excli2018-1174>.
- (8) Bergmeier, S. C. The Synthesis of Vicinal Amino Alcohols. *Tetrahedron* **2000**, *56* (17), 2561–2576. [https://doi.org/10.1016/S0040-4020\(00\)00149-6](https://doi.org/10.1016/S0040-4020(00)00149-6).
- (9) Burchak, O. N.; Py, S. Reductive Cross-Coupling Reactions (RCCR) between CN and CO for β -Amino Alcohol Synthesis. *Tetrahedron* **2009**, *65* (36), 7333–7356. <https://doi.org/10.1016/j.tet.2009.06.003>.
- (10) Karjalainen, O. K.; Koskinen, A. M. P. Diastereoselective Synthesis of Vicinal Amino Alcohols. *Org Biomol Chem* **2012**, *10* (22), 4311–4326. <https://doi.org/10.1039/c2ob25357g>.
- (11) Brooks, W. H.; Guida, W. C.; Daniel, K. G. The Significance of Chirality in Drug Design and Development. *Curr Top Med Chem* **2011**, *11* (7), 760–770. <https://doi.org/10.2174/156802611795165098>.
- (12) Agrawal, T.; Sieber, J. D. Recent Developments in C–C Bond Formation Using Catalytic Reductive Coupling Strategies. *Synthesis (Stuttg)* **2020**, *52* (18), 2623–2638. <https://doi.org/10.1055/s-0040-1707128>.
- (13) Reichard, H. A.; McLaughlin, M.; Chen, M. Z.; Micalizio, G. C. Regioselective Reductive Cross-Coupling Reactions of Unsymmetrical Alkynes. *European J Org Chem* **2010**, 391–409. <https://doi.org/10.1002/ejoc.200901094>.
- (14) Jackson, E. P.; Malik, H. A.; Sormunen, G. J.; Baxter, R. D.; Liu, P.; Wang, H.; Shareef, A.-R.; Montgomery, J. Mechanistic Basis for Regioselection and Regiodivergence in Nickel-Catalyzed Reductive Couplings. *Acc Chem Res* **2015**, *48* (6), 1736–1745. <https://doi.org/10.1021/acs.accounts.5b00096>.
- (15) Nguyen, K. D.; Park, B. Y.; Luong, T.; Sato, H.; Garza, V. J.; Krische, M. J. Metal-Catalyzed Reductive Coupling of Olefin-Derived Nucleophiles: Reinventing Carbonyl Addition. *Science (1979)* **2016**, *354* (6310), aah5133. <https://doi.org/10.1126/science.aah5133>.
- (16) Wang, Y.; Ren, Q. DFT Study of the Mechanisms of Transition-Metal-Catalyzed Reductive Coupling Reactions. *Curr Org Chem* **2020**, *24* (12), 1367–1383. <https://doi.org/10.2174/1385272824999200608135840>.

- (17) Nugent, T. C.; El-Shazly, M. Chiral Amine Synthesis - Recent Developments and Trends for Enamide Reduction, Reductive Amination, and Imine Reduction. *Adv Synth Catal* **2010**, 352 (5), 753–819. <https://doi.org/10.1002/adsc.200900719>.
- (18) Evans, D. A. *An Organizational Format for the Classification of Functional Groups. Application to the Construction of Difunctional Relationships*; 1971.
- (19) Evans, D. A.; Andrews, G. C. Allylic Sulfoxides. Useful Intermediates in Organic Synthesis. *Acc Chem Res* **1974**, 7 (5), 147–155. https://doi.org/10.1021/AR50077A004/ASSET/AR50077A004.FP.PNG_V03.
- (20) Rehman, W.; Arfons, L. M.; Lazarus, H. M. The Rise, Fall and Subsequent Triumph of Thalidomide: Lessons Learned in Drug Development. *Ther Adv Hematol* **2011**, 2 (5), 291–308. <https://doi.org/10.1177/2040620711413165>.
- (21) Eriksson, T.; Björkman, S.; Höglund, P. Clinical Pharmacology of Thalidomide. *Eur J Clin Pharmacol* **2001**, 57 (5), 365–376. <https://doi.org/10.1007/s002280100320>.
- (22) Nguyen, L. A.; He, H.; Pham-Huy, C. Chiral Drugs: An Overview. *Int J Biomed Sci* **2006**, 2 (2), 85–100.
- (23) *Development of New Stereoisomeric Drugs*; 2005.
- (24) Kobayashi, S.; Ishitani, H. Catalytic Enantioselective Addition to Imines. *Chem Rev* **1999**, 99 (5), 1069–1094. <https://doi.org/10.1021/cr980414z>.
- (25) Trowbridge, A.; Walton, S. M.; Gaunt, M. J. New Strategies for the Transition-Metal Catalyzed Synthesis of Aliphatic Amines. *Chem Rev* **2020**, 120 (5), 2613–2692. <https://doi.org/10.1021/acs.chemrev.9b00462>.
- (26) Riant, O.; Hannedouche, J. Asymmetric Catalysis for the Construction of Quaternary Carbon Centres: Nucleophilic Addition on Ketones and Ketimines. *Org Biomol Chem* **2007**, 5 (6), 873. <https://doi.org/10.1039/b617746h>.
- (27) *The Nobel Prize in Chemistry 1990 Press Release*.
- (28) Corey, E. J.; Howe, W. J.; Orf, H. W.; Pensak, D. A.; Petersson, G. General Methods of Synthetic Analysis. Strategic Bond Disconnections for Bridged Polycyclic Structures. *J Am Chem Soc* **1975**, 97 (21), 6116–6124. <https://doi.org/10.1021/ja00854a026>.
- (29) Dibrell, S. E.; Tao, Y.; Reisman, S. E. Synthesis of Complex Diterpenes: Strategies Guided by Oxidation Pattern Analysis. *Acc Chem Res* **2021**, 54 (6), 1360–1373. <https://doi.org/10.1021/acs.accounts.0c00858>.
- (30) Seebach, D. Methods of Reactivity Umpolung. *Angewandte Chemie International Edition in English* **1979**, 18 (4), 239–258. <https://doi.org/10.1002/anie.197902393>.
- (31) Ma, J.; Harms, K.; Meggers, E. Enantioselective Rhodium/Ruthenium Photoredox Catalysis En Route to Chiral 1,2-Aminoalcohols. *Chemical Communications* **2016**, 52 (66), 10183–10186. <https://doi.org/10.1039/C6CC04397F>.
- (32) Yoon, U. C.; Kim, D. U.; Lee, C. W.; Choi, Y. S.; Lee, Y.-J.; Ammon, H. L.; Mariano, P. S. Novel and Efficient Azomethine Ylide Forming Photoreactions of N-(Silylmethyl)Phthalimides and Related Acid and Alcohol Derivatives. *J Am Chem Soc* **1995**, 117 (10), 2698–2710. <https://doi.org/10.1021/ja00115a004>.
- (33) Schwarz, J. L.; Kleinmans, R.; Paulisch, T. O.; Glorius, F. 1,2-Amino Alcohols via Cr/Photoredox Dual-Catalyzed Addition of α -Amino Carbanion Equivalents to Carbonyls. *J Am Chem Soc* **2020**, 142 (5), 2168–2174. <https://doi.org/10.1021/jacs.9b12053>.
- (34) Wang, R.; Ma, M.; Gong, X.; Fan, X.; Walsh, P. J. Reductive Cross-Coupling of Aldehydes and Imines Mediated by Visible Light Photoredox Catalysis. *Org Lett* **2019**, 21 (1), 27–31. <https://doi.org/10.1021/acs.orglett.8b03394>.

- (35) Kim, J. Y.; Lee, Y. S.; Choi, Y.; Ryu, D. H. Enantioselective 1,2-Addition of α -Aminoalkyl Radical to Aldehydes via Visible-Light Photoredox Initiated Chiral Oxazaborolidinium Ion Catalysis. *ACS Catal* **2020**, *10* (18), 10585–10591. <https://doi.org/10.1021/acscatal.0c02443>.
- (36) Seebach, D.; Kolb, M. Umpolung (Dipole Inversion) of Carbonyl Reactivity. *Chem Ind* **1974**, 687–692.
- (37) Miller, J. J.; Sigman, M. S. Design and Synthesis of Modular Oxazoline Ligands for the Enantioselective Chromium-Catalyzed Addition of Allyl Bromide to Ketones. *J Am Chem Soc* **2007**, *129* (10), 2752–2753. <https://doi.org/10.1021/ja068915m>.
- (38) Miller, J. J.; Sigman, M. S. Quantitatively Correlating the Effect of Ligand-Substituent Size in Asymmetric Catalysis Using Linear Free Energy Relationships. *Angewandte Chemie International Edition* **2008**, *47* (4), 771–774. <https://doi.org/10.1002/anie.200704257>.
- (39) Kim, I. S.; Ngai, M.-Y.; Krische, M. J. Enantioselective Iridium-Catalyzed Carbonyl Allylation from the Alcohol or Aldehyde Oxidation Level via Transfer Hydrogenative Coupling of Allyl Acetate: Departure from Chirally Modified Allyl Metal Reagents in Carbonyl Addition. *J Am Chem Soc* **2008**, *130* (44), 14891–14899. <https://doi.org/10.1021/ja805722e>.
- (40) Kim, I. S.; Ngai, M.-Y.; Krische, M. J. Enantioselective Iridium-Catalyzed Carbonyl Allylation from the Alcohol or Aldehyde Oxidation Level Using Allyl Acetate as an Allyl Metal Surrogate. *J Am Chem Soc* **2008**, *130* (20), 6340–6341. <https://doi.org/10.1021/ja802001b>.
- (41) Chen, R.-Y.; Dhondge, A. P.; Lee, G.-H.; Chen, C. A Chiral Bipyridyl Alcohol for Catalytic Enantioselective Nozaki-Hiyama-Kishi Allylation of Aldehydes and Ketones. *Adv Synth Catal* **2015**, *357* (5), 961–966. <https://doi.org/10.1002/adsc.201400945>.
- (42) Anslyn, E. v.; Dougherty, D. A. *Modern Physical Organic Chemistry*; University Science Books, 2006.
- (43) Weix, D. J. Methods and Mechanisms for Cross-Electrophile Coupling of C-Sp² Halides with Alkyl Electrophiles. *Acc Chem Res* **2015**, *48* (6), 1767–1775. <https://doi.org/10.1021/acs.accounts.5b00057>.
- (44) Wang, X.; Dai, Y.; Gong, H. Nickel-Catalyzed Reductive Couplings. *Top Curr Chem* **2016**, *374* (4), 43. <https://doi.org/10.1007/s41061-016-0042-2>.
- (45) Richmond, E.; Moran, J. Recent Advances in Nickel Catalysis Enabled by Stoichiometric Metallic Reducing Agents. *Synthesis (Stuttg)* **2018**, *50* (03), 499–513. <https://doi.org/10.1055/s-0036-1591853>.
- (46) Standley, E. A.; Tasker, S. Z.; Jensen, K. L.; Jamison, T. F. Nickel Catalysis: Synergy between Method Development and Total Synthesis. *Acc Chem Res* **2015**, *48* (5), 1503–1514. <https://doi.org/10.1021/acs.accounts.5b00064>.
- (47) Holmes, M.; Schwartz, L. A.; Krische, M. J. Intermolecular Metal-Catalyzed Reductive Coupling of Dienes, Allenes, and Enynes with Carbonyl Compounds and Imines. *Chem Rev* **2018**, *118* (12), 6026–6052. <https://doi.org/10.1021/acs.chemrev.8b00213>.
- (48) Han, S. B.; Kim, I. S.; Krische, M. J. Enantioselective Iridium-Catalyzed Carbonyl Allylation from the Alcohol Oxidation Level via Transfer Hydrogenation: Minimizing Pre-Activation for Synthetic Efficiency. *Chemical Communications* **2009**, No. 47, 7278. <https://doi.org/10.1039/b917243m>.
- (49) Hassan, A.; Krische, M. J. Unlocking Hydrogenation for C–C Bond Formation: A Brief Overview of Enantioselective Methods. *Org Process Res Dev* **2011**, *15* (6), 1236–1242. <https://doi.org/10.1021/op200195m>.
- (50) Brown, H. C.; Singaram, B. Improved Procedures for the Synthesis of Diisopinocampheylborane of High Optical Purity. *J Org Chem* **1984**, *49* (5), 945–947. <https://doi.org/10.1021/jo00179a041>.

- (51) Brown, H. C.; Kim, K. Won.; Cole, T. E.; Singaram, Bakthan. Chiral Synthesis via Organoboranes. 8. Synthetic Utility of Boronic Esters of Essentially 100% Optical Purity. Synthesis of Primary Amines of Very High Enantiomeric Purities. *J Am Chem Soc* **1986**, *108* (21), 6761–6764. <https://doi.org/10.1021/ja00281a050>.
- (52) Brown, H. C.; Desai, M. C.; Jadhav, P. K. Hydroboration. 61. Diisopinocampheylborane of High Optical Purity. Improved Preparation and Asymmetric Hydroboration of Representative Cis-Disubstituted Alkenes. *J Org Chem* **1982**, *47* (26), 5065–5069. <https://doi.org/10.1021/jo00147a004>.
- (53) Yus, M.; González-Gómez, J. C.; Foubelo, F. Catalytic Enantioselective Allylation of Carbonyl Compounds and Imines. *Chem Rev* **2011**, *111* (12), 7774–7854. <https://doi.org/10.1021/cr1004474>.
- (54) Denmark, S. E.; Fu, J. Catalytic Enantioselective Addition of Allylic Organometallic Reagents to Aldehydes and Ketones. *Chem Rev* **2003**, *103* (8), 2763–2794. <https://doi.org/10.1021/cr020050h>.
- (55) Robbins, D. W.; Lee, K.; Silverio, D. L.; Volkov, A.; Torker, S.; Hoveyda, A. H. Practical and Broadly Applicable Catalytic Enantioselective Additions of Allyl-B(Pin) Compounds to Ketones and α -Ketoesters. *Angewandte Chemie* **2016**, *128* (33), 9762–9766. <https://doi.org/10.1002/ange.201603894>.
- (56) Wada, R.; Oisaki, K.; Kanai, M.; Shibasaki, M. Catalytic Enantioselective Allylboration of Ketones. *J Am Chem Soc* **2004**, *126* (29), 8910–8911. <https://doi.org/10.1021/ja0472001>.
- (57) Alam, R.; Vollgraff, T.; Eriksson, L.; Szabó, K. J. Synthesis of Adjacent Quaternary Stereocenters by Catalytic Asymmetric Allylboration. *J Am Chem Soc* **2015**, *137* (35), 11262–11265. <https://doi.org/10.1021/jacs.5b07498>.
- (58) Lou, S.; Moquist, P. N.; Schaus, S. E. Asymmetric Allylboration of Ketones Catalyzed by Chiral Diols. *J Am Chem Soc* **2006**, *128* (39), 12660–12661. <https://doi.org/10.1021/ja0651308>.
- (59) Shi, S.-L.; Xu, L.-W.; Oisaki, K.; Kanai, M.; Shibasaki, M. Identification of Modular Chiral Bisphosphines Effective for Cu(I)-Catalyzed Asymmetric Allylation and Propargylation of Ketones. *J Am Chem Soc* **2010**, *132* (19), 6638–6639. <https://doi.org/10.1021/ja101948s>.
- (60) Denmark, S. E.; Fu, J. Understanding the Correlation of Structure and Selectivity in the Chiral-Phosphoramidate-Catalyzed Enantioselective Allylation Reactions: Solution and Solid-State Structural Studies of Bisphosphoramidate-SnCl₄ Complexes. *J Am Chem Soc* **2003**, *125* (8), 2208–2216. <https://doi.org/10.1021/ja021280g>.
- (61) Hanhan, N. v.; Tang, Y. C.; Tran, N. T.; Franz, A. K. Scandium(III)-Catalyzed Enantioselective Allylation of Isatins Using Allylsilanes. *Org Lett* **2012**, *14* (9), 2218–2221. <https://doi.org/10.1021/ol300496v>.
- (62) Wooten, A. J.; Kim, J. G.; Walsh, P. J. Highly Concentrated Catalytic Asymmetric Allylation of Ketones. *Org Lett* **2007**, *9* (3), 381–384. <https://doi.org/10.1021/ol062264h>.
- (63) Kim, J. G.; Waltz, K. M.; Garcia, I. F.; Kwiatkowski, D.; Walsh, P. J. Catalytic Asymmetric Allylation of Ketones and a Tandem Asymmetric Allylation/Diastereoselective Epoxidation of Cyclic Enones. *J Am Chem Soc* **2004**, *126* (39), 12580–12585. <https://doi.org/10.1021/ja047758t>.
- (64) Teo, Y.-C.; Goh, J.-D.; Loh, T.-P. Catalytic Enantioselective Allylation of Ketones via a Chiral Indium(III) Complex. *Org Lett* **2005**, *7* (13), 2743–2745. <https://doi.org/10.1021/ol051018n>.
- (65) Zhang, X.; Chen, D.; Liu, X.; Feng, X. Enantioselective Allylation of Ketones Catalyzed by *N,N'*-Dioxide and Indium(III) Complex. *J Org Chem* **2007**, *72* (14), 5227–5233. <https://doi.org/10.1021/jo0706325>.
- (66) Ng, S.-S.; Jamison, T. F. Highly Enantioselective and Regioselective Nickel-Catalyzed Coupling of Allenes, Aldehydes, and Silanes. *J Am Chem Soc* **2005**, *127* (20), 7320–7321. <https://doi.org/10.1021/ja0521831>.

- (67) McInturff, E. L.; Yamaguchi, E.; Krische, M. J. Chiral-Anion-Dependent Inversion of Diastereo- and Enantioselectivity in Carbonyl Crotylation via Ruthenium-Catalyzed Butadiene Hydrohydroxyalkylation. *J Am Chem Soc* **2012**, *134* (51), 20628–20631. <https://doi.org/10.1021/ja311208a>.
- (68) Liang, T.; Nguyen, K. D.; Zhang, W.; Krische, M. J. Enantioselective Ruthenium-Catalyzed Carbonyl Allylation via Alkyne–Alcohol C–C Bond-Forming Transfer Hydrogenation: Allene Hydrometalation vs Oxidative Coupling. *J Am Chem Soc* **2015**, *137* (9), 3161–3164. <https://doi.org/10.1021/jacs.5b00747>.
- (69) Grayson, M. N.; Krische, M. J.; Houk, K. N. Ruthenium-Catalyzed Asymmetric Hydrohydroxyalkylation of Butadiene: The Role of the Formyl Hydrogen Bond in Stereochemical Control. *J Am Chem Soc* **2015**, *137* (27), 8838–8850. <https://doi.org/10.1021/jacs.5b04844>.
- (70) Nguyen, K. D.; Herkommer, D.; Krische, M. J. Ruthenium-BINAP Catalyzed Alcohol C–H *Tert*-Prenylation via 1,3-Enyne Transfer Hydrogenation: Beyond Stoichiometric Carbanions in Enantioselective Carbonyl Propargylation. *J Am Chem Soc* **2016**, *138* (16), 5238–5241. <https://doi.org/10.1021/jacs.6b02279>.
- (71) Holmes, M.; Nguyen, K. D.; Schwartz, L. A.; Luong, T.; Krische, M. J. Enantioselective Formation of CF₃-Bearing All-Carbon Quaternary Stereocenters via C–H Functionalization of Methanol: Iridium Catalyzed Allene Hydrohydroxymethylation. *J Am Chem Soc* **2017**, *139* (24), 8114–8117. <https://doi.org/10.1021/jacs.7b04374>.
- (72) Zhang, W.; Chen, W.; Xiao, H.; Krische, M. J. Carbonyl *Anti*-(α -Amino)Allylation via Ruthenium Catalyzed Hydrogen Autotransfer: Use of an Acetylenic Pyrrole as an Allylmetal Pronucleophile. *Org Lett* **2017**, *19* (18), 4876–4879. <https://doi.org/10.1021/acs.orglett.7b02336>.
- (73) Schwartz, L. A.; Holmes, M.; Brito, G. A.; Gonçalves, T. P.; Richardson, J.; Ruble, J. C.; Huang, K.-W.; Krische, M. J. Cyclometalated Iridium–PhanePhos Complexes Are Active Catalysts in Enantioselective Allene–Fluoral Reductive Coupling and Related Alcohol-Mediated Carbonyl Additions That Form Acyclic Quaternary Carbon Stereocenters. *J Am Chem Soc* **2019**, *141* (5), 2087–2096. <https://doi.org/10.1021/jacs.8b11868>.
- (74) Skucas, E.; Bower, J. F.; Krische, M. J. Carbonyl Allylation in the Absence of Preformed Allyl Metal Reagents: Reverse Prenylation via Iridium-Catalyzed Hydrogenative Coupling of Dimethylallene. *J Am Chem Soc* **2007**, *129* (42), 12678–12679. <https://doi.org/10.1021/ja075971u>.
- (75) Bower, J. F.; Skucas, E.; Patman, R. L.; Krische, M. J. Catalytic C–C Coupling via Transfer Hydrogenation: Reverse Prenylation, Crotylation, and Allylation from the Alcohol or Aldehyde Oxidation Level. *J Am Chem Soc* **2007**, *129* (49), 15134–15135. <https://doi.org/10.1021/ja077389b>.
- (76) Ngai, M. Y.; Skucas, E.; Krische, M. J. Ruthenium Catalyzed C–C Bond Formation via Transfer Hydrogenation: Branch-Selective Reductive Coupling of Allenes to Paraformaldehyde and Higher Aldehydes. *Org Lett* **2008**, *10* (13), 2705–2708. <https://doi.org/10.1021/ol800836v>.
- (77) *Markets - Mining.com*. <https://www.mining.com/markets/>.
- (78) Yoshida, T.; Negishi, E. I. A Novel Copper-Containing Hydride Species and Its Application to the Reduction of Organic Substances. *J Chem Soc Chem Commun* **1974**, No. 18, 762–763. <https://doi.org/10.1039/C39740000762>.
- (79) Deutsch, C.; Krause, N.; Lipshutz, B. H. CuH-Catalyzed Reactions. *Chem Rev* **2008**, *108* (8), 2916–2927. <https://doi.org/10.1021/cr0684321>.
- (80) Liu, R. Y.; Yang, Y.; Buchwald, S. L. Regiodivergent and Diastereoselective CuH-Catalyzed Allylation of Imines with Terminal Allenes. *Angewandte Chemie International Edition* **2016**, *55* (45), 14077–14080. <https://doi.org/10.1002/anie.201608446>.

- (81) Liu, R. Y.; Zhou, Y.; Yang, Y.; Buchwald, S. L. Enantioselective Allylation Using Allene, a Petroleum Cracking Byproduct. *J Am Chem Soc* **2019**, *141* (6), 2251–2256. <https://doi.org/10.1021/jacs.8b13907>.
- (82) Tsai, E. Y.; Liu, R. Y.; Yang, Y.; Buchwald, S. L. A Regio- and Enantioselective CuH-Catalyzed Ketone Allylation with Terminal Allenes. *J Am Chem Soc* **2018**, *140* (6), 2007–2011. <https://doi.org/10.1021/jacs.7b12271>.
- (83) Li, C.; Liu, R. Y.; Jesikiewicz, L. T.; Yang, Y.; Liu, P.; Buchwald, S. L. CuH-Catalyzed Enantioselective Ketone Allylation with 1,3-Dienes: Scope, Mechanism, and Applications. *J Am Chem Soc* **2019**, *141* (12), 5062–5070. <https://doi.org/10.1021/jacs.9b01784>.
- (84) Agrawal, T.; Martin, R. T.; Collins, S.; Wilhelm, Z.; Edwards, M. D.; Gutierrez, O.; Sieber, J. D. Access to Chiral Diamine Derivatives through Stereoselective Cu-Catalyzed Reductive Coupling of Imines and Allenamides. *Journal of Organic Chemistry* **2021**, *86* (7), 5026–5046. https://doi.org/10.1021/ACS.JOC.0C02971/ASSET/IMAGES/LARGE/JO0C02971_0012.JPEG.
- (85) Murphy, S. K.; Dong, V. M. Enantioselective Ketone Hydroacylation Using Noyori's Transfer Hydrogenation Catalyst. *J Am Chem Soc* **2013**, *135* (15), 5553–5556. <https://doi.org/10.1021/ja4021974>.
- (86) Spielmann, K.; Xiang, M.; Schwartz, L. A.; Krische, M. J. Direct Conversion of Primary Alcohols to 1,2-Amino Alcohols: Enantioselective Iridium-Catalyzed Carbonyl Reductive Coupling of Phthalimido-Allene via Hydrogen Auto-Transfer. *J Am Chem Soc* **2019**, *141* (36), 14136–14141. <https://doi.org/10.1021/jacs.9b08715>.
- (87) Spielmann, K.; Xiang, M.; Schwartz, L. A.; Krische, M. J. Direct Conversion of Primary Alcohols to 1,2-Amino Alcohols: Enantioselective Iridium-Catalyzed Carbonyl Reductive Coupling of Phthalimido-Allene via Hydrogen Auto-Transfer. *J Am Chem Soc* **2019**, *141* (36), 14136–14141. <https://doi.org/10.1021/jacs.9b08715>.
- (88) Li, K.; Shao, X.; Tseng, L.; Malcolmson, S. J. 2-Azadienes as Reagents for Preparing Chiral Amines: Synthesis of 1,2-Amino Tertiary Alcohols by Cu-Catalyzed Enantioselective Reductive Couplings with Ketones. *J Am Chem Soc* **2018**, *140* (2), 598–601. <https://doi.org/10.1021/jacs.7b12213>.
- (89) Shao, X.; Li, K.; Malcolmson, S. J. Enantioselective Synthesis of *Anti*-1,2-Diamines by Cu-Catalyzed Reductive Couplings of Azadienes with Aldimines and Ketimines. *J Am Chem Soc* **2018**, *140* (23), 7083–7087. <https://doi.org/10.1021/jacs.8b04750>.
- (90) Hatano, M.; Ishihara, K. Recent Progress in the Catalytic Synthesis of Tertiary Alcohols from Ketones with Organometallic Reagents. *Synthesis (Stuttg)* **2008**, *2008* (11), 1647–1675. <https://doi.org/10.1055/s-2008-1067046>.
- (91) Shibasaki, M.; Kanai, M. Asymmetric Synthesis of Tertiary Alcohols and α -Tertiary Amines via Cu-Catalyzed C–C Bond Formation to Ketones and Ketimines. *Chem Rev* **2008**, *108* (8), 2853–2873. <https://doi.org/10.1021/cr078340r>.
- (92) Riant, O.; Hannedouche, J. Asymmetric Catalysis for the Construction of Quaternary Carbon Centres: Nucleophilic Addition on Ketones and Ketimines. *Org Biomol Chem* **2007**, *5* (6), 873. <https://doi.org/10.1039/b617746h>.
- (93) Pu, L.; Yu, H.-B. Catalytic Asymmetric Organozinc Additions to Carbonyl Compounds. *Chem Rev* **2001**, *101* (3), 757–824. <https://doi.org/10.1021/cr000411y>.
- (94) Luderer, M. R.; Bailey, W. F.; Luderer, M. R.; Fair, J. D.; Dancer, R. J.; Sommer, M. B. Asymmetric Addition of Achiral Organomagnesium Reagents or Organolithiums to Achiral Aldehydes or Ketones: A Review. *Tetrahedron Asymmetry* **2009**, *20* (9), 981–998. <https://doi.org/10.1016/j.tetasy.2009.03.015>.

- (95) Liu, Y.-L.; Lin, X.-T. Recent Advances in Catalytic Asymmetric Synthesis of Tertiary Alcohols via Nucleophilic Addition to Ketones. *Adv Synth Catal* **2019**, *361* (5), 876–918. <https://doi.org/10.1002/adsc.201801023>.
- (96) Tian, P.; Dong, H.-Q.; Lin, G.-Q. Rhodium-Catalyzed Asymmetric Arylation. *ACS Catal* **2012**, *2* (1), 95–119. <https://doi.org/10.1021/cs200562n>.
- (97) Dub, P. A.; Gordon, J. C. The Role of the Metal-Bound N–H Functionality in Noyori-Type Molecular Catalysts. *Nat Rev Chem* **2018**, *2* (12), 396–408. <https://doi.org/10.1038/s41570-018-0049-z>.
- (98) Noyori, R.; Ohkuma, T. Asymmetric Catalysis by Architectural and Functional Molecular Engineering: Practical Chemo- and Stereoselective Hydrogenation of Ketones. *Angewandte Chemie International Edition* **2001**, *40* (1), 40–73. [https://doi.org/10.1002/1521-3773\(20010105\)40:1<40::AID-ANIE40>3.0.CO;2-5](https://doi.org/10.1002/1521-3773(20010105)40:1<40::AID-ANIE40>3.0.CO;2-5).
- (99) Echeverria, P.-G.; Ayad, T.; Phansavath, P.; Ratovelomanana-Vidal, V. Recent Developments in Asymmetric Hydrogenation and Transfer Hydrogenation of Ketones and Imines through Dynamic Kinetic Resolution. *Synthesis (Stuttg)* **2016**, *48* (16), 2523–2539. <https://doi.org/10.1055/s-0035-1561648>.
- (100) Evans, D. A.; Bartroli, J.; Shih, T. L. Enantioselective Aldol Condensations. 2. Erythro-Selective Chiral Aldol Condensations via Boron Enolates. *J Am Chem Soc* **1981**, *103* (8), 2127–2129. <https://doi.org/10.1021/ja00398a058>.
- (101) Wei, L.-L.; Mulder, J. A.; Xiong, H.; Zifcick, C. A.; Douglas, C. J.; Hsung, R. P. Efficient Preparations of Novel Ynamides and Allenamides. *Tetrahedron* **2001**, *57* (3), 459–466. [https://doi.org/10.1016/S0040-4020\(00\)01014-0](https://doi.org/10.1016/S0040-4020(00)01014-0).
- (102) Takimoto, M.; Gholap, S. S.; Hou, Z. Alkylative Carboxylation of Ynamides and Allenamides with Functionalized Alkylzinc Halides and Carbon Dioxide by a Copper Catalyst. *Chemistry – A European Journal* **2019**, *25* (35), 8363–8370. <https://doi.org/10.1002/chem.201901153>.
- (103) Gholap, S. S.; Takimoto, M.; Hou, Z. Regioselective Alkylative Carboxylation of Allenamides with Carbon Dioxide and Dialkylzinc Reagents Catalyzed by an N-Heterocyclic Carbene-Copper Complex. *Chemistry - A European Journal* **2016**, *22* (25), 8547–8552. <https://doi.org/10.1002/chem.201601162>.
- (104) Díaz-Torres, R.; Alvarez, S. Coordinating Ability of Anions and Solvents towards Transition Metals and Lanthanides. *Dalton Transactions* **2011**, *40* (40), 10742. <https://doi.org/10.1039/c1dt11000d>.
- (105) Tolman, C. A. Steric Effects of Phosphorus Ligands in Organometallic Chemistry and Homogeneous Catalysis. *Chem Rev* **1977**, *77* (3), 313–348. <https://doi.org/10.1021/cr60307a002>.
- (106) Dorta, R.; Scott, N. M.; Costabile, C.; Cavallo, L.; Hoff, C. D.; Nolan, S. P. Steric and Electronic Properties of N-Heterocyclic Carbenes (NHC): A Detailed Study on Their Interaction with Ni(CO)₄. *J Am Chem Soc* **2005**, *127* (8), 2485–2495. <https://doi.org/10.1021/ja0438821>.
- (107) Klake, R. K.; Gargaro, S. L.; Gentry, S. L.; Elele, S. O.; Sieber, J. D. Development of a Strategy for Linear-Selective Cu-Catalyzed Reductive Coupling of Ketones and Allenes for the Synthesis of Chiral γ -Hydroxyaldehyde Equivalents. *Org Lett* **2019**, *21* (19), 7992–7998. <https://doi.org/10.1021/acs.orglett.9b02973>.
- (108) van Leeuwen, P. W. N. M.; Kamer, P. C. J.; Reek, J. N. H. The Bite Angle Makes the Catalyst. *Pure and Applied Chemistry* **1999**, *71* (8), 1443–1452. <https://doi.org/10.1351/pac199971081443>.
- (109) Trost, B. M.; Xie, J.; Sieber, J. D. The Palladium Catalyzed Asymmetric Addition of Oxindoles and Allenes: An Atom-Economical Versatile Method for the Construction of Chiral Indole Alkaloids. *J Am Chem Soc* **2011**, *133* (50), 20611–20622. <https://doi.org/10.1021/ja209244m>.

- (110) Shinisha, C. B.; Sunoj, R. B. Transition State Models for Probing Stereinduction in Evans Chiral Auxiliary-Based Asymmetric Aldol Reactions. *J Am Chem Soc* **2010**, *132* (35), 12319–12330. <https://doi.org/10.1021/ja101913k>.
- (111) Evans, D. A.; Takacs, J. M.; McGee, L. R.; Ennis, M. D.; Mathre, D. J.; Bartroli, J. Chiral Enolate Design. *Pure and Applied Chemistry* **1981**, *53* (6), 1109–1127. <https://doi.org/10.1351/pac198153061109>.
- (112) Evans, D. A.; Nelson, J. v.; Taber, T. R. Stereoselective Aldol Condensations. In *Topics in Stereochem*; 2007; pp 1–115. <https://doi.org/10.1002/9780470147221.ch1>.
- (113) Boreux, A.; Indukuri, K.; Gagosz, F.; Riant, O. Acyl Fluorides as Efficient Electrophiles for the Copper-Catalyzed Boroacylation of Allenes. *ACS Catal* **2017**, *7* (12), 8200–8204. <https://doi.org/10.1021/acscatal.7b02938>.
- (114) Gold, V.; Loening, K. L.; McNaught, A. D.; Shemi, P. The IUPAC Definision of the Curtin-Hammett Principle. *IUPAC Compendium of Chemical Terminology*; Blackwell Science: Oxford, 1997.
- (115) Sommer, W.; Weibel, D. *Asymmetric Catalysis Privileged Ligands and Complexes Features Include: BINAP/SEGPLHOS® Ligands and Complexes Solvias® Ligand Portfolio for Enantioselective Hydrogenation DuPhos and BPE Phospholane Ligands and Complexes*; 2008.
- (116) Nogami, H.; Matsunaga, S.; Kanai, M.; Shibasaki, M. Enantioselective Strecker-Type Reaction Promoted by Polymer-Supported Bifunctional Catalyst. *Tetrahedron Lett* **2001**, *42* (2), 279–283. [https://doi.org/10.1016/S0040-4039\(00\)01923-7](https://doi.org/10.1016/S0040-4039(00)01923-7).
- (117) Zhu, S. S.; Cefalo, D. R.; La, D. S.; Jamieson, J. Y.; Davis, W. M.; Hoveyda, A. H.; Schrock, R. R. Chiral Mo–Binol Complexes: Activity, Synthesis, and Structure. Efficient Enantioselective Six-Membered Ring Synthesis through Catalytic Metathesis. *J Am Chem Soc* **1999**, *121* (36), 8251–8259. <https://doi.org/10.1021/ja991432g>.
- (118) Lee, C.-Y.; Cheon, C.-H. Diastereomeric Resolution of *Rac* -1,1'-Bi-2-Naphthol Boronic Acid with a Chiral Boron Ligand and Its Application to Simultaneous Synthesis of (*R*)- and (*S*)-3,3'-Disubstituted 1,1'-Bi-2-Naphthol Derivatives. *J Org Chem* **2013**, *78* (14), 7086–7092. <https://doi.org/10.1021/jo400928q>.
- (119) Romanov-Michailidis, F.; Guénée, L.; Alexakis, A. Enantioselective Organocatalytic Fluorination-Induced Wagner–Meerwein Rearrangement. *Angewandte Chemie* **2013**, *125* (35), 9436–9440. <https://doi.org/10.1002/ange.201303527>.
- (120) Arnold, L. A.; Imbos, R.; Mandoli, A.; de Vries, A. H. M.; Naasz, R.; Feringa, B. L. Enantioselective Catalytic Conjugate Addition of Dialkylzinc Reagents Using Copper–Phosphoramidite Complexes; Ligand Variation and Non-Linear Effects. *Tetrahedron* **2000**, *56* (18), 2865–2878. [https://doi.org/10.1016/S0040-4020\(00\)00142-3](https://doi.org/10.1016/S0040-4020(00)00142-3).
- (121) Qu, B.; Haddad, N.; Rodriguez, S.; Sieber, J. D.; Desrosiers, J.-N.; Patel, N. D.; Zhang, Y.; Grinberg, N.; Lee, H.; Ma, S.; Ries, U. J.; Yee, N. K.; Senanayake, C. H. Ligand-Accelerated Stereoretentive Suzuki–Miyaura Coupling of Unprotected 3,3'-Dibromo-BINOL. *J Org Chem* **2016**, *81* (3), 745–750. <https://doi.org/10.1021/acs.joc.5b02368>.
- (122) Maruoka, K.; Itoh, T.; Araki, Y.; Shirasaka, T.; Yamamoto, H. Efficient Synthesis of Sterically Hindered Chiral Binaphthol Derivatives. *Bull Chem Soc Jpn* **1988**, *61* (8), 2975–2976. <https://doi.org/10.1246/bcsj.61.2975>.
- (123) Green, J. C.; Zanghi, J. M.; Meek, S. J. Diastereo- and Enantioselective Synthesis of Homoallylic Amines Bearing Quaternary Carbon Centers. *J Am Chem Soc* **2020**, *142* (4), 1704–1709. <https://doi.org/10.1021/jacs.9b11529>.

- (124) Tay, J.-H.; Arguelles, A. J.; Nagorny, P. Direct Interconversion of BINOL and H8-BINOL-Based Chiral Brønsted Acids Using Single-Step Red/Ox Manipulations. *Org Lett* **2015**, *17* (15), 3774–3777. <https://doi.org/10.1021/acs.orglett.5b01754>.
- (125) Erre, G.; Junge, K.; Enthaler, S.; Addis, D.; Michalik, D.; Spannenberg, A.; Beller, M. Synthesis of Novel Monodentate Phosphoramidites and Their Application in Iridium-Catalyzed Asymmetric Hydrogenations. *Chem Asian J* **2008**, *3* (5), 887–894. <https://doi.org/10.1002/asia.200800017>.
- (126) Turlington, M.; DeBerardinis, A. M.; Pu, L. Highly Enantioselective Catalytic Alkyl Propiolate Addition to Aliphatic Aldehydes. *Org Lett* **2009**, *11* (11), 2441–2444. <https://doi.org/10.1021/ol900667g>.
- (127) Zanghi, J. M.; Meek, S. J. Cu-Catalyzed Diastereo- and Enantioselective Reactions of γ,Γ -Disubstituted Allyldiboron Compounds with Ketones. *Angewandte Chemie International Edition* **2020**, *59* (22), 8451–8455. <https://doi.org/10.1002/anie.202000675>.
- (128) Bartoszek, M.; Beller, M.; Deutsch, J.; Klawonn, M.; Köckritz, A.; Nemati, N.; Pews-Davtyan, A. A Convenient Protocol for the Synthesis of Axially Chiral Brønsted Acids. *Tetrahedron* **2008**, *64* (7), 1316–1322. <https://doi.org/10.1016/j.tet.2007.11.067>.
- (129) Zhou, Y.; Wang, J.; Gu, Z.; Wang, S.; Zhu, W.; Aceña, J. L.; Soloshonok, V. A.; Izawa, K.; Liu, H. Next Generation of Fluorine-Containing Pharmaceuticals, Compounds Currently in Phase II–III Clinical Trials of Major Pharmaceutical Companies: New Structural Trends and Therapeutic Areas. *Chem Rev* **2016**, *116* (2), 422–518. <https://doi.org/10.1021/acs.chemrev.5b00392>.
- (130) Purser, S.; Moore, P. R.; Swallow, S.; Gouverneur, V. Fluorine in Medicinal Chemistry. *Chem. Soc. Rev.* **2008**, *37* (2), 320–330. <https://doi.org/10.1039/B610213C>.
- (131) Gillis, E. P.; Eastman, K. J.; Hill, M. D.; Donnelly, D. J.; Meanwell, N. A. Applications of Fluorine in Medicinal Chemistry. *J Med Chem* **2015**, *58* (21), 8315–8359. <https://doi.org/10.1021/acs.jmedchem.5b00258>.
- (132) Meanwell, N. A. Fluorine and Fluorinated Motifs in the Design and Application of Bioisosteres for Drug Design. *J Med Chem* **2018**, *61* (14), 5822–5880. <https://doi.org/10.1021/acs.jmedchem.7b01788>.
- (133) Creary, X. Reaction of Organometallic Reagents with Ethyl Trifluoroacetate and Diethyl Oxalate. Formation of Trifluoromethyl Ketones and α -Keto Esters via Stable Tetrahedral Adducts. *J Org Chem* **1987**, *52* (22), 5026–5030. <https://doi.org/10.1021/jo00231a036>.
- (134) Klake, R. K.; Collins, S. A.; Sieber, J. D. A Unified Approach to the Aminoallylation of Carbonyl Compounds Through Cu-Catalyzed Enantioselective Reductive Coupling of Allenamides. *ChemRXIV* **2022**.
- (135) Creary, X. Reaction of Organometallic Reagents with Ethyl Trifluoroacetate and Diethyl Oxalate. Formation of Trifluoromethyl Ketones and α -Keto Esters via Stable Tetrahedral Adducts. *Journal of Organic Chemistry* **1987**, *52* (22), 5026–5030. <https://doi.org/10.1021/jo00231a036>.
- (136) Bousfield, T. W.; Kimber, M. C. A Simple One-Pot Preparation of N-Allenyl Amides, Ureas, Carbamates and Sulfonamides Using a DMSO/TBuOK Protocol. *Tetrahedron Lett* **2015**, *56* (2), 350–352. <https://doi.org/10.1016/j.tetlet.2014.11.093>.
- (137) Dinev, Z.; Gannon, C. T.; Egan, C.; Watt, J. A.; McConville, M. J.; Williams, S. J. Galactose-Derived Phosphonate Analogues as Potential Inhibitors of Phosphatidylinositol Biosynthesis in Mycobacteria. *Org Biomol Chem* **2007**, *5* (6), 952. <https://doi.org/10.1039/b616450a>.
- (138) Gargaro, S. L.; Klake, R. K.; Burns, K. L.; Elele, S. O.; Gentry, S. L.; Sieber, J. D. Access to a Catalytically Generated Umpolung Reagent through the Use of Cu-Catalyzed Reductive Coupling of Ketones and Allenes for the Synthesis of Chiral Vicinal Aminoalcohol Synthons. *Org Lett* **2019**, *21* (23), 9753–9758. <https://doi.org/10.1021/acs.orglett.9b03937>.

- (139) Haider, S.; Alam, M. S.; Hamid, H.; Shafi, S.; Nargotra, A.; Mahajan, P.; Nazreen, S.; Kalle, A. M.; Kharbanda, C.; Ali, Y.; Alam, A.; Panda, A. K. Synthesis of Novel 1,2,3-Triazole Based Benzoxazolinones: Their TNF- α Based Molecular Docking with in-Vivo Anti-Inflammatory, Antinociceptive Activities and Ulcerogenic Risk Evaluation. *Eur J Med Chem* **2013**, *70*, 579–588. <https://doi.org/10.1016/j.ejmech.2013.10.032>.
- (140) Seebach, D.; Enders, D. Umpolung of Amine Reactivity. Nucleophilic α -(Secondary Amino)-Alkylation via Metalated Nitrosamines. *Angewandte Chemie International Edition in English* **1975**, *14* (1), 15–32. <https://doi.org/10.1002/anie.197500151>.
- (141) Beak, P.; Zajdel, W. J.; Reitz, D. B. Metalation and Electrophilic Substitution of Amine Derivatives Adjacent to Nitrogen: α -Metallo Amine Synthetic Equivalents. *Chem Rev* **1984**, *84* (5), 471–523. <https://doi.org/10.1021/cr00063a003>.
- (142) Peterson, D. J. N,N-Disubstituted Aminomethylithium Compounds. *J Am Chem Soc* **1971**, *93* (16), 4027–4031. <https://doi.org/10.1021/ja00745a034>.
- (143) Palomo, C.; Oiarbide, M.; Laso, A. Recent Advances in the Catalytic Asymmetric Nitroaldol (Henry) Reaction. *European J Org Chem* **2007**, *2007* (16), 2561–2574. <https://doi.org/10.1002/ejoc.200700021>.
- (144) Zhang, S.; Li, Y.; Xu, Y.; Wang, Z. Recent Progress in Copper Catalyzed Asymmetric Henry Reaction. *Chinese Chemical Letters* **2018**, *29* (6), 873–883. <https://doi.org/10.1016/j.ccl.2017.10.001>.
- (145) Hemming, D.; Fritzsche, R.; Westcott, S. A.; Santos, W. L.; Steel, P. G. Copper-Boryl Mediated Organic Synthesis. *Chem Soc Rev* **2018**, *47* (19), 7477–7494. <https://doi.org/10.1039/C7CS00816C>.
- (146) Lipshutz, B. H.; Chrisman, W.; Noson, K. Hydrosilylation of Aldehydes and Ketones Catalyzed by [Ph₃P(CuH)]₆. *J Organomet Chem* **2001**, *624* (1–2), 367–371. [https://doi.org/10.1016/S0022-328X\(00\)00903-7](https://doi.org/10.1016/S0022-328X(00)00903-7).
- (147) Chen, J.-X.; Daeuble, J. F.; Brestensky, D. M.; Stryker, J. M. Highly Chemoselective Catalytic Hydrogenation of Unsaturated Ketones and Aldehydes to Unsaturated Alcohols Using Phosphine-Stabilized Copper(I) Hydride Complexes. *Tetrahedron* **2000**, *56* (15), 2153–2166. [https://doi.org/10.1016/S0040-4020\(99\)01098-4](https://doi.org/10.1016/S0040-4020(99)01098-4).
- (148) Meng, F.; Jang, H.; Jung, B.; Hoveyda, A. H. Cu-Catalyzed Chemoselective Preparation of 2-(Pinacolato)Boron-Substituted Allylcopper Complexes and Their In situ Site-, Diastereo-, and Enantioselective Additions to Aldehydes and Ketones. *Angewandte Chemie - International Edition* **2013**, *52* (19), 5046–5051. <https://doi.org/10.1002/anie.201301018>. Cu-Catalyzed.
- (149) Xiang, M.; Pfaffinger, D. E.; Krische, M. J. Allenes and Dienes as Chiral Allylmetal Pronucleophiles in Catalytic Enantioselective C=X Addition: Historical Perspective and State-of-The-Art Survey. *Chemistry – A European Journal* **2021**, *27* (52), 13107–13116. <https://doi.org/10.1002/chem.202101890>.
- (150) Ho, D.; Gargaro, S. L.; Klake, R.; Sieber, J. Development of a Modified System to Provide Improved Diastereocontrol in the Linear-Selective Cu-Catalyzed Reductive Coupling of Ketones and Allenamides. *J Org Chem* **2022**, *87* (4), 2142–2153. <https://doi.org/10.1021/acs.joc.1c02062>.
- (151) Klake, R. K.; Edwards, M. D.; Sieber, J. D. Synthesis of 1,2-Aminoalcohols through Enantioselective Aminoallylation of Ketones by Cu-Catalyzed Reductive Coupling. *Org Lett* **2021**, *23* (16), 6444–6449. https://doi.org/10.1021/ACS.ORGLETT.1C02258/SUPPL_FILE/OL1C02258_SI_001.PDF.
- (152) Skucas, E.; Zbieg, J. R.; Krische, M. J. Anti-Aminoallylation of Aldehydes via Ruthenium-Catalyzed Transfer Hydrogenative Coupling of Sulfonamido Allenes: 1,2-Aminoalcohols. <https://doi.org/10.1021/ja900827p>.

- (153) Zhang, W.; Chen, W.; Xiao, H.; Krische, M. J. Carbonyl *Anti*-(α -Amino)Allylation via Ruthenium Catalyzed Hydrogen Autotransfer: Use of an Acetylenic Pyrrole as an Allylmetal Pronucleophile. *Org Lett* **2017**, *19* (18), 4876–4879. <https://doi.org/10.1021/acs.orglett.7b02336>.
- (154) Zbieg, J. R.; McInturff, E. L.; Krische, M. J. Allenamide Hydro–Hydroxyalkylation: 1,2-Amino Alcohols via Ruthenium-Catalyzed Carbonyl *Anti* -Aminoallylation. *Org Lett* **2010**, *12* (11), 2514–2516. <https://doi.org/10.1021/ol1007235>.
- (155) Yeung, K.; Ruscoe, R. E.; Rae, J.; Pulis, A. P.; Procter, D. J. Enantioselective Generation of Adjacent Stereocenters in a Copper-Catalyzed Three-Component Coupling of Imines, Allenes, and Diboranes. *Angewandte Chemie* **2016**, *128* (39), 12091–12095. <https://doi.org/10.1002/ange.201606710>.
- (156) Suzuki, A. Organoborates in New Synthetic Reactions. *Acc Chem Res* **1982**, *15* (6), 178–184. <https://doi.org/10.1021/ar00078a003>.
- (157) Pelter, A. Tilden Lecture. Carbon–Carbon Bond Formation Involving Boron Reagents. *Chem. Soc. Rev.* **1982**, *11* (2), 191–225. <https://doi.org/10.1039/CS9821100191>.
- (158) Sandford, C.; Aggarwal, V. K. Stereospecific Functionalizations and Transformations of Secondary and Tertiary Boronic Esters. *Chemical Communications* **2017**, *53* (40), 5481–5494. <https://doi.org/10.1039/C7CC01254C>.
- (159) Matteson, D. S. α -Halo Boronic Esters: Intermediates for Stereodirected Synthesis. *Chem Rev* **1989**, *89* (7), 1535–1551. <https://doi.org/10.1021/cr00097a009>.
- (160) Gargaro, S. L.; Sieber, J. D. Asymmetric Access to Boryl-Substituted Vicinal Aminoalcohols through Cu-Catalyzed Reductive Coupling. *ChemRXIV* **2022**.
- (161) Yang, Y.; Perry, I. B.; Lu, G.; Liu, P.; Buchwald, S. L. Copper-Catalyzed Asymmetric Addition of Olefin-Derived Nucleophiles to Ketones. *Science (1979)* **2016**, *353* (6295), 144–150. <https://doi.org/10.1126/science.aaf7720>.
- (162) Miyaura, Norio.; Suzuki, Akira. Palladium-Catalyzed Cross-Coupling Reactions of Organoboron Compounds. *Chem Rev* **1995**, *95* (7), 2457–2483. <https://doi.org/10.1021/cr00039a007>.
- (163) Johansson Seechurn, C. C. C.; Kitching, M. O.; Colacot, T. J.; Snieckus, V. Palladium-Catalyzed Cross-Coupling: A Historical Contextual Perspective to the 2010 Nobel Prize. *Angewandte Chemie International Edition* **2012**, *51* (21), 5062–5085. <https://doi.org/10.1002/anie.201107017>.
- (164) Miyaura, N. Organoboron Compounds. In *Cross-Coupling Reactions, Topics in Current Chemistry*; Miyaura, N., Ed.; Springer Berlin Heidelberg: Berlin, Heidelberg, 2002; Vol. 219. <https://doi.org/10.1007/3-540-45313-X>.
- (165) Shing, T. K. In *Comprehensive Organic Synthesis*; Trost, B. M., Fleming, I., Eds.; Pergamon Press: Oxford, 1991; Vol. 7.
- (166) Paterson, I.; McClure, C. K. Studies in Macrolide Synthesis: Aldol Condensations of Chiral Ethylketones via Boron Enolates. *Tetrahedron Lett* **1987**, *28* (11), 1229–1232. [https://doi.org/10.1016/S0040-4039\(00\)95333-4](https://doi.org/10.1016/S0040-4039(00)95333-4).
- (167) Meng, F.; Jung, B.; Haeffner, F.; Hoveyda, A. H. NHC–Cu-Catalyzed Protoboration of Monosubstituted Allenes. Ligand-Controlled Site Selectivity, Application to Synthesis and Mechanism. *Org Lett* **2013**, *15* (6), 1414–1417. <https://doi.org/10.1021/ol4004178>.
- (168) Jang, H.; Jung, B.; Hoveyda, A. H. Catalytic Enantioselective Protoboration of Disubstituted Allenes. Access to Alkenylboron Compounds in High Enantiomeric Purity. *Org Lett* **2014**, *16* (17), 4658–4661. <https://doi.org/10.1021/ol5022417>.

- (169) Houk, K. N.; Rondan, N. G.; Wu, Y.-D.; Metz, J. T.; Paddon-Row, M. N. Theoretical Studies of Stereoselective Hydroborations. *Tetrahedron* **1984**, *40* (12), 2257–2274. [https://doi.org/10.1016/0040-4020\(84\)80009-5](https://doi.org/10.1016/0040-4020(84)80009-5).
- (170) Suzuki, A. Recent Advances in the Cross-Coupling Reactions of Organoboron Derivatives with Organic Electrophiles, 1995–1998. *J Organomet Chem* **1999**, *576* (1–2), 147–168. [https://doi.org/10.1016/S0022-328X\(98\)01055-9](https://doi.org/10.1016/S0022-328X(98)01055-9).
- (171) Alonso, F.; Beletskaya, I. P.; Yus, M. Non-Conventional Methodologies for Transition-Metal Catalysed Carbon–Carbon Coupling: A Critical Overview. Part 2: The Suzuki Reaction. *Tetrahedron* **2008**, *64* (14), 3047–3101. <https://doi.org/10.1016/j.tet.2007.12.036>.
- (172) Dumrath, A.; Lübbe, C.; Beller, M. Palladium-Catalyzed Cross-Coupling Reactions - Industrial Applications. In *Palladium-Catalyzed Coupling Reactions*; Wiley-VCH Verlag GmbH & Co. KGaA: Weinheim, Germany, 2013; pp 445–489. <https://doi.org/10.1002/9783527648283.ch12>.
- (173) Torborg, C.; Beller, M. Recent Applications of Palladium-Catalyzed Coupling Reactions in the Pharmaceutical, Agrochemical, and Fine Chemical Industries. *Adv Synth Catal* **2009**, *351* (18), 3027–3043. <https://doi.org/10.1002/adsc.200900587>.
- (174) L. Budarin, V.; S. Shuttleworth, P.; H. Clark, J.; Luque, R. Industrial Applications of C-C Coupling Reactions. *Curr Org Synth* **2010**, *7* (6), 614–627. <https://doi.org/10.2174/157017910794328529>.
- (175) Kurti, L.; Czako, B. *Strategic Applications of Named Reactions in Organic Synthesis*; 2005. <https://doi.org/10.1002/ardp.19122500151>.
- (176) Blakemore, D. Chapter 1. Suzuki-Miyaura Coupling. In *Synthetic Methods in Drug Discovery*; Royal Society of Chemistry, 2015; Vol. 1, pp 1–69. <https://doi.org/10.1039/9781782622086-00001>.
- (177) Schreiner, P. R. Metal-Free Organocatalysis through Explicit Hydrogen Bonding Interactions. *Chem Soc Rev* **2003**, *32* (5), 289. <https://doi.org/10.1039/b107298f>.
- (178) Adamo, C.; Amatore, C.; Ciofini, I.; Jutand, A.; Lakmini, H. Mechanism of the Palladium-Catalyzed Homocoupling of Arylboronic Acids: Key Involvement of a Palladium Peroxo Complex. *J Am Chem Soc* **2006**, *128* (21), 6829–6836. <https://doi.org/10.1021/ja0569959>.
- (179) Moreno-Mañas, M.; Pérez, M.; Pleixats, R. Palladium-Catalyzed Suzuki-Type Self-Coupling of Arylboronic Acids. A Mechanistic Study. *J Org Chem* **1996**, *61* (7), 2346–2351. <https://doi.org/10.1021/jo9514329>.
- (180) Aramendía, M. A.; Lafont, F.; Moreno-Mañas, M.; Pleixats, R.; Roglans, A. Electrospray Ionization Mass Spectrometry Detection of Intermediates in the Palladium-Catalyzed Oxidative Self-Coupling of Areneboronic Acids. *J Org Chem* **1999**, *64* (10), 3592–3594. <https://doi.org/10.1021/jo982210o>.
- (181) Yoshida, H.; Yamaryo, Y.; Ohshita, J.; Kunai, A. Base-Free Oxidative Homocoupling of Arylboronic Esters. *Tetrahedron Lett* **2003**, *44* (8), 1541–1544. [https://doi.org/10.1016/S0040-4039\(03\)00023-6](https://doi.org/10.1016/S0040-4039(03)00023-6).
- (182) Wong, M. S.; Zhang, X. L. Ligand Promoted Palladium-Catalyzed Homo-Coupling of Arylboronic Acids. *Tetrahedron Lett* **2001**, *42* (24), 4087–4089. [https://doi.org/10.1016/S0040-4039\(01\)00637-2](https://doi.org/10.1016/S0040-4039(01)00637-2).
- (183) Busacca, C. A.; Fandrick, D. R.; Song, J. J.; Senanayake, C. H. The Growing Impact of Catalysis in the Pharmaceutical Industry. *Adv Synth Catal* **2011**, *353* (11–12), 1825–1864. <https://doi.org/10.1002/ADSC.201100488>.
- (184) Blaser, H.; Pugin, B.; Studer, M. *Chiral Catalyst Immobilization and Recycling*; de Vos, D. E., Vankelecom, I. F. J., Jacobs, P. A., Eds.; Wiley, 2000. <https://doi.org/10.1002/9783527613144>.

- (185) Côté, A. P.; Benin, A. I.; Ockwig, N. W.; O’Keeffe, M.; Matzger, A. J.; Yaghi, O. M. Porous, Crystalline, Covalent Organic Frameworks. *Science (1979)* **2005**, *310* (5751), 1166–1170. <https://doi.org/10.1126/science.1120411>.
- (186) Sharma, R. K.; Yadav, P.; Yadav, M.; Gupta, R.; Rana, P.; Srivastava, A.; Zbořil, R.; Varma, R. S.; Antonietti, M.; Gawande, M. B. Recent Development of Covalent Organic Frameworks (COFs): Synthesis and Catalytic (Organic-Electro-Photo) Applications. *Mater Horiz* **2020**, *7* (2), 411–454. <https://doi.org/10.1039/C9MH00856J>.
- (187) Feng, X.; Ding, X.; Jiang, D. Covalent Organic Frameworks. *Chem Soc Rev* **2012**, *41* (18), 6010–6022. <https://doi.org/10.1039/C2CS35157A>.
- (188) Ding, S. Y.; Wang, W. Covalent Organic Frameworks (COFs): From Design to Applications. *Chem Soc Rev* **2013**, *42* (2), 548–568. <https://doi.org/10.1039/C2CS35072F>.
- (189) Hu, H.; Yan, Q.; Ge, R.; Gao, Y. Covalent Organic Frameworks as Heterogeneous Catalysts. *Chinese Journal of Catalysis* **2018**, *39* (7), 1167–1179. [https://doi.org/10.1016/S1872-2067\(18\)63057-8](https://doi.org/10.1016/S1872-2067(18)63057-8).
- (190) Geng, K.; He, T.; Liu, R.; Dalapati, S.; Tian Tan, K.; Li, Z.; Tao, S.; Gong, Y.; Jiang, Q.; Jiang, D. Covalent Organic Frameworks: Design, Synthesis, and Functions. *Chem Rev* **2020**, *120*, 8814–8933. <https://doi.org/10.1021/acs.chemrev.9b00550>.
- (191) Dolbier, W. R. Fluorine Chemistry at the Millennium. *J Fluor Chem* **2005**, *126* (2), 157–163. <https://doi.org/10.1016/j.jfluchem.2004.09.033>.
- (192) Müller, K.; Faeh, C.; Diederich, F. Fluorine in Pharmaceuticals: Looking Beyond Intuition. *Science (1979)* **2007**, *317* (5846), 1881–1886. <https://doi.org/10.1126/science.1131943>.
- (193) O’Hagan, D. Understanding Organofluorine Chemistry. An Introduction to the C–F Bond. *Chem. Soc. Rev.* **2008**, *37* (2), 308–319. <https://doi.org/10.1039/B711844A>.
- (194) Yale, H. L. The Trifluoromethyl Group in Medical Chemistry. *J Med Pharm Chem* **1959**, *1* (2), 121–133. <https://doi.org/10.1021/jm50003a001>.
- (195) Arnott, J. A.; Planey, S. L. The Influence of Lipophilicity in Drug Discovery and Design. *Expert Opin Drug Discov* **2012**, *7* (10), 863–875. <https://doi.org/10.1517/17460441.2012.714363>.
- (196) Shah, P.; Westwell, A. D. The Role of Fluorine in Medicinal Chemistry. *J Enzyme Inhib Med Chem* **2007**, *22* (5), 527–540. <https://doi.org/10.1080/14756360701425014>.
- (197) Dehnen, S.; Schafer, L. L.; Lectka, T.; Togni, A. Fluorine: A Very Special Element and Its Very Special Impacts on Chemistry. *Inorg Chem* **2021**, *60* (23), 17419–17425. <https://doi.org/10.1021/acs.inorgchem.1c03509>.
- (198) Miyaura, N.; Yamada, K.; Suzuki, A. A New Stereospecific Cross-Coupling by the Palladium-Catalyzed Reaction of 1-Alkenylboranes with 1-Alkenyl or 1-Alkynyl Halides. *Tetrahedron Lett* **1979**, *20* (36), 3437–3440. [https://doi.org/10.1016/S0040-4039\(01\)95429-2](https://doi.org/10.1016/S0040-4039(01)95429-2).
- (199) Miyaura, N.; Yanagi, T.; Suzuki, A. The Palladium-Catalyzed Cross-Coupling Reaction of Phenylboronic Acid with Haloarenes in the Presence of Bases. *Synth Commun* **1981**, *11* (7), 513–519. <https://doi.org/10.1080/00397918108063618>.
- (200) Miyaura, N.; Suzuki, A. Stereoselective Synthesis of Arylated (E)-Alkenes by the Reaction of Alk-1-Enylboranes with Aryl Halides in the Presence of Palladium Catalyst. *J Chem Soc Chem Commun* **1979**, No. 19, 866. <https://doi.org/10.1039/c39790000866>.

- (201) Bellina, F.; Carpita, A.; Rossi, R. Palladium Catalysts for the Suzuki Cross-Coupling Reaction: An Overview of Recent Advances. *Synthesis (Stuttg)* **2004**, *2004* (15), 2419–2440. <https://doi.org/10.1055/s-2004-831223>.
- (202) Christmann, U.; Vilar, R. Monoligated Palladium Species as Catalysts in Cross-Coupling Reactions. *Angewandte Chemie International Edition* **2005**, *44* (3), 366–374. <https://doi.org/10.1002/anie.200461189>.
- (203) Lundgren, R. J.; Stradiotto, M. Addressing Challenges in Palladium-Catalyzed Cross-Coupling Reactions Through Ligand Design. *Chemistry - A European Journal* **2012**, *18* (32), 9758–9769. <https://doi.org/10.1002/chem.201201195>.
- (204) Miura, M. Rational Ligand Design in Constructing Efficient Catalyst Systems for Suzuki–Miyaura Coupling. *Angewandte Chemie International Edition* **2004**, *43* (17), 2201–2203. <https://doi.org/10.1002/anie.200301753>.
- (205) Martin, R.; Buchwald, S. L. Palladium-Catalyzed Suzuki–Miyaura Cross-Coupling Reactions Employing Dialkylbiaryl Phosphine Ligands. *Acc Chem Res* **2008**, *41* (11), 1461–1473. <https://doi.org/10.1021/ar800036s>.
- (206) DeAngelis, A. J.; Gildner, P. G.; Chow, R.; Colacot, T. J. Generating Active “L-Pd(0)” via Neutral or Cationic π -Allylpalladium Complexes Featuring Biaryl/Bipyrazolylphosphines: Synthetic, Mechanistic, and Structure–Activity Studies in Challenging Cross-Coupling Reactions. *J Org Chem* **2015**, *80* (13), 6794–6813. <https://doi.org/10.1021/acs.joc.5b01005>.
- (207) Kinzel, T.; Zhang, Y.; Buchwald, S. L. A New Palladium Precatalyst Allows for the Fast Suzuki–Miyaura Coupling Reactions of Unstable Polyfluorophenyl and 2-Heteroaryl Boronic Acids. *J Am Chem Soc* **2010**, *132* (40), 14073–14075. <https://doi.org/10.1021/ja1073799>.
- (208) Yang, Y.; Oldenhuis, N. J.; Buchwald, S. L. Mild and General Conditions for Negishi Cross-Coupling Enabled by the Use of Palladacycle Precatalysts. *Angewandte Chemie International Edition* **2013**, *52* (2), 615–619. <https://doi.org/10.1002/anie.201207750>.
- (209) Bruno, N. C.; Tudge, M. T.; Buchwald, S. L. Design and Preparation of New Palladium Precatalysts for C–C and C–N Cross-Coupling Reactions. *Chem. Sci.* **2013**, *4* (3), 916–920. <https://doi.org/10.1039/C2SC20903A>.
- (210) Li, H.; Johansson Seechurn, C. C. C.; Colacot, T. J. Development of Preformed Pd Catalysts for Cross-Coupling Reactions, Beyond the 2010 Nobel Prize. *ACS Catal* **2012**, *2* (6), 1147–1164. <https://doi.org/10.1021/cs300082f>.
- (211) Gildner, P. G.; Colacot, T. J. Reactions of the 21st Century: Two Decades of Innovative Catalyst Design for Palladium-Catalyzed Cross-Couplings. *Organometallics* **2015**, *34* (23), 5497–5508. <https://doi.org/10.1021/acs.organomet.5b00567>.
- (212) Littke, A. F.; Dai, C.; Fu, G. C. Versatile Catalysts for the Suzuki Cross-Coupling of Arylboronic Acids with Aryl and Vinyl Halides and Triflates under Mild Conditions. *J Am Chem Soc* **2000**, *122* (17), 4020–4028. <https://doi.org/10.1021/ja0002058>.
- (213) Carrow, B. P.; Hartwig, J. F. Distinguishing Between Pathways for Transmetalation in Suzuki–Miyaura Reactions. *J Am Chem Soc* **2011**, *133* (7), 2116–2119. <https://doi.org/10.1021/ja1108326>.
- (214) Miyaura, N. Cross-Coupling Reaction of Organoboron Compounds via Base-Assisted Transmetalation to Palladium(II) Complexes. *J Organomet Chem* **2002**, *653* (1–2), 54–57. [https://doi.org/10.1016/S0022-328X\(02\)01264-0](https://doi.org/10.1016/S0022-328X(02)01264-0).

- (215) Amatore, C.; Pfluger, F. Mechanism of Oxidative Addition of Palladium(0) with Aromatic Iodides in Toluene, Monitored at Ultramicroelectrodes. *Organometallics* **1990**, *9* (8), 2276–2282. <https://doi.org/10.1021/om00158a026>.
- (216) Lennox, A. J. J.; Lloyd-Jones, G. C. Transmetalation in the Suzuki-Miyaura Coupling: The Fork in the Trail. *Angewandte Chemie International Edition* **2013**, *52* (29), 7362–7370. <https://doi.org/10.1002/anie.201301737>.
- (217) Masamune, S.; Choy, W.; Petersen, J. S.; Sita, L. R. Double Asymmetric Synthesis and a New Strategy for Stereochemical Control in Organic Synthesis. *Angewandte Chemie International Edition in English* **1985**, *24* (1), 1–30. <https://doi.org/10.1002/anie.198500013>.
- (218) Lennox, A. J. J.; Lloyd-Jones, G. C. The Slow-Release Strategy in Suzuki-Miyaura Coupling. *Isr J Chem* **2010**, *50* (5–6), 664–674. <https://doi.org/10.1002/ijch.201000074>.
- (219) Cox, P. A.; Leach, A. G.; Campbell, A. D.; Lloyd-Jones, G. C. Protodeboronation of Heteroaromatic, Vinyl, and Cyclopropyl Boronic Acids: PH–Rate Profiles, Autocatalysis, and Disproportionation. *J Am Chem Soc* **2016**, *138* (29), 9145–9157. <https://doi.org/10.1021/jacs.6b03283>.
- (220) Cox, P. A.; Reid, M.; Leach, A. G.; Campbell, A. D.; King, E. J.; Lloyd-Jones, G. C. Base-Catalyzed Aryl-B(OH)₂ Protodeboronation Revisited: From Concerted Proton Transfer to Liberation of a Transient Aryl Anion. *J Am Chem Soc* **2017**, *139* (37), 13156–13165. <https://doi.org/10.1021/jacs.7b07444>.
- (221) Balmond, E. I.; Galan, M. C.; McGarrigle, E. M. N,N'-Bis[3,5-Bis(Trifluoromethyl)Phenyl]Thiourea. In *Encyclopedia of Reagents for Organic Synthesis*; John Wiley & Sons, Ltd: Chichester, UK, 2014; pp 1–4. <https://doi.org/10.1002/047084289X.rn01642>.
- (222) Lippert, K. M.; Hof, K.; Gerbig, D.; Ley, D.; Hausmann, H.; Guenther, S.; Schreiner, P. R. Hydrogen-Bonding Thiourea Organocatalysts: The Privileged 3,5-Bis(Trifluoromethyl)Phenyl Group. *European J Org Chem* **2012**, *2012* (30), 5919–5927. <https://doi.org/10.1002/ejoc.201200739>.
- (223) Birkholz (née Gensow), M.-N.; Freixa, Z.; van Leeuwen, P. W. N. M. Bite Angle Effects of Diphosphines in C–C and C–X Bond Forming Cross Coupling Reactions. *Chem Soc Rev* **2009**, *38* (4), 1099. <https://doi.org/10.1039/b806211k>.
- (224) Liu, Q.; Lan, Y.; Liu, J.; Li, G.; Wu, Y.-D.; Lei, A. Revealing a Second Transmetalation Step in the Negishi Coupling and Its Competition with Reductive Elimination: Improvement in the Interpretation of the Mechanism of Biaryl Syntheses. *J Am Chem Soc* **2009**, *131* (29), 10201–10210. <https://doi.org/10.1021/ja903277d>.
- (225) Wang, J.; Meng, G.; Xie, K.; Li, L.; Sun, H.; Huang, Z. Mild and Efficient Ni-Catalyzed Biaryl Synthesis with Polyfluoroaryl Magnesium Species: Verification of the Arrest State, Uncovering the Hidden Competitive Second Transmetalation and Ligand-Accelerated Highly Selective Monoarylation. *ACS Catal* **2017**, *7* (11), 7421–7430. <https://doi.org/10.1021/acscatal.7b02618>.
- (226) Ingold, C. K.; Shaw, F. R. CCCLXXXVIII.—The Nature of the Alternating Effect in Carbon Chains. Part XXII. An Attempt Further to Define the Probable Mechanism of Orientation in Aromatic Substitution. *J. Chem. Soc.* **1927**, *0* (0), 2918–2926. <https://doi.org/10.1039/JR9270002918>.
- (227) O'Duill, M.; Engle, K. Protodepalladation as a Strategic Elementary Step in Catalysis. *Synthesis (Stuttg)* **2018**, *50* (24), 4699–4714. <https://doi.org/10.1055/s-0037-1611064>.
- (228) Thomas, A. A.; Zahrt, A. F.; Delaney, C. P.; Denmark, S. E. Elucidating the Role of the Boronic Esters in the Suzuki–Miyaura Reaction: Structural, Kinetic, and Computational Investigations. *J Am Chem Soc* **2018**, *140* (12), 4401–4416. <https://doi.org/10.1021/jacs.8b00400>.

- (229) Thomas, A. A.; Wang, H.; Zahrt, A. F.; Denmark, S. E. Structural, Kinetic, and Computational Characterization of the Elusive Arylpalladium(II)Boronate Complexes in the Suzuki–Miyaura Reaction. *J Am Chem Soc* **2017**, *139* (10), 3805–3821. <https://doi.org/10.1021/jacs.6b13384>.
- (230) Thomas, A. A.; Denmark, S. E. Pre-Transmetalation Intermediates in the Suzuki–Miyaura Reaction Revealed: The Missing Link. *Science (1979)* **2016**, *352* (6283), 329–332. <https://doi.org/10.1126/science.aad6981>.
- (231) Braga, A. A. C.; Morgon, N. H.; Ujaque, G.; Lledós, A.; Maseras, F. Computational Study of the Transmetalation Process in the Suzuki–Miyaura Cross-Coupling of Aryls. *J Organomet Chem* **2006**, *691* (21), 4459–4466. <https://doi.org/10.1016/j.jorganchem.2006.02.015>.
- (232) Braga, A. A. C.; Morgon, N. H.; Ujaque, G.; Maseras, F. Computational Characterization of the Role of the Base in the Suzuki–Miyaura Cross-Coupling Reaction. *J Am Chem Soc* **2005**, *127* (25), 9298–9307. <https://doi.org/10.1021/ja050583i>.
- (233) Braga, A. A. C.; Ujaque, G.; Maseras, F. A DFT Study of the Full Catalytic Cycle of the Suzuki–Miyaura Cross-Coupling on a Model System. *Organometallics* **2006**, *25* (15), 3647–3658. <https://doi.org/10.1021/om060380i>.
- (234) Sicre, C.; Braga, A. A. C.; Maseras, F.; Cid, M. M. Mechanistic Insights into the Transmetalation Step of a Suzuki–Miyaura Reaction of 2(4)-Bromopyridines: Characterization of an Intermediate. *Tetrahedron* **2008**, *64* (30–31), 7437–7443. <https://doi.org/10.1016/j.tet.2008.05.018>.
- (235) Ortuño, M. A.; Lledós, A.; Maseras, F.; Ujaque, G. The Transmetalation Process in Suzuki–Miyaura Reactions: Calculations Indicate Lower Barrier via Boronate Intermediate. *ChemCatChem* **2014**, *6* (11), 3132–3138. <https://doi.org/10.1002/cctc.201402326>.
- (236) Amatore, C.; Jutand, A.; Le Duc, G. Kinetic Data for the Transmetalation/Reductive Elimination in Palladium-Catalyzed Suzuki–Miyaura Reactions: Unexpected Triple Role of Hydroxide Ions Used as Base. *Chemistry - A European Journal* **2011**, *17* (8), 2492–2503. <https://doi.org/10.1002/chem.201001911>.
- (237) Walker, S. D.; Barder, T. E.; Martinelli, J. R.; Buchwald, S. L. A Rationally Designed Universal Catalyst for Suzuki–Miyaura Coupling Processes. *Angewandte Chemie International Edition* **2004**, *43* (14), 1871–1876. <https://doi.org/10.1002/anie.200353615>.
- (238) Mešková, M.; Putala, M. Highly Sterically Hindered Binaphthalene-Based Monophosphane Ligands: Synthesis and Application in Stereoselective Suzuki–Miyaura Reactions. *Tetrahedron Asymmetry* **2013**, *24* (15–16), 894–902. <https://doi.org/10.1016/j.tetasy.2013.06.007>.
- (239) Genov, M.; Almorín, A.; Espinet, P. Efficient Synthesis of Chiral 1,1'-Binaphthalenes by the Asymmetric Suzuki–Miyaura Reaction: Dramatic Synthetic Improvement by Simple Purification of Naphthylboronic Acids. *Chemistry - A European Journal* **2006**, *12* (36), 9346–9352. <https://doi.org/10.1002/chem.200600616>.
- (240) Jensen, J. F.; Johannsen, M. New Air-Stable Planar Chiral Ferrocenyl Monophosphine Ligands: Suzuki Cross-Coupling of Aryl Chlorides and Bromides. *Org Lett* **2003**, *5* (17), 3025–3028. <https://doi.org/10.1021/ol034943n>.
- (241) Uozumi, Y.; Matsuura, Y.; Arakawa, T.; Yamada, Y. M. A. Asymmetric Suzuki–Miyaura Coupling in Water with a Chiral Palladium Catalyst Supported on an Amphiphilic Resin. *Angewandte Chemie International Edition* **2009**, *48* (15), 2708–2710. <https://doi.org/10.1002/anie.200900469>.
- (242) Bermejo, A.; Ros, A.; Fernández, R.; Lassaletta, J. M. C2-Symmetric Bis-Hydrazones as Ligands in the Asymmetric Suzuki–Miyaura Cross-Coupling. *J Am Chem Soc* **2008**, *130* (47), 15798–15799. <https://doi.org/10.1021/ja8074693>.

- (243) Cammidge, A. N.; Crépy, K. V. L. Synthesis of Chiral Binaphthalenes Using the Asymmetric Suzuki Reaction. *Tetrahedron* **2004**, *60* (20), 4377–4386. <https://doi.org/10.1016/j.tet.2003.11.095>.
- (244) Cammidge, A. N.; Crépy, K. V. L. The First Asymmetric Suzuki Cross-Coupling Reaction. *Chemical Communications* **2000**, No. 18, 1723–1724. <https://doi.org/10.1039/b004513f>.
- (245) Shen, X.; Jones, G. O.; Watson, D. A.; Bhayana, B.; Buchwald, S. L. Enantioselective Synthesis of Axially Chiral Biaryls by the Pd-Catalyzed Suzuki–Miyaura Reaction: Substrate Scope and Quantum Mechanical Investigations. *J Am Chem Soc* **2010**, *132* (32), 11278–11287. <https://doi.org/10.1021/ja104297g>.
- (246) Yin, J.; Buchwald, S. L. A Catalytic Asymmetric Suzuki Coupling for the Synthesis of Axially Chiral Biaryl Compounds. *J Am Chem Soc* **2000**, *122* (48), 12051–12052. <https://doi.org/10.1021/ja005622z>.
- (247) Patel, N. D.; Sieber, J. D.; Tcyrulnikov, S.; Simmons, B. J.; Rivalti, D.; Duvvuri, K.; Zhang, Y.; Gao, D. A.; Fandrick, K. R.; Haddad, N.; Lao, K. S.; Mangunuru, H. P. R.; Biswas, S.; Qu, B.; Grinberg, N.; Pennino, S.; Lee, H.; Song, J. J.; Gupton, B. F.; Garg, N. K.; Kozlowski, M. C.; Senanayake, C. H. Computationally Assisted Mechanistic Investigation and Development of Pd-Catalyzed Asymmetric Suzuki–Miyaura and Negishi Cross-Coupling Reactions for Tetra- *Ortho* -Substituted Biaryl Synthesis. *ACS Catal* **2018**, *8* (11), 10190–10209. <https://doi.org/10.1021/acscatal.8b02509>.
- (248) Bulfield, D.; Huber, S. M. Synthesis of Polyfluorinated Biphenyls; Pushing the Boundaries of Suzuki–Miyaura Cross Coupling with Electron-Poor Substrates. *J Org Chem* **2017**, *82* (24), 13188–13203. <https://doi.org/10.1021/acs.joc.7b02267>.

VITA

Samantha Leigh Gargaro (Ginter) was born in May 1996 to Kevin and Jamie Ginter, in Bremerton, Washington. She graduated from Deep Creek High School in Chesapeake, Virginia in 2014. After high school, she set out to study chemistry at Washington State University in Pullman, Washington, where she received her Bachelor of Science in Chemistry in May 2018. During her undergraduate studies, Samantha conducted undergraduate research under the guidance of graduate student Dawanna White (now Ph.D.), in Dr. Cliff Berkman's lab at WSU, synthesizing a library of potential inhibitors for beta-lactamase C of *Mycobacterium tuberculosis*.

In August of 2018, Samantha began her doctoral studies at Virginia Commonwealth University, where she, and Raphael Klake, were the first graduate students to join the Sieber lab. While at Virginia Commonwealth University, Samantha was elected President of the Chemistry Graduate Student Organization for two consecutive years, was awarded the Altria Fellowship for 2021-2022, and also completed an internship with the Innovation Gateway, VCU's Office of Technology Transfer. Samantha completed her graduate studies in December 2022 and is set to begin her new career as a Technical Specialist at an Intellectual Property law firm in Boston, Massachusetts.

SAMANTHA L. GARGARO

EDUCATION



Ph.D. in Organic Chemistry (2018-2022)

Virginia Commonwealth University, Richmond, VA

Advisor: Prof. Joshua D. Sieber

Research Focus: Cu-catalyzed Asymmetric Reductive Coupling using Alleneamides

Committee: Prof. Joshua D. Sieber, Prof. Julio Alvarez,

Prof. Brian Fuglestad, Prof. Frank Gupton

B.S. in Chemistry (2014-2018)



Washington State University, Pullman, WA

Research Advisor: Prof. Clifford Berkman

Research Focus: Synthesis of library of potential inhibitors for Beta-Lactamase C from *Mycobacterium tuberculosis* (Mtb)

PUBLICATIONS

7. **Gargaro, S.**; Sieber, J. Asymmetric Access to Boryl-Substituted Vicinal Aminoalcohols through Cu-Catalyzed Reductive Coupling. *Preprint available at ChemRxiv*: [10.26434/chemrxiv-2022-lmkp8](https://doi.org/10.26434/chemrxiv-2022-lmkp8).
6. Ho, D.; **Gargaro, S.**; Klake, R.; Sieber, J. Development of a Modified System to Provide Improved Diastereocontrol in the Linear-Selective Cu-Catalyzed Reductive Coupling of Ketones and Allenamides. *J. Org. Chem.* **2022**, *87*, 2142–2153.
5. **Gargaro, S.**; Dunson, B.; Sieber, J. Identification of a Surprising Boronic Acid Homocoupling Process in Suzuki-Miyaura Cross-Coupling Reactions Utilizing a Hindered Fluorinated Arene. *Synlett.* **2021**, *32*, 511-516.
 - Special Edition in Honor of Prof. Barry Trost's 80th Birthday.

4. Sieber, J.; Klake, R.; Agrawal, T.; Binh Ho, D.; **Gargaro, S.**; Collins, S.; Edwards, M. Cross-Coupling of Allenamides and C-Based Nucleophiles by Pd-Catalyzed Allylic Alkylation. *Isr. J. Chem.* **2020**, *60*.
 - Special Edition in Honor of Prof. Barry Trost's 80th Birthday.
3. **Gargaro, S.**; Klake, R.; Burns, K.; Elele, S.; Gentry, S.; Sieber, J. Access to a Catalytically Generated Umpolung Reagent Through the use of Cu-Catalyzed Reductive Coupling of Ketones and Allenes for the Synthesis of Chiral Vicinal Aminoalcohol Synthons. *Org. Lett.* **2019**, *21*, 9753–9758.
2. Klake, R.; **Gargaro, S.**; Gentry, S.; Elele, S.; Sieber, J. Development of a Strategy for Linear-Selective Cu-Catalyzed Reductive Coupling of Ketones and Allenes for the Synthesis of Chiral γ -Hydroxyaldehyde Equivalents. *Org. Lett.* **2019**, *21*, 7992-7998.
1. White, D.; Choy, C.; Moural, T.; Martin, S.; Wang, J.; **Gargaro, S.**; Kang, C.; Berkman, C. Bis(benzoyl) Phosphate Inactivators of Beta-Lactamase C from Mtb. *Bioorg. Med. Chem. Lett.* **2019**, *29*, 2116-2118.

HONORS AND AWARDS

- Altria Fellowship (VCU, 2021-2022)
- McFadden/Yount Undergraduate Chemistry Scholarship (WSU, 2017-2018)
- Harvey K. & Clarissa Murer Memorial Scholarship (WSU, 2016-2017)
- Art & Helen Brunstad Endowed Chemistry Scholarship (WSU, 2016-2017)
- Dr. Edwin J. Hart Chemistry Scholarship (WSU, 2015-2016)

PRESENTATIONS

2. *Regiodivergent Cu-Catalyzed Reductive Coupling of Ketones and Allenamides.* **Gargaro, S.**; Sieber, J. D. *et al.* Presented at the 10th Annual Out in STEM: Out to Innovate Conference, Virtual. November 12th, 2020, Poster.
1. *Regiodivergent Cu-Catalyzed Reductive Coupling of Ketones and Allenamides.* Klake, R. K.; **Gargaro, S.**; Sieber, J. D. *et al.* Presented at the 8th Annual Alliance for Diversity in Science and Engineering (ADSE) Young Researcher Conference, The University of Maryland, College Park. October 5th, 2019, Poster.

TEACHING EXPERIENCE

Teaching Assistant for the following courses at Virginia Commonwealth University:

- Organic Chemistry Laboratory I/II, *Spring and Fall 2019, Spring and Fall 2020, and Spring 2021*
- General Chemistry I/II, *Fall 2018*

WORK EXPERIENCE

- Undergraduate Researcher, *Washington State University* (January 2016 – May 2018) *Advisor:* Prof. Berkman
- Graduate Assistant, *Virginia Commonwealth University* (August 2018 – December 2022), *PI:* Prof. J. D. Sieber
- Licensing Liaison, Innovation Manager *VCU Innovation Gateway – Office of Technology Transfer* (June 2022 – September 2022)

LEADERSHIP

- **President**, Chemistry Graduate Student Organization, VCU, 2020-2021, 2021-2022
- **Initiated Community Outreach Programs**, Proposed and implemented community outreach, Sieber Lab, 2021
- **Mentor – Graduate Student Supervisor**, Research Experience for High School Seniors, VCU, Spring 2020
- **Ambassador and Mentor**, Project SEED, ACS, VCU, Summer 2019
- **Co-President**, Chemistry Club, WSU, 2017-2018

PROFESSIONAL AFFILIATIONS

- Out in STEM, 2020-2022
- American Chemical Society, 2020-2022
- ACS Younger Chemists Committee, Virginia Chapter, 2019-2022
- Chemistry Graduate Student Organization, Virginia Commonwealth University, 2018-2022
- Chemistry Club, Washington State University, 2014-2018